Volume I

Evaluation of Coal Minerals and Metal Residues as Coal-Liquefaction Catalysts

Final Report

Work Performed by

**Air Products and Chemicals, Inc.
P.O. Box 538
Allentown, Pennsylvania 18105**

February 1982

DISCLAIMER

This report was prepared as an account of work sponsored by an agency of the United States Government. Neither the United States Government nor any agency Thereof, nor any of their employees, makes any warranty, express or implied, or assumes any legal liability or responsibility for the accuracy, completeness, or usefulness of any information, apparatus, product, or process disclosed, or represents that its use would not infringe privately owned rights. Reference herein to any specific commercial product, process, or service by trade name, trademark, manufacturer, or otherwise does not necessarily constitute or imply its endorsement, recommendation, or favoring by the United States Government or any agency thereof. The views and opinions of authors expressed herein do not necessarily state or reflect those of the United States Government or any agency thereof.

DISCLAIMER

Portions of this document may be illegible in electronic image products. Images are produced from the best available original document.

Volume I

Evaluation of Coal Minerals and Metal Residues as Coal-Liquefaction Catalysts

MASTER

Final Report

Air Products and Chemicals, Inc.

    D. Garg

    E. N. Givens

    F. K. Schweighardt

Auburn University

    A. R. Tarrer

    J. A. Guin

    C. W. Curtis

    W. J. Huang

    K. Shridharani

    J. H. Clinton

February 1982

Prepared for

The U. S. Department of Energy

Under Contract No. DE-AC22-79ET14806

ABSTRACT

The catalytic activity of various minerals, metallic wastes, and transition metals was investigated in the liquefaction of various coals. The effects of coal type, process variables, coal cleaning, catalyst addition mode, solvent quality, and solvent modification on coal conversion and oil production were also studied.

Coal conversion and oil production improved significantly by the addition of pyrite, reduced pyrite, speculite, red mud, flue dust, zinc sulfide, and various transition metal compounds. Impregnation and molecular dispersion of iron gave higher oil production than particulate incorporation of iron. However, the mode of molybdenum addition was inconsequential. Oil production increased considerably both by adding a stoichiometric mixture of iron oxide and pyrite and by simultaneous impregnation of coal with iron and molybdenum.

Hydrogenation activity of disposable catalysts decreased sharply in the presence of nitrogen compounds. The removal of heteroatoms from process solvent improved thermal as well as catalytic coal liquefaction. The improvement in oil production was very dramatic with a catalyst.

ACKNOWLEDGEMENT

NOMENCLATURE

C	Atomic percent carbon, %
C_{AR}	Fractional aromatic carbon
C_n	Concentration of naphthalene, g mole
f_a	Fraction of aromatic carbon or aromaticity
H	Atomic percent hydrogen, %
H_a	Fractional alpha protons defined as protons on carbon atoms adjacent to an aromatic ring
H_{AR}	Fractional aromatic protons
H_o	Fractional beta and higher protons defined as those protons residing on two or more carbon atoms removed from an aromatic ring
H_{OH}	Percent hydroxyl hydrogen, %
k	Pseudo first-order rate constant, g solvent/g catalyst min.
K_a	First-order rate constant for the conversion of asphaltenes, hr^{-1}
K_p	First-order rate constant for the conversion of preasphaltenes, hr^{-1}
$\overline{n}MW$	Number average molecular weight
r	Reaction rate, g mole/min.
R_a	Number of aromatic condensed ring
t	Reaction time, min.
W_c	Weight of the catalyst, g
W_s	Weight of the solvent, g
x	Fractional conversion
X	A parameter
Y	Atomic ratio
σ	Degree of substitution on aromatic ring

SUMMARY

This is the final report under contract number DE-AC22-79ET14806 titled "Evaluation of Coal Minerals and Metal Residues as Coal Liquefaction Catalysts". This contract with Air Products and Chemicals, Inc. included a subcontract with Auburn University to provide screening and evaluation testing in support of larger scale continuous PDU studies at Air Products. The contract was begun on 1 September 1979 and ended on 1 February 1982.

This report is comprised of three volumes. In the present volume, Volume I, all of the work conducted at Air Products plus significant results from work conducted both at Auburn University and the University of Toledo are incorporated. The work conducted at Auburn University is discussed in detail in Volume II. Volume III compiles the work conducted at the University of Toledo sponsored under separate contract under this program. Because of the extensive amount of work conducted under this contract, in addition to the summary, the highlights of the program are discussed in greater detail in the Program Synopsis.

The objective of this program was to investigate options for the development of low-cost disposable catalysts to enhance coal conversion and oil production in coal liquefaction. Studies yielded significant results concerning the catalytic effects of different minerals, metallic wastes, and transition metals on the liquefaction behavior of various coals. Some of the important findings are listed below.

o Pyrite, speculite, red mud, and flue dust were very active in catalyzing coal liquefaction reactions, although they did not show significant activity in solvent hydrogenation; this indicates that a synergistic effect exists between these additives and coal during liquefaction.

o Addition of pyrite, iron oxide, red mud, flue dust and zinc sulfide significantly increased coal conversion and oil production; in addition oil production, hydrogen consumption and rates of conversion of asphaltenes and preasphaltenes increased with increasing temperature. Although pyrite showed the highest catalytic activity of these additives, it yielded the highest hydrogen consumption as well.

o Catalytic activity of various mineral-grade pyrites was very similar.

o Activity of reduced pyrite was comparable to that of pyrite. However, reduced pyrite required less hydrogen consumption and yielded lower hydrocarbon gas production than pyrite.

o Oil production increased considerably when pyrite was mixed with stoichiometric amount of iron oxide. In addition, hydrogen consumption was lower with a mixture of pyrite and iron oxide than with pyrite alone.

o Impregnation and molecular dispersion of iron gave higher oil and lower hydrocarbon gas production than did particulate incorporation of iron.

o Addition of calcium was detrimental to coal liquefaction.

o Cobalt, nickel, and molybdenum impregnation yielded similar levels of oil production, coal conversion, hydrogen consumption, and SRC sulfur content.

o Whereas the mode of iron addition affected liquefaction performance, the mode of molybdenum addition was inconsequential.

o Simultaneous impregnation of coal with iron and molybdenum significantly increased oil production.

o Several minerals and metallic wastes like chrome ore concentrate, phosphate slime, and metal grindings significantly increased coal conversion and oil production.

o Transition metals like nickel, vanadium, tin, and molybdenum also significantly increased coal conversion and oil production.

o Sulfiding of iron oxide with either hydrogen sulfide or mixture of hydrogen and hydrogen sulfide significantly increased its naphthalene hydrogenation activity.

o   Basic and nonbasic nitrogen compounds poisoned the naphthalene hydrogenation
    activity of sulfided iron oxide and Co-Mo-Al catalysts.

o   Removal of heteroatoms from process solvent significantly improved oil
    production in thermal as well as catalytic coal liquefaction.

TABLE OF CONTENTS

TABLE OF CONTENTS (Continued)

TABLE OF CONTENTS (Continued)

TABLE OF CONTENTS (Continued)

TABLE OF CONTENTS (Continued)

LIST OF TABLES

LIST OF TABLES (Continued)

LIST OF TABLES (Continued)

LIST OF TABLES (Continued)

LIST OF FIGURES

Page

PROGRAM SYNOPSIS

Currently, both catalytic and noncatalytic coal liquefaction processes are being examined to establish the technological data base needed for future commercialization. The primary goal of any coal liquefaction process is to give high yield of distillate oils using a minimum amount of hydrogen. In all the liquefaction concepts presently under investigation, a high yield of distillate oils is obtained by using either an expensive catalyst like Co-Mo-Al, or severe reaction conditions (e.g., high temperature and pressure). Furthermore, high yield of distillate oils is obtained at the expense of high hydrocarbon gas production and concomitantly high hydrogen consumption which makes the liquefaction processes less economically attractive. In the literature, inexpensive coal minerals have been reported to catalyze coal liquefaction reactions, and to be active even at less severe reaction conditions. Conceptually, the use of milder reaction conditions together with added inexpensive minerals should increase oil production and reduce hydrocarbon gas production, and therefore hydrogen consumption. If this is true, such inexpensive minerals would greatly improve the above-mentioned conventional coal liquefaction processes. Therefore, the objective of this research program was to investigate options for the identification of low-cost disposable catalysts for use in enhancing the performance and economics of coal liquefaction.

During this program, most of the work was conducted on Kentucky coals using SRC-II heavy distillate solvent. High volatile A bituminous eastern Kentucky coals, which have low intrinsic liquefaction activity, as well as low ash and pyrite contents, were selected as base coals to study the catalytic activity of various minerals, metal-containing by-products, waste materials, transition metal sulfides, and organic compounds of transition metals. In addition, a high volatile B bituminous western Kentucky #9 coal having high liquefaction activity, and higher ash and pyrite contents, was included in the program to study the effect of coal reactivity on liquefaction, as well as mineral catalysis. The program also included two high volatile C bituminous eastern Ohio coals from two different locations to study their liquefaction behavior.

1

SRC-II heavy distillate (550-850°F) received from the SRC-II Pilot Plant at
Fort Lewis, Washington, was selected as a process solvent for the program
because it was thought that high-boiling, heavy-distillate solvent was of
better quality than normal-boiling (450-850°F) solvent and that the yield of
more desirable products like distillate oils increased with solvent quality.
Low boiling process solvent (450-850°F) recovered by distillation of product
slurry was used in some experiments to determine the effect of solvent quality
on coal liquefaction.

Kentucky Coal Liquefaction

Three eastern Kentucky Elkhorn coals were tested to determine their liquefaction
behavior. - The coals were from different counties but had similar rank, and
were therefore expected to display similar liquefaction behavior. However,
the experimental results showed that they had very different liquefaction
characteristics. Overall conversion to pyridine solubles varied from 72 to
85%, and oil yields varied from 8 to 27% at the same processing conditions.
Hydrogen consumption and SRC contents also differed.

Because the intrinsic liquefaction reactivity of the western Kentucky coal
used in the program was higher than that of eastern Kentucky coals, it was
expected to give superior product distribution. Indeed, western Kentucky coal
showed higher conversion to pyridine solubles. Excepting overall coal conversion,
no major differences in product distribution were noted. A strong correlation
was observed between SRC sulfur and initial total sulfur contents of all the
Kentucky coals, excluding Elkhorn #2 coal. No definite trends in overall coal
conversion and product distributions were noted with the variations in ash and
pyritic sulfur contents.

Ohio Coal Liquefaction

To further test the effect of mineral matter and pyritic sulfur contents on
coal liquefaction, four samples of Ohio coals having similar rank but different
mineral matter and pyritic sulfur contents were tested. The coal having high
mineral and pyritic sulfur contents showed slightly higher overall coal conversion
and oil production than the coal having low mineral and pyrite sulfur contents.
No other major differences in product distribution were noted.

2

Since the rank of both Ohio coals (high volatile C bituminous) was lower than that of western Kentucky coal (high volatile B bituminous), liquefaction reactivity should have been higher in the Ohio coal. However, the experimental data showed no significant differences between the overall conversion of Ohio and western Kentucky coals. Furthermore, no definite trend in oil production was noted.

Effect of Process Variables on Kentucky Coal Liquefaction

Different Kentucky coals not only showed different liquefaction behavior as discussed earlier, but also responded differently to reaction temperature. With increasing temperature, Elkhorn #3 coal (Letcher County) showed an increase in overall conversion, whereas the other three Kentucky coals (Floyd County Elkhorn #3, Elkhorn #2, and Kentucky #9) showed either no change or a decrease in overall conversion. Oil, hydrocarbon gas, and water production increased with temperature with all coals except Elkhorn #2. Mixed results were noted in the production of asphaltenes and preasphaltenes. Although their product distributions were different, variations in hydrogen consumption, and SRC sulfur and hydrogen contents of the generated oil fraction with temperature were uniform for all Kentucky coals.

Process solvent quality plays an important role in coal liquefaction. Experiments on Elkhorn #3 (Floyd County) coal showed that overall conversion was higher with low-hydrogen-content (high-boiling-range) solvent than with high-hydrogen-content (low-boiling-range) solvent. The quality of solvent determined by the combined concentration of H_a and H_o protons was higher for high-hydrogen-content solvent than for low-hydrogen-content solvent. Despite higher solvent quality, this high-hydrogen-content solvent resulted in increased hydrogen consumption and decreased desulfurization. The only advantage in using high-quality solvent was that it did aid in improving oil production. Therefore, the use of high- or low-hydrogen-content solvent in coal liquefaction reactions will be governed by the process economics and desired product slate.

Another process variable, hydrogen partial pressure, has been reported to affect oil yield in coal liquefaction. An experiment with Kentucky Elkhorn #2 coal was carried out to simulate the effect of hydrogen partial pressure on

liquefaction by increasing the total hydrogen flow rate. The increase in flow rate showed no effect on overall coal conversion, but increased oil production, as well as the rates of conversion of asphaltenes and preasphaltenes. Hydrogen consumption, hydrogen content, and quality of the generated oil increased, and SRC sulfur content decreased with increasing flow rate. These observations indicate that higher hydrogen flow rate and presumably higher hydrogen partial pressure are advantageous in noncatalytic coal liquefaction.

Mineral Catalysis in Solvent Hydrogenation

Extensive research has been performed in the area of mineral catalysis in coal liquefaction. It is well known that in coal liquefaction, high-molecular-weight compounds rupture thermally, producing unstable free radicals. These free radicals can react with hydrogen donated by hydrogen donor species present in the process solvent to form stable species. Therefore, the presence of sufficient hydrogen donor compounds in the coal liquefaction reaction mixture prevents the repolymerization of free radicals and aids in producing low-molecular-weight products like oils and asphaltenes. It has been speculated that mineral matter catalyzes coal liquefaction reactions by enhancing the transfer of hydrogen from the gas to liquid phase and maintaining the hydrogen donor capability of the process solvent. To better understand the role of minerals and metallic wastes in coal liquefaction reactions, these materials were mixed with the process solvent and passed through the process system at typical coal liquefaction reaction conditions. The original process solvent and reactor effluent streams were analyzed by solvent separation to determine the concentration of oils, asphaltenes, and preasphaltenes. The hydrogen content and the hydrogen donor capability of process solvent increased slightly without additive. However, addition of pyrite, zinc sulfide, and flue dust to the feed solvent yielded a greater increase in hydrogen content and hydrogen donor capability of the process solvent. The addition of these minerals also promoted the conversion of the small amount of residual insolubles (asphaltenes) in the process solvent to oils and hydrocarbon gases. These results help confirm that mineral matter plays an important role in maintaining the quality of the process solvent during coal liquefaction.

Although pyrite, speculite, red mud, and flue dust promoted conversion of the small amounts of asphaltenes to oils, they did not show significant activity in converting the very small amount of preasphaltenes in the solvent to asphaltenes and oils. Overall they were very weak catalysts for solvent hydrogenation compared with Co-Mo-Al or Ni-Mo-Al catalysts. In contrast, the reaction rates of conversion of the asphaltenes and preasphaltenes were significantly higher with the catalysts in the coal liquefaction reaction than with solvent hydrogenation. These observations indicate that synergism exists between these various additives and coal during the liquefaction reaction.

Experiments on solvent hydrogenation were also instrumental in determining changes that might occur in the mineral form of various additives during coal liquefaction. Pyrite was completely converted to pyrrhotite during the reaction, causing an increase in total hydrogen consumption; otherwise, hydrogen consumption was very similar to that of no-additive and various-additive runs. Speculite and red mud containing Fe_2O_3 as the major phase were transformed to Fe_3O_4, FeS, and elemental iron during solvent hydrogenation runs, but no additional hydrogen consumption resulted from this transformation. No changes in the composition and phases of zinc sulfide and flue dust were noted when they were used in solvent hydrogenation.

Catalysis in Coal Liquefaction

This program also involved the catalytic activity of various minerals, metallic wastes, and transitional metals in the liquefaction of Kentucky coals. Catalytic activity was measured in terms of oil production and hydrogen consumption.

Pyrite. Addition of pyrite to the coal liquefaction reaction mixture significantly increased overall coal conversion and oil production compared with no-additive runs. However, the increase in oil production was achieved at the expense of a significant increase in hydrogen consumption. Preasphaltene production decreased with pyrite, but no clear trend was observed for asphaltene production. Hydrogen content and the quality of the generated solvent was higher with pyrite compared with baseline runs. These results further verify that mineral matter catalyzes the coal liquefaction reaction by maintaining or improving solvent quality during liquefaction. No significant trend was noted

in SRC sulfur content with pyrite addition. Analysis of the coal liquefaction residue showed complete conversion of pyrite to pyrrhotite. Similar results were noted in solvent hydrogenation with pyrite.

Process variables such as reaction temperature, pressure, and reaction time have been known to influence both catalytic and noncatalytic coal liquefaction reactions. Increasing reaction temperature and pressure have been shown to increase oil production and hydrogen consumption in noncatalytic coal liquefaction. It is therefore important to know how different process variables affect oil production and hydrogen consumption in the catalytic coal liquefaction process. This information will help both in identifying critical process variables and in optimizing the catalytic coal liquefaction process.

In addition to increasing oil production, hydrogen consumption, and the rates of conversion of asphaltenes and preasphaltenes, higher reaction temperature with pyrite increased overall conversion of Kentucky coals. Therefore, considerably higher oil production can be obtained with pyrite at a higher reaction temperature, but at the expense of increased hydrogen consumption.

Increasing hydrogen flow rate did not significantly change the overall conversion of Kentucky coals in the presence of pyrite. However, higher flow rate yielded higher oil production (and lower hydrogen consumption) with western Kentucky coal, whereas it yielded no significant improvement in oil production with eastern Kentucky coals. As discussed earlier, oil production improved significantly with increasing hydrogen flow rate in the noncatalytic liquefaction of an eastern Kentucky coal. These data suggest that the noncatalytic liquefaction of eastern Kentucky coal and catalytic liquefaction of western Kentucky coal are somehow mass-transfer-limited. More work is needed to positively determine whether the above differences are due to mass transfer or to reactor configuration.

All the above experiments were carried out using a very high concentration of pyrite (10 wt % based on slurry) to positively identify the catalytic activity of pyrite in coal liquefaction. Because the use of such a high concentration in a true plant situation would be unrealistic, the concentration of added

pyrite was reduced to a level of 2.5 wt % based on slurry, which would represent an upper limit for any added disposable catalyst in coal liquefaction. Lowering the concentration of pyrite did not change the overall conversion of both Elkhorn #2 and #3 coals. With decreasing pyrite concentration, oil production decreased for Elkhorn #3 coal, but remained unchanged for Elkhorn #2 coal. Hydrogen consumption also decreased with decreasing pyrite concentration.

The sample of pyrite used in the above experiments was separated from Pittsburgh #8 seam coal. It has been reported in the literature that pyrite from different sources behaves differently. However, data obtained in the present program using various mineral-grade pyrites and those separated from various coals showed no significant differences in overall coal conversion. Oil production, however, was higher with mineral-grade pyrites than with those separated from various coals; these results could be related to the relative purity of the; pyrite samples.

In summary, significant pyrite catalytic activity was observed in coal lique-faction. Pyrite addition increased oil production as well as hydrogen consumption, both for high volatile A bituminous eastern and B bituminous western Kentucky coals. Although variations in oil production and hydrogen consumption with different process variables in the presence of pyrite were different, an increase in oil production was always associated with an increase in hydrogen consumption. Reaction temperature had the most pronounced effect on oil production and hydrogen consumption. Hydrogen consumption was also sensitive to the concentration of the added pyrite and could be reduced by carefully controlling the amount of added pyrite. Finally, oil production and hydrogen consumption could be optimized by carefully selecting the various process variables in the coal liquefaction reaction.

Reduced Pyrite. Addition of pyrite to the coal liquefaction reaction undoubtedly increased oil production over that of noncatalytic runs, but this increase was achieved at the expense of greater hydrogen consumption. Part of the increased consumption was due to the reduction of pyrite to pyrrhotite. Since pyrite reduces to pyrrhotite at coal liquefaction reaction conditions, it was thought that the true catalytic activity of pyrite may be due to some active form of pyrrhotite produced in situ. In addition, the amount of hydrogen normally

consumed to reduce pyrite to pyrrhotite could be saved by adding pyrrhotite instead of pyrite. Experimental results obtained with the addition of reduced pyrite showed coal conversion and oil production comparable with that obtained with pyrite. No significant differences were noted in product distribution with the addition of either pyrite or reduced pyrite. As expected, hydrogen consumption was lower with reduced pyrite than with pyrite. Therefore, the above data indicate that an improvement in process economics can be realized with reduced pyrite instead of pyrite. In spite of this improvement, certain problems with reduced pyrite must be considered, since it is not readily available in the mineral form and has to be produced either by hydrogen reduction or pyrolysis of pyrite. Hydrogen reduction of pyrite is not desirable because it will offset the savings in hydrogen consumption achieved by using reduced pyrite instead of pyrite. Pyrolysis of pyrite seems to be the only other choice, but nothing is known about the activity of this material in coal liquefaction. Thus, more work is needed to study the activity of the reduced pyrite produced by pyrolysis.

Iron Oxide. A considerable amount of work on iron oxide catalysis has been reported. Like pyrite, iron oxide is inexpensive, available in large quantities, and is a potential candidate for use as a disposable catalyst in coal liquefaction. Iron oxide addition increased overall coal conversion and oil production, as well as hydrogen consumption, in the liquefaction of eastern Kentucky coals. Asphaltene production decreased, but mixed results were noted in hydrocarbon gas and preasphaltene production. The activity of reagent-grade iron oxide was far superior to that of mineral-grade iron oxide. All H_2S generated by desulfurization of coal was removed by reagent-grade Fe_2O_3, whereas it was not with mineral-grade Fe_2O_3. X-ray diffraction analysis revealed complete conversion of both grades of Fe_2O_3 to Fe_3O_4, FeS, and elemental iron. SRC sulfur content decreased with reagent-grade Fe_2O_3, while the opposite result was noted with mineral-grade Fe_2O_3. Hydrogen content and thus quality of the generated solvent decreased with the addition of iron oxide.

Overall coal conversion did not change by increasing reaction temperature in the presence of iron oxide. However, oil production and hydrogen consumption increased with temperature. Asphaltene production was unchanged and preasphaltene production decreased with temperature. An increase in iron oxide concentration showed no beneficial effect on coal liquefaction.

Iron Oxide vs. Pyrite. A study was conducted to determine the relative activity of iron oxide and pyrite in coal liquefaction. Experimental data showed that pyrite addition gave higher overall coal conversion and oil production than did iron oxide. Hydrogen consumption, however, was four times higher with pyrite compared with iron oxide. All the H_2S present in the gas phase was removed by iron oxide, which would result in lowering the capital required for a product gas treatment facility. In contrast, the amount of H_2S in the product gas increased with pyrite addition. The quality (hydrogen donor capability) of the generated solvent was higher with pyrite than with iron oxide. These observations show that pyrite and iron oxide have both advantages and disadvantages in coal liquefaction. Therefore, the use of pyrite and iron oxide as disposable catalysts will depend mainly on the process economics.

Iron Oxide/Pyrite Combined. Because both pyrite and iron oxide tend to form pyrrhotite, an active catalyst, during the coal liquefaction reaction, they should improve the liquefaction reaction if added simultaneously. Pyrite will reduce to active pyrrhotite during liquefaction and the H_2S gas liberated by its reduction will be removed by iron oxide to produce an additional amount of active pyrrhotite. Therefore, several runs using a stoichiometric iron oxide/ pyrite mixture were made to test this theory. The mixture did not improve coal conversion compared with pyrite alone, but increased it considerably over iron oxide alone. Oil production increased with the mixture compared with pyrite or iron oxide alone. Significant improvement in hydrogen consumption was also noted with this mixture over pyrite alone. These observations show the tremendous potential of using this mixture in coal liquefaction.

Iron Dispersion. Earlier, oil production and hydrogen consumption were shown to increase with an increase in the concentration of the added pyrite. It is well known that an increase in the concentration of the disposable catalyst reduces the processing capacity of the plant and increases the load on the solid/liquid separation unit. Also, the loss in recoverable carbonaceous material increases with an increase in the concentration of solids in the feed slurry to the separation unit, which ultimately affects the overall efficiency of the plant. All these factors therefore encourage the use of the lowest possible concentration of the catalyst in the reaction.

If catalyst activity is not sufficiently high at low concentration, it may be possible to increase activity by increasing catalyst surface area. Particulate iron catalysts, such as pyrite and iron oxide, have very low surface-area-to-weight ratio (1 to 10 m^2/g). Therefore, iron must be finely dispersed in the coal liquefaction reaction mixture to be effective.

Two methods were used to finely disperse the iron catalyst in the reaction mixture, namely, impregnation and molecular dispersion. A water-soluble iron compound, thermally unstable at coal liquefaction reaction conditions, was impregnated into coal to increase the contact between iron and coal. To effect molecular dispersion, a thermally unstable, process-solvent-soluble compound was used.

Both impregnation and molecular dispersion of iron did not change overall coal conversion, but increased oil production by over a factor of two compared with the no-additive run. Coal conversion was somewhat lower with both methods than with particulate addition of pyrite, but oil production was comparable. However, hydrogen consumption and hydrocarbon gas production were significantly lower with impregnation and molecular dispersion of iron than with pyrite addition. Furthermore, the total concentration of iron used in the two dispersion methods was an order of magnitude lower than that used in the pyrite run. These results show the significance of iron impregnation and molecular dispersion in coal liquefaction reactions.

Metallic Wastes. Like iron compounds, many other inexpensive industrial metallic wastes such as red mud, flue dust, and zinc sulfide are available in large quantities that can be used as disposable catalysts in coal liquefaction. Therefore, it is of great interest to determine their catalytic activity in coal liquefaction, as well as to compare their activity with that of pyrite.

Some of the metallic waste samples tested in the program have already been reported to catalyze coal liquefaction reactions. For example, red mud was extensively used in World War II by the Germans to liquefy brown coal. However, the activity of red mud has never been tested in the liquefaction of U.S coals.

Addition of red mud to the liquefaction of U.S. coal increased overall conversion and produced more oils and hydrocarbon gases compared with no-additive runs. In addition, hydrogen consumption increased, and SRC sulfur content and asphaltene and preasphaltene production decreased. Increasing reaction temperature in the presence of red mud increased the overall conversion of coal and production of hydrocarbon gases and asphaltenes; however, oil production decreased, while hydrogen consumption increased. Therefore, to maximize oil production and minimize hydrogen consumption, lower reaction temperature should be used with red mud.

Since the flue dust tested contained significant quantities of iron, nickel, and molybdenum metals, it was expected to have very high catalytic activity in coal liquefaction reactions. As expected, flue dust addition increased overall coal conversion and oil production. However, hydrogen consumption also increased. An increase in the reaction temperature decreased oil production and increased hydrocarbon gas production and hydrogen consumption, again indicating that lower reaction temperature is preferable.

Zinc compounds in the form of Lewis acids have been reported to significantly catalyze coal liquefaction reactions, but they are expensive and cause severe corrosion problems. However, zinc sulfide mineral is inexpensive and readily available, and therefore can be used as a disposable catalyst. The liquefaction of Elkhorn #3 coal with zinc sulfide addition yielded increased conversion; however, no change was noted in the liquefaction of Elkhorn #2 coal. Oil production, hydrogen consumption, and rate of conversion of asphaltenes increased with ZnS addition for both coals. Asphaltene production decreased with ZnS addition due to the increased rate of conversion of asphaltenes. The hydrogen content and quality of the generated solvent was either maintained or increased with ZnS addition.

Pyrite vs. Metallic Wastes. The comparison of the catalytic activity of various metallic wastes with that of pyrite showed that coal conversion was very similar among all the additives. However, pyrite addition yielded highest oil production and the lowest hydrocarbon gas and asphaltene production among all the additives. It also resulted in the highest hydrogen consumption, SRC

sulfur content, and hydrogen content of the generated solvent. In summary, pyrite showed the highest activity in coal liquefaction among the various metallic wastes tested.

Calcium. U.S. coals contain varying amounts of calcium, which is known to cause scaling problems in heat exchangers. To avoid scaling, several researchers have proposed the removal of calcium from coal before it is liquefied. However, the role of calcium in coal liquefaction is not well known. In the present program, several calcium-containing materials, including lime, were added to the reaction mixture to determine their effect. Although most of the calcium materials had little effect on liquefaction, lime addition yielded decreased coal conversion and oil and asphaltene production. Hydrogen consumption and hydrocarbon gas production increased with lime addition. In addition, the quality of generated solvent was lower compared with the no-additive run. Although it can be concluded that lime addition is detrimental to coal lique-faction, the result is probably more related to the basicity of the lime than to the presence of the calcium ion.

Transition Metals. Transition metals like cobalt, nickel, and molybdenum were reported to have significant catalytic activity in coal liquefaction. The use of some of these metals is restricted because they are not available in large quantities. However, at very low concentrations (~250 ppm based on coal), these metals can be used economically, either by adding them as particulate oxides and sulfides to the feed slurry or by impregnating them into the coal in the form of water-soluble compounds. The catalytic activity of various transition metals in the liquefaction of Elkhorn #2 coal was studied to determine their relative effectiveness and to identify the effect of mode of catalyst addition on liquefaction.

Addition of particulate molybdic oxide and molybdenite increased coal conversion, oil and asphaltene production, and hydrogen consumption. However, the production of hydrocarbon gases was not greatly affected by molybdic oxide and molybdenite addition compared with the no-additive run; SRC sulfur content remained unchanged. Oil and hydrocarbon gas production, as well as hydrogen consumption, increased with increasing temperature in the presence of molybdic oxide. Impregnation of coal with molybdenum increased the production of oils and conversion of

12

asphaltenes and preasphaltenes over no-additive runs; however, hydrocarbon gas production was not greatly affected. The most important observation was that the increase in oil production with molybdenum impregnation was not obtained at the expense of increased hydrogen consumption; in fact, hydrogen consumption was lower than in the no-additive run.

The comparison of catalytic activity of molybdenum impregnated into coal to that of particulate addition of molybdenum showed that the production of oils and hydrocarbon gases was independent of the mode of catalyst addition. In contrast, the catalytic activity of iron was highly dependent on the mode of its addition in coal liquefaction.

Impregnation of coal with cobalt, nickel, and molybdenum gave very similar coal conversion, oil production, hydrogen consumption, and SRC sulfur content. These data indicate that expensive molybdenum catalysts can be replaced by less expensive catalysts like cobalt and nickel without significantly altering the liquefaction performance.

Iron-Molybdenum Impregnation. Simultaneous impregnation of coal with iron and molybdenum showed significant synergism; the production of oils was considerably higher compared with either of them alone. Hydrogen consumption also increased with simultaneous iron/molybdenum impregnation, but the increase was not as dramatic as the increase in oil production. The iron/molybdenum mixture yielded lower production of asphaltenes and preasphaltenes and higher SRC sulfur content than with either used separately. These results show the great potential in using iron and molybdenum together as disposable catalysts in coal liquefaction.

Other Catalysts. Several other potential minerals, metallic wastes, and transition metal catalysts were tested for their catalytic activity using a microautoclave reactor. Addition of the minerals to the coal liquefaction reaction mixture at very high concentrations did increase overall coal conversion and oil production compared with the no-additive run, but the magnitude of the increase in oil production was not great enough to consider

13

them possible disposable catalysts. However, chrome ore concentrate, gypsum, and kaolinite had noticeable catalytic activity in oil production. More data are needed on the catalytic activity of these minerals at lower concentration levels.

Metallic wastes like phosphate slime, metal grindings, and flue dust significantly improved overall coal conversion and oil production. However, their use depends on their availability in large quantities, as well as their cost. Coal liquefaction residues like filter cake and Kerr-McGee ash concentrate were also active catalysts in coal liquefaction.

Most of the transition metal sulfides studied in the program improved coal conversion and oil production. The catalytic activity of nickel, vanadium, and tin sulfides was especially noticeable. Again, the amount of catalyst used in the program was very high and would not represent a realistic situation. Sulfides of iron, nickel, tin, and molybdenum were also active at low concentrations. Still more work is needed at much lower transition metal concentrations to economically justify their use.

Fundamental Studies

Activation of Catalyst. Earlier, pyrite and iron oxide were shown to have significant catalytic activity. To better understand the role of these minerals in coal liquefaction, hydrogenation of a pure model compound, naphthalene, was studied in the presence of these minerals. Although both minerals were noted to be inactive, the naphthalene hydrogenation activity of iron oxide was significantly improved by first sulfiding it with either H_2S or a mixture of H_2 and H_2S gases.

The hydrogenation activity of a commercial catalyst like Ni-Mo-Al has been reported to increase with sulfiding. Iron catalyst, which normally has low hydrogenation activity, showed unexpectedly high hydrogenation activity with sulfiding. More work in this area revealed that the hydrogenation activity of sulfided iron oxide was a function of two important variables, namely,

composition of sulfiding gas and sulfiding temperature. Iron oxide sulfided with pure H_2S was much more active than that sulfided with a mixture of H_2 and H_2S gases. Surface area, as well as the hydrogenation activity of the material sulfided at lower temperatures, was higher than that sulfided at a higher temperature. In addition, this high-surface-area sulfided iron oxide showed naphthalene hydrogenation activity comparable to that observed with sulfided Co-Mo-Al catalyst. X-ray diffraction analysis of the sulfided iron oxide sample having the highest surface area and naphthalene hydrogenation activity showed that it resembled pyrite.

Poisoning of Activated Catalyst. The high-surface-area sulfided iron oxide sample showing very high hydrogenation activity was tested for its catalytic activity in coal liquefaction. Surprisingly, its catalytic activity was similar to that of low-surface-area Robena pyrite. This observation suggested that the sulfided iron oxide catalyst was somehow poisoned in the coal lique-faction system. More work in this area revealed that basic and nonbasic nitrogen compounds, when added to the naphthalene hydrogenation reaction mixture, poisoned both sulfided iron oxide and Co-Mo-Al catalysts, and severely limited their naphthalene hydrogenation activity.

Based on the naphthalene hydrogenation experiments, nitrogen compounds were removed from the process solvent to determine whether the catalytic activity of the sulfided iron oxide would improve. Indeed, the production of oils increased significantly with catalyst when the basic nitrogen compounds were removed from the process solvent. A similar observation was noted with phenol removal. When both nitrogen compounds and phenols were removed from the process solvent, a dramatic increase in oil production was noted in the thermal as well as catalytic coal liquefaction processes. These results show that catalytic and noncatalytic coal liquefaction processes can be greatly improved by pretreating the process solvent.

Recommendations for Further Investigation

In this program, several factors critical to the development of low-cost disposable catalyst were identified. However, the following work is needed to fully understand their role in coal liquefaction:

15

(1) Investigate the relative effectiveness of pyrite and reduced pyrite in overall coal conversion, oil production, and hydrogen consumption.

(2) Investigate the most effective way of dispersing iron and other transition metal catalysts in the reaction mixture.

(3) Investigate the synergistic effect of iron and molybdenum, as well as iron and other transition metals.

(4) Investigate the effect of coal beneficiation on liquefaction with disposable catalysts.

(5) Investigate poisoning of disposable catalyst by nitrogen and oxygen compounds.

OBJECTIVE

The objective of this research program was to investigate options for the development of low-cost disposable catalysts for use in enhancing the performance and economics of coal liquefaction. Various minerals, metal containing by-products, and waste materials were studied to determine whether coal conversion and product quality were affected by their addition as catalysts. The research program was divided into six major tasks with several subtasks within each group. An outline of the program is given below.

1. Select and acquire minerals and metal-containing waste materials.
2. Examine these materials both chemically and physically for uniformity, composition, foreign matter, moisture, and cleanliness.
3. Select methods and prepare samples based on physical and chemical results and prior experience in evaluating catalytic materials.
4. Evaluate additives in preliminary autoclave screening tests, both alone and in the presence of iron sulfide.
5. Prepare additional samples for screening tests in the continuously stirred tank reactor (CSTR) when warranted.
6. Evaluate promising materials under realistic conditions where operating parameters approximate commercial design conditions.

EXPERIMENTAL PROGRAM

Coal Feedstocks

Several different coals (Elkhorn #2, Elkhorn #3, Kentucky #9 and two Ohio
coals) were tested in the program. A low-ash and low-pyrite Elkhorn #3 coal
was used in the screening tests. The choice of Elkhorn #3 coal was based upon
the results of Granoff and Thomas (3) who found that conversion levels were
quite low for this low-pyrite coal. The Pennsylvania State Coal Data Base
(PSDB) contains numerous examples of Elkhorn coals that, as shown below, have
low ash and mineral contents with low levels of pyrite.

Sample I.D.	% ash	% pyrite sulfur
PSOC-001	3.96	0.10
PSOC-002	3.90	0.02
PSOC-003	4.65	0.01
PSOC-004	2.07	0.18
PSOC-005	4.78	0.77
PSOC-006	4.50	0.02

Therefore, to build a reaction network around a low-pyrite coal that also
gives low conversion, an Elkhorn #3 coal was selected to determine mineral
effects on liquefaction.

The University of Kentucky Institute of Mining and Minerals Research (IMMR)
supplied information regarding the Elkhorn coals and provided both low-and
high-ash samples. Numerous channel samples of Ohio coals were supplied by
Ohio DOE through Professor William A. Kneller of the University of Toledo and
Professor Robert Savage of Ohio University.

The selection and analysis of several coals tested in the program are discussed
below. Complete chemical analyses of the Elkhorn and Kentucky coals are
provided in Table 1.

Elkhorn #3. A sample of run-of-mine (ROM) Elkhorn #3 coal obtained from Floyd
County, Kentucky was crushed and sieved to -200 U.S. mesh before use. The
ground coal contained 14.6% ash. This coal sample was extensively evaluated
both at Air Products and Auburn University.

18

Table 1

Proximate and Ultimate Analysis of Kentucky Coal Samples

	wt.%			
	Floyd County Elkhorn #3	Letcher County Elkhorn #3	Letcher County Elkhorn #2	Kentucky #9
Proximate Analysis				
Moisture	1.81	1.80	1.55	1.60
Dry Ash	14.60	33.34	6.29	13.10
Volatile	37.56	---	--	36.13
Fixed Carbon	46.03	---	--	48.90
Ultimate Analysis				
C	69.40	52.88	77.84	70.42
H	4.88	3.67	5.24	4.76
N	1.00	0.95	1.75	1.50
S	1.94	1.63	1.08	3.30
O	8.18	7.73	7.20	6.07
Distribution of Sulfur				
Total Sulfur	1.98	ND[1]	1.08	3.30
Sulfate Sulfur	0.04	ND	0.04	0.10
Pyrite Sulfur	1.19	ND	0.25	1.60
Organic Sulfur	0.75	ND	0.79	1.60

[1]Not Determined

Another sample of Elkhorn #3 coal was obtained from Letcher County, Kentucky, based on the PSDB number PSOC-001. This ROM sample was selected from a mine close to the location where the original sample was taken and represented a close approximation of that location. This coal was found to contain 33.3% ash as opposed to 3-4% ash reported for PSOC-001. The unexpectedly high ash content in the coal was due to the scraping of the mine ceiling the day the sample was collected.

Elkhorn #2. Since the samples of Elkhorn #3 coals from Floyd and Letcher counties, Kentucky, were found to contain high concentrations of ash, additional supplies of low-ash Elkhorn coal were sought for testing. A sample of washed Elkhorn #2 coal from Letcher County, Kentucky, was obtained with the help of IMMR. This sample was crushed and sieved to -150 U.S. mesh before use. The coal contained 6.3% ash compared with high-ash contents of the other two Elkhorn #3 coals described earlier (14.6 and 33.3%, respectively).

Kentucky #9. A sample of Kentucky #9 coal was obtained from the Pyro mine in Union County. The sample contained 13.1% ash and 1.6% pyrite sulfur.

Ohio Coals. Professors Savage and Kneller obtained several Ohio coal samples representing a wide range of total sulfur, pyrite sulfur and ash contents. The detailed analyses of the Ohio coal samples are reported in Volume II. Ohio coal samples from two different seams, Clarion #4A and Pittsburgh #8, were processed in a continuous coal processing development unit (CPDU) to evaluate their liquefaction behavior. The maceral analyses of the Ohio coal samples from the two seams are summarized in Table 2.

The detailed analyses of the Ohio coal samples from the two different seams are reported in Table 3. The Clarion #4A sample (CPDU-132) was obtained from one mine, whereas the other sample CPDU-128A from the same seam was a mixture of coal from two different mines. The relationship of the coals from these two different mines in the sample is unknown. That two samples were from the same seam but from two different mines could explain the differences in their ash content and sulfur distribution. The two samples of Pittsburgh #8 coal were also from the same seam, but were collected from two different mines.

Table 2

Maceral Content of Ohio Coal Samples

Volume Percent

Sample No.	Clarion #4A		Pittsburgh #8 (Belmont County)	
	CPDU[1]-132	CPDU-128A	CPDU-131	CPDU-131A
Vitrinite	83.8	86.7	86.9	87.3
Resinite	2.3	1.5	0.9	1.9
Exinite	5.3	4.3	2.7	2.8
Fusinite	3.3	3.0	3.7	1.1
Semifusinite	4.2	3.4	4.7	6.1
Sclerotinite	0.4	0.2	0.8	0.3
Micrinite	0.6	0.9	0.3	0.5
Inertodetrinite	0.1	0.0	0.0	0.0

[1]CPDU - continuous process development unit

Table 3
Analysis of Ohio Coals

	Clarion #4A		Pittsburgh #8	
	CPDU[1]-132	CPDU-128A	CPDU-131	CPDU-131A
		wt.%		
Proximate Analysis				
Moisture	3.98	2.79	1.69	1.44
Ash	15.09	25.00	14.47	12.65
Volatile Matter	38.38	35.21	38.70	39.94
Fixed Carbon	42.55	37.00	45.14	45.97
Ultimate Analysis				
C	62.31	56.60	66.71	68.31
H	4.95	4.50	4.95	4.97
O	11.33	10.10	8.59	8.15
N	1.18	1.02	1.18	1.18
S	3.71	3.74	4.56	5.06
Sulfur Distribution				
Sulfate Sulfur	0.28	0.15	0.17	0.06
Pyrite Sulfur	1.49	1.82	2.00	2.32
Organic Sulfur	1.94	1.77	2.39	2.68

[1]Air Products sample number

Cleaned Coals - Coal samples from the Ireland mine were cleaned and supplied by Richard P. Killmeyer of DOE's Pittsburgh Mining Technology Center (PMTC). The analyses of the raw and cleaned coal samples are given in Table 4.

Minerals, Metallic Wastes and Metal-Containing By-Product Samples

Samples of various minerals and metallic wastes were obtained for preparation and characterization. The list of samples and their sources is given in Table 5.

Robena pyrite sample was dried at 110°C and ground to 99.9% -325 U.S. mesh in nitrogen. The chemical analysis of Robena pyrite is given in Table 6. The sample was comprised of 75% pyrite, 5% carbonaceous organic material and 20% magnetite, quartz and other inorganic materials. The surface area of the pyrite was 1.0 m^2/g. and the sample was relatively nonporous.

The detailed chemical analysis of the various pyrite samples, and some of the minerals and metallic wastes are presented in Tables 7 to 18. In addition, the detailed thermal analysis of various minerals and metallic wastes are presented in Appendix G.

Process Solvent

SRC-II fuel oil blend (FOB), SRC-II heavy distillate, and distillates recovered from product liquid slurry were used as process solvents in the program. The SRC-II FOB and heavy distillate were received from the Pittsburg and Midway Coal Mining Company (PAMCO) Solvent-Refined-Coal Pilot Plant at Fort Lewis, Washington. The analysis of the SRC-II FOB as supplied by PAMCO is given in Table 19. The FOB was reported to have approximately 20 wt % 550°F+ fraction. The FOB was distilled in a 125-gal batch vacuum distillation unit into two fractions, initial temperature to 550°F (obtained as overhead product) and 550°F+ (obtained as bottoms). The conditions and material balance of a particular distillation run are given in Table 20. The 550°F+ fraction was used as a process solvent and is identified as FOB #1 in this report. A typical analysis of FOB #1 is given in Table 21. The gas chromatography (GC) simulated distillation of FOB #1 provided in Table 22 showed that 11 wt % of the material boiled below 550°F. The difference between vacuum distillation and the GC

Table 4

Pyrite, Ash, and Sulfur Analyses of Ireland Mine Coal Sample[1]

	wt.%		Sulfur Content,%			
Sample	Pyrite	Ash	Pyritic	Sulfate	Organic	Total
Raw Coal	3.98	35.04	2.13	0.10	2.08	4.31
Deep Cleaned Coal (Float 1.30)	0.17	2.48	0.09	<0.01	2.68	2.77
Deep Cleaned Coal (Float 1.30) and Concentrated Pyrite Mixture	3.83	15.47	2.05	0.02	2.85	4.92
Oil Agglomeration Clean Coal	5.08	10.32	2.72	0.35	2.57	5.64
Concentrated Pyrite	46.82	73.86	25.05	0.36	1.16	26.57

[1] Samples obtained from Mr. Richard Killmeyer of Pittsburgh Mining Technology Center, DOE.

24

Table 5

Sources of Minerals and Metal Containing By-Product Samples

Robena Pyrite
$[FeS_2]$

U. S. Steel Corporation
Robena Mine
Angelica, Pennsylvania

South Dakota Pyrite.
$[FeS_2]$

Wards Natural Science Establishment
Rochester, New York

Mexican Pyrite
$[FeS_2]$

Auburn University Geology Department
Auburn, Alabama

Pyrite Separated from
Molybdenum Ore
$[FeS_2]$

Climax Molybdenum Company
Greenwich, Connecticut

Other Pyrite Samples
$[FeS_2]$

Air Products and Chemicals, Inc.
Allentown, Pennsylvania

Magnetite
$[Fe_3O_4]$

U. S. Steel Corporation
Angelica, Pennsylvania

Albanian Chrome Ore Concentrates

Interlake, Inc.
Beverly, Ohio

Kaolinite
$[Al_2SiO_5 \cdot (H_2O)_n]$

Burgess Pigment Company
P. O. Box 349
Sandersville, Georgia

Montmorillonite
$[Al_2Si_4O_{10}(OH)_2]$

Georgia Kaolin Company
433 N. Broad Street
Elizabeth, New Jersey

Table 5

(Continued)

Sources of Minerals and Metal Containing By-Product Samples

Apatite [Calcium Phosphate]	Stauffer Chemical Company Westport, Connecticut
Ilmenite [$FeTiO_3$]	Pesses Company 296505 Hall St. & Cochran Solon, Ohio
Zircon [$ZrSiO_4$]	Chemalloy P.O. Box 350 Bryn Mawr, Pennsylvania
Rutile [TiO_2]	Pesses Company 296505 Hall St. & Cochran Solon, Ohio
Gypsum [$CaSO_4 \cdot 2H_2O$]	C. A. Wagner Philadelphia, Pennsylvania
Feldspar [$KAlSi_3O_8$]	Feldspar Corporation Spruce Pine, North Carolina
Lime [CaO]	Pfizer Minerals Chicago, Illinois
Bornite [Cu_5FeS_4]	The Anaconda Company Geological Department 520 Hennessy Building P.O. Box 621 Butte, Montanna

Table 5

(Continued)

Sources of Minerals and Metal Containing By-Product Samples

Calcite   Auburn University Chemical Engineering
$[CaCO_3]$ Department, Auburn, Alabama

Illite   Department of Geology
$[KAl_2(AlSi_3O_{10})(OH)_2]$ University of Missouri
                                            Columbia, Missouri

Quartz   Sawyer Research Products
$[SiO_2]$ 35400 Lakeland Boulevard
                                            East Lake, Ohio

Pea Ridge Magnetite Concentrates   Bethlehem Steel Corporation
$[Fe_3O_4]$ Bethlehem, Pennsylvania

Blast Furnace Slag   Bethlehem Steel Corporation
                                            Bethlehem, Pennsylvania

Molybdenite   Wards Natural Science Establishment
$[MoS_2]$ Rochester, New York

Molybdenite Concentrate   Climax Molybdenum Company
$[MoS_2]$ Greenwich, Connecticut

Molybdic Oxide   Climax Molybdenum Company
$[Mo_2O_3]$ Greenwich, Connecticut

Flue dust   Air Products and Chemicals, Inc.
                                            Greenville, Pennsylvania

27

Table 5
(Continued)

Sources of Minerals and Metal Containing By-Product Samples

Super Alloy Grindings	Air Products and Chemicals, Inc. Greenville, Pennsylvania
Alnico Grindings	Air Products and Chemicals, Inc. Greenville, Pennsylvania
Dolomite $[CaMg(CO_3)]$	David New Minerals Providence, Utah
Potassium Carbonate $[K_2CO_3]$	Fisher Scientific Co. Fair Lawn, New Jersey
Sodium Carbonate $[Na_2CO_3]$	Fisher Scientific Co. Fair Lawn, New Jersey
Oil Shale	John Ward Smith, Manager Div. of Resource Characterization U.S. Department of Energy Laramie Energy Technology Center P.O. Box 3395 University Station, Wyoming
Zinc Oxide $[ZnO]$	J. T. Baker Chemical Co. Phillipsburg, New Jersey
X-Type Molecular Sieve	W. R. Grace and Company Upper Darby, Pennsylvania
Mordenite	W. R. Grace and Company Upper Darby, Pennsylvania

Table 5

(Continued)

Sources of Minerals and Metal Containing By-Product Samples

Chabazite   W. R. Grace and Company
                                         Upper Darby, Pennsylvania

Speculite   Chemalloy Company, Inc.
$[Fe_2O_3]$ Bryn Mawr, Pennsylvania

Red Oxide   Ferro
$[Fe_2O_3]$ Ottawa Chemical Division
                                         Toledo, Ohio

Reagent Grade Fe_2O_3 Fischer Scientific Company
                                         Fair Lawn, New Jersey

Red Mud   U.S. Department of Interior
                                         Bureau of Mines
                                         Tuscaloosa Research Center
                                         University of Alabama
                                         Tuscaloosa, Alabama

Zinc Sulfide   Metals and Minerals Research
Concentrate   Zerba Research Center
$[ZnS]$ Bethlehem, Pennsylvania

Zinc Flue Dusts   Laclede Flue Dust
(low zinc and high zinc content)   Courtesy Dave Taschler
                                         Air Products and Chemicals, Inc.
                                         Greenville, Pennsylvania

Table 5
(Continued)

Sources of Minerals and Metal Containing By-Product Samples

Copperas   Textile Chemical Company
$[FeSO_4 \cdot 7H_2O]$ Reading, Pennsylvania

Phosphate Slime   E. I. Field
                                          U.S. Bureau of Mines
                                          Tuscaloosa, Alabama

Brown Fly and Bottom Ashes   Alan E. Bland
                                          IMMR, University of Kentucky
                                          Lexington, Kentucky

Green River Fly and Bottom Ashes   Alan E. Bland
(blend and high)   IMMR, University of Kentucky
                                          Lexington, Kentucky

Paradise Fly and Bottom Ashes   Alan E. Bland
                                          IMMR, University of Kentucky
                                          Lexington, Kentucky

Coal Preparation Plant   Alan E. Bland
Refuse Materials   IMMR, University of Kentucky
                                          Lexington, Kentucky

Various Fe_2O_3 Catalysts   Air Products and Chemicals, Inc.
                                          Allentown, Pennsylvania

Metal Sulfides   ICN Pharmaceuticals, Inc.
                                          Plainview, New York

Table 6

Chemical Analysis of Robena Pyrite

	wt. %
Carbon	4.48
Hydrogen	0.34
Nitrogen	0.61
Sulfur	41.34
Oxygen	5.97
Iron	42.30
Other Impurities (by difference)	4.96
Total	100.00
Ash	67.9

Surface Area = 1.0 m^2/g

Table 7

Chemical Analysis of Various Pyrite Samples

Sample	wt.%				
	Fe	Ash	Pyritic Sulfur	Sulfate Sulfur	Pyrite Content Calculated from Pyrite Sulfur
McDowell Country, West Virginia	22.2	83.6	19.8	0.1	37.1
Washington County, Pennsylvania	20.9	70.3	19.7	0.4	36.9
Union County, Kentucky	44.4	68.5	41.8	0.8	78.4
Cambria County, Pennsylvania	27.3	73.9	26.9	0.1	50.1
Webster County, Kentucky	43.4	69.9	46.6	0.3	87.3
Robena, Pennsylvania	42.3	67.9	40.4	0.7	75.7

Table 8

Chemical Analyses of Speculite Sample

	wt.%
Fe	65.1
Fe_2O_3	94.1
SiO_2	5.0
Al_2O_3	0.75
Mn	0.03
P	0.025
S	0.03

Table 9

Chemical Analyses of Pea Ridge Magnetite Concentrate

	wt.%
Fe	69.7
Fe_3O_4	96.2
SiO_2	2.27
Al_2O_3	0.3
CaO	0.36
MgO	0.29
S	0.015
P	0.084

Table 10

Chemical Analyses of Flue Dust,
Superalloy Grindings and Alnico Grindings

	wt.%		
	Superalloy	Flue Dust	Alnico
Ni	55.9	10.98	9.26
Cr	12.5	5.31	0.02
Mo	3.62	0.61	0.01
Co	9.27	7.66	15.71
W	3.10	--	--
Fe	0.53	20.32	42.13
C	--	3.00	1.05
Mn	--	0.52	0.13
S	--	0.50	0.08
SiO_2	--	5.36	--
Cu	--	1.01	1.78
Pb	--	0.57	0.01
Sn	--	0.01	0.05
Al	--	2.46	4.92
Ti	--	0.30	0.45
V	--	0.05	0.01
Moisture	--	0.01	--
Mg	--	3.00	--
Acid Insoluble	9.13	9.09	23.39

Table 11

Chemical Analyses of Red Mud

	wt. %
Al_2O_3	15.0
Fe_2O_3	51.5
SiO_2	1.7
TiO_2	6.7
CaO	7.0
Na_2O	1.0
Loss on Ignition at 1000°C	9.3

Table 12

Chemical Analyses of Zinc Sulfide Concentrate

	wt. %
Zn	62.6
S	31.2
Pb	0.54
Cu	0.21
Fe	1.0
CaO	0.28
MgO	0.14
SiO_2	2.45
Al_2O_3	0.03

Table 13

Elemental Analyses of Zinc Flue Dust Samples

Elements	Low Zinc Sample, wt.%	High Zinc Sample, wt.%
Al	0.30	0.35
Ca	5.00	4.80
Zn	11.60	33.60
Cu	0.18	0.17
Fe	32.10	22.50
Mg	2.30	1.41
Mn	4.80	3.00
Na	0.50	0.65
Pb	1.00	1.60
O (by difference)	42.10	31.90
Total	100.00	100.00

Table 14

Chemical Analyses[1] of Copperas (Ferrous Sulfate)

	wt. %
Ferrous Sulfate, $FeSO_4$	53.78
Iron, Fe_2O_3	0.06
Titanium, TiO_2	0.33
Magnesium Sulfate, $MgSO_4$	1.80
Copper, Cu	0.0004
Lead, Pb	0.0005
Water Insoluble Matter	0.28
Water of Crystallization	43.28

---

[1]Analysis provided by Textile Chemical Company, Reading, Pennsylvania

Table 15

Chemical Analysis of Lime

	wt.%
CaO	94.0
MgO	0.7
SiO_2	1.8
Al_2O_3	0.4
Fe_2O_3	0.1

Table 16

Chemical Analysis of Phosphate Slime

	wt.%
CaO	16.2
P_2O_5 Equivalent	12.0
MgO	2.9
Fe_2O_3	3.4
SiO_2	36.5
Na_2O	0.3
K_2O	0.8
F	1.5
C	1.0
CO_2	2.3
S	0.2

Loss on Ignition at 500°C   10.3

Table 17

Chemical Composition of Various Fe_2O_3 Catalysts

Number	Source of Fe_2O_3	Support	Heat Treatment
705x8-5x1	25% Pure	75% Fly Ash	Calcined
813x1-1x4	75% Pure	25% Fly Ash	Calcined
831x1-1	75% Pure	25% Fly Ash	Not Calcined
705x9-3x2	25% U.S. Steel	75% Fly Ash	Calcined
705x9-3	25% U.S. Steel	75% Fly Ash	Not Calcined
814x1-1x12	50% U.S. Steel	50% Fly Ash	Calcined
705x16-1x6	25% U.S. Steel	75% Silica	Calcined
705x16-1	25% U.S. Steel	75% Silica	Not Calcined
814x3-2x2	50% U.S. Steel	50% Silica	Calcined

Table 18
Analysis of Molybdenite Concentrate

		wt.%
Molybdenum Desulfide		86-96
Molybdenum	51-57	
Sulfur	35-28	
Copper		0.2 Max
Balance		Mainly Siliceous Material

Table 19

Analyses of the SRC II Fuel Oil Blend[1]

Sp. Gravity 60/60°F	0.999	% Pyridine Insolubles	0.02
°API @ 60°F	10.14	% Conradson Carbon	0.34
Viscosity @ 100°F, cSt	4.527	% Ash	0.02
@ 210°F, cSt	1.289	% Water	trace
Pour Point, °F	-55	% Carbon	86.21
Flash Point, °F ASTM D93	160	% Hydrogen	8.64
Btu/lb	17590	% Nitrogen	0.95
Coal Tar Acid, ml/100 g	25.9	% Sulfur	0.21
		% Oxygen	3.99

Distillation Yield	ASTM D1160	ASTM D86
Effective Pressure	2 mm Hg °F	760 mm Hg °F
I.B.P.	---	338
5%	138	398
10%	145	398
20%	155	431
30%	168	445
40%	180	463
50%	191	480
60%	205	498
70%	221	523
		(550°F @ 77%)
80%	254	563
90%	327	669
95%	383	---
E.P.	455	700
Recovery, %	98.5	93
Residue, %	1.5	6
Lost, %	0	1

---

[1] Analysis provided by Mr. R. E. Perrussel of the Pittsburg & Midway Coal Mining Co., DuPont, Washington

Table 20

Distillation of SRC II Fuel Oil Blend

Conditions of the Vacuum Distillation

No. of theoretical plates	15-20
Reflux Ratio	10-1
Pressure	100 mmHg

This material was charged to the still using pressurized N_2; the vacuum during distillation was maintained by a controlled N_2 bleed.

Material Balance:

Total Charge/Batch	=	903 lbs
Overhead Product (550°F-)	=	672 lbs
Bottom Product (550°F+)	=	221 lbs
Total Recovery	=	893 lbs/98.9%
Bottom Product (550°F+)	=	24.5% of the total charge

Table 21
Detailed Analysis of Process Solvents

	wt.%			
	FOB[1] #1	FOB #3	FOB #4	FOB #11
Element				
Carbon	88.79	89.53	88.67	89.44
Hydrogen	7.40	7.20	7.64	7.21
Oxygen	1.96	1.56	2.06	1.70
Nitrogen	1.20	1.07	1.11	1.10
Sulfur	0.48	0.64	0.52	0.55
Solvent Separation				
Oils	90.8	100.0	100.0	93.8
Asphaltenes	8.9	0.0	0.0	5.0
Preasphaltenes	0.4	0.0	0.0	0.4
Insoluble Organic Material (IOM)	0.0	0.0	0.0	0.8
Distribution of Hydrogen in the Oil Fraction				
$H_{Aromatic}$ (H_{Ar})	42.0	52.8	41.0	44.4
$H_{Benzylic}$ (H_a)	29.3	25.0	30.6	28.0
H_{other} (H_o)	28.7	22.2	28.4	27.6

[1] FOB - fuel oil blend

**FIGURE 1
SIMULATED DISTILLATION OF THE
PROCESS SOLVENTS**
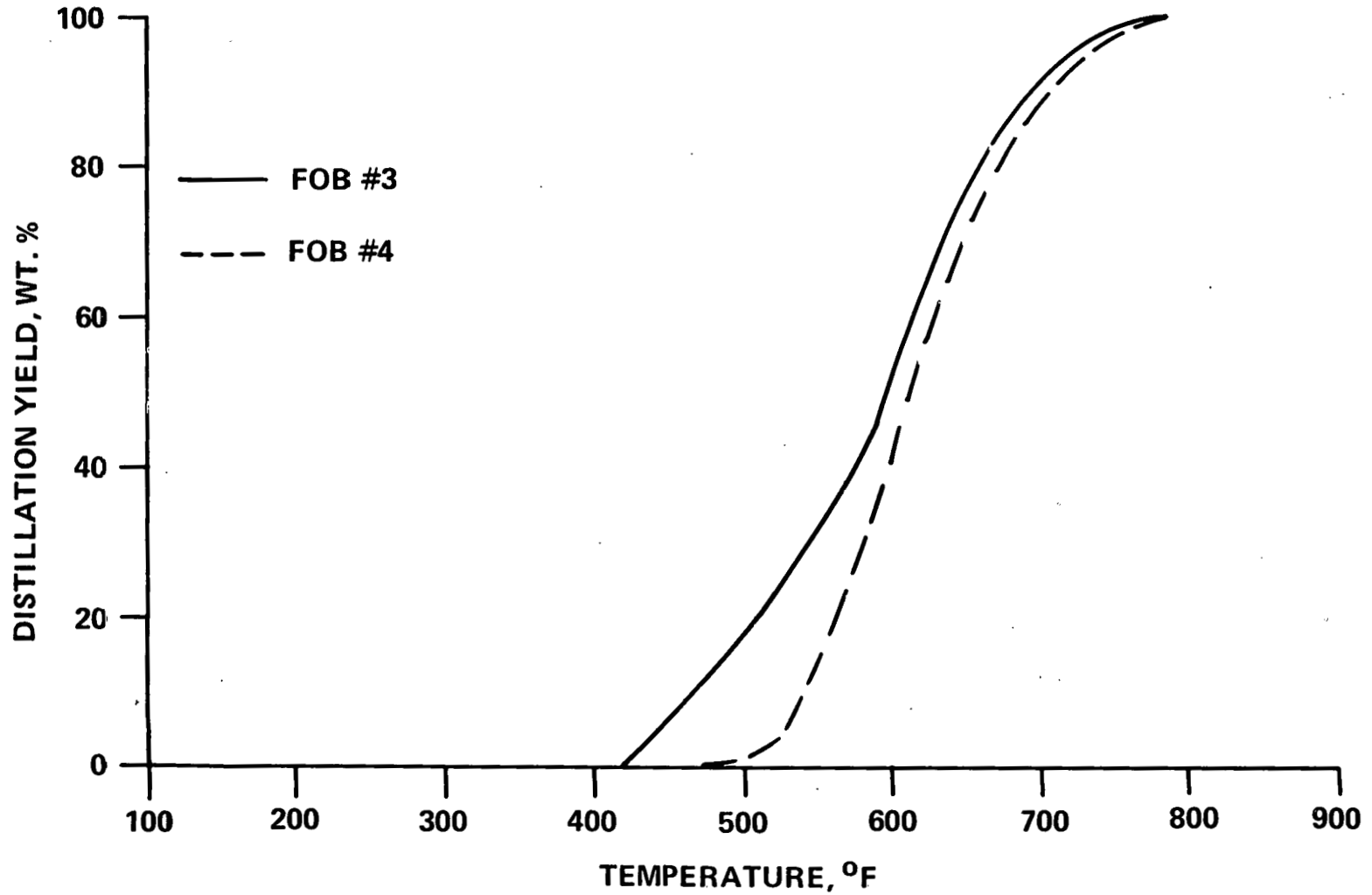
Table 22

Simulated Distillation of Process Solvents

	Temperature, °F			
wt. % Distilled	FOB[1] #1	FOB #3	FOB #4	FOB #11
I.B.P.	513	407	449	519
5%	536	443	531	548
10%	547	460	540	569
20%	576	512	561	590
30%	597	543	580	607
40%	615	573	595	627
50%	638	596	611	648
60%	663	614	630	673
70%	690	635	654	699
80%	721	663	678	732
90%	773	693	709	788
95%	820	718	736	835
97%	850	737	753	845
99%	900	770	781	898
F.B.P.	921	787	792	911

---

[1] FOB - fuel oil blend

simulated distillation can be explained by the larger number of theoretical distillation plates in simulated distillation as opposed to crude vacuum distillation; the simulated distillation column had 200 theoretical plates, whereas the vacuum distillation unit had only 15-20 plates. The solvent separation data (see Appendix C for detailed solvent separation procedure) given in Table 21 showed that FOB #1 contained approximately 90.8 wt % oil.

Two different batches of product slurry taken from the coal processing development unit (CPDU) run 25 were distilled to recover the process solvent. The distillation cut points were mistakenly set at 450 and 850°F instead of 550 and 850°F, respectively. The detailed analysis of these two solvents (100% pentane-soluble oil), FOB #3 and #4, are given in Table 21. The hydrogen and oxygen contents of FOB #4 were higher than those of FOB #3. The simulated distillation of the solvents (Figure 1 and Table 22) showed that FOB #4 contained a slightly larger amount of high boiling point compounds than FOB #3. Table 23 showed that the distribution of nitrogen groups was similar in both the solvents, but the distribution of oxygen groups was drastically different. FOB #4 contained a considerably higher concentration of hydroxyl groups compared with FOB #3. The distribution of protons in the two solvents was determined by proton nuclear magnetic resonance (H'NMR) and is shown in Table 21. FOB #4 to contained higher hydrogen content and a greater proportion of hydrogen-donatable compounds (H_a and H_o) than did FOB #3. This observation suggests that FOB #4 is a better hydrogen donor solvent than FOB #3 and would show higher coal liquefaction activity. Since the amount of 450-850°F process solvent was limited, a decision was made to use it exclusively for the dissolution study of the Ohio coal samples.

SRC-II heavy distillate, identified as FOB #11, was used for most of the program. A detailed chemical and solvent separation analysis of FOB #11, which is summarized in Table 21, agrees well with FOB #1. The GC simulated distillation of FOB #11, presented in Table 22, showed that 6% of the material boiled below 550°F and 3% above 850°F.

Table 23

Distribution of Oxygen and Nitrogen Compounds
in the Process Solvent

	FOB[1] #3		FOB #4	
Total Oxygen, wt.%	1.56		2.06	
	Absolute	Relative	Absolute	Relative
O as ether O	0.81	52.0	0.27	13.0
O as OH	0.75	48.0	1.79	87.0
Total Nitrogen, wt.%	1.07		1.11	
	Absolute	Relative	Absolute	Relative
N as N	0.79	74.0	0.80	72.0
N as NH	0.28	26.0	0.31	28.0

[1] FOB - fuel oil blend

45

Equipment Description

Thermal Analyzer - The thermal stabilities of the minerals and metallic wastes was evaluated by thermal gravimetric analysis (TGA) and differential thermal analysis (DTA) in the presence of helium or nitrogen using Perkin-Elmer* TGS-1, DuPont 990, and Premco Model 50 thermal analyzers. The reactivity of the material with hydrogen was evaluated in the TGA at atmospheric pressure and in the pressurized thermal gravimetric reactor (PTGR) at higher hydrogen pressures. See Appendix A for the design and operation of the PTGR.

Sulfiding Reactor - Samples of iron oxide were sulfided either with pure hydrogen sulfide or with a mixture of hydrogen and hydrogen sulfide gases to produce active iron sulfide catalyst. The detailed description of the equipment and sulfiding procedure are described in Appendix E.

Tubing-Bomb Reactor - Two small tubing-bomb reactors (17.5 and 46.3-mL volume) were designed and assembled at Auburn University for preliminary screening studies of the catalytic activity of various minerals and metallic wastes. The reactor assembly is shown in Figure 2. A reaction mixture containing 3 g coal, 6 g process solvent and a predetermined amount of catalyst was used in most of the experiments. The reactor was pressurized with hydrogen to 1250 psig at 25°C, leak tested, and placed in a preheated fluidized sand bath. Typically, less than 2 minutes were required to heat the reactor to the reaction temperature. The reactor was agitated at 860 strokes per minute with the help of a variable speed motor. The reactor was maintained at the reaction temperature for a specified amount of time and then cooled by placing it in a water bath. Product gases were vented and weighed. Product slurry was solvent-separated to determine the product distribution. A summary of the solvent separation procedure used at Auburn University is given in Appendix B.

Duplicate runs were carried out in the 17.5-mL reactor to test the reproducibility of the system. Hydrogenation runs of process solvent (FOB #1) were conducted three times and the reaction products were solvent separated. The reaction conditions and the solvent separation results are given in Table 24. Similarily, six different coal liquefaction runs were made and the results are

---

Mention of trade name does not imply endorsement by DOE or the contractor.

FIGURE 2
REACTOR SYSTEM USED IN
LIQUEFACTION EXPERIMENTS

VARIABLE
SPEED
ELECTRIC
MOTOR

FLYWHEEL
&
PUSHROD

BEARING

TACHOMETER

AGITATOR SHAFT

MICROREACTOR (TUBING BOMB)

FLUIDIZED SAND BATH

TEMPERATURE CONTROLLER
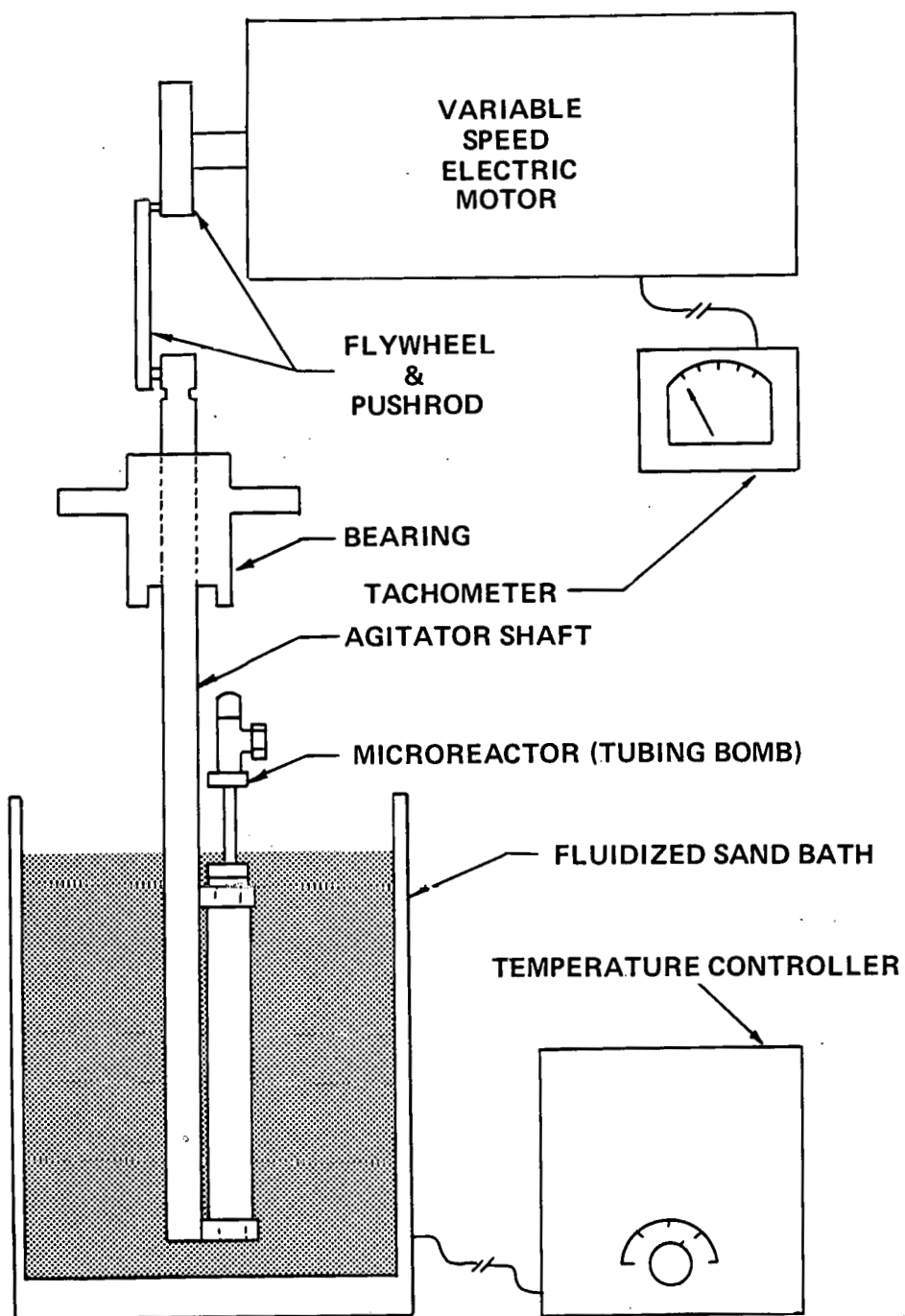
Table 24
Reproducibility Test of Solvent Hydrogenation Runs

	wt.%	
	Mean	Standard Deviation
Oils	90.68	0.87
Asphaltenes	8.66	1.21
Preasphaltenes	0.46	0.31
Residue	0.19	0.06

Reaction Conditions: Reactor - 17.5-mL tubing-bomb
Solvent - FOB #1
Temperature - 410°C
Pressure - 1250 psig H_2 at 25°C
Reaction Time - 30 minutes
Catalyst - None

Table 25
Reproducibility Test of Coal Liquefaction Runs

	Total Product Liquid, wt.%	
	Mean	Standard Deviation
Oils	62.92	0.62
Asphaltenes	12.28	0.80
Preasphaltenes	9.65	0.53
Residue	15.14	0.42

Reaction Conditions: Solvent - 6g
Coal (Elkhorn #3, Floyd County) - 3g
Reactor - 17.5-mL tubing-bomb
Temperature - 410°C
Pressure - 1250 psig H_2 at 25°C
Reaction Time - 30 minutes

summarized in Table 25. Maximum standard deviations of 14.0 and 6.5% were observed in the asphaltene fraction of the solvent hydrogenation and coal liquefaction runs, respectively. A maximum standard deviation of 6.5% in the case of coal liquefaction runs is well within the range of experimental error.

Coal Processing Development Unit (CPDU) - Process studies were done in a continuous 100-lb/day coal liquefaction unit equipped with a continuous stirred autoclave. The use of a stirred tank reactor ensured that solvent vaporization matched that of an actual SRC-I dissolver and that coal minerals did not accumulate. Since there was no slurry preheater, all of the sensible heat was provided by resistance heaters on the reactor. Because of the high heat flux, the reactor wall was about 27°F hotter than the bulk slurry. Multiple thermo-couples revealed that the slurry temperature inside the reactor varied by only 9°F from top to bottom. The products were quenched to 320°F before flowing to a gas/liquid separator that was operated at system pressure. The slurry was throttled into the product receiver while the product gases were cooled to recover the product water and organic condensate. Detailed schematic and operation of the CPDU are given in Appendix H.

Coal liquefaction runs were performed at different reaction conditions. At least 10 reactor volumes of the product were discarded before product samples were collected. A complete sample set consisted of one 0.5 lb product slurry, one 1-liter product slurry as back-up sample, a light condensate sample, and a product gas sample.

Product slurry was solvent-separated into four fractions: (1) pentane-soluble material (oil), (2) pentane-insoluble and benzene-soluble material (asphaltene), (3) benzene-insoluble and pyridine-soluble material (preasphaltene) and (4) pyridine-insoluble material. The latter contains insoluble organic material (IOM) and mineral residue. The solvent separation scheme is described in Appendix C. Each fraction was further subjected to detailed elemental analysis, as well as to nuclear magnetic resonance spectroscopy (NMR), near infrared analysis, and simulated distillation (ASTM D2886). Product gases were analyzed by on-line gas chromatography up to C_4 hydrocarbon gases including other nonhydrocarbon gases (H_2S, NH_3, CO and CO_2). The product water was a combination of the condensed water collected at the unit plus the amount calculated by assuming the water vapor exiting the process unit was in equili- brium with the condensed water.

Test of Reproducibility of CPDU - The reproducibility of the coal liquefaction
reaction and product work-up results was tested using 5.0 wt% pyrite in the
feed slurry. Two different samples taken from CPDU runs 4 hours apart were
analyzed independently; the data are presented in Table 26. The production of
hydrocarbon gases, CO, CO_2 and H_2S, was reproducible. The variation in the
hydrocarbon gases production was less than 3% of the value reported. The
production of oils, preasphaltenes, I.O.M. and water also reproducible.
Significant variation in the production of asphaltenes was noted. The increase
in asphaltenes in sample no. 31-113 was offset by a corresponding decrease in
oils and preasphaltenes.

The conversion of coal was unchanged, and the total hydrogen consumption and
SRC sulfur content were almost identical (Table 26). The distribution of
elements in the various fractions shown in Table 27 was also similar except
for slight variations in oxygen and nitrogen contents. From these results it
could be concluded that the data obtained from the CPDU and work-up laboratory
were reproducible. Slight variations in the production of oils, asphaltenes,
preasphaltenes, and elemental distribution were noted. The variation in the
oils production was only 2.4 wt % (absolute).

Brown-Ladner Calculation - NMR, NIR, and elemental analyses of the oils were
used in the modified Brown-Ladner equations (1,8) to calculate average structural
parameters for the oil molecules. These parameters provide a sensitive measure
of determining the changes in the distribution or rearrangement of the carbon
and hydrogen skeleton in the oils. The structural parameters defined by the
modified Brown-Ladner equations are as follows:

$$f_a = \frac{\frac{C}{H} - \frac{H_a{}^*}{X} - \frac{H_o{}^*}{Y}}{\frac{C}{H}} \qquad \text{(Eqn. 1)}$$

$$\sigma = \frac{\frac{H_a{}^*}{X} + H_{AR}{}^* + \frac{H_{OH}}{H}}{\frac{H_a{}^*}{X} + H_{AR}{}^* \quad \frac{H_{OH}}{H}} \qquad \text{(Eqn. 2)}$$

Table 26
Liquefaction of Floyd County
Elkhorn #3 Coal in the Presence of Pyrite

Sample No.	31-109	31-113
Feed Composition	65% Solvent + 30% Coal + 5% Pyrite	
Temperature, °F	850	850
Residence Time, Min.	38	38
Pressure, psig	2000	2000
Product Distribution, wt.% MAF Coal		
HC	10.4	10.1
CO, CO_2	1.5	1.5
H_2S	0.3	0.3
Oils	30.4	28.0
Asphaltenes	23.6	28.3
Preasphaltenes	19.9	17.7
I.O.M.	9.1	9.1
Water	4.8	5.0
Conversion, %	90.9	90.9
H_2 Consumption, wt.% MAF Coal		
Total	2.24	2.29
From Gas	2.58	2.92
From Solvent	(0.34)[1]	(0.63)
By Pyrite	0.25	0.25
SRC Sulfur, %	0.67	0.67

_____

[1] ( ) = negative value

51

Table 27

Distribution of Elements in Fractions of Liquefaction
Product from Floyd County Elkhorn #3 Coal in the Presence of Pyrite

Sample No.	31-109	31-113
Pyrite, wt.% of Feed Slurry	5.0	5.0
Oil Fractions, wt.%		
C	89.3	89.1
H	7.4	7.5
O	1.9	1.8
N	0.8	0.9
S	0.6	0.7
$\bar{n}$ MW	205	250
Asphaltene Fraction, wt.%		
C	86.5	85.5
H	6.4	6.0
O	5.2	5.7
N	1.3	2.1
S	0.6	0.7
$\bar{n}$ MW	385	375
Preasphaltene Fraction, wt.%		
C	85.7	85.4
H	5.4	5.4
O	5.5	6.1
N	2.4	2.4
S	0.7	0.7

$$\frac{H_{AR}}{C_{AR}} = \frac{\dfrac{H_a{}^*}{X} + H_{AR}{}^* + \dfrac{H_{OH}}{H}}{\dfrac{C}{H} - \dfrac{H_a{}^*}{X} - \dfrac{H_o{}^*}{Y}} \qquad \text{(Eqn. 3)}$$

where $H_a{}^*$ = fractional alpha protons defined as protons on carbon atoms immediately adjacent to an aromatic ring

$H_o{}^*$ = fractional beta and higher protons defined as those protons residing on two or more carbon atoms removed from an aromatic ring

H_{AR} = fractional aromatic protons

$Y = \dfrac{H_o}{C_o}$ atomic ratio

C = atomic percent carbon

H = atomic percent hydrogen

H_{OH} = percent hydroxyl hydrogen

C_{AR} = fractional aromatic carbon

σ = degree of substitution on aromatic rings

f_a = fraction of aromatic carbon

The parameter Y represents the average number of H_o hydrogen atoms on the carbon atoms that are two or more carbons away from the aromatic ring. A fixed value of 2.0 was chosen for Y in the calculation. The parameter X, the average number of hydrogen atoms on carbons alpha to an aromatic ring, was found by trial and error using equation 1 and the additional equation 4.

$$X_{BEST} = \frac{H_a{}^* + H_o{}^*}{\dfrac{C}{H} - \dfrac{C}{H} f_a} \qquad \text{(Eqn. 4)}$$

All calculated X_{BEST} values were in the range 2.0 ± 0.2. The simplified equations described above assume that bridge-head hydrogens are an insignificant fraction of the total hydrogen and that all of the oxygens are attached directly to the ring, either as phenols or as cyclic ethers. The bridge-head hydrogens are defined as hydrogens attached to an ethylene link to two condensed aromatic rings such as acenaphthalene.

The f_a, carbon aromaticity, is defined as the ratio of aromatic carbon atoms to total carbon atoms. Since carbon atom data are not available, f_a is indirectly derived from proton data and elemental analyses using equation 1. H_{AR}/C_{AR} is the ratio of hydrogen atoms at the periphery of the aromatic ring structure to the aromatic carbon atoms. This number is a useful indicator of the degree of condensation of the compounds; for example, H_{AR}/C_{AR} values for benzene (one ring aromatic compound), naphthalene (two-ring condensed aromatic compound) and phenanthrene (three-ring condensed aromatic compound)

$$\text{are} \quad \frac{6 \text{ aromatic protons}}{6 \text{ aromatic carbons}} = 1, \quad \frac{8 \text{ aromatic protons}}{10 \text{ aromatic carbons}} = 0.8$$

$$\text{and} \quad \frac{10 \text{ aromatic protons}}{14 \text{ aromatic carbons}} = 0.71, \text{ respectively.} \quad \text{Therefore } H_{AR}/C_{AR}$$

decreasesas the number of condensed aromatic rings in the compound increases. Sigma (σ) is defined as the ratio of substituents on the aromatic ring to the total available sites for the ring substitution. This provides a rough idea of the degree of aromatic ring substitutions by alkyl and naphthenic and/or phenolic groups. Sigma (σ) for xylenes, methylnaphthalene, and phenol are $2/6 = 0.33$, $1/10 = 0.1$, and $1/6 = 0.17$, respectively.

Combining the above parameters with the molecular weight data, the size of the aromatic ring system can be calculated using Equation 5:

$$R_a = \left(\frac{C_{AR} - H_{AR}}{2} \right) + 1 \qquad \text{(Eqn. 5)}$$

where R_a = number of aromatic condensed ring
C_{AR} = aromatic carbon atoms per molecule
H_{AR} = aromatic proton atoms per molecule

Experimental Procedure

Tubing Bomb Reaction Conditions - Several coal liquefaction runs with and without a catalyst were conducted to establish baseline data. Reaction conditions were sought which would give a sizeable difference in oil production between a noncatalyzed and a strongly catalyzed coal liquefaction system. These reaction conditions were used in evaluating the catalytic activity of various coal minerals and metallic wastes.

Initially a 17.5-mL tubing-bomb reactor was employed. The reactor was charged with 3 g coal, 6 g solvent, and 1 g additive (if any). The reactor was pressurized with hydrogen to 1250 psig at 25°C. This mixture was then reacted at 410°C for 30 minutes and the product was analyzed by solvent separation to determine the product distribution. The results of the reactions in the absence of catalyst, as well as in the presence of presulfided Co-Mo-Al catalyst, are presented in Table 28. Oil production was found to increase from 14% in the case of no-catalyst run to 23% in the Co-Mo-Al runs. Although Co-Mo-Al somewhat improved oil production over the base coal run, the difference was not large enough to accommodate the experimental error and to demonstrate clearly the effect of added catalysts. It was then thought that the coal liquefaction reaction might be hydrogen-starved in the small tubing-bomb (17.5 mL) reactor. A new, larger tubing-bomb (46.3 mL) reactor was assembled and used with a Co-Mo-Al catalyst under the same reaction conditions and amounts of solvent and coal. Oil yield increased to 61% with the larger reactor (Table 29). The amount of hydrogen consumed from the gas phase, as determined by GC analysis, was 0.05 g in the small reactor and 0.14 g in the large reactor. The total amount of hydrogen available in the smaller reactor was 0.065 g. Consumption amounted to 77% of the total available hydrogen. Hydrogen consumption in the larger reactor was significantly higher than the total available hydrogen in the smaller reactor. The reaction in the smaller reactor did not consume all the available hydrogen, although the results from the larger reactor indicated that all of the available hydrogen could have been easily consumed. In addition, the coal conversion increased to 92% with the use of the larger reactor. The increase in coal conversion could be due to better mixing in the larger bomb

Table 28

Preliminary Data for Base Case Determination

| | Product Distribution Based on MAF Coal,% | |
	No-Catalyst	Co-Mo-Al
Oils	14	23
Asphaltenes	17	23
Preasphaltenes	33	32
Residue	36	22
Conversion	64	78

Reaction Conditions:	Reactor - 17.5-mL tubing-bomb
	Solvent - 6g
	Coal (Elkhorn #3, Floyd County) - 3g
	Catalyst - 1g
	Temperature - 410°C
	Pressure - 1250 psig H_2 at 25°C
	Reaction Time - 30 minutes

Table 29

Effect of Reactor Size on Liquefaction

| | Product Distribution Based on MAF Coal,% | |
	Small Reactor (17.5-mL)	Large Reactor (46.3-mL)
Oils	22	61
Asphaltenes	41	19
Preasphaltenes	15	12
Residue	22	8
Conversion	78	92

Reaction Conditions: Solvent - 6g

Coal (Elkhorn #3, Floyd County) - 3g

Catalyst - 1g Co-Mo-Al

Temperature - 450°C

Pressure - 1250 psig H_2 at 25°C

Reaction Time - 30 minutes

(large volume of reactor available for the same volume of reaction mixture) and improved gas/liquid mass transfer. The above observation indicated that the amount of available hydrogen was an important factor in limiting or encouraging the reaction and that a larger bomb was necessary to provide sufficient hydrogen for reaction, as well as to increase oil production.

To study the influence of increased amounts of available hydrogen, another coal liquefaction run in the absence of a catalyst was performed in the large bomb at the same reaction conditions. The results of runs in the presence of a Co-Mo-Al catalyst and in its absence were compared and are presented in Table 30. The 55% difference in oil production (see Table 30) in the larger reactor was significant enough to accommodate the experimental error and to demonstrate clearly the effect of added minerals. The net effect was increased conversion of coal and asphaltene to oil. However, the preasphaltene production remained constant.

The search for an optimum temperature for baseline conditions was conducted in the large tubing-bomb reactor in the presence of a Co-Mo-Al catalyst. The objective was to increase coal conversion and oil production. Table 31 summarizes the results obtained at various reaction temperatures. Oil production increased with reaction temperature up to 475°C, but above 475°C, it suddenly dropped. This occurred because significant coking was observed in the reactor at 500°C. The reaction temperature of 475°C gave significantly higher oil production compared with 450°C, but it showed slightly lower coal conversion. The reaction temperature of 450°C was preferred over 475°C because of ease of CPDU operation at 450°C compared with 475°C. To offset the lower oil production at 450°C compared to 475°C, the reaction time was increased from 30 minutes to 60 minutes; Table 32 shows the effect of reaction time on oil production at 450°C. Oil production increased from 61 to 79%, while coal conversion remained practically the same. Thus, a tubing-bomb reactor of 46.3-mL volume, a reaction temperature of 450°C, and 60 minutes reaction time were chosen as baseline reaction conditions to evaluate the catalytic activity of various minerals and metallic wastes.

Table 30

Effect of Catalyst on Liquefaction

	Product Distribution Based on MAF Coal,%	
	No-Catalyst	Co-Mo-Al
Oils	6	61
Asphaltenes	. 44	19
Preasphaltenes	23	12
Residue	27	8
Conversion	73	92

Reaction Conditions: Reactor - 46.3-mL tubing-bomb

Solvent - 6g

Coal (Elkhorn #3, Floyd County) - 3g

Catalyst - 1g

Temperature - 450°C

Pressure - 1250 psig H_2 at 25°C

Reaction Time - 30 minutes

Table 31

Effect of Reaction Temperature on Coal Liquefaction
in the Presence of Co-Mo-Al

| Temperature, °C | Product Distribution Based on MAF Coal, % | | | |
	425	450	475	500
Oils	28	61	71	42
Asphaltenes	35	19	16	31
Preasphaltenes	27	12	2	2
Residue	10	8	11	25
Conversion	90	92	89	75

Reaction Conditions: Reactor - 46.3-mL tubing-bomb
Pressure - 1250 psig H_2 at 25°C
Reaction Time - 30 Minutes
Coal (Elkhorn #3, Floyd County) - 3g
Solvent - 6g
Catalyst - 1g

Table 32

Effect of Reaction Time on Liquefaction
in the Presence of Co-Mo-Al

Reaction Time Min.	Product Distribution Based on MAF Coal, %	
	30	60
Oils	61	79
Asphaltenes	19	12
Preasphaltenes	12	2
Residue	8	7
Conversion	92	93

Reaction Conditions:
Reactor - 46.3-mL tubing-bomb
Pressure - 1250 psig H_2 at 25°C
Coal (Elkhorn #3, Floyd County) - 3g
Solvent - 6g
Catalyst - lg

NONCATALYTIC COAL LIQUEFACTION

Liquefaction of Kentucky Coals

The liquefaction behavior of several Kentucky coals was studied to establish the baseline data. The baseline data were much needed to determine the relative liquefaction activity of various coals as well as the catalytic activity of various minerals and metallic wastes in coal liquefaction.

Floyd County Elkhorn #3 Coal - The liquefaction of Floyd County Elkhorn #3 coal was studied at two different temperatures in the CPDU and the results are summarized in Table 33. Coal conversion was almost the same at the two different temperatures, but significant differences were found in gas production, product distribution and hydrogen consumption. Hydrocarbon gases, CO, CO_2, H_2S, NH_3, and water production increased as reaction temperature increased from 800 to 850°F; hydrocarbon gas production increased from 2.4 to 4.2%. A net loss of 3.2 wt% in oil production was noted at 800°F. Increasing temperature from 800 to 850°F increased the oil production from a net loss of 3.2 wt % to a net gain of 27.3 wt %. Preasphaltenes were the major reaction product at 800°F, as shown in Table 33. Increasing the temperature to 850°F increased the conversion of preasphaltenes to oil and gases. The first-order rate constants for the conversion of asphaltenes and preasphaltenes, defined in Appendix F, also increased with increasing temperature. The increase in temperature increased the hydrogen consumption from 0.5 to 1.4%; 0.4% of this increase was due to greater gas formation and 0.5% was accounted for in the conversion of preasphaltenes to oil.

The hydrogen content of oil decreased significantly at 850°F; at 800°F, the hydrogen content of oil was higher than the starting value (Table 34). Some differences in hydrogen content of asphaltene and preasphaltene fractions were also noted. The difference in SRC yield given in Table 35 was due to increased conversion to oil. SRC sulfur content also decreased from 0.8 to 0.6% as the temperature increased from 800 to 850°F.

Table 33

Liquefaction Behavior of Kentucky Coals

	Floyd County Elkhorn #3		Letcher County Elkhorn #3	
Sample No.	25-40	25-52	25-100	25-88
Feed	70% Solvent/30% Coal		70% Solvent/30% Coal	
Temperature, °F	850	800	800	850
Pressure, psig	2000	2000	2000	2000
Hydrogen Treat Rate, Mscf/T	19.9	18.2	19.9	20.1
Residence Time, min.	38	38	41	41
Product Distribution, wt.% MAF Coal				
HC	4.2	2.4	2.4	6.8
CO, CO_2	1.0	0.8	1.0	1.3
H_2S, NH_3	1.3	0.9	0.7	0.8
Oils	27.3	(3.2)[1]	--	--
Asphaltenes	14.8	17.6	--	--
Benzene Solubles (Oils & Asphaltenes)	--	--	17.2	15.9
Preasphaltenes	30.1	58.0	38.6	44.8
Insoluble Organic Matter (IOM)	18.1	20.6	37.7	28.4
Water	3.2	2.9	2.4	2.0
Conversion, % MAF Coal	81.9	79.4	62.3	71.6
Hydrogen Consumption, wt.% MAF Coal				
Total	1.40	0.51	(0.16)	0.31
From Gas	0.82	0.61	(0.09)	0.14
From Solvent	0.58	(0.10)	(0.07)	0.17
First Order Rate Constants, hr^{-1}				
K_a	1.09	-0.12	--	--
K_p	2.14	0.39	--	--

[1] ( ) = negative value

Table 33 (Cont'd)

Liquefaction Behavior of Kentucky Coals

	Pyro Kentucky #9		Elkhorn #2 Coal	
Sample No.	28-11	28-22	31-128	31-139
Feed	70% Solvent/30% Coal		70% Solvent/30% Coal	
Temperature, °F	825	850	825	850
Pressure, psig	2000	2000	2000	2000
Hydrogen Treat Rate, Mscf/T	19.8	20.6	18.9	19.9
Residence Time, min.	37	37	35	37
Product Distribution, wt.% MAF Coal				
HC	3.2	5.0	5.2	7.0
CO, CO_2	0.5	0.6	0.7	0.6
H_2S, NH_3	1.4	1.7	0.3	0.3
NH_3	0.0	0.0	0.0	0.0
Oils	7.9	15.3	12.2	8.3
Asphaltenes	26.6	30.0	21.2	21.6
Preasphaltenes	47.0	28.1	44.2	43.4
Insoluble Organic Matter (IOM)	9.4	12.8	14.7	15.7
Water	4.0	6.5	1.5	3.1
Conversion, % MAF Coal	90.6	87.2	85.3	84.3
Hydrogen Consumption, wt.% MAF Coal				
Total	1.34	1.51	0.64	0.53
From Gas	0.69	0.47	0.59	0.44
From Solvent	0.65	1.04	0.05	0.09
First Order Rate Constants, hr^{-1}				
K_a	0.25	0.83	0.62	0.39
K_p	0.17	2.78	1.27	1.09

[1] ( ) = negative value

64

Table 34

Hydrogen Concentration in Feed and Product

Sample No.	25-40	25-52	25-88	25-100	28-11	28-22	31-128	31-139
Coal	Elkhorn #3 - Floyd		Elkhorn #3-Letcher		Kentucky #9-Pyro		Elkhorn #2	
Reaction Temperature, °F	850	800	850	800	825	850	825	850
Hydrogen Content, wt.%								
Feed Oil	7.72	7.72	7.72	7.72	7.72	7.72	7.20	7.20
Product:								
Oils	7.49	7.76	7.61	7.65	7.46	7.30	7.20	7.20
Asphaltenes	6.48	6.77	6.29	6.72	6.42	6.41	6.30	6.10
Preasphaltenes	5.50	5.38	5.20	5.54	5.46	5.39	5.20	4.90

Table 35

SRC Production and Its Sulfur Content

Sample No.	25-40	25-52	25-88	25-100	28-11	28-22	31-128	31-139
Reaction Temperature, °F	850	800	850	800	825	850	825	850
Product Distribution, wt.% MAF Coal								
Asphaltenes	14.8	17.6	39.4	20.5	26.6	30.0	21.2	21.6
Preasphaltenes	30.2	58.0	44.8	38.6	47.0	28.1	44.2	43.4
Total (SRC)	45.0	75.6	84.2	59.1	73.6	58.1	65.4	65.0
SRC Sulfur, Wt.%	0.6	0.8	0.5	0.8	1.16	0.97	0.61	0.55

The simulated distillations of the oil fractions obtained at two different temperatures are shown in Figure 3. No differences in the initial and final boiling points of the two oil fractions were apparent.

Letcher County Elkhorn #3 Coal - The results of liquefaction of Letcher County Elkhorn #3 coal at two different temperatures are summarized in Table 33. Coal conversion increased from 62 to 72% as temperature increased from 800 to 850°F. Hydrocarbon gas production also increased with temperature. No significant difference was found in the production of benzene solubles. Preasphaltene production increased slightly with an increase in temperature. Hydrogen consumption increased from -0.16 to 0.31% as reaction temperature increased; this was due mainly to a higher hydrocarbon gas production and coal conversion.

The distribution of hydrogen in feed oil and various products is given in Table 34. The oil fraction lost some hydrogen at both temperatures. Also, the hydrogen contents of the asphaltenes and preasphaltenes were higher at the lower temperature (800°F). The SRC sulfur content was considerably lower at 850 than at 800°F (i.e., 0.5% at 850°F compared to 0.8% at 800°F) as shown in Table 35. The simulated distillations of the oil fractions obtained at two different temperatures are shown in Figure 4. At 850°F, the oil fraction showed a higher boiling point distribution than did the oil at 800°F, which was probably due to the generation of a higher proportion of higher molecular weight oil from the coal at 850°F than at 800°F.

Kentucky #9 (Pyro) Coal - The conversion of Kentucky #9 (Pyro) coal, studied at two different temperatures (Table 33), decreased slightly with an increase in temperature from 825 to 850°F. With increasing reaction temperature from 825 to 850°F, hydrocarbon gas, H_2S and water production increased from 3.2 to 5.0%, 1.4 to 1.7% and from 4.0 to 6.5%, respectively. Significant differences in oil and preasphaltenes production were noted with an increase in temperature. At 825°F, most of the coal was converted to asphaltene and preasphaltene fractions, as shown in Table 33. Oil production of approximately 8% was noted at 825°F. Increasing the reaction temperature from 825 to 850°F increased the conversion of preasphaltenes to asphaltenes, oils and gases. The oil fraction increased two-fold from 8 to 15%. A slight increase in asphaltene formation from 26 to 30% was noted, but a significant decrease in preasphaltene formation

66

FIGURE 3
EFFECT OF REACTION TEMPERATURE ON SIMULATED DISTILLATION OF OIL FRACTIONS OBTAINED FROM FLOYD COUNTY ELKHORN #3 COAL LIQUEFACTION

Legend:
- 850° F (CCL-25-40)
- 800° F (CCL-25-52)

Y-axis: DISTILLATION YIELD, WT. %
X-axis: TEMPERATURE, °F

FIGURE 4
EFFECT OF REACTION TEMPERATURE ON
SIMULATED DISTILLATION OF OIL FRACTIONS
OBTAINED FROM LETCHER COUNTY ELKHORN #3
COAL LIQUEFACTION

850° F (CCL-25-88)
800° F (CCL-25-100)
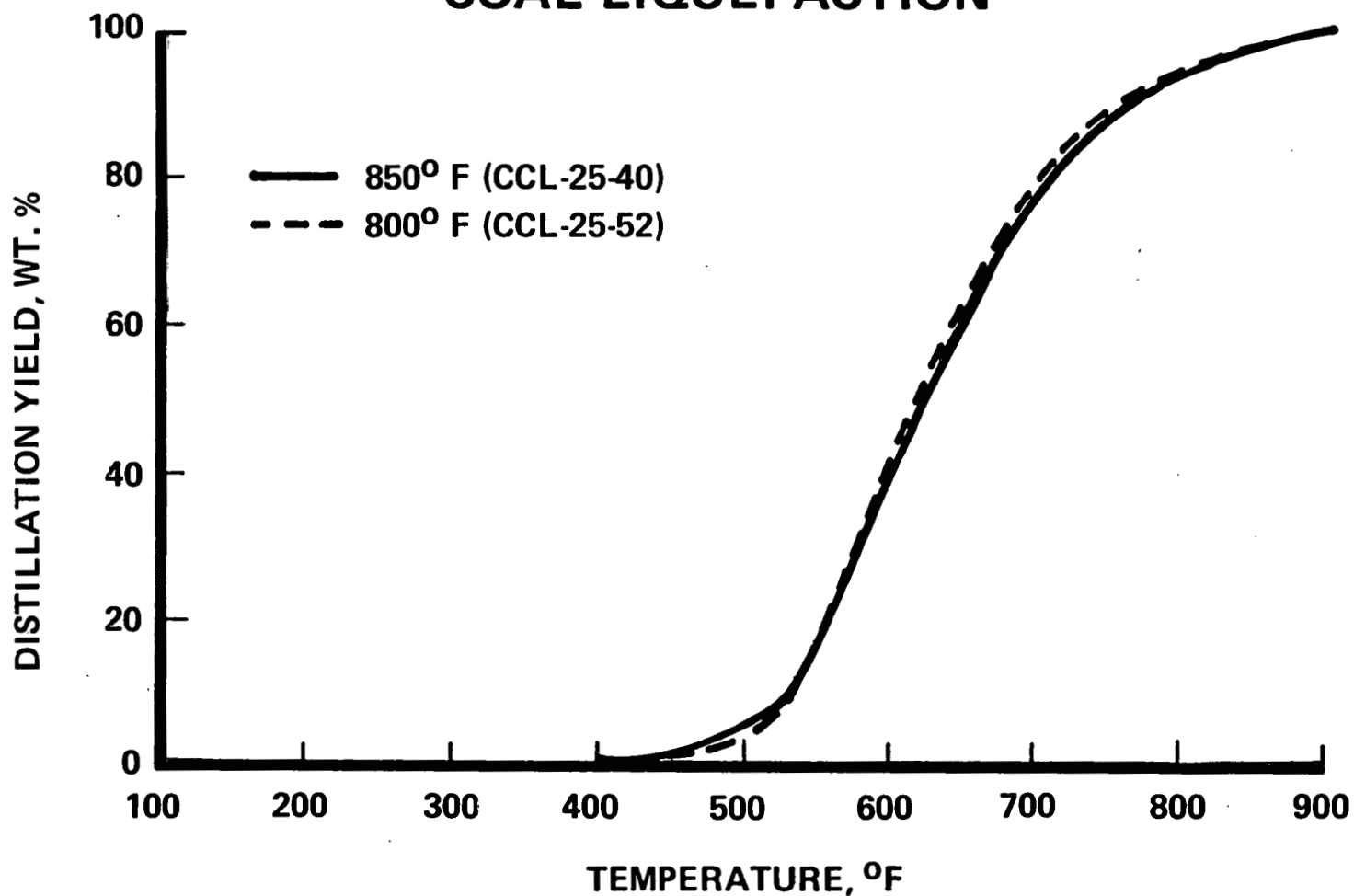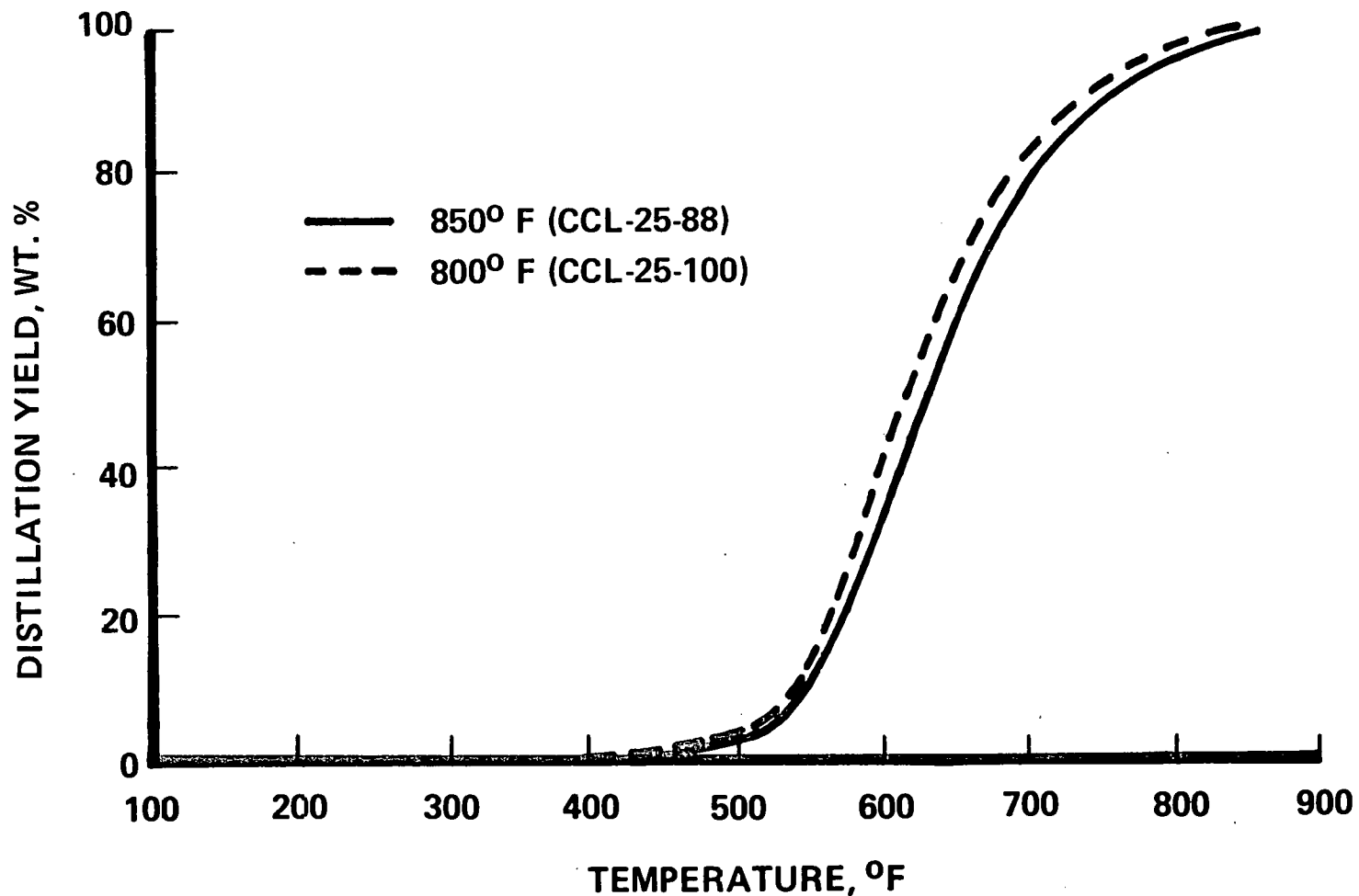
from 47 to 28% was observed. Also, as temperature increased, hydrogen consumption increased from 1.34 to 1.51%, as calculated by elemental hydrogen balance. Increases of 0.02, 0.41 and 0.02 wt% hydrogen based on MAF coal were due to the increased production of gases, oils and water, respectively.

Data on hydrogen content in the various fractions summarized in Table 34 show that the hydrogen content of oil fraction decreased significantly both at 825 and 850°F compared with the hydrogen content of the original solvent. Insignificant differences in the hydrogen contents of asphaltene and preasphaltene fractions were noted at the two temperatures. The sulfur contents of the oil fraction obtained at both temperatures were identical; lower sulfur contents in asphaltenes and preasphaltenes were noted at 850°F than at 825°F. This is indicative of increased desulfurization at higher temperatures.

The simulated distillations of the product oil fractions obtained at both temperatures are shown in Figure 5. No significant differences were noted in the initial and final boiling points of both fractions.

Letcher County Elkhorn #2 Coal - The conversion of Elkhorn #2 coal (Table 33) remained at 85% with an increase in temperature from 825 to 850°F. The production of hydrocarbon gases and water increased from 5.2 to 7.0% and from 1.5 to 3.1%, respectively, with increasing reaction temperature. Oil production decreased significantly from 12.2 to 8.3% with an increase in temperature. No differences were noted in the production of asphaltenes and preasphaltenes with temperature. With increasing temperature, the rate constants for the conversion of asphaltenes and preasphaltenes decreased from 0.62 to 0.39 hr^{-1} and from 1.27 to 1.09 hr^{-1}, respectively. These data indicate that the formation of oils and asphaltenes is not enhanced at 850°F compared with 825°F. Hydrogen consumption, as calculated by elemental hydrogen balance, changed insignificantly with an increase in temperature.

Data on the hydrogen content in the various fractions summarized in Table 34 showed no changes in all fractions. SRC sulfur content did not change with temperature (Table 35). The simulated distillations of the product oil fractions obtained at both temperatures (Figure 6) revealed no significant differences.

FIGURE 5
EFFECT OF REACTION TEMPERATURE ON SIMULATED DISTILLATION OF OIL FRACTIONS OBTAINED FROM LIQUEFACTION OF KENTUCKY #9 COAL

825°F (CCL - 28 - 11)
850°F (CCL - 28 - 22)

DISTILLATION YIELD, WT. %
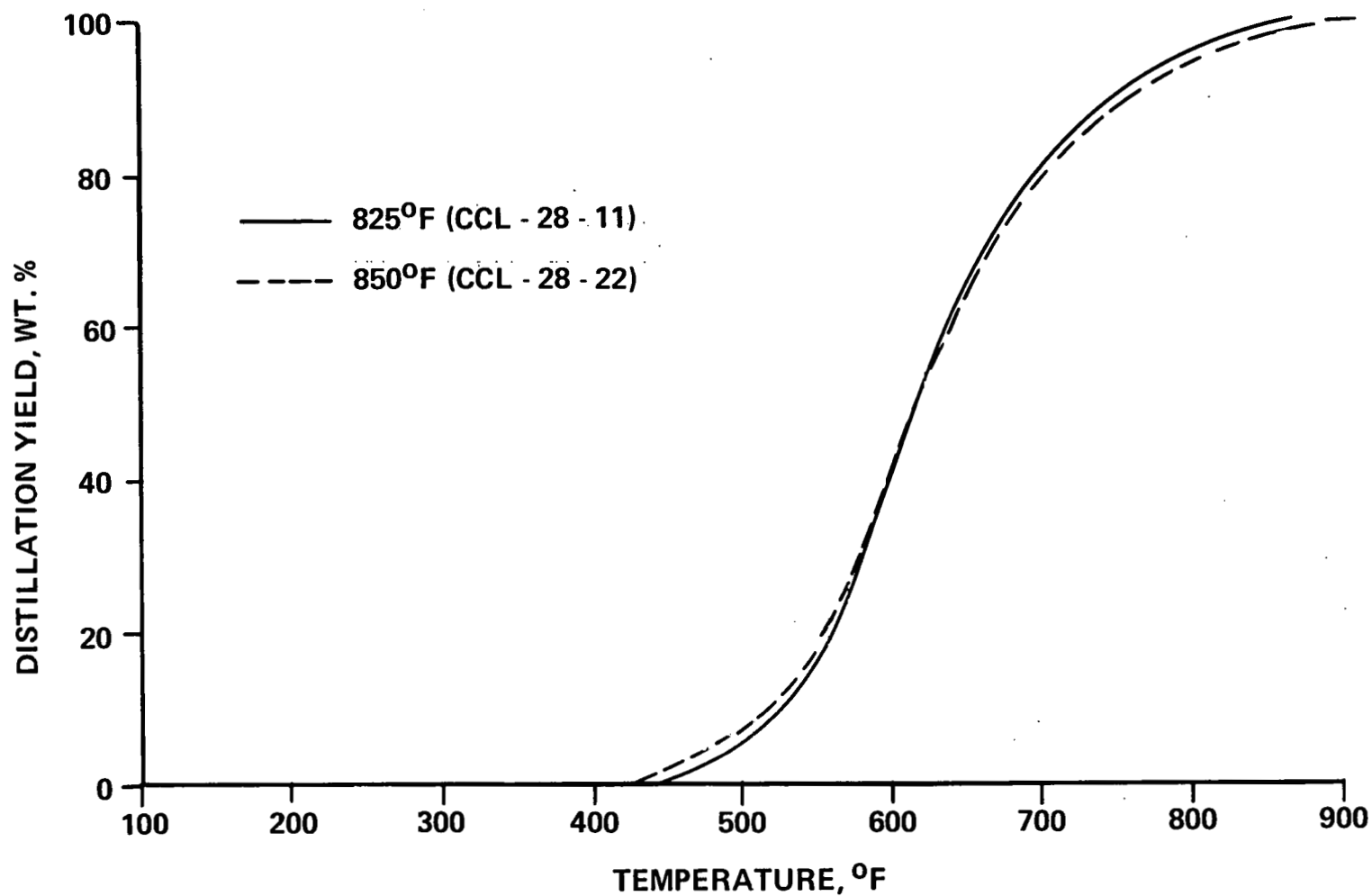
TEMPERATURE, °F

FIGURE 6
EFFECT OF REACTION TEMPERATURE ON SIMULATED DISTILLATION OF OIL FRACTIONS OBTAINED BY LIQUEFACTION OF ELKHORN #2 COAL

Legend:
- —— 31–128 (825°F)
- – – – 31–139 (850°F)

X-axis: TEMPERATURE, °F (100 to 900)
Y-axis: DISTILLATION YIELD, WT. % (0 to 100)
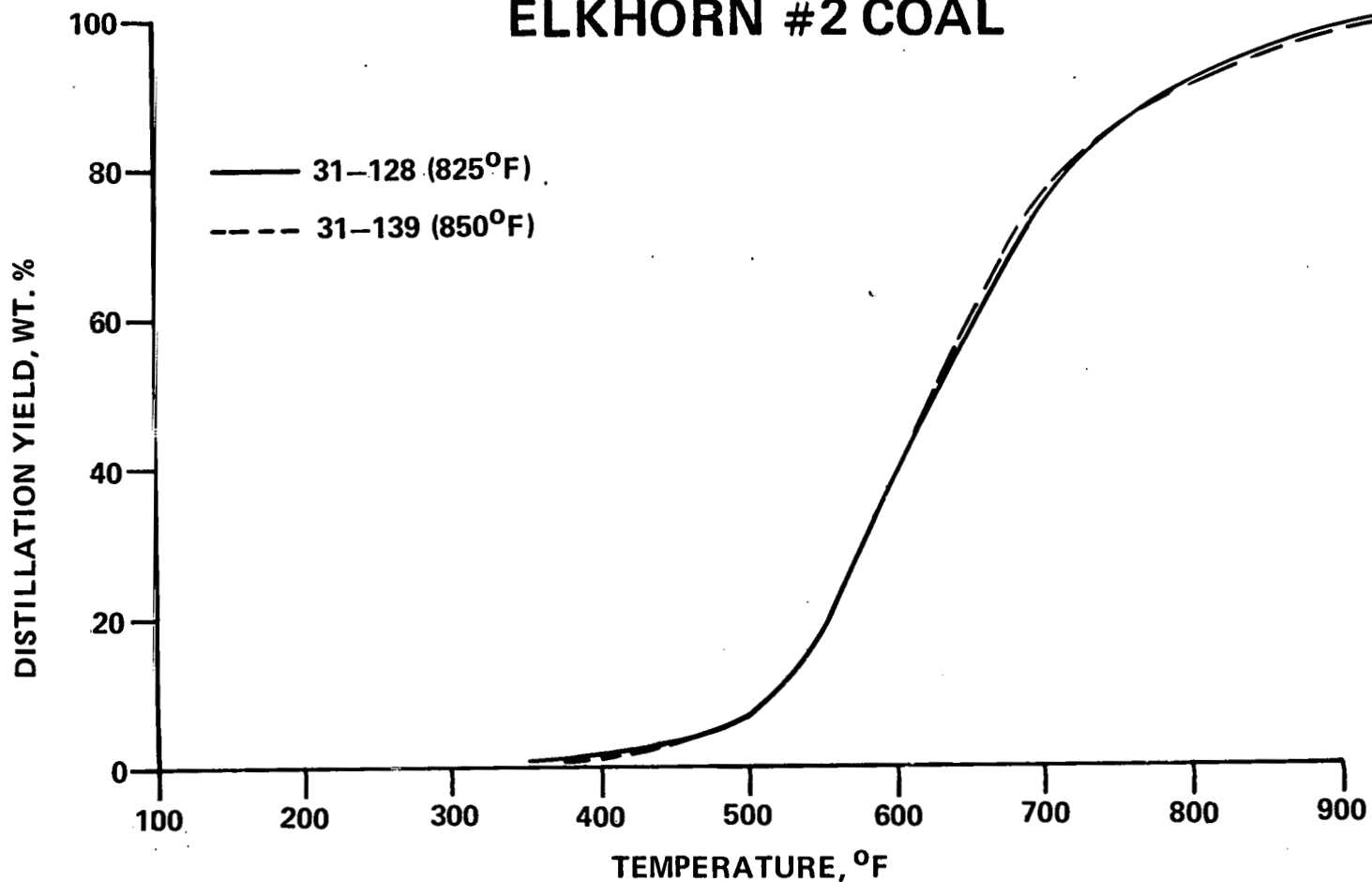
From this data it can be concluded that increasing the reaction temperature in the liquefaction of Elkhorn #2 coal increases the formation of hydrocarbon gases and water, decreases the production of oils, and does not change coal conversion, hydrogen consumption, production of asphaltenes and preasphaltenes, and SRC sulfur content.

Effect of Solvents on Noncatalytic Liquefaction - Two different boiling range process solvents, FOB #1 and FOB #11, were used to study the effect of process solvent on liquefaction of Floyd County Elkhorn #3 coal. The properties of initial solvents and solvents generated by coal liquefaction are discussed below. In addition the results from coal liquefaction runs are also provided.

The solvent separation of the two solvents showed entirely different product distribution (see Table 36). FOB #11 contained more oils and less asphaltenes compared with FOB #1. There was no residue in the FOB #1, while FOB #11 had 0.8% residue. The distribution of elements in the oil fraction of both the solvents presented in Table 37 showed only minor variations in oxygen, nitrogen, and sulfur contents. Significant differences were noted in the hydrogen content of the two oil fractions; FOB #1 contained 7.7% hydrogen compared with 7.2% in FOB #11. The distribution of protons given in Table 38 showed identical H_{AR} values for both solvents. FOB #1 had slightly higher concentrations of H_o and H_a than FOB #11. This information suggests that FOB #1 had slightly higher hydrogen donor capability (better solvent quality) than FOB #11 and, hence, should perform better than FOB #11. FOB #1 had lower aromaticity and degree of aromatic ring substitution and higher degree of condensation than did FOB #11 (Table 39). The two solvents had the same average number of condensed aromatic rings. Simulated distillation of the oil fraction of the two process solvents is compared in Figure 7. The oil fraction of the FOB #11 contained considerably higher boiling point compounds than that of FOB #1. The two oil fractions also exhibited different initial and final boiling points.

Table 36

Distribution of Soluble Fractions in Two Different Process Solvents

	wt.%	
Sample	FOB #1[1]	FOB #11[2]
Oils	90.8	93.8
Asphaltenes	8.9	5.0
Preasphaltenes	0.4	0.4
Insoluble Organic Material	0.0	0.8

[1] 550°F+ cut of SRC-II Fuel Oil Blend

[2] SRC-II Heavy Distillate

Table 37

Elemental Distribution in the Solubility
Fractions from Liquefaction of Elkhorn #3 Coal

Sample No.	FOB #11		FOB #1	
	Feed	Product (31-81)	Feed	Product (25-40)
Temperature, °F	--	850	--	850
Oil Fraction		wt.%		
C	89.7	89.7	89.6	89.1
H	7.2	7.3	7.7	7.5
O	1.4	1.7	1.3	1.8
N	1.1	0.7	0.9	1.3
S	0.6	0.6	0.5	0.3
$\bar{n}$ MW	208	220	220	--
Asphaltene Fraction				
C	ND[1]	86.1	ND	86.1
H	ND	6.1	ND	6.5
O	ND	4.9	ND	4.5
N	ND	2.4	ND	2.2
S	ND	0.5	ND	0.7
Preasphaltene Fraction				
C	ND	86.1	ND	84.1
H	ND	5.0	ND	5.5
O	ND	5.9	ND	5.5
N	ND	2.5	ND	3.3
S	ND	0.5	ND	0.6

[1] Not Determined

Table 38

Distribution of Protons in the Oil Fractions
from Liquefaction of Elkhorn #3 Coal

Sample No.	FOB #11		FOB #1	
	Feed	Product (31-81)	Feed	Product (25-40)
Feed Composition		70% Solvent+ 30% Coal		70% Solvent + 30% Coal
Temperature, °F	--	850	--	850
Pressure, psig	--	2000	--	2000
Total Hydrogen wt.%	7.2	7.3	7.7	7.5

Distribution of Protons, %

	Abs.[1]	Rel.[2]	Abs.	Rel.	Abs.	Rel.	Abs.	Rel.
H_{AR}	3.2	44.4	3.5	47.0	3.2	42.0	3.2	42.1
H_a	2.0	28.0	2.0	28.0	2.3	29.3	2.1	28.2
H_o	2.0	27.6	1.8	25.0	2.2	28.7	2.2	29.7

[1] Abs. - Absolute

[2] Rel. - Relative

Table 39

Modified Brown-Ladner Structural Parameters for the
Oil Fractions from Liquefaction of Elkhorn #3 Coal

Sample No.	FOB #11	Product (31-81)	FOB #1
f_a	0.71	0.72	0.70
σ	0.28	0.27	0.27
H_{AR}/C_{AR}	0.80	0.85	0.83
R_a	3.23	3.18	3.23

75

FIGURE 7
COMPARISON OF SIMULATED DISTILLATION OF OIL FRACTIONS OF TWO DIFFERENT PROCESS SOLVENTS

FOB #11

FOB #1

DISTILLATION YIELD, WT. %

TEMPERATURE, °F
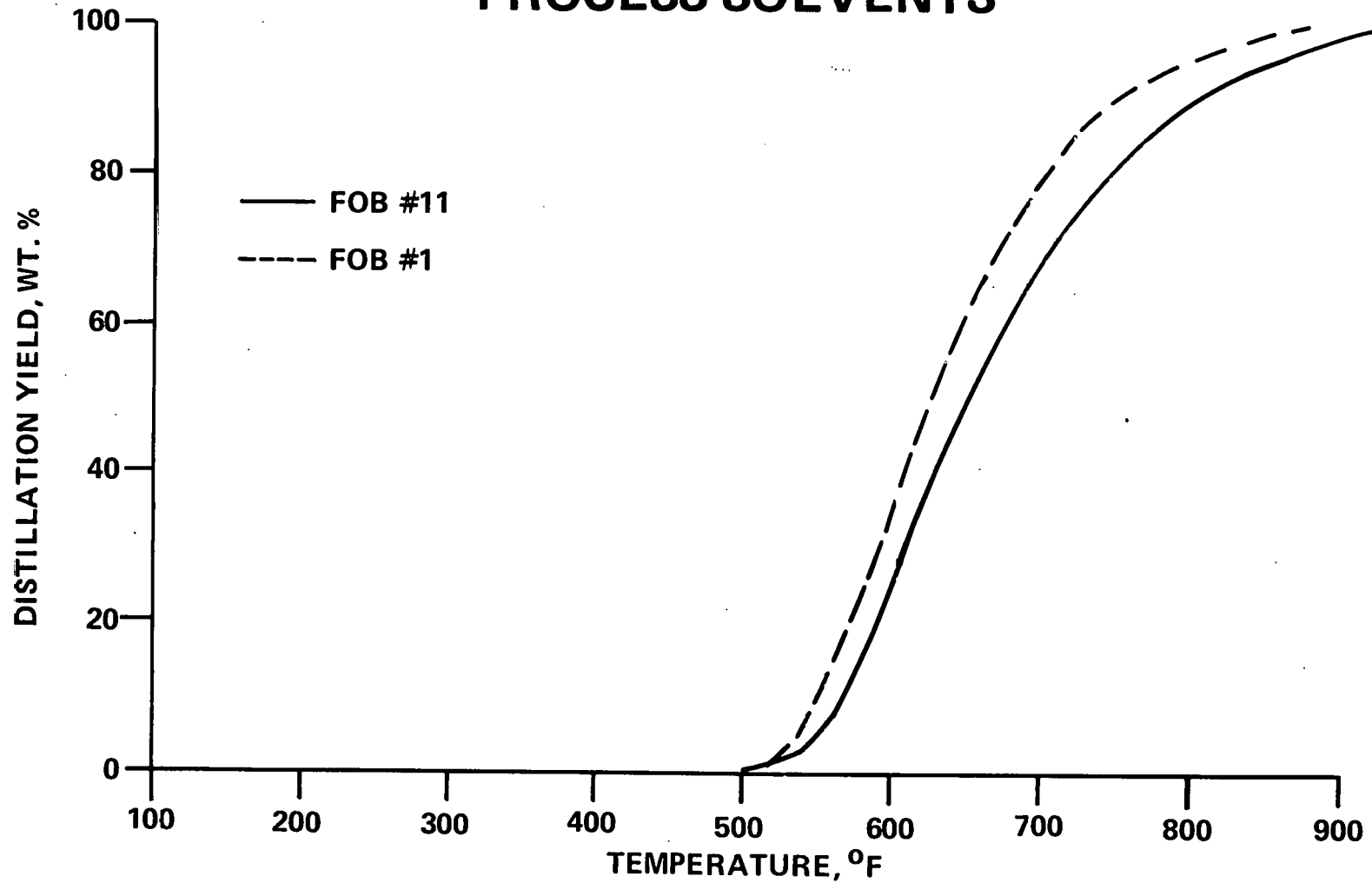
Simulated distillations of the oil fractions (pentane solubles) generated by liquefaction of Elkhorn #3 coal using two different solvents is compared in Figure 8. As noted for the starting solvents (Figure 7), the generated solvents had different boiling point distribution. However, the difference between the boiling point distribution of the generated solvents was less severe than that of original solvents (Figure 7), indicating that generated solvents were approaching a steady-state boiling point distribution.

The liquefaction behavior of Elkhorn #3 coal using the two solvents is presented in Table 40. The lower hydrogen content solvent (FOB #11) yielded a higher coal conversion and hydrocarbon gas production, i.e., 84.2 and 6.8%, respectively, with FOB #11 compared with 81.9 and 4.2% with FOB #1. Oil production, however, was lower with FOB #11 compared to FOB #1 (Table 40). Lower production of H_2S + NH_3 and water was noted with FOB #11 than with FOB #1 (Table 40). The difference in H_2S + NH_3 gas production could be due to the use of the sample bomb with FOB #11 solvent (on-line GC not operational) rather than on-line GC as with FOB #1. The H_2S gas can react either with the walls of the bomb or with other compounds in the gas sample with time. These reactions would eventually lower the concentration of H_2S determined by GC analysis. Higher asphaltenes and lower oil and preasphaltenes production were noted with FOB #11 than with FOB #1. A difference in SRC sulfur content was also apparent. Hydrogen consumption was 0.91% MAF coal with FOB #11 compared with 1.40% with FOB #1. The hydrogen content of oils decreased with FOB #1; i.e., 7.5% hydrogen content in the generated oils compared with 7.7% in the original solvent (Table 37). The hydrogen content of generated solvent was slightly higher than the original solvent when FOB #11 solvent was used. The difference in the total hydrogen consumption was mainly due to that consumed by the solvent. One interesting observation was that when the original solvent hydrogen content was 7.2%, a higher hydrogen content was found in the generated solvent, and when the original solvent hydrogen content was 7.7%, the hydrogen content dropped to 7.5%. These observations tentatively suggest that the solvent was approaching a common hydrogen concentration value between 7.2 and 7.7%.

FIGURE 8
COMPARISON OF SIMULATED DISTILLATION
OF OIL FRACTIONS OBTAINED BY LIQUEFACTION
OF FLOYD COUNTY ELKHORN #3 COAL
USING TWO DIFFERENT SOLVENTS
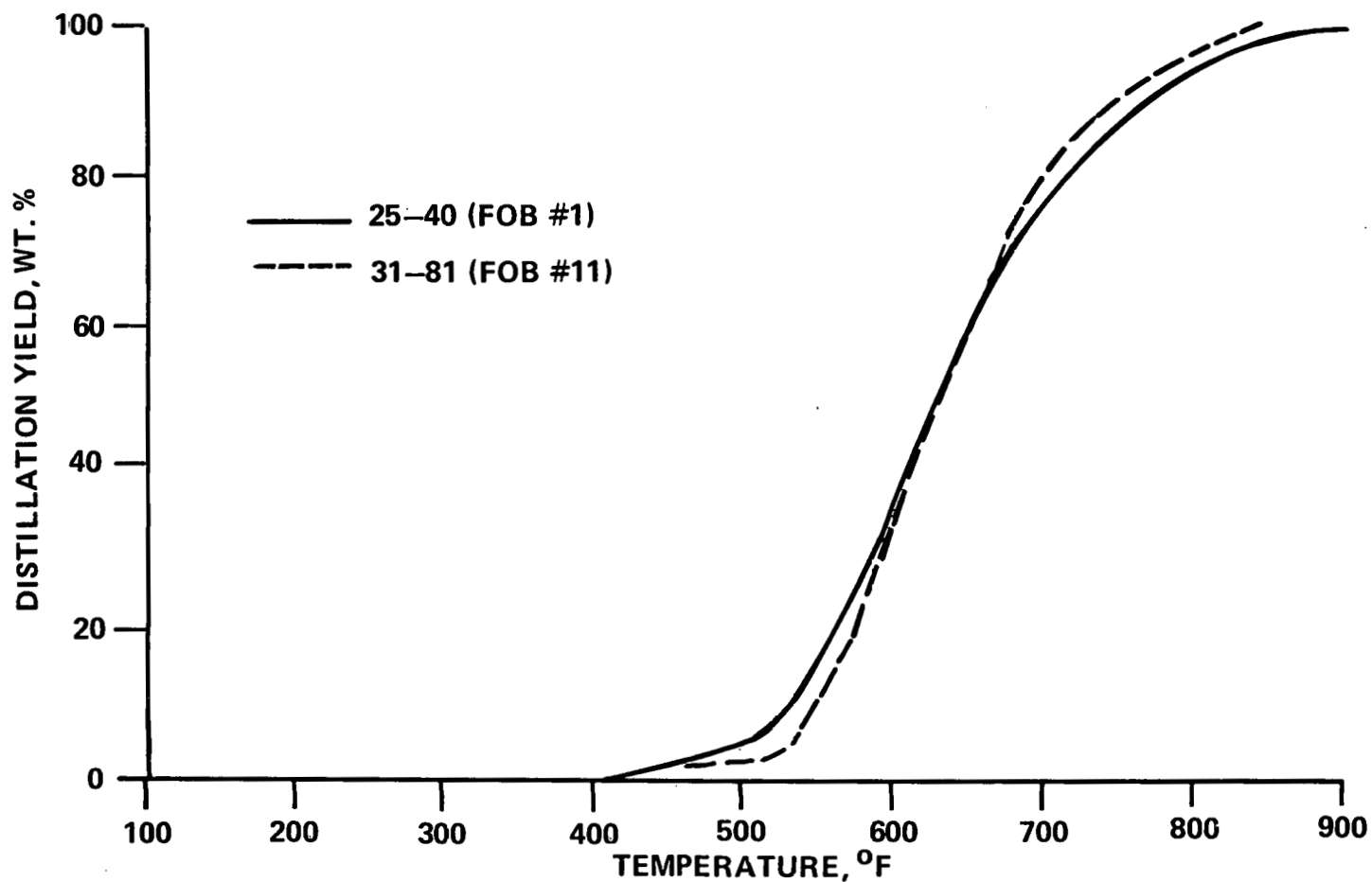
Table 40

Floyd County Elkhorn #3 Coal Liquefaction
Product Distribution

Sample No.	25-40	31-81
Feed Composition	70% Solvent + 30% Coal	
Solvent	FOB #1	FOB #11
Temperature, °F	850	850
Pressure, psig	2000	2000
Time, Min.	38	38
Product Distribution, Wt.% MAF Coal		
HC	4.2	6.8
CO, CO_2	1.0	1.0
H_2S + NH_3	1.3	0.2
Oils	27.3	20.4
Asphaltenes	14.8	29.2
Preasphaltenes	30.1	25.4
I.O.M.	18.1	15.8
Water	3.2	1.2
Conversion, Wt. % MAF Coal	81.9	84.2
SRC Sulfur, %	0.61	0.50
Hydrogen Consumption, Wt.% MAF Coal		
Total	1.40	0.91
From Gas	0.82	0.92
From Solvent	0.58	(0.01)[1]

[1] ( ) = negative value

The concentrations of H_a and H_o were higher in FOB #1 than in FOB #11; higher concentrations of these protons generally indicate higher solvent quality. The concentration of H_{AR} was the same in both the solvents. The distribution of protons in the solvents generated from the two original solvents (Table 38) showed that the difference in the H_a concentration had decreased by 0.3 wt% (2.3 vs 2.0) and 0.1 wt% (2.1 vs. 2.0). The concentrations of H_o and H_{AR} in the generated solvent using F.O.B. #1 were unchanged, while H_{AR} increased for the generated solvent using FOB #11.

Mixed results were obtained with the use of two different hydrogen content and boiling range solvents in the liquefaction of coal. Low hydrogen content solvent resulted in the production of higher hydrocarbon gases, asphaltenes and conversion of coal than high hydrogen content solvent. Oil and water production, however, was lower. SRC sulfur and hydrogen consumption were also considerably lower with low hydrogen content solvent than with high hydrogen content solvent.

Effect of Hydrogen Flow Rate on Noncatalytic Liquefaction - The impact of the increased amount of available hydrogen on the liquefaction of Elkhorn #2 coal was evaluated by increasing the hydrogen flow rate.

The results of liquefaction of Elkhorn #2 coal at two different hydrogen flow rates are compared in Table 41. Coal conversion was unchanged with increasing hydrogen flow rate. The production of hydrocarbon gases and oils increased from 7.0 to 8.2% and from 8.3 to 17.5%, respectively, with increasing hydrogen flow rates from 19.9 to 38.3 mscf/t of coal. The production of preasphaltenes decreased from 43.4 to 35.9% because of increased conversion to oil and gases. The rates of conversion of asphaltenes and preasphaltenes increased significantly with the increase in hydrogen flow rate, i.e, from 0.39 to 0.94% and from 1.09 to 1.71%, respectively. Hydrogen consumption increased slightly from 0.53 to 0.88% and SRC sulfur content was unchanged with increasing hydrogen flow rate.

As summarized in Table 42, all fractions showed only minor changes in the elemental composition with hydrogen flow rate. The simulated distillation of oil fractions obtained at two different flow rates were also very similar, as shown in Figure 9. The distribution of nitrogen and oxygen compounds in the

Table 41

Effect of Hydrogen Flow Rate on
Liquefaction of Elkhorn #2 Coal

Sample No.	31-139	31-149
Temperature, °F	850	850
Pressure, psig	2000	2000
Residence Time, Min.	37	35
Hydrogen Treat Rate, MSCF/T	19.9	38.3
Product Distribution, wt.% MAF Coal		
HC	7.0	8.2
CO, CO_2	0.6	0.7
H_2S	0.3	0.3
NH_3	0.0	0.0
Oils	8.3	17.5
Asphaltenes	21.6	19.4
Preasphaltenes	43.4	35.9
I.O.M.	15.7	16.2
Water	3.1	1.8
Conversion, wt. % MAF Coal	84.3	83.8
Hydrogen Consumption, wt.% MAF Coal		
Total	0.53	0.88
From Gas	0.44	1.00
From Solvent	0.09	(0.12)[1]
SRC Sulfur	0.55	0.48
First Order Rate Constant, hr^{-1}		
K_a	0.39	0.94
K_p	1.09	1.71

[1] ( ) - negative value

Table 42

Effect of Hydrogen Flow Rate on the Distribution of Elements in the
Solubility Fractions from Liquefaction of Elkhorn #2 Coal

Sample No.	31-139	31-149
Temperature, °F	850	850
Hydrogen Treat Rate, MSCF/T	19.9	38.3
Oil Fraction, wt.%		
C	89.7	89.5
H	7.2	7.3
O	1.8	1.7
N	0.7	0.8
S	0.6	0.7
Asphaltene Fraction, wt.%		
C	87.0	86.7
H	6.1	5.8
O	5.0	4.9
N	1.4	2.1
S	0.5	0.5
Preasphaltene Fraction, wt.%		
C	86.6	86.9
H	4.9	4.8
O	5.4	5.1
N	2.4	2.3
S	0.6	0.5

FIGURE 9
EFFECT OF HYDROGEN FLOW RATE ON SIMULATED DISTILLATION OF OIL FRACTIONS OBTAINED BY LIQUEFACTION OF ELKHORN #2 COAL

HYDROGEN FLOW RATE
——— 19.9 MSCF/T (31-139)
– – – 38.3 MSCF/T (31–149)

DISTILLATION YIELD, WT. %
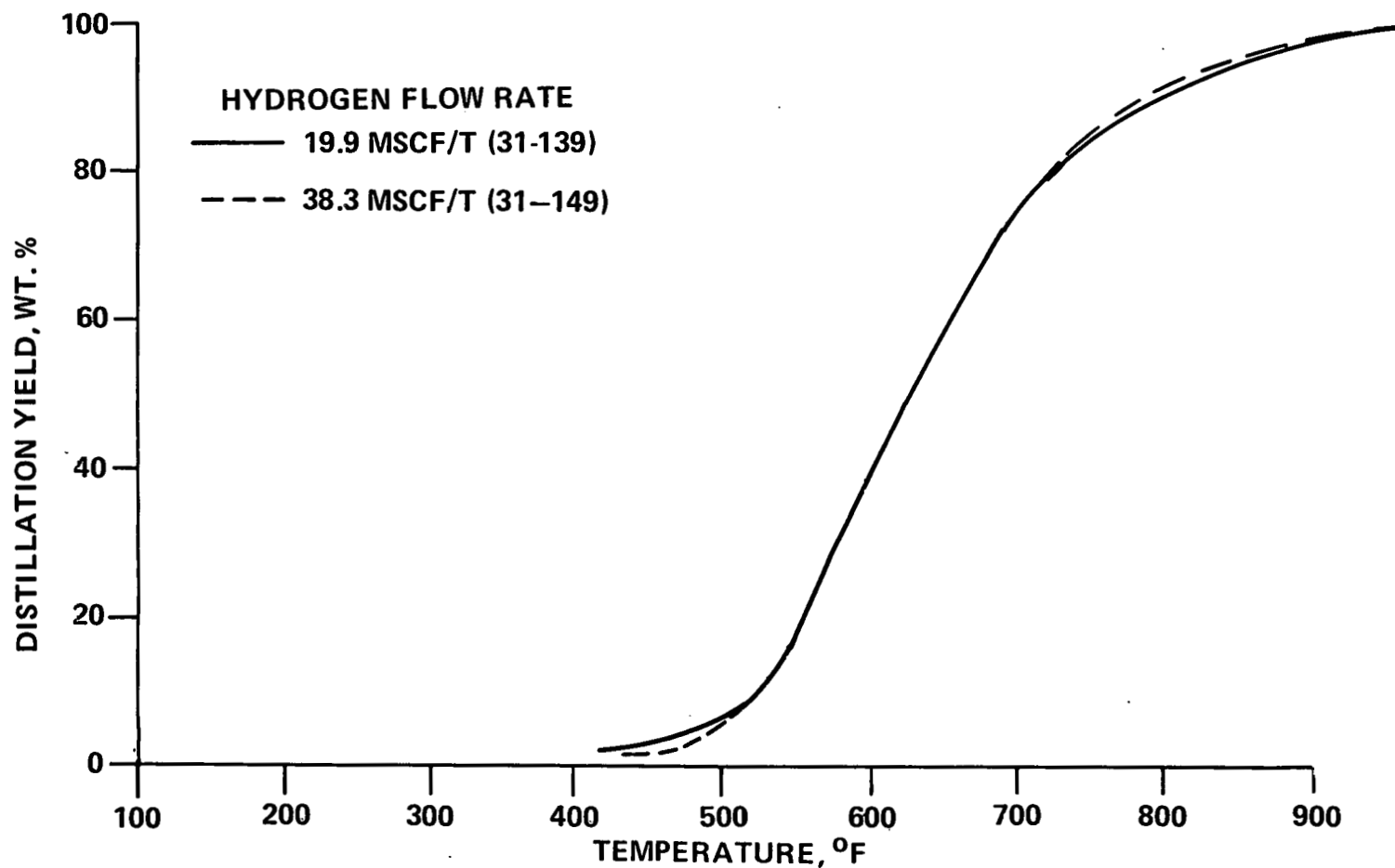
TEMPERATURE, °F

THIS PAGE

WAS INTENTIONALLY

LEFT BLANK

Table 43

Distribution of Nitrogen and Oxygen Compounds in
the Oil Fractions Obtained at Two Different Hydrogen Flow Rates

Sample No.		31-139			31-149	
Temperature, °F		850			850	
H_2 Flow Rate, MSCF/T		19.9			38.3	
Total Nitrogen, wt.%		0.66			0.80	
Total Oxygen, wt.%		1.79			1.70	

Nitrogen Distribution, wt.%

		Abs.[1]	Rel.[2]		Abs.	Rel.
N as N		0.27	40.9		ND[3]	ND
N as NH		0.32	48.5		0.33	48.5
N as NH_2		0.07	10.6		ND	ND

Oxygen Distribution, wt.%

		Abs.	Rel.		Abs.	Rel.
O as O		1.14	63.7		1.02	60.0
O as OH		0.65	36.3		0.68	40.0

[1] Abs. - Absolute

[2] Rel. - Relative

[3] Not Determined

Table 44

Distribution of Protons in the Oil Fractions
Obtained at Two Different Hydrogen Flow Rates

Sample No.	31-139		31-149	
H_2 Flow Rate, MSCF/T	19.9		38.3	
Total Hydrogen, wt.%	7.2		7.3	

Proton Distribution, %

	Abs.[1]	Rel.[2]	Abs.	Rel.
H_{AR}	3.38	46.9	3.31	45.3
H_a	2.01	27.9	2.10	28.7
H_o	1.81	25.2	1.89	26.0

[1] Abs. - Absolute
[2] Rel. - Relative

Table 45

Variation of Brown-Ladner Structural Parameters for
Oil Fractions Obtained at Two Different Hydrogen Flow Rates

Sample No.	31-139	31-149
H_2 Flow Rate, MSCF/T	19.9	38.3
f_a	0.72	0.72
σ	0.27	0.28
H_{AR}/C_{AR}	0.84	0.83
R_a	3.07	3.30

Both samples of Pittsburgh #8 (CPDU-131 and CPDU-131A) collected from Belmont County were from the same seam but from two different mines. The CPDU-131 had a higher concentration of ash than CPDU-131A, while the total pyritic plus organic sulfur content of the CPDU-131A was higher than that of the CPDU-131.

Product Work-Up - In the study with the Ohio coals the product slurries from the coal liquefaction experiments were vacuum distilled to recover the IBP-450°F (cut #1) and 450-780°F (cut #2) solvent fractions. The bottom products, which consisted of SRC, insoluble organic material and mineral matter, were mixed with pyridine, heated and filtered to separate the pyridine solubles and insolubles. The pyridine solubles were vacuum-distilled to remove pyridine and recover solid SRC, and the pyridine insolubles were washed with methylene chloride and dried in an inert atmosphere. The vacuum distillations were essentially single-plate flashes, since a Vigreux column equivalent to no more than two theoretical plates was used to achieve adequate reflux. Distillate cuts overlapped each other in boiling point range to a significant degree. The boiling point distribution of one of the samples, as determined by GC-simulated distillation, is shown in Figure 10. Note that cut #1 contained 16 wt % material boiling above 450°F and cut #2 contained 6 wt % material boiling below 450°F.

A serious difficulty with the laboratory distillation was the irreproducibility of the 780°F end point. Although an 850°F end point was the target in the laboratory batch distillation, 780°F was the maximum end point that could be achieved. Even this end point could not be reached consistently. The distillation work-up procedure was used only for the liquefaction of Ohio coal samples.

The GC-simulated distillation procedure was used to determine the boiling point distribution for the distillate liquid, so that the yield of a standard 450-740°F solvent fraction could be mathematically determined. Since 749°F was the minimum end point achieved by one sample, an end point of 740°F was selected for calculation purposes.

Coal Liquefaction Experiments - A summary of the sample numbers and process conditions used for the liquefaction of Ohio coals is given in Table 46. FOB #3 solvent was used for three coal samples and FOB #4 for the fourth one.

FIGURE 10
SIMULATED DISTILLATION OF SOLVENT FRACTIONS OBTAINED BY LIQUEFACTION OF CLARION #4A COAL SAMPLE

SAMPLE NO. CCL-28-84

CUT #1

CUT #2

DISTILLATION YIELD, WT. %
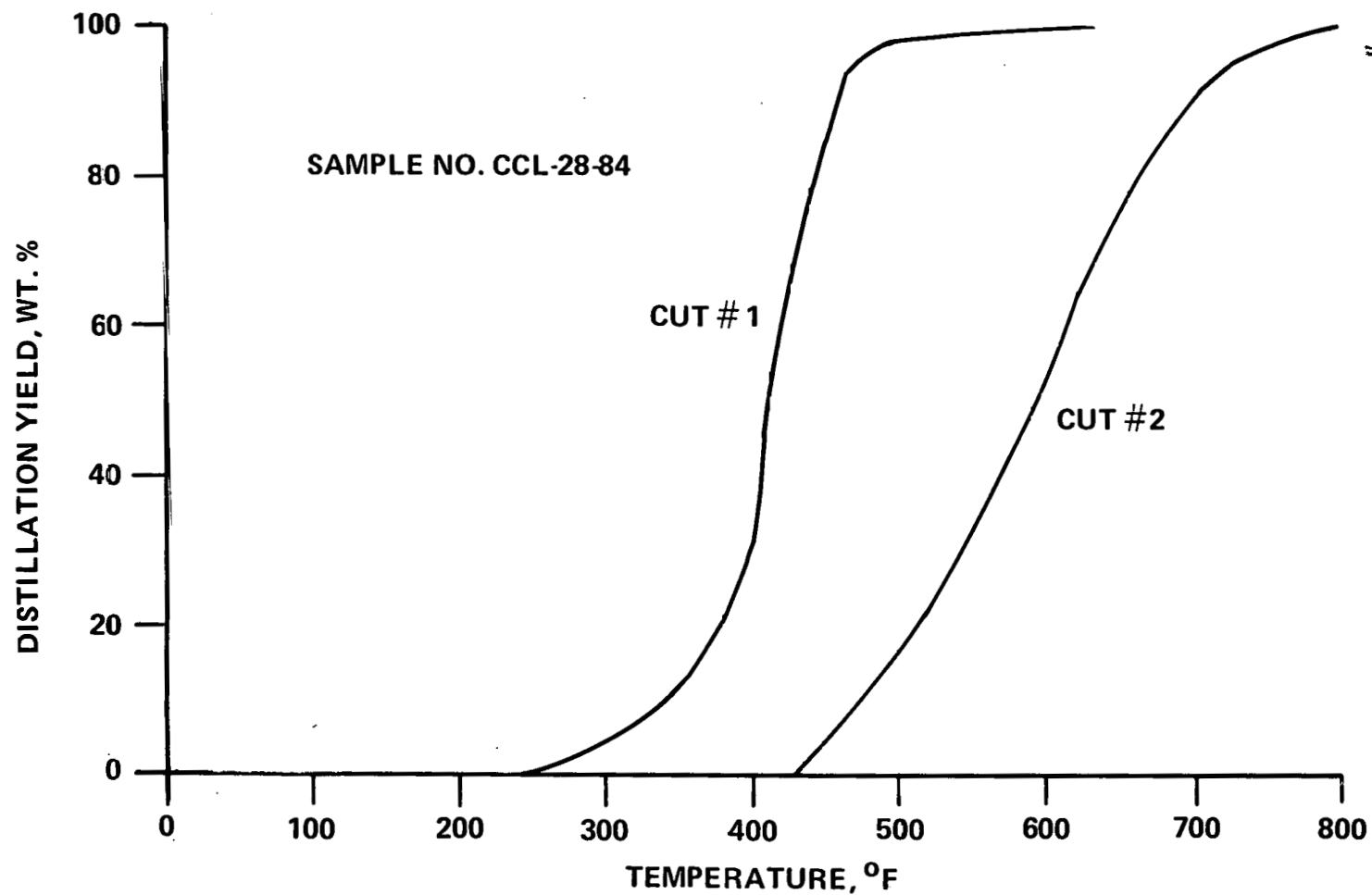
TEMPERATURE, °F

Table 46

Summary of Process Conditions for Liquefaction of Ohio Coals

Sample No.	Coal	Solvent	Temperature, °F	Pressure, psig	Time, Min.	Solvent/Coal By Weight	Hydrogen Feed Rate, MSCF/T
28-84	Clarion #4A CPDU-132	FOB #3	850	2000	36	70/30	19.60
28-96	Clarion #4A CPDU-128A	FOB #3	850	2000	37	70/30	20.32
28-110	Pittsburgh #8 CPDU-131	FOB #3	850	2000	37	70/30	20.82
28-123	Pittsburgh #8 CPDU-131A	FOB #4	850	2000	37	70/30	19.97

The product slurry from the coal liquefaction experiments was separated into the following fractions by the vacuum distillation and GC-simulated distillation data:

IBP-420°F	Light oil
420-450°F	Light solvent
450-740°F	Process solvent
740°F +	SRC
Pyridine-insoluble-residue	

Complete analytical and work-up data for the Ohio coals are presented in Appendix D. The product distribution based on vacuum distillation and GC-simulated distillation was calculated and is discussed below.

Boiling Point Distribution of Feed and Product Liquids - The original solvents (FOB #3 and FOB #4) and the vacuum distillation fractions (cuts #1 and #2) from the product were mathematically subdivided into IBP to minus 420°F, 420-450°F and 450-740°F fractions based on GC-simulated distillation data. The distribution of original solvent into various boiling cuts is calculated and presented in Table 47. The GC-simulated distillation data of the coal liquefaction products (cuts #1 and #2) are shown in Table 48. The distribution of distillation cuts into various boiling point ranges is calculated from GC-simulated distillation data and is shown in Table 49.

Liquefaction of Clarion #4A Coal - The conversions of the two Clarion #4A coals were similar at the same reaction conditions (Table 50). The distillate IBP-740°F was higher for the higher ash sample (CPDU-128A) than CPDU-132. The CPDU-128A sample (high-ash) showed a significant loss in the 420-450°F fraction compared with the CPDU-132 (low-ash) sample. Although no loss in process solvent was observed with the CPDU-128A sample, an 11.0% loss in process solvent was noted with the CPDU-132 sample. This loss in solvent was reflected in higher SRC production (Table 50) compared with the CPDU-128A coal. The production of HC gases and light oil (IBP-420°F) was identical for both samples. Hydrogen consumption was also identical in both the cases and slightly lower SRC sulfur was noted for the CPDU-128A coal sample.

Table 47

Distillation Distribution of Original Solvents for Liquefaction of Ohio Coals

	Weight %	
	FOB #3	FOB #4
I.B.P.-420°F	1.0	0.0
420-450°F	7.0	0.0
450-740°F	90.0	96.0
740°F+	2.0	4.0
Total	100.0	100.0

Table 48

GC-Simulated Distillation Data for Products from Liquefaction of Ohio Coals

wt.% Distilled	Temperature °F							
	28-84		28-96		28-110		28-123	
	Cut #1	Cut #2	Cut #1	Cut #2	Cut #1	Cut #2	Cut #1	Cut #2
I.B.P.	244	423	274	435	247	423	244	433
5	306	447	341	455	326	450	294	493
10	342	468	363	479	353	476	328	528
20	377	512	395	520	393	520	355	551
30	399	541	406	546	405	546	378	577
40	407	570	411	574	410	575	393	595
50	412	594	416	595	415	596	405	611
60	416	611	423	612	421	615	411	631
70	430	634	443	631	442	638	419	654
80	447	663	452	655	451	666	441	680
90	455	695	457	683	457	698	452	712
95	466	722	464	701	464	725	468	738
97	483	742	481	713	475	742	482	756
99	541	756	490	736	496	773	516	788
F.B.P.	631	798	499	749	511	789	537	805

Table 49

Distillation Distribution of Products
from Liquefaction of Ohio Coals

	wt.%							
	28-84		28-96		28-110		28-123	
	Cut #1	Cut #2	Cut #1	Cut #2	Cut #1	Cut #2	Cut #1	Cut #2
I.B.P.-420°F	66.0	0.0	57.0	0.0	59.0	0.0	70.0	0.0
420-450°F	18.0	6.0	21.0	4.0	20.0	5.0	18.0	2.0
450-740°F	16.0	91.0	22.0	96.0	21.0	93.0	12.0	93.0
740°F+	0.0	3.0	0.0	0.0	0.0	2.0	0.0	5.0
Total	100.0	100.0	100.0	100.0	100.0	100.0	100.0	100.0

Table 50

Product Distribution from Liquefaction of Ohio Coals

Sample No.	Clarion #4A Coal		Pittsburgh #8 Coal	
	28-84	28-96	29-110	28-123
Coal	CPDU-132	CPDU-128A	CPDU-131	CPDU-131A
Feed Composition	70% Solvent + 30% Coal		70% Solvent + 30% Coal	
Temperature, °F	850	850	850	850
Solvent	F.O.B #3	F.O.B. #3	F.O.B. #3	F.O.B #4
Pressure, psig	2000	2000	2000	2000
Time, Min.	36	37	37	37
H_2 Flow Rate, MSCF/T	19.6	20.3	20.8	20.0
Product Distribution, wt.% MAF				
HC	4.0	3.7	2.8	3.3
CO, CO_2	1.0	1.1	0.7	0.7
H_2S	1.7	2.2	2.6	2.4
NH_3	0.0	0.1	0.3	0.4
I.B.P.-740°F	0.2	5.3	16.0	7.7
I.B.P.-420°F	11.6	11.0	10.8	10.3
420-450°F	(0.4)[1]	(6.1)	(1.7)	7.7
450-740°F	(11.0)	0.4	6.9	(10.3)
740°F + SRC	81.2	71.3	66.9	75.9
I.O.M.	11.1	12.4	7.0	6.8
Water	0.8	3.9		2.8
Conversion, wt.% MAF Coal	88.9	87.6	93.0	93.2
SRC Sulfur, %	1.1	0.93	1.42	1.94
H_2 Consumption, % MAF Coal	1.07	1.06	1.12	1.52

---

[1] (   ) - negative number

Similar hydrogen content was observed in all three fractions obtained from the two coal samples (Table 51). No differences were noted in the nitrogen, oxygen and sulfur contents of cuts #1 and #2. However, some differences in the nitrogen and oxygen contents were noted in SRC obtained from the two coal samples. The hydrogen content and proton distribution of the process solvent (cut #2) obtained with the coal samples were very similar to that of starting solvent, as shown in Table 52.

Petrographic analysis showed that the CPDU-128A sample had slightly higher reactive maceral content (vitrinite and exinite) compared with the CPDU-132 sample, i.e., 92.5% and 91.4%, respectively. The fusinite content in the CPDU-128A and CPDU-132 coal samples was 7.5 and 8.6%, respectively. The differences between the reactive maceral and fusinite contents of and the two coal samples were not great enough to cause any major variation in the conversion of the two coal samples, as shown in Table 50. Finally, from the available data it can be concluded that lower pyrite and mineral matter containing sample yielded lower production of process solvent. However it is not certain whether the loss in process solvent was due to the differences in pyrite or mineral matter.

<u>Liquefaction of Pittsburgh #8 Coal</u> - The conversions of Pittsburgh #8 coals were identical as was the production of the IBP-420°F fraction (Table 50). The production of hydrocarbon gases was also similar with both coals. Major differences were noted in the production of 420-450°F, 450-740°F and SRC. Both SRC and SRC sulfur content were higher in the high-sulfur containing sample (CPDU-131A). The CPDU-131A coal showed net loss of 10.3% process solvent (450-740°F) while the CPDU-131 showed a gain of 6.9%. A net gain of 7.7% light solvent (420-450°F) was noted with the CPDU-131A, whereas a net loss of 1.7% occurred with the CPDU-131 sample. Combining the light solvent (420-450°F) and process solvent (450-740°F) gave a net loss of 2.6% solvent with the high-sulfur containing sample (CPDU-131A) and a net gain of 5.2% solvent with the CPDU-131A. The two samples had almost similar ash contents, but the CPDU-131 had a slightly higher pyrite content. It is not clear whether this difference is due to mineral contents or to the use of two different process solvents. Hydrogen consumption was higher with the CPDU-131A than with the CPDU-131. The petrographic analysis discussed earlier showed that the CPDU-131 contained slightly higher amounts of reactive macerals (vitrinite

Table 51

Elemental Distribution in the Distillation
Fractions from Liquefaction Product of Ohio Coals

Sample No.	Clarion #4A		Pittsburgh #8	
	28-84	28-96	28-110	28-123
Coal	CPDU-132	CPDU-128A	CPDU-131	CPDU-131A
Cut #1, Wt.%				
C	87.7	88.0	89.0	89.2
H	8.4	8.4	8.2	7.6
O	2.4	2.1	1.7	1.6
N	0.7	0.6	0.4	1.1
S	0.8	0.9	0.7	0.5
Cut #2, Wt.%				
C	89.9	89.7	89.9	85.4
H	7.2	7.3	7.2	--
O	1.4	1.6	1.6	3.9
N	1.1	0.9	0.8	0.8
S	0.5	0.5	0.6	0.7
SRC, Wt.%				
C	85.3	85.7	84.1	84.3
H	5.8	6.1	5.9	6.1
O	5.2	4.1	5.3	5.7
N	2.2	3.1	3.1	2.1
S	1.1	0.9	1.4	1.9

Table 52

Distribution of Protons in the Recycle Solvent
Obtained By Liquefaction of Ohio Coals

Sample No.	FOB #3	28-84	28-96	FOB #3	28-110	FOB #4	28-123
		Clarion #4A			Pittsburgh #8		Pittsburgh #8
Coal	--	CPDU-132	CPDU-128A	--	CPDU-131	--	CPDU-131A
Solvent	--	Cut #2	Cut #2	--	Cut #2	--	Cut #2
Total H, wt.%	7.20	7.16	7.26	7.20	7.21	7.64	--
Absolute							
H_{AR}	3.80	3.78	3.55	3.80	3.65	3.13	4.04
H_a	1.80	1.99	1.97	1.80	2.03	2.34	2.89
H_o	1.60	1.39	1.74	1.60	1.53	2.17	2.39
Relative							
H_{AR}	52.8	52.8	48.9	52.8	50.6	41.0	43.3
H_a	25.0	27.8	27.1	25.0	28.1	30.6	31.0
H_o	22.2	19.4	24.0	22.2	21.3	28.4	25.7

and exinite) than the CPDU-131A, i.e., 92.0% and 90.5%, respectively. The difference in the reactive maceral contents of the two coal samples was, in fact, not great enough to cause any significant difference in the conversion of these two coal samples (Table 50).

The distribution of elements in the various fractions summarized in Table 51 showed no major differences. The distribution of protons in the original solvent and cut #2 showed no differences (Table 52).

From these results it can be concluded that Pittsburgh #8 coal obtained from two different mines yielded similar conversion of coal and production of hydrocarbon gases and light oil. However, these coals showed a relatively different production of 420-450°F, 450-740°F, and SRC. The SRC sulfur content for both coal samples was unusually high, i.e, 1.4 to 1.9% compared with 1.0% for many other coals studied. More work is needed to understand the reason for the high SRC sulfur content and to evaluate other ways of reducing it. The differences in the liquefaction behavior of the Pittsburgh #8 coal could be attributed to the use of different solvents for the liquefaction process.

CATALYTIC EFFECT OF MINERALS AND METALLIC WASTES

During several CPDU runs, both solvent hydrogenation and coal liquefaction experiments were carried out using various minerals and metallic wastes to establish their catalytic activity in coal conversion reactions. Complete analytical and work-up data for all samples collected during the runs are presented in Appendix D. The results are discussed below.

Solvent Hydrogenation Catalysis

The hydrogenation of process solvent was studied in the absence of catalyst and in the presence of pyrite, zinc sulfide, speculite, red mud, and flue dust to assess the catalytic activity of the different mineral additives. The chemistry of transformation of the above minerals and metallic wastes during hydrogenation of process solvent was also studied. Table 53 summarizes the process conditions and product distribution for the hydrogenation of process solvent runs with different minerals and metallic wastes. The first column of

Table 53

Product Distribution for SRC-II Heavy Distillate
Process Solvent Hydrogenation Runs

Sample No.	FOB #11	31-10	31-24	31-34
Feed Composition	Original Solvent	100% Solvent	90% Solvent + 10% Pyrite	90% Solvent + 10% ZnS
Temperature, °F	--	850	850	850
Pressure, psig	--	2000	2000	2000
Hydrogen Treat Rate, Wt.% Solvent	--	1.08	1.31	1.33
Reaction Time, Min.	--	38	38	39
Product Distribution, Wt.%				
HC	--	0.9	1.2	0.8
CO, CO_2	--	0.0	0.1	0.0
H_2S	--	0.0	0.4	0.1
NH_3	--	0.0	0.0	0.0
Oils	93.8	93.4	94.0	92.8
Asphaltenes	5.0	3.4	1.6	4.7
Preasphaltenes	0.4	0.8	0.9	0.9
Insoluble Organic Material	0.8	1.0	1.4	0.5
Water	--	0.5	0.4	0.2
Hydrogen Consumption, Wt.% Solvent	--	0.24	0.42	0.28

Table 53
(continued)

Sample No.	31-45	31-55	31-66
Feed Composition	90% Solvent + 10% Speculite	90% Solvent + 10% Red Mud	90% Solvent + 10% Flue Dust
Temperature, °F	850	850	850
Pressure, psig	2000	2000	2000
Hydrogen Treat Rate, Wt.% Solvent	1.44	1.27	1.31
Reaction Time, Min.	41	39	38
Product Distribution, Wt.%			
HC	0.8	1.0	0.7
CO, CO_2	0.0	0.0	0.0
H_2S	0.0	0.0	0.0
NH_3	0.0	0.0	0.0
Oils	95.2	95.1	96.8
Asphaltenes	2.5	1.6	1.2
Preasphaltenes	0.5	1.0	0.6
Insoluble Organic Material	0.4	0.9	0.4
Water	0.5	0.4	0.3
Hydrogen Consumption, Wt.% Solvent	0.23	0.23	0.26

Table 53 presents the analysis of the original (starting) solvent, and the other six columns present the product distribution for hydrogenation of process solvent in the presence and absence of various additives.

The composition of the original solvent shows a sizable fraction of pentane-insoluble asphaltenes, which are distillate materials. The insolubility cannot be attributed to chemical similarity to typical coal-derived asphaltene materials, since these materials are typically not distillable. The actual chemical composition and relationship to the typical coal-derived asphaltenes is still uncertain, although previously it was suggested that these materials be termed asphaltene-derived oils, suggesting they are easily soluble in heptane or heavier paraffinic solvents. However, the classification of these materials as typical asphaltenes is not inconsistent with the behavior observed for all asphaltenes generated during this study.

The treatment of this process solvent in the absence of any mineral additive resulted in only a very slight shift in product distribution. Other than the easily recognizable hydrocarbon gas make, the shift in the product distribution was well within the range of experimental error. A hydrogen consumption of 0.24 wt% of solvent based on elemental hydrogen balance was noted, which was primarily due to the production of hydrocarbon gases and water. No significant differences were noted in the distribution of elements, shown in Table 54, before and after the reaction.

As will become evident from the extensive data developed in this program, solvent hydrogenation or dehydrogenation very readily occurs during the lique-faction reaction. The seeming inactivity of these solvents to change in the presence of hydrogen gas and the absence of coal suggest that the presence of coal greatly affects solvent interaction with the gaseous hydrogen. That these runs were made in a well-stirred, highly turbulent reactor system reflects the inherent role of the coal or its constituents in the overall conversion process rather than the lack of adequate mass transfer effects.

Pyrite - The role of pyrite (FeS_2) as a hydrogenation catalyst has never been precisely defined. Reference to the properties of this material and its use as a catalyst in various hydrogenation systems has appeared in the literature.

Table 54
Distribution of Elements in the Various Fraction
from the Process Solvent Hydrogenation Runs

Sample No.	FOB #11	31-10	31-24	31-34	31-45	31-55	31-66
Additive	Original Solvent	None	Pyrite	ZnS	Speculite	Red Mud	Flue Dust
Oil Fraction, Wt.%							
C	89.7	89.5	89.5	89.7	89.2	89.6	89.5
H	7.2	7.3	7.5	7.5	7.4	7.4	7.4
O	1.4	1.6	1.3	1.5	2.0	1.5	1.5
N	1.1	0.9	1.0	0.7	0.8	0.9	1.0
S	0.6	0.7	0.7	0.6	0.6	0.6	0.6
$\bar{n}MW$	208	210	200	235	220	210	225
Asphaltene Fraction, Wt.%							
C	ND[1]	87.1	87.1	87.5	86.5	85.0	85.2
H	ND	6.4	6.5	6.6	6.2	6.1	6.3
O	ND	3.9	3.8	3.2	4.8	5.5	5.1
N	ND	2.1	2.1	2.2	2.2	3.0	3.0
S	ND	0.5	0.5	0.5	0.3	0.4	0.4

---

[1] Not determined because of small sample size

To better define the intrinsic activity of pyrite in liquefaction, a definite examination of its activity in the hydrogenation of solvent was necessary. The major change was the formation of 0.4 wt% hydrogen sulfide from reduction of pyrite to pyrrhotite. No change was noted in the oils concentration, while the asphaltenes decreased significantly from 5 to 1.6%. The hydrogen consumption based on elemental hydrogen balance was 0.42 wt% of solvent compared with 0.24 wt% for the no-additive run. Most of the increased hydrogen consumption with pyrite present, namely 0.13 wt%, was due to the reduction of pyrite to pyrrhotite. Complete reduction of pyrite during the hydrogenation reaction was assumed in calculating hydrogen consumption. This assumption was consistent with the X-ray diffraction analysis which showed the formation of pyrrhotite $FeS_{1.085}$ during the reaction. The distribution of elements in the oils and asphaltenes given in Table 54 showed an increase in hydrogen content of oils when pyrite was present. No significant changes were noted in the distribution of elements in asphaltenes with or without pyrite.

The continuous addition of pyrite to the reactor in the presence of process solvents enabled a considerable amount of the pyrrhotite formed to be isolated, washed, and dried for evaluation in subsequent coal liquefaction run. Initial testing was done in the tubing bomb; later continuous process runs were made using this material. Those results will be reported below.

Zinc Sulfide - The addition of zinc sulfide (Table 12) to the process solvent hydrogenation reaction did not result in any marked improvement over the no-additive run. Hydrogen consumption was also very similar to that of the no-additive run. Table 55 shows the X-ray diffraction analysis of the mineral sample before the reaction contained ZnS and FeS (sphalerite-type structure). The sample analyzed after the reaction (see Table 55) showed only minor changes. A slight shift in FeS sphalerite-type structure to a pyrrhotite/troilite-type structure was observed. Analysis of the reaction products showed that the hydrogen contents in the oil fraction were higher than without an additive. Hydrocarbon gas make was the same as in the thermal treatment of the solvent alone. Hydrogen consumption was mainly due to the hydrogen gas make.

Table 55

X-Ray Diffraction Analysis of the Minerals and Metallic Wastes
Before and After the Solvent Hydrogenation Reactions

Additive	Phase	Original Minerals or Metallic Wastes	Analysis of Minerals or Metallic Wastes After Reaction
Pyrite	Major	Pyrite (FeS_2)	Phrrhotite ($FeS_{1.085}$)
	Minor	Marcasite, Fe_3O_4, Quartz	Quartz
Zinc Sulfide	Major	ZnS, FeS (sphalerite type structure)	ZnS, FeS (sphalerite type structure)
	Minor		Pyrrhotite/Troilite
Speculite	Major	Fe_2O_3	FeS (sphalerite type), Fe_3O_4, Fe
	Minor	Silica, Quartz	Silica, Quartz
Red Mud	Major	Fe_2O_3	Fe_3O_4
	Minor	Quartz, $CaCO_3$, Al_2O_3	$CaCO_3$, FeS (sphalerite type), Quartz, Fe, Fe_2O_3
Flue Dust	Major	Fe_3O_4, $NiFe_2O_4$, $FeCr_2O_4$	Fe_3O_4, $NiFe_2O_4$, $FeCr_2O_4$
	Minor	FeS, ZnS (sphalerite type structure)	FeS, ZnS (sphalerite type structure)

Speculite - In addition to the many pyritic and reduced pyrite samples, several different iron materials were used in this program, i.e., iron as ores, as pigment, and as components in waste materials. Speculite is a rather pure mineral that contains 95% Fe_2O_3 (Table 8). Because of its crystalline form, it is used in pigment applications.

Solvent hydrogenation by the addition of speculite to process solvent gave results very similar to the thermal reaction alone. The oil concentration in the resulting product liquid increased slightly from 93.4 to 95.2%, while asphaltenes decreased from 5.0 to 2.5%. No significant variation in gases production was noted. Hydrogen consumption based on elemental hydrogen balance, calculated to be 0.23%, was similar to that of the no-additive run. The X-ray diffraction analysis presented in Table 55 indicated that most of the Fe_2O_3 had transformed to FeS (sphalerite-type structure), Fe_3O_4, and elemental iron. This transformation should have resulted in increased water production and hydrogen consumption, but the data in Table 52 were not sufficiently sensitive to show any such increase. The hydrogen and nitrogen contents of oils and asphaltenes generated with speculite were only slightly different from the base run (Table 54). Also, speculite addition resulted in lower sulfur contents in both the oils and asphaltenes. The reduction of sulfur content indicated some desulfurization activity of speculite through its scrubbing of the sulfur generated from the desulfurization of process solvent.

Red Mud - This iron-rich waste is a by-product of the refining of bauxite ore to produce aluminum. In the ore-refining process, caustic is used to dissolve alumina hydrates which results in separation of the aluminum from impurities. The impurities are then decanted or separated from the solubilized material. These waste muds, referred to as red mud because of the iron present in the ore, will contain varying amounts of residual caustic which results in waste materials that are basic in nature. During the operation of their liquefaction facilities from 1930-1940, the Germans successfully used red mud as a catalyst. Because of inherent differences in red muds and coals from the U.S. and Germany, an examination of red mud generated in the U.S. was deemed appropriate. The composition of the red mud used in this program is shown in Table 11. The addition of red mud to the reaction mixture showed almost the same activity as that of speculite, although the concentration of iron oxide in the same was

104

much lower. On addition of 10% red mud to the reaction mixture the oils concentration in the total product liquid increased from 93.4 to 95.1% and asphaltene concentration decreased from 5.0 to 1.6%. The production of hydrocarbon gases and consumption of hydrogen with red mud were similar to that with speculite (Table 53), and essentially the same as the thermal solvent run in terms of asphaltenes.

The distribution of elements in the oil and asphaltene fractions was also very similar to that with speculite, except that higher oxygen content in asphaltenes was noted with red mud. The X-ray diffraction analysis shown in Table 55 indicated that most of the Fe_2O_3 was transformed to FeS, Fe_3O_4, and elemental iron. Once again, no-additional hydrogen gas was consumed due to the reduction of Fe_2O_3 to Fe_3O_4 and elemental iron.

Flue Dust - Numerous samples of flue dusts were evaluated during this program. The most promising results were obtained with a flue dust supplied by Air Products, as shown in Table 10. This material was rich in nickel, chromium, and cobalt in addition to iron, which was the major metal present in the sample. The addition of this flue dust to the process solvent yielded highest final oil concentration among all the minerals and metallic wastes tested. The production of hydrocarbon gases was identical to that of the no-additive run. Oils concentration increased from 93.4 to 96.8%, while asphaltenes decreased from 5.0 to 1.2%. The concentrations of preasphaltenes and insoluble organic matter in the sample were small; the distribution of elements in the oils and asphaltenes are shown in Table 54. The hydrogen consumption calculated on the basis of elemental hydrogen balance was 0.26%. X-ray diffraction analysis showed no change in the chemical form of compounds present in the flue dust before and after the reaction.

Product Oils - As seen in Table 56, simulated distillation showed that both the final boiling point and the 50% point of the oil fraction of the original solvent were always higher than those of oil fractions of the treated solvent. This trend could not be seen in the number average molecular weight of different oil fractions (see Table 54). The boiling point distribution of the oil fractions from the runs using the different catalysts were very similar except for the lower boiling point region; the differences in the lower region were

Table 56

Simulated Distillation of the Oil Fractions
from the Process Solvent Hydrogenation Runs

Sample No.	FOB #11	31-10	31-24	31-34	31-45	31-55	31-66
Additive	O.S.	None	Pyrite	ZnS	Speculite	Red Mud	Flue Dust
Yield, wt %				Temperature, °F			
I.B.P.	27	-77	-73	-80	-73	-73	-71
2	527	451	502	458	434	87	106
5	547	476	536	512	476	535	536
10	568	501	549	543	535	553	555
20	592	551	575	574	567	580	580
30	609	580	591	591	586	594	594
40	629	597	606	606	602	615	614
50	650	617	624	626	621	634	632
60	675	637	644	647	645	659	656
70	701	665	668	671	668	681	676
80	735	689	691	697	695	712	704
90	793	730	730	734	737	758	749
95	842	763	764	768	773	796	784
98	887	797	799	801	809	831	817
F.B.P.	925	831	836	835	838	862	845

O.S. - Original Solvent

undoubtedly a result of the analytical separation method, wherein different
levels of trace pentane (solvent used for solvent separation) remained behind
from the solvent separation procedure.

The oxygen content and the distribution of oxygen compounds as ethers and
phenols were very similar for all the oil fractions except for the one obtained
with speculite (Table 57). The difference in the oxygen content could be due
to analytical error. The nitrogen content and the distribution of nitrogen
compounds were also very similar in all the oil fractions except for zinc
sulfide; lower nitrogen content in the oil fraction was noted with ZnS. The
reduction in the nitrogen content was accompanied by an increase in ammonia
production, although the total amount of ammonia produced was still less than
0.1% of solvent. The difference in the nitrogen content could be due to
analytical error.

Table 58 shows the total hydrogen content and the distribution of protons as
H_{AR}, H_a, and H_o in the various oil fractions. Slightly higher hydrogen content
was noted in the generated oil fractions than in the original solvent. No
significant differences between the generated oil fractions and original
solvent were noted in the distribution of protons, the carbon aromaticity
(f_a), degree of condensation (H_{AR}/C_{AR}), degree of aromatic ring substitution
(σ) and the average ring size (R_a) as shown in Table 59.

Liquefaction Catalysis

Extensive research has been performed in the field of mineral catalysis in
coal liquefaction. It has been speculated that mineral matter catalyzes coal
liquefaction reaction by enhancing the transfer of hydrogen from gas to
liquid phase and maintaining the hydrogen donor capability of the process
solvent. Solvent hydrogenation experiments with different minerals and metallic
wastes discussed earlier showed definite improvement in hydrogen content and
hydrogen donor capability of process solvent. Asphaltenes conversion, however,
was not significantly catalyzed by these minerals and metallic wastes. These
observations suggest that various minerals and metallic wastes are poor catalysts
for solvent hydrogenation. In order to explore the interaction of solvent in

Table 57

Distribution of Oxygen and Nitrogen Compounds in the
Oil Fractions from the Process Solvent Hydrogenation Runs

Sample No.	FOB #11	31-10	31-24	31-34	31-45	31-55	31-66
Additive		None	Pyrite	ZnS	Speculite	Red Mud	Flue Dust
Oxygen Distribution, Wt.%							
Absolute							
Total Oxygen	1.42	1.55	1.30	1.54	2.05	1.51	1.55
O as Ether Oxygen	0.90	0.94	0.77	0.94	1.41	0.94	0.93
O as OH	0.52	0.61	0.53	0.60	0.64	0.57	0.62
Relative							
O as Ether Oxygen	63.4	60.6	59.2	61.0	68.8	62.2	60.0
O as OH	36.6	39.4	40.8	39.0	31.2	37.8	40.0
Nitrogen Distribution, Wt.%							
Absolute							
Total Nitrogen	1.05	0.91	1.02	0.68	0.82	0.87	1.00
N as Pyridine Type	0.61	0.50	0.66	0.18	0.44	0.42	0.56
N as NH	0.38	0.32	0.32	0.39	0.33	0.36	0.35
N as NH_2	0.06	0.09	0.04	0.11	0.05	0.09	0.09
Relative							
N as Pyridine Type	58.1	55.0	64.7	26.5	53.7	48.3	56.0
N as NH	36.2	35.1	31.4	57.4	40.2	41.4	35.0
N as NH_2	5.7	9.9	3.9	16.1	6.1	10.3	9.0

Table 58

Distribution of Protons in the Oil Fractions
from the Process Solvent Hydrogenation Runs

Sample No.	FOB #11	31-10	31-24	31-34	31-45	31-55	31-66
Additive		None	Pyrite	ZnS	Speculite	Red Mud	Flue Dust
Total Hydrogen, Wt.%	7.2	7.3	7.5	7.5	7.4	7.4	7.4
Distribution of Protons, %							
Relative							
H_{AR}	44.4	42.9	42.9	45.0	47.0	44.9	44.4
H_a	28.0	29.2	29.2	29.0	29.2	27.4	29.0
H_o	27.6	27.9	27.9	26.0	23.8	27.7	26.6
Absolute							
H_{AR}	3.20	3.13	3.22	3.38	3.48	3.32	3.29
H_a	2.02	2.13	2.19	2.18	2.16	2.03	2.15
H_o	1.98	2.04	2.09	1.94	1.76	2.05	1.96

H_{AR} - Aromatic Protons
H_a - Alpha Protons
H_o - Beta and Other Protons

Table 59

Brown-Ladner Structural Parameters for the Oil
Fractions from the Process Solvent Hydrogenation Runs

Sample No.	FOB #11	31-10	31-24	31-34	31-45	31-55	31-66
Additive		None	Pyrite	ZnS	Speculite	Red Mud	Flue Dust
f_a	0.71	0.71	0.71	0.71	0.72	0.72	0.71
σ	0.28	0.28	0.28	0.27	0.27	0.26	0.27
H_{AR}/C_{AR}	0.80	0.80	0.82	0.84	0.87	0.82	0.82
R_a	3.23	3.27	3.10	3.33	3.11	3.20	3.34

the presence of coal, various metallic wastes, and transition metals were used in the liquefaction of Kentucky coals. The chemistry of the transformation of the above materials during coal liquefaction was also studied. The results of the above study are described in detail below.

Catalysis by Pyrite

Pyrite is the most logical disposable catalyst that can be used in U.S. lique-faction plants. Pyrite is found in most eastern U.S. coals, and is readily available at coal beneficiation facilities. The major drawback of the pyrite catalyst system is the additional H_2S generation. Nevertheless, the easy recovery of pyrite coupled with a simple preparation step is unequaled.

The use of pyrite in liquefaction has been recognized for some time. However, the rapidity of the decomposition of pyrite, both thermally and in the presence of hydrogen, was not known. Hence, the following series of studies was carried out.

Thermal Properties - The pyrolysis of pyrite begins at about 930°F (11) and proceeds according to Equation 6.

$$FeS_2 = FeS + \frac{1}{n} S_n \qquad \text{(Eqn. 6)}$$

The thermogram of Robena pyrite under flowing helium gas is shown in Figure 11. Robena pyrite samples of different particle sizes began to decrease in weight at about 400°C (750°F). The samples continued to lose weight until a temperature of 640°C (1185°F) was reached, after which the change in weight was insignificant. Similar pyrolysis behavior of pyrite was observed by Richardson (9). It can be seen that pyrite of particle sizes +40, 40 x 80, 140 x 200 and -325 mesh showed similar thermograms. The maximum weight loss for all three samples was between 22 to 23%, which is nearly stoichiometric according to Equation 6. The pyrite sample of particle size -200 mesh gave an entirely different thermogram compared with the other particle size ranges. The maximum weight loss for -200 mesh sample was only 18.5% compared with 22 to 23% for the others because it contained less available sulfur for thermal distillation (Table 60).

FIGURE 11
TGA OF ROBENA PYRITE
IN THE PRESENCE OF He GAS

—·—·— +40 MESH
————— 40 X 80 MESH
————— 140 X 200 MESH
— — — — -200 MESH
—··—··— -325 MESH

HEATING RATE = 20°C/MIN.
HELIUM FLOW RATE = 40 ML./MIN.

WEIGHT LOSS, %

TEMPERATURE, °C
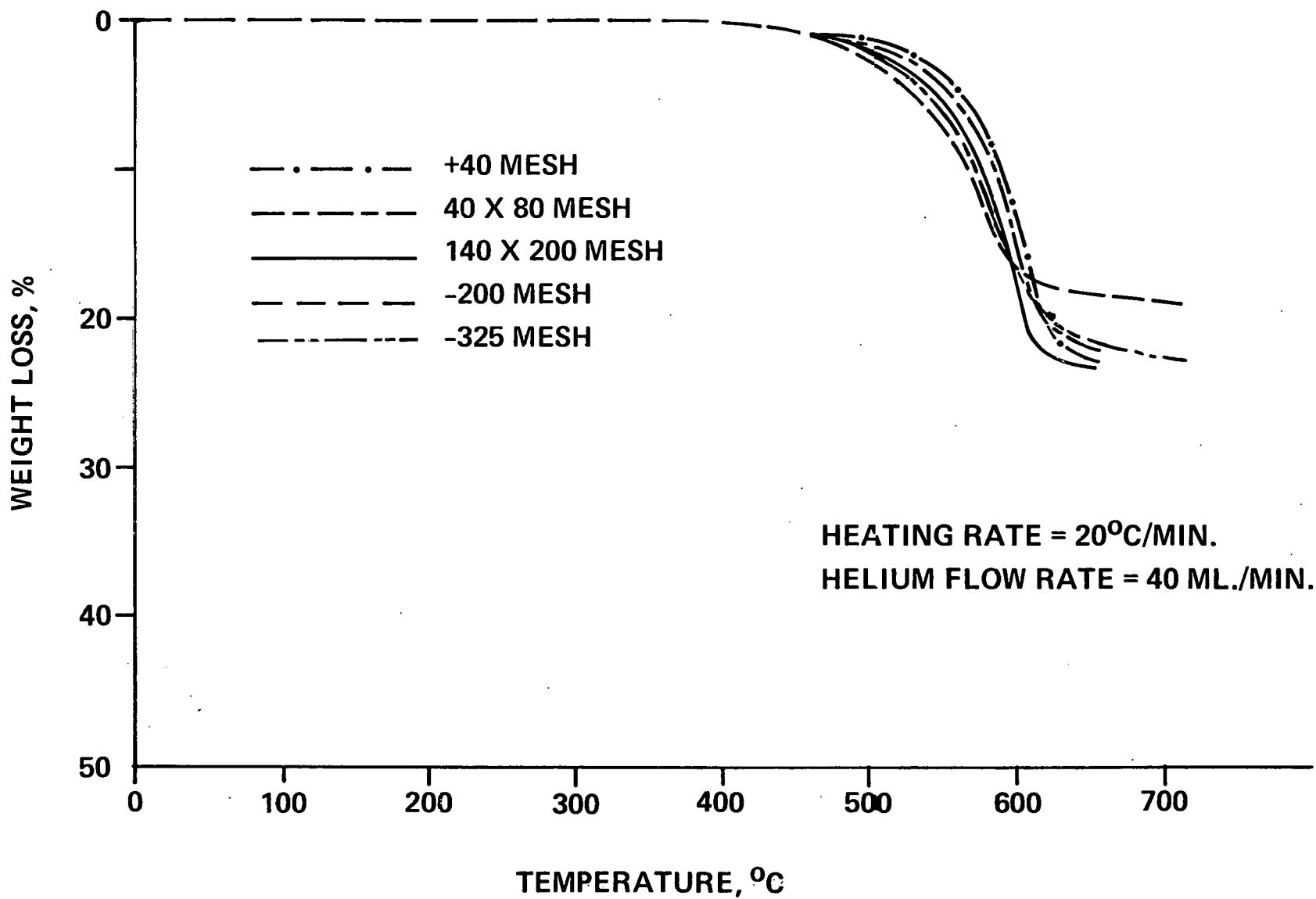
Table 60

Iron and Sulfur Distribution in the
Different Fractions of Robena Pyrite[1] Sample

Fractions U.S. Mesh	wt.%	
	Fe	Total Sulfur
+40	42.5	42.8
40 x 80	43.7	44.3
80 x 140	41.1	43.7
140 x 200	48.8	47.0
-200	50.6	35.8
-325[2]	42.3	41.3

---

[1] See Table 6 for the analysis of various impurities
[2] Total sample was ground to -325 U.S. Mesh

Reduction of pyrite with hydrogen was reported in the literature to take place at about 930°F (11) and to proceed according to Equation 7.

$$FeS_2 + H_2 = FeS + H_2S \qquad \text{(Eqn. 7)}$$
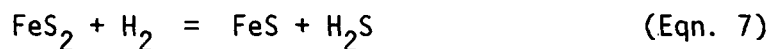
A constant weight loss of 24% was reported at temperatures up to 500°C (930°F) with no further reduction to Fe (11).

Figure 12 presents the thermogram for Robena pyrite in the presence of flowing hydrogen. Weight loss began about 610°F with maximum reduction (close to 20.0%) attained at around 600°C (1110°F). Comparison of pyrolysis with reduction of pyrite (Figures 11 and 12) revealed that pyrite was more temperature-sensitive to hydrogen reduction than to pyrolysis; in hydrogen, pyrite reduction began at 320°C (610°F) compared with 380°C (715°F) for pyrolysis. Overall weight reduction was completed at about 600°C (1100°F) in the presence of hydrogen, compared with 650°C (1200°F) in pyrolysis. In both cases overall weight loss was approximately the same.

The reduction of -200 and -325 mesh Robena pyrite samples in hydrogen was studied in detail in the PTGR (see Appendix A for operating procedures). The PTGR was heated to the required reaction temperature and pressurized with hydrogen to the operating pressure before the sample was lowered into the reaction zone. Fast heating of the sample was attained and the reduced sample was removed after the prescribed reaction time. The gaseous products were collected in a stainless steel bomb they were passed through an ice trap. Both the condensed and gaseous products in the ice trap were analyzed to determine composition and provide a material balance.

Table 61 and Figure 13 show the variation in weight reduction of Robena pyrite and the products obtained with temperature at a randomly selected constant hydrogen pressure of 1,000 psig. The weight of pyrite was found to decrease linearly with the increase in reaction temperature (see Figure 13). Table 61 shows substantial differences between the overall weight loss and the overall weight of the product recovered. The major source of error was the determination of H_2S in the product gas.

114

FIGURE 12
TGA OF PYRITE IN THE
PRESENCE OF HYDROGEN GAS

ROBENA PYRITE = -200 MESH
HEATING RATE = 10°C/MIN.
HYDROGEN FLOW = 200 ML./MIN.

WEIGHT LOSS, %
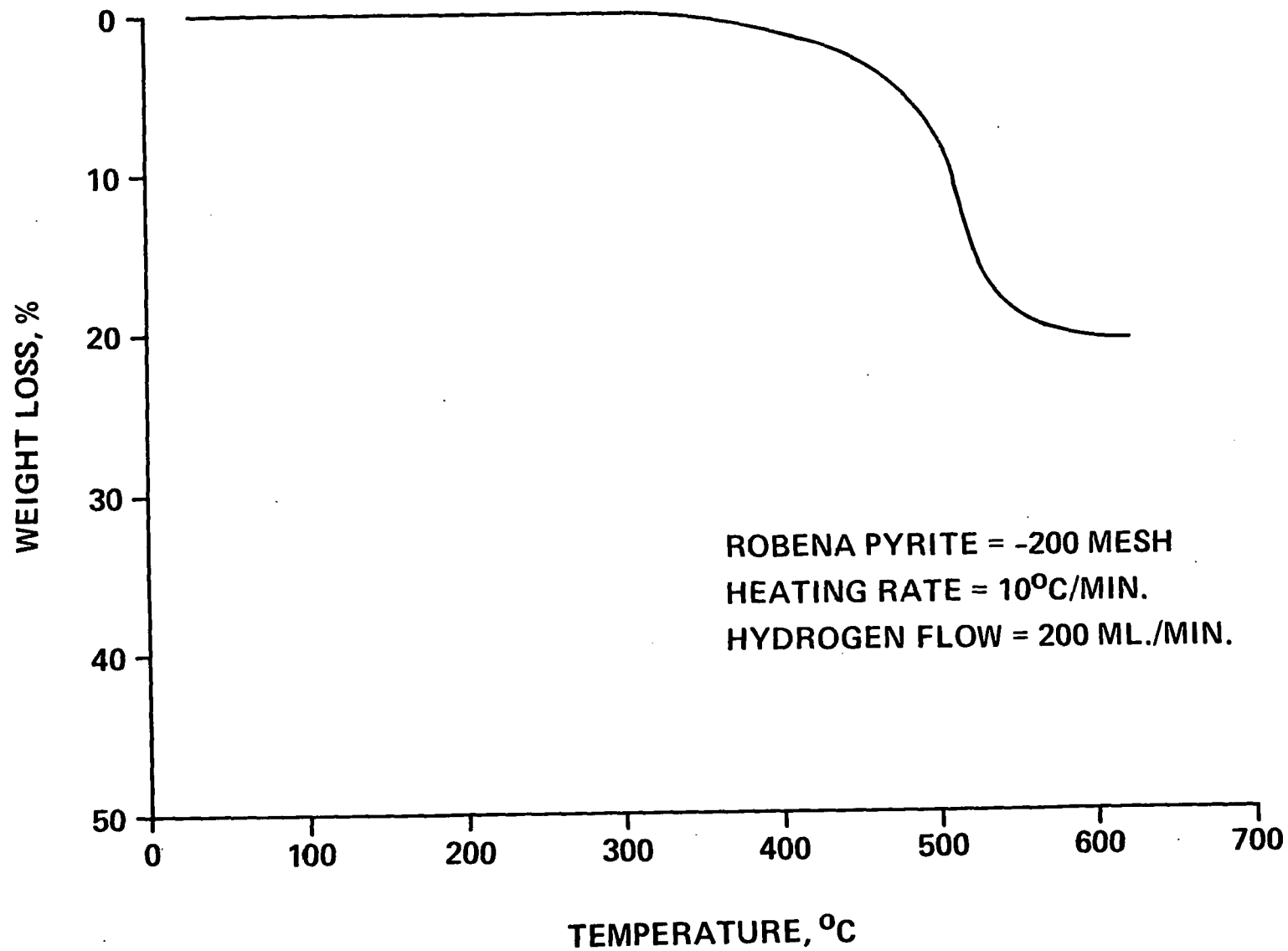
TEMPERATURE, °C

Table 61

Effect of Temperature on Robena Pyrite (-200 Mesh) Reduction

Reaction Time = 10 Minutes, Pressure = 1000 psig H_2

Temp. °C	Initial Weight g	Final Weight g	Weight Loss g	Weight Loss %	N_2	H_2S	Gas Analyses, g H_2O	CH_4	CO	Liquid Analyses,[1] Sulfur	Total Recovered Product g	% Recovery of the Lost Wt.
400	3.0	2.50	0.50	16.67	0.0081	0.0330	0.0572	-	-	0.0259	0.1242	24.8
450	3.0	2.48	0.52	17.33	0.0050	0.0654	0.0289	-	-	0.0095	0.1088	20.92
500	3.0	2.43	0.57	19.0	0.0210	0.0785	0.0537	-	-	0.0136	0.1668	29.26
600	3.0	2.44	0.56	18.67	0.0011	0.0595	0.0272	0.0063	0.0024	0.0133	0.1098	19.6

[1] Condensed in the ice trap.

Table 62

Effect of Hydrogen Pressure on Robena Pyrite (-200 Mesh) Reduction

Reaction Time = 10 Minutes, Temperature = 450°F

Pres. psig	Initial Weight g	Final Weight g	Weight Loss g	Weight Loss %	N_2	H_2S	Gas Analyses, g H_2O	CH_4	CO	Liquid Analyses,[1] Sulfur	Total Recovered Product g	% Recovery of the Lost Wt.
500	3.0	2.49	0.51	17.00	-	0.1851	0.0483	-	-	0.0006	0.2394	47.0
1000	3.0	2.48	0.52	17.33	0.005	0.0654	0.0289	-	-	0.0095	0.1088	21.0
1500	3.0	2.50	0.50	16.67	-	-	-	-	-	0.0090	-	-

[1] Condensed in the ice trap.

FIGURE 13
EFFECT OF REACTION TEMPERATURE
ON ROBENA PYRITE (-200 MESH) REDUCTION

REACTOR = PTGR
PRESSURE = 1,000 PSIG
REACTION TIME = 10 MIN.

WEIGHT LOSS, %

TEMPERATURE, °C
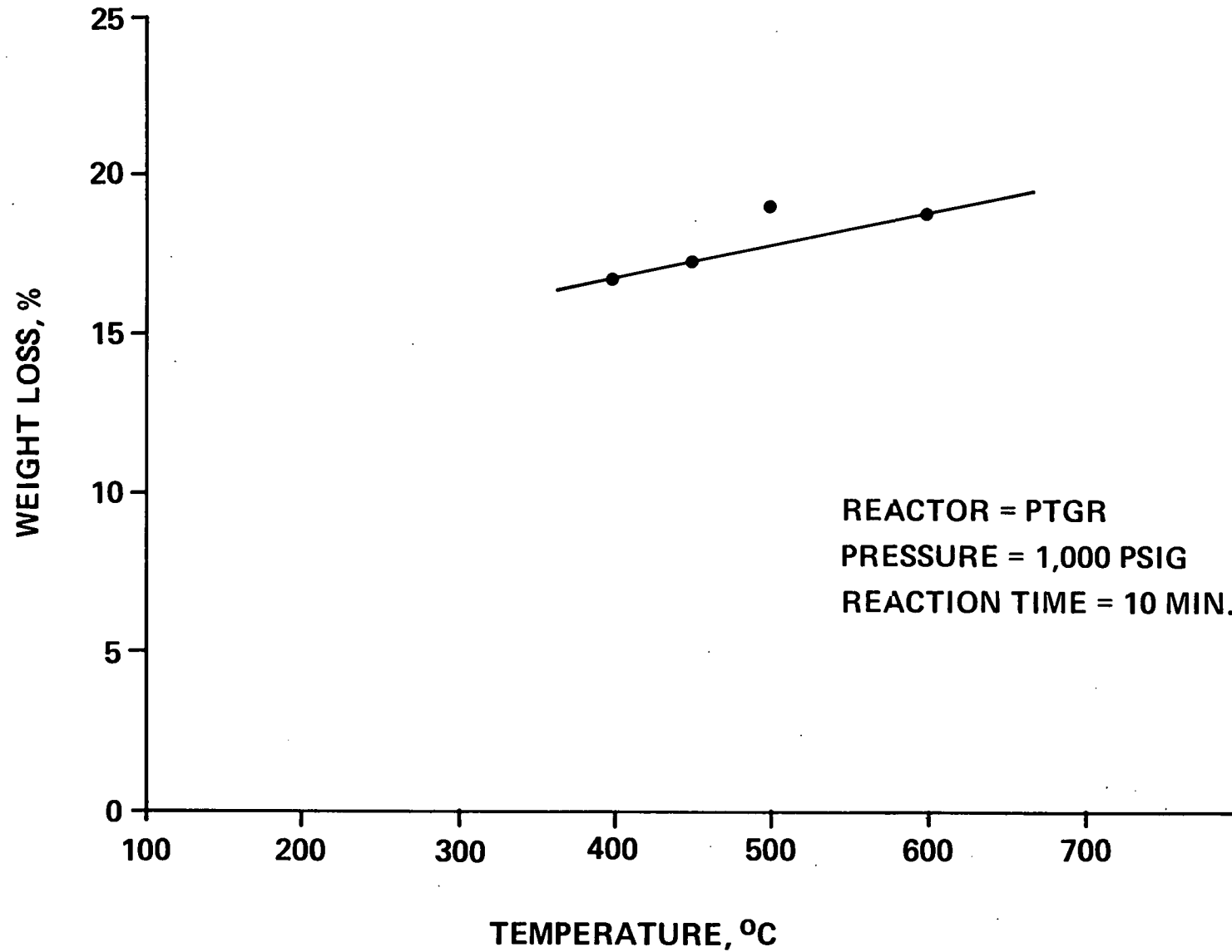
FIGURE 14
EFFECT OF REACTION PRESSURE ON
ROBENA PYRITE (-200 MESH) REDUCTION

REACTOR = PTGR
TEMPERATURE = 450° C
REACTION TIME = 10 MIN.

WEIGHT LOSS, %

REACTION PRESSURE, PSIG
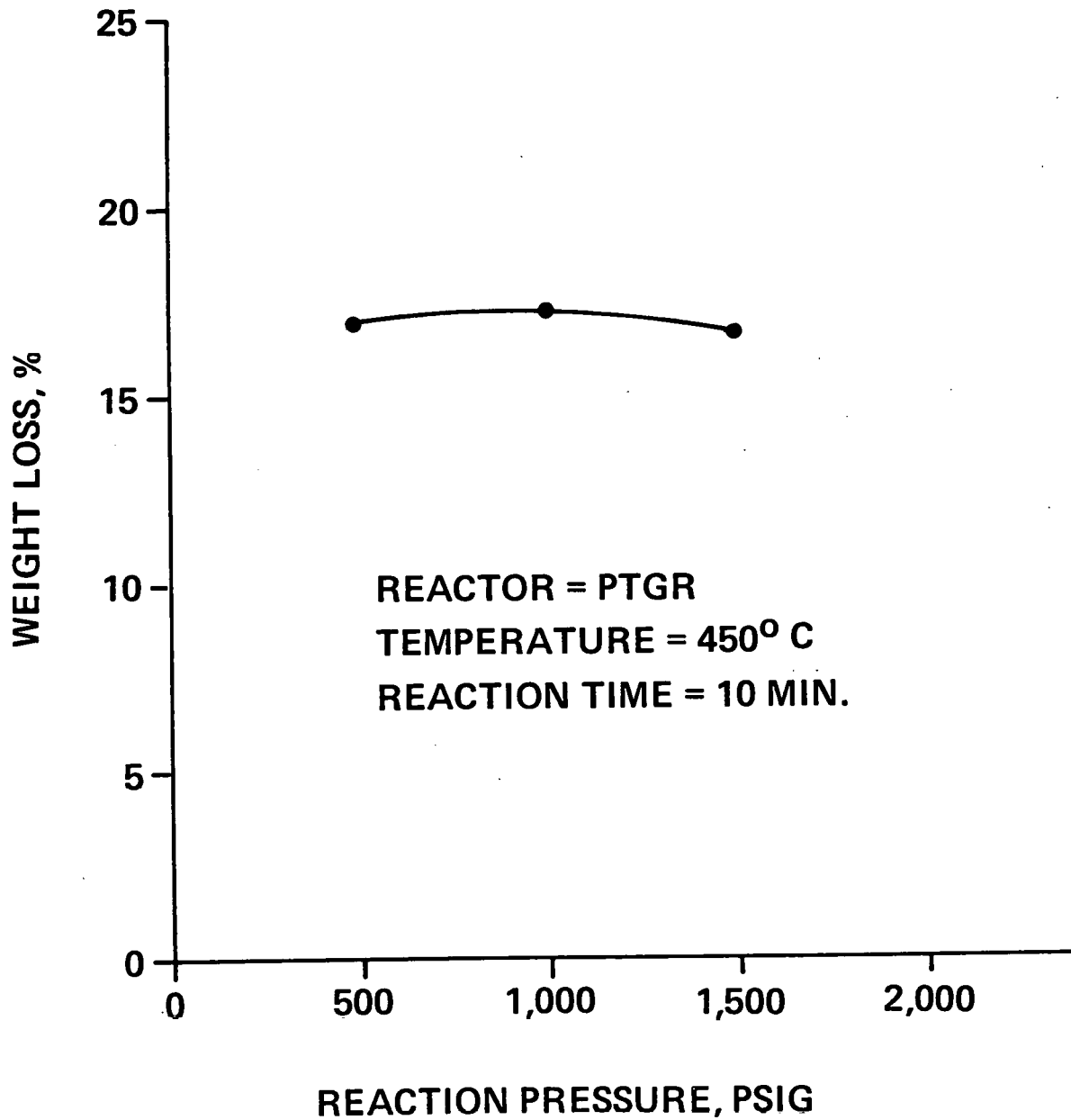
Table 62 and Figure 14 show no significant difference in the weight reduction of pyrite with variations in hydrogen pressure. As shown in Figure 15, -325 mesh pyrite, which had a considerably higher total sulfur content than the -200 mesh pyrite (41.3% as opposed to 35.8%), showed greater weight loss at all temperatures than did the -200 mesh fraction.

The hydrogen reduction kinetics of the -325 mesh fraction of Robena pyrite studied in the PTGR are shown in Figure 16. It can be seen that as temperature increased, the rate of pyrite reduction increased. At typical coal liquefaction reaction conditions of 450°C (840°F) and 1,000 psig, all of pyrite was reduced to pyrrhotite within 4 minutes. The reaction conditions, however, differ from coal liquefaction because of the absence of liquid phase. The samples of Robena pyrite reduced at different reaction temperatures were analyzed by X-ray diffraction (XRD) to determine the nature of the phases present. The results of XRD analysis, summarized in Table 63, identified the major phase in all the samples as troilite. Pyrrhotite could not be positively identified in these samples.

Pyrite Catalysis of Eastern Kentucky Coals - High volatile A bituminous eastern Kentucky coals having low intrinsic liquefaction activity (i.e., low pyrite concentration) were chosen as the base coals for the study of catalytic activity of the various minerals, metal containing by-products, waste materials, transition metal sulfides, and organic compounds for transition metals. Table 1 presents the data on three samples taken from Floyd and Letcher counties on three occasions without coal preparation. The amount of pyrite in the Floyd County sample was higher than expected; data from the Penn State data base originally suggested that the pyrite content should be considerably lower. Another sample taken from Letcher County showed a pyrite content of 0.25%. A more complete discussion of the selection of the coals from the eastern Kentucky coal region is given under the section on "Coal Feedstocks." The response of each of these particular coals to the presence of added pyrite is discussed below.

Floyd County Elkhorn #3 Coal - The liquefaction of Floyd County Elkhorn #3 coal, both in the presence and absence of Robena pyrite, was studied at two temperatures as shown in Table 64. Addition of pyrite at the level of 10% of the feed slurry increased coal conversion at both 800 and 850°F. A significant

FIGURE 15
HYDROGEN REDUCTION OF ROBENA
PYRITE IN PTGR

PRESSURE = 1,000 PSIG H_2

REACTION TIME = 10 MINUTES
FAST HEATING

△ -325 MESH (41.3% TOTAL SULFUR)
O -200 MESH (35.7% TOTAL SULFUR)

WEIGHT LOSS, %
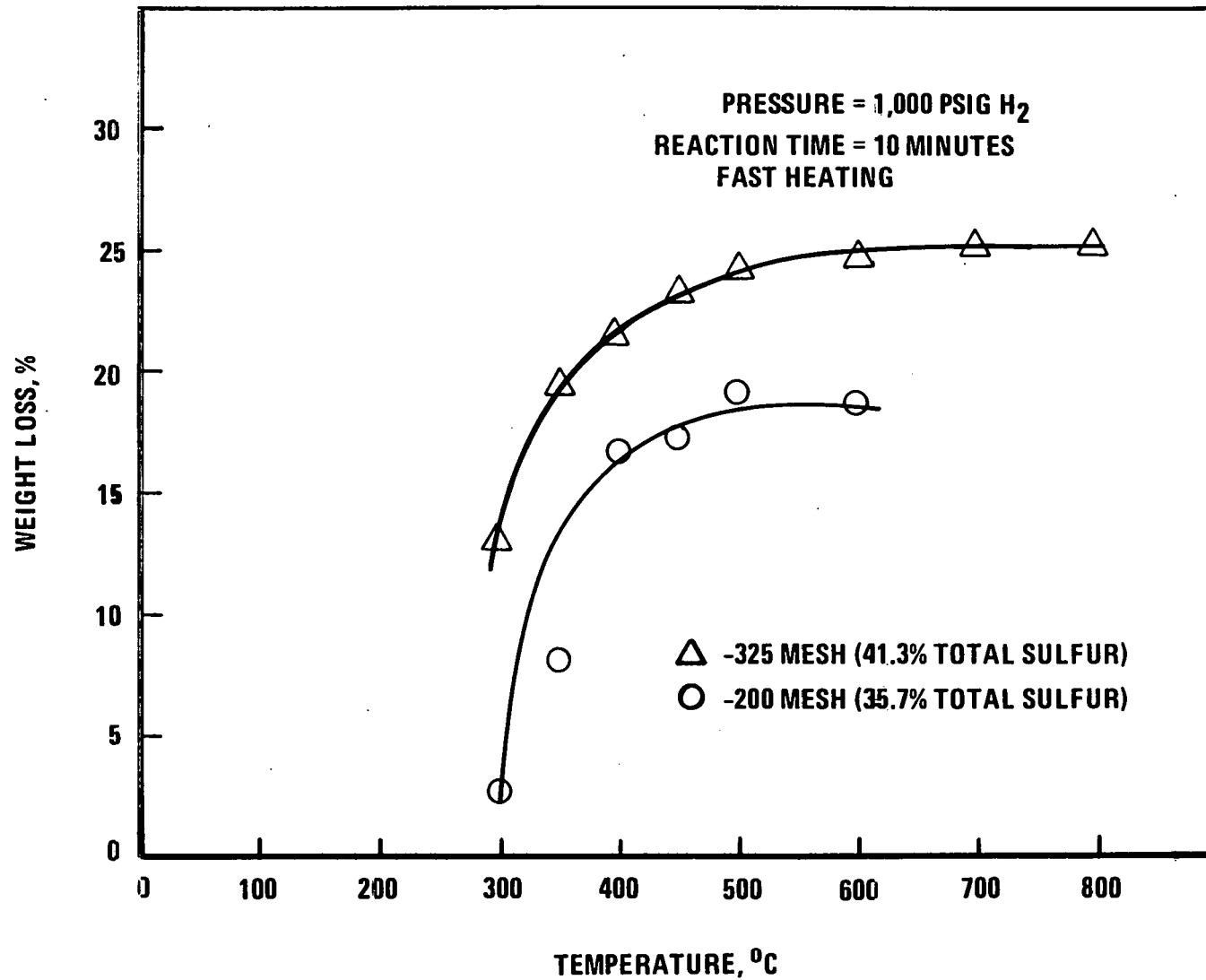
TEMPERATURE, °C

FIGURE 16
REDUCTION OF -325 MESH ROBENA PYRITE IN THE PTGR

PRESSURE = 1,000 PSIG H_2

700°C
500°C
450°C
400°C
350°C

300°C

WEIGHT LOSS, %
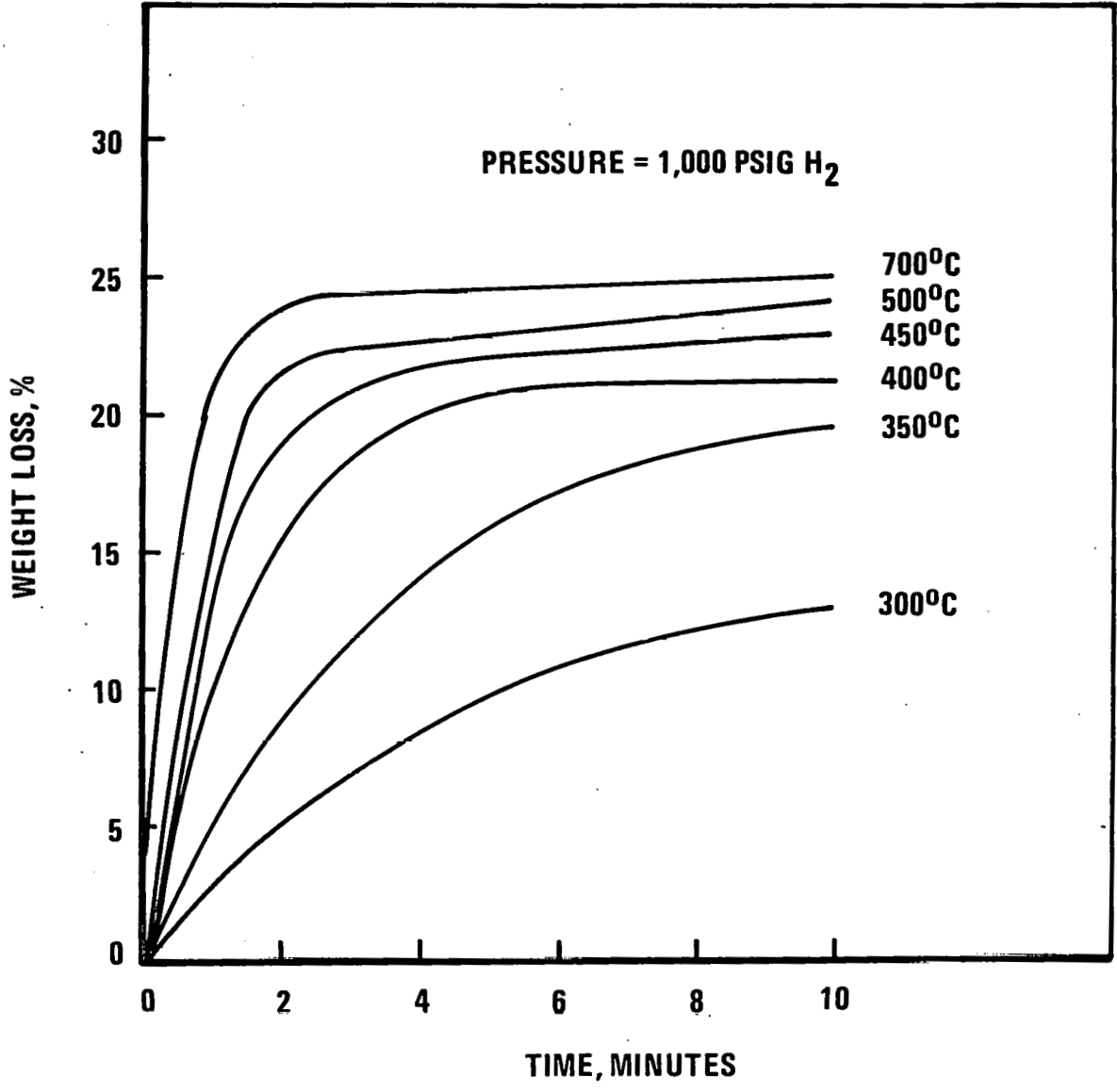
TIME, MINUTES

Table 63

Reduction of -325 Mesh Robena Pyrite in the PTGR[1]

Reaction Time = 10 Minutes

H_2 Pressure = 1000 psig

Rapid Heating

Reaction Temperature, °C	Weight Loss, wt.%	XRD Analysis
400	21.3	FeS (troilite) major phase. No Fe detected. One extra line at 3.34Å probably due to pyrrhotite.
450	23.0	FeS (troilite) major phase. No Fe detected. Possible presence of pyrrhotite (less than in the sample treated at 400°C). Extra lines at 3.35, 3.03, and 1.95Å were not identified.
500	24.0	FeS (troilite) major phase. No Fe detected. Extra unidentified lines at 3.33, 3,38, 3.02, 5.14, and 1.95Å. Possible presence of pyrrhotite.
600	23.3	FeS (troilite) major phase. Possible presence of pyrrhotite and elemental Fe. Unidentified lines at 5.14, 3.33 and 1.95Å.
700	25.0	FeS (troilite) major phase. Possible presence of pyrrhotite and Fe. Unidentified lines at 5.18, 3.36 and 1.95Å.
800	25.0	FeS (troilite) major phase. Possible presence of pyrrhotite and Fe. Unidentified lines at 3.33, 2.85 and 1.95Å.

---

[1] PTGR - pressurized thermal gravimetric reactor

Table 64

Liquefaction Behavior of Floyd County Elkhorn #3 Coal

Sample No. Feed	25-52 70% Solvent[2]/30% Coal	25-40	25-48 60% Solvent[2] + 30% Coal + 10% Pyrite	25-136	28-71 63.6% Solvent[2] + 27.3% Coal + 9.1% Pyrite
Temperature, °F	800	850	800	850	850
Pressure, psig	2000	2000	2000	2000	2000
Hydrogen Treat Rate, Mscf/T	18.2	19.9	20.8	21.9	47.2
Residence Time, min.	38	38	38	41	35
Product Distribution, wt.% MAF Coal					
HC	2.4	4.2	2.0	5.3	3.1
CO, CO_2	0.8	1.0	0.9	1.2	0.8
H_2S, NH_3	0.9	1.3	0.9	3.0	0.7
Oils	(3.2)[1]	27.3	(10.0)	41.0	42.1
Asphaltenes	17.6	14.8	40.5	11.3	18.5
Preasphaltenes	58.0	30.1	49.3	24.1	18.8
Insoluble Organic Matter (IOM)	20.6	18.1	13.7	10.1	9.9
Water	2.9	3.2	2.7	3.5	6.1
Conversion, % MAF Coal	79.4	81.9	86.3	89.9	90.1
Hydrogen Consumption, wt.% MAF Coal					
Total	0.51	1.40	1.65	2.53	2.85
From Gas	0.61	0.82	1.82	2.49	2.88
From Solvent	(0.10)	0.58	(0.17)	0.04	(0.03)
By Pyrite	--	--	0.50	0.50	0.50
First Order Rate Constants, hr^{-1}					
K_a	-0.12	1.09	-0.26	1.84	--
K_p	0.39	2.14	0.96	3.05	--

[1] ( ) = negative value

[2] Solvent = F.O.B. #1

increase in oil production from 27 to 41% was noted at the higher temperatures. At 800°F, a net loss in oil yield occurred with the coal alone, as well as with the added pyrite. At both temperatures, the production of preasphaltenes decreased with pyrite. Asphaltene production increased significantly at 800°F, whereas it decreased slightly at 850°F with pyrite addition. Similarly, the production of hydrocarbon gases and water decreased at 800°F, but increased at 850°F with pyrite. The first-order rate constants for the conversions of asphaltenes and preasphaltenes increased with the addition of pyrite. Hydrogen consumption also increased significantly at both 800 and 850°F with added pyrite. Part of the increased hydrogen consumption, 0.5 wt%, was consumed in reducing the added pyrite. The increase in hydrogen consumption was due mainly to the increased production of oil. A significant observation was that the oil hydrogen content was depleted in the absence of pyrite, while it was maintained in its presence (Table 65).

Coal conversion with pyrite was similar at the two temperatures. The yield of hydrocarbon gases, CO, CO_2, H_2S, NH_3, and water increased with temperature. The most significant differences were in the distribution of oil, asphaltene, and preasphaltene fractions. At 800°F, most of the dissolved coal was found in the asphaltene and preasphaltene fractions. At the higher temperature the conversion of asphaltenes and preasphaltenes increased; the asphaltene and preasphaltene fractions decreased from 41 to 11% and from 49 to 24%, respectively. A net loss of 10 wt.% oil was noted at 800°F, whereas at 850°F, a net oil production of 41% occurred (Table 64). The reaction rates of conversion of asphaltenes and preasphaltenes increased with increasing temperature. The above information shows that the conversions of asphaltenes and preasphaltenes are more sensitive to the reaction temperature in the presence of pyrite. The increase in temperature not only increased oil production, but also increased the hydrogen consumption, i.e., 1.7 to 2.5%.

The hydrogen content of the oil fraction given in Table 65 decreased with an increase in temperature. Likewise, the hydrogen content of asphaltenes and preasphaltenes decreased with temperature. The conversion of SRC increased considerably with temperature in both the presence and absence of pyrite (Table 66). SRC sulfur content also decreased with the increase in temperature.

Table 65

Hydrogen Concentration in Feed and Product

Sample No.	25-52	25-40	25-148	25-136	28-71
Reaction Temperature, °F	800	850	800	850	850
Hydrogen Content, wt.%					
Feed Oil	7.72	7.72	7.72	7.72	7.72
Product:					
Oils	7.76	7.49	7.80	7.70	7.73
Asphaltenes	6.77	6.48	7.10	6.24	7.43
Preasphaltenes	5.38	5.50	5.84	5.65	5.68

Table 66

SRC Production and its Sulfur Content

Sample No.	25-52	25-40	25-148	25-136
Reaction Temperature, °F	800	850	800	850
Product Distribution, wt.% MAF Coal				
Asphaltenes	17.6	14.8	39.8	10.9
Preasphaltenes	58.0	30.2	48.6	24.1
Total (SRC)	75.6	45.0	88.4	35.0
SRC Sulfur, Wt.%	0.8	0.6	0.8	0.7

The simulated distillation of the oil fractions obtained with and without pyrite at 800 and 850°F showned no significant differences (Figures 17 and 18).

The oil fractions generated from the liquefaction of Floyd County Elkhorn #3 coal in the presence and absence of Robena pyrite were analyzed by NMR to determine the distribution of protons (see Table 67). The concentration of aromatic protons decreased and that of beta and other protons increased with the addition of pyrite at 800 and 850°F. No conclusion could be drawn in concerning the concentration of H_a. An attempt was then made to identify and differentiate the chemical structure of the solvent generated in the presence and absence of Robena pyrite in coal liquefaction mixtures at 800°F using Brown-Ladner structural parameters modified by H. L. Retcofsky et al. (8).

The calculated values of the structural parameters for the oil fractions are provided in Table 68. The calculated value of f_a, carbon aromaticity, decreased slightly with pyrite, suggesting that pyrite is aiding in the hydrogenation of the aromatic ring compounds. Similarly, the degree of condensation of H_{AR}/C_{AR} decreased slightly with pyrite addition. The small decrease in the value of H_{AR}/C_{AR} could be due to experimental error. To verify a decrease in ring size, the value of R_a was calculated and is presented in Table 68. The calculated value of R_a showed no difference in the average ring size in the oil fractions obtained in the presence and absence of Robena pyrite. The value of σ increased with the addition of pyrite, indicating the increase in the degree of substitution by alkyl, naphthenic, and/or phenolic groups. The increase in the value of H_o (Table 67) suggested the substitutions were mainly due to alkyl groups. A comparison of the values for the starting solvent (FOB #1) and solvent generated after reaction (Table 68) showed that the aromaticity, H_{AR}/C_{AR}, and average ring size decrease and the degree of substitution (σ) increased with the reaction, both in the presence and absence of pyrite.

From the above data it can be concluded that the addition of Robena pyrite to Floyd County Elkhorn #3 coal increases coal dissolution, promotes solvent hydrogenation, and improves conversion of preasphaltenes and asphaltenes to oil and gases.

126

FIGURE 17
COMPARISON OF SIMULATED DISTILLATION OF OIL FRACTIONS OBTAINED FROM FLOYD COUNTY ELKHORN #3 COAL LIQUEFACTION AT 850° F
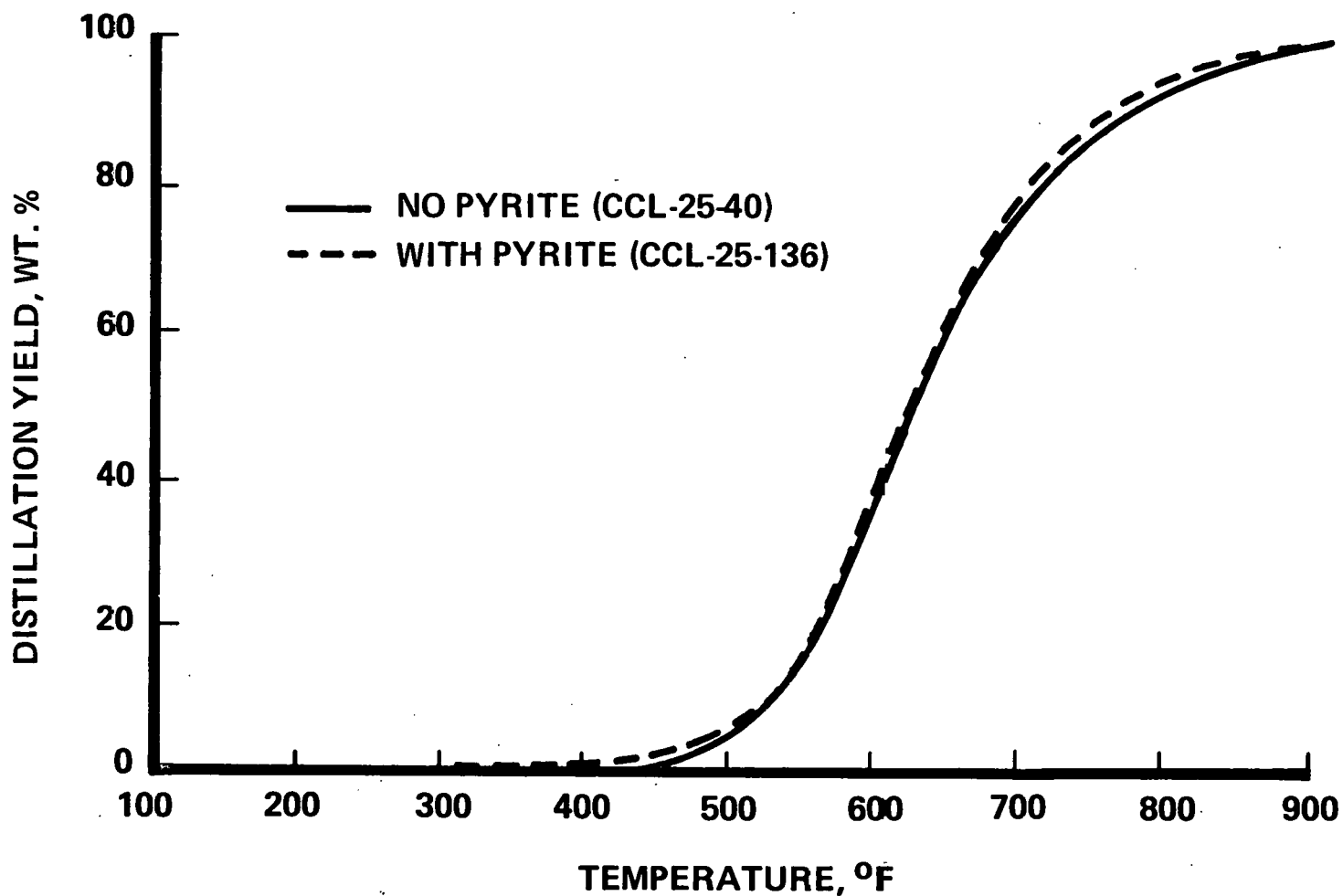
FIGURE 18
COMPARISON OF SIMULATED DISTILLATION OF OIL FRACTIONS OBTAINED FROM FLOYD COUNTY ELKHORN #3 COAL LIQUEFACTION AT 800°F

128
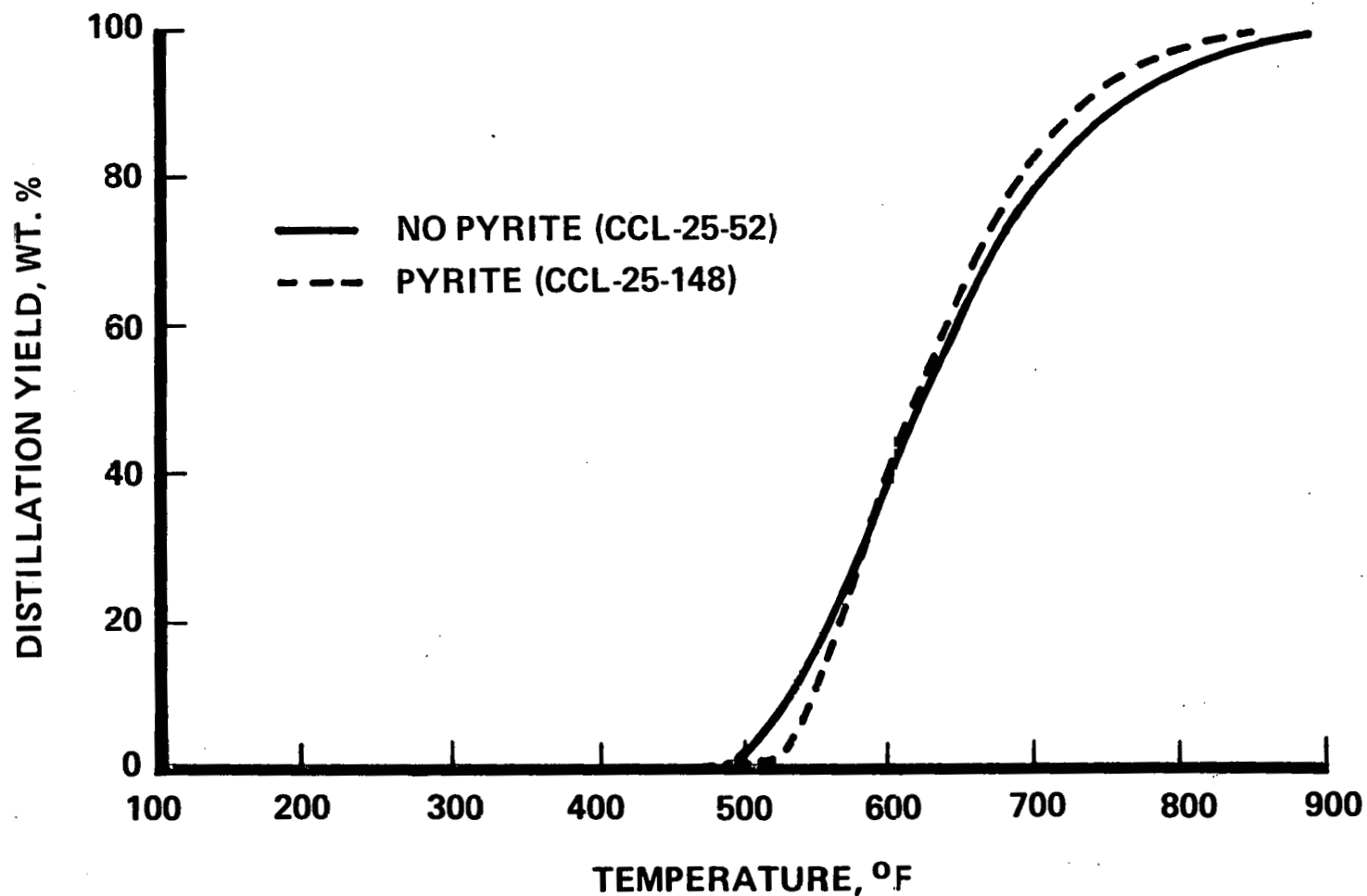
Table 67

Distribution of Protons in the Oil Fraction from the
Coal Liquefaction Product in the Presence and Absence of Robena Pyrite

Sample		25-52	25-40	25-148	25-136
Feed Composition	Original Solvent (FOB#1)	70% Solvent + 30% Elkhorn #3 Coal		60% Solvent + 30% Elkhorn #3 Coal + 10% Robena Pyrite	
Temp., °F		800	850	800	850
Pressure, psig		2000	2000	2000	2000
Total Hydrogen, wt. %		7.76	7.49	7.80	7.70
Distribution of Protons, %					
Absolute					
H_{AR}[1]	3.24	3.20	3.15	3.00	3.10
H_a[2]	2.26	2.32	2.11	2.18	2.18
H_o[3]	2.22	2.24	2.23	2.62	2.42
Relative					
H_{AR}	42.0	41.3	42.1	38.5	40.3
H_a	29.3	29.9	28.2	27.9	28.3
H_o	28.7	28.8	29.7	33.6	31.4

[1] H_{AR} - Aromatic protons
[2] H_a - Alpha protons
[3] H_o - Beta and other protons

129

Table 68

Brown-Ladner Structural Parameters for the Oil Fractions

Sample		25-52	25-148
			60% Solvent +
		70% Solvent +	30% Elkhorn #3
	Original Solvent	30% Elkhorn	Coal + 10%
Feed Composition	(FOB#1)	#3 Coal	Robena Pyrite
Temp., °F	-	800	800
Pressure, psig	-	2000	2000
f_a	0.702	0.697	0.674
σ	0.271	0.287	0.294
H_{AR}/C_{AR}	0.834	0.838	0.825
R_a	3.23	3.12	3.13

Letcher County Elkhorn #3 Coal - The liquefaction of Letcher County Elkhorn #3 coal was studied at 800 and 850°F, both in the presence and absence of Robena pyrite and the results are tabulated in Table 69. With pyrite, coal conversion increased significantly at both temperatures. Hydrogen consumption increased significantly with pyrite at both the temperatures. The increase in hydrogen consumption was due to pyrite reduction, increased coal conversion, and increased benzene solubles yield. The hydrogen content of the oil fractions were unchanged with the addition of pyrite (Table 70).

In the presence of pyrite, coal conversion increased from 75 to 91% with an increase in temperature from 800 to 850°F. The yield of hydrocarbon gases and benzene solubles also increased with temperature. Hydrogen consumption increased from 2.0 to 3.0% with temperature; this increase was due to increased production of hydrocarbon gases and conversion of coal. The hydrogen contents of asphaltenes and preasphaltenes were higher at 800 than at 850°F (see Table 70). SRC production decreased greatly with temperature, as shown in Table 71. SRC sulfur content decreased slightly with an increase in temperature from 800 to 850°F. The simulated distillations of the oil fractions obtained in the presence and absence of pyrite showed no significant differences both at 800 and 850°F (Figures 19 and 20).

Elkhorn #2 Coal - The liquefaction of Elkhorn #2 coal was studied at 825 and 850°F in the presence of Robena pyrite and the results are summarized in Table 72. Coal conversion increased with pyrite at both temperatures. Oil production increased by more than a factor of two with pyrite at both temperatures. The production of hydrocarbon gases also increased with pyrite (Table 72). Addition of pyrite significantly reduced the production of preasphaltenes, but no significant change in the production of asphaltenes was noted with pyrite. Pyrite addition significantly increased the rates of conversion of asphaltenes and preasphaltenes at 825 and 850°F. Hydrogen consumption increased from 0.64 to 1.68 wt% and from 0.53 to 2.41 wt% at 825 and 850°F, respectively, with pyrite. The increased hydrogen consumption was due to the reduction of pyrite to FeS and to the increased production of oils and hydrocarbon gases. The sulfur content of the SRC remained unchanged with pyrite addition (Table 72).

·ᶅ

Table 69

Liquefaction Behavior of Letcher County Elkhorn #3 Coal

Sample No.	25-88	25-100	25-184	25-196
Feed	70% Solvent/30% Coal		60.8% Solvent/30.6% Coal/8.6% Pyrite	
Temperature, °F	850	800	850	800
Pressure, psig	2,000	2,000	2,000	2,000
Hydrogen Treat Rate, Mscf/T	20.1	19.9	33.1	22.1
Residence Time, Min.	41	41	41	41
Product Distribution, wt.% MAF Coal				
HC	6.8	2.4	6.2	2.2
CO, CO_2	1.3	1.0	1.3	1.0
H_2S, NH_3	0.8	0.7	7.4	6.0
Benzene Solubles (Oils & Asphaltenes)	15.9	17.2	45.6	24.8
Preasphaltenes	44.8	38.6	27.0	38.8
I.O.M.	28.4	37.7	8.7	24.9
Water	2.0	2.4	3.8	2.3
Conversion, wt.% MAF Coal	71.6	62.3	91.3	75.1
Hydrogen Consumption, wt. % MAF Coal				
Total	0.31	(0.16)[1]	2.97	1.98
From Gas	0.14	(0.09)	2.79	2.34
From Solvent	0.17	(0.07)	0.18	(0.36)
By Pyrite	--	--	0.55	0.55

[1] ( ) = negative value

Table 70

Hydrogen Content in Feed and Product

Sample No.	25-88	25-100	25-184	25-196
Temperature, °F	850	800	850	800
Hydrogen Content, wt.%				
Feed Oil	7.72	7.72	7.72	7.72
Product:				
Oils	7.61	7.65	7.60	7.72
Asphaltenes	6.29	6.71	6.35	8.02
Preasphaltenes	5.20	5.54	5.34	5.89

Table 71

SRC Production and Its Sulfur Content

Sample No.	25-88	25-100	25-184	25-196
Temperature, °F	850	800	850	800
Product Distribution, wt.% MAF				
Asphaltenes	39.4	20.5	14.2	22.1
Preasphaltenes	44.8	38.6	27.0	38.8
Total (SRC)	84.2	59.1	41.2	60.9
SRC Sulfur, wt.%	0.5	0.8	0.5	0.6

FIGURE 19
COMPARISON OF SIMULATED DISTILLATION OF OIL FRACTIONS OBTAINED FROM LETCHER COUNTY ELKHORN #3 COAL LIQUEFACTION AT 850° F
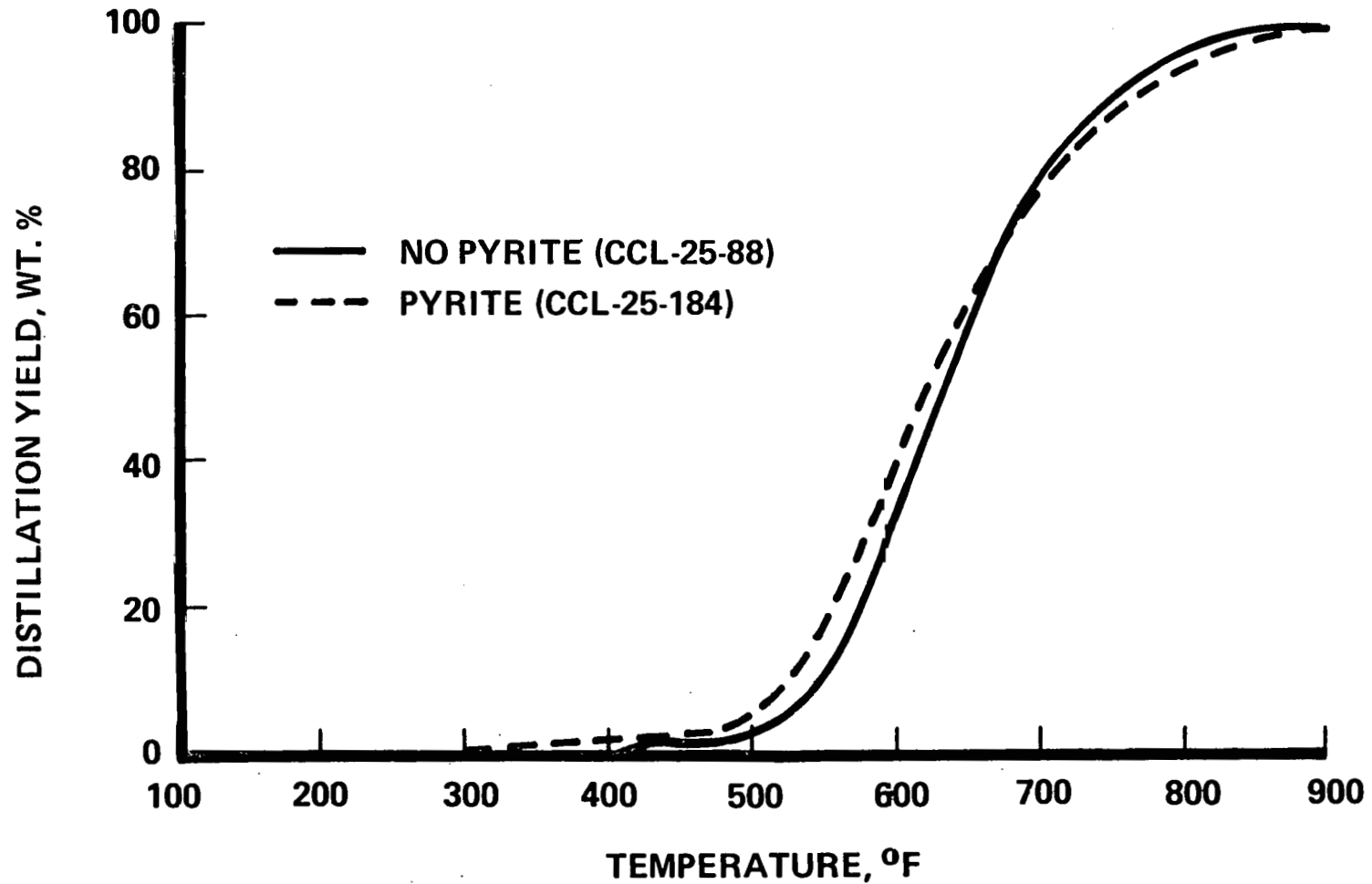
FIGURE 20
COMPARISON OF SIMULATED DISTILLATION OF OIL FRACTIONS OBTAINED FROM LETCHER COUNTY ELKHORN #3 COAL LIQUEFACTION AT 800° F

Legend:
- NO PYRITE (CCL-25-100)
- PYRITE (CCL-25-196)

X-axis: TEMPERATURE, °F
Y-axis: DISTILLATION YIELD, WT. %
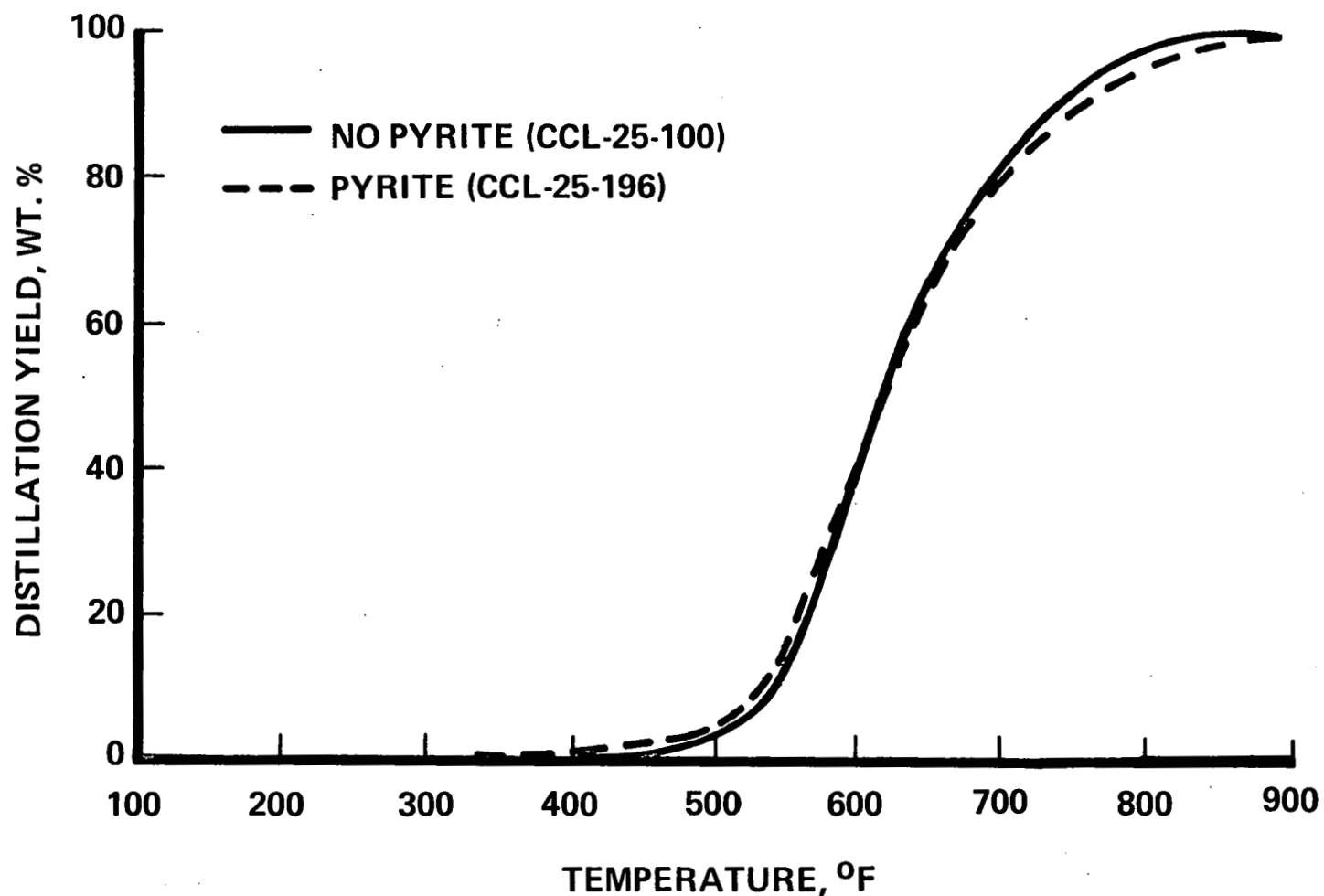
Table 72

Liquefaction Behavior of Elkhorn #2 Coal

Sample No.	31-128	31-139	31-186	31-196
Feed	70% Solvent[2] + 30% Coal		60% Solvent[2] + 30% Coal + 10% Robena Pyrite	
Temperature, °F	825	850	825	850
Pressure, psig	2000	2000	2000	2000
Hydrogen Treat Rate, MSCF/T	18.9	19.9	23.0	22.5
Residence Time, Min.	35	37	39	39
Product Distribution, wt.% MAF Coal				
HC	5.2	7.0	5.7	10.6
CO, CO_2	0.7	0.6	0.9	1.2
H_2S	0.3	0.3	0.0	0.0
NH_3	0.0	0.0	0.0	0.0
Oils	12.2	8.3	28.2	27.0
Asphaltenes	21.2	21.6	24.3	22.3
Preasphaltenes	44.2	43.4	29.6	25.6
I.O.M.	14.7	15.7	8.1	9.3
Water	1.5	3.1	3.2	4.0
Conversion, wt.% MAF Coal	85.3	84.3	91.9	90.7
Hydrogen Consumption, wt.% MAF Coal				
Total	0.64	0.53	1.68	2.41
From Gas	0.59	0.44	2.29	2.92
From Solvent	0.05	0.09	(0.61)[1]	(0.51)
By Pyrite	--	--	0.50	0.50
SRC Sulfur, %	0.61	0.55	0.60	0.57
First Order Rate Constants, hr^{-1}				
K_a	0.62	0.39	1.24	1.25
K_p	1.27	1.09	2.65	2.86

[1] ( ) = negative value
[2] Solvent = F.O.B.#11

136

As depicted in Figures 21 and 22, the oil fractions obtained with and without pyrite had similar boiling point distributions. As seen in Table 73, oil fractions obtained in the presence of pyrite contained more hydrogen than did those obtained in the absence of pyrite; the hydrogen content of the oil fractions obtained in the absence of pyrite was similar to that of starting solvent. Therefore, the oil hydrogen content is improved in the presence of pyrite, whereas it is maintained in its absence. Some differences were noted in the nitrogen and oxygen contents of all the fractions obtained with and without the addition of pyrite.

No definite trend in the distribution of oxygen compounds with or without pyrite was apparent (Table 74). However, lower concentrations of pyridine types of compounds and more NH_2 type compounds were noted with pyrite compared to a no-additive run. The concentration of NH type compounds was not changed with the addition of pyrite.

A higher concentration of H_{AR} in the oil fractions obtained without pyrite and in the original solvent was observed compared with oil fractions obtained with pyrite (Table 75); this indicated that more aromatic hydrocarbons were hydrogenated with pyrite. The concentrations of H_a and H_o protons were higher with pyrite than without pyrite and in the original solvent, which indicated increased production of side chain and hydrogenated aromatic compounds with pyrite. The solvent quality, estimated by the concentration of H_a and H_o, remained unchanged for solvent generated without pyrite and improved for that generated with pyrite. The Brown-Ladner structural parameters, given in Table 75, indicated no significant changes in aromaticity (f_a) and degree of substitution (σ) of oils obtained with pyrite compared with original solvent and those obtained without pyrite. Some variations in the degree of condensation (H_{AR}/C_{AR}) and the average number of condensed aromatic rings were also noticed.

The conversion of coal changed only slightly with an increase in temperature from 825 to 850°F with pyrite (Table 72). The production of hydrocarbon gases increased from 5.7 to 10.6% with an increase in temperature from 825°F to 850°F. No significant change in the production of oils and asphaltenes was noted with increasing reaction temperature. The rate constants for the

FIGURE 21
COMPARISON OF SIMULATED DISTILLATION OF OIL FRACTIONS OBTAINED BY LIQUEFACTION OF ELKHORN #2 COAL AT 825° F
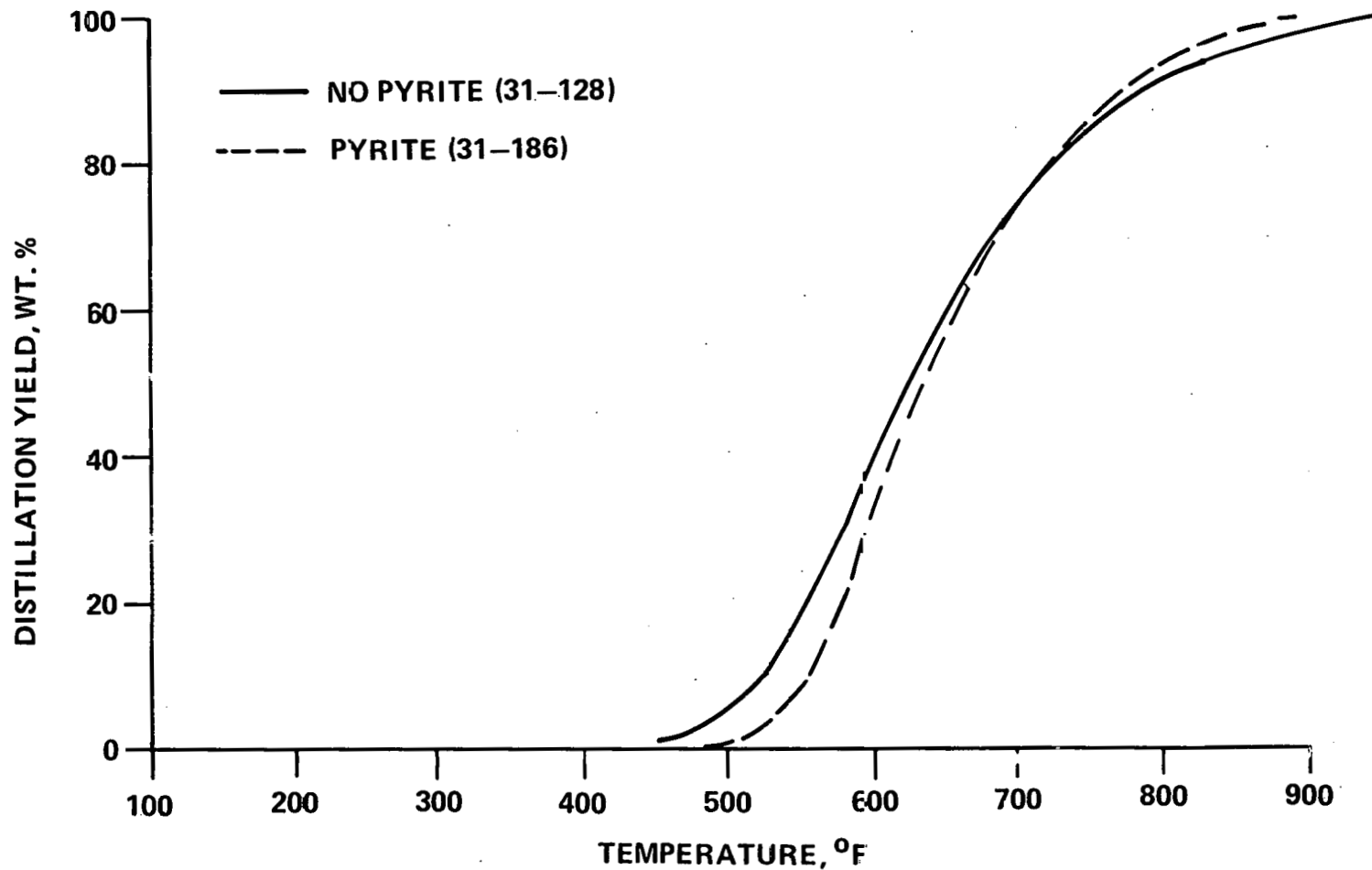
FIGURE 22
COMPARISON OF SIMULATED DISTILLATION OF OIL FRACTIONS OBTAINED BY LIQUEFACTION OF ELKHORN #2 COAL AT 850° F
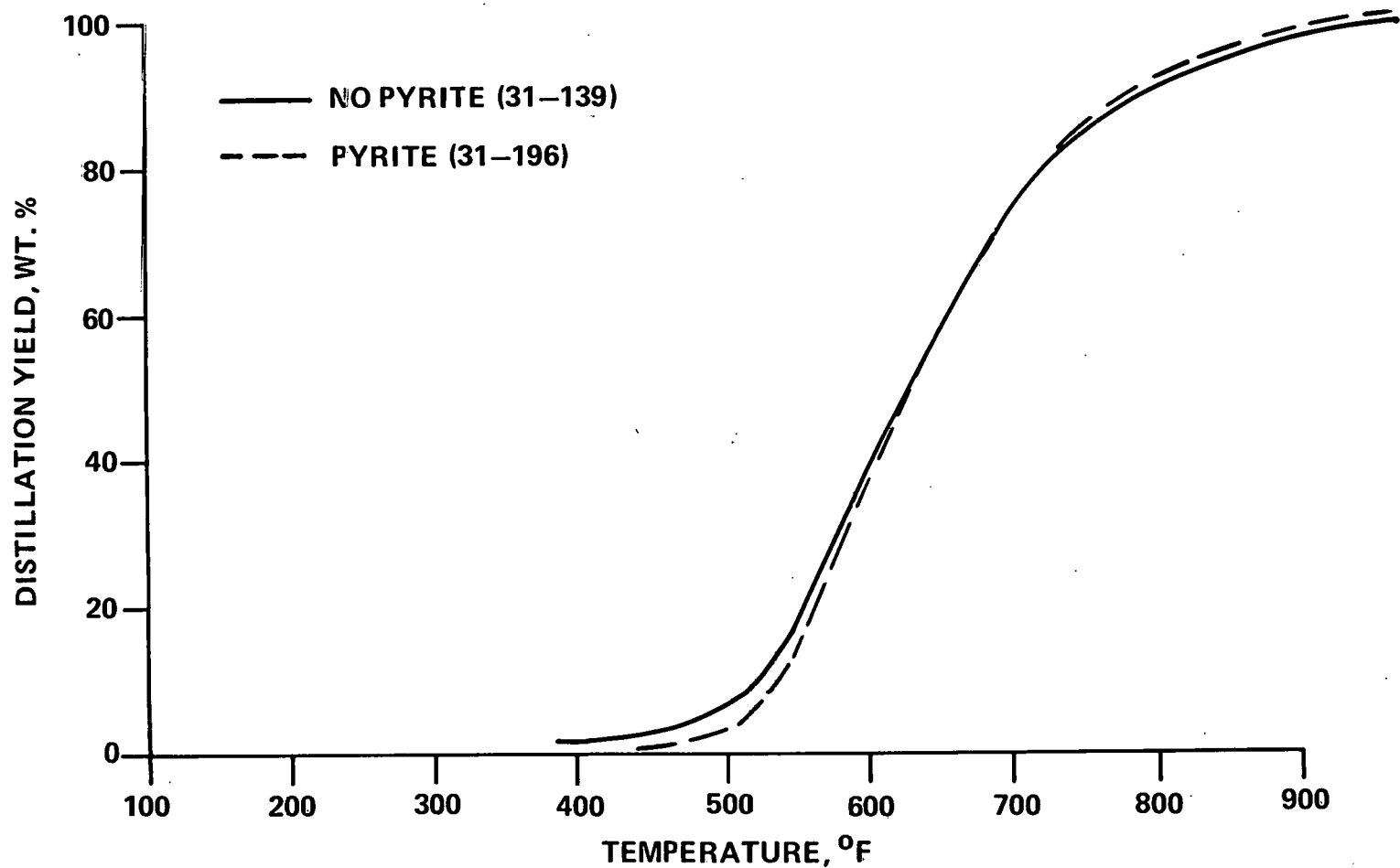
Table 73

Elemental Distribution in the Liquefaction Products of
Elkhorn #2 Coal in the Presence and Absence of Robena Pyrite

Sample No.	(FOB #11)	31-128	31-186	31-139	31-196
Temperature, °F	--	825	825	850	850
Pyrite	--	No	Yes	No	Yes
Oil Fraction, Wt.%					
C	89.7	89.5	89.2	89.7	89.4
H	7.2	7.2	7.5	7.2	7.5
O	1.4	1.7	1.8	1.8	1.6
N	1.1	0.9	0.8	0.7	0.9
S	0.6	0.7	0.7	0.6	0.6
$\bar{n}MW$	208	220	225	205	210
Asphaltene Fraction, Wt.%					
C	--	85.9	85.6	87.0	87.3
H	--	6.3	5.7	6.1	6.0
O	--	5.8	5.9	5.0	5.1
N	--	1.4	2.3	1.4	--
S	--	0.6	0.5	0.5	0.5
Preasphaltene Fraction, Wt. %					
C	--	85.3	85.4	86.6	85.8
H	--	5.2	5.2	4.9	5.0
O	--	6.2	6.1	5.4	5.7
N	--	2.2	2.3	2.4	2.3
S	--	0.6	0.7	0.6	0.6

Table 74

Distribution of Nitrogen and Oxygen Compounds
in Oil Fractions of Elkhorn #2 Liquefaction
in the Presence and Absence of Robena Pyrite

Sample No.	FOB #11		31-128		31-186		31-139		31-196	
Temperature, °F	--		825		825		850		850	
Pyrite	--		No		Yes		No		Yes	
Oxygen Distribution, Wt. %										
Total	1.42		1.69		1.81		1.79		1.65	
	Abs.[1]	Rel.[2]	Abs.	Rel.	Abs.	Rel.	Abs.	Rel.	Abs.	Rel.
O as O	0.90	63.4	1.07	63.3	1.10	60.8	1.14	63.7	0.99	60.0
O as OH	0.52	36.6	0.62	36.7	0.71	39.2	0.65	36.3	0.66	40.0
Nitrogen Distribution, Wt.%										
Total	1.05		0.86		0.81		0.66		0.86	
	Abs.	Rel.	Abs.	Rel.	Abs.	Rel.	Abs.	Rel.	Abs.	Rel.
N as N	0.61	58.	0.50	58.1	0.43	53.1	0.27	40.9	--	--
N as NH	0.38	36.2	0.32	37.2	0.31	38.3	0.32	48.5	0.33	38.4
N as NH_2	0.06	5.7	0.04	4.7	0.07	8.6	0.07	10.6	--	--

[1] Abs. - Absolute
[2] Rel. - Relative

Table 75
Distribution of Protons in the Oil Fractions of Elkhorn #2 Coal Liquefaction in the Presence and Absence of Robena Pyrite

Sample No.	(FOB #11)		31-128		31-186		31-139		31-196	
Temperature, °F	--		825		825		850		850	
Pyrite	--		No		Yes		No		Yes	
Total Hydrogen, wt.%	7.2		7.2		7.5		7.2		7.5	
Distribution of Protons, %										
	Abs.[1]	Rel.[2]	Abs.	Rel.	Abs.	Rel.	Abs.	Rel.	Abs.	Rel.
H_{AR}	3.20	44.4	3.26	45.3	2.90	38.7	3.38	46.9	3.20	42.6
H_a	2.02	28.0	1.95	27.1	2.47	32.9	2.01	27.9	2.15	28.7
H_o	1.98	27.6	1.99	27.6	2.13	28.4	1.81	25.2	2.15	28.7

[1] Abs. - Absolute
[2] Rel. - Relative

Table 76
Brown-Ladner Structural Parameters of the Oil Fractions of Elkhorn #2 Coal Liquefaction in the Presence and Absence of Robena Pyrite

Sample No.	(FOB #11)	31-128	31-186	31-319	31-196
Temperature, °F	--	825	825	850	850
Pyrite	--	No	Yes	No	Yes
f_a		0.71	0.72	0.70	0.72	0.70
σ		0.28	0.27	0.31	0.27	0.28
H_{AR}/C_{AR}		0.80	0.81	0.79	0.84	0.80
R_a		3.23	3.36	3.56	3.07	3.19

the conversion of asphaltenes and preasphaltenes were not significantly changed from 825 to 850°F in the presence of pyrite. This information indicates that pyrite catalyzes preasphaltene conversion, whereas it has no influence on the conversion of asphaltenes. The increase in temperature increased the hydrogen consumption from 1.68 to 2.41 wt% on the basis of MAF coal; this increase was due to increased production of hydrocarbon gases and water. The sulfur content of the SRC was not significantly changed.

The distribution of elements in the various fractions (Table 73) showed lower oxygen content in all fractions at 850°F than at 825°F. This is in agreement with higher water production at 850°F than at 825°F. Minor variations in the concentrations of hydrogen and nitrogen in all fractions at both temperatures were noted.

The concentration of the total oxygen in the oil fraction with pyrite was lower at 850°F than at 825°F, as were the concentrations of ether and hydroxyl type compounds, but the relative distribution of the oxygen compounds was the same (Table 74). The concentration of NH type compounds was very similar at both temperatures.

The distribution of protons (Table 75) showed an increase in H_{AR}, a decrease in H_a, and no change in H_o with an increase in reaction temperature from 825 to 850°F in the presence of pyrite. This is indicative of lower solvent quality of generated oil at the higher temperature. The aromaticity (f_a) of the two solvents was identical and a slight decrease in the degree of substitution by alkyl or other groups was noted with increasing temperature. The value of H_{AR}/C_{AR} was very similar at both temperatures. The average number of condensed aromatic rings decreased from 3.56 to 3.19 with an increase in temperature from 825 to 850°F (Table 76).

These results indicated that the addition of Robena pyrite to Elkhorn #2 coal increased the conversion of coal and preasphaltenes, increased the production of oils, hydrocarbon gases, promoted hydrogenation of solvent, improved the quality of generated solvent, increased the consumption of hydrogen, but did not alter the sulfur content of SRC. Increasing the reaction temperature in the presence of pyrite increased the production of hydrocarbon gases, increased

hydrogen consumption, did not effect sulfur content of SRC, and decreased the production of oils. If the objective of coal liquefaction is to increase oils production with minimum hydrogen consumption, lower reaction temperatures should be used with pyrite.

Pyrite Catalysis of Western Kentucky Coal - A high volatile B bituminous western Kentucky coal having high intrinsic liquefaction activity was chosen for the study of catalytic activity of pyrite. Table 1 presents the data on the samples (Kentucky #9) taken from Pyro mine. The analysis of the sample showed a pyrite content of 1.6% which was higher than that of eastern Kentucky coals. The response of this particular coal to the presence of added pyrite is discussed below.

Kentucky #9 (Pyro) Coal - The liquefaction of Kentucky #9 coal was studied at two temperatures in the presence of Robena pyrite and the results are summarized in Table 77. Coal conversion increased slightly with pyrite addition, both at 825 and 850°F. Oil production increased by over a factor of two with pyrite at both temperatures. The production of asphaltenes remained unchanged with pyrite at 825°F, but decreased from 30 to 20% at 850°F. A significant decrease in the production of preasphaltenes was noted with pyrite at 825°F. The rates of conversion of asphaltenes and preasphaltenes increased significantly with pyrite addition. Hydrogen consumption also increased with pyrite at both temperatures. A part of the increased hydrogen consumption, i.e., 0.5 wt%, was consumed in reducing the added pyrite; the remaining increased hydrogen consumption increased oil yield.

The simulated distillations of the oil fractions obtained with and without pyrite at 825 and 850°F, as shown in Figures 23 and 24, had similar initial and final boiling points but different boiling point distributions. The oils obtained with pyrite contained consistently higher boiling point compounds compared with oils generated without pyrite.

The distribution of elements in the various fractions obtained at 825 and 850°F (Table 78) showed that the oil fractions obtained in the absence of pyrite had considerably lower hydrogen content than those obtained with pyrite.

Table 77

Liquefaction Behavior of Kentucky #9 Coal from Pyro Mine

Sample No.	28-11	28-22	28-35	28-46	28-56
Feed	70% Solvent/30% Coal		60% Solvent/30% Coal/10% Robena Pyrite		
Temperature, °F	825	850	825	850	850
Pressure, psig	2,000	2,000	2000	2000	2000
Hydrogen Treat Rate MSCF/T	19.8	20.6	21.5	21.8	45.9
Residence Time, Min.	37	37	35	35	37
Product Distribution, wt.% MAF Coal					
HC	3.2	5.0	2.9	4.9	3.4
CO, CO_2	0.5	0.6	0.6	0.7	0.7
H_2S	1.4	1.7	0.6	0.4	2.7
NH_3	0.0	0.0	0.0	0.3	0.0
Oils	7.9	15.3	23.9	34.9	41.3
Asphaltenes	26.6	30.0	28.2	19.8	22.5
Preasphaltenes	47.0	28.1	31.5	25.6	20.2
Insoluble Organic Matter (I.O.M.)	9.4	12.8	6.7	7.4	4.1
Water	4.0	6.5	5.6	5.9	5.1
Conversion, wt.% MAF Coal	90.6	87.2	93.3	92.6	95.9
Hydrogen Consumption, wt.% MAF Coal					
Total	1.34	1.51	2.16	2.90	2.61
From Gas	0.69	0.47	2.12	2.88	2.70
From Solvent	0.65	1.04	0.04	0.02	(0.09)[1]
By Pyrite	--	--	0.50	0.50	0.50
First-Order Rate Constants, hr^{-1}					
K_a	0.25	0.83	0.46	1.47	
K_p	0.17	2.78	2.53	3.57	

[1] ( ) = negative value

FIGURE 23
COMPARISON OF SIMULATED DISTILLATION OF OIL FRACTIONS OBTAINED FROM KENTUCKY #9 COAL LIQUEFACTION AT 825° F
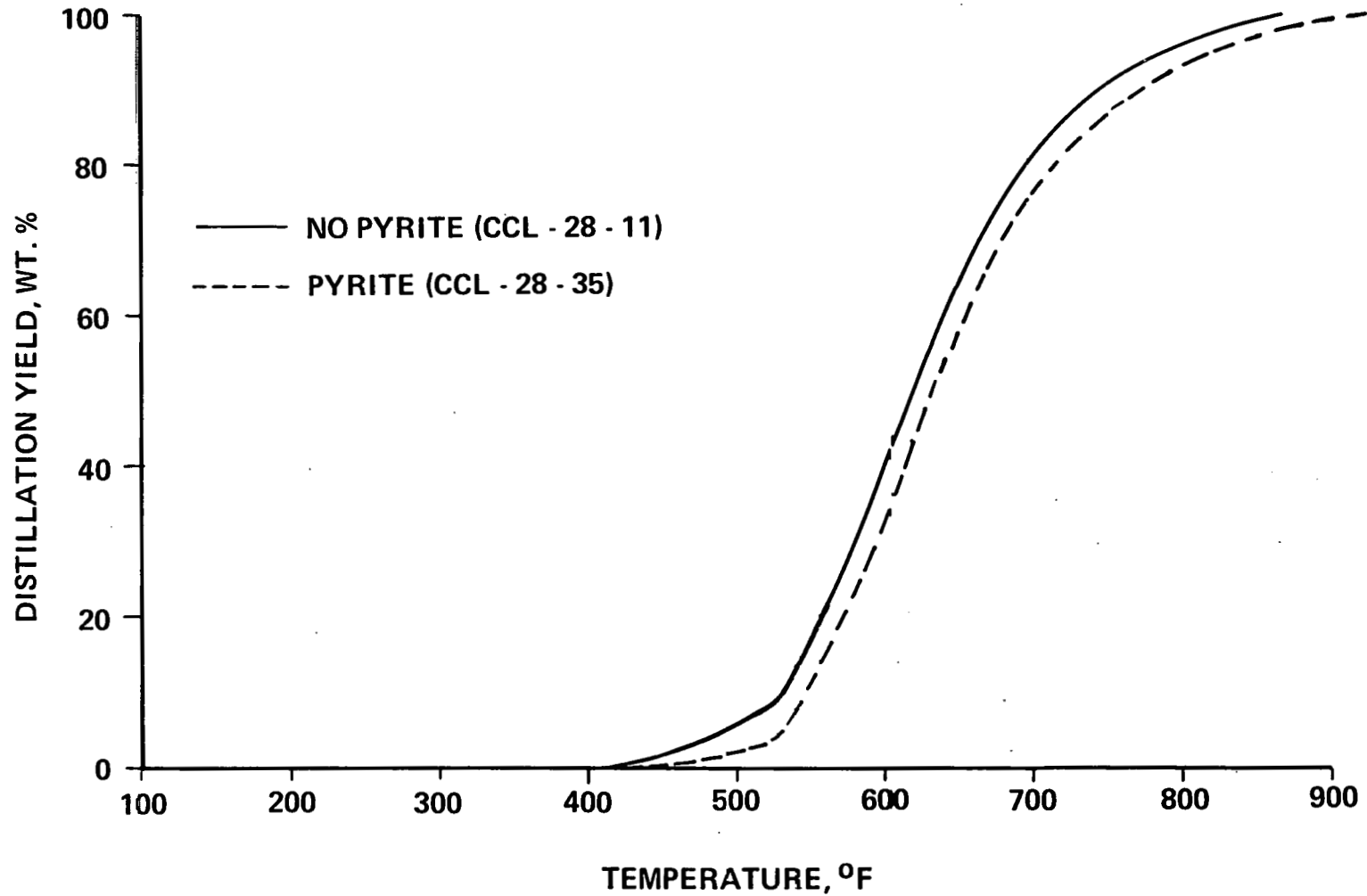
FIGURE 24
COMPARISON OF SIMULATED DISTILLATION OF OIL FRACTIONS OBTAINED FROM KENTUCKY #9 COAL LIQUEFACTION AT 850° F

NO PYRITE (CCL - 28 - 22)

PYRITE (CCL - 28 - 46)
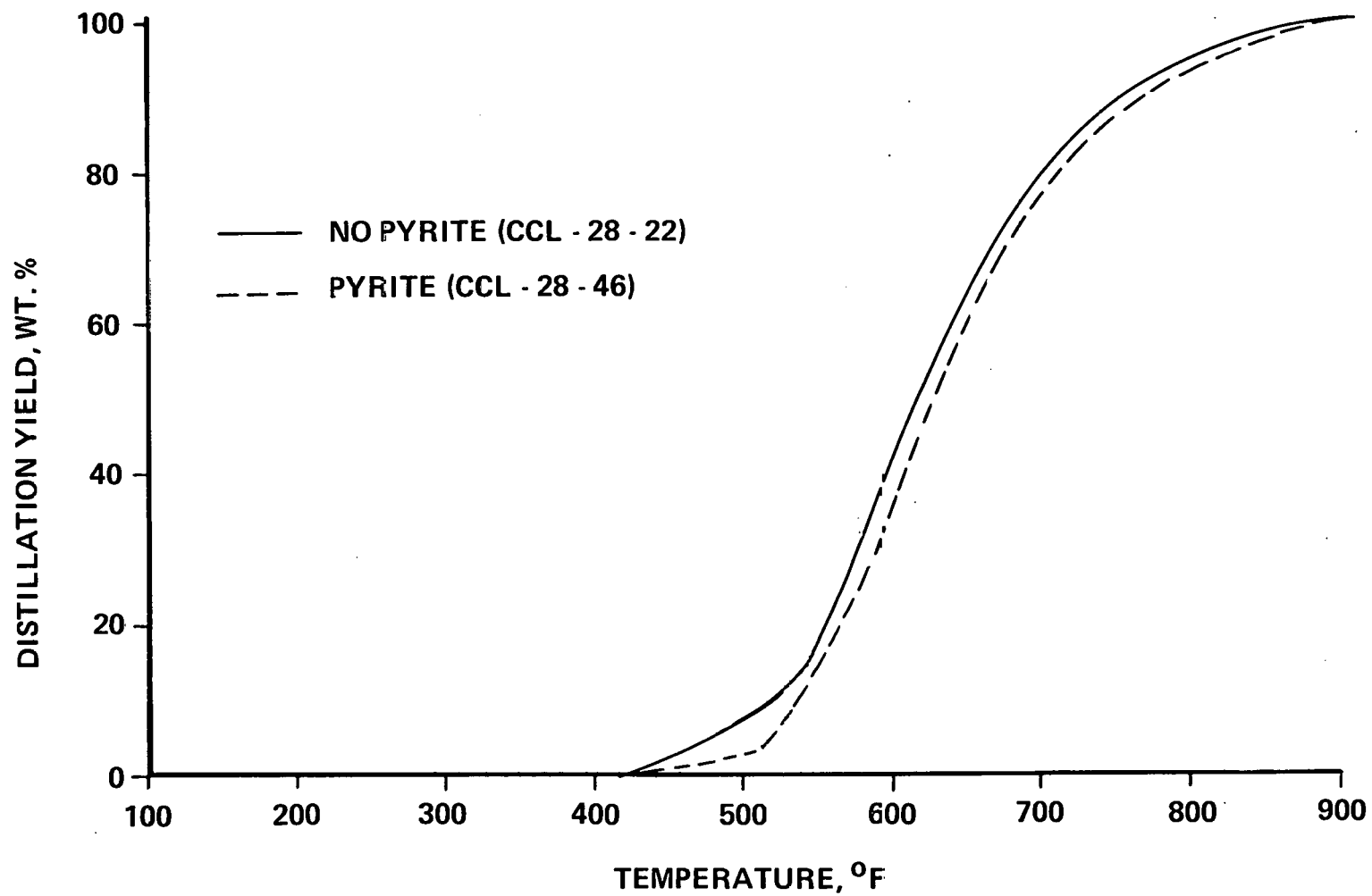
Table 78

Elemental Distribution in the Solubility Fractions
of the Liquefaction of Kentucky #9 Coal
in the Presence and Absence of Robena Pyrite

Sample No.	(FOB #1)	28-11	28-35	28-22	28-46	28-56
Temperature, °F	--	825	825	850	850	850
Pyrite	--	No	Yes	No	Yes	Yes
H_2 Flow Rate, MSCF/T	--	19.8	21.5	20.6	21.8	45.9
Oil Fraction, wt.%						
C	89.6	89.5	88.8	89.5	89.1	89.1
H	7.7	7.5	7.7	7.3	7.7	7.8
O	1.3	1.5	1.8	1.7	1.7	1.5
N	0.9	0.9	1.1	0.7	1.0	1.2
S	0.5	0.6	0.5	0.6	0.5	0.5
$\bar{n}$MW	220	208	212	204	208	208
Asphaltene Fraction, wt.%						
C	-	85.8	84.0	86.2	85.4	86.0
H	-	6.4	6.3	6.4	6.8	6.4
O	-	4.3	6.2	4.6	4.4	4.4
N	-	2.5	2.3	2.2	2.4	2.4
S	-	1.0	1.3	1.0	1.0	1.0
$\bar{n}$MW	-	341	698	342	557	423
Preasphaltene Fraction, wt.%						
C	-	83.7	82.5	83.9	83.5	84.1
H	-	5.5	5.6	5.4	5.7	5.6
O	-	6.0	7.6	6.0	5.8	5.5
N	-	2.4	2.4	2.4	2.5	2.7
S	-	1.4	1.4	1.2	1.7	1.1
$\bar{n}$MW	-	1583	8178	1772	1426	1142

The hydrogen content of oil fractions obtained in the presence of pyrite was similar to that of starting solvent, indicating the the oil hydrogen content was depleted in the absence of pyrite, whereas it was maintained in its presence. The hydrogen contents of asphaltenes and preasphaltenes obtained with pyrite were generally higher than those without pyrite. Some variations in nitrogen, oxygen, and sulfur contents of all the fractions were also noted with and without pyrite.

The distribution of nitrogen and oxygen compounds present in the oil fractions (Table 79) showed that the concentration of pyridine type compounds increased slightly and that NH type compounds decreased slightly with the addition of pyrite. The latter was probably due to the hydrogenation of NH to NH_2 types of compounds and finally to ammonia.

Higher concentrations of H_{AR} in the oil fractions obtained without pyrite and lower values in the oil fractions obtained with pyrite were observed compared with the original solvent (Table 80); this indicated that more aromatics were hydrogenated with pyrite. The concentrations of H_a and H_o protons decreased without pyrite, while they increased with pyrite; this was indicative of increased production of side chain and hydrogenated aromatic compounds. Solvent quality, estimated by the concentration of H_a and H_o, improved for the solvents generated in the presence of pyrite and declined for that generated in its absence. The Brown-Ladner structural parameters for the oil fractions are listed in Table 81. The aromaticity, f_a, of the oils obtained without pyrite was higher, and that of the oils obtained with pyrite was lower than the original solvent. This was also supported by a higher value of H_{AR} without pyrite and a lower valve with pyrite. The increase in the value of H_o with pyrite was also verified by an increased degree of substitution (σ). Although some variation in the degree of condensation (H_{AR}/C_{AR}) was observed with and without pyrite, no significant change in the average number of aromatic rings (R_a) was noted.

Coal conversion was similar at the two different temperatures with pyrite, but significant differences were found in hydrocarbon gas production, product distribution, and hydrogen consumption. Hydrocarbon gases production increased with increasing reaction temperature from 825 to 850°F. Increasing the

Table 79

Distribution of Nitrogen and Oxygen Compounds in O⁻1 Fractions from the
Liquefaction of Kentucky #9 Coal in the Presence and Absence of Robena Pyrite

Sample No.	28-11	28-35	28-22	28-46	28-56
Temperature, °F	825	825	850	850	850
Pyrite	No	Yes	No	Yes	Yes
H_2 Flow Rate, MSCF/T	19.8	21.5	20.6	21.8	45.9
Total Nitrogen, wt.%	0.92	1.14	0.96	1.03	1.23
Total Oxygen, wt.%	1.54	1.79	1.65	1.74	1.49
Distribution of Nitrogen, %					
Absolute					
N as N	0.54	0.85	0.60	0.71	0.91
N as NH	0.35	0.26	0.33	0.25	0.26
N as NH_2	0.03	0.03	0.03	0.07	0.06
Relative					
N as N	58.7	74.6	62.5	68.9	74.0
N as NH	38.0	22.8	34.4	24.3	21.
N as NH_2	3.3	2.6	3.1	6.8	4.9
Distribution of Oxygen, %					
Absolute					
O as O	0.89	1.0	0.96	0.90	0.67
O as OH	0.65	0.79	0.69	0.84	0.82
Relative					
O as O	57.8	55.9	58.2	51.7	45.0
O as OH	42.2	44.1	41.8	48.3	55.0

Table 80

Distribution of Protons in the Oil Fractions from the
Liquefaction of Kentucky #9 Coal in the Presence and Absence of Robena Pyrite

Sample No.	(FOB #1)	28-11	28-35	28-22	28-46	28-56
Temperature, °F	-	825	825	850	850	850
Pyrite	-	No	Yes	No	Yes	Yes
H_2 Flow Rate, MSCF/T		19.8	21.5	20.6	21.8	45.9
Total Hydrogen, wt.%	7.62	7.46	7.70	7.30	7.71	7.76
Distributions of Protons, %						
Absolute						
H_{AR}	3.24	3.27	2.96	3.30	2.98	2.96
H_a	2.26	2.08	2.42	2.09	2.35	2.31
H_o	2.22	2.11	2.32	1.91	2.38	2.49
Relative						
H_{AR}	42.0	43.8	38.5	45.2	38.7	38.2
H_a	29.3	27.9	31.5	28.6	30.5	29.8
H_o	28.7	28.3	30.0	26.2	30.8	32.0

Table 81

Brown-Ladner Structural Parameters for
the Oil Fractions from the Liquefaction of
Kentucky #9 Coal in the Presence and Absence of Pyrite

Sample No.	(FOB #1)	28-11	28-35	28-22	28-46
Temperature, °F	-	825	825	850	850
Pyrite	-	No	Yes	No	Yes
f_a	0.702	0.722	0.685	0.733	0.693
σ	0.271	0.259	0.306	0.264	0.290
H_{AR}/C_{AR}	0.834	0.809	0.834	0.800	0.804
R_a	3.23	3.23	3.26	3.24	3.27

temperature from 825 to 850°F increased the conversion of both asphaltenes and preasphaltenes to oils and gases; oil production increased from 24 to 35% and asphaltenes and preasphaltenes decreased from 28 to 20 and from 31 to 26%, respectively. Also, an increase in temperature increased the hydrogen consumption from 2.2 to 2.9 wt% on the basis of MAF coal.

The distribution of elements of the various fractions obtained with pyrite (Table 78) indicated that the hydrogen contents of the oil fractions obtained at 825 and 850°F were identical. The number average molecular weights of the oil, asphaltene, and preasphaltene fractions decreased with increasing temperature. No significant differences were noted in the nitrogen contents of oil, asphaltenes, and preasphaltenes. With increasing temperature, the sulfur contents changed as follows: the oil remained unchanged, the asphaltenes decreased from 1.28 to 0.95%, and the preasphaltenes increased from 1.36 to 1.68%. The oxygen contents of asphaltenes decreased from 6.16 to 4.41% and the preasphaltenes decreased from 7.49 to 5.76%.

The distribution of protons was unaffected by reaction temperatures as shown in Table 80. The concentration of H_{AR} was lower and that of H_a and H_o was higher in the generated oil fractions compared with the original solvent; this was indicative of higher solvent quality of generated oils than the original solvent. Lower aromaticity and a higher degree of substitution by alkyl or other groups was found for generated solvents than for the original solvent. Although the value of H_{AR}/C_{AR} decreased considerably with increasing reaction temperatures, no change in the average number of condensed aromatic rings was noted (see Table 81).

The above results showed that the addition of Robena pyrite to Kentucky #9 coal increased coal dissolution, promoted solvent hydrogenation, increased oil production and improved solvent quality.

Effect of Pyrite Concentration on Liquefaction - The effect of Robena pyrite concentration was examined in the liquefaction of Elkhorn #2 and #3 coals and the results are discussed below.

Elkhorn #3 Coal - The catalytic activity of 10 wt% Robena pyrite in the lique-
faction of Elkhorn #3 coal was discussed earlier. The effect of the pyrite
concentration in the liquefaction of Elkhorn #3 coal was also examined at both
2.5 and 5.0 wt% and the results were compared to a no-additive run. Coal
conversion increased from 84.2% with no-additive to ~89% with the addition of
pyrite at all concentrations (Table 82). Conversion was not affected by
adding different amounts of pyrite. The production of hydrocarbon gases
increased with increasing concentration of pyrite (Table 82 and Figure 25).
However, the production of hydrocarbon gases with 10 wt% pyrite was lower
compared with the 2.5 and 5.0 wt% addition of pyrite. These differences could
be due to the use of a different solvent (FOB #1) when 10 wt% pyrite was added
to the feed slurry. Significant increases in the production of oils occurred
with an increase in pyrite concentration, as shown in Table 82 and Figure 26.
The increase in oil production with pyrite was due either to the increased
conversion of coal, to the conversion of asphaltenes, or both. The conversion
of asphaltenes and preasphaltenes increased with increasing concentrations of
pyrite (see Figure 27). The concentration of preasphaltenes at 10 wt.% addition
of pyrite seemed to be in error, but it could be due to the use of different
process solvent (FOB #1). The first-order rate constants for the conversion
of asphaltenes and preasphaltenes also increased with increasing pyrite concen-
tration. The rate of conversion of asphaltenes increased from 0.75 to 1.31
hr^{-1} with the addition of 5 wt% pyrite, and the rate of preasphaltene conversion
increased from 2.95 to 4.07 hr^{-1}. These increases reflect the activity of
pyrite in catalyzing asphaltene and preasphaltene conversion. The X-ray
diffraction analysis of the coal liquefaction residue material showed complete
reduction of pyrite to pyrrhotite. This reduction results in the production
of hydrogen sulfide gas, and the partial pressure of hydrogen sulfide gas
produced during the reaction increases with increasing the concentration of
pyrite. The increased concentration of this gas increases its back reaction
with organic compounds, producing organic sulfur compounds. The high molecular
weight fractions, e.g., asphaltenes and preasphaltenes, are more susceptible
to H_2S back reaction. Higher asphaltene and preasphaltene sulfur content with
pyrite than without pyrite verified this (Table 83). No change in the sulfur
content of oils was noted with the addition of pyrite compared to a no-pyrite
run as shown in Table 83. The increase in sulfur contents of asphaltenes and
preasphaltenes with pyrite resulted in higher SRC content (Table 83 and Figure 28).

Table 82
Floyd County Elkhorn #3 Coal Liquefaction
Product Distribution in the Presence of Pyrite

Sample No.	31-81	31-93	31-109	25-136
Feed Composition	70% Solvent + 30% Coal	67.5% Solvent + 30% Coal + 2.5% Pyrite	65% Solvent + 30% Coal + 5% Pyrite	60% Solvent + 30% Coal + 10% Pyrite
Solvent	FOB #11	FOB #11	FOB #11	FOB #1
Temperature, °F	850	850	850	850
Residence Time, Min.	38	40	38	41
Pressure, psig	2000	2000	2000	2000
Product Distribution, wt.% MAF Coal				
HC	6.8	9.4	10.4	5.3
CO, CO_2	1.0	1.3	1.5	1.2
H_2S	0.2	0.3	0.3	2.8
NH_3	0.0	0.0	0.0	0.2
Oils	20.4	22.3	30.4	41.0
Asphaltenes	29.2	29.7	23.6	11.1
Preasphaltenes	25.4	22.7	19.9	24.1
I.O.M.	15.8	11.2	9.1	10.4
Water	1.2	3.1	4.8	3.5
Conversion, %	84.2	88.8	90.9	89.9
H_2 Consumption, wt.% MAF Coal				
Total	0.91	1.75	2.24	2.53
From Gas	0.92	2.30	2.58	2.49
From Solvent	(0.01)[1]	(0.55)	(0.34)	0.04
By Pyrite	--	0.13	0.25	0.50
SRC Sulfur, %	0.50	0.55	0.67	0.66
First Order Rate Constants, hr^{-1}				
K_a	0.75	0.78	1.31	1.84
K_p	2.95	3.28	4.07	3.05

---

[1] ( ) = negative value

155

FIGURE 25
VARIATION IN THE PRODUCTION OF GASES WITH THE CONCENTRATION OF PYRITE
(ELKHORN #3 COAL)
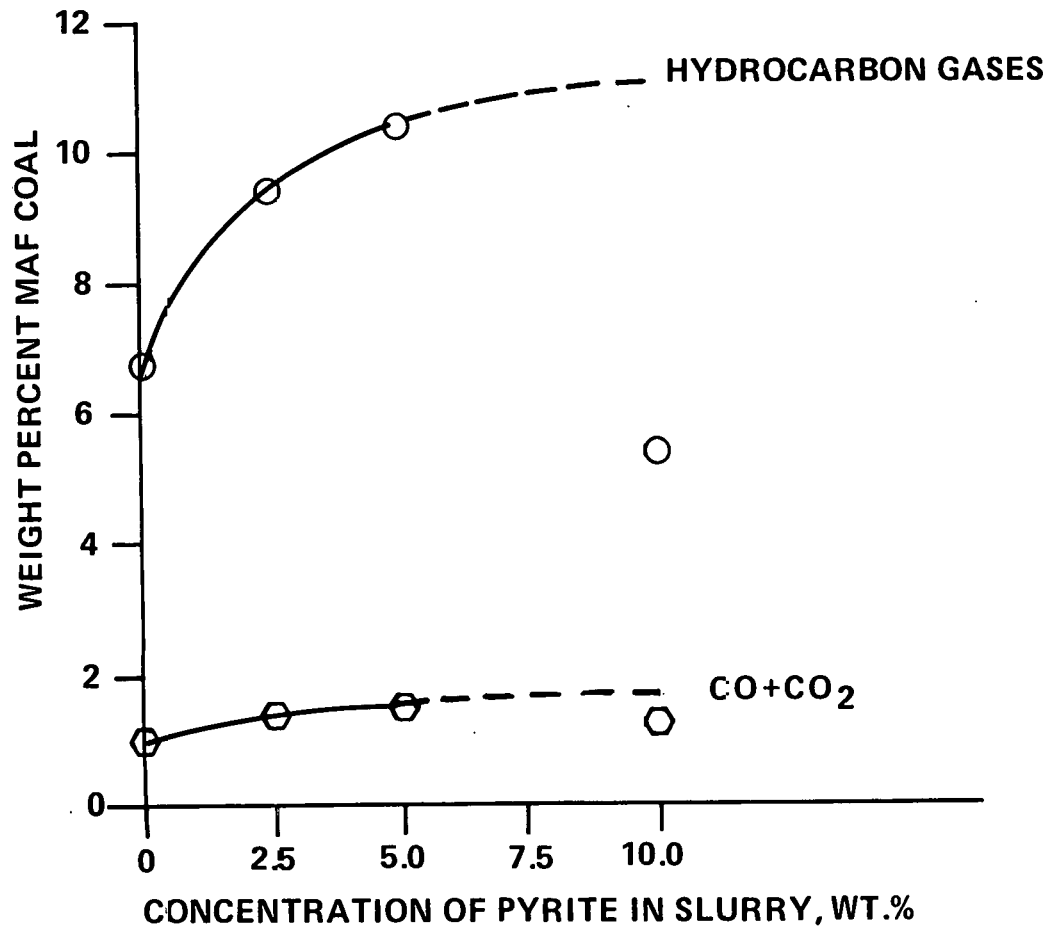
FIGURE 26
VARIATION IN THE PRODUCTION OF OILS WITH THE CONCENTRATION OF PYRITE
(ELKHORN #3 COAL)
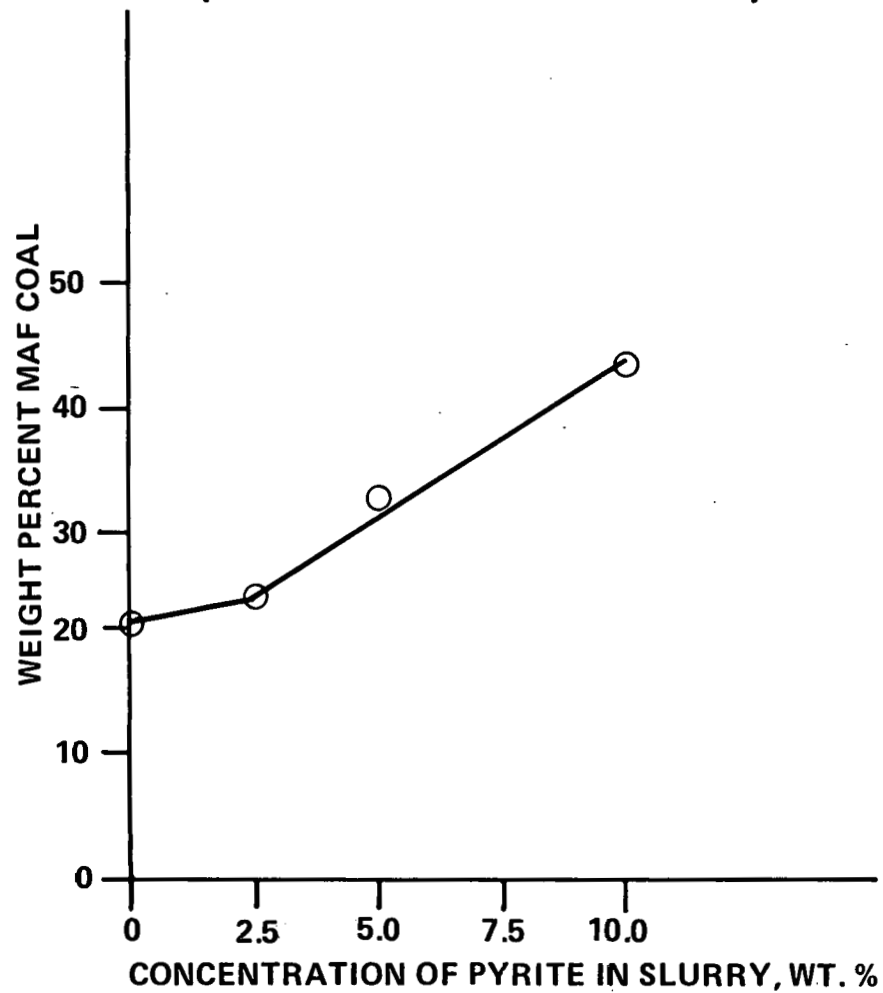
FIGURE 27
VARIATION IN THE PRODUCTION OF ASPHALTENES AND PREASPHALTENES WITH CONCENTRATION OF PYRITE (ELKHORN #3 COAL)
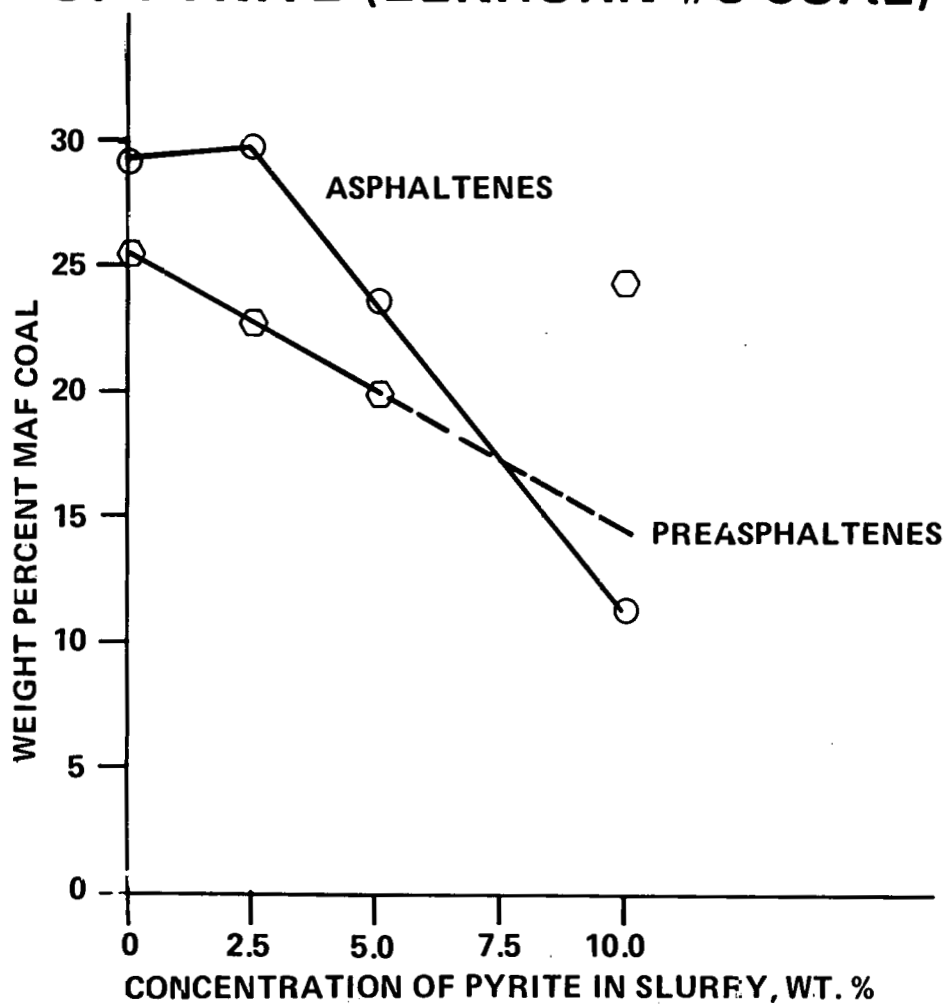
Table 83
Elemental Distribution in the Liquefaction Products
of Floyd County Elkhorn #3 Coal in the Presence of Pyrite

Sample No.	31-81	31-93	31-109	25-136
Pyrite, Wt.%	0.5	2.5	5.0	10.0
Temperature, °F	850	850	850	850
Solvent	FOB #11	FOB #11	FOB #11	FOB #1
Oil Fraction, Wt.%				
C	89.7	89.3	89.3	89.1
H	7.3	7.5	7.4	7.7
O	1.7	1.9	1.9	1.8
N	0.7	0.7	0.8	1.0
S	0.6	0.6	0.6	0.5
$\bar{n}$ MW	220	230	205	205
Asphaltene Fraction, Wt.%				
C	86.1	86.2	86.5	85.1
H	6.1	6.4	6.4	6.2
O	4.9	4.8	5.2	5.7
N	2.4	2.1	1.3	2.4
S	0.5	0.5	0.6	0.6
$\bar{n}$ MW	390	--	384	490
Preasphaltene Fraction, Wt.%				
C	86.1	86.0	85.7	83.2
H	5.0	5.1	5.4	5.7
O	5.9	5.8	5.5	--
N	2.5	2.4	2.4	3.3
S	0.5	0.6	0.7	0.7
$\bar{n}$ MW	990	--	--	984

FIGURE 28
VARIATION OF SRC SULFUR WITH THE
CONCENTRATION OF PYRITE
(ELKHORN #3 COAL)
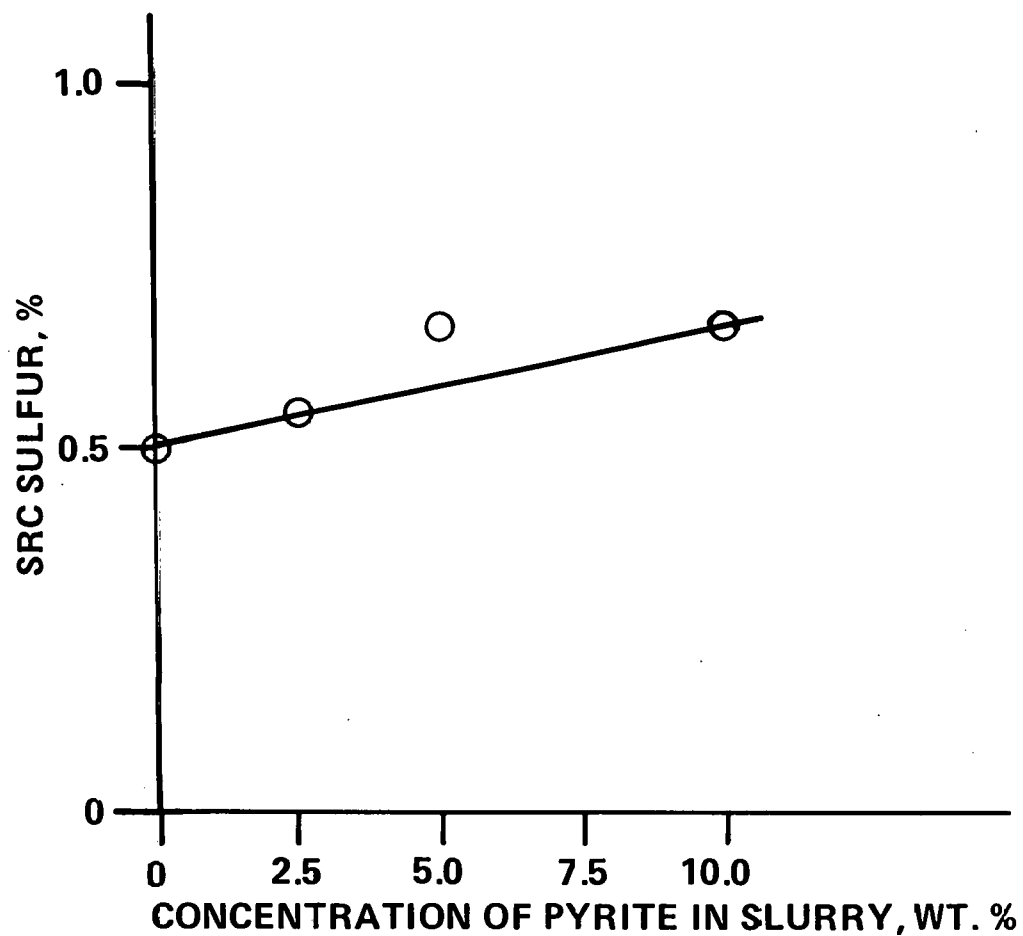
The hydrogen contents of oils, asphaltenes and preasphaltenes were consistently higher with pyrite than without it (Table 83). The higher hydrogen content in the oils and the additional hydrogen consumed to increase oils production plus the additional hydrogen consumed to reduce pyrite to pyrrhotite resulted in higher overall hydrogen consumption. The total hydrogen consumption increased consistently with increasing amounts of added pyrite as shown in Table 82 and Figure 29. The total hydrogen consumed increased very rapidly with the amount of pyrite added, but the total hydrogen consumed minus hydrogen required for pyrite reduction values approached an upper limit and did not increase significantly with the addition of pyrite.

The simulated distillations of the oils obtained using different concentrations of pyrite are shown in Figure 30. Other than slight variations in the initial boiling points and the boiling point distribution of the lower boiling point materials, no major differences were noted.

The distribution of nitrogen and oxygen compounds in the oils (Table 84) showed a slight change in oxygen and nitrogen contents in the presence of pyrite. No significant difference was noted in the distribution of total oxygen as ether or phenols with or without pyrite. An increase in pyridine type compounds was noted with pyrite compared to the no-additive run; this increase occurred at the expense of NH_2 type compounds.

The concentration of H_{AR} decreased with pyrite, while that of H_a and H_o increased with pyrite. A higher concentration of H_a and H_o is indicative of higher solvent quality of generated oils. No significant differences occurred in the distribution of protons (Table 85) with an increase in the pyrite concentration in the feed slurry from 2.5 to 5.0 wt%. No major changes were noted in the values of Brown-Ladner structural parameters with and without pyrite (Table 86).

Elkhorn #2 Coal - The effect of different pyrite concentration levels, namely 2.5, 5.0 and 10.0 wt% based on feed slurry, was studied in the liquefaction of Elkhorn #2 coal at 850°F. The production of hydrocarbon gases and oils increased with pyrite addition as did the conversion of coal and preasphaltenes (see Table 87). Coal conversion was almost identical at all three pyrite concentrations. The production of hydrocarbon gases and oils were also similar at

FIGURE 29
VARIATION OF HYDROGEN CONSUMPTION WITH THE CONCENTRATION OF PYRITE (ELKHORN #3 COAL)

TOTAL H_2 CONSUMPTION

(TOTAL $-$ H_2 CONSUMED TO REDUCE FeS_2 TO FeS)

Y-axis: HYDROGEN CONSUMPTION, WT. % MAF COAL

X-axis: CONCENTRATION OF PYRITE IN SLURRY, WT. %
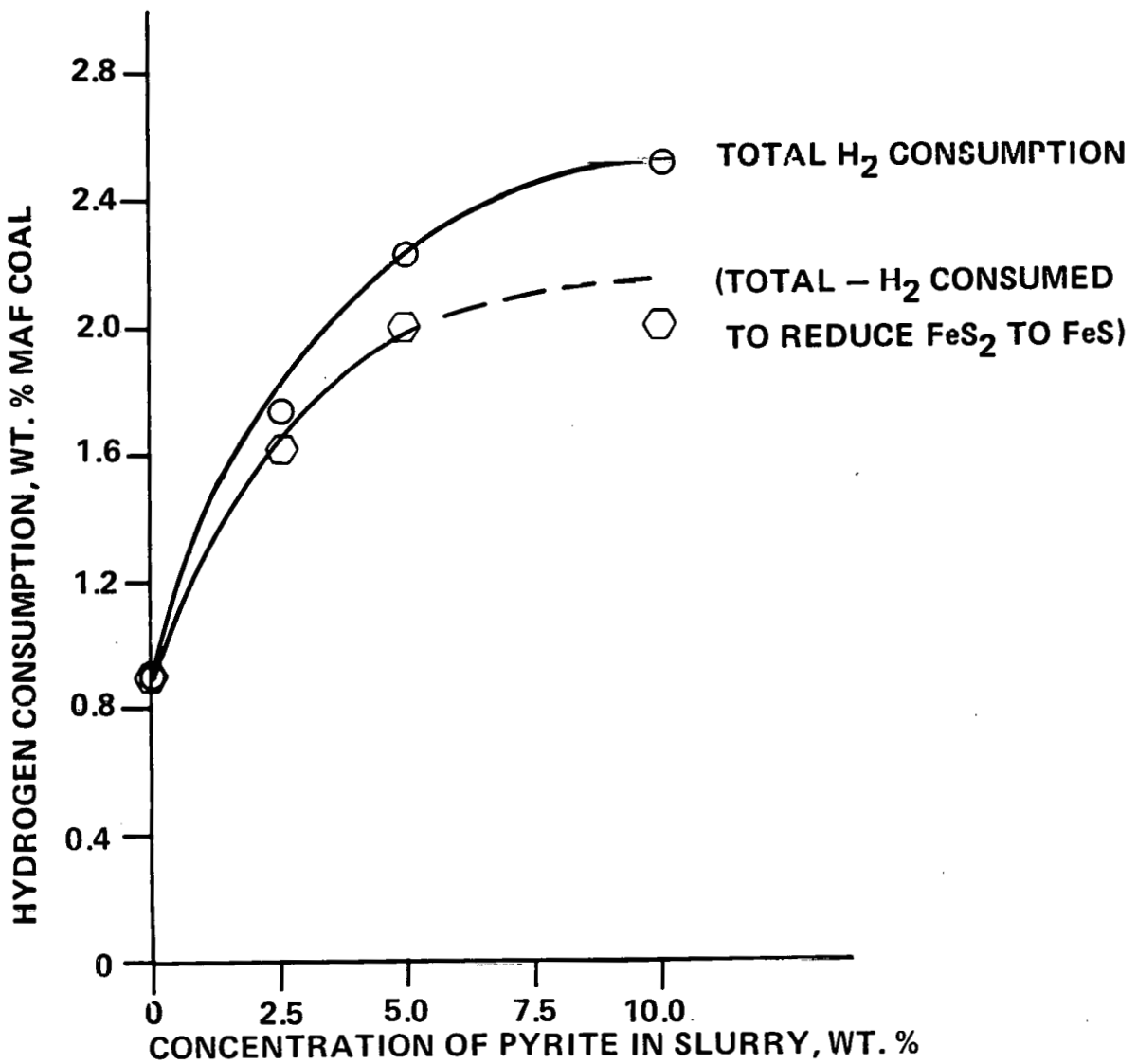
FIGURE 30
EFFECT OF CONCENTRATION OF PYRITE ON SIMULATED DISTILLATION OF OILS
(ELKHORN #3 COAL)

Legend:
- 31–81 (0.0 % PYRITE)
- 31–93 (2.5% PYRITE)
- 31–109 (5.0 % PYRITE)

X-axis: TEMPERATURE, °F
Y-axis: DISTILLATION YIELD, WT. %
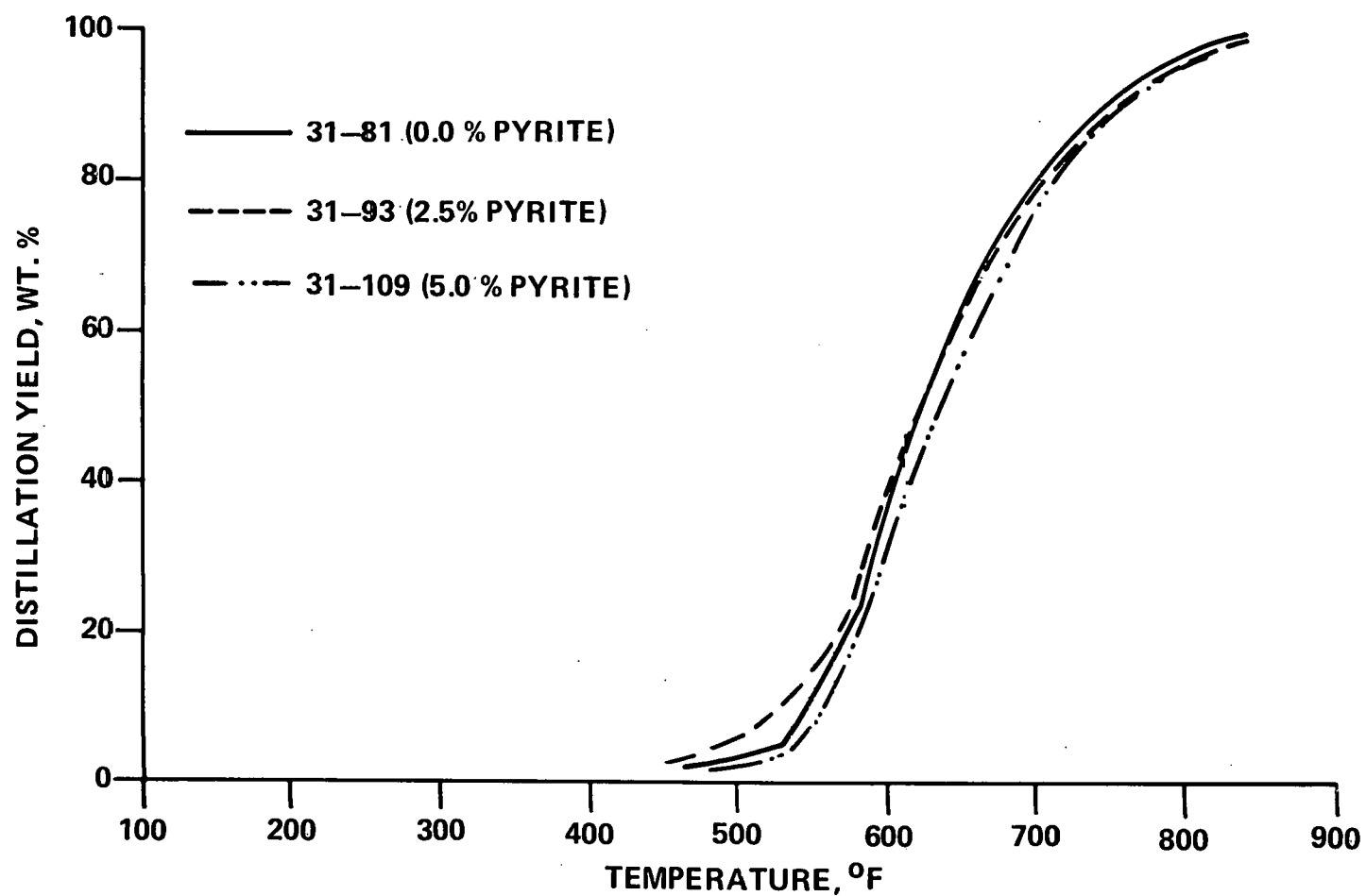
Table 84

Distribution of Oxygen and Nitrogen Compounds in the
Oil Fractions from the Liquefaction of Floyd County
Elkhorn #3 Coal in the Presence of Different Concentration Levels of Pyrite

Sample No.	31-81		31-93		31-109	
Pyrite Conc., wt.% of Slurry	0.0		2.5		5.0	
Oxygen Distribution, wt.%						
Total Oxygen	1.72		1.88		.185	
	Abs.	Rel.	Abs.	Rel.	Abs.	Rel.
O as O	1.09	63.4	1.17	62.2	1.14	61.6
O as OH	0.63	36.6	0.71	37.8	0.71	38.4
Nitrogen Distribution, wt.%						
Total Nitrogen	0.73		0.76		0.78	
	Abs.	Rel.	Abs.	Rel.	Abs.	Rel.
N as N	0.30	41.1	0.43	56.6	0.40	51.2
N as NH	0.32	43.8	0.33	33.4	0.32	41.0
N as NH_2	0.11	15.1	--	--	0.06	7.8

Table 85

Distribution of Protons in the Oil Fraction from the
Liquefaction of Floyd County Elkhorn #3 Coal in
the Presence of Different Concentration Levels of Pyrite

Sample No.		31-81		31-93		31-109	
Pyrite Conc.,							
wt.% of Slurry		0.0		2.5		5.0	
Total Hydrogen, wt.%		7.3		7.5		7.4	
Distribution of Protons, wt.%							
		Abs.	Rel.	Abs.	Rel.	Abs.	Rel.
H_{AR}		3.43	47.0	3.14	41.8	3.08	41.6
H_a		2.04	28.0	2.44	32.5	2.26	30.5
H_o		1.83	25.0	1.92	25.7	2.06	27.9

Table 86

Brown-Ladner Structural Parameters for the
Oil Fractions from the Liquefaction of Floyd County
Elkhorn #3 Coal In the Presence of Different Concentration Levels of Pyrite

Sample No.	31-81	31-93	31-109
Pyrite Conc.,			
wt.% of Feed Slurry	0.0	2.5	5.0
f_a	0.72	0.70	0.71
σ	0.27	0.29	0.28
H_{AR}/C_{AR}	0.85	0.83	0.80
R_a	3.18	3.41	3.26

Table 87

Effect of Concentration of Robena Pyrite On Liquefaction of Elkhorn #2 Coal

Sample No.	31-139	31-161	31-175	31-196
Temperature, °F	850	850	850	850
Feed Composition	70% Solvent + 30% Coal	67.5% Solvent + 30% Coal + 2.5% Pyrite	65% Solvent + 30% Coal + 5.0% Pyrite	60% Solvent + 30% Coal + 10.0% Pyrite
Solvent	FOB #11	FOB #11	FOB #11	FOB #11
Pressure, psig	2,000	2,000	2,000	2,000
Hydrogen Treat Rate, MSCF/T	19.9	24.2	22.2	22.5
Residence Time, Min.	37	38	38	39
Product Distribution, wt.% MAF Coal				
HC	7.0	10.2	9.9	10.6
CO, CO_2	0.6	0.9	1.0	1.2
H_2S	0.3	0.3	0.0	0.0
Oils	8.3	25.6	24.3	27.0
Asphaltenes	21.6	22.3	18.6	22.3
Preasphaltenes	43.4	28.2	32.3	25.6
I.O.M.	15.7	9.3	10.4	9.3
Water	3.1	3.2	3.5	4.0
Conversion	84.3	90.7	89.6	90.7
Hydrogen Consumption, wt.% MAF Coal				
Total	0.53	1.75	1.81	2.4
From Gas	0.44	1.96	2.30	2.92
From Solvent	0.09	(0.2)[1]	(0.49)	(0.51)
By Pyrite	--	0.13	0.25	0.50
SRC Sulfur, %	0.55	0.49	0.50	0.57
First Order Rate Constants, hr^{-1}				
K_a	0.39	1.71	1.26	1.25
K_p	1.09	2.59	2.04	2.86

[1] ( ) = negative value

166

all three in pyrite concentrations (Table 87 and Figures 31 and 32). The production of asphaltenes was unaffected by the concentration of pyrite, whereas the conversion of preasphaltenes increased with increasing concentration of pyrite (Table 87 and Figure 33). The rates of conversion of asphaltenes and preasphaltenes increased with pyrite. However, the rate constants were insensitive to the variations in the concentration of pyrite. SRC sulfur was unchanged with the addition of pyrite (Table 87 and Figure 34). The total hydrogen consumption increased consistently with the increase in the concentration of pyrite (Table 87 and Figure 35), but the total hydrogen consumed minus the hydrogen required to reduce pyrite to pyrrhotite increased only marginally.

Table 88 shows an increase in the hydrogen content of the oil fractions with increasing pyrite concentration. Simulated distillation of the oil fractions, illustrated in Figure 36, showed no significant differences with increasing pyrite concentration.

Table 89 shows higher concentrations of pyridine-type compounds with increasing pyrite addition. However, no significant differences were noted in the distribution of nitrogen and oxygen compounds with increasing concentrations of pyrite from 2.5 to 10.0 wt%.

The concentration of H_{AR} decreased and that of H_o and H_a increased with the addition of pyrite (Table 90). Solvent quality as determined by H_a and H_o was higher for solvent generated with pyrite than without pyrite. The concentration of H_{AR}, H_a, and H_o did not change significantly with increasing pyrite concentration from 2.5 to 10.0 wt%. No changes in the values of Brown-Ladner structural parameters were noted (Table 91).

Effect of Hydrogen Flow Rate on Liquefaction - Hydrogen partial pressure has been reported to influence both catalytic and noncatalytic coal liquefaction (12, 13). The results from an experiment with Kentucky Elkhorn #2 simulating the effect of hydrogen partial pressure on liquefaction by increasing the total hydrogen flow rate in the absence of a catalyst, which was discussed on page 80, showed no effect on coal conversion, but increased oil production, as well as the rates of conversion of asphaltenes and preasphaltenes. It was

FIGURE 31
VARIATION IN THE PRODUCTION OF GASES AND
WATER WITH THE CONCENTRATION OF PYRITE
(ELKHORN #2 COAL)
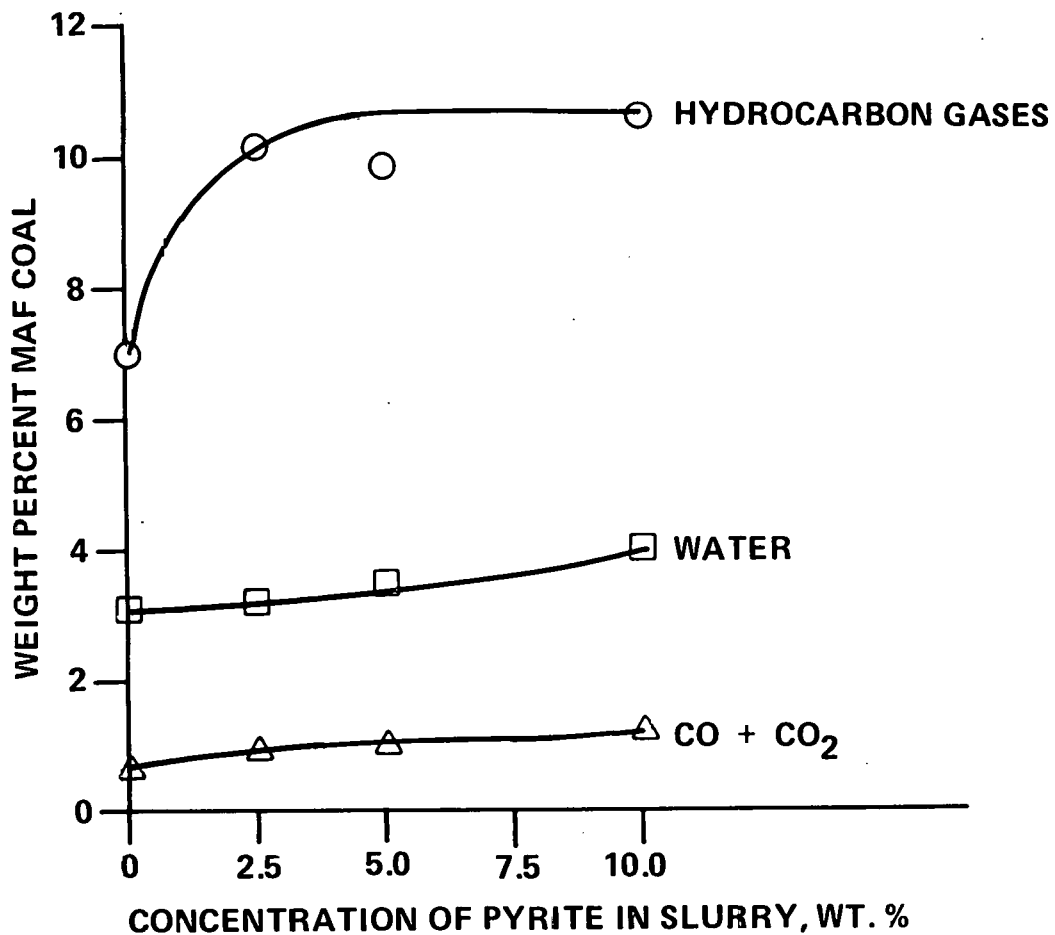
FIGURE 32
VARIATIONS IN THE PRODUCTION OF OILS
WITH THE CONCENTRATION OF PYRITE
(ELKHORN #2 COAL)
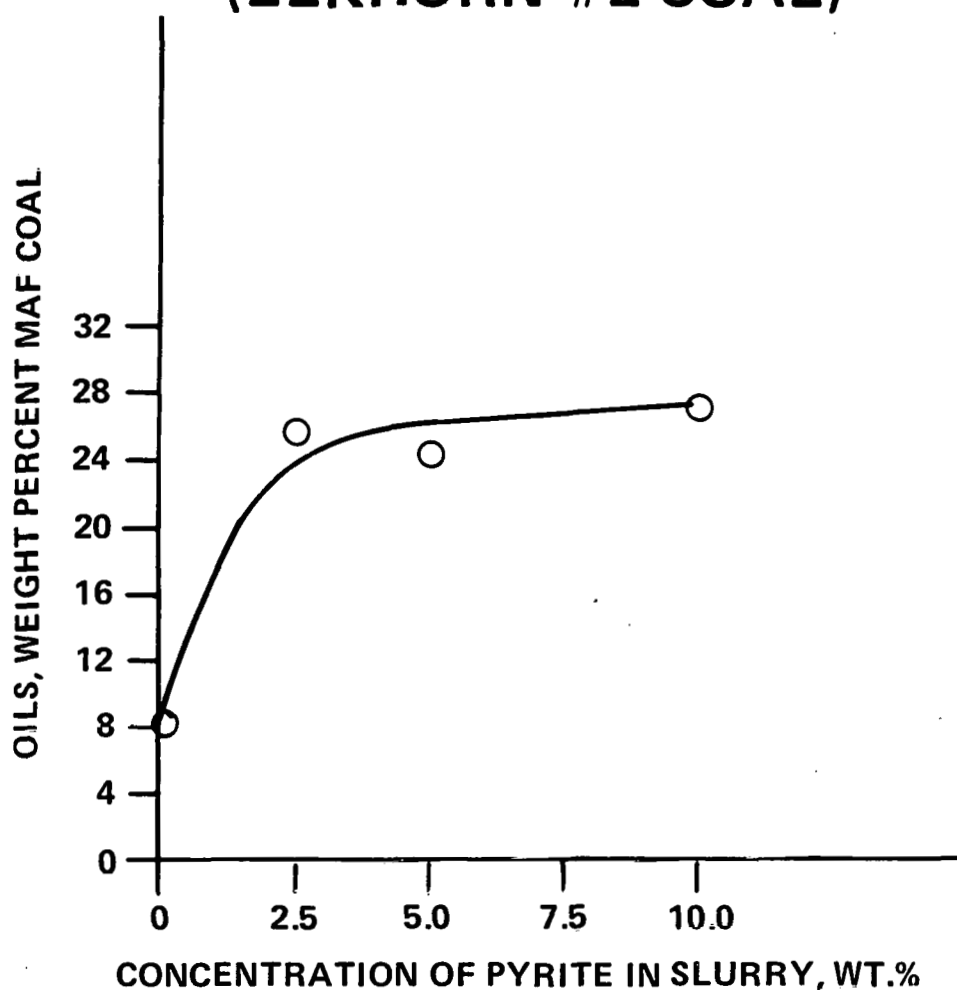
FIGURE 33
VARIATION IN THE PRODUCTION OF ASPHALTENES
AND PREASPHALTENES WITH THE CONCENTRATION
OF PYRITE (ELKHORN #2 COAL)
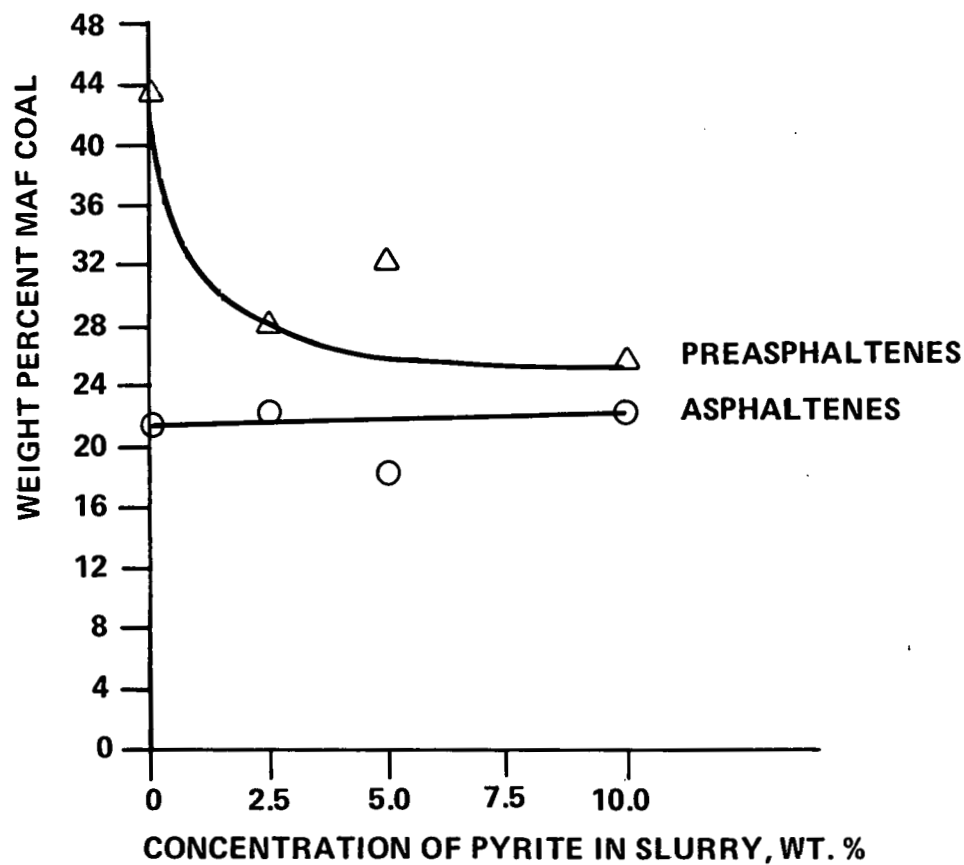
FIGURE 34
VARIATION OF SRC SULFUR CONTENT WITH THE CONCENTRATION OF PYRITE
(ELKHORN #2 COAL)
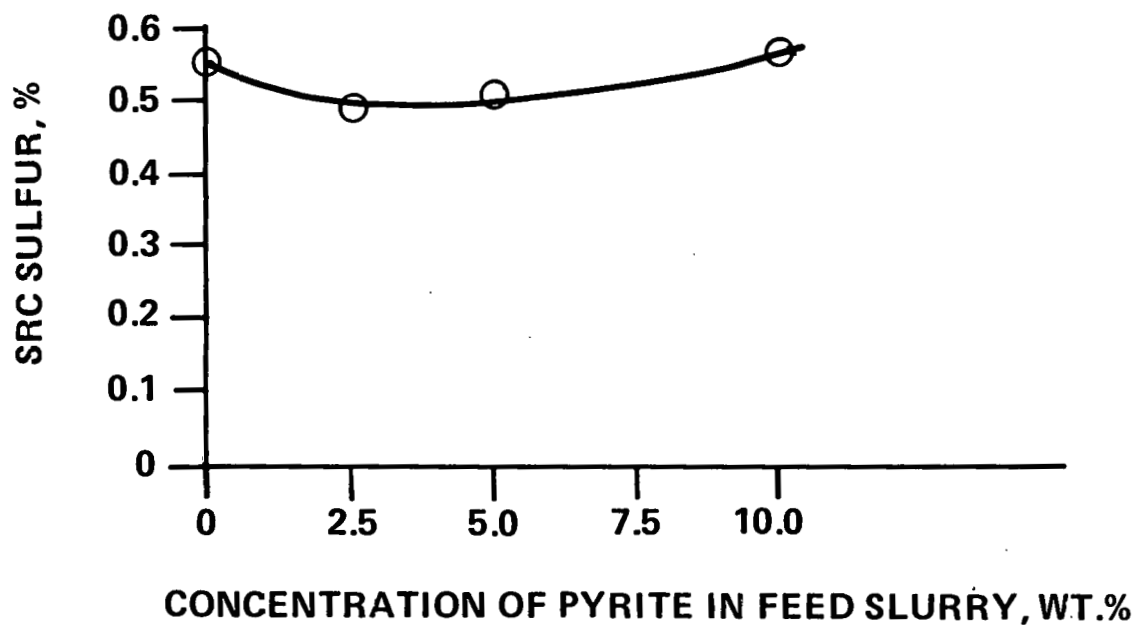
FIGURE 35
VARIATION OF HYDROGEN CONSUMPTION WITH
THE CONCENTRATION OF PYRITE
(ELKHORN #2 COAL)
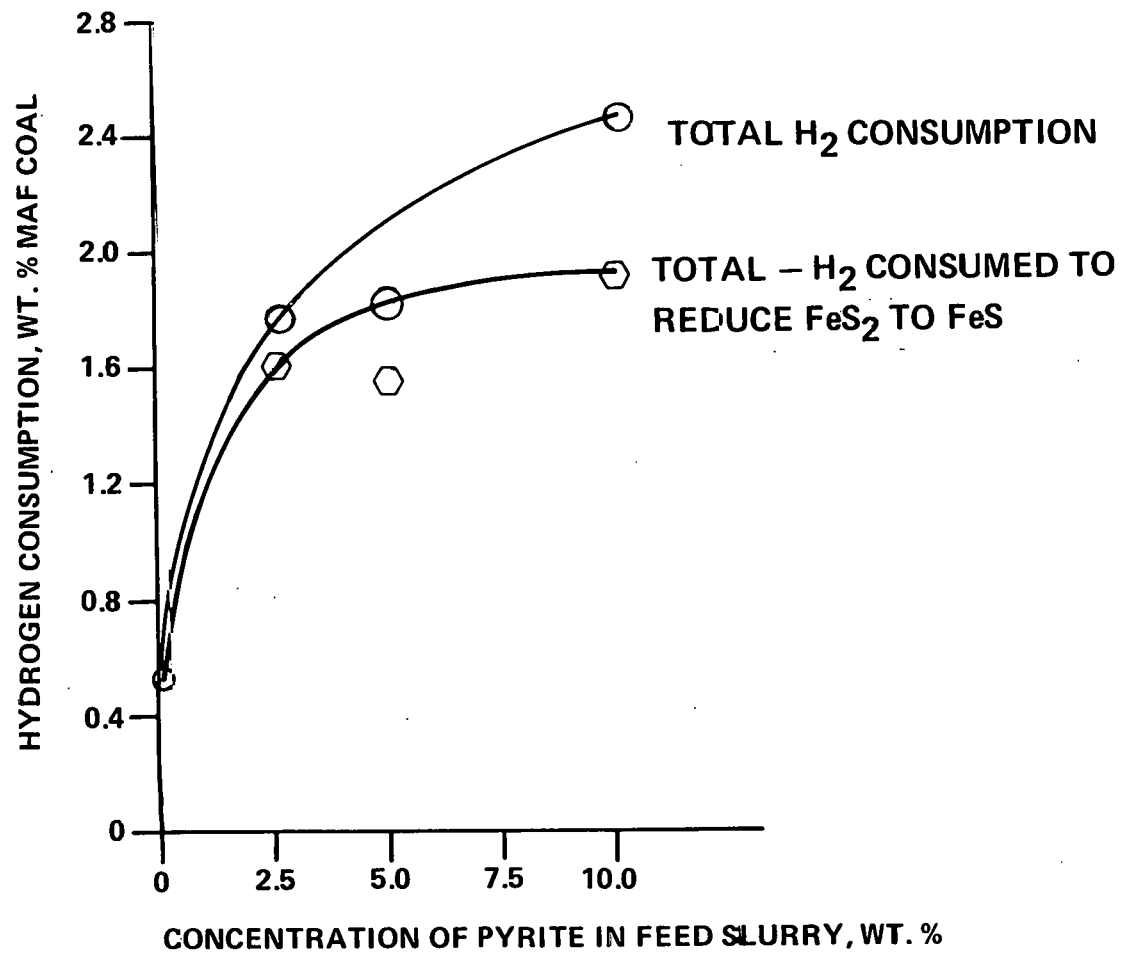
Table 88

Elemental Distribution in the
Elkhorn #2 Coal Liquefaction Products in the
Presence of Different Amounts of Robena Pyrite

Sample No.	31-139	31-161	31-175	31-196
Pyrite Concentration, wt.% of Feed Slury	0.0	2.5	5.0	10.0
Oil Fraction, Wt.%				
C	89.7	89.5	89.4	89.4
H	7.2	7.3	7.5	7.5
O	1.8	1.7	1.7	1.6
N	0.7	0.8	0.8	0.9
S	0.6	0.6	0.6	0.6
$\bar{n}$ MW	205	220	245	210
Asphaltene Fraction, Wt.%				
C	87.0	86.6	86.4	87.3
H	6.1	5.8	5.9	6.0
O	5.0	4.8	5.0	5.1
N	1.4	2.4	2.2	--
S	0.5	0.5	0.5	0.5
Preasphaltene Fraction, Wt.%				
C	86.6	86.1	86.6	85.8
H	4.9	4.8	5.0	5.0
O	5.4	5.8	5.6	5.7
N	2.4	2.4	2.3	2.3
S	0.6	0.5	0.5	0.6

FIGURE 36
EFFECT OF CONCENTRATION OF PYRITE ON SIMULATED DISTILLATION OF OIL FRACTIONS (ELKHORN #2 COAL)
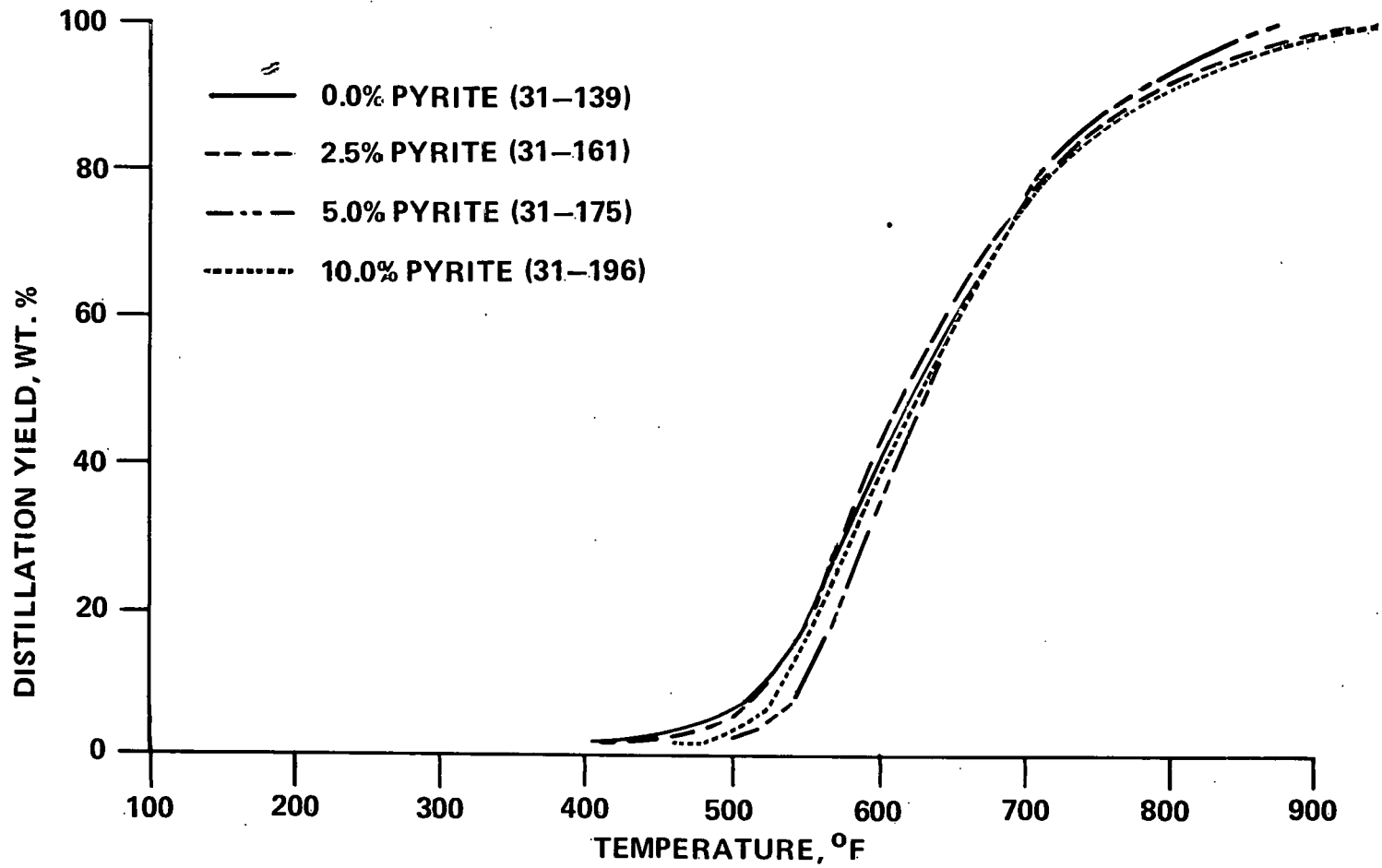
Table 89

Distribution of Oxygen and Nitrogen Compounds in the
Oil Fractions from the Liquefaction of Elkhorn #2 Coal
in the Presence of Different Concentration Level of Pyrite

Sample No.	31-139		31-161		31-175		31-196	
Pyrite Conc., wt.% of Slurry	0.0		2.5		5.0		10.0	
Oxygen Distribution, wt.%								
Total Oxygen	1.79		1.73		1.71		1.65	
	Abs.[1]	Rel.[2]	Abs.	Rel.	Abs.	Rel.	Abs.	Rel.
O as O	1.14	63.7	1.02	60.0	1.04	60.8	0.99	60.0
O as OH	0.65	36.3	0.71	40.0	0.67	39.2	0.66	40.0
Nitrogen Distribution, wt.%								
Total Nitrogen	0.66		0.81		0.78		0.86	
	Abs.	Rel.	Abs.	Rel.	Abs.	Rel.	Abs.	Rel.
N as N	0.27	40.9	0.41	50.6	0.38	48.7	--	--
N as NH	0.32	48.5	0.33	40.7	0.33	42.3	0.33	38.4
N as NH_2	0.07	10.6	0.07	8.7	0.07	9.0	--	--

[1] Abs. - Absolute
[2] Rel. - Relative

Table 90

Distribution of Protons in the Oil Fractions
from the Liquefaction of Elkhorn #2 Coal in the
Presence of Different Concentration Levels of Pyrite

Sample No.	31-139		31-161		31-175		31-196	
Pyrite Conc., wt.% of Feed Slurry	0.0		2.5		5.0		10.0	
Total Hydrogen, wt.%	7.2		7.3		7.5		7.5	

Distribution of Protons, %

	Abs.[1]	Rel.[2]	Abs.	Rel.	Abs.	Rel.	Abs.	Rel.
H_{AR}	3.38	46.9	3.19	43.7	3.30	44.0	3.20	42.6
H_a	2.01	27.9	2.13	29.2	2.27	30.3	2.15	28.7
H_o	1.81	25.2	1.98	27.0	1.93	25.7	2.15	28.7

[1] Abs. - Absolute
[2] Rel. - Relative

Table 91

Brown-Ladner Structural Parameters for the
Oil Fractions from the Liquefaction of Elkhorn #2 Coal
in the Presence of Different Concentration Levels of Pyrite

Sample No.	31-139	31-161	31-175	31-196
Pyrite Concentration, wt.% of Feed Slurry	0.0	2.5	5.0	10.0
f_a	0.72	0.71	0.71	0.70
σ	0.27	0.28	0.29	0.28
H_{AR}/C_{AR}	0.84	0.82	0.84	0.80
R_a	3.07	3.30	3.46	3.19

also shown earlier (page 119) that the addition of pyrite to coal liquefaction increased the coal conversion as well as oil production. Therefore it was of great value to know whether further increase in oil production could be attained by increasing hydrogen flow rate in the presence of pyrite.

Several experiments were performed with different Kentucky coals to evaluate the impact of total available hydrogen on their liquefaction in the presence of pyrite. The results obtained from the above experiments are discussed below.

Elkhorn #3 Coal - Elkhorn #3 coal conversion and oil production was unchanged with increasing hydrogen flow rate in the presence of pyrite (Table 64). Hydrocarbon gas production decreased and water production, preasphaltene conversion, and asphaltene production increased with flow rate. Hydrogen consumption appeared to increase slightly with increasing flow rate. Hydrogen content in asphaltenes increased with increasing hydrogen flow rate as shown in Table 65.

The above results show that increased hydrogen flow rate with Elkhorn #3 coal did not alter conversion or oils make, but increased the yield of asphaltenes.

Kentucky #9 Coal - The effect of hydrogen flow rate on the liquefaction of Kentucky #9 coal in the presence of pyrite is shown in Table 77. Coal conversion and oils make increased while preasphaltene yield decreased with increasing flow rate. Hydrogen consumption decreased slightly with increasing flow rate.

The distribution of elements in the various fractions given in Table 78 showed insignificant change in the hydrogen contents of oils, asphaltenes and preasphaltenes with increasing hydrogen flow rate. The oxygen and sulfur contents in some fractions were lower at the higher hydrogen flow rate. Although all fractions showed insignificant variations in nitrogen contents, the number average molecular weights were consistently lower at the higher hydrogen flow rate.

The concentration of quinoline-type compounds in the oil fraction increased with higher hydrogen flow rate as shown in Table 79; no other significant differences were noted. The concentration of oxygen compounds, like ethers, decreased with increasing hydrogen flow rate from 0.90 to 0.67%, which was indicative of improved deoxygenation. The NMR data for the oil fractions obtained at the two flow rates were similar (Table 80). The simulated distillation of the oil fractions obtained at different hydrogen flow rates showed a sizable difference as depicted in Figure 37.

Elkhorn #2 Coal - Increasing the hydrogen flow rate when running Elkhorn #2 coal from 22.5 to 49.7 Mscf per ton of coal in the presence of pyrite did not alter conversion of coal or the production of oils. Likewise, the production of hydrocarbon gases and asphaltenes remained the same (Table 92). Hydrogen consumption increased slightly with increasing flow rate. No significant difference were noted in the simulated distillation of oil fractions obtained at the two hydrogen flow rates in the presence of pyrite (see Figure 38).

The distribution of elements in the various fractions obtained at the two rates (Table 93) showed higher hydrogen contents in all the fractions at the higher rate. No significant differences were noted in the distribution of oxygen and nitrogen compounds in the oil fractions (Table 94). The concentrations of H_{AR} decreased and H_a and H_o increased with flow rate (Table 95). The values of f_a and σ did not change with an increase in rate.

The effect of the hydrogen flow rate in the presence of pyrite revealed that increasing flow rate did not change the overall conversion of Kentucky coals. However, higher flow rate yielded higher oil production with Kentucky #9 coal, whereas it showed no significant improvement in oil production with either Elkhorn #2 or Elkhorn #3 coal. No conclusion could be drawn regarding the effect of hydrogen flow rate on hydrogen consumption because it increased with flow rate in some cases and decreased in others. On the contrary, increasing hydrogen flow rate in the absence of pyrite increased the oil production and

FIGURE 37
EFFECT OF HYDROGEN FLOW RATE ON SIMULATED DISTILLATION OF OIL FRACTIONS OBTAINED FROM LIQUEFACTION OF KY #9 COAL IN THE PRESENCE OF ROBENA PYRITE

HYDROGEN FLOW RATE
- - - - 21.83 MSCF/T (CCL - 28 - 46)
——— 45.89 MSCF/T (CCL - 28 - 56)

DISTILLATION YIELD, WT. %
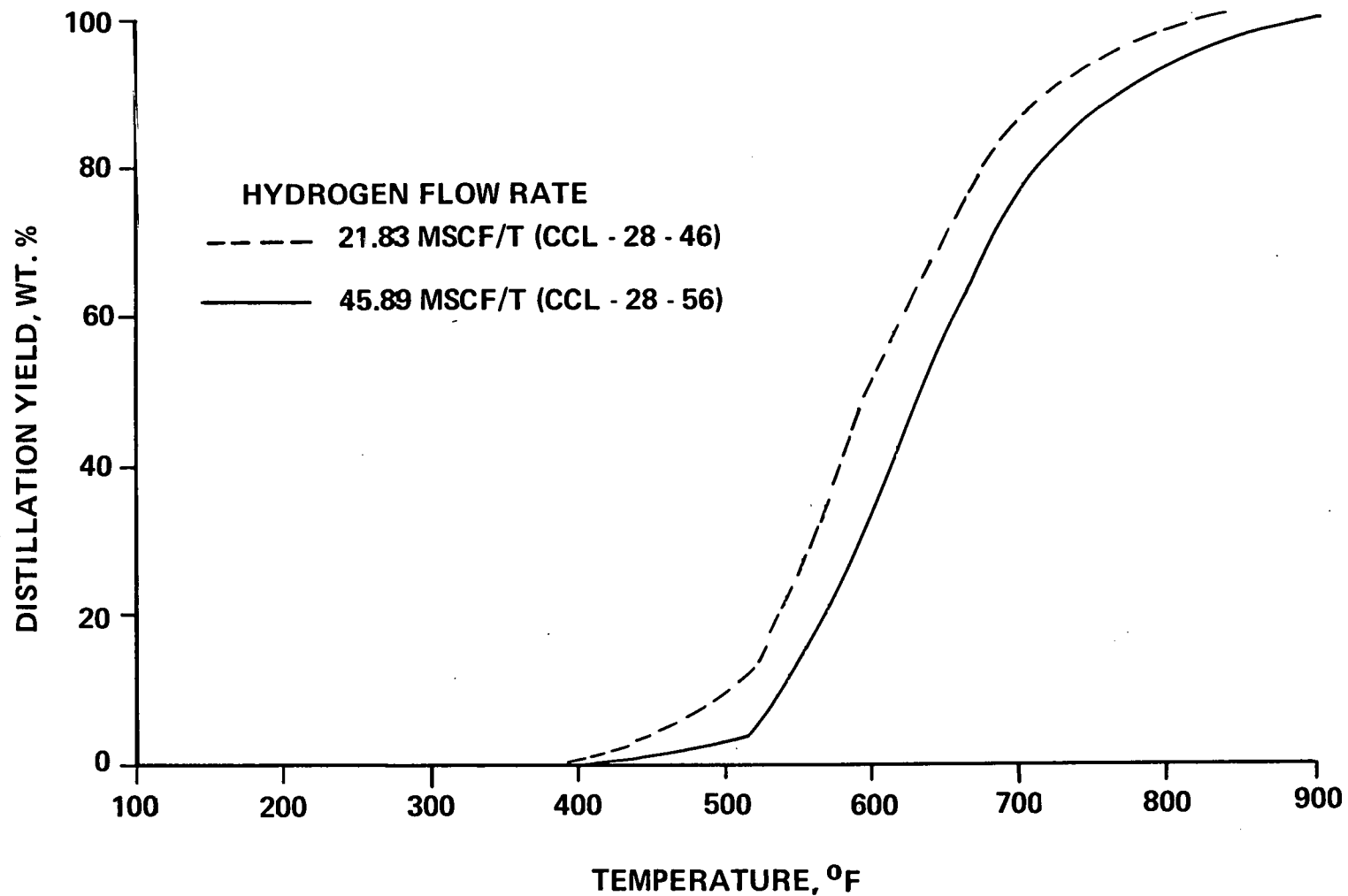
TEMPERATURE, °F

Table 92

Effect of Hydrogen Flow Rate on Liquefaction of
Elkhorn #2 Coal in The Presence of Robena Pyrite

Sample No.	31-196	31-206
Temperature, °F	850	850
Pressure, psig	2000	2000
Residence Time, Min.	39	41
Hydrogen Treat Rate, MSCF/T	22.5	49.7
Product Distribution, wt.% MAF Coal		
HC	10.6	10.6
CO, CO_2	1.2	1.1
H_2S	0.0	0.0
NH_3	0.0	0.1
Oils	27.0	28.1
Asphaltenes	22.3	22.7
Preasphaltenes	25.6	23.6
I.O.M.	9.3	9.4
Water	4.0	4.4
Conversion, wt. % MAF Coal	90.7	90.6
Hydrogen Consumption, wt.% MAF Coal		
Total	2.41	2.63
From Gas	2.92	3.55
From Solvent	(0.51)	(0.92)
By Pyrite	0.50	0.50
SRC Sulfur	0.57	0.58
First Order Rate Constant, hr^{-1}		
K_a	1.25	1.23
K_p	2.86	3.05

[1] ( ) - negative value

180

FIGURE 38
EFFECT OF HYDROGEN FLOW RATE ON SIMULATED DISTILLATION OF OIL FRACTIONS OBTAINED BY LIQUEFACTION OF ELKHORN #2 COAL IN THE PRESENCE OF PYRITE

HYDROGEN FLOW RATE

——— 22.5 MSCF/T (31–196)

– – – 49.7 MSCF/T (31–206)
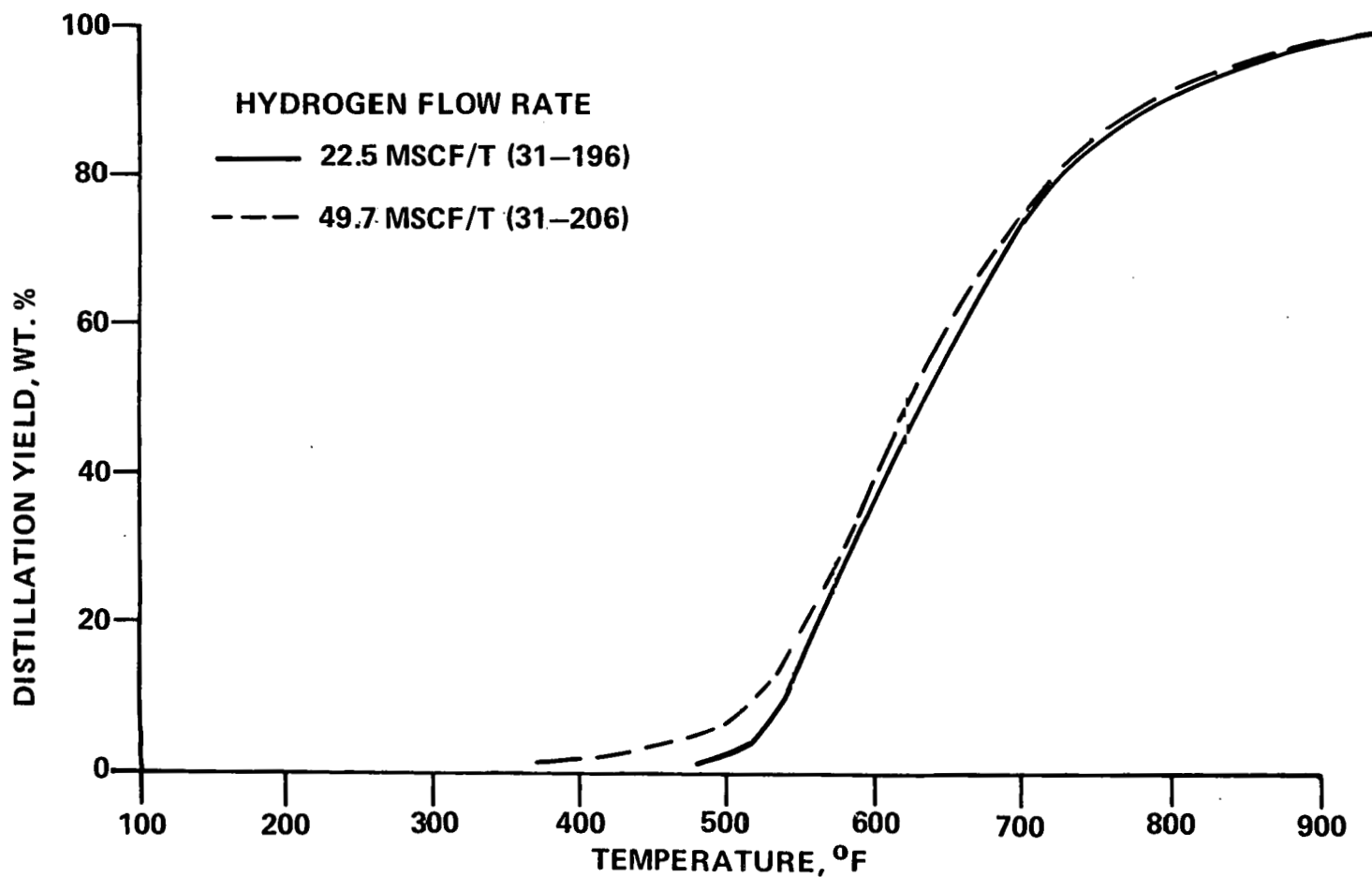
Table 93

Effect of Hydrogen Flow Rate on the Distribution of Elements
in the Solubility Fractions from the Liquefaction
of Elkhorn #2 Coal in the Presence of Robena Pyrite

Sample No.	31-196	31-206
Temperature, °F	850	850
Hydrogen Treat Rate, MSCF/T	22.5	49.7
Oil Fraction, wt.%		
C	89.4	89.3
H	7.5	7.7
O	1.6	1.6
N	0.9	0.8
S	0.6	0.6
$\bar{n}$ MW	210	235
Asphaltene Fraction, wt.%		
C	87.3	86.8
H	6.0	6.3
O	5.1	4.4
N	--	2.0
S	0.5	0.5
Preasphaltene Fraction, wt.%		
C	85.8	85.4
H	5.0	5.3
O	5.7	5.3
N	2.3	2.7
S	0.6	0.7

Table 94

Distribution of Nitrogen and Oxygen Compounds in the Oil
Fractions from the Liquefaction of Elkhorn #2 Coal
at Two Different Hydrogen Flow Rates

Sample No.			31-196			31-206	
Temperature, °F			850			850	
H_2 Flow Rate, MSCF/T			22.5			49.7	
Total Nitrogen, wt.%			0.66			0.68	
Total Oxygen, wt.%			1.65			1.57	

Nitrogen Distribution, wt.%

	Abs.	Rel.		Abs.	Rel.
N as N	0.33	50.0		0.35	51.5
N as NH	0.33	50.0		0.33	48.5
N as NH_2	--	--		--	--

Oxygen Distribution, wt.%

	Abs.	Rel.		Abs.	Rel.
O as O	0.99	60.0		0.89	56.7
O as OH	0.66	40.0		0.68	43.3

---

[1] Abs. - Absolute

[2] Rel. - Relative

Table 95

Distribution of Protons in the Oil Fractions from the
Liquefaction of Elkhorn #2 Coal at Two Different H_2 Flow Rates

Sample No.	31-196		31-206	
H_2 Flow Rate, MSCF/T	22.5		49.7	
Total Hydrogen, wt.%	7.5		7.7	
Proton Distribution, %				
	Abs.	Rel.	Abs.	Rel.
H_{AR}	3.20	42.6	3.00	39.0
H_a	2.15	28.7	2.39	31.0
H_o	2.15	28.7	2.31	30.0

[1] Abs. - Absolute
[2] Rel. - Relative

Table 96

Variation of Brown-Ladner Structural Parameters for
Oil Fractions from the Liquefaction of
Elkhorn #2 Coal at Two Different Hydrogen Flow Rates

Sample No.	31-196	31-206
H_2 Flow Rate, MSCF/T	22.5	49.7
f_a	0.70	0.69
σ	0.28	0.29
H_{AR}/C_{AR}	0.80	0.79
R_a	3.19	3.54

hydrogen consumption in Elkhorn #2 coal liquefaction (see page 80). These observations seem to indicate that noncatalytic coal liquefaction is more sensitive to flow rate (effective hydrogen partial pressure) than is catalytic coal liquefaction.

Various Mineral Pyrites - Pyrite samples from various sources were tested in a tubing-bomb reactor for their catalytic activity in Floyd County Elkhorn #3 coal liquefaction. Since Elkhorn #3 coal was used in establishing base-line, it was decided to continue using it for testing the catalytic activity of minerals and metallic wastes. The conversion of coal increased with the addition of all the pyrites, as shown in Table 97. Coal conversion on the order of 85% was noted with all the mineral pyrite samples. Oil production increased from 16 to ~47% with various pyrites. Asphaltene and preasphaltene production were similar with pyrites from Mexico, South Dakota, and Matheson Coleman Bell (MCB). The increase in oil production with these pyrites was due to increased conversion of asphaltenes to oils.

Various Pyrite Samples Separated from Coal - Pyrite samples separated from various coals were tested in a tubing-bomb reactor for their catalytic activity in coal liquefaction. Coal conversion increased with the addition of all the pyrites, as shown in Table 98. Oil production increased by more than a factor of two with addition of some of the pyrite samples (i.e., 16% to more than 31%). Asphaltene production decreased with pyrites except for Robena pyrite compared to the no-additive run. The increased production of oil was due to increased conversion of asphaltenes to oil. The production of gas and preasphaltenes was not greatly affected by the addition of various pyrite samples.

Effect of Coal Cleaning on Liquefaction - Ireland mine coal and beneficiated products provided by DOE were studied to determine the effect of coal cleaning on liquefaction. The coal sample was cleaned by flotation using a 1.30 specific gravity media. A sample of coal prepared by adding pyrite separated from coal to the deep-cleaned coal was also provided to study the catalytic activity of pyrite. Another sample of Ireland coal cleaned by oil agglomeration was supplied to study the effect of selective cleaning of coal. The detailed analyses on raw and cleaned coals from Ireland mine summarized in Table 4

185

Table 97

Catalytic Activity of Different Mineral Pyrites in Coal Liquefaction

| | | Product Distribution, wt.% MAF Coal | | |
| | | Siniola, Mexico | South Dakota | MCB |
Additive	None	Pyrite	Pyrite	Pyrite
Oils	16	47	48	46
Asphaltenes	48	29	29	28
Preasphaltenes	13	9	10	10
I.O.M.	23	15	13	16
Conversion	77	85	87	84

Reaction Mixture: Coal - 3 g (Floyd County Elkhorn #3)
                     Solvent - 6 g
                     Additive - 1 g

Reaction Condition: Temperature - 450°C
                     Pressure - 1250 psig H_2 at 25°C
                     Time - 60 Minutes

Reactor: Tubing-Bomb
           Volume - 46.3 ml.

For the purpose of calculations, all pyrites (FeS_2) are assumed to form FeS during reaction.

Table 98

Catalytic Activity of Pyrite Samples Separated from Various Coals

Product Distribution, wt.% MAF Coal

Additive	None	McDowell County, WV	Union County, Ky.	Cambria County, Pa.	Washington County, Pa.	Webster County, Ky.	Ireland Mine	Robena Pyrite, Pa
Purity of Pyrites	--	37.1	78.4	50.1	36.9	87.3	46.8	75.7
Gas	11	13	12	13	14	11/a	8	9
Oils	16	33	40	39	33	31	42	35
Asphaltenes	39	26	29	26	29	30	26	40
Preasphaltenes	14	13	11	12	13	14	11	7
I.O.M.	20	15	8	10	11	14	13	9
Conversion	80	85	92	90	89	86	87	91

Reaction Mixture: Coal - 3 g (Floyd County Elkhorn #3)
Solvent - 6 g
Additive - 1g

Reaction Condition: Temperature - 450°C
Pressure - 1250 psig H_2 at 25°C
Time - 60 Minutes

Reactor: Tubing-Bomb
Volume - 46.3 ml.

showed significant variations in the concentration of pyrite among different samples. The liquefaction behavior of raw, deep-cleaned, deep-cleaned-plus-pyrite, and coal cleaned by oil agglomeration is shown in Table 99. The raw coal sample (ash = 35.04%) showed a conversion of 85%. Oil and asphaltene production were 14 and 42%, respectively. Conversion of the deep-cleaned coal (ash = 2.48%; pyrite = 0.17%) was very similar to that of raw coal, but oil production decreased significantly from 14 to 2%. The decrease in oil production was due to lower ash and pyrite contents in the deep-cleaned coal than raw coal. Preasphaltene and asphaltene production increased from 15 to 21% and from 42 to 46%, respectively. When part of the recovered pyrite was again added to the deep-cleaned coal sample (ash = 15.47%, pyrite = 3.83%), the liquefaction behavior of the combined mixture approached that of raw coal, showing that pyrite catalyzes the conversion of asphaltenes and preasphaltenes to oils. The coal cleaned by oil agglomeration contained the highest amount of pyrite (pyrite = 5.08%) and therefore showed the highest coal conversion and oil production among all the raw and cleaned coal samples (Table 99). Part of this increased coal conversion and oil production could be due to physical adsorption of kerosene on the oil agglomerated coal sample.

Catalysis by Reduced Pyrite

A large sample of Robena pyrite was reduced at 842°F for 3 hours with hydrogen gas in a reduction unit. The X-ray diffraction analysis of the treated material showed that it was composed of approximately 60% pyrrhotite ($FeS_{1.074}$) and 40% troilite (FeS). Results on the catalytic activity of the reduced pyrite sample in the liquefaction of Elkhorn #2 coal at 825°F are summarized in Table 100. Conversion of coal and preasphaltenes and the production of oils increased significantly with the addition of reduced pyrite compared with the no-additive run; oil production increased by over a factor of two. Rates of conversion of asphaltenes and preasphaltenes also increased considerably with reduced pyrite. The production of asphaltenes decreased slightly, and that of hydrocarbon gases, CO, CO_2, and water were unchanged with reduced pyrite over the no-additive run. Hydrogen consumption and SRC sulfur content increased marginally with reduced pyrite addition.

Table 99

Liquefaction Behavior of Raw and Cleaned Ireland Mine Coal Samples

Product Distribution, wt.% MAF Coal

Coal	Raw	Deep Cleaned	Deep Cleaned + Pyrite	Cleaned by Oil Agglomeration
Gas	14	14	11	12
Oils	14	2	16	23
Asphaltenes	42	46	39	37
Preasphaltenes	15	21	17	15
I.O.M.	15	17	17	13
Conversion	85	83	83	90

Reaction Mixture: Coal - 3 g
Solvent - 6 g

Reaction Conditions: Temperature - 450°C
Pressure - 1250 psig H_2 at 25°C
Time - 60 Minutes

Reactor: Tubing-Bomb
Volume - 46.3 m.

Table 100

Catalytic Activity of Reduced Robena Pyrite in
Liquefaction of Elkhorn #2 Coal

Sample No.	31-128	44-20
Feed Composition	70% Solvent + 30% Coal	67.5% Solvent + 30% Coal + 2.5% Reduced Pyrite
Temp., °F	825	825
H_2 Flow Rate, MSCF/T	18.9	24.3
Pressure, psig	2000	2000
Reaction Time, Min.	35	39.5
Product Distribution, wt.% MAF Coal		
HC	5.2	5.0
CO, CO_2	0.7	0.8
H_2S	0.3	1.0
Oils	12.2	29.6
Asphaltenes	21.2	17.3
Preasphaltenes	44.2	34.5
I.O.M.	14.7	10.3
Water	1.5	1.5
Conversion	85.3	89.7
Hydrogen Consumption, wt.% MAF Coal		
Total	0.64	0.83
From Gas	0.59	0.69
From Solvent	0.05	0.14
SRC Sulfur, %	0.61	0.64
First Order Rate Constants, hr^{-1}		
K_a	0.62	1.52
K_p	1.27	2.01

190

Distribution of elements in the various fractions given in Table 101 showed no significant differences in hydrogen, oxygen, nitrogen, and sulfur contents of various fractions obtained with and without reduced pyrite. Higher concentrations of H_{AR} and H_a and a lower value of H_o was noted in the oil fraction obtained with reduced pyrite, as shown in Table 102. No positive conclusions could be drawn about solvent quality from the proton distribution data.

From the above data it can be concluded that the addition of reduced pyrite to coal during liquefaction increases oil production and the rate of conversion of asphaltenes and preasphaltenes. Reduced pyrite also marginally increases the overall hydrogen consumption, but does not have any impact on production of gases and removal of SRC sulfur.

Catalysis by Iron Oxide

The catalytic activity of pyrite was discussed in detail in the previous section. Like pyrite, iron oxide is inexpensive and available in large quantities, making it a potential disposable catalyst in coal liquefaction.

Thermal Properties - The TGA of iron oxide (Fe_2O_3) in the presence of hydrogen gas showed complete reduction to elemental iron at approximately 550°C (1022°F). Iron oxide, however, showed a weight loss of 21% when reduced in hydrogen in the PTGR at 842°F and 1000 psig pressure instead of the 30% weight loss necessary for stoichiometric reduction of Fe_2O_3 to elemental iron. This suggests that incomplete reduction of iron oxide (Fe_2O_3) to elemental iron may occur at typical coal liquefaction reaction temperatures. On the contrary, complete conversion of iron oxide to iron sulfide may occur due to the presence of H_2S in coal liquefaction reaction.

Activity of Iron Oxide - Two different samples of iron oxide, mineral-grade and reagent-grade, were studied for their catalytic activity in coal liquefaction. Speculite, mineral-grade iron oxide, is a rather pure mineral and it contains 95% Fe_2O_3 (Table 8). Reagent-grade iron oxide, on the contrary, is 100% Fe_2O_3. Both samples were ground to -200 mesh before use in coal liquefaction. The catalytic activity of these iron oxide samples is discussed below.

Table 101

Effect of Reduced Pyrite on Distribution of
Elements in Liquefaction Products from Elkhorn #2 Coal

Sample No.	Original Solvent (FOB #11)	31-128	44-20
Catalyst	--	None	Reduced Pyrite
Oil Fraction, wt.%			
C	89.7	89.5	89.6
H	7.2	7.2	7.2
O	1.4	1.7	1.7
N	1.1	0.9	0.9
S	0.6	0.7	0.6
Asphaltene Fraction, wt.%			
C	ND[1]	85.9	84.5
H	ND	6.3	5.9
O	ND	5.8	6.6
N	ND	1.4	2.4
S	ND	0.6	0.6
Preasphaltene Fraction, wt.%			
C	ND	85.3	--
H	ND	5.2	4.8
O	ND	6.2	10.0
N	ND	2.2	2.3
S	ND	0.6	0.7

Oxygen is determined by difference

[1] Not determined

Table 102

Effect of Reduced Pyrite on Distribution of Protons in the
Oil Fractions from Liquefaction of Elkhorn #2 Coal

Sample No.	Original Solvent (FOB #11)	31-128	44-20
Catalyst	--	None	Reduced Pyrite
Total Hydrogen	7.2	7.2	7.2
Distribution of Protons, %			
Absolute			
H_{AR}	3.20	3.26	3.37
H_a	2.02	1.95	2.03
H_o	1.98	1.99	1.80
Relative			
H_{AR}	44.4	45.3	46.8
H_a	28.0	27.1	28.2
H_o	27.6	27.6	25.0

Speculite (Mineral-Grade Fe_2O_3) - The catalytic activity of speculite was studied at both 825 and 850°F (Table 103). A concentration of 10 wt% speculite based on feed slurry was used to positively identify its catalytic activity. Data on liquefaction in the presence of speculite at 850°F showed that the production of hydrocarbon gases, oils, preasphaltenes, and water increased from 6.8 to 9.6%, 20.4 to 25.4%, 25.4 to 31.0% and 1.2 to 4.6%, respectively, coal conversion increased from 84 to 90% (Table 103). The rate of asphaltene conversion increased from 0.75 to 1.37, whereas that of preasphaltene conversion decreased from 2.95 to 2.13. Speculite apparently catalyzes the asphaltene conversion to oils but has a negative effect on preasphaltene conversion. The SRC sulfur content was very similar in both the cases. A significant increase in hydrogen consumption occurred from 0.91% with no-additive to 1.84% with speculite. The increased hydrogen consumption was due mainly to increased production of hydrocarbon gases, oils, and water, as well as to supplying the hydrogen required to reduce Fe_2O_3 to Fe_3O_4 and elemental iron.

No major differences in the hydrogen, oxygen, nitrogen and sulfur contents in the oils were noted with speculite (see Table 104); lower ether and higher hydroxyl-type compound concentrations were observed with speculite compared with the no-additive run, as shown in Table 105. Some variation in the distribution of nitrogen compounds with and without speculite is shown in Table 105. Table 106 shows no significant variation in the distribution of protons with and without speculite addition. The values of the Brown-Ladner structural parameters were very similar with and without the addition of speculite. However, the simulated distillation of oil fractions (Figure 39) showed marked differences in the boiling point distribution in that the oils obtained with speculite covered a wider boiling point range compared with the no-additive run.

The temperature sensitivity to speculite showed that the conversion of coal was essentially unchanged. Increasing the reaction temperature from 825 to 850°F also had almost no effect on oil production (23.8 vs. 25.4%). Hydrocarbon gas production increased from 4.9 to 9.6%. No change in asphaltene production was noted, but preasphaltenes decreased from 39.8 to 31.0% with the increase in temperature. Most of the converted preasphaltenes were found in the gaseous hydrocarbon fraction. The reaction rates for asphaltene and

Table 103

Liquefaction of Elkhorn #3 Coal in the Presence of Mineral-Grade Iron Oxide

Sample No.	31-81	31-248	31-258
Feed Composition	70% Solvent +	60% Solvent +	
	30% Coal	30% Coal +	
		10% Speculite	
Temperature, °F	850	825	850
Pressure, psig	2000	2000	2000
Hydrogen Flow Rate, MSCF/T	18.6	22.5	23.8
Reaction Time, Min.	38	38	38
Product Distribution, wt.% MAF Coal			
HC	6.8	4.9	9.6
CO, CO_2	1.0	1.2	1.4
H_2S	0.2	0.1	0.1
NH_3	0.0	0.0	0.0
Oils	20.4	23.8	25.4
Asphaltenes	29.2	17.8	17.5
Preasphaltenes	25.4	39.8	31.0
I.O.M.	15.8	8.9	10.4
Water	1.2	3.5	4.6
Conversion	84.2	91.1	89.6
Hydrogen Consumption, wt.% MAF Coal			
Total	0.91	1.38	1.84
From Gas	0.92	1.31	1.69
From Solvent	(0.01)[1]	0.07	0.15
By Additive	--	0.17	0.17
SRC Sulfur, %	0.50	0.64	0.54
First Order Rate Constants, hr^{-1}			
K_a	0.75	1.26	1.37
K_p	2.95	1.61	2.13

[1] ( ) - means negative value

195

Table 104

Distribution of Elements in the Liquefaction Products of
Elkhorn #3 Coal in the Presence of Mineral-Grade Iron Oxide

Sample No.	31-81	31-248	31-258
Additive	None	Speculite	
Temperature, °F	850	825	850
Oil Fraction, wt.%			
C	89.7	89.7	89.9
H	7.3	7.2	7.2
O	1.7	1.6	1.6
N	0.7	0.8	0.7
S	0.6	0.7	0.7
$\bar{n}$ MW	220	195	240
Asphaltene Fraction, wt.%			
C	86.1	86.3	87.1
H	6.1	6.0	5.8
O	4.9	5.6	5.2
N	2.4	1.6	1.3
S	0.5	0.6	0.5
$\bar{n}$ MW	390	--	480
Preasphaltene Fraction, wt.%			
C	86.2	85.2	86.4
H	5.1	4.9	4.7
O	5.9	6.4	5.6
N	2.5	2.6	2.5
S	0.5	0.7	0.6
$\bar{n}$ MW	990	1930	1820

Table 105

Distribution of Oxygen and Nitrogen
Compounds in the Oil Fraction from the Liquefaction
Product of Elkhorn #3 Coal in the Presence of Mineral-Grade Iron Oxide

Sample No.	FOB #11 Original Solvent		31-81		31-248		31-258	
Additive	--		None		Speculite		Speculite	
Temperature, °F	--		850		825		850	
Oxygen Distribution, wt.%								
Total	1.42		1.72		1.64		1.60	
	Abs.	Rel.	Abs.	Rel.	Abs.	Rel.	Abs.	Rel.
O as O	0.90	63.4	1.09	63.4	0.98	59.8	0.92	57.5
O as OH	0.52	36.6	0.63	36.6	0.66	40.2	0.68	42.5
Nitrogen Distribution, wt.%								
Total	1.05		0.73		0.78		0.65	
	Abs.	Rel.	Abs.	Rel.	Abs.	Rel.	Abs.	Rel.
N as N	0.61	58.1	0.30	41.1	0.40	51.3	0.28	43.1
N as NH	0.38	36.2	0.32	43.8	0.32	41.0	0.32	49.2
N as NH_2	0.06	5.7	0.11	15.1	0.06	7.7	0.05	7.7

Table 106

Distribution of Protons in the Oil Fractions from the Liquefaction
of Elkhorn #3 Coal in the Presence of Mineral-Grade Iron Oxide

	FOB #11			
Sample No.	Original Solvent	31-81	31-248	31-258
Additive	--	None	Speculite	
Temperature, °F	--	850	825	850
Total Hydrogen, Wt.%	7.2	7.3	7.2	7.2
Distribution of Protons, %				
Relative				
H_{AR}	44.4	47.0	45.7	46.8
H_a	28.0	28.0	28.3	28.7
H_o	27.6	25.0	26.0	24.5
Absolute				
H_{AR}	3.20	3.43	3.29	3.37
H_a	2.02	2.04	2.04	2.07
H_o	1.98	1.83	1.87	1.76

Table 107

Brown-Ladner Structural Parameters for the Oil
Fractions from the Liquefaction Product of Elkhorn #3
Coal in the Presence of Mineral-Grade Iron Oxide

	FOB #11			
Sample No.	Original Solvent	31-81	31-248	31-258
Additive	--	None	Speculite	
Temperature, °F	--	850	825	850
f_a	0.71	0.72	0.72	0.72
σ	0.28	0.27	0.28	0.29
H_{AR}/C_{AR}	0.80	0.85	0.83	0.84
R_a	3.23	3.18	3.03	3.45

FIGURE 39
COMPARISON OF SIMULATED DISTILLATION OF OIL
FRACTIONS OBTAINED BY LIQUEFACTION OF
ELKHORN #3 COAL IN THE PRESENCE AND ABSENCE
OF SPECULITE AT 850° F
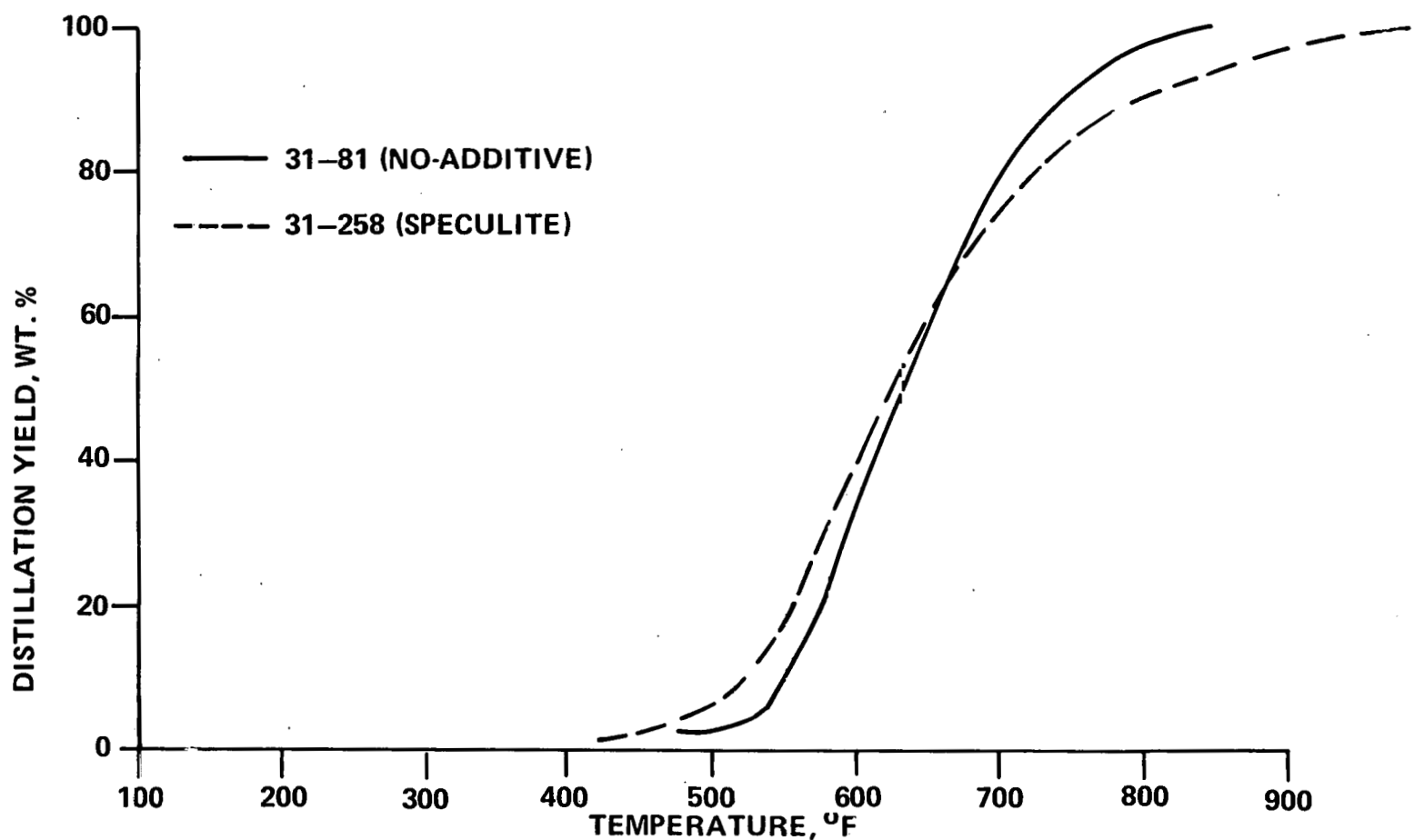
preasphaltene conversion increased from 1.26 to 1.37 and from 1.61 to 2.13, respectively, with increasing temperature. The conversion of preasphaltenes seemed to be more sensitive to temperature than to asphaltenes. Hydrogen consumption increased from 1.38 to 1.84% as temperature increased from 825 to 850°F. The X-ray diffraction analysis of the coal liquefaction residue material showed it was a mixture of Fe_3O_4, FeS, and elemental iron. A part of the total hydrogen consumed was due to reduction of Fe_2O_3; 0.17 wt% hydrogen based on MAF coal was calculated to be consumed to completely reduce Fe_2O_3 to Fe_3O_4. The SRC sulfur content decreased from 0.64 to 0.54% at the higher reaction temperature.

The distribution of elements in the oils (Table 104) showed no significant changes with reaction temperature, whereas that of asphaltenes and preasphaltenes showed only minor changes. The distribution of oxygen compounds (Table 105) in the oils were unchanged at 825 and 850°F. No significant variations in the distribution of protons and the values of Brown-Ladner structural parameters were noted with the increase in temperature (see Tables 106 and 107).

The above data point out that increasing the coal liquefaction reaction temperature in the presence of speculite increases the production of hydrocarbon gases and oils, increases hydrogen consumption, and decreases the production of preasphaltenes and the sulfur content of SRC. The increase in production of hydrocarbon gases with temperature is much greater than the increase in oils production, and the increase in production of hydrocarbon gases is achieved at the expense of increased hydrogen consumption. In terms of hydrogen consumption, the use of lower temperature is preferred.

Reagent-Grade Iron Oxide - The catalytic activity of reagent-grade Fe_2O_3 in Elkhorn #2 coal liquefaction reaction was studied at 850°F at two iron oxide concentrations. Coal conversion remained unchanged and the production of oil increased with the addition of Fe_2O_3 over the noncatalytic run; oil production increased from 8.3 to 23.7%. The production of asphaltenes and preasphaltenes decreased with Fe_2O_3 addition (Table 108), whereas the rates of conversion of both the preasphaltenes and asphaltenes increased. Hydrogen consumption and SRC sulfur content were essentially unchanged. All the H_2S produced during coal liquefaction was removed by Fe_2O_3. The x-ray diffraction analysis of the liquefaction residue showed complete conversion of Fe_2O_3 to Fe_3O_4 and pyrrhotite.

Table 108

Effect of Reagent-Grade Iron Oxide on Liquefaction of Elkhorn #2 Coal

Sample No.	31-139	38-28	38-40
Feed Composition	70% Solvent+ 30% Coal	68.3% Solvent+ 30% Coal + 1.7% Fe_2O_3	66.6% Solvent+ 30% Coal + 3.4% Fe_2O_3
Temperature, °F	850	850	850
Pressure, psig	2,000	2,000	2,000
Hydrogen Flow Rate, MSCF/T	19.9	27.6	26.0
Reaction Time, Min.	37	42.6	40.6
Product Distribution, Wt.% MAF Coal			
HC	7.0	4.7	6.5
CO, CO_2	0.6	0.6	0.6
H_2S	0.3	0.0	0.0
Oils	8.3	23.7	22.6
Asphaltenes	21.6	18.9	19.1
Preasphaltenes	43.4	35.0	35.7
I.O.M.	15.7	13.8	13.2
Water	3.1	3.3	2.3
Conversion	84.3	86.6	86.8
Hydrogen Consumption, Wt.% MAF Coal			
Total	0.53	0.46	0.68
From Gas	0.44	0.00	0.50
From Solvent	0.09	0.49	0.23
By Fe_2O_3	-	(0.03)[1]	(0.05)
SRC Sulfur, %	0.55	0.48	0.52
First Order Rate Constants, hr^{-1}			
K_a	0.39	1.07	1.08
K_p	1.09	1.66	1.68

---

[1] (   ) means negative value

The distribution of elements in various fractions given in Table 109 showed some changes in the hydrogen and nitrogen contents in all the fractions obtained with iron oxide. Higher H_{AR} and lower H_a and H_o concentrations were noted with Fe_2O_3, as shown in Table 110.

Effect of Fe_2O_3 Concentration - The catalytic activity of Fe_2O_3 in coal liquefaction was studied at two different concentrations, namely, 1.7 and 3.4 wt percent of slurry. The distribution of products and the concentrations of elements in the various fractions are summarized in Tables 108 and 109. The conversion of coal and the production of oils, asphaltenes, and preasphaltenes were unchanged by increasing the concentration of Fe_2O_3. The production of hydrocarbon gases increased from 4.7 to 6.5% with increasing Fe_2O_3 concentration. Hydrogen consumption increased slightly with increasing Fe_2O_3 concentration. Reaction rates for conversion of asphaltenes and preasphaltenes given in Table 108 were not changed by increasing Fe_2O_3 concentration; in addition, no significant differences in the distribution of elements in the various fractions were noted. The concentration of H_{AR} decreased and that of H_a and H_o increased by increasing Fe_2O_3 concentration (Table 110). This information suggests that the quality of the generated solvent increases with increasing Fe_2O_3 concentration. However, the quality of solvent generated with Fe_2O_3 was lower than that generated with no-addition.

It can be concluded from the above data that the coal liquefaction reaction is not greatly improved by increasing the concentration of Fe_2O_3 from 1.7 to 3.4 wt% of slurry.

Activity of Supported Fe_2O_3 Catalysts - Study of the catalytic activity of iron oxide (Fe_2O_3) showed that addition of Fe_2O_3 slightly increased the conversion of coal and significantly increased the production of oil. These increases indicated the potential of Fe_2O_3 as one of the most important candidates for the disposable catalyst study.

To study the activity of Fe_2O_3 in more detail, various iron oxide catalysts supported on either fly ash or silica with varying concentrations of iron oxide (either in the pure form or iron ore obtained from U.S. Steel) were prepared at Air Products and added to coal during liquefaction. The results are shown in Table 111.

Table 109

Effect of Reagent-Grade Iron Iron Oxide on Elemental
Distribution in the Liquefaction Products of Elkhorn #2 Coal

Sample No.	31-139	38-28	38-40
Temperature, °F	850	850	850
Fe_2O_3 Concentration, Wt.%	0.0	1.7	3.4
Oil Fraction, Wt.%			
C	89.7	90.1	89.9
H	7.2	7.0	7.2
O	1.8	-	-
N	0.7	0.9	0.9
S	0.6	0.7	0.7
Asphaltene Fraction, Wt.%			
C	87.0	86.4	87.2
H	6.1	5.6	5.7
O	5.0	-	-
N	1.4	2.5	2.4
S	0.5	0.5	0.5
Preasphaltene Fraction, Wt.%			
C	86.6	85.0	85.7
H	4.9	4.5	4.6
O	5.4	-	-
N	2.4	2.7	2.6
S	0.6	0.5	0.5

Table 110

Effect of Reagent-Grade Iron Oxide on Distribution of Protons in
the Oil Fractions from the Liquefaction of Elkhorn #2 Coal

Sample No.	31-139		38-28		38-40	
Temperature, °F	850		850		850	
Fe_2O_3 Concentration, Wt.%	0.0		1.7		3.4	
Total Hydrogen, Wt.%	7.2		7.0		7.2	
Distribution of Protons, %						
	Rel.	Abs.	Rel.	Abs.	Rel.	Abs.
H_{AR}	46.9	3.38	51.8	3.63	48.4	3.48
H_a	27.9	2.01	26.3	1.84	27.3	1.96
H_o	25.2	1.81	21.9	1.53	24.3	1.76

Table 111

Catalytic Activity of Various Supported Fe_2O_3 Catalysts

Product Distribution, wt.% MAF Coal

Catalyst No.			705x8-5x1	813x1-1x4	813x1-1
Description of Catalyst	None	Speculite (Fe_2O_3)	25% Fe_2O_3 on Fly Ash	75% Fe_2O_3 on Fly Ash	75% Fe_2O_3 on Fly Ash
Calcined	No	No	Yes	Yes	No
Gas					
Oils	16	40	37	29	34
Asphaltenes	48	35	31	33	30
Preasphaltenes	13	11	15	20	17
I.O.M.	23	14	17	18	19
Conversion	77	86	83	82	81

Reaction Mixtures: 3 g Elkhorn #3 Coal
6 g Solvent
1 g Catalyst

Reaction Condition: Temp. - 450°C
Time - 60 Minutes
Pressure - 1,250 psig H_2 at 25°C
Reactor - Tubing-Bomb

Table 111

(Continued)

Catalytic Activity of Various Supported Fe_2O_3 Catalysts

Product Distribution, wt.% MAF Coal

Catalyst No.	705x-9-3x2	705x9-3	814x1-12	705x16-1x6	705x16-1	814x3-2x2
Description	25% U.S. Steel Fe_2O_3 on Fly Ash	75% U.S. Steel Fe_2O_3 on Fly Ash	75% U.S. Steel Fe_2O_3 on Fly Ash	25% U.S. Steel Fe_2O_3 on Silica	25% U.S. Steel Fe_2O_3 On Silica	50% U.S. Steel Fe_2O_3 on Silica
Calcination	Yes	No	Yes	Yes	No	Yes
Oils	31	34	39	34	36	40
Asphaltenes	32	32	31	32	31	31
Preasphaltenes	14	13	16	13	13	12
I.O.M.	23	21	14	21	20	17
Conversion	77	79	86	79	80	83

Reaction Mixtures: 3 g Elkhorn #3 Coal
6 g Solvent
1 g Catalyst

Reaction Condition: Temp. - 450°C
Time - 60 Minutes
Pressure - 1,250 psig H_2 at 25°C
Reactor - Tubing-Bomb

At a constant catalyst concentration, the following changes did not cause any definite trend in liquefaction: increasing the concentration of iron oxide from 25 to 75%; changing from pure iron oxide to impure iron oxide obtained from U.S. Steel; changing the support from fly ash to pure silica and calcining the catalyst before use.   Coal conversion and the oil production were lower in all the cases except for the one obtained with pure Fe_2O_3.

Comparison of the Catalytic Activity of Pyrite and Iron Oxide

The catalytic activity of pyrite and iron oxide in the liquefaction of Elkhorn #2 coal is compared and presented in Table 112.   The addition of pyrite yielded higher overall conversion of coal and production of hydrocarbon gases and asphaltenes compared with iron oxide.   Preasphaltene yield was lower with pyrite than with iron oxide.   The rates of conversion of asphaltenes and preasphaltenes were also higher with pyrite.   Furthermore, the hydrogen content and the quality of generated solvent, shown in Table 113, were higher with pyrite than with iron oxide.   In spite of all the benefits of pyrite over iron oxide, there are disadvantages.   Hydrogen consumption with pyrite was almost four times that of iron oxide.   Also, the addition of iron oxide removed all the H_2S generated in the coal liquefaction reaction, eliminating the need of a sulfur recovery unit for the plant.   The use of pyrite or iron oxide in coal liquefaction reaction as a disposable catalyst will depend mainly on process economics.

Catalysis by Combinations of Different Iron Compounds

Reduced pyrite was shown to catalyze coal liquefaction by improving coal conversion and oil production.   Catalysis by pyrite and reduced pyrite is little understood.   Thus, to understand the transformation of pyrite to pyrrhotite, an in-situ preparation of pyrrhotite from a pyrite and iron oxide mixture was conducted.   In addition, the catalytic activity of pyrrhotite prepared in-situ was tested in coal liquefaction reactions.

Table 112

Comparison of Catalytic Activity of Pyrite
and Iron Oxide in Liquefaction of Elkhorn #2 Coal

Sample No.	31-161	38-28
Additive	Pyrite	Iron Oxide
Fe Concentration, wt.% Coal	3.53	3.97
Temperature, °F	850	850
Pressure, psig	2000	2000
Hydrogen Flow Rate, MSCF/T	24.2	27.6
Reaction Time, Min.	38	42.6
Product Distribution, wt.% MAF Coal		
HC	10.2	4.7
CO, CO_2	0.9	0.6
H_2S	0.3	0.0
Oils	25.6	23.7
Asphaltenes	22.3	18.9
Preasphaltenes	28.2	35.0
I.O.M.	9.3	13.8
Water	3.2	3.3
Conversion	90.7	86.6
Hydrogen Consumption, wt.% MAF Coal	1.75	0.46
SRC Sulfur, %	0.49	0.48
First Order Rate Constants, hr^{-1}		
K_a	1.71	1.07
K_p	2.59	1.66

Table 113

Comparison of the Properties of Solvent Generated
by Liquefaction of Elkhorn #2 Coal in the
Presence of Pyrite and Iron Oxide

Sample No.	31-161	38-28
Additive	Pyrite	Iron Oxide
H Content of Oil, %	7.3	7.0
Distribution of Protons, wt.% Absolute		
H_{AR}	3.19	3.63
H_a	2.13	1.84
H_o	1.98	1.53

In-Situ Preparation of Pyrrhotite - Robena pyrite samples were treated with
process solvent in the presence of hydrogen gas at 450°C at 1-, 3-, and
30-minute reaction times in a tubing-bomb reactor. The reaction product was
filtered and washed to recover the solid residue. X-ray diffraction analysis
of the solid residue showed complete conversion of pyrite to pyrrhotite 11C in
less than 3 minutes. This observation indicated that the transformation of
pyrite to pyrrhotite in coal liquefaction was very rapid.

In another set of experiments, a mixture of Robena pyrite and iron oxide was
treated at the same reaction conditions. Both Fe_2O_3 and pyrite were used so
as to remove all the H_2S evolved during pyrite reduction with the Fe_2O_3 and at
the same time generate, in-situ, active pyrrhotite. A reaction time of 30
minutes was used for the experiment. Iron oxide, when treated alone, completely
reduced to elemental iron. The mixture of iron oxide and pyrite formed FeS
(troilite) instead of elemental iron and pyrrhotite 11C ($FeS_{1.099}$), as observed
with iron oxide and pyrite, respectively. Therefore, a mixture of pyrite and
iron oxide resulted in a different form of iron sulfide than did pyrite alone.
The formation of different forms of iron sulfide was probably due to differences
in H_2S partial pressures in the liquefaction reactor.

Activity of Pyrrhotite - The catalytic activity of a pyrrhotite prepared
in-situ by the simultaneous addition of iron oxide and pyrite to the coal
liquefaction feed slurry was studied. A mixture of 1.7% Fe_2O_3 and 2.5% pyrite
based on feed slurry was used. The ratio was determined by calculating the
amount of Fe_2O_3 required to remove all the H_2S generated by the hydrogen
reduction of pyrite. The results are summarized in Table 114.

Coal conversion was not greatly affected by using a mixture of Fe_2O_3 and
pyrite over pyrite alone, but improved measurably compared with Fe_2O_3 alone.
Oil production increased with a mixture of Fe_2O_3 and pyrite over pyrite and
iron oxide alone, as shown in Table 114. A significant reduction in the
production of hydrocarbon gases was noted with the Fe_2O_3/pyrite mixture compared
with the run using pyrite alone. All the H_2S produced during liquefaction as
well as that generated by pyrite reduction was removed by Fe_2O_3. X-ray
diffraction analysis of the liquefaction residue showed complete conversion of
pyrite and iron oxide to troilite (FeS). Hydrogen consumption with the iron

210

Table 114

Liquefaction of Elkhorn #2 Coal in the Presence of
A Mixture of Pyrite and Iron Oxide

Sample No.	31-161	38-28	38-83
Feed Composition	67.5% Solvent + 30% Coal + 2.5% Pyrite	68.3% Solvent + 30% Coal + 1.7% Fe_2O_3	65.8% Solvent + 30% Coal + 2.5% Pyrite + 1.7%Fe_2O_3
Temperature, °F	850	850	850
Pressure, psig	2,000	2,000	2,000
Hydrogen Flow Rate, MSCF/T	24.2	27.6	27.2
Residence Time, Min.	38	42.6	46.1
Product Distribution, wt.% MAF Coal			
HC	10.2	4.7	5.8
CO,CO_2	0.9	0.6	0.8
H_2S	0.3	0.0	0.0
Oils	25.6	23.7	28.0
Asphaltenes	22.3	18.9	24.1
Preasphaltenes	28.2	35.0	29.8
I.O.M.	9.3	13.8	9.0
Water	3.2	3.3	2.5
Conversion	90.7	86.6	91.0
Hydrogen Consumption, wt.% MAF Coal			
Total	1.75	0.46	0.93
From Gas	1.96	0.00	1.31
From Solvent	(0.21)[1]	0.49	(0.22)
By Additive	0.13	(0.03)	(0.16)
SRC Sulfur, %	0.49	0.48	0.48

---

[1] ( ) - means negative value

211

oxide/pyrite mixture was higher than with Fe_2O_3, but was lower than with pyrite. The above differences could partly be due to slight increases in hydrogen flow rate, residence time and the total concentration of iron sulfide with the use of mixture of FeS_2/Fe_2O_3 than either of them alone.

The hydrogen content of the oil fraction obtained with a mixture of iron compounds was higher than that generated with iron oxide, but was similar to that generated with pyrite (see Table 115). Similar observations were noted for the generated solvent quality, represented by the concentrations of H_a and H_o (Table 116). No other major differences were noted in the distribution of elements in the various fractions.

It can be concluded that the coal liquefaction reaction is improved by using a iron oxide/pyrite mixture. The mixture gave lower hydrocarbon gas production and slightly higher oil and asphaltene yield compared with using either of them alone. Hydrogen consumption with the mixture was significantly reduced compared with the run with pyrite, though the SRC sulfur content was not greatly affected by using the iron oxide/pyrite mixture.

Effect of Reaction Variables on Coal Liquefaction - The effect of various process variables on the liquefaction of Elkhorn #2 coal using the mixture of Robena pyrite and iron oxide was studied. The process variables studied were the concentration of catalysts, reaction temperature, total pressure, reaction time and hydrogen flow rate.

Concentration - Three different combinations of Fe_2O_3 and Robena pyrite (i.e., 0.5% Fe_2O_3 + 0.75% pyrite, 1.7% Fe_2O_3 + 2.5% pyrite and 3.4% Fe_2O_3 + 5% pyrite) were used to study the effect of their concentration on coal liquefaction at 850°F. Once again the ratio of iron oxide and pyrite was determined by the amount of iron oxide required to remove all the H_2S generated by hydrogen reduction of pyrite. The results are summarized in Table 117. Coal conversion and hydrocarbon gas production were not greatly affected by using different concentrations of a specific mixture having a set ratio of Fe_2O_3 and pyrite. However, oil production increased from 25 to 38% by increasing the Fe_2O_3/pyrite concentration from 1.25 to 8.4 wt%. Asphaltene and preasphaltene production was unaffected at lower concentrations of Fe_2O_3 and pyrite, but decreased at

Table 115

Elemental Distribution in the Liquefaction Products from
the Liquefaction of Elkhorn #2 Coal in the Presence
of a Mixture of Iron Oxide and Pyrite

Sample No.	31-161	38-28	38-83
Temperature, °F	850	850	850
Additive	Pyrite	Iron Oxide	Pyrite/Iron Oxide
Oil Fraction, wt.%			
C	89.5	90.1	89.6
H	7.3	7.0	7.4
N	0.8	0.9	1.0
S	0.6	0.7	0.7
O	1.8	1.3	1.3
Asphaltene Fraction, wt.%			
C	86.6	86.4	86.5
H	5.8	5.6	5.8
N	2.4	2.5	2.4
S	0.5	0.5	0.5
O	4.7	5.0	4.8
Preasphaltene Fraction, wt.%			
C	86.1	85.0	84.5
H	4.8	4.5	4.7
N	2.4	2.7	2.7
S	0.5	0.5	0.5
O	6.2	7.3	7.6

Oxygen was determined by difference

Table 116

Distribution of Protons in Oil Fractions from the Liquefaction
of Elkhorn #2 Coal in the Presence of a Mixture of Iron Oxide and Pyrite

Sample No.	31-161	38-28	38-83
Temp., °F	850	850	850
Additive	Pyrite	Iron Oxide	Pyrite/Iron Oxide
Total Hydrogen, wt.%			
	7.3	7.0	7.4
Distribution of Protons, %			
Relative			
H_{AR}	43.7	51.8	44.5
H_a	29.2	26.3	29.6
H_o	27.0	21.9	25.9
Absolute			
H_{AR}	3.19	3.63	3.29
H_a	2.13	1.84	2.19
H_o	1.98	1.53	1.92

Table 117

Effect of Concentration of Robena Pyrite and
Iron Oxide on Elkhorn #2 Coal Liquefaction

Sample No.	45-39	38-83	38-102
Feed Composition	68.75% Solvent + 30% Coal + 0.5% Fe_2O_3 + 0.75% Pyrite	65.8% Solvent + 30% Coal + 1.7% Fe_2O_3 + 2.5% Pyrite	61.6% Solvent + 30% Coal + 3.4% Fe_2O_3 + 5% Pyrite
FeS_2/Fe_2O_3 (mole ratio)	1/1	1/1	1/1
Temperature, °F	850	850	850
Pressure, psig	2000	2000	2000
H_2 Flow Rate, MSCF/T	23.5	27.2	30.6
Residence Time, Min.	36.9	46.1	50.6
Product Distribution, wt.% MAF Coal			
HC	7.3	5.8	5.9
CO, CO_2	1.0	0.8	0.7
H_2S	0.1	0.0	0.0
Oils	24.8	28.0	38.4
Asphaltenes	24.0	24.1	21.6
Preasphaltenes	29.5	29.8	20.1
I.O.M.	11.9	9.0	11.6
Water	1.4	2.5	1.7
Conversion	88.1	91.0	88.4
Hydrogen Consumption, wt.% MAF Coal			
Total	0.85	0.93	1.16
From Gas	0.85	1.31	1.75
From Solvent	0.05	(0.22)	(0.25)
By Additive	(0.05)	(0.16)	(0.34)
SRC Sulfur, %	0.30	0.48	0.48

[1]( ) - means negative value

215

higher concentrations. All H_2S produced during liquefaction, as well as generated by pyrite reduction, was removed by Fe_2O_3. Hydrogen consumption based on elemental hydrogen balance increased slightly with catalyst concentration (see Table 117). Some of the above differences, once again, could be due to increased hydrogen flow rate and residence time with increase in concentration of the mixture.

The distribution of elements given in Table 118 showed minor variations in hydrogen, nitrogen, and sulfur contents of the various fractions obtained with different catalyst concentrations. The aromatic hydrogen content (H_{AR}) increased and H_o decreased with increasing catalyst concentration (see Table 119). No positive conclusion about the quality of the generated solvent could be made from the above data.

It can be concluded that increasing the concentration of both iron oxide and pyrite in the reaction mixture improves oil production, increases conversion of asphaltenes and preasphaltenes, and increases hydrogen consumption, but does not have a significant effect on hydrocarbon gas production or SRC sulfur content.

Reaction Time - Results from the study of reaction times of 38 and 54 minutes on coal liquefaction in the presence of a mixture of iron oxide and Robena pyrite are summarized in Table 120. The conversion of coal and preasphaltenes and production of hydrocarbon gases and water were not greatly affected by increasing reaction time. Oil production increased from 19 to 25% with increasing reaction time. The increase in oil production was accompanied by a decrease in asphaltene production from 23 to 19% (Table 120). Rate of asphaltene conversion remained constant, whereas that of preasphaltene conversion decreased from 1.8 to 1.3 hr^{-1}. Hydrogen consumption increased marginally with time. No significant difference was noted in SRC sulfur content.

Distribution of elements in various fractions (Table 121) showed no major changes with increasing reaction time. Also, distribution of protons in the oil fraction was unchanged (Table 122).

It can be concluded that increasing reaction time increases oil production and hydrogen consumption, decreases asphaltene production and does not have any significant effect on SRC sulfur content or on the production of gases and water.

216

Table 118

Effect of Concentration of Robena Pyrite and Iron Oxide
on Elemental Distribution of Elkhorn #2 Coal Liquefaction Products

Sample No.	45-30	38-83	38-102
Temperature, °F	850	850	850
Additive	0.5% Fe_2O_3 + 0.75% Pyrite	1.7% Fe_2O_3 + 2.5% Pyrite	3.4% Fe_2O_3 + 5.0% Pyrite
C	89.7	89.6	89.6
H	7.2	7.4	7.4
N	0.9	1.0	1.0
S	0.6	0.7	0.6
O	1.6	1.3	1.4
Asphaltene Fraction, wt.%			
C	86.5	86.5	86.7
H	5.8	5.8	5.9
N	2.6	2.4	2.4
S	0.3	0.5	0.4
O	4.8	4.8	4.6
Preasphaltene Fraction, wt.%			
C	85.4	84.5	84.7
H	4.8	4.7	4.8
N	2.4	2.7	2.6
S	0.4	0.5	0.6
O	7.0	6.6	7.3

Oxygen is determined by difference

217

Table 119

Effect of Distribution of Robena Pyrite and Iron Oxide on Proton
Distribution in the Oil Fractions from Elkhorn #2 Coal Liquefaction

Sample No.	45-39	38-83	38-102
Temperature, °F	850	850	850
Additive	0.5% Fe_2O_3 + 0.75% Pyrite	1.7% Fe_2O_3 + 2.5% Pyrite	3.4% Fe_2O_3 + 5.0% Pyrite
Total Hydrogen, wt.%	7.2	7.4	7.4
Distribution of Protons, %			
Relative			
H_{AR}	39.4	44.5	45.9
H_a	30.4	29.6	28.2
H_o	30.2	25.6	25.9
Absolute			
H_{AR}	2.84	3.29	3.40
H_a	2.19	2.19	2.09
H_o	2.17	1.92	1.91

Table 120

Effect of Process Variables on Liquefaction of Elkhorn #2 Coal
in the Presence of a Mixture of Iron Oxide and Robena Pyrite

Sample No.	45-23	45-62	45-52	45-23	45-31	45-23	45-39	45-23	45-79
Feed Composition	68.75% Solvent + 30% Coal + 0.5% Fe_2O_3 + 0.75% Pyrite								
Temperature, °F	825	825	825	825	800	825	850	825	825
Pressure, psig	2000	2000	1000	2000	2000	2000	2000	2000	2000
Residence Time, Min.	38.0	53.8	35.8	38.0	37.4	38.0	36.9	38.0	36.9
H_2 Flow Rate, MSCF/T	25.6	24.1	22.7	25.6	25.7	25.6	23.5	25.6	47.1
Process Variable	Reaction Time		Pressure			Temperature		H_2 Flow Rate	
Product Distribution, wt.% MAF Coal									
HC	5.1	5.9	3.3	5.1	3.4	5.1	7.3	5.1	5.1
CO, CO_2	0.6	0.8	0.7	0.6	0.5	0.6	1.0	0.6	0.7
H_2S	0.1	0.0	0.0	0.1	0.0	0.1	0.1	0.1	0.1
Oils	19.3	25.0	10.7	19.3	13.0	19.3	24.8	19.3	24.8
Asphaltenes	23.5	19.2	22.7	23.5	24.5	23.5	24.0	23.5	22.8
Preasphaltenes	37.1	36.3	40.9	37.1	41.6	37.1	29.5	37.1	33.2
I.O.M.	12.8	11.3	20.7	12.8	15.8	12.8	11.9	12.8	12.0
Water	1.5	1.5	1.0	1.5	1.2	1.5	1.4	1.5	1.3
Conversion	87.2	88.7	79.3	87.2	84.2	87.2	88.1	87.2	88.0
Hydrogen Consumption, wt.% MAF Coal									
Total	0.65	0.85	0.16	0.65	0.37	0.65	0.85	0.64	0.85
From Gas	0.82	1.06	0.00	0.82	0.58	0.82	0.85	0.85	1.25
From Solvent	(0.12)[1]	(0.16)	0.21	(0.12)	(0.16)	(0.12)	0.05	(0.12)	(0.35)
By Additive	(0.05)	(0.05)	(0.05)	(0.05)	(0.05)	(0.05)	(0.05)	(0.05)	(0.05)
SRC Sulfur, %	0.41	0.38	0.38	0.41	0.42	0.41	0.30	0.41	0.42
First Order Rate Constants, hr^{-1}									
K_a	0.85	0.88	0.51	0.85	0.57	0.85	1.12	0.85	1.14
K_p	1.78	1.32	1.34	1.78	1.41	1.78	2.61	1.78	2.26

[1]( ) - means negative value

Table 121

Effect of Process Variables on Elemental Distribution of Liquefaction
Products in the Presence of a Mixture of Iron Oxide Robena Pyrite

Sample No.	45-23	45-62	45-52	45-23	45-31	45-23	45-39	45-23	45-79
Temperature, °F	825	825	825	825	800	825	850	825	825
Pressure, psig	2000	2000	2000	1000	2000	2000	2000	2000	2000
Residence Time, Min.	38.0	53.8	35.8	38.0	37.4	38.0	36.9	38.0	36.9
H_2 Flow Rate, MSCF/T	25.6	24.1	22.7	25.6	25.7	25.6	23.5	25.6	47.1
Process Variable	Reaction Time		Pressure			Temperature		H_2 Flow Rate	
Oil Fraction, wt.%									
C	89.8	89.5	90.0	89.8	89.7	89.8	89.7	89.8	89.5
H	7.3	7.3	7.2	7.3	7.3	7.3	7.2	7.3	7.4
N	0.9	0.8	0.9	0.9	0.9	0.9	0.9	0.9	0.9
S	0.6	0.6	0.6	0.6	0.6	0.6	0.6	0.6	0.6
O	1.4	1.8	1.3	1.4	1.5	1.4	1.6	1.4	1.6
Asphaltene Fraction, wt.%									
C	85.9	85.8	86.4	85.9	85.8	85.9	86.5	85.9	85.8
H	5.9	5.8	5.8	5.9	6.1	5.9	5.8	5.9	6.0
N	2.3	2.5	2.3	2.3	2.2	2.3	2.6	2.3	2.4
S	0.4	0.3	0.3	0.4	0.3	0.4	0.3	0.4	0.4
O	5.5	5.6	5.2	5.5	5.6	5.5	4.8	5.5	5.4
Preasphaltene Fraction, wt.%									
C	83.9	84.3	85.2	83.9	83.4	83.9	85.4	83.9	83.9
H	4.9	4.8	4.8	4.9	5.1	4.9	4.8	4.9	5.0
N	2.3	2.5	2.6	2.3	2.3	2.3	2.4	2.3	2.4
S	0.5	0.4	0.4	0.5	0.5	0.5	0.4	0.5	0.4
O	8.4	8.0	7.0	8.4	8.7	8.4	7.0	8.4	8.3

Oxygen is determined by difference

Table 122

Effect of Process Variables on Proton Distribution in
the Oil Fraction from the Liquefaction of Elkhorn #2 Coal
with a Mixture of Iron Oxide and Robena Pyrite

Sample No.	45-23	45-62	45-52	45-23	45-31	45-23	45-39	45-23	45-79
Temp., °F	825	825	825	825	800	825	850	825	825
Pressure, psig	2000	2000	1000	2000	2000	2000	2000	2000	2000
Residence Time, Min.	38.0	53.8	35.8	38.0	37.4	38.0	36.9	38.0	36.9
H_2 Flow Rate, MSCF/T	25.6	24.1	22.7	25.6	25.7	25.6	23.5	25.6	47.1
Process Variables	Reaction Time		Pressure			Temperature		H_2 Flow Rate	
Total Hydrogen, wt.%	7.3	7.3	7.2	7.3	7.3	7.3	7.2	7.3	7.4
Distribution of Protons, %									
Relative									
H_{AR}	36.9	36.8	39.0	36.9	36.4	36.9	39.4	36.9	35.9
H_a	31.5	32.0	30.1	31.5	30.7	31.5	30.4	31.5	32.4
H_o	31.6	31.2	30.9	31.6	32.9	31.6	30.2	31.6	31.7
Absolute									
H_{AR}	2.69	2.67	2.81	2.69	2.66	2.69	2.84	2.69	2.66
H_a	2.30	2.34	2.17	2.30	2.24	2.30	2.19	2.30	2.40
H_o	2.31	2.29	2.22	2.31	2.40	2.31	2.17	2.31	2.34

Total Pressure - Increasing the total pressure from 1000 to 2000 psig using 100% hydrogen feed increased conversion from 79 to 87% (see Table 120). Likewise, the yields of oils and hydrocarbon gases increased at the higher pressure; (oil production increased from 11 to 19%). The conversion of asphaltenes and preasphaltenes changed slightly (Table 120) such that the rates of conversion increased from 0.5 to 0.9 hr^{-1} and from 1.3 to 1.8 hr^{-1}, respectively. Hydrogen consumption increased from 0.2 to 0.7 wt%, but SRC sulfur content remained constant.

No significant variations were noted in the distribution of elements in the various fractions, as shown in Table 121. The concentration of H_{AR} decreased slightly and that of H_a and H_o increased slightly (Table 122), indicating that the quality of generated solvent increases at higher hydrogen partial pressures.

Overall, the increase in pressure increased the conversion of coal, increased the yield of hydrocarbon gases and oils, increased the consumption of hydrogen, and did not affect the sulfur content of SRC.

Reaction Temperature - The liquefaction of Elkhorn #2 coal was evaluated at 800, 825 and 850°F in the presence of a mixture of iron oxide and Robena pyrite (Table 120). Coal conversion and hydrocarbon gas production increased as reaction temperature was increased from 800 to 850°F. Simultaneously, oil production increased from 13 to 25% (Table 120). As temperature increased asphaltene production remained constant, but preasphaltene yield decreased. Rates of conversion of asphaltenes and preasphaltenes also increased with temperature as shown in Table 120. Hydrogen consumption increased and with increasing temperature. SRC sulfur content decreased with increasing temperature from 825 to 850°F.

The distribution of elements in various fractions (Table 121) showed essentially no variations in nitrogen and sulfur contents with increase in temperature except for a small decrease in hydrogen contents of asphaltenes and preasphaltenes. The concentration of H_{AR} increased slightly and that of H_a and H_o decreased slightly, indicating that the quality of generated solvent decreases with increasing reaction temperature.

In summary, the increase in liquefaction temperature from 800 to 850°F in the presence of a mixture of iron oxide and Robena pyrite increased the conversion of coal and preasphaltenes, and increased the yield of oils and hydrocarbon gases; in addition, hydrogen consumption increased and SRC desulfurization improved slightly.

Hydrogen Flow Rate - An increase in hydrogen flow rate from 26 to 47 mscf/ton in the presence of a mixture of iron oxide and Robena pyrite did not significantly change coal conversion or hydrocarbon gas, asphaltene and water production. Oil production, however, increased from 19 to 25% (see Table 120). Production of preasphaltenes decreased from 37 to 33%. The rates of conversion of asphaltenes and preasphaltenes increased from 0.9 to 1.1 hr^{-1} and from 1.8 to 2.3 hr^{-1}, respectively. Hydrogen consumption based on elemental hydrogen balance increased and SRC sulfur content remained constant.

Hydrogen contents in the various fractions given in Table 121 were unchanged with increasing flow rate. No other major differences were noted. The quality of the solvent generated based on H_a and H_o was increased slightly with higher hydrogen flow rate (see Table 122).

It can be concluded that hydrogen flow rate does have some impact on coal liquefaction in that it improves oil production and preasphaltene conversion. However, coal conversion and SRC sulfur content are not affected.

Effect of Catalyst Addition Mode

Earlier, oil production and hydrogen consumption were shown to increase with the addition of pyrite, iron oxide and a combination of pyrite and iron oxide. It was also shown that oil production increased with increasing their concentration in the reaction mixture. It is well known that an increase in the concentration of the disposable catalyst reduces the processing capability of the plant and increases the load on the solid/liquid separation unit. Also, it is known that the loss in recoverable carbonaceous material increases with an increase in the concentration of solids in the feed slurry to the separation unit,

which ultimately affects the overall efficiency of the plant. All these factors therefore encourage the use of the lowest possible concentration of the catalyst in the reaction.

If the catalyst activity is not sufficiently high at low concentration, it may be possible to increase activity by increasing catalyst surface area. Particulate iron catalyst, for example, pyrite and iron oxide, has a very low surface-area-to-weight ratio (1 to 10 m^2/g). Therefore, iron must be finely dispersed in the coal liquefaction reaction mixture to be effective.

Two methods were used to finely disperse the iron catalyst in the reaction mixture, namely, impregnation and molecular dispersion. A water-soluble iron compound, thermally unstable at coal liquefaction reaction conditions, was impregnated into coal to increase the contact between iron and coal. to effect molecular dispersion, a thermally unstable process-solvent-soluble compound was used. The results of catalyst dispersion study are discussed below.

Iron Impregnated on Coal - A sample of Elkhorn #2 coal impregnated with 1 wt% iron in the form of iron sulfate was liquefied at 825 and 850°F. The product distributions obtained from the iron-impregnated coal are summarized in Table 123. The production of oil increased by over a factor of two at both temperatures, although coal conversion was not significantly affected. Preasphaltene yield decreased while the rate of preasphaltene conversion increased considerably with iron impregnation. The production of hydrocarbon gases decreased considerably at both 825 and 850°F. X-ray diffraction analysis of coal lique-faction residue showed complete conversion of iron sulfate to pyrrhotite. Hydrogen consumption based on elemental hydrogen balance and SRC sulfur content was not significantly affected by iron impregnation.

The distribution of elements in the various fractions summarized in Table 124 was not greatly affected by iron impregnation. Proton distribution (Table 125) showed an increase in H_{AR} and decrease in H_a and H_o values, suggesting that the solvent generated by iron impregnated coal would have lower solvent quality than that generated without impregnation.

Table 123

Effect of Iron Impregnation on
Liquefaction of Elkhorn #2 Coal

Sample No.	31-128	31-139	38-10	38-17
Iron Impregnation	No	No	Yes	Yes
Fe Conc., wt.% Coal	--	--	1.0	1.0
Feed Composition	70% Solvent + 30% Coal			
Temperature, °F	825	850	825	850
Pressure, psig	2000	2000	2000	2000
Hydrogen Flow Rate, MSCF/T	18.9	19.9	20.6	27.3
Reaction Time, Min.	35.0	37.0	32.8	40.8
Production Distribution, wt.% MAF Coal				
HC	5.2	7.0	3.5	4.4
CO, CO_2	0.7	0.6	0.6	0.5
H_2S	0.3	0.3	0.2	0.2
Oils	12.2	8.3	25.0	30.3
Asphaltenes	21.2	21.6	19.1	20.8
Preasphaltenes	44.2	43.4	35.8	27.5
I.O.M.	14.7	15.7	13.5	13.1
Water	1.5	3.1	2.3	3.2
Conversion	85.3	84.3	86.5	86.9
Hydrogen Consumption, wt.% MAF Coal				
Total	0.64	0.53	0.40	0.60
From Gas	0.59	0.44	0.04	0.00
From Solvent	0.05	0.09	0.36	0.60
SRC Sulfur, %	0.61	0.55	0.61	0.57
First Order Rate Constants, hr^{-1}				
K_a	0.62	0.39	1.45	1.33
K_p	1.27	1.09	2.19	2.63

Table 124

Effect of Iron Impregnation on Elemental Distribution
of Liquefaction Products from Elkhorn #2 Coal

Sample No.	Original Solvent FOB #11	31-128	31-139	38-10	38-17
Temperature, °F	-	825	850	825	850
Iron Impregnation	-	No	No	Yes	Yes
Oil Fraction, wt.%					
C	89.7	89.5	89.7	90.0	89.8
H	7.2	7.2	7.2	7.1	7.0
O	1.4	1.7	1.8	1.4	1.6
N	1.1	0.9	0.7	0.8	1.0
S	0.6	0.7	0.6	0.7	0.6
Asphaltene Fraction, wt.%					
C	-	85.9	87.0	85.6	86.6
H	-	6.3	6.1	6.0	5.8
O	-	5.8	5.0	5.5	4.7
N	-	1.4	1.4	2.4	2.4
S	-	0.6	0.5	0.5	0.5
Preasphaltene Fraction, wt%					
C	-	85.3	86.6	82.9	84.9
H	-	5.2	4.9	4.9	4.6
O	-	6.2	5.4	7.9	7.4
N	-	2.2	2.4	2.6	2.5
S	-	0.6	0.6	0.7	0.6

Oxygen is determined by difference

226

Table 125

Effect of Iron Impregnation on Distribution of Protons in the
Oil Fractions from the Liquefaction of Elkhorn #2 Coal

Sample No.	31-128	31-139	38-10	38-17
Temperature, °F	825	850	825	850
Iron Impregnation	No	No	Yes	Yes
Total Hydrogen, wt.%	7.2	7.2	7.1	7.0
Distribution of Protons, %				
Relative				
H_{AR}	45.3	46.9	51.3	50.0
H_a	27.1	27.9	25.3	27.1
H_o	27.6	25.2	23.4	22.9
Absolute				
H_{AR}	3.26	3.38	3.64	3.50
H_a	1.95	2.01	1.80	1.90
H_o	1.99	1.81	1.66	1.60

The conversion of impregnated coal was not changed by increasing the reaction temperature from 825 to 850°F. Oil and hydrocarbon gas production increased with increasing temperature, the former from 25 to 30%. The difference in oil production at 825 and 850°F could be due partly to the difference in reaction time (see Table 123). Asphaltene production was unchanged and that of preasphaltenes decreased with increasing reaction temperature. The rate of conversion of asphaltenes decreased slightly, but that of preasphaltenes increased from 2.19 to 2.63 hour^{-1}. Hydrogen consumption increased slightly, and SRC sulfur content decreased marginally.

The distribution of elements in various fractions (Table 124) was not significantly changed by reaction temperature; the concentration of H_{AR} in the generated oil fraction decreased and that of H_a and H_o increased slightly (Table 125).

In conclusion, the impregnation of Elkhorn #2 coal with 1% iron reduced hydrocarbon gas and preasphaltene production and increased oil production. However, it did not affect asphaltene production, hydrogen consumption, and SRC sulfur content.

Molecular Dispersion of Iron in Feed Slurry - The catalytic activity of iron improved when it was impregnated into coal rather than added as particulate pyrite. Therefore, catalyst activity can be improved by providing sufficient contact between catalyst and coal. One method is to disperse the catalyst at the molecular level.

Molecular dispersion of iron can be attained by using iron naphthenate mixed in coal-oil slurry. Because it is unstable at coal liquefaction reaction conditions iron naphtenate decompose to generate elemental iron, which reacts with H_2S gas generated by desulfurization of coal to produce finely dispersed active iron sulfide catalyst.

Catalytic activity from the molecular dispersion of iron in the liquefaction of Elkhorn #2 coal was studied by using 1 wt% iron naphthenate based on coal at 825°F. As shown in Table 126, coal conversion was not affected by iron dispersion. However, oil production increased by over a factor of two with

Table 126

Effect of Molecular Dispersion of Iron
on Liquefaction of Elkhorn #2 Coal

Sample No.	31-128	47-10
Feed Composition	70% Solvent + 30% Coal	65% Solvent + 30% Coal + 5% Fe-Naphthenate
Fe Conc., wt.% Coal	--	1.0
Temperature, °F	825	825
Pressure, psig	2000	2000
H_2 Flow Rate, MSCF/T	18.9	23.3
Reaction Time, Min.	35.0	38.0
Product Distribution, wt.% MAF Coal		
HC	5.2	3.0
CO, CO_2	0.7	1.0
H_2S	0.3	0.0
Oils	12.2	32.5
Asphaltenes	21.2	18.1
Preasphaltenes	44.2	30.4
I.O.M.	14.7	14.0
Water	1.5	1.0
Conversion	85.3	86.0
H_2 Consumption, wt.% MAF Coal		
Total	0.64	0.99
From Gas	0.59	0.00
From Solvent	0.05	0.99
SRC Sulfur, %	0.61	0.53
First Order Rate Constants, hr^{-1}		
K_a	0.62	1.74
K_p	1.27	2.45

iron dispersion compared with the no-additive run. Production of hydrocarbon gases and preasphaltenes decreased considerably, while reaction rates of conversion of asphaltenes and preasphaltenes increased dramatically with iron dispersion (see Table 127). Hydrogen consumption based on elemental hydrogen balance and SRC sulfur content also increased. The distribution of elements in the various fractions summarized in Table 127 showed minor variations.

In summary, molecular dispersion of 1 wt% iron in coal liquefaction feed slurry significantly reduced hydrocarbon gas and preasphaltene production, increased oil production and hydrogen consumption.

Comparison of Iron Impregnation, Particulate Addition and Molecular Dispersion - Comparison of liquefaction results of Elkhorn #2 coal catalyzed by impregnated iron, molecularly dispersed iron, and particulate iron at 825°F reveals a significant difference in the magnitude of iron loading in the three different modes of iron addition (Table 128). As discussed earlier, oil production increased with pyrite concentration. Therefore, pyrite addition data was used for comparison.

Coal conversion was considerably lower with iron impregnation and molecular dispersion compared with pyrite addition, but was higher than that of the no-additive run, as discussed earlier. The hydrocarbon gas production and hydrogen consumption were significantly lower with iron impregnation and molecular dispersion compared with pyrite addition, although oil production was comparable. Lower asphaltene production and higher asphaltene and lower preasphaltene rates of conversion were noted with impregnation and molecular dispersion of iron than with particulate addition. SRC sulfur content was similar with iron impregnation, molecular dispersion and particulate pyrite addition.

The hydrogen content and quality of generated solvent based on H_a and H_o values were higher with pyrite than with iron impregnation, as shown in Tables 129 and 130. Solvent generated with impregnation and molecular dispersion of iron lost hydrogen, whereas it gained hydrogen with pyrite. No other differences were noted in the distribution of elements in the various fractions.

Table 127

Effect of Molecular Dispersion of Iron on Elemental
Distribution in the Liquefaction Products of Elkhorn #2 Coal

Sample No.	Original Solvent FOB #11	31-128	47-10
Temperature, °F	--	825	825
Iron	--	No	Yes
Oil Fraction, wt.%			
C	89.7	89.5	90.4
H	7.2	7.2	7.1
O	1.4	1.7	1.1
N	1.1	0.9	0.8
S	0.6	0.7	0.6
Asphaltene Fraction, wt.%			
C	--	85.9	85.5
H	--	6.3	6.0
O	--	5.8	5.8
N	--	1.4	2.2
S	--	0.6	0.5
Preasphaltene Fraction, wt.%			
C	--	85.3	85.3
H	--	5.2	4.8
O	--	6.2	7.0
N	--	2.2	2.4
S	--	0.6	0.5

Table 128

Effect of Iron Impregnation, Molecular Dispersion and Particulate Addition on Liquefaction of Elkhorn #2 Coal

Sample No.	31-186	38-10	47-10
Additive	Pyrite	Iron Impregnation	Molecular Dispersion
Feed	60% Solvent/30% Coal/ 10% Pyrite	70% Solvent/30% Impregnated Coal	65% Solvent + 30% Coal + 5% Iron Naphthenate
Temperature, °F	825	825	825
Pressure, PSIG	2,000	2,000	2,000
Hydrogen Flow Rate, MSCF/T	23.0	20.6	23.3
Residence Time, Min.	39	32.8	38.0
Product Distribution, wt.% MAF Coal			
HC	5.7	3.5	3.0
CO, CO_2	0.9	0.6	1.0
H_2S	0.0	0.2	0.0
Oils	28.2	25.0	32.5
Asphaltenes	24.3	19.1	18.1
Preasphaltenes	29.6	35.8	30.4
I.O.M	8.1	13.5	14.0
Water	3.2	2.3	1.0
Conversion	91.9	86.5	86.0
Hydrogen Consumption, wt.% MAF Coal			
Total	1.68	. 0.40	0.99
From Gas	2.29	0.04	0.00
From Solvent	(0.61)[1]	0.36	0.99
By Pyrite	0.50	-	-
SRC Sulfur, %	0.60	0.61	0.53
First Order Rate Constants, hr^{-1}			
K_a	1.24	1.45	1.74
K_p	2.65	2.19	2.45

[1] ( ) - means negative value

232

Table 129

Effect of Iron Impregnation, Molecular Dispersion and Particulate
Addition on Distribution of Elements in Elkhorn #2 Coal Liquefaction Products

Sample No.	Original Solvent FOB #11	31-186	31-196	38-10	38-17	47-10
Temperature, °F	-	825	850	825	850	825
Additive	-	Pyrite		Iron Impregnation		Molecular Dispersion
Oil Fraction, wt.%						
C	89.7	89.2	89.4	89.9	89.8	90.4
H	7.2	7.5	7.5	7.1	7.0	7.1
O	1.4	1.8	1.6	-	-	1.1
N	1.1	0.8	0.9	0.8	1.0	0.8
S	0.6	0.7	0.6	0.7	0.6	0.6
Asphaltene Fraction, wt.%						
C	-	85.6	87.3	85.6	86.6	85.5
H	-	5.7	6.0	6.0	5.8	6.0
O	-	5.9	5.1	-	-	5.8
N	-	2.3	-	2.4	2.4	2.2
S	-	0.5	0.5	0.5	0.5	0.5
Preasphaltene Fraction, wt.%						
C	-	85.4	85.8	82.9	84.9	85.3
H	-	5.2	5.0	4.9	4.6	4.8
O	-	6.1	5.7	-	-	7.0
N	-	2.3	2.3	2.6	2.5	2.4
S	-	0.7	0.6	0.7	0.6	0.6

Table 130

Effect of Iron Impregnation and
Particulate Addition on Distribution of
Protons in Oil Fractions from Elkhorn #2 Coal Products

Sample No.	31-186		31-196		38-10		38-17	
Temperature, °F	825		850		825		850	
Additive	Pyrite				Iron Impregnation			
Total Hydrogen, wt.%	7.5		7.5		7.1		7.0	
Distribution of Protons, %								
	Abs.	Rel.	Abs.	Rel.	Abs.	Rel.	Abs.	Rel.
H_{AR}	2.90	38.7	3.20	42.6	3.64	51.3	3.50	50.0
H_a	2.47	32.9	2.15	28.7	1.80	25.3	1.90	27.1
H_o	2.13	28.4	2.15	28.7	1.66	23.4	1.60	22.9

Abs. - Absolute
Rel. - Relative

The above data show that the mode of catalyst addition plays an important role in coal liquefaction. The effectiveness of a metal catalyst can be enhanced significantly by finely dispersing it in the coal liquefaction reaction mixture. In addition, the concentration of the metal catalyst can be reduced through more effective dispersion techniques without significantly affecting product distribution. The reduction in catalyst loading will eventually increase the overall throughput of the plant, drastically reduce the load in the solid-liquid separation unit, and improve overall process economics.

Catalysis by Metallic Wastes

Like iron compounds, many other inexpensive industrial metallic wastes such as red mud, flue dust, and zinc sulfide are available in large quantities that can be used as disposable catalysts in coal liquefaction. Therefore, it is of great interest to determine their catalytic activity in coal liquefaction, as well as to compare their activity with that of pyrite.

Some of the metallic waste samples tested in the program have already been reported to catalyze coal liquefaction reactions. For example, red mud was extensively used in World War II by Germans to liquefy brown coal. However, the activity of red mud has never been tested in the liquefaction of U.S. coals.

Catalysis by Red Mud - The liquefaction of Elkhorn #3 coal was studied at 825 and 850°F in the presence of red mud. Red mud addition at 850°F increased coal conversion and oil production from 84 to 87% and from 20 to 34%, respectively (Table 131). Addition of red mud also increased the production of hydrocarbon gases from 6.8 to 8.7%. Asphaltenes production decreased from 29.2 to 18.5%, and that of the preasphaltenes decreased from 25.4 to 22.1%. The addition of red mud increased significantly the conversion of asphaltenes. The rate constants for asphaltene and preasphaltene conversion increased from 0.75 to 1.70 hr^{-1} and from 2.95 to 3.48 hr^{-1}, respectively. The increase in hydrogen consumption from 0.92 to 2.51% with red mud was due to an increased production of hydrocarbon gases, oils, and water, and to the reduction of Fe_2O_3 to Fe_3O_4. The sulfur content of SRC decreased marginally, and all hydrogen sulfide gas produced by desulfurization of coal was removed by red mud.

Table 131
Liquefaction of Elkhorn #3 Coal in the Presence
of Various Minerals and Metallic Wastes

Sample No.	31-81	31-268	31-278	31-301	31-312	31-321
Feed Composition	70% Solvent + 30% Coal	60% Solvent + 30% Coal + 10% Red Mud		60% Solvent + 30% Coal + 10% Flue Dust		67.5% Solvent + 30% Coal + 2.5% Lime
Temperature, °F	850	825	850	825	850	850
Pressure, psig	2000	2000	2000	2000	2000	2000
Hydrogen Flow Rate, MSCF/T	18.5	24.1	24.8	22.8	23.5	21.8
Reaction Time, Min.	38	39	39	37	38	38
Product Distribution, wt.% MAF Coal						
HC	6.3	5.3	8.7	4.5	9.2	8.9
CO, CO_2	1.0	1.3	1.7	1.3	1.7	0.3
H_2S	0.2	0.0	0.0	0.0	0.0	0.0
NH_3	0.0	0.0	0.0	0.0	0.0	0.0
Oils	20.4	35.9	33.6	30.9	25.5	15.1
Asphaltenes	29.2	10.6	18.5	26.3	33.7	14.2
Preasphaltenes	25.4	28.4	22.1	19.6	18.8	31.6
I.O.M.	15.8	16.6	12.8	14.2	7.1	27.9
Water	1.2	1.9	2.6	3.2	4.0	2.0
Conversion	84.2	83.4	87.2	85.8	92.9	72.1
Hydrogen Consumption, wt.% MAF Coal						
Total	0.91	1.06	1.86	1.43	2.19	1.04
From Gas	0.92	2.13	2.51	2.32	3.08	0.66
From Solvent	(0.01)	(1.07)	(0.65)	(0.89)	(0.89)	0.38
By Additive	--	0.08	0.08	--	--	--
SRC Sulfur, %	0.50	0.56	0.46	0.59	0.46	0.84
First Order Rate Constants, hr^{-1}						
K_a	0.75	2.45	1.70	1.31	0.88	0.86
K_p	2.95	2.44	3.48	4.51	4.73	1.41

( ) - means negative value

236

Table 132

X-Ray Diffraction Analysis of the Minerals and Metallic Wastes
Before and After the Use as Additives in Elkhorn #3 Coal Liquefaction

Additive	Phase	Original Minerals or Metallic Waste	Analysis of Minerals and Metallic Wastes After Coal Liquefaction Reaction
Red Mud	Major	Fe_2O_3	Fe_3O_4
	Minor	Quartz, $CaCO_3$, Al_2O_3	Quartz, FeS (sphalerite type), Troilite, Fe_2O_3, $CaCO_3$, Al_2O_3
Flue Dust	Major	Fe_3O_4, $NiFe_2O_4$, $FeCr_2O_4$	Fe_3O_4, $NiFe_2O_4$, $FeCr_2O_4$
	Minor	FeS, ZnS (sphalerite type)	FeS, ZnS (sphalerite type)
Lime	Major	CaO	$CaCO_3$
	Minor	--	$CaSO_4 \cdot 2H_2O$

237

The distribution of elements in various fractions (Table 133) showed minor changes in sulfur content of asphaltenes and preasphaltenes obtained with red mud compared with the no-additive case. Minor variations were also noted in other elements in the oils, asphaltenes, and preasphaltenes. Minor variations in the distribution of oxygen compounds were noted with red mud (Table 134). The distribution of nitrogen compounds in the oils showed an increase in pyridine type compounds. Proton distribution (Table 135) showed a decrease in H_{AR} and an increase in H_a and H_o, which could signify higher quality of solvent generated with red mud than with no additive. The values of the Brown-Ladner structural parameters shown in Table 136 presented insignificant variations with red mud addition.

With both an increase in temperature from 825 to 850°F and red mud, coal conversion increased from 83 to 87%. The production of hydrocarbon gases and asphaltenes increased from 5.3 to 8.7% and 10.6 to 18.5%, respectively. Oil and preasphaltene production decreased from 35.9 to 33.6% and from 28.4 to 22.1% with an increase in temperature (see Table 131). The increase in conversion of coal and preasphaltenes resulted in a net increase of asphaltene and hydrocarbon gas production. The rate of asphaltene conversion decreased from 2.45 to 1.70 hr^{-1} and that of preasphaltene conversion increased from 2.44 to 3.48 hr^{-1} with an increase in temperature. These observations suggest that preasphaltene conversion is favored and that of asphaltene is retarded by increasing the temperature in the presence of red mud. It should be noted that no H_2S was observed in the gas phase. The hydrogen consumption calculated on the basis of elemental hydrogen balance increased from 2.13 to 2.51%; this increase was due mainly to increased production of hydrocarbon gases and water. The X-ray diffraction analysis of the coal liquefaction residue (Table 132) showed partial conversion of Fe_2O_3 present in red mud to Fe_3O_4 and FeS. Part of the total hydrogen consumption was due to the reduction of Fe_2O_3 to Fe_3O_4, i.e., 0.08 wt% hydrogen on an MAF coal basis.

No significant differences in the elemental distribution of various fractions were noted (Table 133). Simulated distillation of the oil fractions obtained at 850 and 825°F (Figure 40) showed no major differences.

Table 133

Distribution of Elements in the Liquefaction Products of
Elkhorn #3 Coal in the Presence of Various Minerals and Metallic Wastes

Sample No.	31-81	31-268	31-278	31-301	31-312	31-321
Additive	None	Red Mud		Flue Dust		Lime
Temperature, °F	850	825	850	825	850	850
Oil Fraction, wt.%						
C	89.7	89.3	89.3	89.1	89.1	89.9
H	7.3	7.7	7.5	7.7	7.7	7.1
O	1.7	1.6	1.7	1.7	1.7	1.5
N	0.7	0.8	0.9	0.9	1.0	0.8
$\underline{S}$	0.6	0.6	0.6	0.6	0.6	0.6
n MW	220	195	230	230	215	220
Asphaltene Fraction, wt.%						
C	86.1	86.1	85.5	85.7	85.9	86.3
H	6.1	6.2	6.2	6.5	6.2	5.8
O	4.9	5.6	5.6	5.8	5.2	5.2
N	2.4	1.6	2.3	1.4	2.3	2.1
$\underline{S}$	0.5	0.6	0.4	0.6	0.4	0.6
n MW	390	--	450	535	380	410
Preasphaltene Fraction, wt.%						
C	86.2	85.0	85.4	85.1	85.4	82.1
H	5.1	4.8	5.0	5.6	5.3	4.6
O	5.9	6.5	6.3	6.2	6.2	7.1
N	2.5	2.5	2.8	2.5	2.6	2.4
$\underline{S}$	0.5	0.6	0.5	0.6	0.6	0.7
n MW	990	--	--	--	1225	1105

Table 134

Distribution of Oxygen and Nitrogen Compounds in the Oil
Fraction from the Liquefaction Products anc Elkhorn #2 Coal
in the Presence of Various Minerals and Metallic Wastes

Sample No.	FOB #11		31-81		31-268		31-278		31-301		31-312		31-321	
Additive	--		None		Red Mud				Flue Dust				Lime	
Temperature, °F	--		850		825		850		825		850		850	
Oxygen Distribution, wt.%														
Total	1.42		1.72		1.63		1.71		1.73		1.74		1.52	
	Abs.	Rel.	Abs.	Rel.	Abs.	Rel.	Abs.	Rel.	Abs.	Rel.	Abs.	Rel.	Abs.	Rel.
O as O	0.90	63.4	1.09	63.4	1.02	62.6	1.01	59.1	1.05	60.7	1.03	59.2	0.91	59.9
O as OH	0.52	36.6	0.63	36.6	0.61	37.4	0.70	40.9	0.68	39.3	0.71	40.8	0.61	40.1
Nitrogen Distribution, wt.%														
Total	1.05		0.73		0.76		0.89		0.89		0.95		0.83	
	Abs.	Rel.	Abs.	Rel.	Abs.	Rel.	Abs.	Rel.	Abs.	Rel.	Abs.	Rel.	Abs.	Rel.
N as N	0.61	58.1	0.30	41.1	0.41	54.0	0.50	56.2	0.53	59.6	0.55	57.9	0.44	53.0
N as NH	0.38	36.2	0.32	43.8	0.30	39.5	0.33	37.1	0.31	34.8	0.32	33.7	0.35	42.2
N as NH_2	0.06	5.7	0.11	15.1	0.05	6.5	0.06	6.7	0.05	5.6	0.08	8.4	0.04	4.8

Table 135

Distribution of Protons in the Oil Fractions
from the Liquefaction of Elkhorn #3 Coal in the
Presence of Various Minerals and Metallic Wastes

Sample No.	FOB #11	31-81	31-268	31-278	31-301	31-312	31-321
Additive	--	None	Red Mud		Flue Dust		Lime
Temperature, °F	--	850	825	850	825	850	850
Total Hydrogen, wt.%	7.2	7.3	7.7	7.5	7.7	7.7	7.1

Distribution of Protons, %

Relative

	FOB #11	31-81	31-268	31-278	31-301	31-312	31-321
H_{AR}	44.4	47.0	43.6	43.5	39.9	41.4	48.8
H_a	28.0	28.0	28.5	28.3	30.3	25.9	26.3
H_o	27.6	25.0	27.9	28.2	29.8	32.7	24.9

Absolute

	FOB #11	31-81	31-268	31-278	31-301	31-312	31-321
H_{AR}	3.20	3.43	3.36	3.26	3.07	3.19	3.46
H_a	2.02	2.04	2.19	2.12	2.33	1.99	1.87
H_o	1.98	1.83	2.15	2.12	2.30	2.52	1.77

FIGURE 40
SIMULATED DISTILLATION OF OIL FRACTIONS OBTAINED BY LIQUEFACTION OF ELKHORN #3 COAL IN THE PRESENCE OF RED MUD

——— 31–268 (RED MUD, 825°F)

- - - - 31–278 (RED MUD, 850°F)

DISTILLATION YIELD, WT. %

TEMPERATURE, °F

242
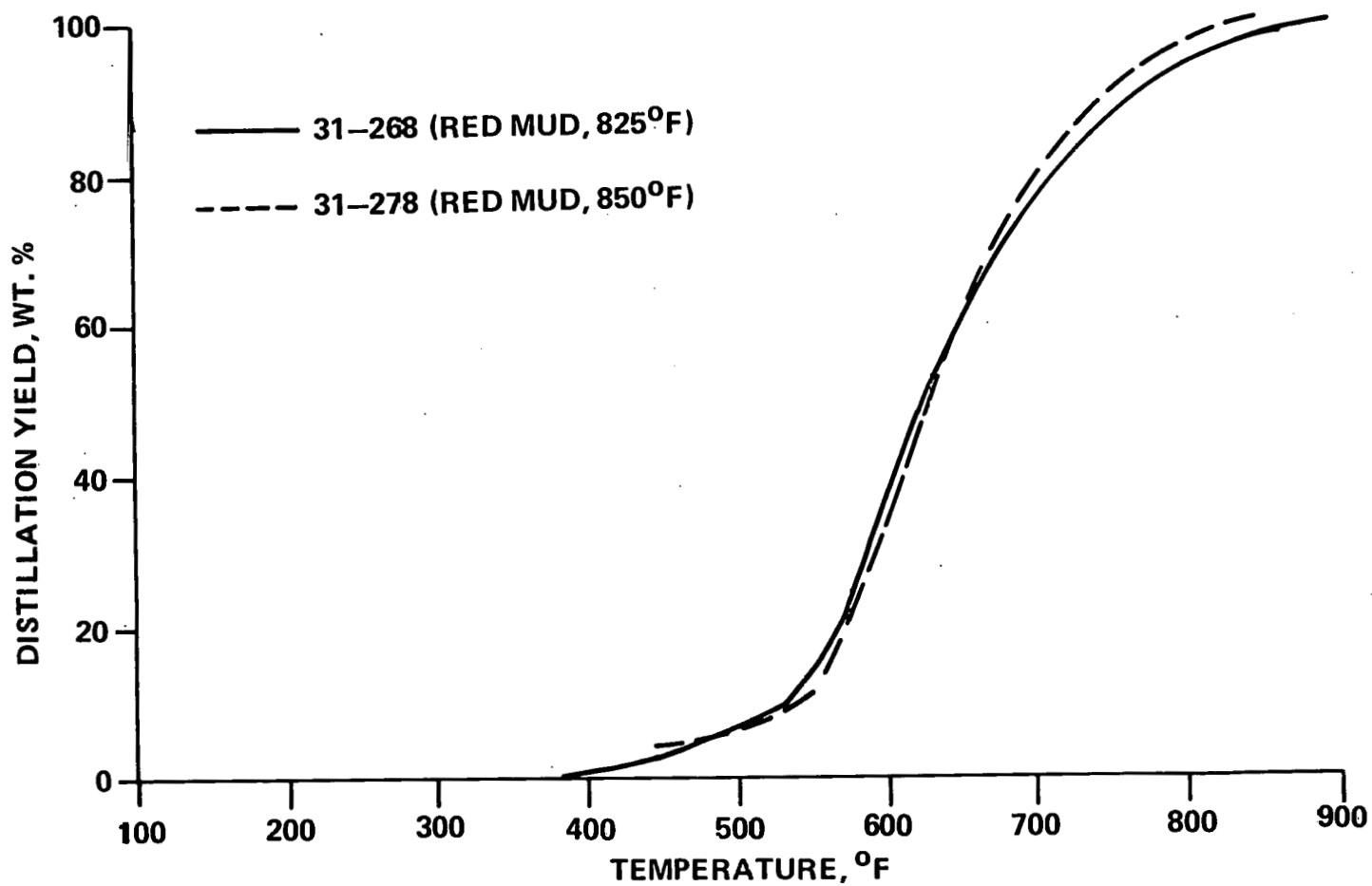
The distribution of nitrogen and oxygen compounds in the oil fraction presented in Table 134 showed insignificant variations with the increase in temperature. At 850°F, the hydrogen content was lower than at 825°F, but the distribution of protons (Table 135) was very similar at both temperatures. In addition, the Brown-Ladner structural parameters were very similar at both temperatures.

It can be concluded that the addition of red mud to the coal liquefaction reaction mixture increases oil and hydrocarbon gas production, improves coal conversion, increases hydrogen consumption, and decreases asphaltene and preasphaltene production. Increasing the reaction temperature in the presence of red mud increases coal conversion, hydrocarbon gas and asphaltene production, and hydrogen gas consumption, and decreases oil production. Therefore, if the goal of coal liquefaction is to maximize oil production and minimize hydrogen consumption, lower temperature should be used when red mud is added to the reaction mixture.

As presented earlier, red mud consists of approximately 50% Fe_2O_3; the balance is Al_2O_3, quartz, and other impurities, however speculite consists primarily of Fe_2O_3. Alumina and quartz were found to be inactive in the batch coal liquefaction tests. It is not known why the iron oxide present in red mud is different from that in speculite, which is pure iron oxide. Attempting to ascertain the reasons for the difference in the catalytic activity of red mud and speculite, the nitrogen BET surface area of the two materials was determined. Speculite and red mud differed by an order of magnitude, i.e., and 35 m^2/g, respectively. This variation could be one of the factors responsible for the higher oil yield with red mud.

Catalysis by Flue Dust - Since the flue dust tested contained significant quantitites of iron, nickel, and molybdenum metals, it was expected to have very high activity in coal liquefaction reactions. As expected, coal conversion increased from 84 to 93% on addition of flue dust at 850°F (Table 131). Flue dust addition also increased the production of hydrocarbon gases and oils from 6.8 to 9.2% and 20.4 to 25.5%, respectively. Preasphaltene production decreased from 25.4 to 18.8%. The increased conversion of coal and

Table 136

Brown-Ladner Structural Parameters for the Oil Fractions
from the Liquefaction of Elkhorn #3 Coal in the
Presence of Various Minerals and Metallic Wastes

Sample No.	FOB #11	31-81	31-268	31-273	31-301	31-312	31-321
Additive	--	None	Red Mud		Flue Dust		Lime
Temperature, °F	--	850	825	850	825	850	850
f_a	0.71	0.72	0.71	0.71	0.70	0.70	0.73
σ	0.28	0.27	0.27	0.26	0.28	0.25	0.26
H_{AR}/C_{AR}	0.80	0.85	0.85	0.83	0.80	0.79	0.84
R_a	3.23	3.18	2.86	3.29	3.49	3.24	3.22

preasphaltenes resulted in added production of hydrocarbon gases, oils and asphaltenes. The addition of flue dust increased the rates of conversion of asphaltenes only marginally from 0.75 to 0.88 hr^{-1} and of preasphaltenes from 2.95 to 4.73 hr^{-1}. Preasphaltene conversion was found to be more sensitive to flue dust addition than was asphaltene conversion. The sulfur content of SRC was unchanged. The total hydrogen consumption increased from 0.91 to 2.19%.

The distribution of elements in the various fractions obtained with and without the addition of flue dust is summarized in Table 133. No differences were noted in the sulfur content of oils and preasphaltenes, but the sulfur content of asphaltenes decreased from 0.6 to 0.4% on addition of flue dust. Higher nitrogen content in oils and minor differences in the nitrogen contents of the asphaltenes and preasphaltenes were noted the dust addition. Higher hydrogen contents were observed in all the fractions with flue dust over no-additive run.

The distribution of nitrogen and oxygen compounds in the oils showed higher concentration of hydroxyl and pyridine-type compounds with flue dust (see Table 134). Lower concentration of H_{AR} and higher concentration of H_a and H_o were noted with flue dust, as shown in Table 135; the lattter indicates better quality of solvent generated with flue dust than that generated with no-additive. No significant differences were noted in the values of aromaticity (f_a), degree of substitution (σ), and H_{AR}/C_{AR} with flue dust (see Table 136).

Coal conversion increased from 86 to 93% and oil production decreased from 30.9 to 25.5% with increasing temperature in the presence of flue dust. No significant change was noticed in preasphaltene production with temperature. The increased conversion of coal resulted in added production of asphaltenes. Hydrocarbon gas production increased from 4.5 to 9.2% as the temperature increased from 825 to 850°F. The decrease in oil production with temperature was balanced by a corresponding increase in the production of hydrocarbon gases. The rate of conversion of asphaltenes decreased from 1.31 to 0.88, and the rate of preasphaltene conversion increased slightly from 4.51 to 4.75. No H_2S was detected in the product gas at both temperatures and the sulfur content

of the SRC decreased from 0.59 to 0.46% with an increase in temperature. Hydrogen consumption calculated on the basis of elemental hydrogen balance increased from 1.43 to 2.19%. The X-ray diffraction analysis of the coal liquefaction residue material (Table 132) showed no change in the chemical nature of flue dust before and after the reaction.

The distribution of elements in the oils (Table 133) showed no changes with reaction temperature. Lower hydrogen contents were noted in the asphaltenes and preasphaltenes at 850°F than at 825°F. Otherwise, no significant differences were noted in the asphaltenes and preasphaltenes with increasing temperature.

The distribution of nitrogen and oxygen compounds (Table 134) showed insignificant variations with temperature. The concentration of H_{AR} in the oils was unchanged with temperature (see Table 135), whereas significant changes in H_a and H_o were noted; H_a decreased from 2.33 to 1.99% (absolute) and H_o increased from 2.30 to 2.52%. It is not known what effect a shift in the concentration of H_a and H_o would have on the solvent quality. The degree of substitution (σ) and average number of condensed aromatic rings decreased from 0.28 to 0.25 and from 3.49 and 3.24, respectively, with an increase in temperature (see Table 136). The simulated distillation of the oil fractions obtained at 825 and 850°F were very similar, as shown in Figure 41.

It can be concluded that the addition of flue dust to coal liquefaction reaction increases the production of oils, hydrocarbon gases, and asphaltenes, increases conversion of coal and consumption of hydrogen, and improves the quality of the solvent generated by the reaction. The increase in reaction temperature in the presence of flue dust decreases the oil production and increases hydrocarbon gas production and hydrogen consumption. Since the objective of the program is to maximize oil production with minimum hydrocarbon gas production and hydrogen consumption, a lower temperature is preferred. The reaction temperature of 825°F in no case represents the optimum reaction temperature.

Catalysis by Lime - U.S. coals contain varying amounts of calcium, which is known to cause scaling problems in heat exchangers. To avoid scaling, several researchers have proposed the removal of calcium from coal before it is liquefied.

FIGURE 41
SIMULATED DISTILLATION OF OIL FRACTIONS OBTAINED BY LIQUEFACTION OF ELKHORN #3 COAL IN THE PRESENCE OF FLUE DUST

——— 31–301 (FLUE DUST, 825°F)

– – – 31–312 (FLUE DUST, 850°F)
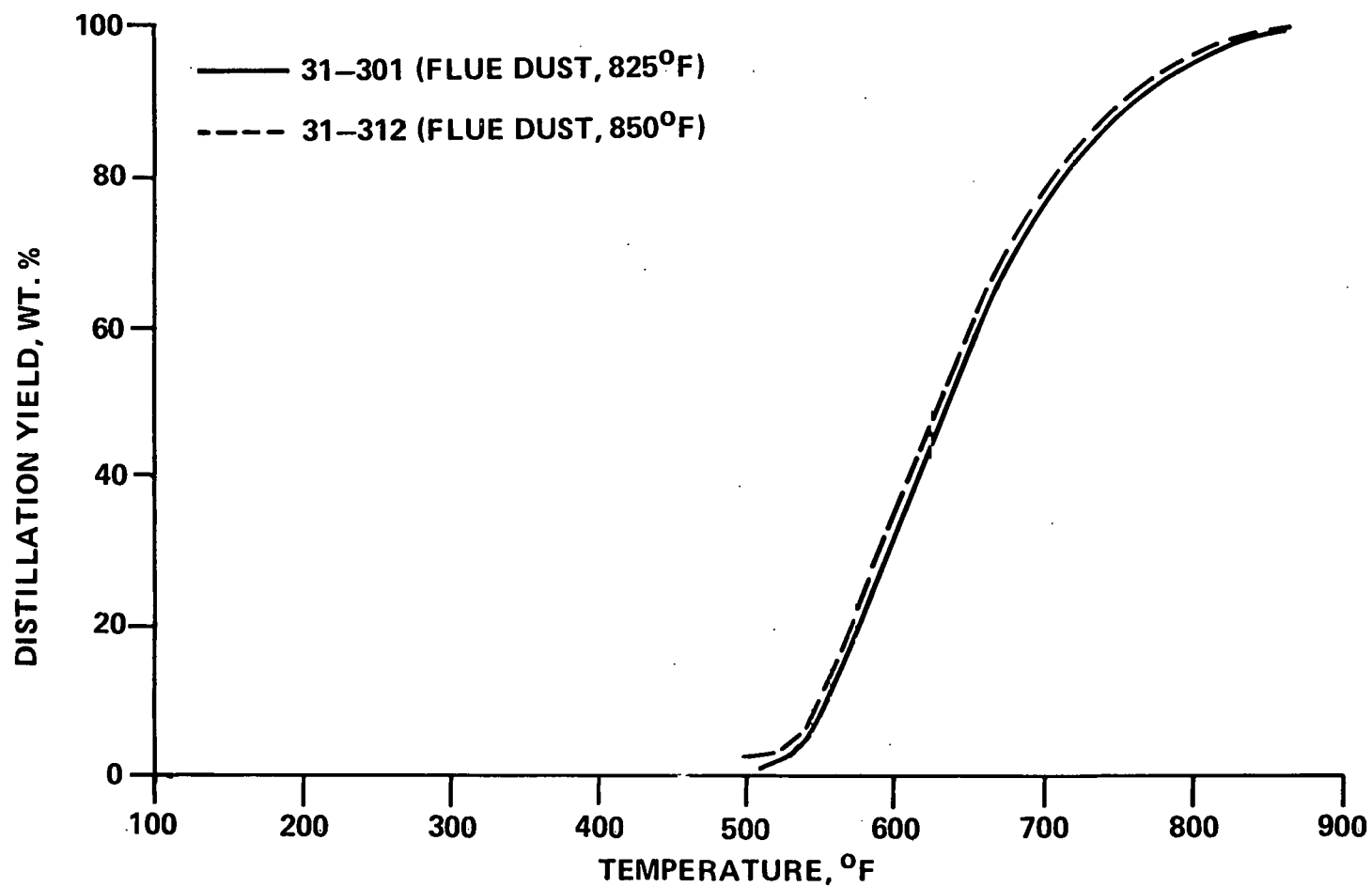
However, the role of calcium in coal liquefaction is not well known. Therefore, calcium in the form of lime was added to the reaction mixture to study its role in coal liquefaction and the results are discussed below.

The liquefaction of coal in the presence of 2.5 wt% lime based on feed slurry at 850°F resulted in a coal conversion of 72% as shown in Table 131. Comparing the liquefaction of coal in the presence and absence of lime (Table 131) shows that lime addition was detrimental to coal liquefaction because it decreased coal conversion. Hydrocarbon gas increased and oil and asphaltene production decreased simultaneously. Lime addition dramatically reduced the rate of preasphaltene conversion from 2.95 to 1.41 hr^{-1}. Asphaltene conversion rates changed slightly. Hydrogen consumption based on elemental hydrogen balance changed slightly from 0.91 to 1.04% with lime addition. The SRC sulfur content increased significantly from 0.50 to 0.84%. The production of $CO + CO_2$ was reduced considerably from 1.0 to 0.3%, and no hydrogen sulfide was detected in the gas phase with lime. The X-ray diffraction analysis of the coal liquefaction residue (Table 132) showed complete conversion of CaO to $CaCO_3$ and $CaSO_4$.

The distribution of elements in the various fractions obtained with and without lime are compared in Table 133. The hydrogen content was lower in all the fractions obtained with lime. Higher sulfur contents were noted in asphaltenes and preasphaltenes with lime, whereas no change was noted in the oils. Minor variations were noted in the nitrogen and oxygen contents of all the fractions. In addition, lower concentrations of ether and higher concentrations of pyridine-type compounds were observed in the oils obtained with lime compared to the no-additive run (see Table 134). Table 135 shows no significant difference in the concentration of H_{AR} with or without lime addition, whereas the concentration of H_a and H_o decreased with lime. This could indicate low quality solvent generated with lime addition compared with the no-additive run. The Brown-Ladner structural parameters were not significantly different with or without lime (see Table 136).

The simulated distillation of the oil fractions obtained with and without lime are shown in Figure 42. Lower initial and higher final boiling points of the oil were noted with lime. The two boiling point distribution curves crossed each other at 670°F.

FIGURE 42
COMPARISON OF SIMULATED DISTILLATION OF
OIL FRACTIONS OBTAINED BY LIQUEFACTION OF
ELKHORN #3 COAL IN THE PRESENCE AND
ABSENCE OF LIME AT 850° F
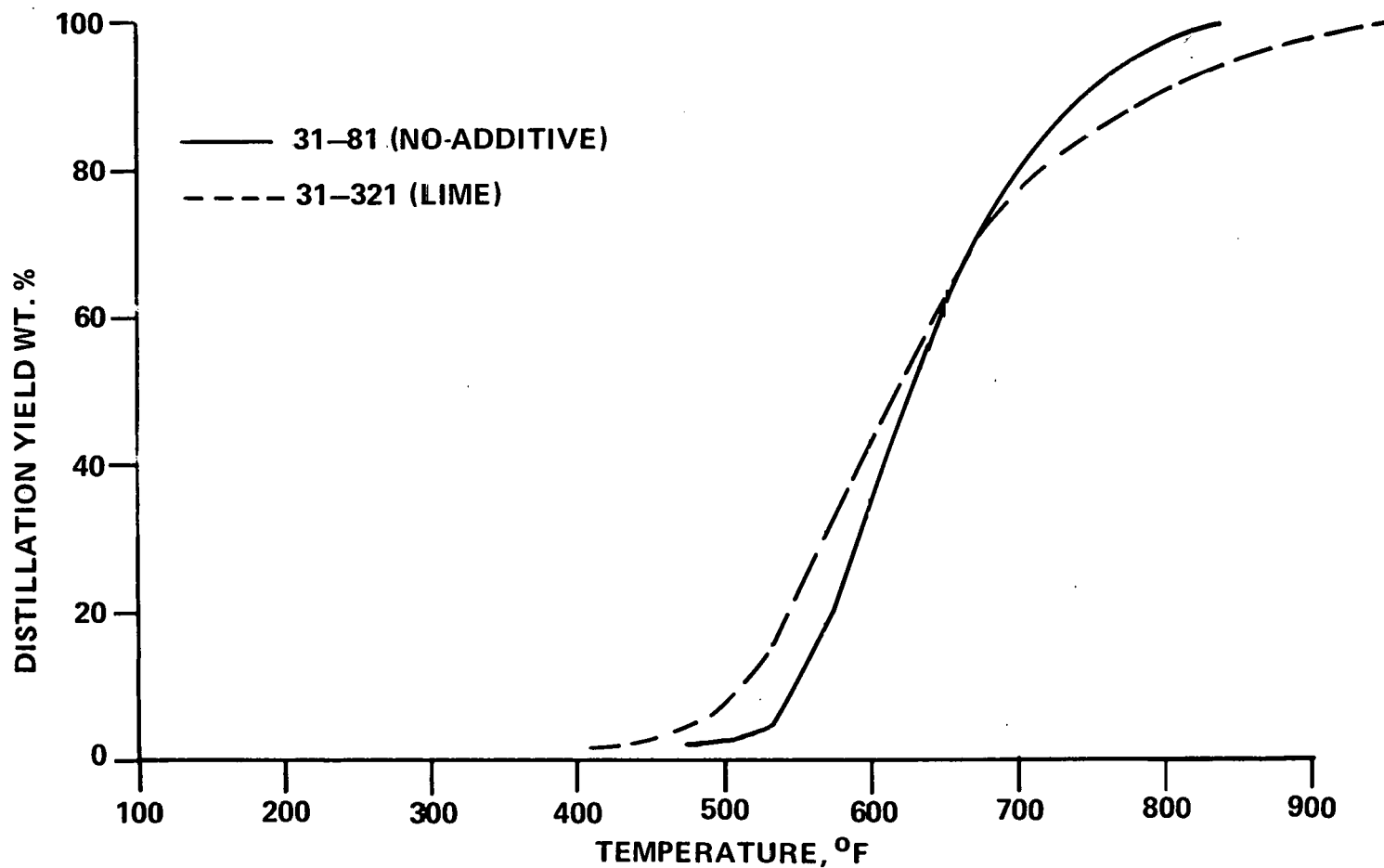
From the above data it can be concluded that lime added to the coal liquefaction reaction mixture is detrimental, since it decreases coal conversion and oil and asphaltene production, increases hydrogen consumption and lowers the quality of solvent generated by the reaction.

Catalysis by Zinc Sulfide - Zinc compounds in the form of Lewis acids have been reported to significantly catalyze coal liquefaction reactions, but they are expensive and cause severe corrosion problems. On the contrary, zinc sulfide mineral is inexpensive and readily available, and therefore can be used as a disposable catalyst. Therefore, the catalytic activity of zinc sulfide was studied in coal liquefaction reaction and the results are discussed below.

Elkhorn #3 Coal - Addition of zinc sulfide at 850°F increased coal conversion from 84 to 92% and increased oil and hydrocarbon gas production from 20.4 to 29.3% and from 6.8 to 8.9%, respectively (Table 137). Asphaltenes decreased from 29.2 to 22.3%. The rate of conversion of asphaltenes increased from 0.75 to 1.31 hr^{-1} and that of preasphaltene conversion did not change significantly. These data show that preasphaltene conversion was not catalyzed by zinc sulfide, whereas it catalyzed the conversion of asphaltenes to oils. Hydrogen consumption based on elemental hydrogen balance increased from 0.92 to 1.93% with zinc sulfide.

Coal conversion increased from 89 to 92% as temperature increased from 825 to 850°F in the presence of zinc sulfide. Hydrocarbon gas production increased with increasing reaction temperature from 5.8 to 8.9% Oil, asphaltene and preasphaltene production was not greatly changed. The rates of asphaltene and preasphaltene conversion increased slightly with increasing the temperature. Hydrogen consumption increased from 1.43 to 1.93%, and SRC sulfur content decreased slightly with the increase in temperature.

The distribution of elements in the various fractions (Table 138) showed no change in the oils at the two temperatures, but minor variations were noted in the asphaltenes and preasphaltenes. X-ray diffraction analysis of the coal liquefaction residue showed no change in the chemical form of zinc sulfide before and after the reaction.

Table 137

Catalytic Activity of Zinc Sulfide in Coal Liquefaction

Sample No.	31-81	31-219	31-234	31-128	44-10
Feed Composition	70% Solvent + 30% Elkhorn #3 Coal	60% Solvent + 30% Elkhorn #3 Coal + 10% ZnS		70% Solvent + 30% Elkhorn #2 Coal	69% Solvent + 30% Elkhorn #2 Coal + 1% ZnS
Temperature, °F	850	825	850	825	825
Pressure, psig	2000	2000	2000	2000	2000
Hydrogen Flow Rate, MSCF/T	18.6	26.4	24.0	18.9	23.5
Reaction Time, Min.	38	41	39	35	37.3
Product Distribution, Wt.% MAF Coal					
HC	6.8	5.8	8.9	5.2	4.3
CO, CO_2	1.0	1.4	1.5	0.7	1.0
H_2S	0.2	0.2	0.2	0.3	0.2
NH_3	0.0	0.0	0.0	0.0	0.0
Oils	20.4	27.3	29.3	12.2	23.0
Asphaltenes	29.2	24.1	22.3	21.2	18.5
Preasphaltenes	25.4	27.3	27.5	44.2	36.8
I.O.M.	15.8	11.2	7.6	14.7	14.7
Water	1.2	2.7	2.7	1.5	1.5
Conversion	84.2	88.8	92.4	85.3	85.3
Hydrogen Consumption, Wt.% MAF Coal					
Total	0.91	1.43	1.93	0.64	0.41
From Gas	0.92	1.52	1.93	0.59	0.46
From Solvent	(0.01)[1]	(0.09)	0.00	0.05	(0.05)
SRC Sulfur, %	0.50	0.65	0.55	0.61	0.76
First Order Rate Constants, hr^{-1}					
K_a	0.75	1.11	1.31	0.62	1.61
K_p	2.95	2.66	2.79	1.27	2.13

[1] ( ) - means negative value

251

Table 138

Distribution of Elements in the
Zinc Sulfide Catalyzed Liquefaction Products

Sample No.	31-81	31-219	31-234	31-128	44-110
Coal	Elkhorn #3			Elkhorn #2	
Additive	None	ZnS		None	ZnS
Temperature, °F	850	825	850	825	825
Oil Fraction, wt.%					
C	89.7	89.4	89.4	89.5	89.3
H	7.3	7.3	7.3	7.2	7.3
O	1.7	1.8	1.8	1.7	1.9
N	0.7	0.9	0.9	0.9	0.9
S	0.6	0.7	0.7	0.7	0.6
$\bar{n}$ MW	220	230	250	--	--
Asphaltene Fraction, wt.%					
C	86.1	85.2	86.2	85.9	84.6
H	6.1	6.3	5.9	6.3	5.8
O	4.9	5.8	5.1	5.8	6.3
N	2.4	2.1	2.4	1.4	2.6
S	0.5	0.6	0.5	0.6	0.7
$\bar{n}$ MW	390	470	465	--	--
Preasphaltene Fraction, wt.%					
C	86.2	84.4	86.6	85.3	82.6
H	5.1	5.5	4.8	5.2	4.8
O	5.9	6.6	5.5	6.2	9.4
N	2.5	2.8	2.5	2.2	2.4
S	0.5	0.7	0.6	0.6	0.8
$\bar{n}$ MW	990	1210	1775	--	--

The distribution of oxygen and nitrogen compounds presented in Table 139 showed no significant difference with an increase in temperature. In addition, the distribution of protons was very similar at both temperatures as shown in Table 140. The Brown-Ladner structural parameters (Table 141) were very similar at both reaction temperatures.

In conclusion, coal liquefaction in the presence of zinc sulfide at 825 and 850°F showed only minor variations in product distribution, element composition, nitrogen compound, oxygen compound and proton distribution and variation in Brown-Ladner structural parameters. Hydrogen consumption was lower at the lower temperature, whereas oil production was higher with zinc sulfide at 825°F (27.3%) than with no additive at 850°F (20.4%). These data suggest a lower reaction temperature with zinc sulfide addition to the reaction mixture to best utilize its catalytic activity.

Elkhorn #2 Coal - The liquefaction of Elkhorn #2 coal in the presence of one wt% ZnS based on feed slurry at 825°F is compared to the baseline run in Table 137. The addition of ZnS did not alter overall coal conversion, but improved the conversion of preasphaltenes and production of oils. Preasphaltene production decreased from 44 to 37% and that of oils increased from 12 to 23% with the addition of ZnS compared with the no-additive run. Rates of conversion of asphaltenes and preasphaltenes increased significantly from 0.62 to 1.61 hr^{-1} and from 1.27 to 2.13 hr^{-1}, respectively. The production of hydrocarbon gases, H_2S, CO, CO_2, asphaltenes, and water was not greatly affected, although hydrogen consumption based on elemental hydrogen balance decreased and SRC sulfur content increased slightly with ZnS addition.

The distribution of elements in the various fractions given in Table 138 showed higher sulfur and lower hydrogen contents in the asphaltene and preasphaltene fractions with ZnS compared with the no-additive run. Otherwise, no major differences were noted. The distribution of protons (Table 140) showed a decrease in H_{AR} value and a corresponding increase in the concentrations of H_a and H_o with ZnS, indicating that the quality of solvent generated with ZnS was higher than that generated with no-additive.

It can be concluded that zinc sulfide can be selectively used in coal liquefaction to increase the production of oils; higher SRC sulfur content is the only disadvantage.

Table 139

Distribution of Oxygen and Nitrogen Compounds
in the Oil Fraction of Zinc Sulfide Catalyzed Liquefaction

Sample No.	FOB #11		31-81		31-219		31-234	
Additive	--		None		Zinc Sulfide			
Temperature, °F	--		850		825		850	
Oxygen Distribution, Wt.%								
Total	1.42		1.72		1.75		1.78	
	Abs.	Rel.	Abs.	Rel.	Abs.	Rel.	Abs.	Rel.
O as O	0.90	63.4	1.09	63.4	1.14	65.1	1.14	64.0
O as OH	0.52	36.6	0.63	36.6	0.61	34.9	0.64	36.0
Nitrogen Distribution, Wt.%								
Total	1.05		0.73		0.86		0.88	
	Abs.	Rel.	Abs.	Rel.	Abs.	Rel.	Abs.	Rel.
N as N	0.61	58.1	0.30	41.1	0.51	59.3	0.44	50.0
N as NH	0.38	36.2	0.32	43.8	0.30	34.9	0.34	38.6
N as NH_2	0.06	5.7	0.11	15.1	0.05	5.8	0.10	11.4

Table 140

Distribution of Protons in the Oil
Fractions of Zinc Sulfide Catalyzed Liquefaction

Sample No.	FOB #11	31-81	31-219	31-234	31-128	44-10
Coal	--	Elkhorn #3			Elkhorn #2	
Additive		None	Zinc Sulfide		None	Zinc Sulfide
Temperature, °F	--	850	825	850	825	825
Total Hydrogen, Wt.%	7.2	7.3	7.3	7.3	7.2	7.3
Distribution of Protons, %						
Relative						
H_{AR}	44.4	47.0	46.7	47.3	45.3	40.2
H_a	28.0	28.0	29.5	28.3	27.1	30.2
H_o	27.6	25.0	23.8	24.4	27.6	29.6
Absolute						
H_{AR}	3.20	3.43	3.41	3.45	3.26	2.93
H_a	2.02	2.04	2.15	2.07	1.95	2.20
H_o	1.98	1.83	1.74	1.78	1.99	2.16

Table 141

Brown-Ladner Structural Parameters for the Oil Fractions
of Zinc Sulfide Catalyzed Liquefaction of Elkhorn #3 Coal

Sample No.	FOB #11	31-81	31-219	31-234
Additive	--	None	Zinc Sulfide	
Temperature, °F	--	850	825	850
f_a	0.71	0.72	0.72	0.72
σ	0.28	0.27	0.28	0.27
H_{AR}/C_{AR}	0.80	0.85	0.87	0.85
R_a	3.23	3.18	3.26	3.47

Activity Comparison of Various Minerals and Metallic Wastes in Liquefaction

The catalytic activity of various minerals and metallic wastes in the liquefaction of Elkhorn #3 coal is compared in Table 142. The most desirable functions of a catalyst in coal liquefaction are high oil production, high coal conversion, good solvent quality, low hydrocarbon gas production, and low hydrogen consumption. The performance of the various minerals and metallic waste samples tested was rated on the basis of the above criteria and produced a classification as follows:

Hydrocarbon gases:	pyrite > red mud > ZnS > lime > flue dust > speculite
Oil:	pyrite > red mud > ZnS > flue dust > speculite > lime
Conversion:	flue dust > ZnS > pyrite > speculite > red mud > lime
H_2 Consumption:	lime > speculite > red mud > ZnS > flue dust > pyrite
Solvent Quality:	pyrite > flue dust > red mud > ZnS > speculite > lime

Based on the above analyses, the overall performance of various minerals and metallic wastes can be rated as follows: pyrite > red mud > flue dust > ZnS > speculite > lime.

Catalysis by Transition Metals

Transition metals like cobalt, nickel, and molybdenum were reported to have significant catalytic activity in coal liquefaction. The use of some of these metals is restricted because they are not available in large quantitities. However, at very low concentrations (~250 ppm based on coal), these metals can be used economically, either by adding them as particulate oxides and sulfides to the feed slurry or by impregnating them into coal in the form of water-soluble compounds. The catalytic activity of various transition metals in the liquefaction of Elkhorn #2 coal was studied to determine their relative effectiveness and to identify the effect of mode of catalyst addition on liquefaction.

Catalysis by Molybdenum Compounds - The catalytic activity of molybdic oxide and molybdenum disulfide was studied in the liquefaction of Elkhorn #2 coal. Both molybdenum disulfide (enriched molybdenite) and molybdic oxide (oxidized, enriched molybdenite) were supplied by Climax Molybdenum Company.

Table 142
Comparison of Catalytic Activity of Various Minerals and
Metallic Wastes in Liquefaction of Elkhorn #3 Coal

Reaction Condition: Temperature = 850°F,   Time = 40 Min.
Total Pressure = 2000 psig, Hydrogen Flow Rate = 20 MSCF/T
and Catalyst Concentration = 10 wt.% of Slurry (2.5 wt.% Lime)

Additive	Pyrite	Speculite	Red Mud	ZnS	Flue Dust	Lime
Product Distribution, wt.% MAF Coal						
HC	5.3	9.6	8.7	8.9	9.2	8.9
Oils	41.0	25.4	33.6	29.3	25.5	15.1
Asphaltenes	11.3	17.5	18.5	22.3	33.7	14.2
Preasphaltenes	24.1	31.0	22.1	27.5	18.8	31.6
Conversion	89.9	89.6	87.2	92.4	92.9	72.1
H_2 Consumption, wt.% MAF Coal	2.53	1.84	1.86	1.93	2.19	1.04
SRC Sulfur	0.70	0.54	0.46	0.55	0.46	0.84
First Order Rate Constants, hr^{-1}						
K_a	1.84	1.37	1.70	1.31	0.88	0.86
K_p	3.05	2.13	3.48	2.79	4.73	1.41
H Content of Oil	7.7	7.2	7.5	7.3	7.7	7.1
Distribution of Protons, %						
H_{AR}	3.10	3.37	3.26	3.45	3.19	3.46
H_a	2.18	2.07	2.12	2.07	1.99	1.87
H_o	2.42	1.76	2.12	1.78	2.52	1.77

Activity of Molybdic Oxide - Comparing coal liquefaction in the presence of 1 wt % molybdic oxide to baseline runs showed that molybdic oxide increased coal conversion from ~85 to ~90% both at 825 and 850°F (Table 143). Molybdic oxide increased oil production from 12 to 25% at 825°F and from 8 to 29% at 850°F, respectively. At 825 and 850°F, the catalyst yielded lower production of hydrocarbon gases compared with baseline runs. Production of asphaltenes increased and that of preasphaltenes decreased at both temperatures. Hydrogen consumption was higher with molybdic oxide (see Table 143). Rates of conversion of asphaltenes and preasphaltenes increased considerably with catalyst addition at both temperatures, showing that catalysis occurred independent of temperature. SRC sulfur content was not greatly affected by the catalyst addition. A higher hydrogen content was noted in the oil fractions obtained with molybdic oxide than without it, as shown in Table 144. In addition, higher H_a and H_o and the lower H_{AR} contents were noted in oil fractions obtained at 850°F with molybdic oxide. No major differences were noted in the distribution of elements in various fractions and in the distribution of protons in oil fractions.

As shown in Table 143, the overall effect of temperature was quite small. The distribution of elements in the various fractions (Table 144) showed minor variations in all fractions. Molybdic oxide and molybdenum sulfide could not be detected in the reaction product. X-ray fluorescence analysis showed the presence of more than 5% molybdenum in the coal liquefaction residue. Distribution of protons in the oil fraction (Table 145) showed a decrease in concentrations of H_{AR} and H_a and an increase in that of H_o with increasing reaction temperature. Solvent generated with molybdic oxide definitely contained more hydrogen than the no-additive run indicating strong hydrogenation activity. No positive conclusions could be drawn about solvent quality from the proton distribution data.

Activity of Molybdenite - The catalytic activity of molybdenum was evaluated by using molybdenite containing 90% molybdenum disulfide. A molybdenite concentration of 0.03% based on slurry (0.05 wt% molybdenum based on coal) was used in the experiment, and the results are summarized in Table 143. Addition of molybdenite marginally changed the coal conversion over the no-additive run. It increased the conversion of preasphaltenes and production of oils,

259

Table 143

Effect of Molybdenum Compounds on Liquefaction of Elkhorn #2 Coal

Sample No.	31-128	31-139	38-120	38-129	44-32	45-108
Feed Composition	70% Solvent + 30% Coal		69% Solvent+ 30% Coal+ 1% Molybdic Oxide[1]		69.97% Solvent + 30% Coal + 0.03% Molybdenite	70% Solvent 30% Molybdenum Impregnated Coal
Temp., °F	825	850	825	850	825	825
Pressure, psig	2,000	2,000	2,000	2,000	2,000	2,000
Hydrogen Flow Rate, MSCF/T	18.9	19.9	25.6	24.4	23.2	23.7
Reaction Time, Min.	35	37	40.7	38.3	36.3	36.5
Product Distribution, wt.% MAF Coal						
HC	5.2	7.0	4.5	4.8	4.8	4.1
CO, CO_2	0.7	0.6	0.7	0.5	0.6	0.7
H_2S	0.3	0.3	0.4	0.4	0.4	0.6
Oils	12.2	8.3	25.2	29.2	25.2	21.7
Asphaltenes	21.2	21.6	34.9	26.0	18.0	17.6
Preasphaltenes	44.2	43.4	22.3	24.2	36.3	40.3
I.O.M.	14.7	15.7	9.2	11.5	12.9	13.2
Water	1.5	3.1	2.8	3.4	1.8	1.8
Conversion	85.3	84.3	90.8	88.5	87.1	86.8
Hydrogen Consumption, wt.% MAF Coal						
Total	0.64	0.53	1.03	1.12	0.52	0.40
From Gas	0.59	0.44	1.45	1.61	0.09	0.17
From Solvent	0.05	0.09	(0.42)[2]	(0.49)	0.43	0.23
SRC Sulfur, %	0.61	0.55	0.60	0.52	0.55	0.61
First Order Rate Constants, hr^{-1}						
K_a	0.62	0.39	0.79	1.19	1.36	1.19
K_p	1.27	1.09	3.80	3.44	1.92	1.57

[1]Molybdic Oxide contained 90% MoO_3 and 10% Silica
[2]( ) - means negative value

260

Table 144

Effect of Molybdenum Compounds on Elemental
Distribution of Elkhorn #2 Coal Liquefaction Products

Sample No.	Original Solvent FOB #11	31-128	31-139	38-120	38-129	44-32	45-108
Temperature, °F	-	825	850	825	850	825	825
Catalyst	-	None		Molybdic Oxide		Molybdenite	Ammonium Molybdate
Oil Fraction, wt.%							
C	89.7	89.5	89.7	89.7	89.7	89.9	89.5
H	7.2	7.2	7.2	7.4	7.5	7.1	7.2
O	1.4	1.7	1.8	1.2	1.3	1.6	1.7
N	1.1	0.9	0.7	1.0	0.9	0.8	0.9
S	0.6	0.7	0.6	0.7	0.6	0.6	0.7
Asphaltene Fraction, wt.%							
C	-	85.9	87.0	85.6	85.8	85.7	85.3
H	-	6.3	6.1	6.1	6.1	5.8	5.9
O	-	5.8	5.0	5.2	5.2	5.7	6.0
N	-	1.4	1.4	2.5	2.4	2.3	2.2
S	-	0.6	0.5	0.6	0.5	0.5	0.6
Preasphaltene Fraction, wt.%							
C	-	85.3	86.6	84.4	85.0	84.0	83.4
H	-	5.2	4.9	5.1	5.3	4.7	5.1
O	-	6.2	5.4	7.5	6.7	8.4	8.3
N	-	2.2	2.4	2.3	2.5	2.3	2.6
S	-	0.6	0.6	0.7	0.5	0.6	0.6

Oxygen is determined by difference

Table 145

Effect of Molybdenum Compounds on Distribution of Protons in the Oil Fractions from the Liquefaction of Elkhorn #2 Coal

Sample No.	31-128		31-139		38-120		38-129		44-32		45-108	
Temp., °F	825		850		825		850		825		825	
Catalyst	None				Molybdic Oxide				Molybdenite		Ammonium Molybdate	
Total Hydrogen, Wt.%	7.2		7.2		7.4		7.5		7.1		7.2	
Distribution of Protons, %	Rel.	Abs.	Rel.	Abs.	Rel.	Abs.	Rel.	Abs.	Rel.	Abs.	Rel.	Abs.
H_{AR}	45.3	3.26	46.9	3.38	44.3	3.28	41.7	3.13	42.8	3.04	38.2	2.75
H_a	27.1	1.95	27.9	2.01	29.6	2.19	28.6	2.15	29.0	2.06	32.2	2.32
H_o	27.6	1.99	25.2	1.81	26.1	1.93	29.7	2.22	28.2	2.00	29.6	2.13

Rel. - Relative

Abs. - Absolute

the latter by over a factor of two. Rates of conversion of asphaltenes and preasphaltenes increased from 0.62 to 1.36 hr^{-1} and from 1.27 to 1.92 hr^{-1}, respectively, with molybdenite. Production of hydrocarbon gases and asphaltenes were not greatly affected, as were hydrogen consumption and SRC sulfur content.

Distribution of elements in various fractions (Table 144) showed insignificant differences compared with the no-additive run. Only lower H_{AR} concentration in the oil fraction was noted with molybdenite (Table 145).

It can be concluded that molybdenite addition to the coal liquefaction reaction mixture greatly improved oil production. However, hydrocarbon gas production was not greatly affected.

Molybdenum Impregnation - A sample of Elkhorn #2 coal impregnated with 0.02 wt% molybdenum in the form of ammonium molybdate was studied for its liquefaction behavior. Impregnation of coal with molybdenum did not change overall coal conversion, but increased the conversion of preasphaltenes and asphaltenes, as shown in Table 143. Oil production increased from 12 to 22% with molybdenum impregnation over the no-additive run. Hydrocarbon gas production was not greatly affected, although hydrogen consumption was lower with impregnated coal compared with the original coal. SRC sulfur content decreased slightly with molybdenum impregnation.

Distribution of elements in the various fractions given in Table 144 showed lower hydrogen contents in asphaltene and preasphaltene fractions with molybdenum-impregnated coal compared with original coal. Otherwise, no major differences were noted. The higher concentrations of H_a and H_o observed in the oil fraction obtained with impregnated coal (Table 145) were indicative of a higher quality of solvent than that generated with the original coal.

Impregnation Versus Particulate Molybdenum Addition - The liquefaction of Elkhorn #2 coal impregnated with 0.02 wt% molybdenum was compared with 0.05 and 2.0 wt% molybdenum added as molybdenite and molybdic oxide, respectively, to the coal-oil slurry. Coal conversion was slightly higher at the higher molybdenum concentration, as shown in Table 146. The conversion of preasphaltenes and the production asphaltenes increased with increasing molybdenum

Table 146

Effect of Molybdenum Impregnation and Particulate Addition on Liquefaction of Elkhorn #2 Coal

Sample No.	38-120	44-32	45-108
Additive	Molybdic Oxide	Molybdenite	Ammonium Molybdate
Mo Concentration, wt. % Coal	2.0	0.05	0.02
Feed Consumption	60% Solvent + 30% Coal + 1% Molybdic Oxide	69.97% Solvent + 30% Coal + 0.03% Molybdenite	70% Solvent + 30 % Impregnated Coal
Temp., °F	825	825	825
Pressure, psig	2000	2000	2000
Hydrogen Flow Rate, MSCF/T	25.6	23.2	23.7
Reaction Time, Min.	40.7	36.3	36.5
Product Distribution, wt.% MAF Coal			
HC	4.5	4.8	4.1
CO, CO_2	0.7	0.6	0.7
H_2S	0.4	0.4	0.6
Oils	25.2	25.2	21.7
Asphaltenes	34.9	18.0	17.6
Preasphaltenes	22.3	36.3	40.3
I.O.M.	9.2	12.9	13.2
Water	2.8	1.8	1.8
Conversion	90.8	87.1	86.8
Hydrogen Consumption, wt.% MAF Coal			
Total	1.03	0.52	0.40
From Gas	1.45	0.09	0.17
From Solvent	(0.42)	0.43	0.23
SRC Sulfur, %	0.60	0.55	0.61
First Order Rate Constants, hr^{-1}			
K_a	0.79	1.36	1.19
K_p	3.80	1.92	1.57

concentration. The production of hydrocarbon gases was independent of the mode of catalyst addition. The rate of preasphaltene conversion increased with molybdenum concentration, but no positive trend was observed in the rate of asphaltene conversion. Hydrogen consumption increased with molybdenum concentration, but the SRC sulfur content was independent of both the concentration of the catalyst and its mode of addition.

The distribution of elements summarized in Table 147 showed some variations in hydrogen contents in the oil, asphaltene and preasphaltene fractions with particulate addition and impregnation. In various fractions, minor variations in the distribution of elements other than hydrogen were observed. Higher H_{AR} and lower H_a and H_o values were noted with particulate addition than with impregnation (see Table 148). These data indicate that the quality of solvent generated in the reaction (based on H_a and H_o values) is higher with molybdenum impregnation than with particulate addition.

The above data suggest that oil production is not greatly affected by the mode of molybdenum catalyst addition. More experimental work using identical concentrations of molybdenum metal based on coal are needed to define the effect of the mode of catalyst addition on coal liquefaction.

Catalysis by Impregnation of Transition Metals - Samples of Elkhorn #2 coal impregnated with 0.02 wt% metal in the form of cobalt nitrate, nickel nitrate and ammonium molybdate were studied for their liquefaction behavior. Impregnation of the coal did not change overall coal conversion, but increased the conversion of preasphaltenes and asphaltenes, as shown in Table 149. Oil production increased on the average from 12 to 20% with metal impregnation. Hydrocarbon gas production was not greatly affected with impregnation. Hydrogen consumption was lower with impregnated coals compared with the original coal. SRC sulfur content was either unchanged or decreased marginally with metal impregnation.

Distribution of elements in various fractions (Table 150) showed lower hydrogen contents in asphaltenes and preasphaltenes with metal impregnated coals compared with the original coal. No other major differences were noted. Higher H_a and

265

Table 147

Effect of Molybdenum Impregnation and Particulate Addition on
Distribution of Elements in Elkhorn #2 Coal Liquefaction Products

Sample	Original Solvent FOB #11	38-120	44-32	45-108
Catalyst	--	Molybdic Oxide	Molybdenite	Mo Impregnation
Oil Fraction, wt.%				
C	89.7	89.7	89.9	89.5
H	7.2	7.4	7.1	7.2
O	1.4	1.2	1.6	1.7
N	1.1	1.0	0.8	0.9
S	0.6	0.6	0.6	0.7
Asphaltene Fraction, wt.%				
C	--	85.6	85.7	85.3
H	--	6.1	5.8	5.9
O	--	5.2	5.7	6.0
N	--	2.5	2.3	2.2
S	--	0.6	0.5	0.6
Preasphaltene Fraction, wt.%				
C	--	84.4	84.0	83.4
H	--	5.1	4.7	5.1
O	--	7.5	8.4	8.3
N	--	2.3	2.3	2.6
S	--	0.7	0.6	0.6

Oxygen is determined by difference

266

Table 148

Effect of Molybdenum Impregnation and Particulate Addition on
Proton Distribution in Oil Fractions from Elkhorn #2 Coal Liquefaction

Sample No.	Original Solvent FOB #11	38-120	44-32	45-108
Catalyst	--	Molybdic Oxide	Molybdenite	Mo Impregnation
Total Hydrogen, Wt.%	7.2	7.4	7.1	7.2
Distribution of Protons, %				
Absolute				
H_{AR}	3.20	3.28	3.04	2.75
H_a	2.02	2.19	2.06	2.32
H_o	1.98	1.93	2.00	2.13
Relative				
H_{AR}	44.4	44.3	42.8	38.2
H_a	28.0	29.6	29.0	32.2
H_o	27.6	26.1	28.2	29.6

Table 149

Effect of Metal Impregnation on Liquefaction of Elkhorn #2 Coal

Sample No.	31-128	45-89	45-98	45-108
Metal Salt Used	None	Cobalt Nitrate	Nickel Nitrate	Ammonium Molybdate
Metal Concentration, wt.% Coal	-	0.02	0.02	0.02
Feed Composition	70% Solvent + 30% Coal	70% Solvent + 30% Impregnated Coal		
Temp., °F	825	825	825	825
Pressure, psig	2000	2000	2000	2000
Hydrogen Flow Rate, MSCF/T	18.9	23.8	23.8	23.7
Reaction Time, Min.	35	36.7	37.0	36.5
Product Distribution, wt.% MAF Coal				
HC	5.2	3.8	4.8	4.1
CO, CO_2	0.7	0.7	0.7	0.7
H_2S	0.3	0.4	0.6	0.6
Oils	12.2	21.5	20.0	21.7
Asphaltenes	21.2	17.7	17.0	17.6
Preasphaltenes	44.2	40.2	38.5	40.3
I.O.M.	14.7	14.3	16.5	13.2
Water	1.5	1.4	1.9	1.8
Conversion	85.3	85.7	83.7	86.8
Hydrogen Consumption, wt.% MAF Coal				
Total	0.64	0.39	0.33	0.40
From Gas	0.59	0.00	0.00	0.17
From Solvent	0.05	0.39	0.33	0.23
SRC Sulfur, %	0.61	0.57	0.51	0.61
First Order Rate Constants, hr^{-1}				
K_a	0.62	1.16	1.09	1.19
K_p	1.27	1.56	1.52	1.57

Table 150

Effect of Metal Impregnation on Elemental
Distribution of Elkhorn #2 Coal Liquefaction Products

Sample No.	Original Solvent FOB #11	31-128	45-89	45-98	45-108
Catalyst	--	None	Cobalt	Nickel	Molybdenum
Oil Fraction, Wt.%					
C	89.7	89.5	89.6	89.8	89.5
H	7.2	7.2	7.2	7.1	7.2
O	1.4	1.7	1.7	1.7	1.7
N	1.1	0.9	0.8	0.8	0.9
S	0.6	0.7	0.7	0.6	0.7
Asphaltene Fraction, Wt.%					
C	--	85.9	85.6	85.0	85.3
H	--	6.3	5.8	5.9	5.9
O	--	5.8	5.7	6.2	6.0
N	--	1.4	2.3	2.4	2.2
S	--	0.6	0.6	0.5	0.6
Preasphaltene, Fraction, Wt.%					
C	--	85.3	83.5	83.6	83.4
H	--	5.2	4.7	4.6	5.1
O	--	6.2	8.9	9.0	8.3
N	--	2.2	2.3	2.3	2.6
S	--	0.6	0.6	0.5	0.6

Oxygen is determined by difference

H_o values observed in the oil fraction obtained with impregnated coals (Table 151) was indicative of a higher quality of solvent generated with impregnated coals.

These data indicate that the impregnation of coal with low concentrations of cobalt, nickel, and molybdenum yields very similar coal conversion, product distribution, hydrogen consumption, and SRC sulfur content. The rates of conversion of asphaltenes and preasphaltenes are also nearly identical with these metals.

Synergism in Coal Liquefaction - The liquefaction behavior of coal impregnated with 1 wt% iron and 0.02 wt% molybdenum was discussed earlier in this report. Both the iron and molybdenum were shown to catalyze the coal liquefaction reaction and increase oil production. Data from liquefaction of an Elkhorn #2 coal impregnated simultaneously with a mixture of 1 wt% iron and 0.02 wt% molybdenum based on coal are summarized in Table 152.

Coal conversion improved considerably with the iron/molybdenum mixture over iron or molybdenum alone. Oil production increased significantly compared with that of both individual iron and molybdenum runs, as shown in Table 152; this increase indicated a significant synergistic effect of the two metals. The production of hydrocarbon gas was not greatly affected by using the mixture. Lower asphaltene and preasphaltene production, higher asphaltene and preasphaltene conversion rates, higher hydrogen consumption, and higher SRC sulfur content were observed with the iron/molybdenum mixture.

Hydrogen content of the oil fraction obtained with the mixture was either equivalent to or higher than that obtained with either of the metals alone (see Table 153). No other major differences were noted in the distribution of elements in the various fractions. Aromatic hydrogen content in the oil fraction obtained with the mixture was higher than with molybdenum and lower than that with iron alone (see Table 154). Quality of the generated solvent with the iron/molybdenum mixture was higher than that with iron, but was lower than that with molybdenum alone.

Table 151

Effect of Metal Impregnation on Distribution of
Protons in the Oil Fractions from Liquefaction of Elkhorn #2 Coal

| | Original Solvent | | | | |
Sample No.	FOB #11	31-128	45-89	45-98	45-108
Catalyst	--	None	Cobalt	Nickel	Molybdenum
Total Hydrogen, Wt.%	7.2	7.2	7.2	7.1	7.2
Distribution of Protons, %					
Absolute					
H_{AR}	3.20	3.26	2.90	2.88	2.75
H_a	2.02	1.95	2.12	2.24	2.32
H_o	1.98	1.99	2.18	1.97	2.13
Relative					
H_{AR}	44.4	45.3	40.3	40.6	38.2
H_a	28.0	27.1	29.5	31.6	32.2
H_o	27.6	27.6	30.2	27.8	29.6

Table 152

Synergistic Effect in Elkhorn #2 Coal Liquefaction

Sample Number	38-10	45-108	45-116
Catalyst, Wt. % Coal	1.0% Iron	0.02% Molybdenum	1.0% Iron + 0.02% Molybdenum
Feed Composition	70% Solvent + 30% Impregnated Coal		
Temp., °F	825	825	825
Pressure, psig	2000	2000	2000
Hydrogen Flow Rate, MSCF/T	20.6	23.7	23.4
Reaction Time, Min	32.8	36.5	37.2
Product Distribution, wt.% MAF Coal			
HC	3.5	4.1	3.1
CO, CO_2	0.6	0.7	0.7
H_2S	0.2	0.6	0.6
Oils	25.0	21.7	36.3
Asphaltenes	19.1	17.6	15.2
Preasphaltenes	35.8	40.3	33.0
I.O.M.	13.5	13.2	9.3
Water	2.3	1.8	1.8
Conversion	86.5	86.8	90.7
Hydrogen Consumption, wt.% MAF Coal			
Total	0.99	0.40	0.59
From Gas	0.04	0.17	0.49
From Solvent	0.99	0.23	0.10
SRC Sulfur, %	0.61	0.61	0.67
First Order Rate Constant, hr^{-1}			
K_a	1.45	1.19	2.09
K_p	2.19	1.57	2.44

Table 153

Synergistic Effect on Iron and Molybdenum on
Elemental Distribution of Elkhorn #2 Coal Liquefaction Products

Sample No.	38-10	45-108	45-116
Catalyst	Iron	Molybdenum	Iron + Molybdenum
Oil Fraction, wt.%			
C	89.9	89.5	89.8
H	7.1	7.2	7.2
O	1.5	1.7	1.6
N	0.8	0.9	0.8
S	0.7	0.7	0.6
Asphaltene Fraction, wt.%			
C	85.6	85.3	85.1
H	6.0	5.9	5.9
O	5.5	6.0	6.0
N	2.4	2.2	2.4
S	0.5	0.6	0.6
Preasphaltene Fraction, wt.%			
C	82.9	83.4	83.7
H	4.9	5.1	4.9
O	8.9	8.3	8.4
N	2.6	2.6	2.3
S	0.7	0.6	0.7

Oxygen is determined by difference

273

Table 154

Synergistic Effect of Iron and Molybdenum on Distribution
of Protons in the Oil Fractions from Liquefaction of Elkhorn #2 Coal

Sample No.	38-10	45-108	45-116
Catalyst	Iron	Molybdenum	Iron + Molybdenum
Total Hydrogen, Wt.%	7.1	7.2	7.2
Distribution of Protons, %			
Absolute			
H_{AR}	3.64	2.75	2.92
H_a	1.80	2.32	2.15
H_o	1.66	2.13	2.13
Relative			
H_{AR}	51.3	38.2	40.5
H_a	25.3	32.2	29.8
H_o	23.4	29.6	29.7

It can be concluded that a synergism exists between iron and molybdenum in the catalysis of the coal liquefaction reaction. The production of oil increased and that of asphaltenes and preasphaltenes decreased, while hydrogen consumption and SRC sulfur content increased marginally.

Catalysis by Other Minerals and By-Product Metallic Wastes (Tubing-Bomb)

Several other different mineral and metallic waste samples were screened in a tubing-bomb reactor for their catalytic activity. The results are discussed below.

Zeolites - Mordenite caused a decrease in coal conversion, as shown in Table 155. Mordenite addition reduced conversion to 69% from a conversion level of 77% of pure coal. Although only a slight change in preasphaltene production was noted, mordenite addition to the coal liquefaction reaction mixture improved oil production from 16 to ~22%, which was due to increased asphaltene conversion. The addition of chabazite did not alter coal conversion, but significantly increased oil production at the expense of asphaltenes.

Clays - Kaolinite and montmorillonite did not improve coal conversion (Table 155), although both of these clay materials increased the conversion of asphaltenes to oils. Oil production increased from 16 (no-additive run) to 32 and 29%, and asphaltenes decreased from 48 (no-additive run) to 33 and 34% with the addition of kaolinite and montmorillonite, respectively. The catalytic activity of silica (Table 155) was also found to be similar to that of montmorillonite.

Minerals - The addition of mica caused a decrease in coal conversion compared with the no-additive run (Table 155). Oil production increased with mica. Although the preasphaltene production was not greatly affected by the addition of the mica, that of asphaltenes decreased sharply from 48% to ~31%, which was due to increased conversion of asphaltenes to oils.

The addition of bornite, feldspar, sodium carbonate, dolomite, apatite, ilmenite, rutile, illite, zircon, and calcite to the reaction mixture gave product distributions similar to that of a no-additive run. Although a slight variation in coal conversion and oil yield was observed, the variation was within the limits of experimental error.

Table 155

Catalytic Activity of Minerals in Coal Liquefaction

Product Distribution, wt.% MAF Coal

Additive	None	Mordenite	Chabazite	Kaolinite	Montmorillonite
Oils	16	22	28	32	29
Asphaltenes	48	33	35	33	34
Preasphaltenes	13	14	13	13	12
I.O.M.	23	31	24	22	25
Conversion	77	69	76	78	75

Reaction Mixture: Coal - 3g (Floyd County Elkhorn #3)
Solvent - 6g
Additive - 1g

Reaction Conditions: Temperature - 450°C
Pressure - 1250 psig H_2 at 25°C
Time - 60 Minutes

Reactor: Tubing-Bomb
Volume - 46.3 ml.

Table 155

(Continued)

Catalytic Activity of Minerals in Coal Liquefaction

Product Distribution, wt.% MAF Coal

Additive	Silica*	Gypsum	Albanian Chrome Ore Concentrate	Mica	Dolomite	Bornite	Rutile
Oils	25	34	33	28	17	17	25
Asphaltenes	37	36	34	31	40	44	41
Preasphaltenes	13	13	13	16	16	12	14
I.O.M.	25	17	20	25	27	27	20
Conversion	75	83	80	75	73	73	80

*Received from Fisher Scientific Company.

Table 155

(Continued)

Catalytic Activity of Minerals in Coal Liquefaction

Product Distribution, wt.% MAF Coal

Additive	Na_2CO_3	Illite	Calcite	Apatite	Feldspar	Zircon	Ilmenite	ZnO
Oils	22	25	25	27	27	28	29	22
Asphaltenes	43	42	43	38	37	39	42	51
Preasphaltenes	8	14	15	12	14	15	13	11
I.O.M.	27	19	17	23	22	18	16	16
Conversion	73	81	83	77	78	82	84	84

Both gypsum and Albanian chrome ore concentrate showed slightly improved catalytic activity compared to mordenite and clay materials. Coal conversion and oil production with these two additives were generally higher compared to the noncatalytic run. The addition of zinc oxide slightly improved coal conversion and the production of oil over the no-additive run (Table 155), but the improvement was marginal.

Metallic Wastes - Addition of high- and low-zinc flue dusts and oil shale to the coal liquefaction reaction mixture increased coal conversion and oil yield slightly over the no-additive run (Table 156). Although the samples of zinc flue dust contained varying concentrations of zinc and iron, the data showed no relationship between catalytic activity and the concentration of zinc in the samples. Also, the presence of iron and zinc in the samples indicated no definite advantage. However, when added to the coal liquefaction reaction mixture alone or in the form of either pyrite or iron oxide, iron showed significant improvement in the coal conversion and the oil production. The above results suggest that iron, if chemically complexed with zinc, loses its catalytic activity in coal liquefaction.

Phosphate slime showed significant improvement in coal conversion from 77 to 92% and in oil production from 16 to 34%. The increase in oil production with phosphate slime could be in error because of large amounts of water present in the sample (oil and water are not distinguished in the tubing-bomb reactor). The addition of flue dust, super alloy, and Alnico grindings to the coal liquefaction reaction mixture significantly improved coal and asphaltene conversion and oil production. The catalytic activity of various metallic wastes could not be correlated to the concentration of iron in the samples.

Fly Ashes - The catalytic activity of various fly ashes in coal liquefaction was evaluated and the data are shown in Table 157. The addition of Brown and Green River fly ashes to coal liquefaction reactions was detrimental to coal conversion (Table 157). The addition of Paradise fly ash did not change coal conversion, but significantly improved oil and asphaltene production; oil yield varied from 14 to 28% and asphaltenes from 31 to 36% with the addition of fly ashes. Examination of chemical analyses of different fly ashes, given in Table 158, revealed no definite trend to explain the above observations.

Table 156

Catalytic Activity of Metallic Waste and Metal-Containing By-Products

Product Distribution, wt.% MAF Coal

Additive	None	Oil Shale	High Zinc Flue Dust	Low Zinc Flue Dust	Phosphate Slime
Oils	16	26	22	28	34
Asphaltenes	48	38	46	42	46
Preasphaltenes	13	16	12	14	8
I.O.M.	23	20	20	16	8
Conversion	77	80	80	84	92

Reaction Mixture: Coal - 3 g (Floyd County Elkhorn #3)
                    Solvent - 6 g
                    Additive - 1 g

Reaction Conditions: Temperature - 450°C
                      Pressure - 1250 psig H_2 at 25°C
                      Time - 60 Minutes

Reactor: Tubing-Bomb
           Volume - 46.3 ml.

Table 156

(Continued)

Catalytic Activity of Metallic Waste and Metal-Containing By-Products

Product Distribution, wt.% MAF Coal

Additive	Super Alloy Grindings	Alnico Grindings	Flue Dust
Oils	35	39	48
Asphaltenes	39	40	37
Preasphaltenes	13	9	7
I.O.M.	13	12	8
Conversion	87	88	92

Table 157

Effect of Fly Ashes on Coal Liquefaction

Product Distribution wt.% MAF Coal

Additive	None	Brown Fly Ash	Green River Fly Ashes Blend	High	Paradise Fly Ash
Oils	16	14	23	24	28
Asphaltenes	48	32	35	31	36
Preasphaltenes	13	22	14	14	14
I.O.M.	23	32	28	31	22
Conversion	77	68	72	69	78

Reaction Mixture: Coal - 3 g Elkhorn #3

                        Solvent - 6 g

                        Additive - 1 g

Reaction Conditions: Temp. - 450°C

                        Pressure - 1,250 psig H_2 at 25°C

                        Time - 60 Minutes

                        Reactor - Tubing-Bomb (46.3 ml.)

Table 158

Chemical Analysis[1] of the Fly Ash Samples

wt.%

Sample	SiO_2	TiO_2	Al_2O_3	Fe_2O_3	CaO	MgO	K_2O	Na_2O	Sulfur	Moisture	High Temp. Ash
Brown	51.9	1.4	29.1	11.6	1.1	1.3	3.3	0.4	0.5	0.3	96.7
Paradise	42.9	1.2	18.5	29.6	2.3	0.9	2.9	0.6	1.0	-	96.7
Greer River											
High	40.9	0.9	16.8	32.3	5.4	0.7	1.8	0.3	0.4	0.1	99.7
Blend	48.1	0.7	14.8	32.2	1.6	0.5	1.6	0.2	0.2	0.2	94.9

[1]Analysis provided by Dr. Alan E. Bland of the Institute of Mining and Minerals, University of Kentucky, Lexington, Kentucky.

Bottom Ashes - The degree of catalytic activity of various bottom ashes in coal liquefaction reactions (Table 159) was determined to be as follows: Green River > Brown > Paradise. The catalytic activity of these bottom ashes could be related to the variation in their sulfur content, as shown in Table 160. The highest sulfur content ash gave the highest activity and vice versa.

Low- and High-Temperature Ashes of SRC-I Filter Cake Residue - SRC-I filter cake residue received from Wilsonville pilot plant was ashed at low temperature (LTA) and at two high temperatures. These ashes were then used as additive in coal liquefaction experiments. The addition of various ashes (Table 161) increased coal conversion from 77 to 83%. The different ashes also catalyzed the conversion of asphaltenes to oils; the highest catalytic activity was obtained with LTA of filter cake residue.

Low- and High-Temperature Ashes of Kerr-McGee (K-M) Ash Concentrate - K-M ash concentrate received from Wilsonville pilot plant was treated in the same manner as the filter cake residue and was used as additive in coal liquefaction experiments. The ashes of K-M ash concentrate were more reactive than that of filter cake residue (Table 162). Again, the addition of ashes increased the dissolution of coal and the conversion of asphaltenes to oils. Highest oil production was also obtained with LTA of Kerr-McGee ash concentrate.

Catalysis by Transition Metals (Tubing-Bomb)

Metal Sulfides - Coal conversion increased significantly with the addition of various metal sulfides, as shown in Table 163. Gas production increased with the addition of all the sulfides. The increase was more pronounced with nickel, vanadium, tungsten, and cobalt sulfides. Preasphaltene production seemed to be unchanged, whereas asphaltene production decreased with the addition of metal sulfides. Although oil production increased with the addition of any sulfide (31 to 49% vs. 16% with no additive), the increase was significant with nickel, vanadium and tin sulfides.

Organic Compounds of Transition Metals - The catalytic activity of metal sulfides can be increased by increasing the exposed surface area of the metals. Molecular dispersion of various metals was achieved by using organic metal

284

Table 159

Effect of Bottom Ashes in Coal Liquefaction

Product Distribution, wt.% MAF Coal

	None	Paradise Bottom Ash	Brown Bottom Ash	Green River Bottom Ash
Oils	16	21	29	38
Asphaltenes	48	31	33	34
Preasphaltenes	13	15	13	14
I.O.M.	23	33	25	14
Conversion	77	67	76	86

Reaction Mixture: Coal - 3 g Elkhorn #3
                     Solvent - 6 g
                     Additive - 1 g

Reaction Conditions: Temp. - 450°C
                      Pressure - 1,250 psig H_2 at 25°C
                      Time - 60 Minutes
                      Reactor - Tubing-Bomb (46.3 ml.)

Table 160

Chemical Analyses[1] of the Bottom Ash Samples

wt.%

Sample	SiO_2	TiO_2	Al_2O_3	Fe_2O_3	CaO	MgO	K_2O	Na_2O	Sulfur	Mois-ture	High Temp. Ash
Paradise	49.8	0.9	19.8	22.6	4.0	0.9	2.2	0.4	0.1	0.0	100.8
Brown	46.8	1.1	23.4	21.8	1.5	0.9	2.3	0.3	2.9	0.2	95.8
Green River	49.7	1.1	20.7	23.7	1.6	0.8	2.2	0.3	3.3	0.6	85.3

[1]Analyses provided by Dr. Alan E. Bland.

Table 161

Catalytic Activity of Low- and High-
Temperature Ashes of SRC-I Filter Cake Residue

Product Distribution, wt.% MAF Coal

Additive	None	Filter Cake Residue		
Ashing Temp., °C	-	800	510	LTA
Oils	16	35	38	46
Asphaltenes	48	34	36	29
Preasphaltenes	13	13	10	8
I.O.M.	23	18	16	17
Conversion	77	82	84	83

Reaction Mixture: 3 g Elkhorn #3 Coal
                   6 g Solvent
                   1 g Additive

Reaction Condition: Temp. - 450°C
                    Pressure - 1,250 psig H_2 at 25°C
                    Time - 60 Minutes
                    Reactor - Tubing-Bomb (46.3 ml.)

Table 162

Catalytic Activity of Low- and High-
Temperature Ashes of Kerr-McGee Ash Concentrate

Product Distribution, wt.% MAF Coal

Additive	None	K-M Ash Concentrate		
Ashing Temp., °C	-	800	510	LTA
Oils	16	41	42	50
Asphaltenes	48	36	34	31
Preasphaltenes	13	10	10	8
I.O.M.	23	13	14	11
Conversion	77	87	86	89

Reaction Mixture: 3 g Elkhorn #3 Coal
                     6 g Solvent
                     1 g Additive

Reaction Condition: Temp. - 450°C
                    Pressure - 1,250 psig H_2 at 25°C
                    Time - 60 Minutes
                    Reactor - Tubing-Bomb (46.3 ml.)

Table 163

Catalytic Activity of Metal Sulfides

Product Distribution, wt.% MAF Coal

Sulfides	None	Mo	Ni	V	Sn	Co	Cr	W
Gas	11	14	17	18	13	18	14	18
Oils	16	31	43	49	47	33	36	34
Asphaltenes	39	29	26	23	23	28	28	27
Preasphaltenes	14	16	12	9	12	12	15	10
I.O.M.	20	10	(2)[1]	(1)	5	9	7	11
Conversion	80	90	98	99	95	91	93	89

Reaction Mixture: 3 g (Floyd County Elkhorn #3)

Solvent - 6 g

Additive - 1g

Reaction Conditions: Temperature - 450°C

Pressure - 1250 psig H_2 at 25°C

Time - 60 Minutes

Reactor: Tubing-Bomb

Volume - 46.3 ml.

[1]( ) - Questionable

Metal sulfide samples were received from ICN Pharmaceuticals, Inc., Plainview, NY.

compounds such as metal naphthenate, octoate, and linoleate. The organic metal compounds are soluble in mineral oil and can be efficiently dispersed in the recycle solvent. These compounds are unstable at coal liquefaction reaction conditions and disintegrate into the corresponding metals.

The catalytic activity of various metals added in the form of metal naphthenate is shown in Table 164. Surprisingly, no significant improvement in coal conversion was noted when metal loading was 0.1 wt% of coal. Lower coal conversions were noted with cobalt and zinc naphthenates at 0.1% concentration than with the no-additive run. However, coal and asphaltene conversion, and oil production increased upon increasing metal concentrations of cobalt, iron, nickel, zinc, and tin from 0.1 to 1.0%. In some cases, preasphaltene production increased while it decreased in others.

The catalytic activity of metal octoate, neo-decanoate, and linoleate is shown in Table 165. Once again, no significant improvements in coal conversion and oil production were noted with all the metals except molybdenum when metal loading was 0.1 wt.% of coal. The addition of molybdenum in the form of molybdenum octoate significantly increased coal conversion and oil production, as shown in Table 165. The production of preasphaltenes was also not affected greatly by the addition of different metals except molybdenum.

OTHER RELATED WORK

As discussed earlier, minerals like pyrite and iron oxide improve overall coal conversion and oil production. To better understand the catalytic activity of these minerals, hydrogenation of a pure model compound, for example naphthalene, was studied in the presence of the above minerals.

The conversion of naphthalene to tetralin and to other hydrogenated reaction products yields tetralin and methyl indane (2). The main hydrogen transfer reactions involved are given in equations 8 and 9.

Table 164

Catalytic Activity of Organic Transition Metal Compounds

Product Distribution, wt.% MAF Coal

Metals Naphthenates	None	Cobalt		Molybdenum		Iron		Nickel		Zinc		Tin	
Conc. of Metal, wt.% Coal	0.00	0.1	1.0	0.1	1.0	0.1	1.0	0.1	1.0	0.1	1.0	0.1	1.0
Gas	11	17	15	15	19	14	14	18	22	16	18	15	12
Oils	16	10	29	24	15	27	30	22	36	10	15	29	46
Asphaltenes	39	32	30	29	29	27	26	28	28	32	30	28	23
Preasphaltenes	14	17	16	14	17	17	21	15	6	16	17	12	7
I.O.M.	20	24	10	18	20	15	9	17	8	26	20	16	12
Conversion	80	76	90	82	80	85	91	83	92	74	80	84	88

Reaction Mixture: Coal - 3 g (Floyd County Elkhorn #3)

                       Solvent - 6 g

Reaction Conditions: Temperature - 450°C

                       Pressure - 1250 psig H_2 at 25°C

                       Time - 60 Minutes

Reactor: Tubing-Bomb

        Volume - 46.3 ml.

Table 165

Catalytic Activity of Organic Transition Metal Compounds

Product Distribution, wt.% MAF Coal

Organic Compounds	None	Neo-Decanoate		Octoate				Linoleate
		Co	Zn	Pb	Ni	Mo	Cr	Co
Gas	11	18	14	9	12	11	16	15
Oils	16	12	15	21	8	39	11	21
Asphaltenes	39	29	31	31	32	29	31	32
Preasphaltenes	14	18	18	16	18	10	18	15
I.O.M.	20	23	22	23	30	11	24	17
Conversion	80	77	78	77	70	89	76	83

Reaction Mixture: Coal - 3 g (Floyd County Elkhorn #3)
Solvent - 6 g
Metal Loading - 0.1 Wt.% of Coal

Reaction Conditions: Temperature - 450°C
Pressure - 1250 psig H_2 at 25°C
Time - 60 Minutes

Reactor: Tubing-Bomb
Volume - 46.3 ml.

Hydrogenation reaction:

$$naphthalene + H_2 \xrightarrow[\text{catalyst}]{\text{minerals}} tetralin \qquad \text{(Eqn. 8)}$$

Dehydrogenation reaction:

$$tetralin \xrightarrow[\text{catalyst}]{\text{minerals}} naphthalene + H_2 \qquad \text{(Eqn. 9)}$$
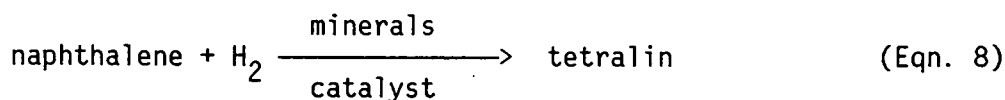
A mixture of 10% naphthalene in hexadecane was subjected to hydrogenation to study the above reaction. The reaction products were vacuum-filtered and analyzed by gas chromatography (GC) to determine the peak areas of different compounds. The hydrogenation activity of the minerals was followed by monitoring the tetralin-to-naphthalene (T/N) ratio and naphthalene conversion.

When iron oxide and pyrite were used in the reaction, they unexpectedly showed very little hydrogenation activity (see Table 166). Commercial catalyst like Co-Mo-Al, on the contrary, hydrogenated almost all the naphthalene to tetralin at the same reaction conditions. Lower catalytic activity of pyrite could be attributed to its low-surface-area-to-weight ratio (1 m^2/g). To verify this, a high-surface-area synthetic pyrite was produced by sulfiding iron oxide and was tested for its catalytic activity in the naphthalene hydrogenation reaction. The results of the above study are discussed below.

Production of High-Surface-Area Synthetic Pyrite

Samples of iron oxide were sulfided either with pure hydrogen sulfide or with a mixture of hydrogen and hydrogen sulfide gases to produce high-surface-area synthetic pyrite. The sulfiding procedure is described in detail in Appendix E. A series of sulfiding temperatures with a constant reaction time of 2.5 hours was employed for sulfiding. The surface area of the material obtained by sulfiding with H_2S and a mixture of H_2S and H_2 was determined using the nitrogen BET method; the data are presented in Table 167 and Figure 43. The surface area of the sulfided iron oxide decreased with increasing sulfiding temperatures,

Table 166

Catalytic Activity of Sulfided Fe_2O_3 in Naphthalene Hydrogenation

Sulfiding Temp., °C	Sulfiding Gas	Naphthalene Conversion, %	Tetralin/ Naphthalene Ratio
No Catalyst	--	--	0.06
Original Fe_2O_3	--	--	0.18
Robena Pyrite	--	--	0.03
Co-Mo-Al	--	79.6	--
Sulfided Fe_2O_3			
125	Pure H_2S	70.4	2.43
210	Pure H_2S	79.0	3.76
275	Pure H_2S	90.0	8.49
350	Pure H_2S	86.6	6.19
425	Pure H_2S	82.9	4.84
500	Pure H_2S	80.2	3.79
135	H_2/H_2S Mixture	6.8	0.08
211	H_2/H_2S Mixture	23.2	0.30
275	H_2/H_2S Mixture	31.2	0.42
350	H_2/H_2S Mixture	75.6	3.13
430	H_2/H_2S Mixture	52.5	1.15
550	H_2/H_2S Mixture	15.0	0.18

Reaction Mixture: 10% naphthalene in hexadecane

Catalyst - 10% by wt. of reaction mixture

Reaction Condition: Temp. - 410°C

Time - 30 Minutes

Pressure - 1250 psig H_2 at 25°C

Reactor - Tubing-Bomb (14.5 ml.)

Table 167

Variation of Surface Area of Sulfided Iron
Oxide with Sulfiding Temperature

Sulfiding Temp, °C	Sulfiding Gas	Surface Area, m^2/g
125	Pure H_2S	14.9
210	Pure H_2S	--
275	Pure H_2S	7.2
350	Pure H_2S	6.5
425	Pure H_2S	5.5
500	Pure H_2S	3.8
135	H_2/H_2S Mixture	15.2
211	H_2/H_2S Mixture	12.7
275	H_2/H_2S Mixture	10.9
350	H_2/H_2S Mixture	6.9
430	H_2/H_2S Mixture	4.6
550	H_2/H_2S Mixture	2.1

295

FIGURE 43
VARIATION OF SURFACE AREA OF SULFIDED Fe$_2$O$_3$ WITH TEMPERATURE
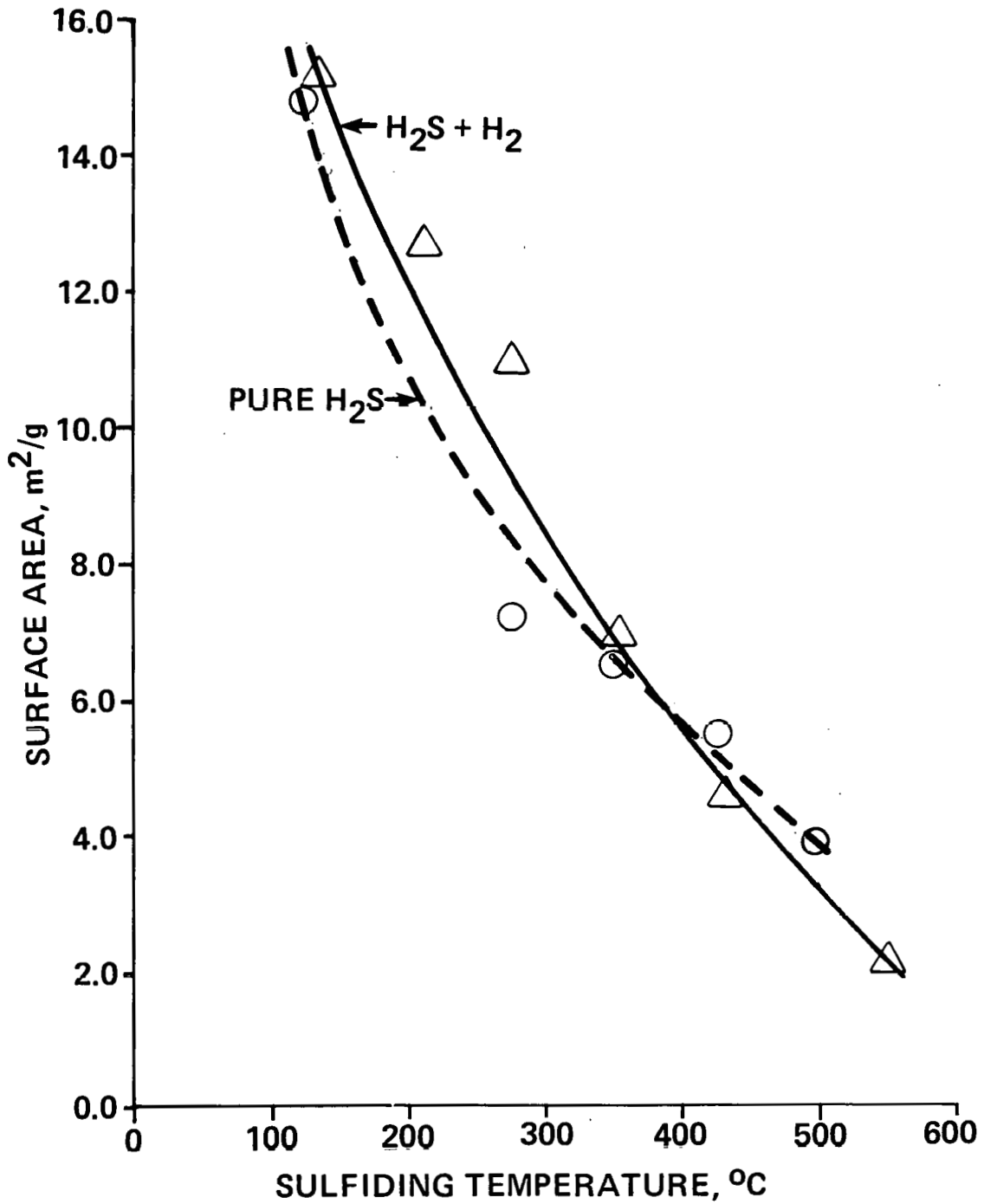
suggesting the use of lower temperatures for producing high-surface-area sulfided material. Two new batches of iron oxide samples sulfided at 275 and 400°C were prepared and analyzed by X-ray diffraction to determine the chemical form of the samples. The material sulfided at 400°C was identified as troilite (FeS), whereas that sulfided at 275°C was primarily pyrite, with traces of unreacted iron oxide. Similar results have been reported by several workers (4,10).

Naphthalene Hydrogenation - The iron oxide samples sulfided at various temperatures with pure H_2S and a mixture of H_2 and H_2S gases were tested for their catalytic activity in a naphthalene hydrogenation reaction.

The sulfided Fe_2O_3 consistently showed much higher naphthalene hydrogenation activity than Fe_2O_3 and pyrite (see Table 166). Furthermore, the material sulfided with pure H_2S was more active than that sulfided using a mixture of H_2S and H_2. There appears to exist an optimum sulfiding temperature close to 275°C for pure H_2S and to 350°C for H_2S/H_2. There also appears to be a relationship between surface area of the material sulfided with pure H_2S and its hydrogenation activity.

The catalytic activity of Fe_2O_3 sulfided at 275°C and that of Co-Mo-Al are compared in Table 168. Comparable naphthalene conversions were observed at 380°C with Co-Mo-Al versus 410°C with Fe_2O_3 sulfided at 275°C (Table 168). The data indicated that the catalytic activity of the Co-Mo-Al at lower temperature (380°C) is about twice that of the Fe_2O_3 sulfided at 275°C. By using higher reaction temperatures the same conversion levels can be achieved by Fe_2O_3 sulfided at 275°C.

It can be concluded that the surface area of pyrite or iron sulfide does affect its hydrogenation activity. Hydrogenation activity comparable to that of sulfided Co-Mo-Al catalyst can be achieved by carefully controlling the sulfiding temperature to produce high-surface-area synthetic pyrite.

Table 168

Comparison of Catalytic Activity of Co-Mo-Al and
Sulfided Iron Oxide in Naphthalene Hydrogenation Reaction

Catalyst	Time, Min.	Temp., °C	Naphthalene Conversion, %
Co-Mo-Al	5	380	61.0
	10	380	80.2
	15	380	88.1
Sulfided Fe_2O_3 at 275°C	5	410	56.2
	10	410	73.6
	15	410	82.0

Reaction Mixture: 5 g (10% Naphthalene in hexadecane)
                     Sulfide Fe_2O_3 - 0.5 g
                     Sulfided Co-Mo-Al - 0.25 g

Reaction Condition: Pressure - 1,250 psig H_2 at 25°C
                    Reactor - Tubing-Bomb (14.5 ml.)

Catalyst Poisoning in Coal Liquefaction

A sample of the iron oxide sulfided at 275°C, which showed the highest naphthalene hydrogenation activity, was tested as a catalyst in coal liquefaction. Surprisingly, the catalytic activities of sulfided iron oxide and Robena pyrite were identical, suggesting that the sulfided iron oxide, high-activity catalyst is somehow poisoned in the coal liquefaction system, and therefore does not show any enhancement over Robena pyrite. The poisoning of this catalyst is discussed in detail below.

Quinoline Poisoning - The effect of the presence of basic nitrogen compounds on naphthalene hydrogenation was studied by adding quinoline to the reaction mixture. Quinoline significantly reduced the hydrogenation activity of both sulfided Fe_2O_3 and Co-Mo-Al (Table 169), but was more severe with the sulfided Fe_2O_3.

The reaction products obtained from the naphthalene hydrogenation reaction with quinoline using Co-Mo-Al and sulfided iron oxide were analyzed by GC/MS. Propylcyclohexane, a denitrogenated product, was identified as the major compound produced from quinoline when Co-Mo-Al was used as a catalyst, whereas 1,2,3,4-tetrahydroquinoline was the major compound obtained from quinoline with sulfided Fe_2O_3. These data may indicate that the Co-Mo-Al catalyst was much more active for denitrogenation than was the sulfided Fe_2O_3.

Since part of the quinoline is denitrogenated with the Co-Mo-Al catalyst, the concentration of basic nitrogen remaining in the reaction mixture decreases with reaction time. This will eventually reduce overall poisoning effect and give more hydrogenation activity. Sulfided Fe_2O_3 hydrogenates the quinoline, but is not active enough to remove nitrogen.

A sensitivity to quinoline poisoning in naphthalene hydrogenation was examined for both sulfided iron oxide (sulfiding temperature 275°C) and the Co-Mo-Al catalyst. The results (Tables 170 and 171 and Figures 44 and 45) showed that poisoning increased with increasing concentrations of quinoline for both sulfided iron oxide and the Co-Mo-Al catalyst, but was more severe with sulfided iron oxide.

Table 169

Effect of Quinoline on Naphthalene Hydrogenation Reaction

| | Naphthalene Conversion, % | |
| Quinoline | Sulfided | Sulfided |
Concentration, wt.%	Fe_2O_3	Co-Mo-Al
0.0	82.0	88.1
0.25	23.4	62.8

Reaction Mixture: 5 g (10% naphthalene in hexadecane)

Catalyst: 0.5 g Sulfided Fe_2O_3
             0.25 g Co Co-Mo-Al

Reaction Condition: Temp. - 380°C (Co-Mo-Al)
                            - 410°C (Sulfided Fe_2O_3)
                      Pressure - 1,250 psig H_2 at 25°C
                      Time - 15 Minutes
                      Reactor - Tubing-Bomb (14.5 ml.)

Table 170

Sensitivity Study of Quinoline Concentration On
Naphthalene Hydrogenation in the Presence of
Sulfided Iron Oxide

Quinoline Concentration, %	Naphthalene Conversion, % For Different Reaction Time, Min.		
	5	10	15
0.0	56.2	73.6	82.0
0.10	13.7	28.9	40.1
0.25	8.0	15.2	23.4
0.52	3.3	7.4	13.0
1.02	2.0	5.8	7.0
2.04	3.0	3.7	8.5

Reaction Mixture: 5 g (10% naphthalene in hexadecane)
                    Catalyst - 0.5 g sulfided Fe_2O_3

Reaction Condition: Temp. - 410°C
                    Pressure - 1,250 psig H_2 at 25°C
                    Reactor - Tubing-Bomb (14.5 ml.)

Table 171

Sensitivity Study of Quinoline Concentration On
Naphthalene Hydrogenation in the Presence of
Sulfided Co-Mo-Al

Quinoline Concentration, %	Naphthalene Conversion, % For Different Reaction Time, Min.		
	5	10	15
0.0	61.0	80.2	88.1
0.26	28.7	55.3	62.8
0.50	24.1	41.1	58.9
1.03	19.4	33.5	44.9
1.97	13.3	23.0	37.6

Reaction Mixture: 5 g (10% naphthalene in hexadecane)
                    Catalyst - 0.25 g sulfided Co-Mo-Al

Reaction Condition: Temp. - 380°C
                    Pressure - 1,250 psig H_2 at 25°C
                    Reactor - Tubing-Bomb (14.5 ml.)

FIGURE 44
QUINOLINE POISONING IN NAPHTHALENE HYDROGENATION REACTION IN THE PRESENCE OF SULFIDED Fe_2O_3

QUINOLINE CONCENTRATION, WT. %

○   0.0
◓   0.10
□   0.25
△   0.52
●   1.02
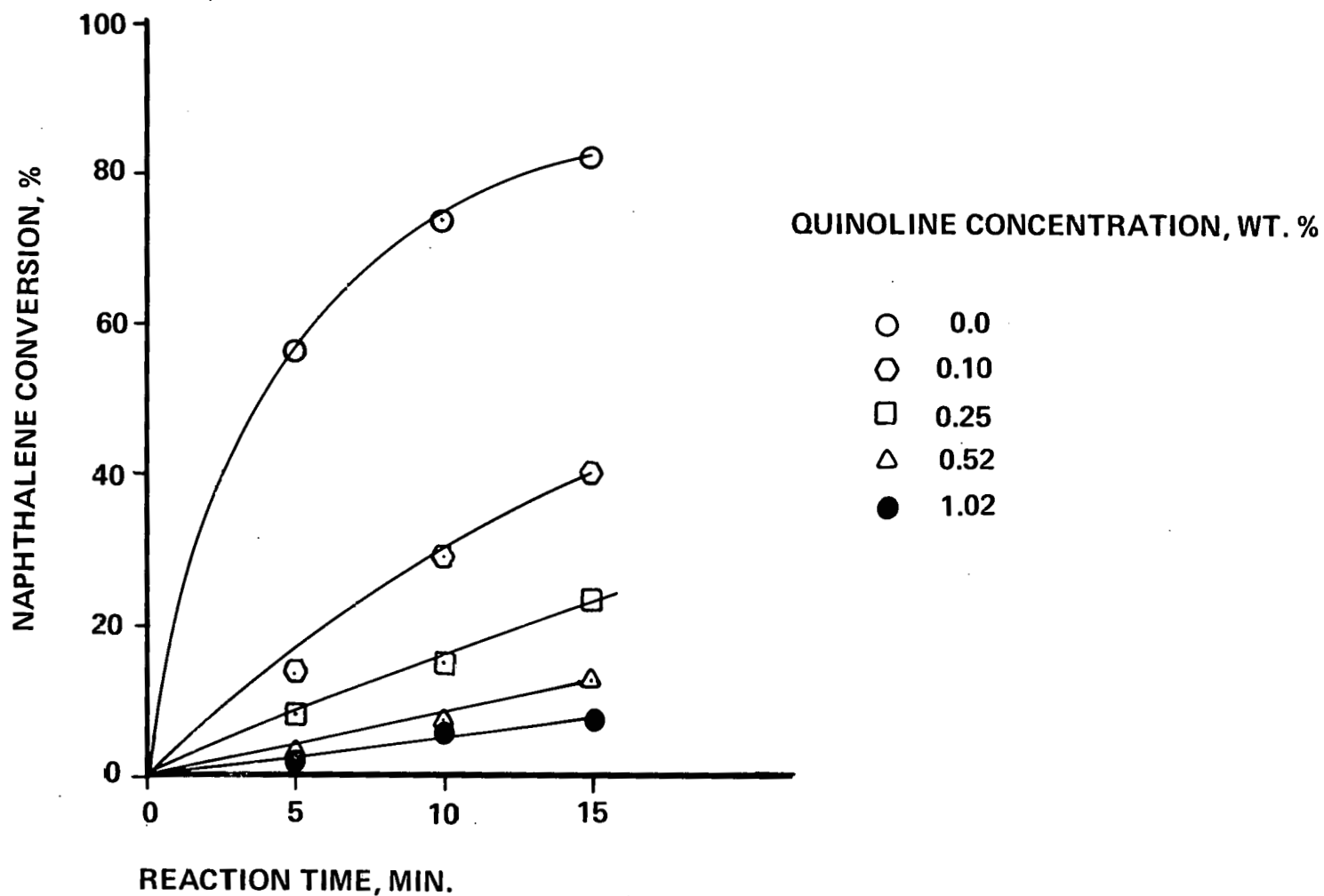
FIGURE 45
QUINOLINE POISONING IN NAPHTHALENE
HYDROGENATION REACTION IN THE PRESENCE
OF SULFIDED Co-Mo-Al
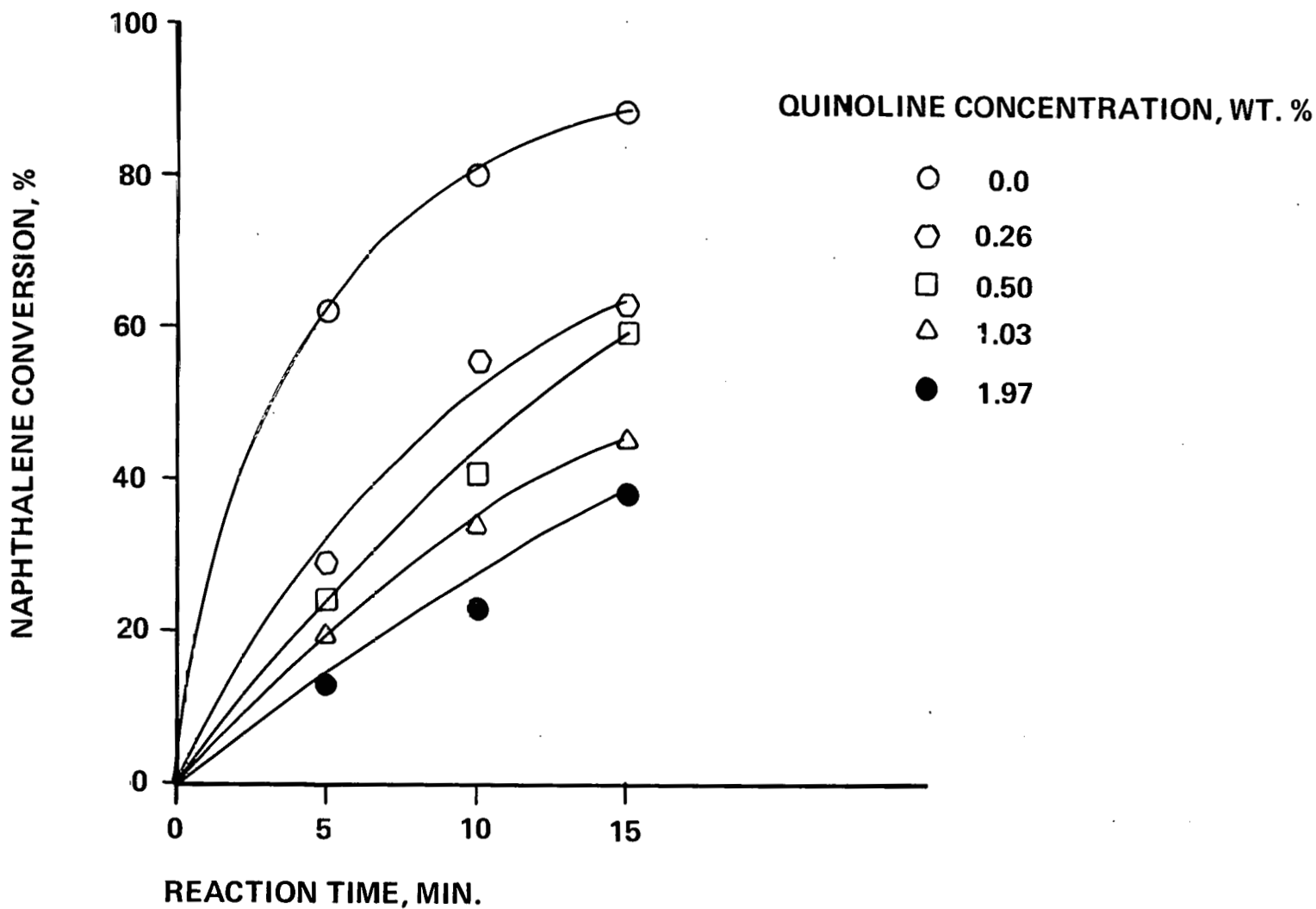
Reaction Kinetics - Data obtained on the conversion of naphthalene with time were used to evaluate the kinetics of the quinoline poisoning reaction. A 10/1 mole ratio of available hydrogen (gaseous hydrogen) to naphthalene was used for the study, indicating that much hydrogen would be left unused, even if complete conversion of naphthalene was achieved. The concentration of hydrogen gas was, therefore, assumed to be constant to simplify the modeling of the reaction kinetics. The rate of naphthalene hydrogenation could be represented by

$$r = k \frac{W_c}{W_s} C_n \qquad (10)$$

where r = reaction rate, g mole/min,

k = pseudo first-order rate constant, g solvent/g catalyst-min,

W_c = mass of the catalyst, g, and

W_s = mass of the solvent (hexadecane), g.

C_n = concentration of naphthalene, g mole

Integration of rate expression (eqn. 10) yields

$$- \ln (1 - x) = k \frac{W_c}{W_s} t \qquad (11)$$

where x = fractional conversion, and

t = reaction time, min.

The fractional conversion of naphthalene plotted against time on semi-log graph paper (Figure 46) shows a linear relationship between fractional naphthalene conversion and time which indicates that a first-order rate expression can describe the naphthalene hydrogenation reaction kinetics. The pseudo first-order rate constants were determined for different concentrations of quinoline using linear regression analysis; the data are presented in Table 172. Similar analysis was performed for the Co-Mo-Al catalyst (Table 173).

FIGURE 46
SEMI-LOG PILOT OF FRACTIONAL CONVERSION VERSUS TIME FOR NAPHTHALENE HYDROGENATION IN THE PRESENCE OF SULFIDED $Fe_2 O_3$

QUINOLINE CONCENTRATION, WT. %

△ 1.02
□ 0.25
○ 0.10
○ 0.00

Y-axis: (1 - FRACTIONAL NAPHTHALENE CONVERSION)

X-axis: REACTION TIME, MIN.

Table 172

First Order Rate Constant for Naphthalene
Hydrogenation Reaction in the Presence of Sulfided Fe_2O_3

Quinoline Conc., wt. %	Rate Constant, g solvent/ g catalyst-min.	Inhibition Factor
0.00	1.10	1.00
0.25	0.16	0.14
0.52	0.08	0.07
1.02	0.05	0.04
2.04	0.05	0.04

Table 173

First Order Rate Constant for Naphthalene
Hydrogenation Reaction in the Presence of Sulfided Co-Mo-Al

Quinoline Conc., wt. %	Rate Constant, g solvent/ catalyst-min.	Inhibition Factor
0.00	2.20	1.00
0.26	1.26	0.47
0.50	1.02	0.38
1.03	0.71	0.26
1.97	0.53	0.19

The measure of quinoline poisoning was determined by an inhibition factor, which was defined as the ratio of the rate constant at some concentration of added poison (quinoline) to the rate constant with no added poison:

$$\text{Inhibition factor} = k_i/k \qquad (12)$$

where k_i = pseudo first-order hydrogenation rate constant at the level of
        quinoline concentration, and
    k = pseudo first-order hydrogenation rate constant without quinoline.

The inhibition factor defined above has a value of one when no quinoline is present in the reaction mixture, i.e., zero inhibition by quinoline. As inhibition by quinoline increases, the value of the inhibition factor becomes smaller such that maximum inhibition approaches a limiting value of zero.

The values of the inhibition factor at different concentration levels of quinoline are also presented in Table 172 and 173. Rapid decline in the value of the inhibition factor was noted with sulfided iron oxide and the Co-Mo-Al catalyst with increasing amounts of quinoline. The decline in the value of the inhibition factor was more pronounced with sulfided iron oxide than with the Co-Mo-Al catalyst. These observations suggest that quinoline has a higher poisoning effect on the sulfided iron oxide than does the Co-Mo-Al catalyst.

Nonbasic Nitrogen Compound Poisoning - The basic nitrogen compound quinoline was shown to poison the naphthalene hydrogenation reaction. To provide more information concerning the poisoning activity of nitrogen compounds, the role of nonbasic nitrogen compounds was studied in the naphthalene hydrogenation reaction.

Nonbasic compounds can form basic nitrogen compounds (5) on hydrogenation; for example, with hydrogenation, pyrrole, a nonbasic nitrogen compound, was reported to form pyrrolidine, a basic nitrogen compound. A series of experiments with three different nitrogen compounds, both basic and nonbasic, was performed to determine the effect of nitrogen compounds on the naphthalene hydrogenation reaction. The experimental conditions were the same as used in the quinoline poisoning study. Fe_2O_3 sulfided at 275°C was used as a catalyst in all the

reactions. The results of the effect of nitrogen compounds on the naphthalene hydrogenation reaction are summarized in Table 174. The presence of aniline, carbazole, and indole reduced (poisoned) significantly the hydrogenation activity of sulfided Fe_2O_3. The pseudo first-order rate constant determined by linear regression and an inhibition factor defined as the ratio of the rate constant at some concentration of nitrogen compound to the rate constant with no nitrogen compound addition are presented in Table 175. The values of the pseudo first-order rate constant and the inhibition factor obtained by quinoline addition are also included for comparison. The rate constants and inhibition factors decreased with the addition of nitrogen compounds. The poisoning effect of nitrogen compounds in the naphthalene hydrogenation reaction was as follows: quinoline > indole > carbazole > aniline.

From the above data it can be concluded that the presence of nitrogen compounds are detrimental to the hydrogenation reaction, and the hydrogenation reaction can be improved by simply removing nitrogen compounds from the reaction mixture.

Solvent Modification Applied to Coal Liquefaction Reaction

The presence of nitrogen compounds is known to inhibit catalyst activity in numerous commercial processes. Earlier it was shown that nitrogen compounds such as quinoline limit the naphthalene hydrogenation activity of sulfided Fe_2O_3 and Co-Mo-Al. Thus, if heteroatoms were removed from the coal-derived liquids, the catalytic activity of the catalyst should excel in coal processing. Experiments were performed to determine the effect of the removal of heteroatoms from process solvent on thermal and catalytic coal liquefaction.

Samples of SRC-II heavy distillate (F.O.B. #11) were treated individually to remove basic nitrogen compounds and phenolic compounds. Another sample was treated separately to remove the nitrogen as well as the oxygen containing compounds. The distribution of elements in the original and treated solvents is given in Table 176. The basic nitrogen-compound-free solvent showed 42 and 15% removal of total nitrogen and oxygen, respectively, from the original solvent. The phenol-free solvent showed 37% removal of total oxygen, whereas the total nitrogen content did not change. The nitrogen-and oxygen-free solvent had zero nitrogen and contained only 25% of the total oxygen present

309

Table 174

Effect of Different Nitrogen Compounds
On Naphthalene Hydrogenation Reaction

Nitrogen Compounds	Naphthalene Conversion, % Different Reaction Time, Min.		
	5	10	15
None	56.2	73.6	82.5
Aniline	30.3	44.4	54.0
Carbazole	18.5	29.1	40.4
Indole	12.0	22.8	25.7

Reaction Mixture: 5 g (10% naphthalene in hexadecane)
                          Catalyst - 0.5 g sulfided Fe_2O_3
                          Nitrogen Compound - 0.025 g

Reaction Condition: Temperature - 410°C
                          Pressure - 1250 psig H_2 at 25°C
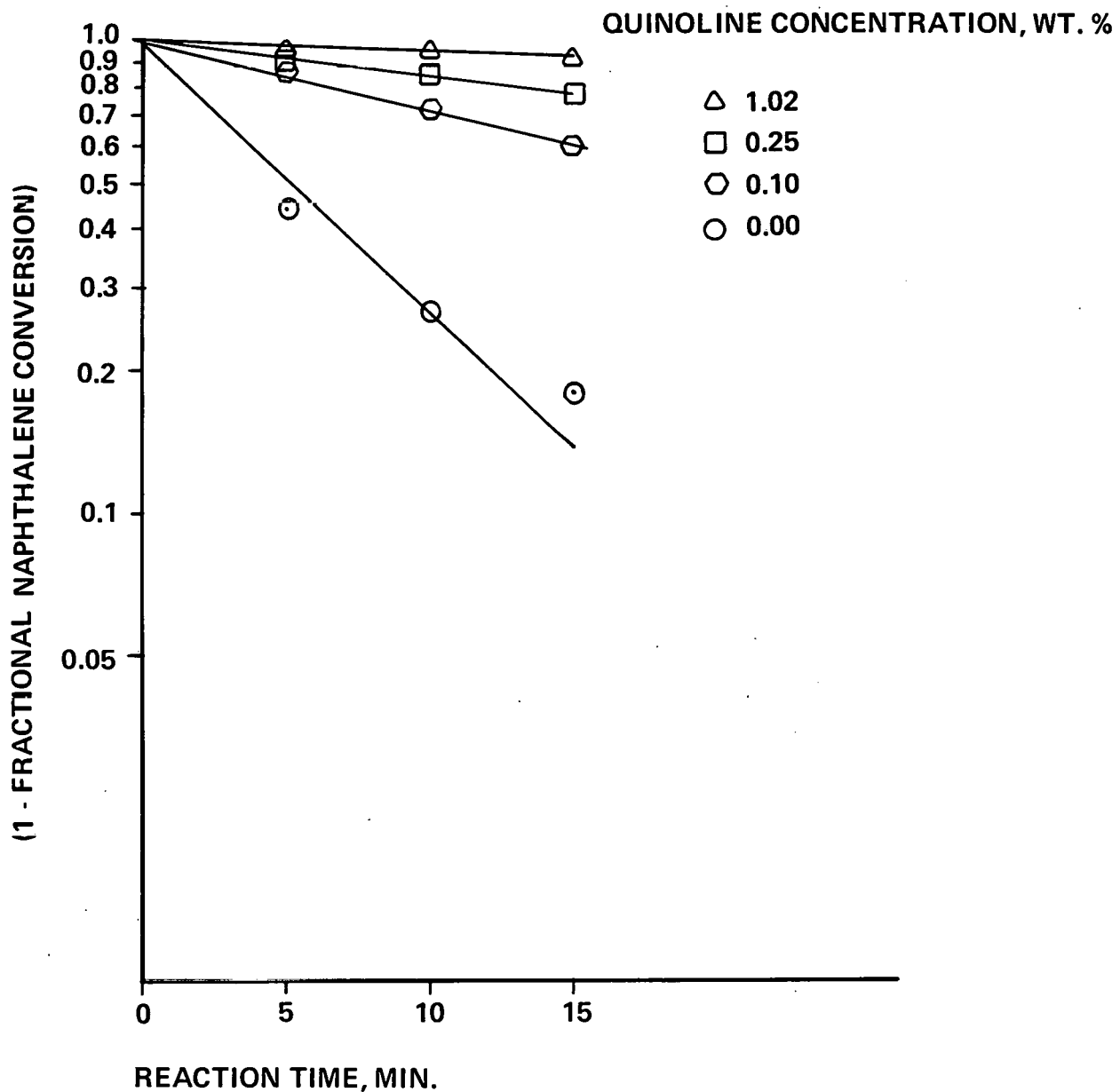   Reactor - Tubing-Bomb (14.5 ml.)

Table 175

Pseudo First Order Rate Constant for Naphthalene
Hydrogenation Reaction in the Presence of Sulfided Fe_2O_3

Nitrogen Compound	Rate Constant g Solvent/g Catalyst, Min.	Inhibition Factor
None	1.01	1.0
Aniline	0.50	0.50
Carbazole	0.31	0.31
Indole	0.19	0.19
Quinoline	0.07	0.07

Table 176

Distribution of Elements in Original and Treated Solvents

	wt.%			
Elements	Original Solvent	N-Base Free Solvent	Phenol Free Solvent	Nitrogen and Oxygen Free Solvent
Carbon	89.44	89.66	89.80	90.36
Hydrogen	7.21	7.53	7.36	8.48
Oxygen	1.70	1.45	1.07	0.42
Nitrogen	1.10	0.64	1.06	0.01
Sulfur	0.55	0.72	0.71	0.73

Table 177

Solvent Separation of Original and Treated Solvents

	wt.%			
Solvent Fractions	Original Solvent	N-Base Free Solvent	Phenol Free Solvent	Nitrogen and Oxygen Free Solvent
Oils	92.8	95.2	94.3	95.8
Asphaltenes	5.8	4.5	5.3	2.2
Preasphaltenes	0.7	0.2	0.4	2.0
I.O.M.	0.7	0.1	0.0	0.0

in the original sample. The hydrogen and sulfur contents of samples increased upon treatment. The original solvent and the treated solvents were separated into oils, asphaltenes, preasphaltenes, and I.O.M. The data are given in Table 177.

The original and treated solvent samples were used with and without sulfided Fe_2O_3 to determine the effect of heteroatom removal on thermal as well as catalytic coal liquefaction. The liquefaction product was solvent-separated into oils, asphaltenes, preasphaltenes, and I.O.M. The product distribution is summarized in Table 178. Conversion of approximately 75% was noted with all solvents in the absence of sulfided Fe_2O_3. Oil, asphaltene and preasphaltene yields were very similar using original, N-base-free and phenol-free solvents; oil yield was negative in all three cases. Significantly higher oil yields were noted with the nitrogen- and oxygen-free solvent without catalyst. The increase in oil yields was due to increased asphaltene and preasphaltene conversion. The above data show relative improvement in thermal conversion of coal using heteroatom-free solvent.

Coal liquefaction was significantly improved by adding sulfided Fe_2O_3 in the coal liquefaction reaction mixture. Coal conversion increased from 75 to 89% with all the solvents using sulfided Fe_2O_3. The conversion of asphaltenes and preasphaltenes was also greatly improved. Higher oil yields were noted in all the experiments with sulfided Fe_2O_3; oils increased from -2 to 24% with original solvent, from -3 to 31% with N-base free solvent, from -6 to 30% with phenol-free solvent and from 23 to 48% with nitrogen- and oxygen-free solvent. Both N-base-free and phenol-free solvents showed an oil production of 30% as opposed to 24% with original solvent using sulfided Fe_2O_3. This information shows that the removal of either nitrogen or oxygen improved catalytic coal lique-faction, whereas the individual removal of heteroatoms seemed to have little effect in thermal coal liquefaction. When both nitrogen and oxygen compounds were removed from process solvent, oil production increased in thermal as well as catalytic liquefaction. The improvement was very dramatic in the case of catalytic coal liquefaction (Table 178); oil production was 48% with sulfided Fe_2O_3 compared with only 23% without additive. Also, the use of sulfided

Table 178

Effect of Solvent Treatment on Coal Liquefaction

Product Distribution, wt.% MAF Coal

| Catalyst | Original Solvent | | N-Base Free Solvent | | Phenol Free Solvent | | Nitrogen and Oxygen Free Solvent | |
	None	Sulfided Fe_2O_3	None	Sulfided Fe_2O_3	None	Sulfided Fe_2O_3	None	Sulfided Fe_2O_3
Gas	9	8	9	6	7	7	10	8
Oils	(2)[1]	24	(3)	31	(6)	30	23	48
Asphaltenes	44	42	42	39	47	35	28	26
Preasphaltenes	22	13	23	13	23	16	13	7
I.O.M.	27	13	29	11	29	12	25	11
Conversion	73	87	71	89	71	88	75	89
Recovery, %	100.5	98.9	98.4	100.5	98.9	101.0	99.2	101.0

Reaction Mixture: Coal - 3 g (Floyd County Elkhorn #3)

Solvent - 6 g

Additive - 1g

Reaction Conditions: Temperature - 425°C

Pressure - 1250 psig H_2 at 25°C

Time - 60 Minutes

Reactor: Tubing-Bomb

Volume - 46.3 ml.

Iron Oxide was sulfided at 275°C

[1]( ) - Indicate negative value

Fe_2O_3 significantly improved the conversion of preasphaltenes over the no-additive run; preasphaltene production decreased from 13 to 7%. The production of gas was not affected by using different solvents in the thermal or catalytic coal liquefaction experiments.

It can be concluded that the removal of heteroatoms from coal-derived process solvent improves oil production and the conversion of asphaltenes and preasphaltenes in thermal as well as catalytic coal liquefaction.

REFERENCES

1. Brown, J. K. and W. R. Ladner, Fuel 39, 87 (1967).

2. Cronauer, D. C., Douglas M. Jewell, Y. T. Shah, and K. A. Kueser, "Hydrogen Transfer Cracking of Dibenzyl in Tetralin and Related Solvents," Ind. Eng. Chem. Fundam., Vol. 17, No. 4, pp. 291, 1978.

3. Granoff, B. and M. Thomas, "Mineral Matter Effects in Coal Liquefaction - Autoclave Screening Study," ACS Division of Fuel Chemistry, paper presented at Chicago Meeting, September 1977.

4. Griffith, R. H. and A. R. Morcom, Journal of Chemical Society, page 786 (1945).

5. Katzer, J. R. and R. Sivasubramanian, Catal. Rev. - Sci. Eng., 20 (2), 155 (1979).

6. Kawa, Walter, R. W. Hiteshue, R. E. Anderson, and Harold Greenfield, "Reactions of Iron and Iron Compounds with Hydrogen Sulfide," A report prepared by the Bureau of Mines (Investigation 5690).

7. Kirk-Othmer, Encyclopedia of Chemical Technology, Volume 12, Page 40, Second Edition, Interscience Publishers.

8. Retcofsky, H. L., F. K. Schweighardt, and M. Hovgh, Anal. Chem., 49, 585 (1977).

9. Richardson, J. T., "Thermomagnetic Studies of Iron Compounds in Coal Char,", Fuel, Vol. 51, pp. 150, April 1972.

10. Sayee, L. A., Journal of Chemical Society, page 2002 (1929).

11. Schwab, George-Maria and J. Philinis, "Reaction of Iron Pyrite: Its Thermal Decomposition, Reduction by Hydrogen and Air Oxidation," J. American Chemical Society, Vol. 69, 1947, pp. 2588 to 2598.

12. Solvent Refined Coal (SRC) Process, Quarterly Technical Progress Report prepared by The Pittsburg and Midway Mining Co. for U.S. Dept. of Energy (FE/496-141), December 1977.

13. Solvent Refined Coal (SRC) Process, Quarterly Technical Progress Report prepared by PAMCO for U.S. Dept. of Energy (FE/496-143), January 1978.

APPENDIX A

Pressurizable Thermogravimetric Reactor (PTGR)

A schematic diagram of the system layout is illustrated in Figures A.1 and
A.2. The primary apparatus used in obtaining data is a 6 gram capacity
thermobalance built specifically for Air Products' laboratories by Spectrum
Products, Inc. This apparatus is capable of operation at pressures up to 1500
psi and at temperatures up to 1000°C. The reactor is a 4-ft. cylindrical
Haynes 188 superalloy tube with 3/4 inch i.d. and 2.5 inch o.d., 3 feet of
which is heated by a Marshall tubular furnace (Model No. 1149).

Thermocouples are located along the outer tube wall, inside the furnace and
inside the reactor tube. The exact locations of the thermocouples are shown
in Figure A.3. The exit gas temperature upstream of the tar trap is also
monitored by a thermocouple. The thermocouple just below the sample basket
was used as a feedback for the heater controller to maintain constant tempera-
ture or heating rate. Process gas enters either through the top or the bottom
of the reactor tube, while the purge gas can be admitted through the microbalance
housing at the top and flows down the dip-tube. The gas flow rates into and
out of the reactor are measured by three Brooks thermal mass flowmeters
(Model 5811). FI-1 and FI-3 in Figure A.2, which measured the flowrate into
and out of the reactor, were calibrated with hydrogen; FI-2, which measured
the flow rate down the reactor, was calibrated with helium. If helium is
flowing through FI-1 and FI-3, the indicated flow rate has to be multiplied by
1.5 to give the actual helium flow rate. The system pressure was measured by
two pressure transducers PI-1 and PI-2 (by Setra Systems, Inc. Model 204),
located at the exit gas line upstream and downstream of the tar trap, respec-
tively. The pressure difference between the inlet and exit gas line was
measured by another pressure transducer PI-3 (Setra Systems, Inc. Model 228).

The 3/8 inch o.d., 5 inch long sample basket (fabricated by Newark Wire Cloth
Company) can hold up to a 3 gram sample. It can be lowered into or raised from
the heated section of the reactor tube by a No. 40 gauge chromel wire attached
to a motorized winch. The microbalance is engaged only when the basket is in

317

its pre-determined final position inside the reactor. The exit gas line upstream of the tar trap is kept hot by heating tapes to prevent tar conden- sation. The pyrolysis gas is passed through the tar trap (immersed in ice) and collected either in a sampling cylinder or in the sample loops of a Valco automatic sampling unit for gas chromatograph analysis. The system pressure was maintained by a back-pressure regulator PCV-1 (Grove Valve and Regulator Company, Model S-91-W) located downstream of the tar trap.

Experimental Procedure

The PTGR has two modes of operation: the hot-start fast heating mode and the cold-start slow heating mode. In the hot-start fast heating mode, the sample in the basket was lowered rapidly into the hot reactor; the heating rate was approximately $15°C/sec$. In the cold-start slow heating mode, the basket was lowered into the reactor at ambient temperature and then the reactor was heated to its final temperature; the heating rate was approximately $8°C/min$.

Experimental Preparation

The PTGR system was leak-tested with helium under pressure. The microbalance transducer was checked and calibrated periodically to assure its accuracy. Before each experiment, the recorder was zeroed and spanned by means of poten- tiometers so that only the sample weight loss was recorded as a percentage of its original weight. The recorder was zeroed while the microbalance was engaged with an empty basket; this was done either with the reactor hot or cold. With the reactor cold, the recorder can be spanned by lowering the basket loaded with a known weight of sample (from direct weighing) into the reactor to engage the microbalance. When the reactor was hot, the recorder was spanned by using a known weight of sand in the basket instead of sample and then replacing the sand with the same weight of sample afterwards. The total percentage weight loss obtained from such thermograms agreed to within 2% of the percentage weight loss obtained from direct weighing. Three or four experiments a day were possible with this spanning procedure. A timer could be preset to turn the furnace on early in the morning so that the reactor was ready at the desired temperature for experimental runs. The timer was used only when all high temperature shut-off controls were functioning. The tar trap was washed and cleaned with tetrahydrofuran (THF) after each experiment and then dried by blowing air through it.

FIGURE A-1
PRESSURIZABLE THERMOGRAVIMETRIC REACTOR (PTGR)

WINDLASS

INERT GAS FEED

TAR TRAP

GAS SAMPLING UNIT

SAMPLING CYLINDER

SAMPLE BASKET

FURNACE

PROCESS GAS FEED

OPERATING CAPABILITIES:

TEMPERATURE: 1000° C
PRESSURE: 1500 PSIG
SAMPLE SIZE: 3 g

FIGURE A-2
DETAILED PTGR SYSTEM

FIGURE A-3
THERMOCOUPLE POSITIONS IN REACTOR

319
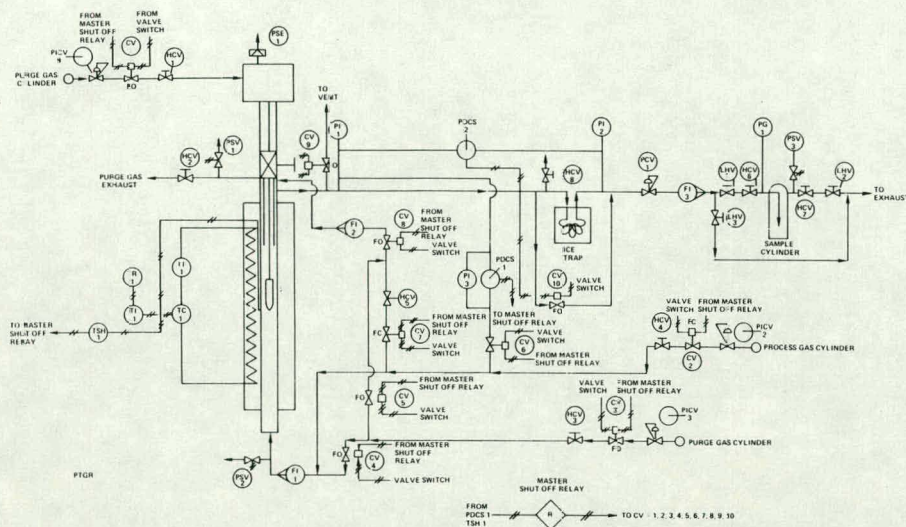
Date Acquisition Procedure

1. Slow heating mode experiments: The basket, with approximately 3g of
    sample, was lowered into the reactor at room temperature. After purging
    the system with helium, the reactor was heated. The temperature, monitored
    by a thermocouple located immediately below the sample basket, the helium
    flow rate and the sample weight were continuously recorded. Gas samples
    were periodically collected by syringes through a septum in the heated
    exit line. These samples were subsequently analyzed using a Perkin-Elmer
    Sigma-1 gas chromatograph.

2. Fast heating mode experiments: Before heating the reactor, the system
    was purged with helium; when hydrogen was used, the hydrogen inlet lines
    were purged with hydrogen to eliminate any trapped air before purging the
    system with helium. The reactor was then heated up to the operating
    temperature. Then the system was pressurized to the operating pressure
    with helium and leak-tested. The system was now ready for experimental
    runs in helium. The loaded sample basket was lowered rapidly into the
    hot reactor and held for the desired residence time. The pressure,
    temperature and volume of the sampling cylinder were recorded. The gas
    in the sampling cylinder was mixed by means of a heat gun before it was
    analyzed by the Perkin-Elmer Sigma-1 gas chromatograph. After the sample
    was cooled down, the system was depressurized and purged with helium.
    The basket was removed from the system and weighed. The tar trap was
    washed with a known volume of THF solution. The treated sample and the
    THF tar washings were analyzed.

    A step-by-step operating procedure for a helium run and a hydrogen run is
    described in the next section in the PTGR operating procedure. After
    putting back the cleaned tar trap and replacing the full sampling cylinder
    with an empty one, the system was ready for the next experimental run.

3. Temperature measurement at center of sample bed: This was done only in
    helium at atmospheric pressure. A sub-miniature thermocouple (Omega
    Engineering, Inc., Catalog #SCAIN-020U-66) was embedded at the center of
    the sample bed. The temperature was recorded as the basket was lowered
    rapidly into the hot reactor with helium flowing. The microbalance

housing was opened to atmosphere for ease of feeding in the thermocouple but the reactor was purged of air by the flow of helium from the bottom of the reactor. In the slow heating mode, the system was closed after the basket was in place, and the temperature at the center of the sample bed and the gas temperature inside the reactor immediately below the basket were recorded during heat-up of the reactor.

Water Analysis

Water from the sampling cylinder was analyzed by the gas chromatograph. Water in the tar trap was washed with a known volume of THF. From the weight percent analyses of water in the THF washing solution and that in the "clean" THF, the volume of the THF used in the washing and from the specific gravity (0.88) of THF, the weight of water in the tar trap can be obtained.

PTGR OPERATING PROCEDURE

Helium Run Procedure

1. After spanning and zeroing the recorder, turn on the He main regulator to 1200 psig.
2. Purge system with He at atmospheric pressure (8 min. with 1 scfh flow rate). The valves (refer to Figure A.2) should be as follows:

CV	Status	HCV	Status	LHV	STATUS
1.	Open/Close*	1	Open	1	Open
2	Close	2	Open/Close	2	Open
3	Open	3	Open	3	Open/Close
4	Open	4	Close		
5	Open/Close*	5	Open		
6	Open	6	Open		
7	Open/Close*	7	Open		
8	Open/Close*	8	Open/Close*		
9	Close				
10	Close				

*Open CV1, CV5, CV7, CV8, HCV2, HCV8, LHV3 temporarily and then close them.

3. Turn on cooling water.

4. Turn on heater and heat up to desired temperature with helium purging.

5. After reaching temperature, set the dome pressure on the back-pressure regulator to the desired operating pressure.

6. After the system has reached operating pressure, purge the sampling cylinder with helium. Add ice to tar trap bath.

7. Record pressure and flow rate on data sheet.

8. Set recorder for weight monitoring:

   (i)   Switch on point 15 and print only point 15.

   (ii) Set Point Scan on recorder to Variable (fastest) print.

   (iii) Set chart speed to 8 inch/min.

9. Lower basket into reactor and simultaneously close LHV2.

10. Raise the basket after holding it in the reactor for the desired residence time.

11. After the calculated pressure has been reached in the sample cylinder, close LHV-1 and LHV-3.

12. Depressurize the system by closing CV3, CV4 and slowing opening up HCV8.

13. Close HCV6, HCV7 and remove sample cylinder.

14. Weigh the basket and its content after letting it cool down in solution. Send the THF tar trap washing and the original clean THF solution for water analysis.

Hydrogen Run Procedure

1. Set dome pressure for H_2 delivery to 1200 psig.

2. Turn on He main to 1200 psig.

3. With reactor cold, purge system with hydrogen at atmospheric pressure (8 min. with 1 scfh flow rate). The valves are as follows:

CV	Status	HCV	Status	LHV	Status
1	Close	1	Open	1	Open
2	Open	2	Close	2	Open
3	Close	3	Open	3	Open
4	Close	4	Open		
5	Close	5	Open		
6	Open	6	Open		
7	Close	7	Open		
8	Close	8	Open		
9	Close				
10	Close				

322

4. Purge system with helium at atmospheric pressure (8 min. with 1 scfh).
    (i)   Close CV2.
    (ii) Open CV1, CV3, CV4, CV5.
    (iii) Open CV7, CV8, CV10, HCV2 temporarily to purge and then close them.
    (iv) Close HCV8 and LHV3.
5. Turn on cooling water and start heating with helium purging.
6. After reaching temperature, set back-pressure regulator's dome pressure and pressurized system to operating pressure with helium. Check for leaks.
7. Depressurize system of helium.
    (i)   Close CV1, CV3, CV4, CV5.
    (ii) Open CV7, CV8.
    (iii) Slowly release back-pressure regulator dome pressure and open HCV8.
8. Set system dome pressure for H_2 inside the high pressure cell.
9. Fill tar trap bath with ice.
10. Purge system with H_2 at atmospheric pressure (8 min. with 1 scfh).
    (i)   Open CV2.
    (ii) Open CV7, CV8, CV10 temporarily to purge and then close them.
    (iii) Close LHV3, HCV8.
    The valves should have the following status:

CV	Status	HCV	Status	LHV	Status
1	Close	1	Open	1	Open
2	Open	2	Open	2	Open
3	Close	3	Open	3	Close
4	Close	4	Open		
5	Close	5	Open		
6	Open	6	Open		
7	Open/Close	7	Open		
8	Open/Close	8	Close		
9	Close				
10	Open/Close				

11. Set back-pressure regulator dome pressure from outside of the high pressure cell.
12. After reaching operating pressure, purge the system with H_2.

13. Record pressure and flow rate on data sheet.
14. Set recorder for weight monitoring (same as Step 8 in helium run procedure).
15. Lower basket into reactor and simultaneously close LHV2.
16. Raise the basket after holding it in the reactor for the desired residence time.
17. After the calculated pressure has been reached in the sample cylinder, close LHV1 and open LHV3.
18. Depressurize the system by closing CV2 and slowly opening up HCV8.
19. After depressurization, purge the system with helium before entering high pressure cell.
    (i) Open CV1, CV3, CV4, CV5, CV7, CV8, CV10.
    (ii) Close CV1, CV3, CV4 after purging.
20. Close HCV6, HCV7 and remove sample cylinder.
21. Weigh the basket and its content after letting it cool down in helium. Save the product for analysis.
22. Remove the tar trap and wash with THF solution (same as Step 15 in helium run procedure).

APPENDIX B

Solvent Separation Procedure (Auburn University)

I. Obtaining Sample Weight

1. Weigh filter paper, beaker, and three 500 ml flasks.

2. Place filter paper into filter (readings to .001 g are presently used).

3. Transfer reaction mixture from tubing-bomb to beaker. Carefully scrape the inside of the bomb and caps to remove all the sample. Do not include drops on the outside edges which may be contaminated with sealing material.

4. Presently two steel balls are used in the tubing-bombs to aid mixing. Remove the steel mixing balls from the mixture in the beaker after stirring well.

5. Wipe off any sample on the top half of the inside of the beaker.

6. Weigh the beaker and sample to obtain sample weight. (The time between step 3 and 5 should be as short as practical because some of the sample is volatile.) The volatile components and oil are calculated from the sample weight less the other components and, thus, after weighing some loss of volatiles does not affect the analysis.

II. Extraction Procedures

Pentane Extraction of Oils

1. Pour 40 to 50 ml pentane into the sample and with a spatula stir the mixture well. Wipe as much as possible of the material adhering to the spatula into the bottom of the beaker.

2. Pour the liquid into two 100 ml centrifuge tubes and centrifuge for 3 to 5 minutes at 500 to 700 rpm. Place a lid (rubber stopper) lightly on the centrifuge tubes before centrifuging. Before centrifuging, wash the remaining mixture in the beaker and beaker walls with pentane from a wash bottle. This liquid also is poured into the centrifuge tubes before centrifuging.

3. After centrifuging pour the fluid directly into the pressure filter and catch the fluid in one of the 500 ml flasks.

4. Spread out the mixture remaining in the flask on the bottom of the flask to facilitate the crushing in step 6 below. Any material remaining on tools (spatula, glass rod, etc.) should be carefully protected and included in the separation procedure at the appropriate time determined by the operator.

5. Fill the beaker with liquid nitrogen and immerse a glass stirring rod (1/2" to 1") with a flat end. Allow the mixture to stop boiling violently before proceding with step 6.

6. Crush the frozen sample to a fine powder under the liquid nitrogen. Five to ten minutes of crushing is required.

7. Allow the liquid N_2 to evaporate to just above the sample. Place a cap on the beaker to minimize splatter loss. The cap may be a funnel cut to allow the sonicator tip to be immersed in the fluid. Material which splatters on the cap, upper part of the beaker, or on the sonifier should be recovered.

8. Place the beaker quickly under the sonifier and turn on the sonifier.

9. Pour enough pentane into the beaker after the sonifier is turned on so that the sonifier tip will be immersed at least 1/2 inch into the fluid.

10. Sonicate at level 5 on the "output control" for five minutes.

11. Let the mixture settle for approximately 2 minutes after removing from the sonifier.

12. Pour the liquid into two 100 ml centrifuge tubes and centrifuge for 3 to 4 minutes (700 rpm). (Allow the solid material to remain in the beaker.)

13. After centrifuging, pour the fluid into the filter.

14. Repeat steps 9-13 twice more (three sonications in all). On the last step allow the solid material to pour into the centrifuge tubes. Wash the material from the beaker thoroughly with pentane, pouring the entire mixture into the centrifuge tubes.

15. Centrifuge for 3 to 4 minutes and pour the fluid into the filters. See step 19 below for the completion of the use of the pressure fillter.

Benzene Extraction of Asphaltenes

16. Pour about 20 ml benzene into each of the centrifuge tubes. Stir with a glas rod (1/4" to 3/8" diameter) and pour into the original beaker. Remove as much of the material from the tubes beaker. Care should be exercised so that material is not spilled.

17. Sonicate the benzene in the beaker for 3 to 5 minutes at "output control" level 3. Use a benzene wash bottle to wash material remaining on the sonicator into the beaker. Pour all the material, liquid and solid, into the centrifuge tubes using a benzene wash bottle as required.

18. Centrifuge for 4 to 5 minutes.

19. To complete the pentane soluble portion collection apply pressure
    to the filter if any liquid remains in the filter. Wash the
    insides of the pressure filter with pentane and pressure it through.
    Repeat. Remove the pentane catch flask and place a clean flask
    for the collection of asphaltenes. Use a little benzene to wash
    the filter and filter paper. A few drops will begin to collect in
    the clean flask.

20. Pour the liquid from the centrifuge in step 18 into the pressure
    filter. The solid material should remain in the centrifuge tubes.

21. Pour some benzene into the beaker and scrape the material remaining
    on the sides of the beaker into the benzene. Wash other tools
    upon which any quantity of sample remains into the benzene in the
    flask. The tools will include glass rods, spatula, and sonifier
    tip after the extraction procedures were begun.

22. Pour the benzene from the beaker into the centrifuge tubes. Wash
    any loose material in the beaker into the centrifuge tubes. Stir
    the material in the centrifuge tubes vigorously with the glass
    rods used in step 15.

23. Centrifuge.

24. Pour the liquid from step 22 into the pressure filter.

25. Repeat steps 21-23 one more time.

Methylene Chloride (90% by volume) - Methyl Alcohol (10% by Volume)
Extraction of Preasphaltenes

26. Repeat steps 15 through 24, but with the methylene chloride-methyl
    alcohol mixture rather than benzene. Step 19 will refer to completing
    the benzene soluble portion collection rather than the "pentane
    soluble portion" collection.

328

27. On the last step wash all the material from the centrifuge tubes into the pressure filter. It will take approximately one hour under 10 lbs pressure to push the liquid through the filter.

III. Removing Solvents from the Respective Fractions

Removing Pentane on Rotovap

1. The flask may be rotated slowly (on the lowest Rotovap setting). Rotovap bath temperature should be 60°C; a small flow of nitrogen should be directed into the oil flask. No stop cock grease is used.

2. Leave the flask on two minutes after pentane ceases to form on the cooling coils. (Drops may still remain on the coils but will not be increasing in size.) Cooling coils are approximately at 0°C. Place a clean flask on the rotovap to avoid condensing Rotovap bath vapors on the cooling coils.

3. Allow the flask now containing only oils to set at room temperature for one half hour, then weigh to obtain weight of oils.

Removing Benzene

1. Rotovap bath temperature 75°C (Up to 90°C is acceptable). A medium nitrogen flow rate is required.

2. Do not evaporate the last 10 to 20 ml of benzene. The benzene is freeze dried as follows:

   a. Swirl the flask in liquid nitrogen to evenly coat the inside two thirds of the flask.

b. Attach immediately to a vacuum pump. A trap immersed in liquid nitrogen is necessary to collect the benzene. The trap is positioned between the flask and the pump. The pump should be exhausted to a hood. The freeze drying requires approximately 1 hour.

3. After freeze drying, dry the outside of the flask as necessary, let set at room temperature for 15 minutes and weigh to obtain the weight of asphaltenes. The appearance of the asphaltenes should be a medium to light tan and obviously dry. If not dry, then repeat the freeze drying step.

Removing Methylene Chloride - Methyl Alcohol

1. Rotovap bath temperature 60°C to 90°C.

2. A low nitrogen flow rate is required; too high a flow rate will result in blowing some of the dry preasphaltenes out of the flask.

3. When the preasphaltene is completely dry, remove the flask, dry the outside, allow to set at room temperature for one half hour and weigh to obtain weight of preasphaltene.

IV. Obtaining the Weight of Residue

1. The residue containing the insoluble organic matter (I.O.M.), coal minerals, and any insoluble material added will accumulate on the filter paper. Carefully remove this material along with the filter paper on to a watch glass. Recover any material adhering to the filter parts. Allow the material to air dry (breaking the material apart will help). After drying (one half hour is generally sufficient if the material is broken into small pieces) weigh to obtain the amount of residue.

V. Sample Weights

1. In spite of repeated scraping and washing with various solvents there will be some small amount of material remaining on the beaker, centrifuge tubes, sonicator tip, filter walls, and tools. This is unavoidable, however, reasonable effort should be made to minimize the loss.

2. The weights of the various fractions are calculated from the fraction less the flask weight.

3. Though the oils amount are weighed, the actual oil value used is obtained by subtracting the sum of the asphaltene, preasphaltene, and residue weights from the original sample weight. The assumption is that if the sum of the four fractions is less than the sample weight, that volatile components from the oil were lost. This assumes that the amount of material lost in 1. is small.

APPENDIX C

Solvent Separation Procedure (Air Products)

It is the purpose of this procedure to provide a rapid and precise
fractionation of the gross coal conversion product into four subfractions
defined by their solubility.

    A) Oils - Pentane Solubles

    B) Asphaltenes - Pentane Insoluble/Benzene Soluble

    C) Preasphaltenes - Pyridine Soluble/Benzene Insoluble

    D) Residue - Pyridine insoluble

This procedure was conducted at room temperature 25°C $\pm$ 3°, under nitrogen gas
pressure, using solvents of the highest quality available. The sample may be
liquid, solid or a mixture, with less than 1% material boiling below 150°C.

Equipment Required:

1. Branson Model 350 Sonicator with 3/4 inch horn

2. Millipore 142 mm pressure filter with 300 ml capacity #XX40-047-00, with
    142 mm filter, 5μ, FSLW-01420

3. Round bottom distilling flasks - 500 ml, 250 ml, 2 each

4. Rotovapor R, Fisher Scientific #9-548-151 (1979)

5. Vacuum pump and trap

6. Nitrogen-Gas (0-20 psi adjustable) pressure filter feed
    Nitrogen-Gas (0-20 psi adjustable) rotovapor feed
    Nitrogen-liquid (1-2L) freeze sample (dewar)

7. a)   n-Pentane -
    b)   Benzene -   Grade of solvent depends upon ultimate
    c)   Pyridine -   use of sample subfractions <u>Pesticide</u>,
    d)   Methanol   <u>Distilled in Glass</u>, or <u>HPCL</u> grade

8. Fume hood 150-200 cfm air rate exchange

9. Cooling water or heater exchange for rotovapor condenser

10. Balance to read weights $\pm$ 0.005 grams or better with maximum load 200 grams.

Safety Features:

Solvents must be used only under the fume hood and transferred from bottle to flask by hand pump. Gloves to protect workers hands, and overalls for laboratory work are required. Clean-up of spills on hands can be completed with Go-Jo, waterless hand-cleaner, mild scrubbing and water wash (warm). All normal safety precautions must be observed during the full operation.

Sample Handling:

The sample chosen for this procedure must be representative of the process unit output. Great care must be given to the isolation of approximately 50 grams of gross product.

The sample, once chosen, must be kept free of air (oxygen), heat and light. Store samples not ready for separation at 4°C under a blanket of nitrogen. Hot samples may be taken in 316 stainless steel bottles (DuPont #03226, 235 ml 61 x 140 mm with screw cap). Samples may be warmed to 65°C in the cans and stirred or shaken to induce good mixing just prior to taking a 5 gram actual work-up sample.

Procedure

The laboratory equipment is prepared in the following order:

a) Ultrasonic unit with 3/4 inch horn adjusted and cleaned with methylene chloride.

b) Millipore filter put in place after taking weight of dry filter element. Ensure that all O-rings fit well with no leaks (test with n-pentane under 10 psi). Use Teflon tape (3/4 inch) to wrap screw fittings and seals.

333

c) Prepare rotovapor-bath temperature at 55-60°F for n-pentane; nitrogen flow rate should just cause 1/4-1/2 inch dimple in liquid of 250 ml flask.

d) Cooling liquid for rotovapor condenser should be 10°C if heater exchanger used -10°C with MeOH.

Step 1   Tare a 150 ml heavy wall Pyrex beaker, add 5 grams read to ± 0.005 grams of the desired coal-derived sample. Add approximately 100 ml of liquid nitrogen slowly to the beaker to maintain a quiet solution. Total volume of liquid nitrogen used may exceed 500 ml.

Step 2   With a (3/81/2 inch) Pyrex glass stirring rod, grind the now frozen sample to a fine powder. This procedure requires 5-8 minutes and no large 1/16 inch lumps should remain. Fill with more liquid nitrogen to maintain at least 30 ml volume while grinding.

Step 3   Allow the liquid nitrogen to evaporate to just above the solid mixture. Add with moderate (micro-probe 1/8 inch/power level 3) sonication 100 ml of n-pentane. Some stirring may be required (keep tools out of beaker while sonic power is on). Sonciate for 5 minutes at level 5.

Step 4   Allow mixture to settle (1-2 minutes) decant supernatant into filter unit, refill beaker with n-pentane and sonicate again for 3-5 minutes. Allow decant liquid to filter into a 250 ml flask - do not allow filter to dry from this time onward.

Step 5   Repeat Step 4 twice for a total of 300 ml n-pentane. If catch flask fills transfer to rotovapor and begin to remove n-pentane under nitrogen at 60°C. Transfer the solids with small portions (25-50 ml) of pentane.

Do not discard beaker; hold for additional transfer of solvents to filter. This assures removal of maximum amount of material and reduces losses.

334

Step 6   Filter the solids, adding nitrogen pressure (5-10 psi) if needed.
          Add new pentane via original beaker as needed for a total of 2 L.
          This amount can be recollected from rotovapor unit during the
          continuous solvent removal steps.

Step 7   Continue solvent filtering (up to 2 L) until the filtrate is a very
          light yellow/green. At the end of the pentane extraction, with
          25 ml pentane in the filter, add 100 ml benzene and continue as in
          Step 6 for 2.5 L. The new filtrate is collected in a new 500 ml
          flask (tare). Continue to transfer filtrate to rotovapor with a
          waterbath temperature of 75°C. Nitrogen flow rate 1/2 inch dimple.

Step 8   The pentane solubles from steps 6 and 7 should be held on rotovapor
          for 2 minutes past the last drop of condensed pentane is in the
          catch flask. Remove, clean and dry outside of the flask containing
          the oils (reddish) and weigh. From the difference on tare:

                    Yield of oils: -------- grams

Step 9   The benzene extraction is carried out in a similar fashion as in
          Steps 6-8. The benzene solubles are removed from the rotovapor when
          10-20 ml of solution remains. The flask is swirled in liquid nitrogen
          to evenly coat 2/3 inner flask and freeze the solution in place.
          Quickly transfer flask to vacuum line (1 mm Hg) with trap and allow
          flask to stand unheated to freeze dry the benzene (sublime) in about
          1 hour.

                    Yield of asphaltenes: -------- grams

Step 10   After the last benzene extraction begin to add pyridine and continue
          extraction as in Steps 6-8. Remove the solvent at 90°C under 1/4-1/2
          inch nitrogen dimple. Two liters of pyridine are required. The
          last wash should be pure methanol (100 ml), followed by nitrogen gas
          at 5 psi for 10 minutes. As the pyridine is just nearly removed
          (5-10 ml) stop and add 10-15 ml benzene. Swirl flask to mix contents
          and freeze-dry as in Step 9 for one hour. If pyridine odor remains,
          add 20 ml benzene and re-freeze dry.

Yield of preasphaltenes: -------- grams

Step 11   The residue will dry in-place. Stop nitrogen, gently remove filter and weigh.

Yield of residue: -------- grams

Step 12   Oils   _____A_____

Asphaltenes   _____B_____

Preasphaltenes   _____C_____

Residue   _____D_____

A + B + C + D = Total recovered

Original mass of sample = MS.

MS - total recovered = net loss or gain.

If gain of weight is observed solvent is present in oils or other fraction.
If loss of weight is observed oils have volatile matter.

Add net loss to mass of oils (A + net loss) and calculate over material recovery.

	Recovered	Corrected	%
Report: Oils	A	A + net loss	_____
Asphaltenes	B	B	_____
Preasphaltenes	C	C	_____
Residue	D	D	_____
Total Recovered		MS	100%

Fractional and Elemental Composition
of the Product Liquid

The product liquid samples collected during the operation of CPDU were solvent separated into various fractions as discussed in Appendix C. The solvent separation and elemental analyses results for the various fractions are summarized below.

		FR	C	H	O	N	S	Ash	Sum	nMw
CCL-25-14	PL	--	89.0	7.28	1.82	1.20	0.47	0.23	100.00	206
	O	88.60	89.64	7.40	1.30	1.17	0.50	--	100.00	198
	A	7.80	80.99	4.68	--	--	--	--	--	--
	P	3.40	--	--	--	--	--	--	--	--
	R	0.20	--	--	--	--	--	--	--	--
	Sum	100.0								
	RCV	98.8								
CCL-25-28	PL	--	82.82	7.28	1.32	0.97	0.46	7.14	100.00	203
	O	88.0	89.25	7.74	1.39	1.19	0.44	--	100.00	205
	A	3.0	84.0	6.76	--	--	0.64	--	--	--
	P	1.0	--	--	--	--	--	--	--	--
	R	8.0	4.55	0.41	3.54	0.33	31.61	85.58	126.02[1]	--
	Sum	100.00								
	RCV	99.60								

---

[1] Sum is more than 100% because coal minerals and added catalysts gain weight upon oxidation.

    C = Carbon
    H = Hydrogen
    O = Oxygen
    N = Nitrogen
    S = Sulfur
  Ash = Oxidized Residue
   PL = Product Liquid
    O = Oil
    A = Asphaltene
    P = Preasphaltene
    R = Residue
  RCV = Solvent Separation Recovery
   FR = Solvent Fractions

Fractional and Elemental Composition
of the Product Liquid

		FR	C	H	O	N	S	Ash	Sum	nMW
CCL-25-40	PL	--	82.22	6.67	2.82	1.17	0.98	6.15	100	238
	O	71.34	89.05	7.49	1.79	1.33	0.34	--	100	--
	A	10.20	86.10	6.48	4.53	2.24	0.66	--	100	404
	P	8.00	84.06	5.50	5.44	3.33	0.58	1.10	100	1205
	R	10.46	30.44	1.88	5.18	0.78	5.01	56.71	100	--
	Sum	100.00								
	RCV	98.06								
CCL-25-52	PL		82.88	6.71	2.89	1.20	0.79	5.52	99.99	276
	O	63.28	88.86	7.76	1.24	1.61	0.53	--	100	214
	A	10.80	84.33	6.77	5.83	2.23	0.84	--	100	521
	P	15.00	82.84	5.38	7.00	2.46	0.77	1.55	100	2409
	R	10.93	34.54	1.97	5.85	0.87	3.05	53.72	100.00	
	Sum	100.01								
	RCV	99.9								
CCL-25-88	PL		78.73	6.32	2.36	1.12	0.86	10.60	100	279
	O	59.0	89.83	7.61	1.24	0.83	0.49	--	100	215
	A	14.0	87.03	6.29	4.20	1.97	0.51	--	100	394
	P	9.0	82.35	5.20	5.26	4.17	0.56	2.46	100	1210
	R	18.0	18.75	1.13	5.30	0.35	1.88	72.59	100	
	Sum	100.0								
	RCV	99.6								
CCL-25-100	PL		73.42	5.88	2.86	0.96	0.73	16.16	100	302
	O	58.2	89.16	7.65	1.87	0.86	0.47	--	100	204
	A	9.5	85.61	6.71	4.85	2.23	0.59	--	100	309
	P	7.2	83.49	5.54	6.88	2.39	0.85	0.85	100	1527
	R	25.1	19.16	1.24	4.83	0.43	1.63	74.89	102.18	
	Sum	100.0								
	RCV	99.7								
CCL-25-136	PL		74.34	6.24	2.47	0.95	2.59	13.41	100	278
	O	67.6	89.12	7.70	1.76	0.96	0.49	--	100	205
	A	8.6	85.12	6.24	5.65	2.37	0.62	--	100	490
	P	6.6	83.17	5.65		3.28	0.71	--		984
	R	17.20	17.06	1.00	4.19	0.39	12.64	74.70	109.98	
	Sum	100.00								
	RCV	99.6								
CCL-25-148	PL	--	75.09	6.39	2.85	1.05	3.10	11.51	100	283
	O	53.8	88.59	7.8	2.02	1.12	0.47	--	100	213
	A	16.1	86.51	7.1	3.67	2.08	0.64	--	100	305
	P	13.0	81.90	5.84	6.49	4.04	0.77	0.10	100	994
	R	17.1	18.9	1.18	4.78	0.74	15.80	70.91	111.40	--
	Sum	100.0								
	RCV	99.0								

Fractional and Elemental Composition
of the Product Liquid

		FR	C	H	O	N	S	Ash	Sum	nMW
CCL-25-184	PL	--	77.30	6.54	2.53	1.12	1.11	11.40	100	--
	O	66.34	88.50	7.60	2.29	1.17	0.44	--	100	208
	A	8.91	86.09	6.35	4.59	2.43	0.54	--	100	454
	P	5.94	82.84	5.34	6.15	2.79	0.59	2.30	100	1239
	R	18.81	15.52	0.99	4.40	0.39	5.89	72.81	100.0	--
	Sum	100.0								
	RCV	100.0								
CCL-25-196	PL	--	69.61	5.74	3.37	0.92	1.85	18.52	100	--
	O	57.0	87.87	7.72	2.64	1.32	0.45	--	100	209
	A	10.0	86.01	8.02	3.52	1.81	0.63	--	100	566
	P	8.0	81.02	5.89	5.68	3.55	0.69	3.18	100	1284
	R	25.0	16.99	1.27	5.49	0.34	6.04	76.21	106.34	--
	Sum	100.0								
	RCV	99.8								
CCL-28-11	PL	--	84.16	6.68	3.18	1.37	0.90	3.71	100.00	290
	O	67.6	89.52	7.43	1.54	1.92	0.56	--	100.00	208
	A	13.5	85.83	6.42	4.30	2.49	0.95	--	100.00	341
	P	12.7	83.74	5.46	5.99	2.40	1.38	1.03	100.00	1583
	R	6.2	28.53	1.65	5.08	0.77	5.01	63.62	104.66	--
	Sum	100.0								
	RCV	98.8								
CCL-28-22	PL	--	83.73	6.55	2.14	1.21	1.17	5.19	100.00	243
	O	68.21	89.53	7.30	1.65	0.96	0.56	--	100.00	204
	A	14.15	86.19	6.41	4.35	2.20	0.86	--	100.00	342
	P	7.56	83.94	5.39	6.03	2.42	1.17	1.04	100.00	1772
	R	10.08	18.04	1.26	4.77	0.53	7.65	74.18	106.43	--
	Sum	100.0								
	RCV	99.44								
CCL-28-35	PL	--	75.14	6.12	2.60	1.22	3.58	11.34	100.00	320
	O	63.8	88.82	7.70	1.79	1.14	0.54	--	100.00	212
	A	13.3	83.99	6.31	6.16	2.26	1.28	--	100.00	698
	P	8.7	82.45	5.62	7.49	2.40	1.36	0.68	100.00	1878
	R	14.2	12.32	0.80	4.27	0.27	20.37	75.34	113.37	--
	Sum	100.0								
	RCV	101.0								
CCL-28-46	PL	--	--	--	--	--	--	--	--	--
	O	66.8	89.05	7.71	1.74	1.03	0.47	--	100.00	208
	A	11.0	85.39	6.83	4.41	2.42	0.95	--	100.00	557
	P	7.1	83.53	5.69	5.76	2.53	1.68	0.81	100.00	1426
	R	15.1	11.13	0.81	3.28	0.27	20.65	80.16	116.30	--
	Sum	100.0								
	RCV	99.57								

APPENDIX D (continued)

Fractional and Elemental Composition
of the Product Liquid

		C	H	O	N	S	Ash	Sum	$\bar{n}$ MW
CCL-28-84	Cut #1	87.65	8.40	2.44	0.68	0.83	--	100.00	156
	Cut #2	89.85	7.16	1.42	1.12	0.46	--	100.00	176
	SRC	85.26	5.84	5.20	2.17	1.11	0.42	100.00	--
	Residue	29.60	1.85	7.40	0.45	5.00	59.60	103.90	--
CCL-28-96	Cut #1	88.00	8.37	2.09	0.62	0.92	--	100.00	190
	Cut #2	89.67	7.26	1.62	0.92	0.53	--	100.00	180
	SRC	85.70	6.11	4.13	3.13	0.93	--	100.00	--
	Residue	18.27	1.31	6.63	0.40	3.82	71.25	101.68	--
CCL-28-110	Cut #1	89.00	8.24	1.71	0.38	0.67	--	100.00	185
	Cut #2	89.87	7.21	1.60	0.77	0.55	--	100.00	190
	SRC	84.09	5.88	5.27	3.05	1.42	0.29	100.00	--
	Residue	21.32	1.35	6.54	0.29	6.83	70.30	106.63	--
CCL-28-123	Cut #1	89.16	7.59	1.64	1.08	0.52	--	100.00	183
	Cut #2	85.35	9.32	3.89	0.75	0.68	--	100.00	--
	SRC	84.15	6.13	5.64	2.14	1.94	--	100.00	--
	Residue	24.39	1.42	5.57	0.29	8.44	68.05	108.16	--

Cut #1 = IBP - 450°F
Cut #2 = 450°F - FBP
SRC = Solvent Refined Coal
Residue = Pyridine Insolubles

APPENDIX D (continued)

Fractional and Elemental Composition
of the Product Liquid

		FR	C	H	O	N	S	Ash	Sum	$\bar{n}$ MW
CCL-28-56	PL	--	76.55	6.45	2.73	1.22	3.01	10.03	100.00	253
	O	69.09	89.05	7.76	1.49	1.23	0.47	--	100.00	208
	A	11.82	85.99	6.40	4.40	2.38	0.83	--	100.00	423
	P	5.70	84.11	5.57	5.52	2.66	1.07	--	100.00	1142
	R	13.39	10.7	0.75	3.74	0.24	20.01	80.20	115.64	--
	Sum	100.0								
	RCV	99.86								
CCL-28-71	PL	--	79.24	6.64	2.49	1.15	2.44	9.18	100.00	271
	O	70.60	89.30	7.73	1.52	1.05	0.40	--	100.00	208
	A	10.40	86.69	7.43	3.09	2.22	0.56	--	100.00	498
	P	4.70	84.19	5.68	5.37	2.60	0.89	1.27	100.00	1649
	R	14.30	15.07	0.97	4.65	0.25	17.66	76.40	115.00	--
Original Solvent (F.O.B. #11)										
	PL	--	89.44	7.21	1.70	1.10	0.55	--	100.00	222
	O	93.8	89.68	7.25	1.42	1.05	0.60	--	100.00	208
	A	5.0	--	--	--	--	--	--	--	--
	P	0.4	--	--	--	--	--	--	--	--
	R	0.8	--	--	--	--	--	--	--	--
	Sum	100.0								
	RCV	100.0								
CCL-31-10	O	93.3	89.51	7.34	1.55	0.91	0.69	--	100.00	210
	A	3.5	87.10	6.41	3.88	2.14	0.47	--	100.00	570
	P	0.2	--	--	--	--	--	--	--	--
	R	1.0	--	--	--	--	--	--	--	--
	Sum	100.0								
	RCV	99.9								
CCL-31-24	O	86.2	89.50	7.49	1.30	1.02	0.68	--	100.00	200
	A	1.5	87.10	6.50	3.80	2.13	0.47	--	100.00	--
	P	0.8	--	--	--	--	--	--	--	--
	R	11.5	3.20	0.10	3.10	--	31.70	85.95	124.05	--
	Sum	100.0								
	RCV	100.0								
CCL-31-34	O	90.9	89.77	7.45	1.54	0.68	0.55	--	100.00	235
	A	4.6	87.48	6.60	3.23	2.24	0.45	--	100.00	--
	P	0.9	--	--	--	--	--	--	--	--
	R	3.6	4.69	0.15	3.55	--	20.65	81.75	110.79	--
	Sum	100.0								
	RCV	99.6								

Fractional and Elemental Composition
of the Product Liquid

		FR	C	H	O	N	S	Ash	Sum	$\bar{n}$MW
CCL-31-45	O	93.8	89.22	7.36	2.05	0.82	0.55	--	100.00	220
	A	2.5	86.46	6.20	4.84	2.16	0.34	--	100.00	330
	P	0.5	--	--	--	--	--	--	--	--
	R	3.2	3.18	0.18	5.91	--	8.02	96.87	114.16	--
	Sum	100.0								
	RCV	99.3								
CCL-31-55	O	82.5	89.65	7.36	1.51	0.87	0.62	--	100.00	210
	A	1.4	85.03	6.07	5.55	2.97	0.38	--	100.00	--
	P	0.9	--	--	--	--	--	--	--	--
	R	15.2	5.46	0.47	12.83	--	17.48	91.91	128.15	--
	Sum	100.0								
	RCV	99.5								
CCL-31-66	O	91.6	89.49	7.37	1.55	1.00	0.59	--	100.00	225
	A	1.1	85.25	6.29	5.08	2.97	0.40	--	100.00	--
	P	0.6	--	--	--	--	--	--	--	--
	R	6.7	6.35	0.43	6.79	--	2.64	96.67	112.88	--
	Sum	100.0								
	RCV	99.5								
CCL-31-81	O	72.80	89.68	7.28	1.72	0.73	0.59	--	100.00	220
	A	11.18	86.11	6.10	4.92	2.36	0.51	--	100.00	390
	P	6.92	86.15	5.05	5.86	2.45	0.49	--	100.00	990
	R	9.10	27.32	1.35	5.61	0.38	4.58	67.20	106.44	--
	Sum	100.00								
	RCV	99.95								
CCL-31-93	O	71.27	89.32	7.47	1.88	0.76	0.57	--	100.00	230
	A	11.26	86.21	6.35	4.86	2.06	0.53	--	100.00	--
	P	6.21	86.03	5.14	5.84	2.39	0.59	--	100.00	--
	R	11.26	22.26	1.09	4.99	0.26	9.67	70.80	100.33	--
	Sum	100.00								
	RCV	98.60								
CCL-31-109	O	71.88	89.35	7.39	1.85	0.78	0.64	--	100.00	205
	A	9.70	86.49	6.42	5.23	1.33	0.64	--	100.00	385
	P	5.56	85.65	5.42	5.48	2.43	0.71	0.31	100.00	--
	R	12.86	18.81	1.04	4.41	0.36	13.69	72.62	110.93	--
	Sum	100.00								
	RCV	98.81								

Fractional and Elemental Composition
of the Product Liquid

		FR	C	H	O	N	S	Ash	Sum	n̄ MW
CCL-31-113	O	71.35	89.06	7.51	1.83	0.94	0.67	--	100.00	250
	A	10.96	85.53	6.00	5.70	2.13	0.65	--	100.00	375
	P	5.00	85.06	5.36	6.10	2.35	0.70	0.43	100.00	--
	R	12.69	18.98	0.94	4.62	0.21	13.75	72.07	110.57	--
	Sum	100.00								
	RCV	98.27								
CCL-31-128	O	70.82	89.55	7.23	1.69	0.86	0.67	--	100.00	220
	A	9.63	85.90	6.29	5.79	1.43	0.59	--	100.00	450
	P	12.86	85.25	5.22	6.22	2.18	0.62	0.51	100.00	2035
	R	6.69	53.36	2.56	5.56	0.86	3.12	36.73	102.19	--
	Sum	100.00								
	RCV	99.31								
CCL-31-139	O	69.9	89.72	7.21	1.79	0.66	0.62	--	100.00	205
	A	9.8	87.04	6.05	5.01	1.38	0.53	--	100.00	--
	P	12.7	86.63	4.93	5.38	2.39	0.56	0.11	100.00	--
	R	7.6	55.29	2.49	4.96	1.16	3.04	35.34	102.28	--
	Sum	100.0								
	RCV	98.8								
CCL-31-149	O	73.0	89.49	7.30	1.70	0.85	0.66	--	100.00	195/240
	A	9.2	86.68	5.81	4.91	2.12	0.47	--	100.00	475
	P	10.6	86.89	4.81	5.11	2.28	0.48	0.42	100.00	1755
	R	7.2	56.90	2.48	5.48	0.91	2.51	33.91	102.19	--
	Sum	100.0								
	RCV	99.2								
CCL-31-161	O	74.00	89.49	7.34	1.73	0.81	0.62	--	100.00	220
	A	10.06	86.59	5.79	4.79	2.36	0.46	--	100.00	410
	P	8.54	86.14	4.81	5.76	2.42	0.51	0.36	100.00	1570
	R	7.40	42.51	1.77	4.92	0.51	9.24	48.38	107.33	--
	Sum	100.00								
	RCV	98.98								
CCL-31-175	O	71.42	89.39	7.47	1.71	0.78	0.64	--	100.00	245
	A	8.91	86.44	5.91	5.02	2.16	0.47	--	100.00	--
	P	9.75	86.56	4.96	5.61	2.29	0.54	0.05	100.00	1450
	R	9.92	32.96	1.35	4.58	0.30	15.04	57.30	111.52	--
	Sum	100.00								
	RCV	98.00								

<u>Fractional and Elemental Composition</u>
<u>of the Product Liquid</u>

		FR	C	H	O	N	S	Ash	Sum	n̄ MW
CCL-31-186	O	68.11	89.16	7.55	1.81	0.81	0.66	--	100.00	225
	A	10.37	85.55	5.72	5.93	2.27	0.54	--	100.00	505
	P	9.00	85.38	5.16	6.14	2.29	0.66	0.38	100.00	1730
	R	12.52	25.05	1.14	4.42	0.32	20.10	64.15	115.18	--
	Sum	100.00								
	RCV	100.00								
CCL-31-196	O	68.25	89.37	7.50	1.65	0.86	0.62	--	100.00	210
	A	9.86	87.33	5.96	5.10	1.08	0.54	--	100.00	--
	P	7.89	85.75	4.95	5.66	2.32	0.61	0.71	100.00	1500
	R	14.00	22.80	0.88	4.19	0.12	21.85	67.38	117.22	--
	Sum	100.00								
	RCV	99.00								
CCL-31-206	O	69.86	89.35	7.70	1.57	0.77	0.60	--	100.00	235
	A	10.18	86.78	6.32	4.42	1.96	0.52	--	100.00	365
	P	7.39	85.41	5.33	5.34	2.68	0.66	0.59	100.00	--
	R	12.57	24.15	0.98	4.20	0.29	20.59	65.98	116.19	--
	Sum	100.00								
	RCV	98.48								
CCL-31-219	O	66.20	89.42	7.29	1.75	0.86	0.68	--	100.00	230
	A	9.50	85.18	6.28	5.82	2.12	0.60	--	100.00	470
	P	7.45	84.43	5.51	6.55	2.81	0.71	--	100.00	1210
	R	16.85	19.02	0.97	3.87	0.28	16.68	69.48	110.30	--
	Sum	100.00								
	RCV	99.94								
CCL-31-234	O	69.40	89.39	7.26	1.78	0.88	0.69	--	100.00	250
	A	9.40	86.16	5.89	5.10	2.35	0.50	--	100.00	465
	P	7.80	86.57	4.80	5.47	2.54	0.62	--	100.00	1775
	R	13.40	23.96	1.14	4.30	0.34	13.23	64.97	107.94	--
	Sum	100.00								
	RCV	100.00								
CCL-31-248	O	67.18	89.69	7.22	1.64	0.78	0.66	--	100.00	195
	A	8.10	86.28	5.97	5.59	1.55	0.62	--	100.00	--
	P	11.10	85.19	4.94	6.36	2.60	0.66	0.25	100.00	1930
	R	13.62	21.42	0.99	9.84	0.24	6.02	72.94	111.45	--
	Sum	100.00								
	RCV	99.22								

Fractional and Elemental Composition
of the Product Liquid

		FR	C	H	O	N	S	Ash	Sum	n̄ MW
CCL-31-258	O	66.77	89.88	7.19	1.60	0.65	0.67	--	100.00	240
	A	7.95	87.14	5.81	5.20	1.31	0.53	--	100.00	480
	P	8.61	86.41	4.67	5.58	2.54	0.55	0.25	100.00	1820
	R	16.67	18.81	0.85	11.76	0.24	4.72	77.29	113.67	--
	Sum	100.00								
	RCV	98.60								
CCL-31-268	O	67.80	89.25	7.73	1.63	0.76	0.64	--	100.00	195
	A	5.94	86.10	6.21	5.55	1.59	0.56	--	100.00	--
	P	7.73	85.02	4.77	6.54	2.52	0.56	0.58	100.00	--
	R	18.53	15.19	0.79	12.56	0.12	3.95	83.34	115.95	--
	Sum	100.00								
	RCV	97.84								
CCL-31-278	O	68.00	89.24	7.54	1.71	0.89	0.62	--	100.00	230
	A	8.10	85.54	6.16	5.59	2.27	0.43	--	100.00	450
	P	6.15	85.43	5.01	6.25	2.79	0.51	--	100.00	--
	R	17.75	15.78	0.88	11.81	0.07	3.80	83.45	115.79	--
	Sum	100.00								
	RCV	99.79								
CCL-31-301	O	65.91	89.09	7.65	1.73	0.89	0.64	--	100.00	230
	A	9.96	85.69	6.48	5.84	1.42	0.57	--	100.00	535
	P	5.36	85.05	5.63	6.22	2.48	0.62	--	100.00	--
	R	18.77	13.64	0.79	7.65	0.06	4.90	87.18	114.22	--
	Sum	100.00								
	RCV	99.81								
CCL-31-312	O	66.61	89.06	7.65	1.74	0.95	0.61	--	100.00	215
	A	12.28	85.89	6.24	5.19	2.25	0.42	--	100.00	380
	P	5.32	85.38	5.28	6.19	2.59	0.55	--	100.00	1225
	R	15.79	14.50	0.70	7.16	0.06	4.69	86.17	113.28	--
	Sum	100.00								
	RCV	99.33								
CCL-31-321	O	69.37	89.90	7.10	1.52	0.83	0.64	--	100.00	220
	A	7.21	86.30	5.75	5.21	2.12	0.62	--	100.00	410
	P	8.53	82.06	4.62	7.06	2.42	0.66	3.18	100.00	1105
	R	14.89	38.58	2.11	11.51	1.05	3.60	53.94	110.79	--
	Sum	100.00								
	RCV	99.44								

Fractional and Elemental Composition
of the Product Liquid

		FR	C	H	O	N	S	Ash	Sum	n̄ MW
CCL-38-10	O	74.01	89.97	7.10	1.44	0.82	0.67	--	100.00	
	A	8.98	85.60	5.96	5.48	2.45	0.51	--	100.00	
	P	10.43	82.94	4.85	8.95	2.56	0.70	--	100.00	
	R	6.58	55.72	2.55	5.81	1.37	4.17	33.07	102.69	
	Sum	100.00								
	RCV	99.64								
CCL-38-17	O	75.59	89.75	7.00	1.61	0.99	0.65	--	100.00	
	A	9.54	86.60	5.79	4.73	2.36	0.52	--	100.00	
	P	8.16	84.92	4.62	7.39	2.45	0.62	--	100.00	
	R	6.51	52.79	2.28	5.08	0.85	4.72	36.70	102.42	
	Sum	100.00								
	RCV	99.96								
CCL-38-28	O	72.51	90.05	7.04	1.35	0.87	0.69	--	100.00	
	A	8.95	86.37	5.56	5.10	2.51	0.46	--	100.00	
	P	10.37	84.96	4.49	7.37	2.68	0.50	--	100.00	
	R	8.17	50.54	2.03	--	1.05	2.87	41.40	--	
	Sum	100.00								
	RCV	99.66								
CCL-38-40	O	70.70	89.89	7.15	1.39	0.88	0.69	--	100.00	
	A	8.93	87.16	5.70	4.19	2.43	0.52	--	100.00	
	P	10.56	85.66	4.56	6.70	2.55	0.53	--	100.00	
	R	9.81	41.72	1.70	11.44	0.89	2.41	52.90	111.06	
	Sum	100.00								
	RCV	99.33								
CCL-38-83	O	70.16	89.56	7.35	1.39	1.00	0.70	--	100.00	
	A	10.14	86.51	5.81	4.82	2.40	0.46	--	100.00	
	P	8.71	84.54	4.71	7.52	2.73	0.50	--	100.00	
	R	10.99	29.72	1.22	--	0.56	10.96	63.43	--	
	Sum	100.00								
	RCV	99.22								
CCL-38-102	O	72.67	89.62	7.37	1.38	1.00	0.63	--	100.00	
	A	9.78	86.71	5.88	4.54	2.44	0.43	--	100.00	
	P	6.24	84.72	4.75	7.40	2.56	0.57	--	100.00	
	R	11.31	23.46	0.92	4.84	0.39	20.98	67.91	118.50	
	Sum	100.00								
	RCV	99.99								

APPENDIX D (continued)

Fractional and Elemental Composition
of the Product Liquid

		FR	C	H	O	N	S	Ash	Sum
CCL-38-120	O	73.57	89.70	7.42	1.20	0.97	0.71	--	100.00
	A	13.57	87.64	6.05	5.23	2.52	0.56	--	100.00
	P	6.69	84.42	5.14	7.43	2.34	0.67	--	100.00
	R	6.17	45.82	2.07	7.39	0.84	3.64	45.79	106.05
	Sum	100.00							
	RCV	99.88							
CCL-38-129	O	73.95	89.69	7.46	1.34	0.91	0.60	--	100.00
	A	10.93	85.79	6.06	5.24	2.39	0.52	--	100.00
	P	7.18	85.00	5.31	6.65	2.51	0.53	--	100.00
	R	6.74	43.40	1.91	7.36	0.62	3.55	48.00	104.84
	Sum	100.00							
	RCV	98.80							
CCL-40-10	O	73.0	89.35	7.27	1.92	0.85	0.61	--	100.0
	A	8.7	84.61	5.81	6.27	2.57	0.74	--	100.0
	P	10.6	82.60	4.80	9.44	2.39	0.77	--	100.0
	R	7.7	42.84	2.14	6.51	1.05	6.12	46.01	104.67
	Sum	100.0							
	RCV	98.2							
CCL-44-20	O	74.1	89.57	7.19	1.72	0.88	0.64	--	100.00
	A	8.4	84.61	5.88	6.56	2.38	0.57	--	100.00
	P	10.1	82.11	4.83	10.02	2.34	0.70	--	100.00
	R	7.4	41.16	1.87	5.98	0.87	9.38	48.04	107.30
	Sum	100.0							
	RCV	98.3							
CCL-44-32	O	74.5	89.92	7.07	1.59	0.77	0.65	--	100.00
	A	8.7	85.70	5.75	5.72	2.33	0.50	--	100.00
	P	10.6	84.00	4.70	8.39	2.32	0.59	--	100.00
	R	6.2	58.68	2.57	6.15	1.19	3.02	30.00	101.55
	Sum	100.0							
	RCV	99.6							
CCL-45-23	O	71.60	89.83	7.30	1.38	0.89	0.60	0.00	100.00
	A	10.20	85.88	5.94	5.68	2.25	0.35	0.00	100.00
	P	10.80	83.93	4.86	8.45	2.30	0.46	0.00	100.00
	R	7.40	50.88	2.37	--	1.07	6.66	38.37	--
	Sum	100.00							
	RCV	99.00							

Fractional and Elemental Composition
of the Product Liquid

		FR	C	H	O	N	S	Ash	Sum
CCL-45-31	O	69.4	89.72	7.32	1.41	0.91	0.64	0.00	100.00
	A	10.4	85.80	6.09	5.55	2.22	0.34	0.00	100.00
	P	12.0	83.35	5.11	8.71	2.34	0.49	0.00	100.00
	R	8.2	53.36	2.57	6.88	0.98	6.30	36.07	106.16
	Sum	100.00							
	RCV	98.98							
CCL-45-39	O	73.7	89.73	7.23	1.51	0.92	0.61	0.00	100.00
	A	10.4	86.45	5.81	4.88	2.60	0.25	0.00	100.00
	P	8.7	85.44	4.76	7.07	2.37	0.36	0.00	100.00
	R	7.2	48.35	2.01	6.59	0.88	7.50	42.34	107.65
	Sum	100.00							
	RCV	98.1							
CCL-45-52	O	68.7	89.98	7.16	1.29	0.93	0.64	0.00	100.00
	A	9.9	86.36	5.77	5.24	2.29	0.34	0.00	100.00
	P	11.8	85.21	4.75	7.05	2.57	0.42	0.00	100.00
	R	9.6	56.79	2.55	6.74	1.44	4.78	32.57	104.87
	Sum	100.00							
	RCV	98.97							
CCL-45-62	O	73.40	89.52	7.32	1.77	0.79	0.60	0.00	100.00
	A	9.00	85.78	5.82	5.61	2.45	0.34	0.00	100.00
	P	10.60	84.27	4.79	8.04	2.48	0.42	0.00	100.00
	R	7.00	47.68	2.02	6.36	0.93	7.08	42.66	106.73
	Sum	100.00							
	RCV	98.20							
CCL-45-79	O	73.20	89.52	7.40	1.60	0.87	0.61	0.00	100.00
	A	10.00	85.83	5.96	5.45	2.35	0.41	0.00	100.00
	P	9.70	83.87	5.00	8.27	2.45	0.43	0.00	100.00
	R	7.20	50.09	2.19	6.66	0.96	6.59	39.97	106.96
	Sum	100.10							
	RCV	98.31							
CCL-45-89	O	73.00	89.69	7.17	1.69	0.80	0.65	--	100.00
	A	8.40	85.61	5.78	5.72	2.31	0.58	--	100.00
	P	11.20	83.48	4.67	8.95	2.33	0.57	--	100.00
	R	7.40	56.77	2.50	6.42	1.10	2.77	32.21	101.77
	Sum	100.00							
	RCV	98.00							

Fractional and Elemental Composition
of the Product Liquid

		FR	C	H	O	N	S	Ash	Sum
CCL-45-98	O	73.10	89.79	7.11	1.69	0.78	8.63	--	100.00
	A	8.60	85.04	5.91	6.19	2.36	0.50	--	100.00
	P	11.70	83.60	4.61	8.97	2.30	0.52	--	100.00
	R	6.60	56.71	2.43	6.58	1.30	1.84	32.89	101.75
	Sum	100.00							
	RCV	98.60							
CCL-45-108	O	73.3	89.63	7.15	1.68	0.85	0.69	--	100.00
	A	8.6	85.34	5.85	6.02	2.22	0.57	--	100.00
	P	11.8	83.34	5.10	8.31	2.61	0.64	--	100.00
	R	6.3	55.08	2.42	6.26	1.02	2.30	34.82	101.90
	Sum	100.0							
	RCV	98.5							
CCL-45-116	O	77.1	89.75	7.21	1.58	0.81	0.65	--	100.00
	A	7.8	85.06	5.91	5.98	2.45	0.60	--	100.00
	P	9.5	83.74	4.87	8.34	2.33	0.72	--	100.00
	R	5.6	48.15	2.17	6.45	0.91	4.82	41.40	103.90
	Sum	100.0							
	RCV	98.1							
CCL-47-10	O	76.9	90.42	7.12	1.03	0.82	0.61	0.00	100.00
	A	8.4	85.50	5.96	5.77	2.23	0.54	0.00	100.00
	P	9.3	85.28	4.83	6.97	2.39	0.53	0.00	100.00
	R	5.4	58.18	2.65	--	1.08	2.73	31.15	--
	Sum	100.00							
	RCV	97.86							

APPENDIX E

Sulfiding of Iron Oxide

The iron sulfide or reduced pyrite (FeS) was prepared at Auburn University by sulfiding ferric oxide (Fe_2O_3) with H_2S in the presence of hydrogen gas. The ferric oxide used was red-anhydrous powder of over 99% purity and was obtained from Fisher Scientific Company. The hydrogen sulfide gas was of commercial purity obtained from Matheson Gas Company. The sulfiding reaction is given in Equation E-1.

$$Fe_2O_3 + 2H_2S + H_2 \longrightarrow 2FeS + 3H_2O \qquad \text{(Eqn. E-1)}$$

The schematic of the apparatus used is shown in Figure E-1. A constant supply pressure of 2 psig was maintained on the H_2 and H_2S cylinders. Rotameters were used to measure the individual gas flow rates and the gas flow rates were controlled by fine metering valves to give a required H_2/H_2S flow ratio. A porcelain boat containing approximately 2-3g of ferric oxide was placed in the center of 1-inch O.D. Pyrex glass tube heated by a Lindberg Electric Furnace (Type 123-12). A thermocouple was installed in the center of the furnace to read and manually control the temperature. The unreacted H_2S gas was scrubbed with the use of caustic solution and the other gases were vented in the hood.

The system was checked and corrected for leaks before turning on the heat. Usually, 50-70 minutes were required to heat the furnace from room temperature to the desired temperature. When the desired temperature was reached, the time was marked as zero time. A reaction time of 150 minutes was used. At the end of the reaction period the heat was turned off and the product was allowed to cool down rapidly to room temperature. The product was then removed, ground, and stored under an inert atmosphere of N_2 for later use as a catalyst.

FIGURE E-1
APPARATUS FOR FeS PREPARATION

351
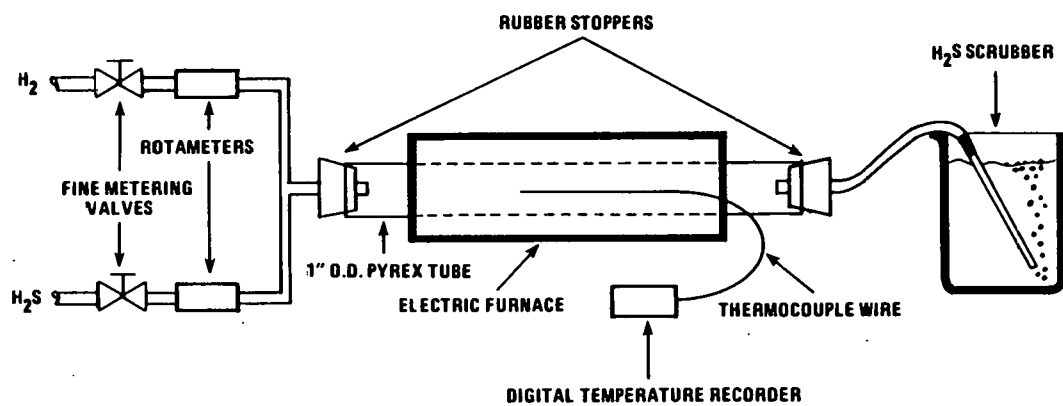
APPENDIX F

Calculation of Reaction Rate Constants

The reaction rate constants for conversion of asphaltene and preasphaltene were calculated assuming sequential reaction, for example,

Coal $\xrightarrow{\quad k_c \quad}$ Preasphaltenes $\xrightarrow{\quad k_p \quad}$ Asphaltenes $\xrightarrow{\quad k_a \quad}$ Oils
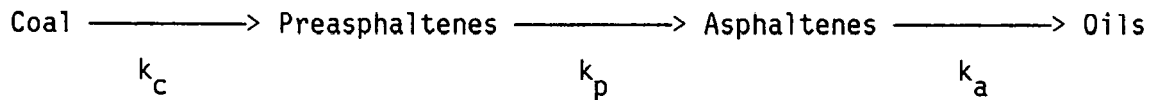
where k_c, k_p, and k_a are first-order rate constants for the conversion of coal, preasphaltenes and asphaltenes, respectively. The rate expression could be written as follows:

$$k_c C_o t = C_i - C_o \qquad \text{(F-1)}$$

$$k_c C_o t - k_p P_o t = P_o - P_i \qquad \text{(F-2)}$$

$$k_p P_o t - k_a A_o t = A_o - A_i \qquad \text{(F-3)}$$

$$\text{and} \qquad k_a A_o t = O_o - O_i \qquad \text{(F-4)}$$

where t = nominal residence time, hr.
     C = concentration of coal, g/hr.
     P = concentration of preasphaltene, g/hr.
     A = concentration of asphaltene, g/hr.
     O = concentration of oil, g/hr.
and subscript i and o refer to inlet and outlet, respectively.

Rearranging the equations F-1 to F-4, to obtain:

$$k_a = \frac{O_o - O_i}{A_o t} \qquad \text{(F-5)}$$

$$k_p = \frac{(A_o - A_i) + (O_o - O_i)}{P_o t} \qquad \text{(F-6)}$$

Equations F-5 and F-6 were used to calculate the first-order reaction rate constants for the conversion of asphaltene and preasphaltene.

Thermal Properties of Various Minerals and Metallic Wastes

Magnetite - The thermogram of magnetite in the presence of flowing helium is shown in Figure G-1. Negligible weight loss was observed suggesting that magentite is thermally stable up to 600°C under inert atmosphere.

The thermogram for magnetite in the presence of flowing hydrogen is also shown in Figure G-1. Magnetite began losing weight (reduction of magnetite) at around 350°C; the rate of weight reduction reached its maximum at around 450°C. The reaction of magnetite with hydrogen is represented by the equation given below.[1]

$$Fe_3O_4 + 4H_2 = 3 Fe + 4H_2O \qquad \text{(Eqn. G-1)}$$
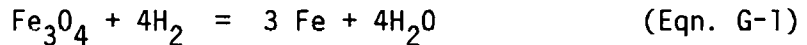
Stoichiometrically, complete reduction of pure magnetite (Fe_3O_4) results in 27.6% weight reduction. The overall observed weight loss at 600°C was 24%. Therefore, the actual and the theoretical weight loss correspond very well (providing the impurities in the magnetite sample are accounted for in the calculation) suggesting that complete reduction of magnetite is achieved at 600°C.

Magnetite when reduced at 450°C under 1000 psig hydrogen pressure for 10 minutes in the PTGR (fast heating) lost approximately 2.7% weight (see Table G-1). This weight loss corresponds to only 10% of the weight loss necessary for complete stoichiometric reduction. Therefore, if magnetite is used as a disposable catalyst in coal liquefaction, only a small fraction of the total hydrogen required for coal liquefaction will be consumed in reducing the magnetite.

---

[1] Kawa, Walter, Hiteshue, R. W., Anderson, R. E. and Harold Greenfield, "Reactions of iron and iron compounds with hydrogen sulfide", A report prepared by the Burea of Mines (Investigation 5690).

FIGURE G-1
TGA OF MAGNETITE IN THE PRESENCE OF
HYDROGEN AND HELIUM GASES

He FLOW RATE = 40 ML./MIN.
HYDROGEN FLOW RATE = 300 ML./MIN.
MAGNETITE = – 200 MESH
HEATING RATE =
H_2 = 10°C/MIN.
He = 20°C/MIN.
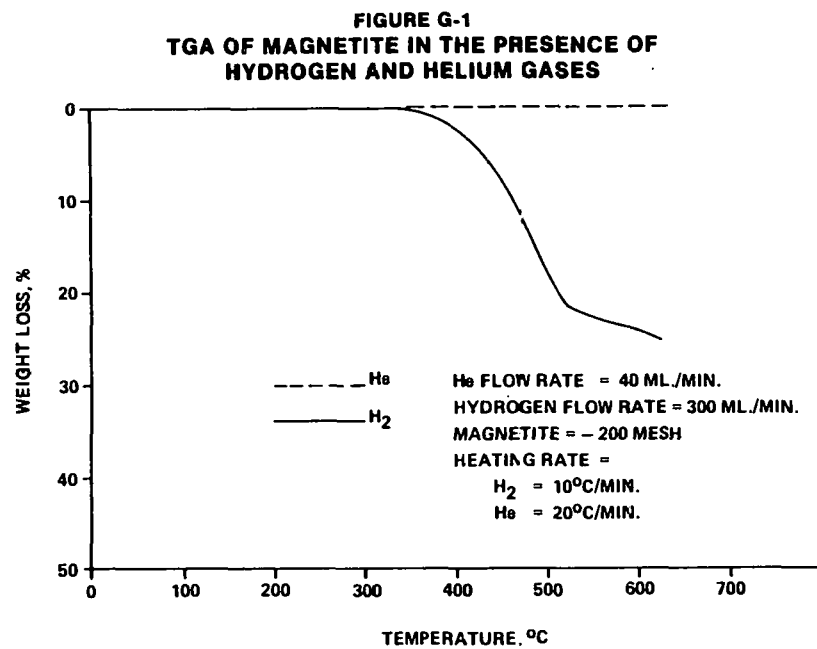
FIGURE G-2
DTA OF MAGNETITE IN THE PRESENCE OF AIR

HEATING RATE = 20° C/MIN.

EXOTHERMIC
PROCESS

ENDOTHERMIC
PROCESS

355
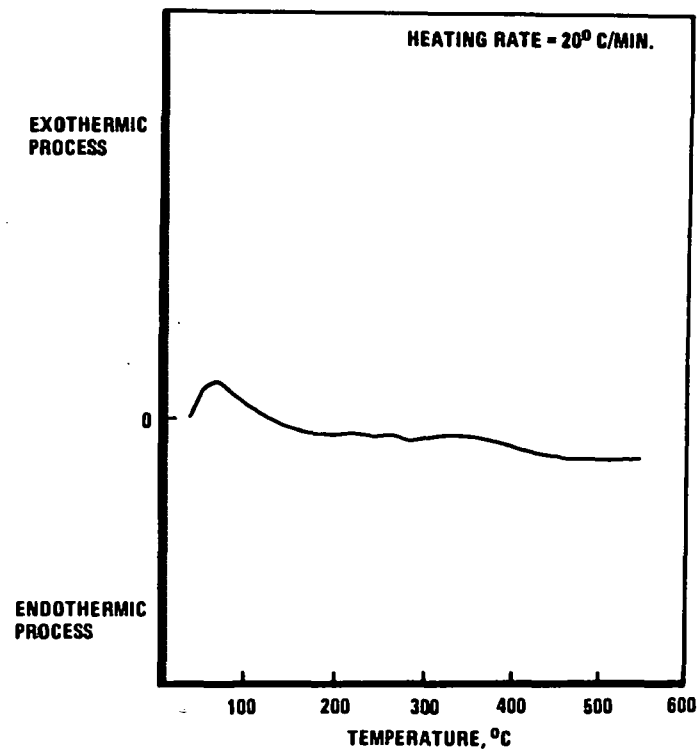
TABLE G-1

Reduction of Minerals and Metallic Wastes in the PTGR

Sample	Initial Weight, g	Final Weight, g	Weight Loss, g	Weight Loss, %	Gas Analyses, % N₂	Gas Analyses, % CO₂	Gas Analyses, % H₂S	H₂O	Total Recovered Product g	Recovery of Lost Weight
Magnetite	3.00	2.92	0.08	2.67	--	--	--	0.0378	0.0378	47.3
Montmorillonite (Thixogell #3)	3.00	2.53	0.47	15.6	0.0045	--	--	0.0564	0.0609	13.0
Montmorillonite (Hydrite PX1672)	1.50	1.47	0.03	2.0	--	--	--	--	--	--
Montmorillonite (Colloid BP1673)	3.00	2.75	0.25	8.3	--	--	--	0.0744	0.0744	29.8
Apatite (Monocalcium Phosphate)	3.00	2.82	0.18	2.7	--	--	--	0.0035	0.0035	1.9
Apatite (Dicalcium Phosphate)	3.00	2.79	0.21	2.8	--	--	--	0.0656	0.0656	31.2
Apatite (Tricalcium Phosphate)	3.00	2.69	0.31	10.3	--	--	--	0.0446	0.0446	14.4
Quick Lime	3.00	3.00	--	--	--	--	--	--	--	--
Gypsum	3.00	2.41	0.59	19.7	0.0025	0.0562	--	0.0497	0.1084	18.4
Bornite	3.00	2.81	0.19	6.3	0.0022	0.0017	--	0.0317	0.0356	10.8
Ilmenite	3.00	2.91	0.09	3.0	--	--	--	--	--	--
Rutile	3.00	3.00	0.00	0.0	--	--	--	--	--	--
Illite	3.00	2.90	0.10	3.3	--	--	--	--	--	--
Molybdenite	3.00	3.00	0.00	0.0	--	--	--	--	--	--
Flue Dust	3.00	2.78	0.22	7.3	0.0033	--	--	0.0496	0.0529	24.1

TABLE G-1 (Continued)

Reduction of Minerals and Metallic Wastes in the PTGR

Sample	Initial Weight, g	Final Weight, g	Weight Loss, g	Weight Loss, %	Gas Analyses, % N_2	CO_2	H_2S	H_2O	Total Recovered Product g	Recovery of Lost Weight,%
Alnico Grindings	3.00	2.96	0.04	1.3	--	--	--	--	--	--
Super Alloy Grindings	3.00	3.00	0.00	0.0	--	--	--	--	--	--
Kaolinite Burgess #10	2.82	2.80	0.02	0.02	--	--	--	--	--	--
Calcite	2.82	2.82	0.00	0.00	--	--	--	--	--	--
Feldspar NC-4	3.00	3.00	0.00	0.00	--	--	--	--	--	--
Albanion Chrome										
Ore Concentrate	3.00	2.98	0.02	0.67	--	--	--	--	--	--
Molybdic Oxide	3.00	2.73	0.27	9.00	--	--	0.081	0.054	0.135	50.0
Phosphate Slime	1.00	0.89	0.11	11.00	--	--	--	0.037	0.037	33.6
Sphalerite (ZnS)	3.00	2.98	0.02	0.67	--	--	--	--	--	--
Dolomite	1.00	1.00	0.00	0.00	--	--	--	--	--	--
Oil Shale	1.00	0.95	0.05	5.00	--	--	--	0.055	0.055	110.0
Red Mud	1.00	0.87	0.13	13.00	--	--	--	0.053	0.053	40.7

Reaction Time = 10 Minutes, Temperature = 450°C
Pressure = 1,000 psig H_2

The DTA of magnetite in the presence of air showed a small exotherm from room temperature to 120°C (see Figure G-2). This exotherm, the only thermal activity that was observed, was apparently due to oxidation of carbon and other impurities present in the sample.

Zinc Flue Dusts - The thermograms of low zinc and high zinc flue dust samples under flowing helium gas are shown in Figures G-3 and G-4. Both samples were noted to be thermally stable in the presence of inert gas; i.e., no weight loss upon heating in the presence of inert atmosphere.

The thermograms of zinc flue dust samples under flowing hydrogen are also presented in Figure G-3 and G-4. Both flue dust samples started losing weight (reduction of flue dust) at around 350°C and continued to do so with the increase in temperature. Complete reduction of flue dust samples was not achieved during the heating period. The overall weight loses for low zinc and high zinc samples at 600°C were 14.5 and 12.5%, respectively.

The DTA's of zinc flue dust samples (low and high zinc contents) in the presence of helium and air are shown in Figures G-5 to G-8. The low zinc and high zinc flue dust samples gave minor endotherms at 133 and 72°C, respectively, in the presence of helium. These endotherms are probably due to the vaporization of moisture present in the samples. Similarly, minor endotherms were observed in the presence of air at somewhat lower temperatures. Also, very minor exotherms at 360°C (low zinc sample) and at 109°C (high zinc sample) were apparently due to the oxidation of the sample. The high zinc sample, in addition to both an endotherm and exotherm at low temperatures, also gave an endotherm at 495°C which was due to fusion of the sample.

The two zinc flue dust samples were reduced at 450°C under 1000 psig hydrogen pressure for 10 minutes in the PTGR (fast heating) to study the reduction of flue dusts and the data are presented in Table G-2. The low zinc and high zinc flue dust samples lost 6.3 and 4.7% weight, respectively. The corresponding weight losses (at 450°C) under flowing hydrogen (1 atm pressure) were 1.5 and 3%. The differences in the weight loss under flowing hydrogen and under pressurized hydrogen could be due to differences in pressure and heating time.

FIGURE G-3
TGA OF ZINC FLUE DUST (LOW ZINC) IN THE PRESENCE OF HELIUM AND HYDROGEN GASES

He FLOW RATE = 40 ML./MIN.
H_2 FLOW RATE = 300 ML./MIN.
HEATING RATE =
H_2 = 10°C/MIN.
He = 20°C/MIN.
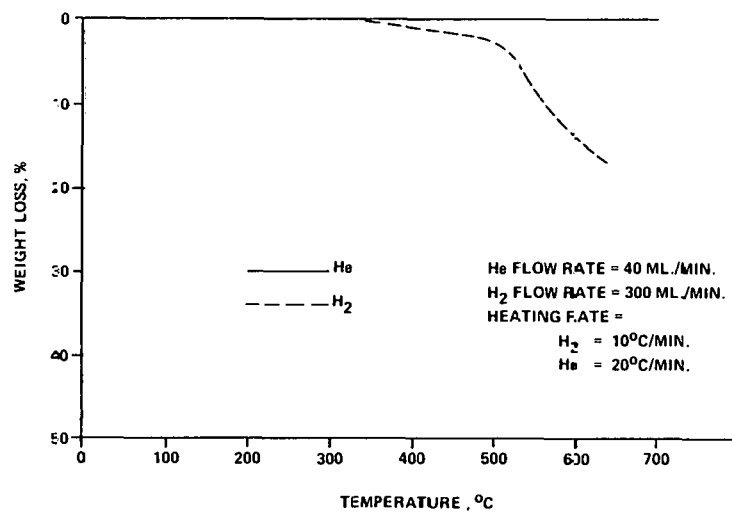
FIGURE G-4
TGA OF ZINC FLUE DUST (HIGH ZINC) IN THE PRESENCE OF HYDROGEN AND HELIUM GASES

He FLOW RATE = 40 ML./MIN.
H_2 FLOW RATE = 300 ML./MIN.
HEATING RATE
H_2 = 10°C/MIN.
He = 20°C/MIN.
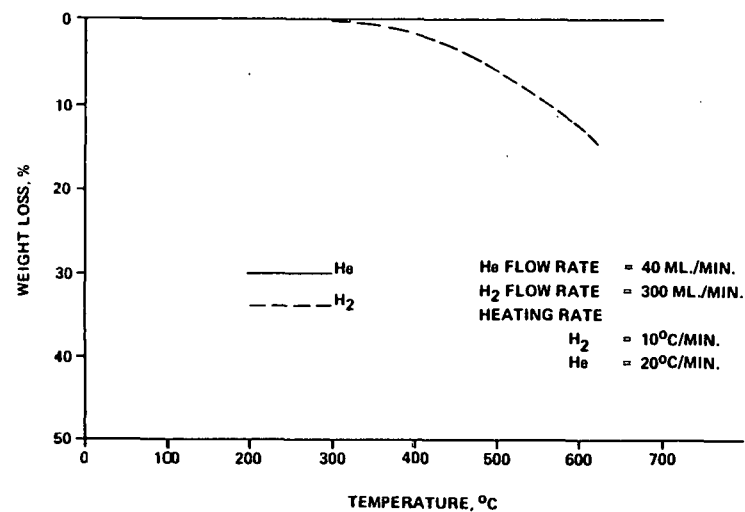
FIGURE G-5
DATA OF LOW ZINC FLUE DUST IN THE PRESENCE OF HELIUM

HEATING RATE = 20° C/MIN.

133° C
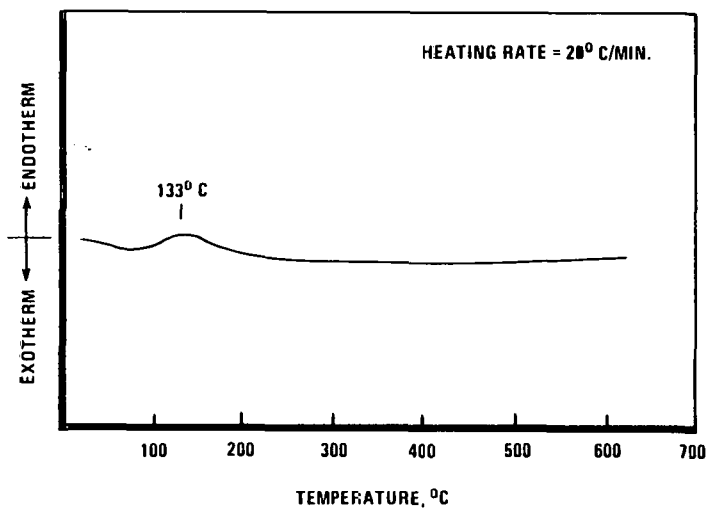
FIGURE G-6
DTA OF HIGH ZINC FLUE DUST IN THE PRESENCE OF HELIUM

HEATING RATE = 20° C/MIN.

72° C

359
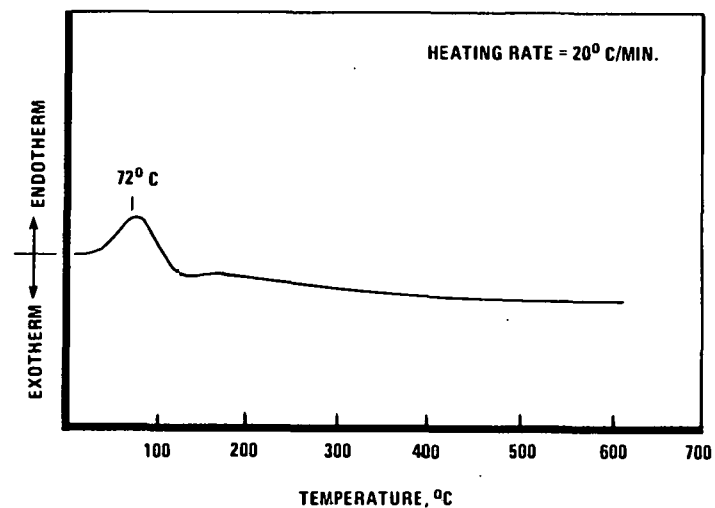
FIGURE G-7
DTA OF LOW ZINC FLUE DUST IN THE PRESENCE OF AIR

HEATING RATE = 20° C/MIN.

30° C

360° C

ENDOTHERM

EXOTHERM

TEMPERATURE, °C
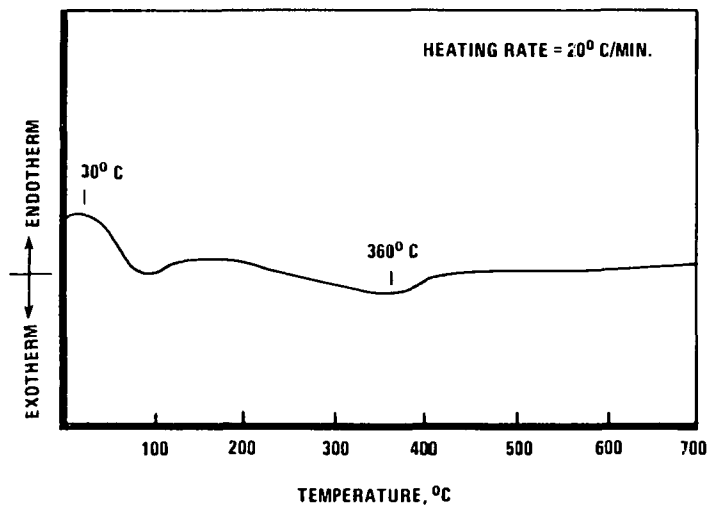
FIGURE G-8
DTA OF HIGH ZINC FLUE DUST IN THE PRESENCE OF AIR

HEATING RATE = 20° C/MIN.

51° C

109° C

495° C

ENDOTHERM

EXOTHERM

TEMPERATURE, °C
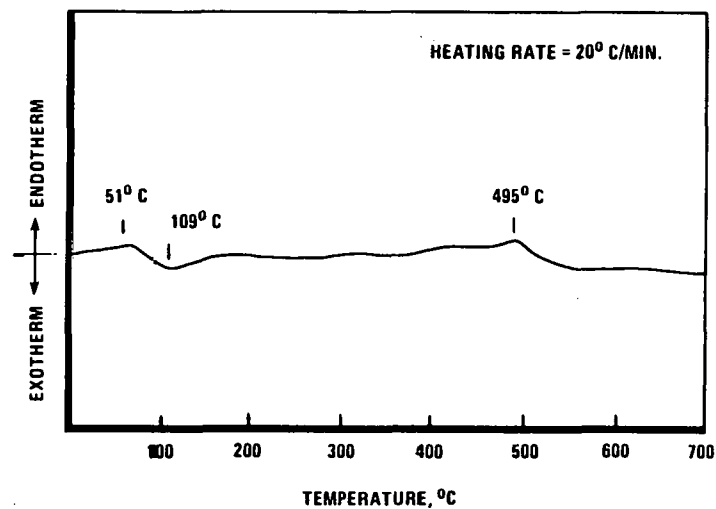
FIGURE G-9
TGA OF ZINC OXIDE IN THE PRESENCE OF HYDROGEN

WEIGHT LOSS, %

HEATING RATE = 20° C/MIN.
FLOW RATE = 300 ML./MIN.

TEMPERATURE, °C
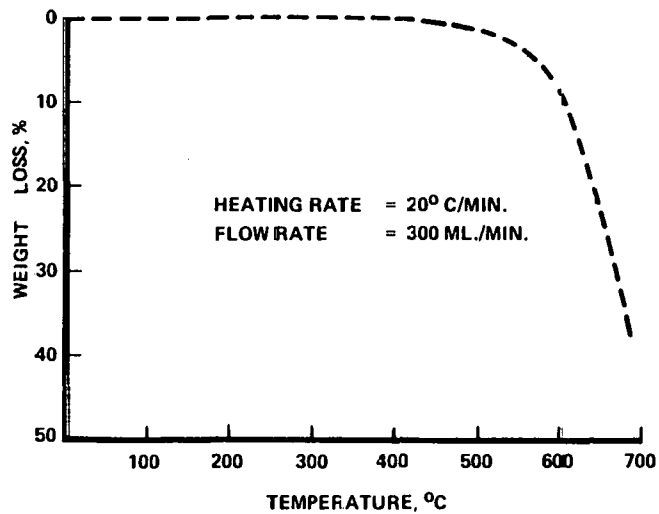
FIGURE G-10
TGA OF COPPERAS IN THE PRESENCE
OF HELIUM GAS

WEIGHT LOSS, %

HEATING RATE = 20°C/MIN.
FLOW RATE = 40 ML./MIN.

TEMPERATURE, °C

360
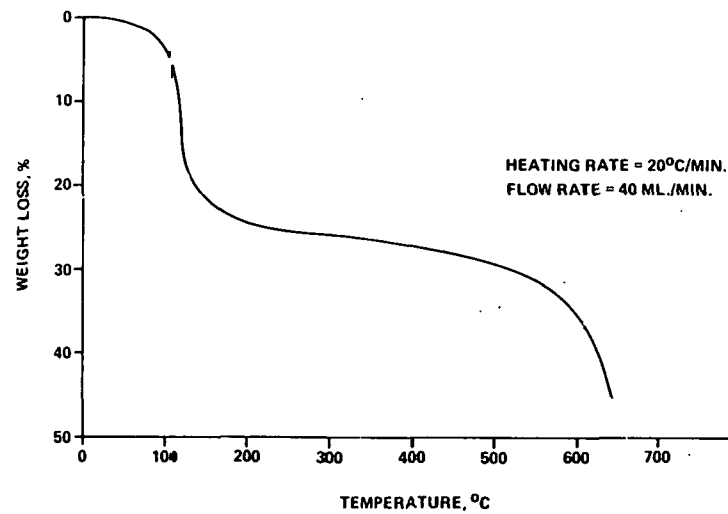
TABLE G-2

Reduction of Zinc Flue Dusts in PTGR

	Low Zinc	High Zinc
Temp., °C	450	450
Pressure, psig	1000	1000
Initial Weight, g	3.0	3.0
Final Weight, g	2.81	2.86
Weight Loss, g	0.19	0.14
Weight Loss, %	6.33	4.67
Gas Analyses, g water	0.02	0.0468
Liquid Analysis,* g, water	0.269	0.2845
Liquid Analysis,* g, sulfur	0.0005	0.0002
Total Recovered Product, g	0.2895	0.3315
% Recovery of Lost Weight	152.0	237.0

---

*Condensed in the ice trap.

The samples of zinc flue dusts before and after hydrogen reduction in the PTGR were analyzed by x-ray diffraction. The major difference between the two zinc samples was the concentration of zinc; the high zinc samples had significantly greater concentration of ZnO than the low zinc sample. The chemical forms of zinc present in the two samples were identified as $ZnFe_2O_4$ and ZnO. After hydrogen reduction the amount of $ZnFe_2O_4$ present in the sample diminished and elemental iron and the FeO isomorph appeared. The concentration of ZnO was not greatly affected by the treatment. Zinc metal was not observed either before or after reduction. Apparently the iron oxide reduced in preference to the zinc oxide. The analysis of various hydrogen reduction products (gas and condensed liquid given in Table G-2 showed that the major product was water. The formation of water further confirmed the reduction of iron oxide to elemental iron.

Zinc Oxide - Zinc oxide on analysis by TGA lost weight at approximately 450°C in the presence of hydrogen gas as shown in Figure G-9. The stoichiometric reduction (24.6% weight loss) of ZnO was obtained at about 660°C. The sample continued to lose weight at temperatures above 660°C. The excess loss in weight (more than the stoichiometric amount) was due to volatilization of zinc. Similar results were obtained by reducing ZnO in the PTGR at 450 and 1000°C and 1000 psig hydrogen pressure. ZnO lost approximately 60% of the inital weight at 1000°C in just ten minutes; whereas no weight loss was observed at 450°C as shown in Table G-3. So, if ZnO is to be reduced to Zn, the reduction temperature used should be in between 450-660°C to assure the reduction of ZnO and to avoid volatilization of elemental zinc. The reduction of the ZnO sample verified earlier work of hydrogen reduction of zinc flue dusts where no reduction of ZnO was reported at 450°C. Furthermore, no weight correction due to the reduction of ZnO would be necessary if it is used as an additive in coal liquefaction under normal operating conditions.

The DTA of ZnO in the presence of air showed no significant features up to 550°C indicating the sample was thermally stable.

Copperas (Ferrous Sulfate) - The thermogram of copperas under an inert atmosphere is shown in Figure G-10. The sample started losing water of crystallization at around 40°C. The rate of water removal reached its maximum value at around

Table G-3

Reduction of Zinc Oxide in PTGR

Temp., °C	1000	450
H_2 Pressure, psig	1000	1000
Reaction Time, min.	10	10
Initial Weight, g	3.00	3.00
Final Weight, g	1.20	3.00
Weight Loss, g	1.80	0.00
Weight Loss, %	60.0	0.0

120°C, dropped substantially above 200°C, once again started to increase at about 500°C, and continued to do so with the increase in temperature. The water of crystallization present in the copperas (43.28%) was removed at 635°C. The sample lost more than 44% weight at and above 640°C. This additional loss of weight (in addition to water of crystallization) at the higher temperature was due to decomposition of $FeSO_4$ to sulfur dioxide, sulfur trioxide, basic iron sulfate ($Fe_2[SO_4]_3$), and other products.[2]

The thermogram of copperas under flowing hydrogen is shown in Figure G-11. The water of crystallization (43.28%) was removed at around 470°C, considerably lower than in the case of pyrolysis. The decomposition of $FeSO_4$ was apparently completed at around 520°C (insignificant change in weight above 520°C). The DTA of copperas run to 550°C in the presence of air showed endotherms that were due to the loss of water at around 75 and 130°C and exotherms that were due to decomposition and oxidation of $FeSO_4$ at 220°C (see Figure G-12). The sample, after cooling, was run again. Most of the endotherms and exotherms disappeared as shown in Figure G-12. Another sample was heated to just below 220°C to remove the water of crystallization and then cooled to room temperature. Again on heating to 200°C, most of the endotherm disappeared as shown in Figure G-13. All the water of crystallization was lost by 200°C without decomposing the material.

Terra Alba F&P Gypsum - The TGA of Terra Alba F&P gypsum ($CaSO_2.2H_2O$) in the presence of hydrogen and nitrogen is shown in Figure G-14. A sharp 19% initial weight loss was observed between 100 and 200°C in the presence of both gases. The weight loss is due to the loss of water of hydration. The combined water present in the gypsum was reported to be 19.8%. The observed weight loss of 19% corresponds well to the amount of combined water present in the sample. The sample lost water of hydration at a lower temperature in the presence of hydrogen than in the presence of nitrogen. The hydrogen reduction of gypsum

---

[2] Kirk - Othmer, Encyclopedia of Chemical Technology, Volume 12, Page 40, Second Edition, Interscience Publishers.

FIGURE G-11
TGA OF COPPERAS IN THE PRESENCE OF HYDROGEN GAS

HEATING RATE = 10°C/MIN.
FLOW RATE = 300 ML./MIN.
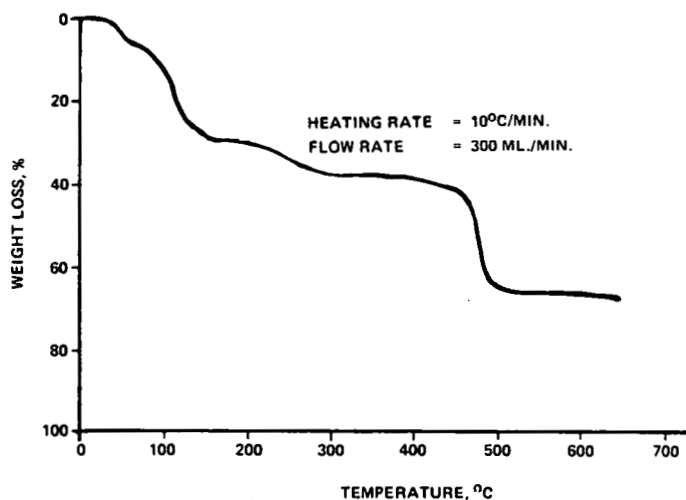
FIGURE G-12
DTA OF COPPERAS (FeSO$_4$ ·7H$_2$O) IN THE PRESENCE OF AIR

—— INITIAL RUN TO 540° C
- - - - RERUN OF SAME SAMPLE AFTER COOLING
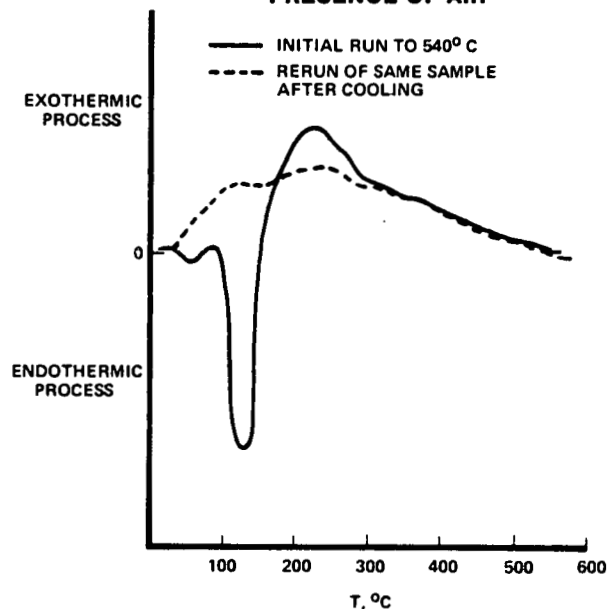
FIGURE G-13
DTA OF COPPERAS (FeSO$_4$ ·7H$_2$O) IN THE PRESENCE OF AIR

—— INITIAL RUN TO 190° C
- - - - RERUN AFTER COOLING
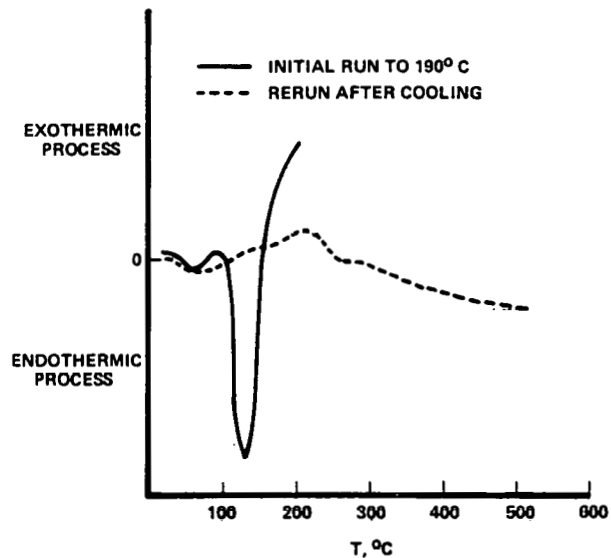
FIGURE G-14
TGA OF GYPSUM (TERRA ALBA F&P) IN THE PRESENCE OF HYDROGEN AND NITROGEN GASES

HEATING RATE = 20° C/MIN.
FLOW RATES:
N$_2$ = 25 ML./MIN.
H$_2$ = 300 ML./MIN.

—— N$_2$
- - - - H$_2$

365
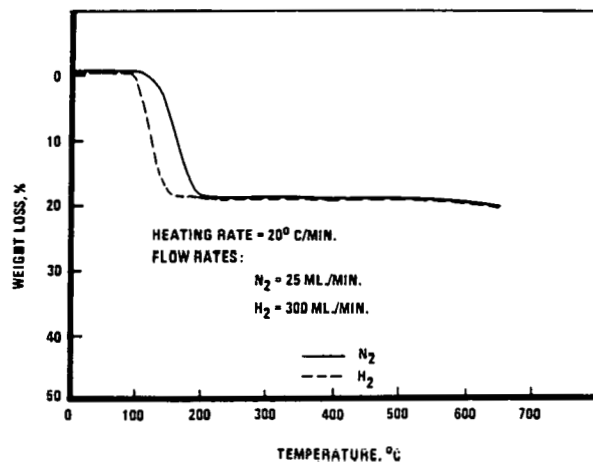
at high hydrogen pressure shown in Table G-1 also gave a weight loss of about 19%. A large portion of the weight loss is due to the removal of water of hydration and the balance due to the decomposition of gypsum.

The DTA of two different gypsums (Terra Alba F&P and Terra Alba #105) gave a large endotherm between 100 and 150°C (see Figures G-15 and G-16). The endotherm is due to the loss of water of hydration. The sample, after losing waters of hydration, was thermally stable in the presence of air up to 550°C.

Kaolinite (Burgess #10) - The sample was stable from room temperature to 300°C both in the presence of hydrogen and nitrogen. The sample lost approximately 13% weight at about 625°C in the presence of both gases, as shown in Figure G-17. The loss in weight is due to the loss of structural water from the clay matrix.

The kaolinite sample was reduced at high hydrogen pressure in the PTGR and the results are reported in the Table G-1. Negligible weight loss was observed at 450°C and 1000 psig hydrogen pressure. Kaolinite is chemically and thermally stable at typical coal liquefaction reaction conditions. The DTA of kaolinite in air is shown in Figure G-18. An endotherm observed around 400°C was very broad and continued beyond the temperature range used in the experiments. The endotherm is due to the loss of lightly bound water in the clay matrix.

Apatite (Monocalcium, Dicalcium, and Tricalcium Phosphate) - Endotherms were observed at around 270 to 290°C due to the loss of water of hydration and condensation of the hydroxyl groups into the oxide (see Figures G-19 to G-20). The monocalcium phosphate showed this process most clearly, whereas the latter process dominated in the dicalcium phosphate. The tricalcium phosphate has no hydroxyl group to lose, hence no endotherms appeared in the DTA trace at the indicated temperature. There is some indication of loss of moisture around 200°C.

The hydrogen reduction results of apatite are shown in Table G-1. The weight loss ranging from two to ten percent was due to the loss of water of hydration. The apatite by itself is insensitive to hydrogen reduction at 450°C.

FIGURE G-15
DTA OF TERRA ALBA F&P GYPSUM
IN THE PRESENCE OF AIR

HEATING RATE = 20° C/MIN.

EXOTHERMIC
PROCESS

0

ENDOTHERMIC
PROCESS

100   200   300   400   500   600

TEMPERATURE, °C
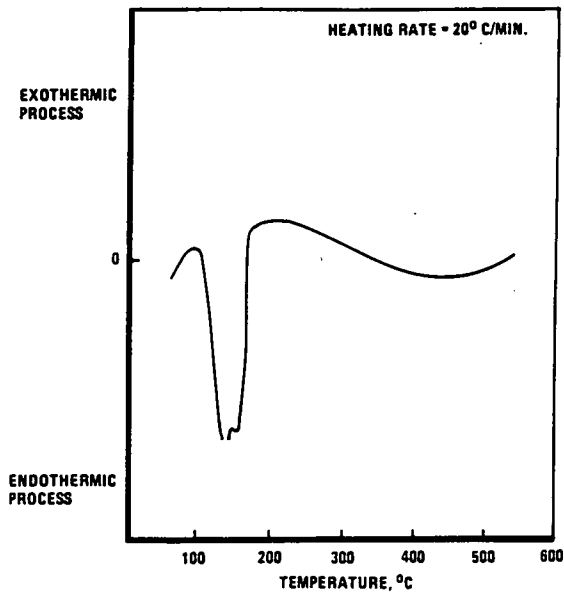
FIGURE G-16
DTA OF TERRA ALBA #105 GYPSUM
IN THE PRESENCE OF AIR

HEATING RATE = 20° C/MIN.

EXOTHERMIC
PROCESS

0

ENDOTHERMIC
PROCESS

100   200   300   400   500   600

TEMPERATURE, °C
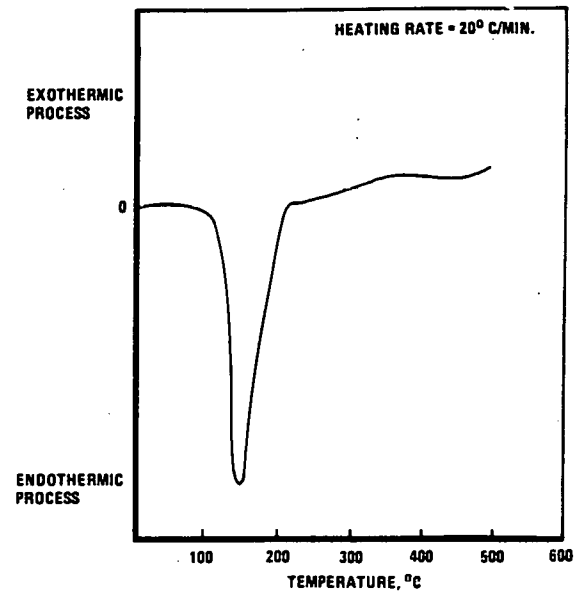
FIGURE G-17
TGA OF KAOLINITE (BURGESS #10) IN THE
PRESENCE OF HYDROGEN AND NITROGEN GASES

0

HEATING RATE = 20° C/MIN.

FLOW RATES:

N_2 = 25 ML./MIN.

H_2 = 300 ML./MIN.

10

20

30

40

50

WEIGHT LOSS, %

—— N_2
---- H_2

0   100   200   300   400   500   600   700

TEMPERATURE, °C
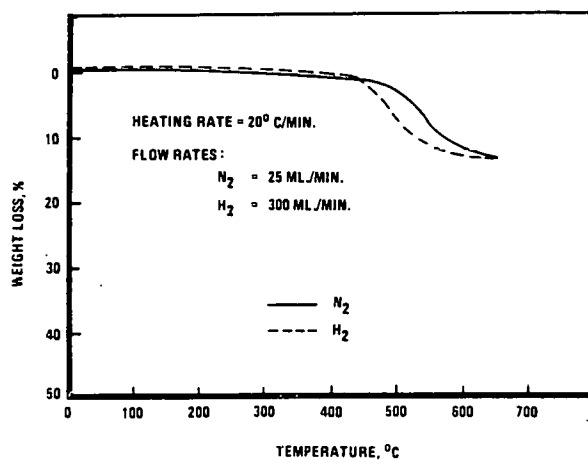
FIGURE G-18
DTA OF KAOLINITE (BURGESS #10)
IN THE PRESENCE OF AIR

HEATING RATE = 20° C/MIN.

---- EXTRAPOLATED

EXOTHERMIC
PROCESS

0

ENDOTHERMIC
PROCESS

100   200   300   400   500   600

TEMPERATURE, °C

367
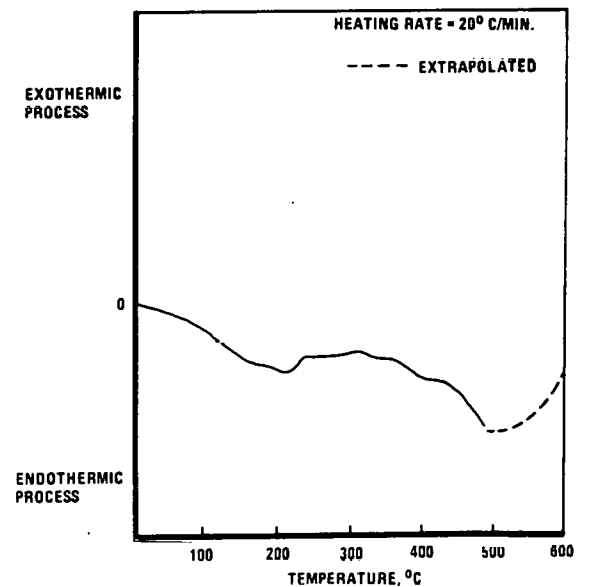
FIGURE G-19
DTA OF APATITE (MONOCALCIUM PHOSPHATE) IN THE PRESENCE OF AIR
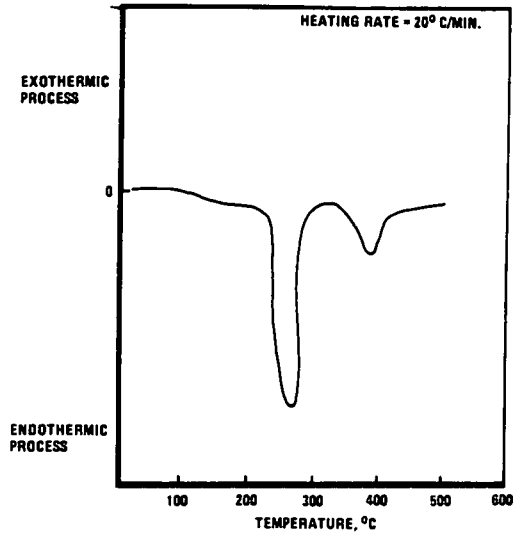
FIGURE G-20
DTA OF APATITE (DICALCIUM PHOSPHATE) IN THE PRESENCE OF AIR
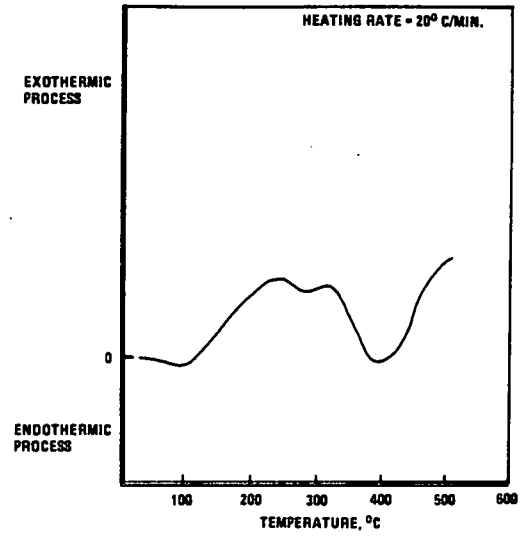
FIGURE G-21
DTA OF APATITE (TRICALCIUM PHOSPHATE) IN THE PRESENCE OF AIR
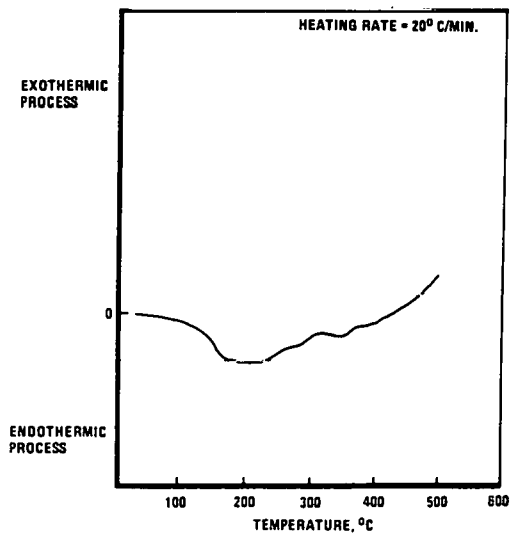
FIGURE G-22
DTA OF RUTILE IN THE PRESENCE OF AIR

368
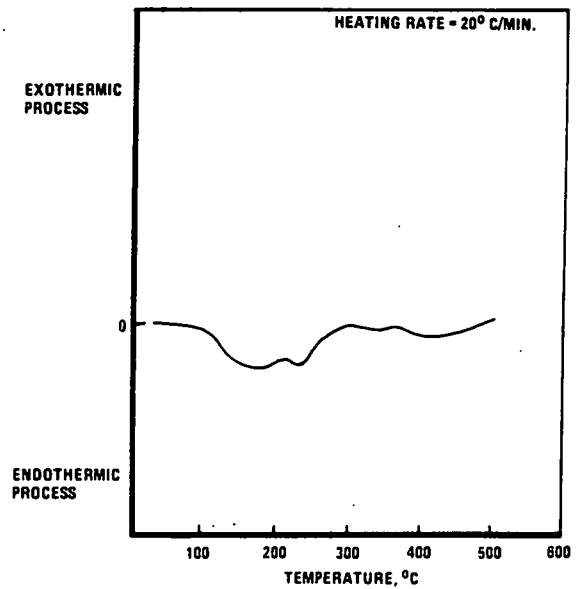
Montmorillonite - Three different samples of montmorillonite were hydrogen reduced at 450°C and 1000 psig pressure. The samples showed weight losses ranging from two to ten percent. The weight loss was mainly due to the removal of water from the samples. Water was the major compound determined in the gas product as reported in Table G-1. The montmorillonite by itself was insensitive to hydrogen reduction at 450°C.

Zircon and Quartz - No thermal activity was observed in the presence of air up to 500°C. The materials were also insensitive to hydrogen treatment at 450°C in the PTGR.

Calcite - The DTA of calcite gave no endothermic or exothermic activities. Also, no reduction of the sample was observed in the PTGR at 1000 psig hydrogen pressure and 450°C, as shown in Table G-1.

Rutile - There were no major features in the DTA of rutile in the presence of air. The small endotherms between 150 to 225°C (Figure G-22) were due to the loss of water adsorbed on the surface of the mineral. The sample was insensitive to hydrogen reduction at 450°C.

Ilmenite - No sharp features were observed in the DTA of ilmenite in air. A broad endotherm around 400°C, as shown in Figure G-23, was due to impurities present in the mineral. The sample was insensitive to hydrogen at 450°C.

Feldspar (NC4) - No major features in the DTA in air (see Figure G-24) were observed. The material was also found to be insensitive to hydrogen reduction at high pressure in the PTGR (see Table G-1).

Illite - Small exotherms were observed in the DTA of illite in the presence of air, as shown in Figure G-25. The exotherms are due to the oxidation of inorganic and iron constituents of the mineral. The sample was insensitive to hydrogen at 450°C.

Chrome Ore Concentrate - The DTA of chrome ore concentrate in the presence of air showed no significant activity over the temperature range used in this study (Figure G-26). The material was insensitive to hydrogen treatment at 450°C in the PTGR (Table G-1).

FIGURE G-23
DTA OF ILMENITE IN THE PRESENCE OF AIR
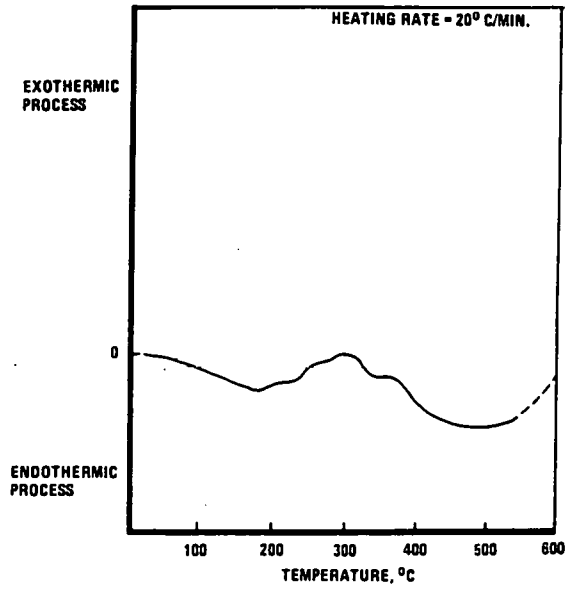
FIGURE G-24
DTA OF FELDSPAR (NC4) IN THE PRESENCE OF AIR
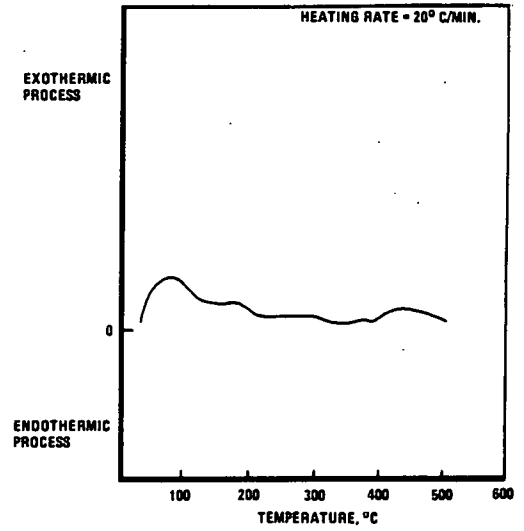
FIGURE G-25
DTA OF ILLITE IN THE PRESENCE OF AIR
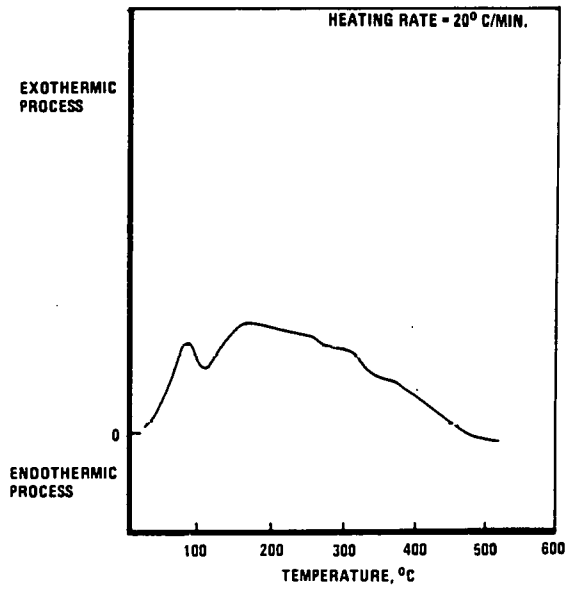
FIGURE G-26
DTA OF CHROME ORE CONCENTRATE IN THE PRESENCE OF AIR

370
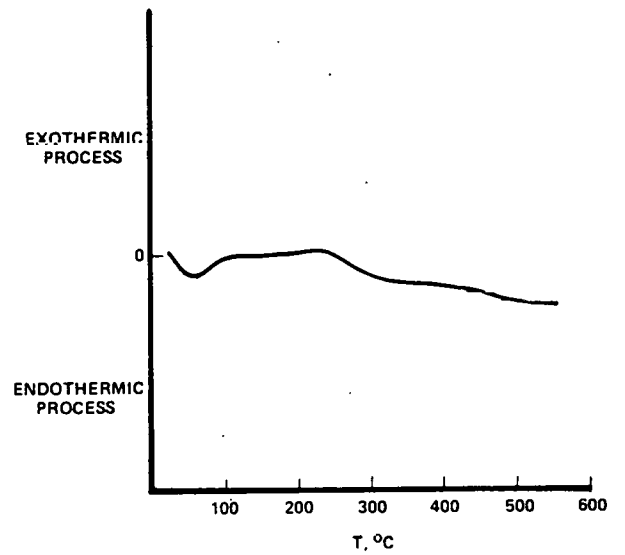
Quick Lime - Quick lime in the presence of air showed no apparent thermal activity up to 550°C. Under hydrogen pressure quick lime did not reduce at 450°C as shown in Table G-1.

Molybdic Oxide - No thermal activity was observed in the presence of air up to 600°C as shown in Figure G-27. Molybdie oxide lost 9% weight when treated in the PTGR, which was mainly due to the reduction of metal oxide.

Mordenite and Chabozite - The thermograms of mordenite and chabozite showed no thermal activity in the presence of air.

X-Type Molecular Sieve - The thermogram of X-type molecular sieve showed a broad and pronounced endotherm starting at room temperature and continuing to about 350°C (see Figure G-28). The endotherm was due to the loss of adsorbed water.

Flue Dust - Ni-Mo-Fe containing flue dust sample showed a broad exotherm in the presence of air (Figure G-29). The exotherm was due to oxidation of various metals present in the sample. The hydrogen reduction of flue dust showed a weight loss of seven percent at 450°C and 1000 psig pressure. The major weight loss was due to the reduction of some of the metal oxides to their corresponding reduced states. The results of hydrogen reduction of flue dust are tablulated in Table G-1.

Bornite - The hydrogen reduction of bornite, shown in Table G-1, gave a six percent weight loss. The weight is mainly due to the reduction of oxides to their corresponding reduced form.

Super Alloy and Alnico Grindings - The DTA's in air of super alloy and Alnico grindings are shown in Figures G-30 and G-31. The samples showed a definite exotherm due to the oxidation of the metals. Since the oxidation is a surface process, the broad peaks are due to a lack of rapid oxygen transfer below the surface. The hydrogen reduction of the above two grindings at 450°C and 1000 psig was conducted in the PTGR. The samples were found to be insensitive to hydrogen reduction as shown in Table G-1. This is due to the presence of metals in the samples in the reduced form.

FIGURE G-27
DTA OF MOLYBDIC OXIDE IN THE
PRESENCE OF AIR

EXOTHERMIC
PROCESS

0

ENDOTHERMIC
PROCESS

100   200   300   400   500   600

T, °C
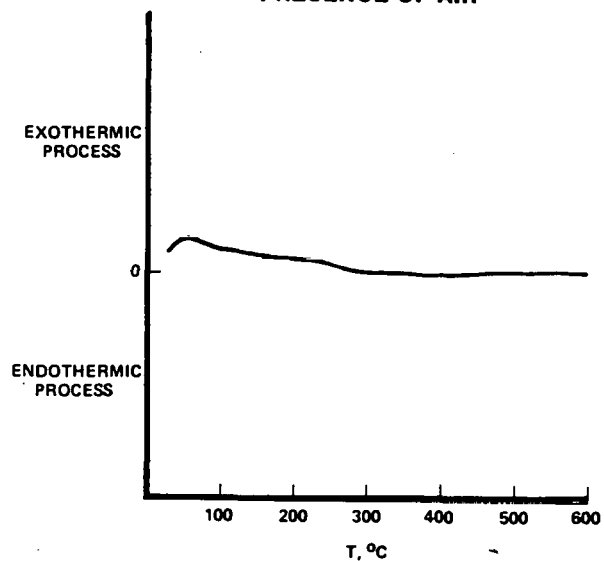
FIGURE G-28
DTA OF X-TYPE MOLECULAR SIEVE
IN THE PRESENCE OF AIR

EXOTHERMIC
PROCESS

0

ENDOTHERMIC
PROCESS

100   200   300   400   500   600

T, °C
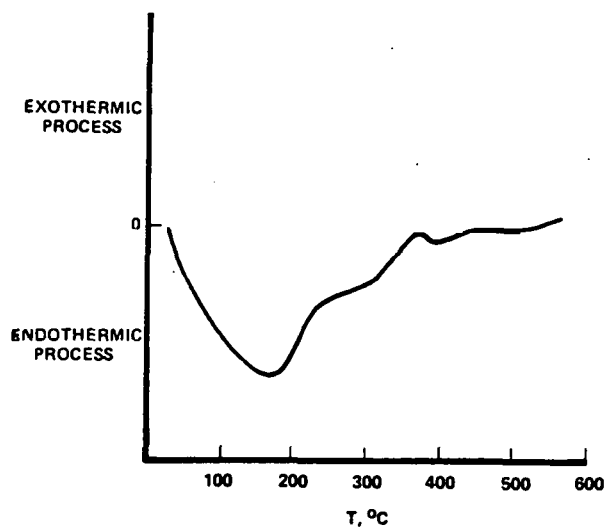
FIGURE G-29
DTA OF FLUE DUST IN THE PRESENCE OF AIR

EXOTHERMIC
PROCESS

0

ENDOTHERMIC
PROCESS

100   200   300   400   500   600

T, °C
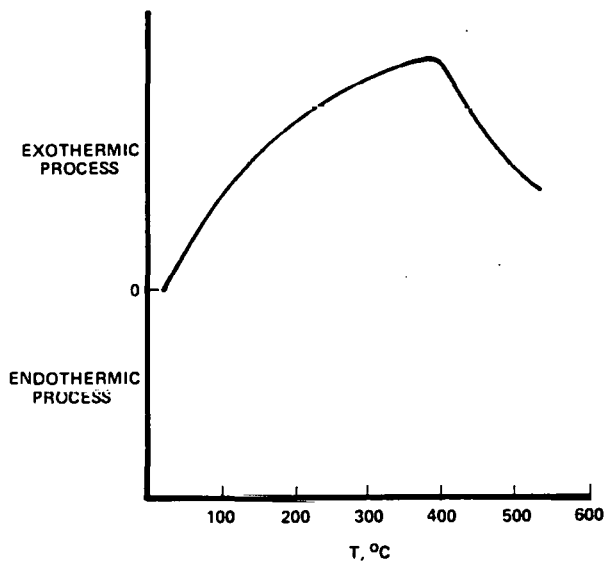
FIGURE G-30
DTA OF SUPER ALLOY GRINDINGS
IN THE PRESENCE OF AIR

EXOTHERMIC
PROCESS

0

ENDOTHERMIC
PROCESS

100   200   300   400   500   600

T, °C

372
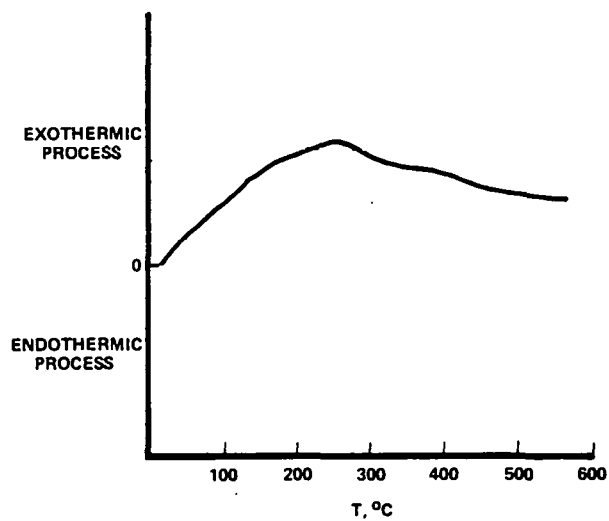
Sphalerite (ZnS) - The TGA of sphalerite under flowing hydrogen and nitrogen gases is shown in Figure G-32. The material was insensitive to thermal treatment (nitrogen) as well as chemical reaction to hydrogen at temperatures up to 600°C. No reaction was noted when the material was heated with hydrogen at 450°C and 1000 psig (Table G-1).

Red Mud - The TGA of red mud under nitrogen (Figure G-33) showed a weight loss of 12% at 700°C. This was due to the loss of volatile material present in the sample. The weight loss of 27% at 650°C in the presence of hydrogen gas was due to the reduction of various oxides that were present in the sample in their respective elemental form. A weight loss of 13% was noted at 450°C in the PTGR (see Table G-1) which matched a corresponding weight loss of 14.5% at 450°C in the TGA. This weight loss under process conditions can have a significant affect on the reaction conditions under continuous flow operation. Since most of the product obtained by hydrogen reduction is water, if this moisture passes through the reaction system, it can severely reduce the hydrogen partial pressure in the system.

Other Materials - Dolomite was insensitive to hydrogen treatment at 450°C in the PTGR (see Table G-1). No weight correction would be required when testing it for its catalytic activity in coal liquefaction. Phosphate slime lost 11% weight which was mainly due to the reduction of metal oxides present in the sample. Oil shale gave 5% weight reduction mainly due to the loss of volatiles.

Fly Ashes
Green River (blend) Fly Ash - This sample was obtained from the Green River power plant located at Moorman, Muhlenberg Co., Kentucky. It was taken when burning a "blend" of two W. Kentucky coals in the power plant. The DTA of the sample in the presence of helium showed no thermal activity (Figure G-34), whereas in the presence of air an exotherm occurred around 587°C (Figure G-35). The exotherm is due to the oxidation of some of the compounds present in the fly ash. Figure G-36 shows the thermograms of Green River (blend) fly ash under flowing helium and hydrogen gases. The fly ash was found to be thermally stable under inert atmosphere (helium); whereas it started losing weight at around 300°C under flowing hydrogen. The weight loss at 600°C was observed to be 6.2%.

FIGURE G-31
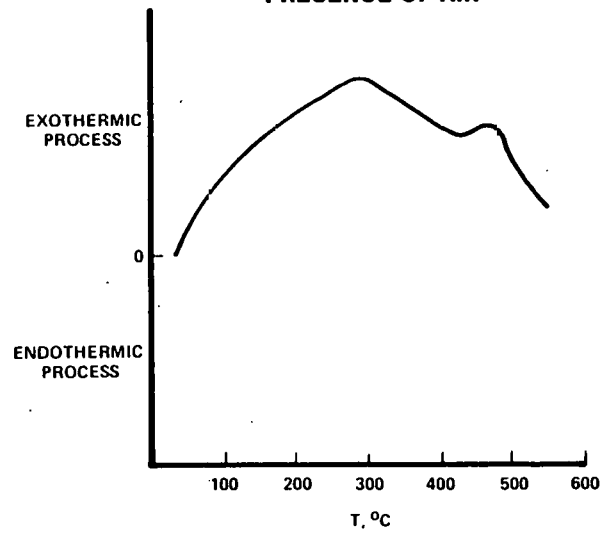DTA OF ALNICO GRINDINGS IN THE
PRESENCE OF AIR

FIGURE G-32
TGA OF SPHALERITE (ZnS) IN THE PRESENCE OF
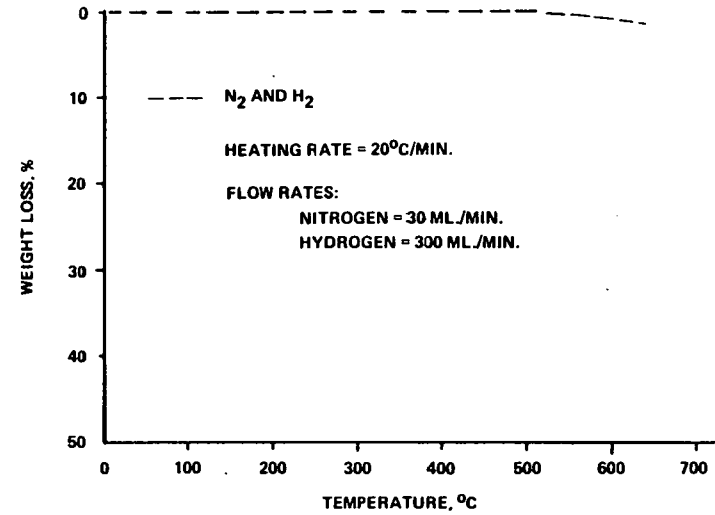HYDROGEN AND NITROGEN GASES

FIGURE G-33
TGA OF RED MUD IN THE PRESENCE OF HYDROGEN
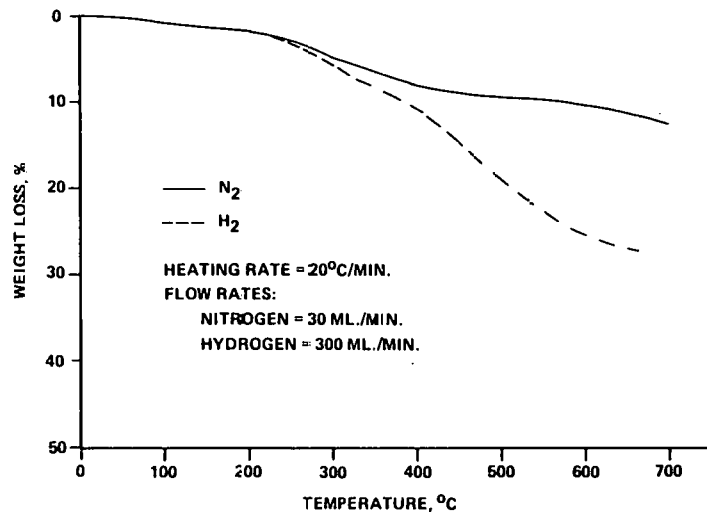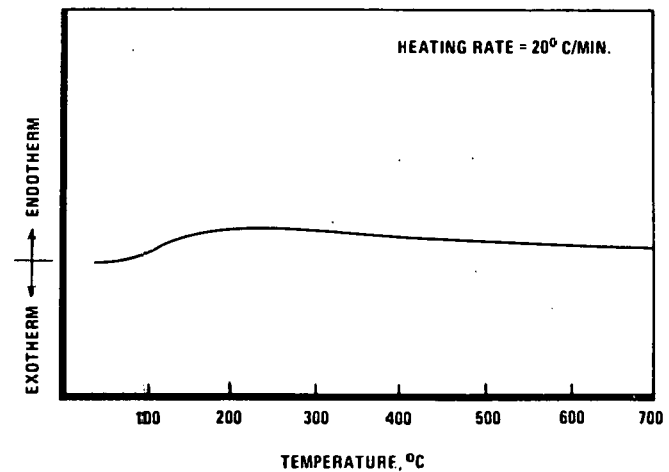AND NITROGEN GASES

FIGURE G-34
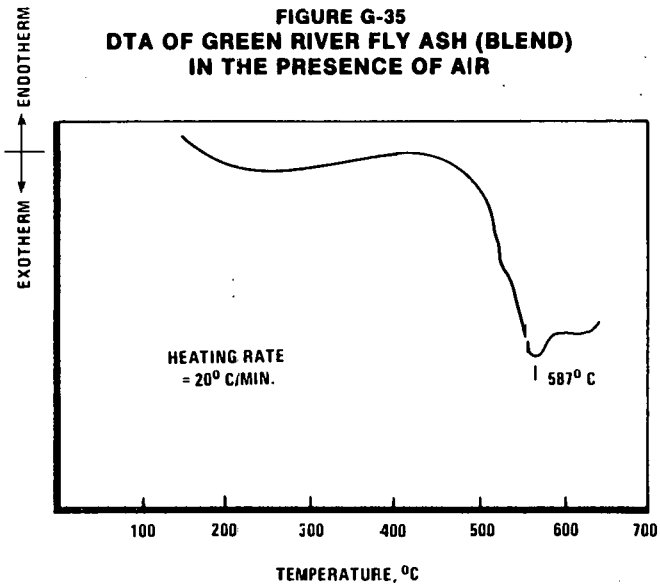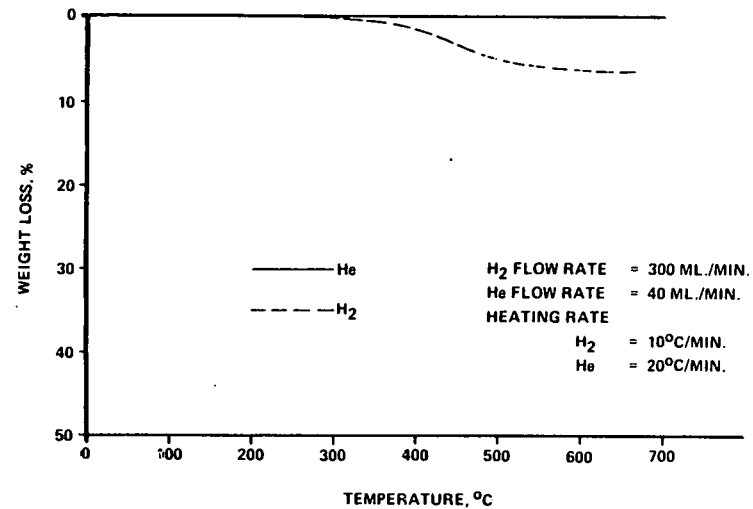DTA OF GREEN RIVER FLY ASH (BLEND)
IN THE PRESENCE OF HELIUM

374

FIGURE G-35
DTA OF GREEN RIVER FLY ASH (BLEND)
IN THE PRESENCE OF AIR

HEATING RATE
= 20° C/MIN.

587° C

FIGURE G-36
TGA OF GREEN RIVER (BLEND) FLY ASH IN THE PRESENCE
OF HELIUM AND HYDROGEN GASES

He

H₂

H_2 FLOW RATE = 300 ML./MIN.
He FLOW RATE = 40 ML./MIN.
HEATING RATE
H_2 = 10°C/MIN.
He = 20°C/MIN.

FIGURE G-37
DTA OF GREEN RIVER FLY ASH (HIGH)
IN THE PRESENCE OF HELIUM

HEATING RATE = 20° C/MIN.
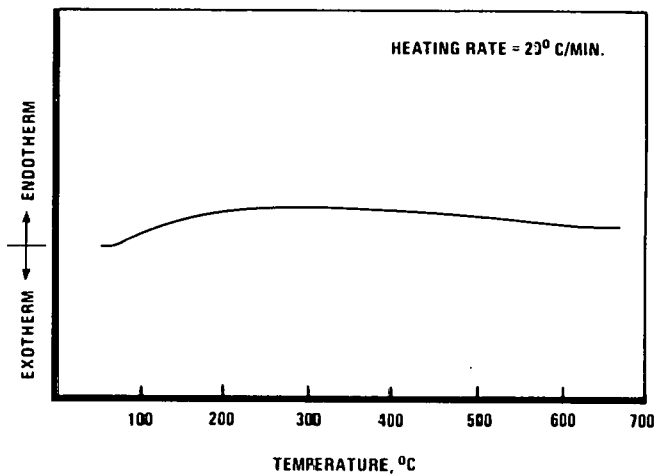
FIGURE G-38
DTA OF GREEN RIVER FLY ASH (HIGH) IN THE
PRESENCE OF AIR

HEATING RATE = 20° C/MIN.

630° C

375
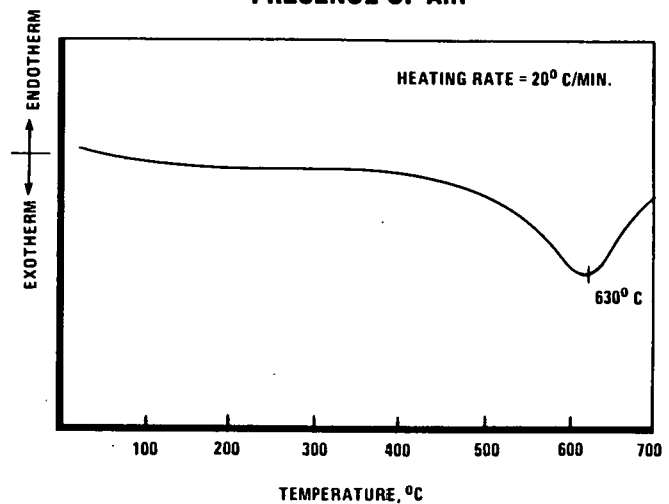
Green River (high) Fly Ash - This sample was also obtained from the Green River power plant. It was taken when burning "high" sulfur W. Kentucky coal in the power plant. The DTA's of Green River (high) Fly Ash were found to be similar to that of the blend except for an exotherm at 630°C instead of 587°C. The DTA's are shown in Figures G-37 and G-38. The Green River (high) ash lost weight at approximately 350°C, both under flowing helium and hydrogen gases (see Figure G-39). The weight losses under flowing helium and hydrogen gases at 600°C were observed to be 1.0 and 3.0%, respectively.

Brown Fly Ash - The fly ash sample was obtained from the E. W. Brown power plant located at Burgin, Mercer Co., Kentucky. The sample was taken when burning E. Kentucky coal in the power plant. The DTA in the presence of helium showed no thermal activity (Figure G-40). The DTA in the presence of air showed an exotherm at 660°C due to the oxidation of the material (Figure G-41). The thermograms for Brown fly ash under flowing helium and hydrogen gases are shown in Figure G-42. The fly ash lost weight at approximately 300°C both in helium and hydrogen gases. The weight losses under flowing helium and hydrogen gases at 600°C were found to be 1.0 and 2.3%, respectively.

Paradise Fly Ash - The fly ash sample was obtained from the Paradise power plant located at Paradise, Muhlenberg Co., Kentucky. The sample was taken when burning E. Kentucky coal. The DTA of Paradise Fly Ash in the presence of helium showed one minor endotherm at approximately 110°C due to the loss of moisture from the sample, whereas in the presence of air a minor exotherm at 631°C was observed due to the oxidation of the sample. The DTA's are shown in Figures G-43 and G-44. The Paradise fly ash began losing weight at approximately 250°C both under flowing helium and hydrogen gases (Figure G-45). The total weight losses under flowing helium and hydrogen gases at 600°C were 2.0 and 7.3%, respectively.

The results from the reduction of the above fly ashes, conducted at high pressure (1000 psig hydrogen) in the PTGR, are summarized in Table G-4. The weight loss was insignificant for all the samples with the maximum weight loss being only 4%. Water, the major product of the reduction, was trapped in the dry ice trap but was not analyzed due to the small sample size. These observations suggest that the fly ashes are not very sensitive to hydrogen reduction.

FIGURE G-39
TGA OF GREEN RIVER (HIGH) FLY ASH IN THE PRESENCE
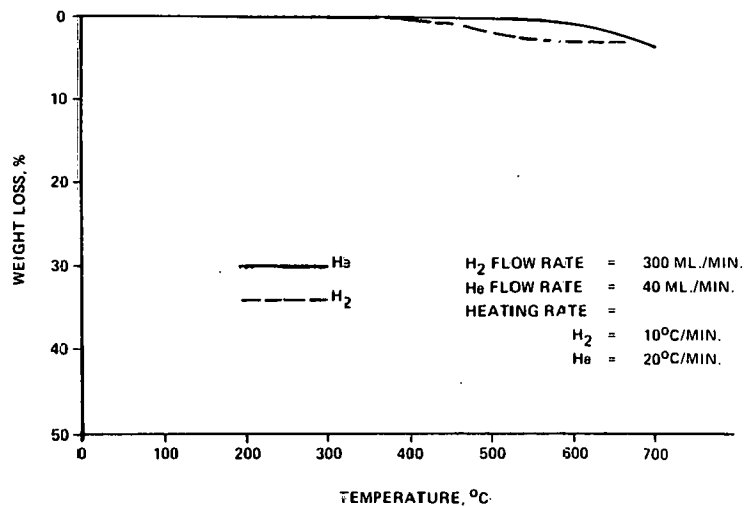OF HELIUM AND HYDROGEN GASES

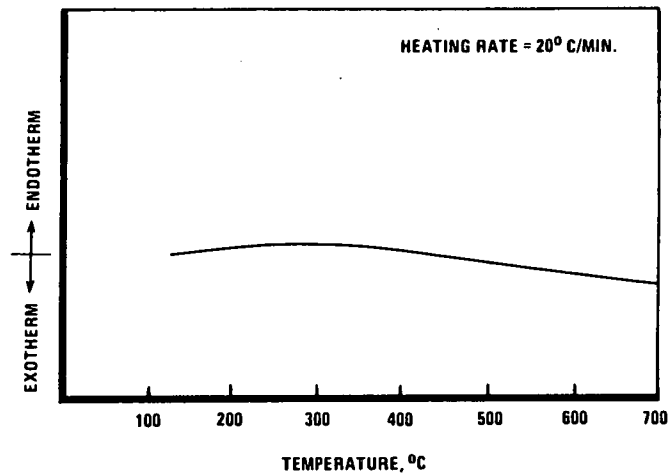FIGURE G-40
DTA OF BROWN FLY ASH IN THE PRESENCE OF HELIUM

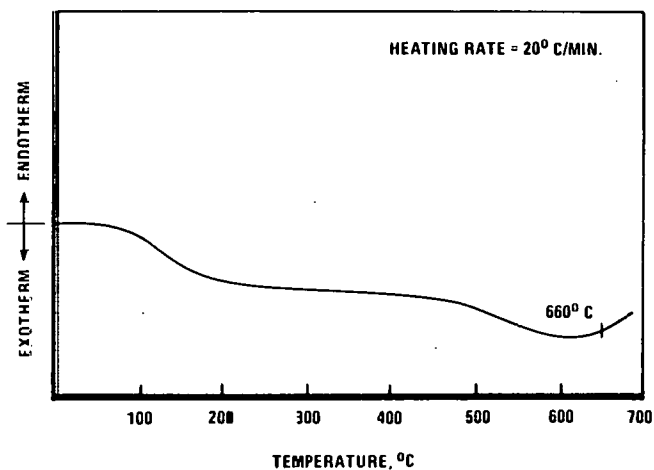FIGURE G-41
DTA OF BROWN FLY ASH IN THE PRESENCE OF AIR

FIGURE G-42
TGA OF BROWN FLY ASH IN THE PRESENCE
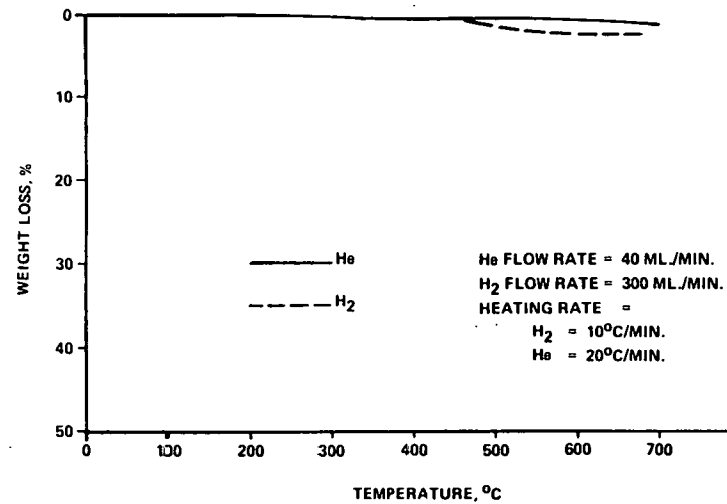OF HELIUM AND HYDROGEN GASES

377

TABLE G-4

Reduction of Fly Ashes in the PTGR

Sample	Initial Weight, g	Final Weight, g	Weight Loss, g	Weight Loss, %	Gas Analyses, g N2	Gas Analyses, g H20	Total Recovered Product, g	Recovery of Lost wt.%
Brown Fly Ash	3.00	3.00	0.0	0.0	--	--	--	--
Paradise Fly Ash	3.00	2.88	0.12	4.0	0.0040	0.0400	0.044	37.0
Green River Fly Ash								
Blend	3.0	2.91	0.09	3.0	0.0030	0.0350	0.038	42.0
High	3.00	2.92	0.08	2.7	0.0036	0.0355	0.040	50.0

Reaction Time = 10 Minutes, Temp. = 450°C

Pressure = 1000 psig H_2

FIGURE G-43
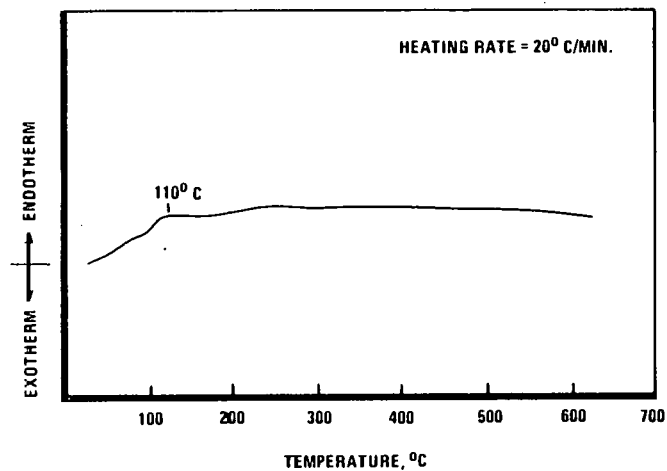DTA OF PARADISE FLY ASH IN THE PRESENCE OF HELIUM

FIGURE G-44
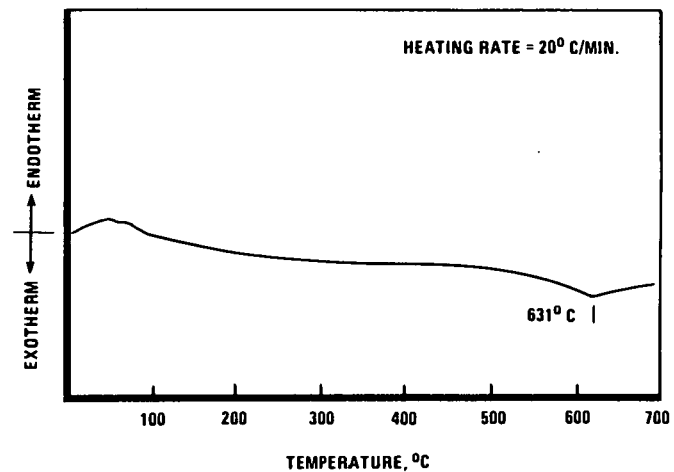DTA OF PARADISE FLY ASH IN THE PRESENCE OF AIR

FIGURE G-45
TGA OF PARADISE FLY ASH IN THE PRESENCE
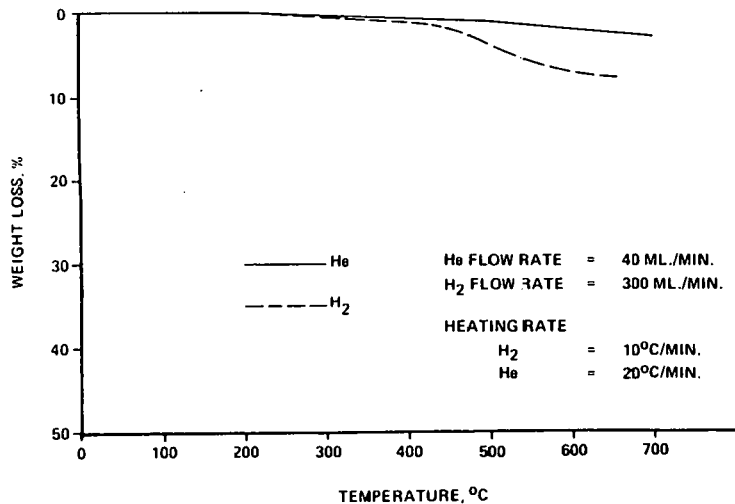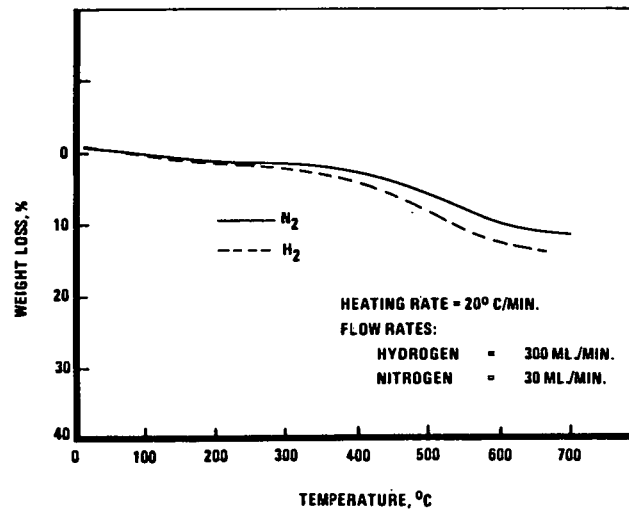OF HELIUM AND HYDROGEN GASES

FIGURE G-46
TGA OF GREEN RIVER BOTTOM ASH IN THE PRESENCE
OF HYDROGEN AND NITROGEN GASES

379

Bottom Ashes

Green River Bottom Ash - The bottom ash sample was obtained from the Green River power plant located at Moorman, Muhlenberg Co., Kentucky. The TGA of the sample in the presence of hydrogen and nitrogen is shown in Figure G-46. The sample began losing weight at approximately 100°C and continued to lose weight up to 700°C. The sample appeared to contain some volatiles because it lost approximately 11% weight by the time it reached 700°C in the presence of nitrogen. The weight loss was even greater in the presence of hydrogen because of reduction in addition to pyrolysis. The sample was analyzed by DTA in the presence of air to determine combustible material in the sample. The sample gave a strong exotherm at around 400°C (see Figure G-47), which verified the presence of volatile/combustible materials in the sample.

Paradise Bottom Ash - The sample was obtained from the Paradise power plant located at Paradise, Muhlenberg Co., Kentucky. The TGA of Paradise Bottom Ash showed no weight loss either in the presence of hydrogen or nitrogen, as shown in Figure G-48. The DTA of the sample in the presence of air, Figure G-49, showed a broad exotherm over much of the temperature range, due to the oxidation of various sample components.

Brown Bottom Ash - The bottom ash sample was obtained from the E. W. Brown power plant located at Burgin, Mercer Co., Kentucky. The sample lost approximately 2 and 5% weight at 600°C in the presence of nitrogen and hydrogen, respectively. The sample began losing weight at around 450°C in the presence of nitrogen and at 200°C in the presence of hydrogen, as shown in Figure G-50. The higher loss in weight in the presence of hydrogen as opposed to nitrogen is due to reduction of the sample in addition to pyrolysis. The DTA of the sample in air (Figure G-51), showed one broad exotherm in the range 100 to 300°C and one sharp exotherm at around 440°C. The sharp exotherm is due to the oxidation of the organic material present in the sample.

The hydrogen reduction of bottom ashes was conducted in the PTGR. The samples lost weight ranging from one to 14% as presented in Table G-5. The major compounds found in the gas phase were methane and water. Brown and Paradise bottom ashes lost insignificant weight (maximum of three percent); whereas Green River bottom ash lost approximately 14% weight. These observations suggest that Green River bottom ash is more hydrogen sensitive than Brown and Paradise bottom ashes.

FIGURE G-47
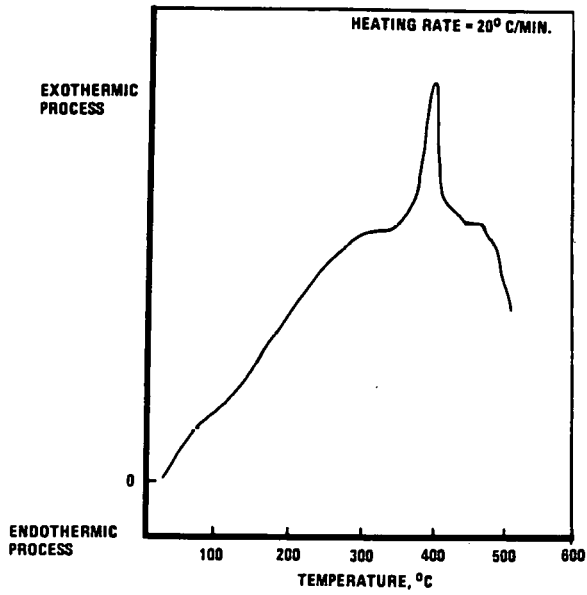**DTA OF GREEN RIVER BOTTOM ASH
IN THE PRESENCE OF AIR**

HEATING RATE = 20° C/MIN.

EXOTHERMIC PROCESS

ENDOTHERMIC PROCESS

TEMPERATURE, °C

FIGURE G-48
**TGA OF PARADISE BOTTOM ASH IN THE PRESENCE
OF HYDROGEN AND NITROGEN GASES**

WEIGHT LOSS, %

N_2
H_2

HEATING RATE = 20° C/MIN.
FLOW RATES:
   HYDROGEN   = 300 ML./MIN.
   NITROGEN   = 30 ML./MIN.

TEMPERATURE, °C
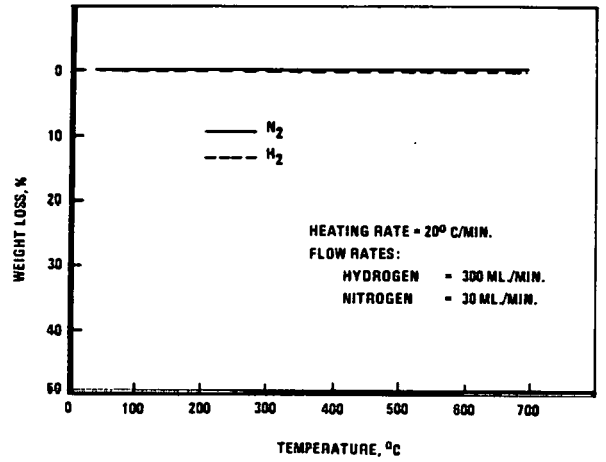
FIGURE G-49
**DTA OF PARADISE BOTTOM ASH IN THE
PRESENCE OF AIR**

HEATING RATE = 20° C/MIN.

EXOTHERMIC PROCESS

ENDOTHERMIC PROCESS

TEMPERATURE, °C
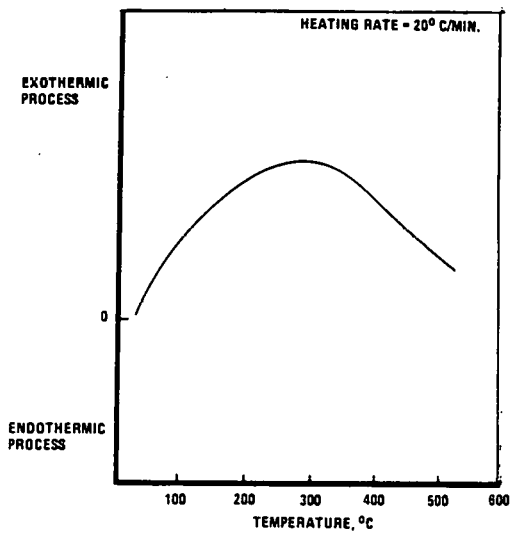
FIGURE G-50
**TGA OF BROWN BOTTOM ASH IN THE PRESENCE
OF HYDROGEN AND NITROGEN GASES**

WEIGHT LOSS, %

N_2 GAS
H_2 GAS

HEATING RATE   = 20° C/MIN.
FLOW RATES:
   NITROGEN = 30 ML./MIN.
   HYDROGEN = 300 ML./MIN.

TEMPERATURE, °C

381
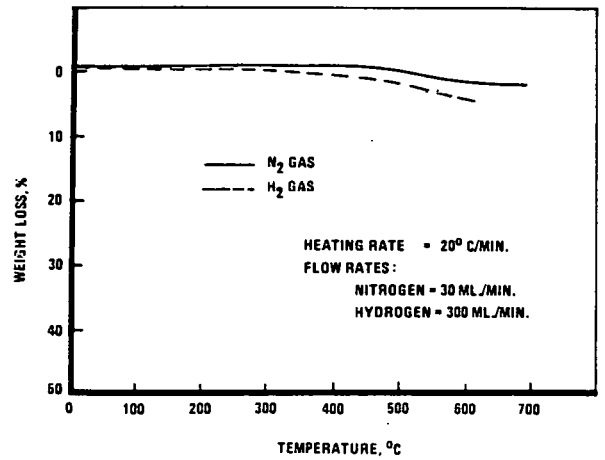
TABLE G-5

Reduction of Bottom Ashes in the PTGR

Sample	Initial Weight, g	Final Weight, g	Weight Loss, g	Weight Loss, %	Gas Analyses, g N2	Gas Analyses, g CH4	Gas Analyses, g H2O	Total Recovered Product, g	Recovery of Lost Wt.
Brown Fly Ash	3.00	2.92	0.02	2.7	0.0031	0.0032	0.0426	0.0489	61
Paradise Bottom Ash	3.00	2.96	0.04	1.3	--	--	--	--	0
Green River Bottom Ash	3.00	2.58	0.42	14.0	0.0043	0.0078	0.0519	0.0640	15

Reaction Time = 10 Minutes, Temp. = 450°C

Pressure = 1000 psig H_2

Coal Preparation Plant Waste Materials - The TGA of the various coal preparation plant waste materials studied in the presence of hydrogen and nitrogen are shown in Figures G-52 to G-59. These materials show very similar thermograms with weight losses varying between 16 and 32% of the initial weight. The weight loss is due to volatile organic matter (coal) present in the samples, and the variation in weight loss is due to the different amounts of organic material present in the samples.

The DTA's of the coal preparation plant waste materials in the presence of air are shown in Figures G-60 to G-65. All these samples show very similar thermograms, with two exothermic peaks, both quite broad and in the temperature range of 325 to 450°C. The exotherms are due to the oxidation of the carbonacious material present in the samples. The DTA of the Colonial/P&M coal preparation plant waste material was repeated to check the reproducibility and is shown in Figure G-65. After the DTA analysis the sample was left in the instrument, cooled down to room temperature, and again analyzed in the presence of air for its thermal activities. On the second pass, the sample was essentially inert (Figure G-65). Once the carbonacious material was oxidized, the oxidized product showed no more thermal activity in the presence of air.

The TGA of the various coal preparation plant waste materials were studied in the presence of air. The samples showed a weight loss ranging from 35 to 68% as shown in Figures G-66 and G-67. The weight loss was primarily due to the oxidation of the organic material present in the samples. The purpose of this study was to determine the oxidation temperature required to remove the organic phase and the weight percent ash present in the samples. The temperature required for complete oxidation was observed to be greater than 500°C.

Pyrite-Magnetite Mixture - The possibility of generating reduced pyrite by reacting a mixture of pyrite and magnetite simultaneously was examined in the PTGR. The individual and coupled reactions of hydrogen reduction of pyrite-magnetite are given by equations G-2 to G-4.

FIGURE G-51
DTA OF BROWN BOTTOM ASH IN THE PRESENCE OF AIR
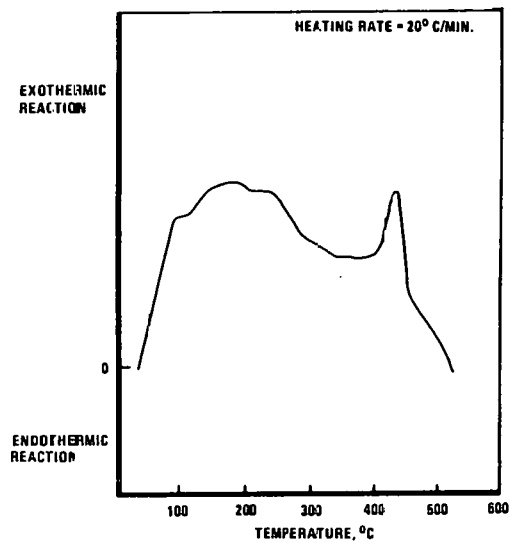
FIGURE G-52
TGA OF HENDRIX/BETH - ELKHORN COAL PREPARATION PLANT WASTE MATERIAL IN THE PRESENCE OF HYDROGEN AND NITROGEN GASES
(SAMPLE NO. BEH-P-C)

FIGURE G-53
TGA OF GUND/ISLAND CREEK COAL PREPARATION PLANT WASTE MATERIAL IN THE PRESENCE OF HYDROGEN GAS
(SAMPLE NO. ICG-P-C)

FIGURE G-54
TGA OF GUND/ISLAND CREEK COAL PREPARATION PLANT WASTE MATERIAL IN THE PRESENCE OF HYDROGEN AND NITROGEN GASES
(SAMPLE NO. ICG-P-F)
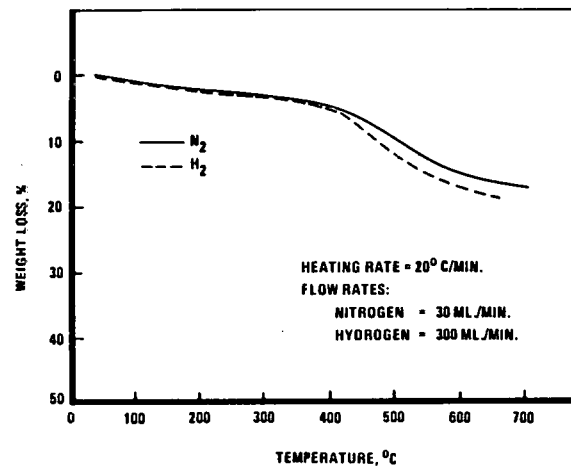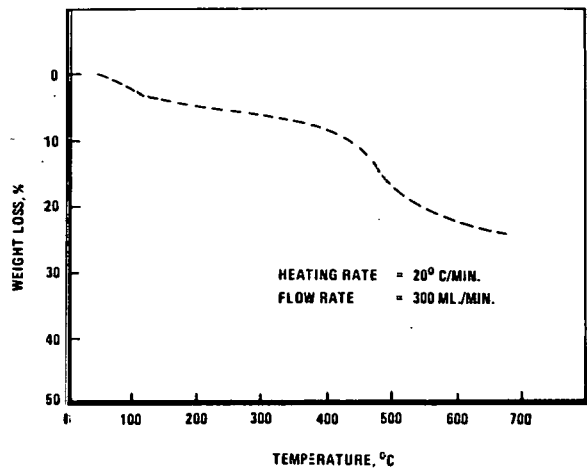

384

FIGURE G-55
TGA OF SPURLOCK/ISLAND CREEK COAL PREPARATION PLANT WASTE MATERIAL IN THE PRESENCE OF HYDROGEN AND NITROGEN GASES (SAMPLE NO. ICS-P-C)

HEATING RATE = 20° C/MIN.
FLOW RATES:
NITROGEN = 30 ML./MIN.
HYDROGEN = 300 ML./MIN.

FIGURE G-56
TGA OF GILBRATOR/AMAX COAL PREPARATION PLANT WASTE MATERIAL IN THE PRESENCE OF NITROGEN AND HYDROGEN GASES (SAMPLE NO. AG-P-M)

HEATING RATE = 20° C/MIN.
FLOW RATES:
NITROGEN = 30 ML./MIN.
HYDROGEN = 300 ML./MIN.
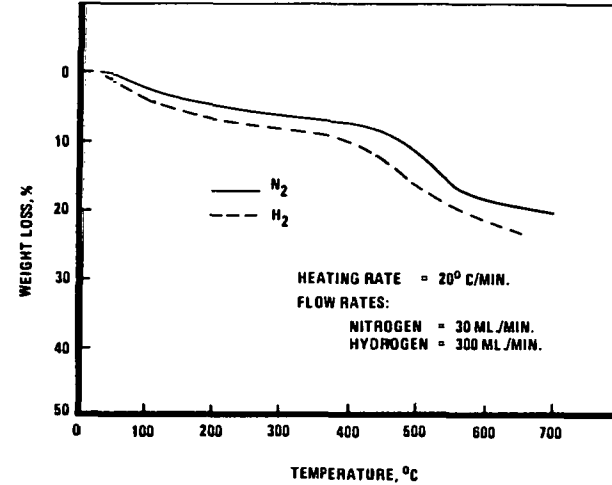
FIGURE G-57
TGA OF FIES/ISLAND CREEK COAL PREPARATION PLANT WASTE MATERIAL IN THE PRESENCE OF HYDROGEN AND NITROGEN GASES (SAMPLE NO. ICF-P-CM)

HEATING RATE = 20° C/MIN.
FLOW RATES:
NITROGEN = 30 ML./MIN.
HYDROGEN = 300 ML./MIN.
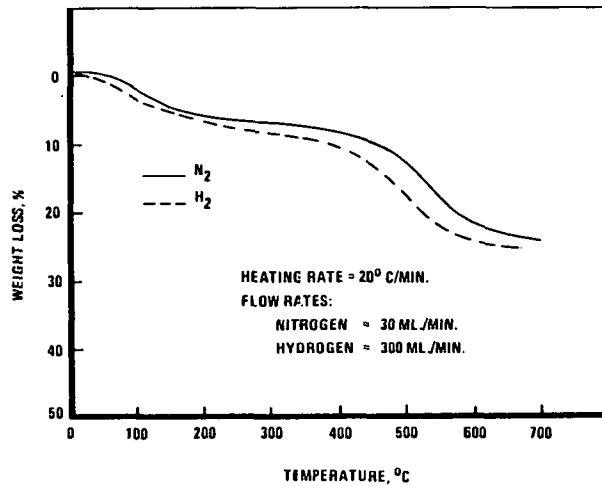
FIGURE G-58
TGA OF HAMILTON #1/ISLAND CREEK COAL PREPARATION PLANT WASTE MATERIAL IN THE PRESENCE OF HYDROGEN AND NITROGEN GASES (SAMPLE NO. ICH1-P-CM)

HEATING RATE = 20° C/MIN.
FLOW RATE:
HYDROGEN = 300 ML./MIN.
NITROGEN = 30 ML./MIN.

385
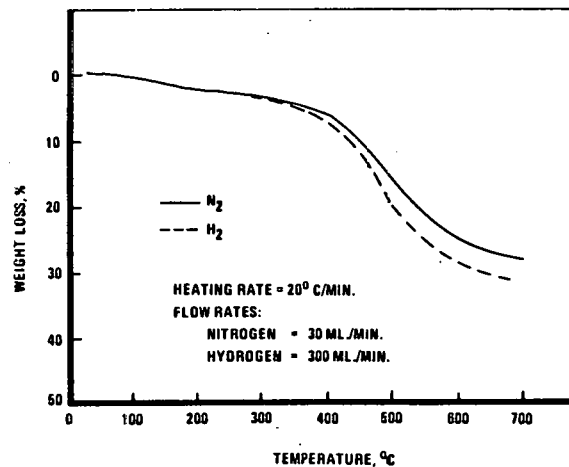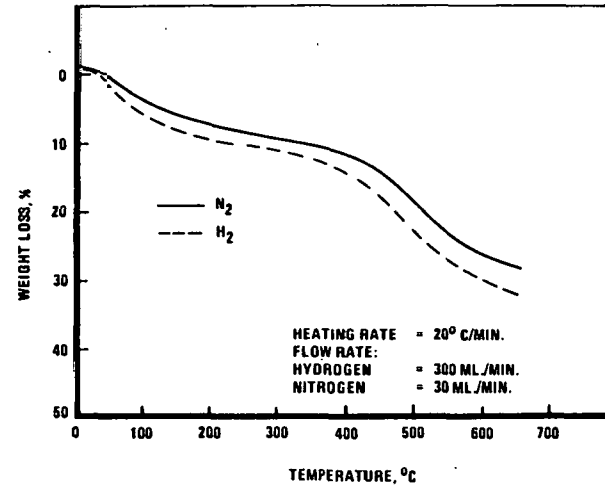
FIGURE G-59
TGA OF COLONIAL/P&M COAL
PREPARATION PLANT WASTE MATERIAL
IN THE PRESENCE OF HYDROGEN AND NITROGEN GASES
(SAMPLE NO. PMC-P-C)
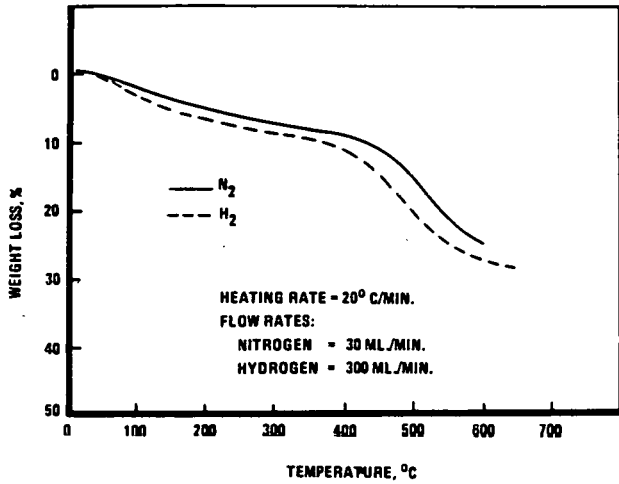
FIGURE G-60
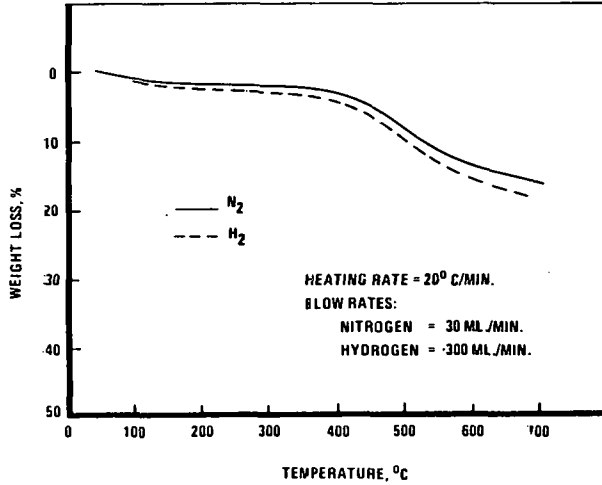DTA OF HENDRIX/BETH ELKHORN
COAL PREPARATION PLANT
WASTE MATERIAL IN THE PRESENCE OF AIR

FIGURE G-61
DTA OF GUND/ISLAND CREEK COAL PREPARATION PLANT
WASTE MATERIAL IN THE PRESENCE OF AIR

FIGURE G-62
DTA OF SPURLOCK/ISLAND CREEK
COAL PREPARATION PLANT
WASTE MATERIAL IN THE PRESENCE OF AIR

386

FIGURE G-63
DTA OF GILBRATOR/AMAX COAL PREPARATION PLANT WASTE MATERIAL IN THE PRESENCE OF AIR

FIGURE G-64
DTA OF FIES/ISLAND CREEK COAL PREPARATION PLANT WASTE MATERIAL IN THE PRESENCE OF AIR

FIGURE G-65
DTA OF COLONIAL/P&M COAL PREPARATION PLANT WASTE MATERIAL IN THE PRESENCE OF AIR
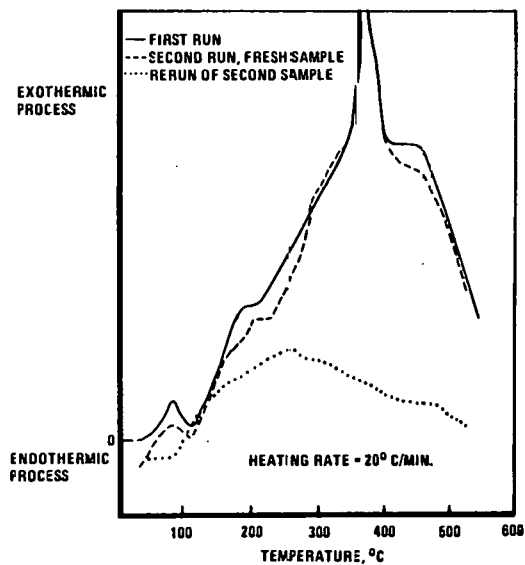
FIGURE G-66
TGA OF GUND/ISLAND CREEK COAL PREPARATION PLANT WASTE MATERIAL IN THE PRESENCE OF AIR
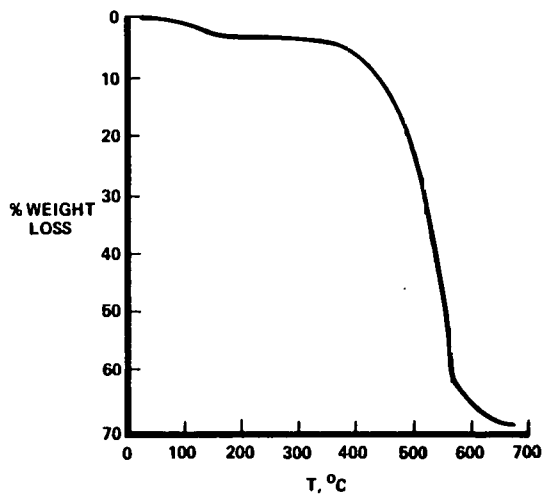
FIGURE G-67
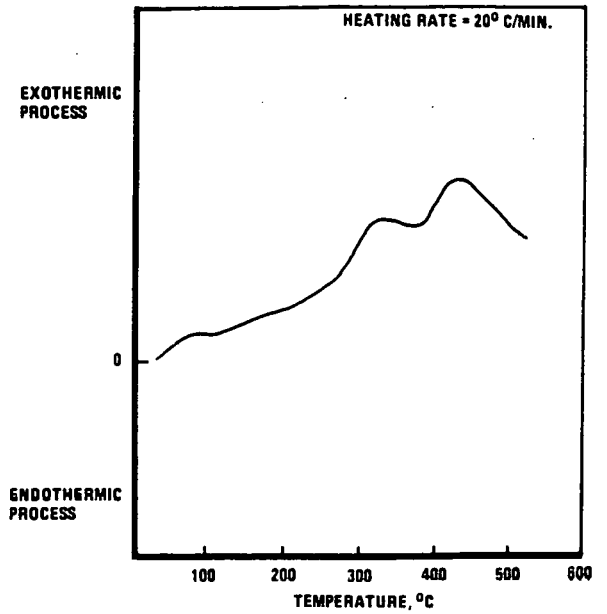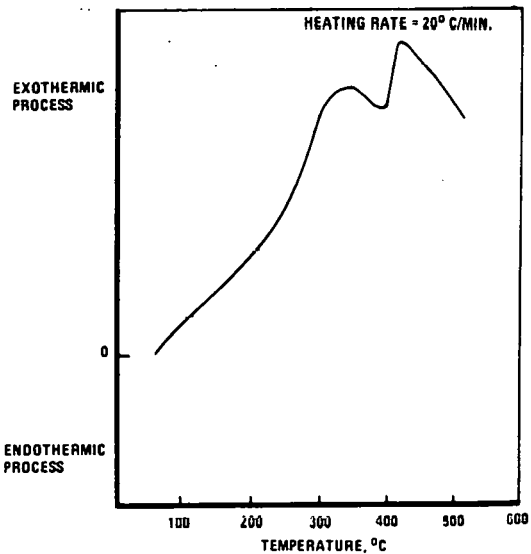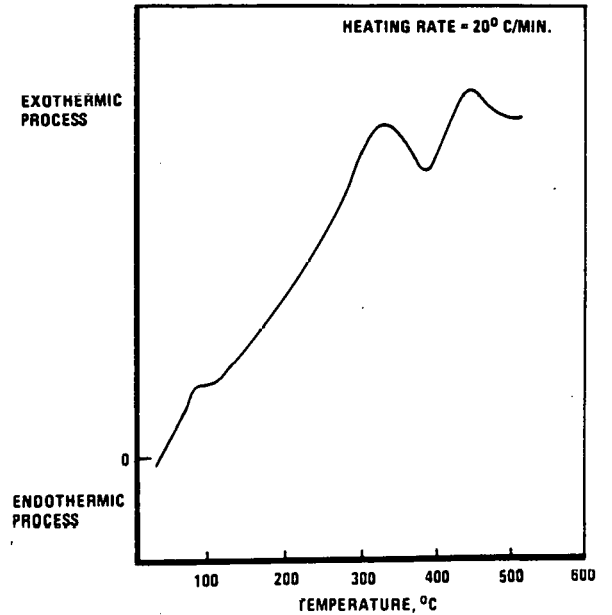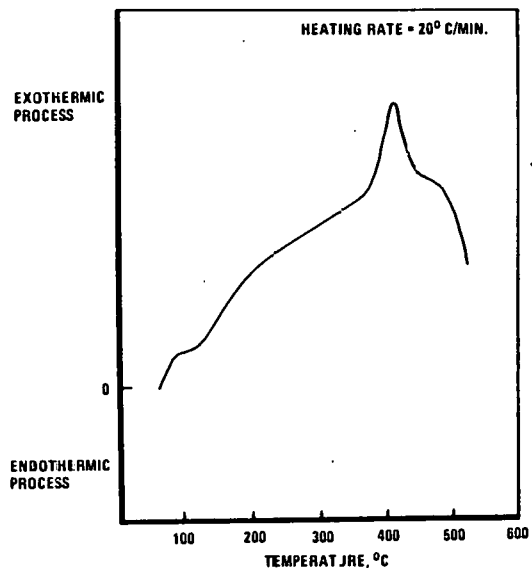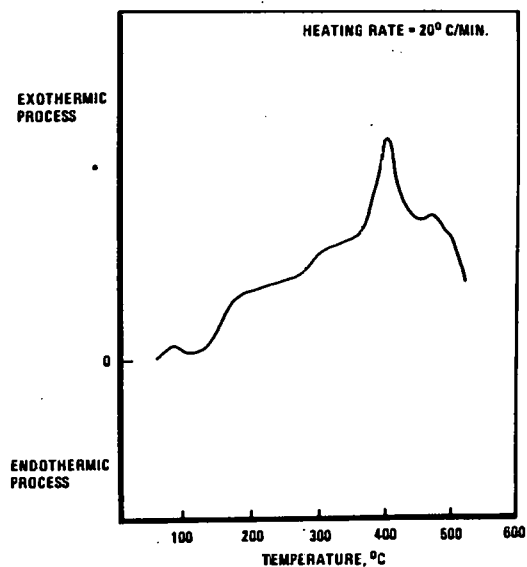**TGA OF FIES/ISLAND CREEK COAL PREPARATION PLANT WASTE MATERIAL IN THE PRESENCE OF AIR**

387

$$3FeS_2 + 3H_2 \longrightarrow 3FeS + 3H_2S \qquad \text{(Eqn. G-2)}$$
$$Fe_3O_4 + 3H_2S + H_2 \longrightarrow 3FeS + 4H_2O \qquad \text{(Eqn. G-3)}$$

$$Fe_3O_4 + 3FeS_2 + 4H_2 \longrightarrow 6FeS + 4H_2O \qquad \text{(Eqn. G-4)}$$
$$\text{M.W.} \quad 232 \qquad 120 \qquad\qquad 88$$
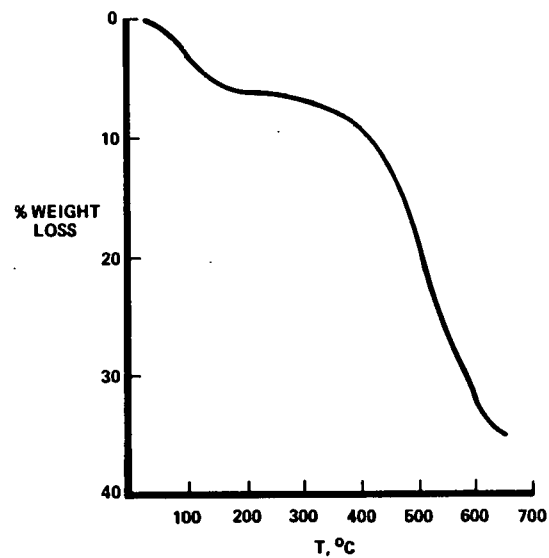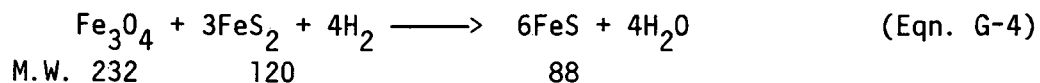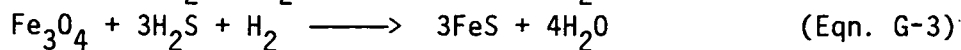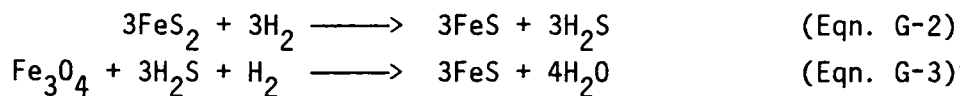
A 50-50 mixture by weight of pyrite and magnetite was treated in the PTGR at 450°C and 1000 psig. The theoretical reaction product distribution obtained was calculated using Equations G-2 to G-4 and the calculation procedure is described below.

$$\text{Feed:} \quad 1.5 \text{ g } FeS_2$$
$$\qquad\qquad 1.5 \text{ g } Fe_3O_4$$

From the Equation G-4 it is evident that pyrite is the limiting reactant in the reaction mixture. The stoichiometric amount of Fe_3O_4 that can react with 1.5 g FeS_2 is calculated to be 0.97 g. Therefore, the remaining 0.53 g of Fe_3O_4 is subjected to direct hydrogen reduction reaction. The direct hydrogen reduction of Fe_3O_4 at 450°C and 1000 psig H_2 pressure resulted in only 2.67% weight reduction in the PTGR. Using this number, the amounts of reduced pyrite, elemental iron and unreacted Fe_3O_4 that would result from the reaction of 1.5 g of FeS_2 and 1.5 g of Fe_3O_3 are given in Table G-6. The relative distribution of iron among various iron species is calculated and presented in Table G-7. The observed distribution of iron determined by Mössbauer is also presented in Table G-7 for comparison. It can be seen that the theoretical and observed distribution of iron vary by an order of magnitude indicating that the reaction of pyrite and magnitude cannot be described by Equation G-4.

The total weight loss assuming no chemical reaction between pyrite and magnetite is calculated and compared to observed total weight loss as shown in Table G-8. The calculated and observed weight losses are noted to be very close. Likewise, the calculated iron distribution for the 50-50 mixture and that determined by Mössbauer are also quite similar. Therefore, on the basis of the above results there seems to be little interaction between pyrite and magnetite under the reaction conditions used in the study. Likewise, these compounds appear to behave as individual compounds in hydrogen reduction reaction.

Table G-6

Reduction of Pyrite-Magnetite Mixture in the PTGR

Reaction Mixture:
Pyrite = 1.5 g
Magnetite = 1.5 g
Reaction Temp. = 450°C
Pressure = 1000 psig H_2

Material	Theoretical Distribution, Wt.%
FeS	80.7
Fe_3O_4	19.1
alpha-Fe	0.2

Table G-7

Distribution of Elemental Iron as Determined by Mössbauer
in the Reaction Product of Pyrite Magnetite Reduction

	Theoretical Distribution Weight %	Observed Distribution Weight %
FeS	78.5	34.0
Fe_3O_4	21.1	49.0
Fe	0.36	13.0
Other	--	4.0

Table G-8

Reduction of Pyrite, Magnetite and 50-50 Mixture

	100% Pyrite	100% Magnetite	Pyrite - Magnetite 50-50
U.S. Mesh Size	-200	-200	-200
Temp., °C	450	450	450
Initial Weight, g	3.00	3.00	3.00
Final Weight, g	2.48	2.92	2.73
Weight Loss, %	17.33	2.67	9.00
Calculated Weight Loss, *%	--	--	10.00

* Calculated on the basis of no other reaction of pyritic sulfur with magnetite.

APPENDIX H

Coal Processing Development Unit (CPDU)

Equipment

Figure H-1 is a simplified flowsheet of the Coal Process Development Unit
(CPDU). The detailed description of various equipments is presented below.

Slurry Feed System - Three 65 gallon charge tanks are used to contain the
start-up solvent and slurry feedstocks for the coal liquefaction experiments.
The tanks are constructed of stainless steel and can be operated at temperatures
of up to 600°F at pressures of up to 1000 psig. Provision is made to blanket
the tanks with nitrogen. Each charge tank is equipped with a high-speed
turbine stirrer. A 15 gpm Moyno pump is employed to recycle the slurry feedstock
in a closed-loop around charge tanks to aid in maintaining a uniform dispersion
of coal or residue in the solvent. A spare Moyno pump is piped into the
recycle loop. The Moyno pump is a progressive cavity pump, equipped with a
stainless steel rotor and stator, which can develop a differential pressure of
about 35 psi.

The liquefaction reactor is fed from a 8-liter slurry feed tank constructed
from 4" stainless steel pipe. Although this feed tank is normally operated at
ambient temperature, it can be heated. A 15 psig blanket of nitrogen is
maintained over the slurry in this tank. Although the tank is not stirred, a
1.5 gpm Moyno pump circulates slurry around the tank to maintain a uniform
solid suspension. A differential pressure transmitter mounted on the feed
tank measure the mass of slurry in the tank. This measurement is used to
calculate the slurry feed rate to the liquefaction reactor. The slurry feed
tank is typically refilled every hour from one of the charge tanks by opening
a pneumatically-operated ball valve in the short length of tubing linking the
feed tank to the charge tank recycle loop.

A separate 10-liter solvent feed tank also is provided. This tank is equipped
with a differential pressure transmitter and may be operated at temperatures
up to 600°F.
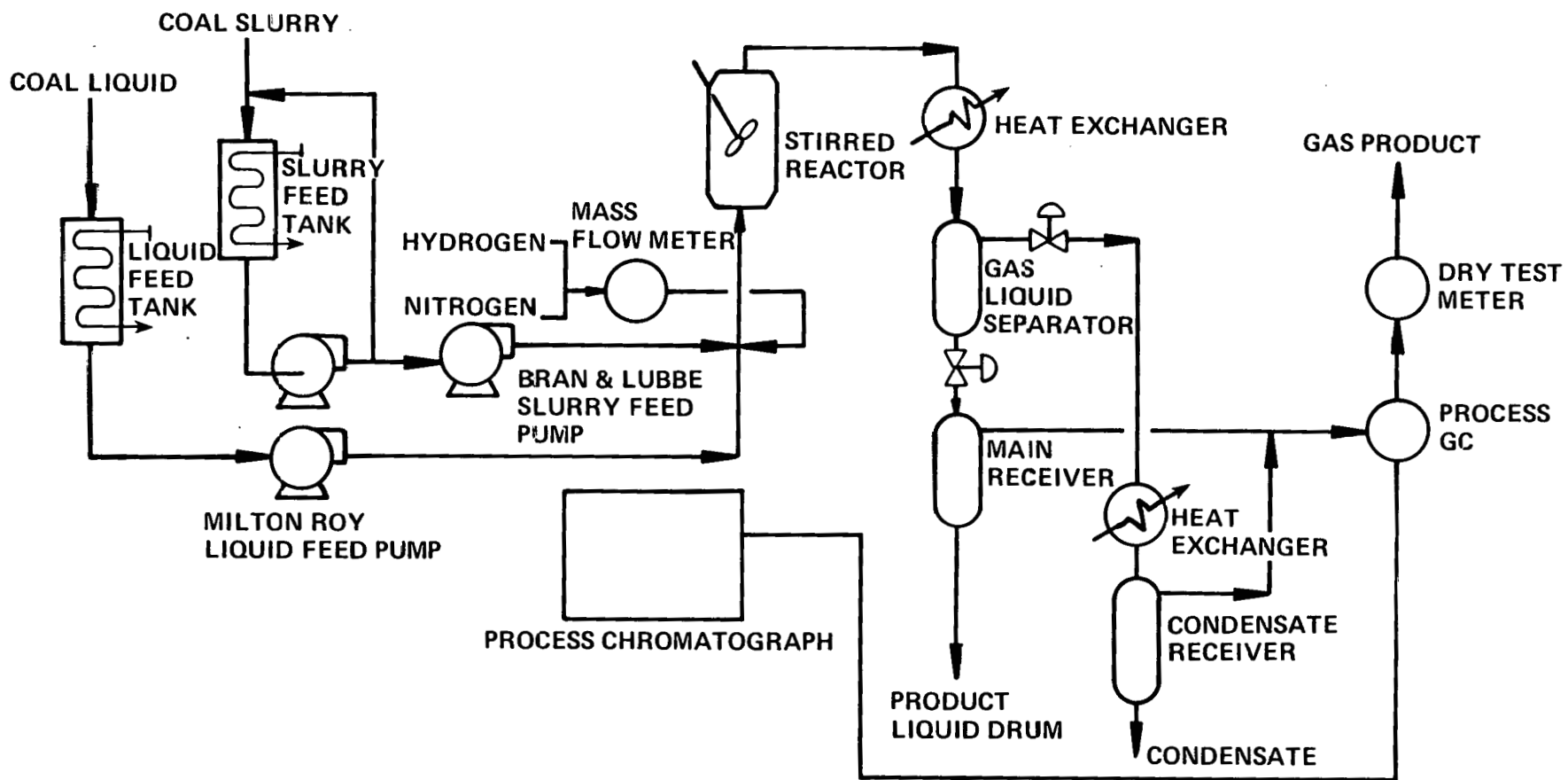
FIGURE H-1. SIMPLIFIED DIAGRAM OF COAL PROCESS DEVELOPMENT UNIT

The CPDU has two high-pressure, positive-displacement slurry feed pumps. The Bran and Lubbe pump is typically used to pump coal slurries, with the Milton Roy pump used as a spare. These are both piston pumps with double ball-and-seat check valves at the inlet and discharge of the pump chamber. A tungsten carbide plunger and balls are used when pumping coal slurries. A variety of plunger sizes are available, permitting pump rates of about 250-7500 cc/hr. However, if -200 mesh coal particles are being processed, the minimum pump rate is about 1000 cc/hr. At lower rates, solids settle in the 9/16" transfer tubing and/or in the flow-through diaphragm isolators. The complex piping and valve arrangement at the inlet or the slurry pumps permits either or both of them to pump from either feed tank.

A high pressure switch is installed at the discharge of each of the high-pressure pumps as a safety device. This switch will shut down the pump if the line pressure exceeds the designated operating pressure by 500 psi. A pressure gauge and rupture disc are also installed in this line. Flow-through isolators are associated with the pressure switch and pressure gauge. Priming lines are provided to facilitate pump start-up. These priming lines are N_2 purged.

Continuous Stirred Tank Reactor (CSTR) - The coal liquefaction reactor is a 1-liter CSTR built by Pressure Products. This vessel is constructed of A-286 alloy steel and has a pressure rating of 5000 psig at 1000°F. The CSTR has an inside diameter of 3 inches and an inside length of 9 inches. Agitation is provided by a 2-inch diameter, 6-blade turbine, which is driven at speeds up to 2000 rpm (typically 1000 rpm) by a sealed magnetic drive. The turbine blades are flat and have a 1/2 inch width. The turbine is 1-1/4 inches above the bottom of the vessel.

Although the CSTR is not baffled, a 3/8" thermowell effectively breaks the vortex at the typical impeller speed of 1000 rpm. A cold-flow model of the vessel and agitator confirms that:

1. solids are fully suspended

2. the vortex is very small

3. the gas void fraction is about 13 percent volume

4. most of the gas/liquid contact occurs in the immediate vicinity of the turbine.

A baffles was tested in the CSTR, but discarded because it tended to collect solid particles, thus leading to coke formation.

Both the hydrogen gas and the feed slurry enter the CSTR at ambient temperature through a 9/16" inlet port centered in the base. Both the product gas and slurry leaving thorugh a 9/16" port at the top of the body. A slow nitrogen purge must be maintained between the stirrer shaft and bearings to protect the graphite bearings from the slurry. The normal nitrogen concentration in the product gas stream is about 2 mole %.

The CSTR is heated by stainless steel-sheathed resistance heaters wrapped around the body and heated. Temperature control is based on reactor wall temperature. Sufficient heating capacity is available to permit operation at 885°F with a slurry space velocity of 5.0. Thermocouples placed at the bottom, middle, and near the top of the thermowell indicate that veritical temperature gradients in the CSTR are small.

Gas-Liquid Separation - The product slurry is quenched to 325°F in a coiled heat exchanger, which is cooled with Mobiltherm on the shell-side. Like all of the transfer tubing and vessels downstream of the CSTR, this tubing is traced with electrical resistance heaters and insluated with fiberglass to avoid product freezing in the tubing during unplanned pump stoppages. The Mobiltherm heat transfer fluid is heated or cooled, as required, to maintain the 325°F process fluid temperature.

The quenched product slurry and gases enter the gas/liquid separator through a dip tube which directs the flow against the vessel wall, about an inch from the bottom. This 316 SS vessel has an inside diameter of 4 inches and an inside length of 22 inches. A 3200 psig rupture disc mounted at the gas outlet from the gas/liquid separator.

A Masoneilan-Annin "Wee Willie" valve with size C tungsten carbide trim serves as the slurry dump valve. A manual bypass valve can be used to drain the separator if a plug develops in the Annin valve. The product slurry is let-down to the 30 psig pressure of the main receiver.

The main receiver is a 4 inch I.D. by 22 inch I.L. 316 SS vessel. It is equipped with a differential pressure transmitter that measures the weight of product slurry held in the receiver. The receiver is typically drained every hour, either to a sample receiver or a 55 gallon product drum. The product rate is calculated from the change in the differential pressure transmitter reading. The product drum is placed on an electronic scale to provide the actual product liquid rate.

Product Gas Train - The product gas is metered out of the gas liuqid separator through the system pressure valve (a Research Control Valve). This pneumatic valve is controlled based upon the system pressure, as measured by a pressure transmitter mounted between the gas/liquid separator and this valve. Because the system pressure valve may be blocked by heavy liquid drops elutriated from the gas/liquid separator, a redundant valve is provided. Block valves are also provided to permit one of the system pressure valves to be isolated for maintenance.

The dissolver gases and water which flash from the product slurry in the main receiver are combined with the main product gas stream immediately downstream of the system pressure valve. A 140 psig rupture disc is installed at this point. The low-pressure product gas train is maintained at 30 psig by a Circle Seal back pressure regulator. The combined product gas stream is routed to a water-cooled condensor for removal of the bulk of the water and the C_5+ hydrocarbons. Two condensors, each with its own condensate receiver

can be operated together in series or singly, with one held in reserve. The gases leaving the condensate receivers are further cooled in a packed vessel placed in an ice bath.

The product gases are routed through a dryer tube to the Beckman process chromatograph. This chromatograph is capable of analyzing 2 gas samples per hour for a total of 15 components (H_2, N_2, O_2, CO, CO_2, NH_3, H_2S, C_1-C_4, iC_4, ethylene and propylene, and C_5+).

The product gas pressure is reduced to less than 1 psig in the back pressure regulator before flowing to the test meter. A pressure transducer and thermocouple are mounted in the product gas line immediately upstream of the dry test meter to permit the flow rate to be converted from actual cubic feed per hour to standard liters per hour. A magnet is mounted on the sweep arm of the dry test meter to permit electronic data logging of the rate. The product gas is passed through an activated carbon scrubber prior to venting.

Inlet Gas Train - Hydrogen from an Air Products tube trailer is compressed to 4000 psig in a Carblin diaphragm compressor. Ballast tanks before and after the compressor stabilize the compressor operation and the hydrogen delivery pressure. Two forward pressure regulators in series are used to maintain a constant hydrogen pressure, typically 3400 psig, in the hydrogen metering loop. A Hoke micrometering needle valve is used to control the hydrogen flow. A Thermal instrument mass flowmeter measures the flow.

The purge nitrogen for the magnetic stirrer on the CSTR is supplied from 6000 psig Air Products cylinders. A forward pressure regulator is used to set the pressure on the stirrer at 100-200 psig above the system pressure. Almost all of this pressure drop occurs across a needle valve in the nitrogen line, which limits the flow due to a few standard liters per hour. The nitrogen can also be used to purge the CSTR and the rest of the CPDU.

Operation

All of the CPDU runs have been conducted with once-through solvent, i.e., no effort has been made to achieve the steady-state solvent composition through solvent recycle. This greatly increased the number of reaction conditions

that can be examined during the course of a single CPDU run. Although none of the data points represent "equilibrium" data points conclusions drawn from those data regarding the effect of catalyst addition are expected to be valid.

The feed slurries are prepared at room temperature, typically in 40-50 kilogram batches, immediately prior to use. The feed slurry is stored in a charge tank equipped with a turbine agitator and a recycle pump which maintain a uniform suspension of the solids. Slurry handling was planned to minimize consumption of recycle solvent. The experiments began by slurrying the catalyst in the solvent. After the catalyst is dispersed in the solvent, coal was added to bring the slurry composition to 30 wt.% coal. Separate base-line experiments were conducted with the coal slurried in solvent, but without added catalyst.

The feed slurry is pumped to the reactor from a feed tank which is maintained at ambient temperature. This feed tank, which is equipped with a recycle pump to mix the slurry, is refilled each hour from the charge tank. Whenever the feed slurry composition is changed, the feed tank is drained and then flushed several times with the new feed slurry. When reaction conditions are altered, at least 10 reactor volumes of slurry are processed through the reactor at the new conditions prior to beginning to collect any product samples for analysis.

A continuously stirred tank reactor was selected from these experiments to insure that the vapor compositon in the reactor, including the partial pressure of light solvent components, matched that of an actual SRC-I dissolver. A stirred-auto-clave design was chosen for this reactor to insure that the coal minerals were well mixed and did not accumulate in the reactor. Cold-flow experiments, conducted in a Plexiglas model, have confirmed that the flat-bladed turbine agitator keeps the solids well distributed throughout the reactor volume, so that coal minerals will not accumulate.

Although a propensity to coking on baffles prohibits baffling of the reactor, the thermowell effectively kills the vortex and the void fraction is only 0.13. Because all of the sensible heat to bring the slurry to reaction temperature is provided by resistance heating of the reactor, the reactor wall is about 25°F hotter than the bulk slurry.

The product gas and slurry leaving the CSTR are quenched to 325°F to freeze
the reactions, before flowing to a gas/liquid separator, at reactor pressure.
The product slurry is throttled into the product receiver, at a rate which
maintains a constant, small inventory in the separator.

Water, light hydrocarbons and gases, which flash from the product slurry in
the 30 psig receiver, are combined with the product gas stream from the separator.
The combined gas stream is cooled to about 60°F to condense the water and
light organics, prior to entering the gas chromatograph and dry test meter for
product gas yields and volume measurement.

Appendix I

Effects of Coal Minerals, By-Product Metallic

Wastes, and Other Additives on Coal Liquefaction

by

W. J. Huang
C. W. Curtis
J. A. Guin
J. H. Clinton
H. L. Barwood
A. R. Tarrer

Auburn University Coal Conversion Laboratory
Department of Chemical Engineering
Auburn University, Alabama 36849

ABSTRACT

The effects of approximately 75 minerals and additives on the conversion of coal to liquids have been examined in tubing bomb liquefaction experiments using an Elkhorn #3 coal in the presence of solvent and hydrogen. The product distribution consisting of gas, oils, preasphaltenes, asphaltenes and insoluble organic material (IOM) on a maf coal basis was obtained for each experiment. Both positive and negative effects (if any) of the various additives on coal conversion to oil were noted. The effects were found to range from virtually nil to more than a 100 percent increase in oil fraction production as compared to a baseline experiment with no additive. Thus, $Co-Mo-Al_2O_3$, ammonium paramolybdate, molybdic oxide, red mud, hematite, ferrous sulfate and pyrite gave oil yields of 66%, 58%, 56%, 49%, 46%, 42%, and 37-44% on a percentage of maf coal basis as compared to an average oil yield of 21% in the baseline no-additive case. Changes undergone by certain of the additives during reaction also were examined.

INTRODUCTION

The dissolution of coal to preasphaltenes and gases is generally considered a thermally produced step. The hydrocracking of preasphaltenes to asphaltenes, oil, and gases is facilitated by commercial catalysts or additives which act catalytically or enter into the reactions. A desired product is the oil fraction since the oil fraction requires the least amount of further processing to convert it or separate it into liquid fuels with desirable qualities. A study of the effects on coal liquefaction of various additives including coal minerals and by-product metallic wastes has been made. The variable of interest has been the amount of lower molecular weight species, i.e., oil, produced as a result of added minerals or waste materials. Results are reported on a maf coal basis as a product distribution of gas, oil (pentane soluble), asphaltenes (benzene solubles, pentane insoluble), preasphaltenes (methylene chloride - methanol solubles, benzene and pentane insoluble), and insoluble organic material (IOM), material which is insoluble in any of the solvents used.

In terms of the minerals associated naturally with coal deposits a number of questions arise. Should the coal minerals be removed before lique- faction reactions if possible or should only certain minerals be removed? Do certain minerals inhibit the desired reactions in coal liquefaction processing? Which, if any, of the minerals are catalytic in nature, and would it be advantageous to include extra quantities of these in a liquefaction reactor? Are there synergetic effects on liquefaction reactions among mineral species? An experimental screening program was performed by adding minerals to coal

liquefaction processing and observing the results on a macroscopic scale.

EXPERIMENTAL

Reaction Equipment. A batch reactor (tubing bomb reactor) agitated while immersed in a heated fluidized sand bath comprises the reaction system used. Figure 1 is a schematic of the equipment. A reactor volume, 46.3 cc, was chosen so that the supply of hydrogen gas is sufficient even in the case of a good hydrogenation catalyst.

The tubing bomb was constructed of 316 seamless stainless steel, 3/4 inch O.D., with a 0.065 inch wall thickness. The reactor was sealed at one end by a Swagelok cap, and the other end was connected to a Nupro fine metering valve through Swagelok fittings. The tubing bomb is agitated at 860 cycles per minute with a vertical stroke of 1-1/2 inches. Two 3/16" diameter steel balls are placed in the tubing bomb to aid mixing of the coal, gas, solvent, and additive. The sand bath in which the tubing bomb is immersed is a Techne Inc. SBL-2D equipped with a Techne TC4D temperature controller.

Reactants. Reactants used are hydrogen, coal, solvent, and the additive of interest. A description and the sources of the additives used are listed in Table I. The hydrogen used was Commercial 2000 psig grade. The coal used was ground bituminous Elkhorn No. 3 from Floyd County, Kentucky. The solvent used was the $550^{\circ}F+$ fraction of an SRC-II fuel oil blend produced using Powhatan No. 5 mine coal. An analysis of the coals and solvent used in this study is given in Table II. Coal and solvent were supplied by Air Products and Chemicals, Inc.

Reaction Conditions. Reaction conditions were sought which would maximize the difference in oils production between experiments where an active catalyst was used and experiments where no additive was used. For

the particular coal and solvent used, it was determined experimentally that at 450°C and one hour reaction time an actively catalyzed reaction would result in approximately 66% of the charged coal being converted to oils. A noncatalyzed reaction, that is, one with no added minerals, would result in an oil make of approximately 21%. Any mineral additives which had a positive effect on oil production would be expected to be between these extremes.

Reaction Procedures and Product Analysis. Before use, the coal and additive are dried overnight in a vacuum oven at 100°C in order to remove moisture. The coal, additive, and solvent are charged to the reactor in a layered configuration. The sealed tubing bomb reactor is attached to the agitation equipment and the reaction is begun. After the reaction, the tubing bomb is quickly quenched by immersing in water at room temperature. After quenching, the gas is collected in a gas sampling bag. The volume of the gas is determined by volume displacement. A sample of the gas is analyzed by gas chromatography for H_2, O_2 and N_2 (air), CH_4, CO_2, C_2H_4, C_2H_6, H_2S, C_3H_6, C_3H_8, $i-C_4H_{10}$, $n-C_4H_{10}$, and C_5H_{12}. The liquid and solid materials in the tubing bomb are collected and the product distribution which is expressed as % oils, % asphaltenes, % preasphaltenes, and % insoluble organic matter (IOM) is determined. To obtain the product distribution, the entire liquid and solid contents from the bomb are used.

The solvent separation procedure is summarized below and is given in schematic form in Figure 2. Pentane is poured over the sample and a Branson 350 sonifier is used to extract the oils fraction by agitating the pentane and sample. The liquid material is then centrifuged, and the supernatant liquid is pressure filtered and collected in a flask. A three to five micron filter paper is used in the filter. The solid material is carefully washed

back into the original beaker with pentane to be further sonicated with more pentane. Four such extractions with pentane are routinely used to extract the oils fraction. On the few occasions where sticky material or large particles remain after the four pentane extractions, liquid nitrogen is carefully poured over the material and the material is crushed with a glass rod to fine particles. Just before the liquid nitrogen evaporates completely, pentane is poured over the sample and sonicated as before.

In order to extract the asphaltenes, benzene is used and one sonication is performed. The sonication is followed by several manually stirred washings with benzene. Before the liquid material is pressure filtered, centrifugation is used to avoid coating the filter paper with suspended preasphaltene particles. After extraction with benzene, the preasphaltenes are collected by sonicating and washing the remaining material with a solution of 90% methylene chloride - 10% methanol by volume. The remaining material is washed with the methylene chloride - methanol solution into the pressure filter, further washed and dried. Nitrogen is the gas used in the pressure filter apparatus. The residue on the filter paper is air dried and contains insoluble organic matter (IOM), coal minerals, and the mineral additive if any. It is assumed that little or none of the additives, coal minerals, or IOM have passed through the filter paper.

The pentane and methylene chloride - methanol solvents are evaporated from their respective fractions of $60^{\circ}C$ under nitrogen. The oils are a reddish liquid and the preasphaltenes are dry black solid particles. The benzene is evaporated at $80^{\circ}C$ from the asphaltenes fraction until about 10 to 20 milli-liters remain. The benzene solution is then freeze-dried, leaving the asphaltenes as a dry, flaky crust.

In this paper, the product distribution is reported in terms of gas, oil, asphaltenes, preasphaltenes and insoluble matter. Previous disclosures of this work included only the liquid portion of the product distribution, excluding the gases produced during the reaction. In reporting the product analyses, the initial product distribution of the solvent is subtracted from the product distribution of the liquid reaction product, putting the results on a solvent free basis. An average value for the gas produced from the solvent is subtracted from the amount of gas produced during reactions with coal and solvent. The amount of minerals in the coal, determined from high temperature ashing, and the amount of additive, if any, are subtracted from the residue obtained after the solvent extractions putting the results on an additive free, ash free basis. Since the coal is dried before use, the results are reported on an additive free, moisture free, ash free, solvent free basis. It has been observed that some water is present after the reactions, presumably due to the oxygen in the original coal and solvent. Experimental results have shown that the water is about 2.5 to 3.5% of the coal. Due to the nature of the separation procedure and the calculations, the water is reported as part of the oil fraction.

Ashing Procedures. The high temperature ashing procedure consists of heating the sample of interest at 800°C for two hours in air. Medium temperature ashing is done at 510°C for two hours in air. Low temperature ashing was accomplished with a L.F.E. Corporation L.T.A. 504. Approximately 50 watts were used with 1.5 to 2.0 gram samples per chamber. The oxygen flow rate was 0.05 cc /min; the oxygen pressure was 1 mm Hg. The ashing is stopped when a constant weight is obtained.

X-ray Diffraction Analysis. Several reacted and unreacted disposable catalysts were analyzed using x-ray powder diffraction methods conducted on a Phillips x-ray diffractometer. The samples were ground to -200 mesh and mounted as an acetone slurry on glass slides. 100 mg of sample was used for both the unreacted and reacted samples and then the pattern of the reacted sample was corrected for dilution by organic residue and residual coal ash. Reaction products were identified using the ASTM powder diffraction index for inorganic substances. Some reaction products could not be identified by this method and were classified as unknowns.

RESULTS AND DISCUSSION

Temperature Dependency of Product Distribution. In determining the conditions to use for the reactions the temperature of reaction was one of the variables considered. Figure 3 shows the temperature dependency of the liquid product distribution in a liquefaction reaction catalyzed by Co-Mo-Al. A maximum appears in oil production around $475^{\circ}C$ for the particular coal and solvent used in this study. At $500^{\circ}C$ coking was observed on the walls of the reactor and the insoluble organic material (IOM) is seen on Figure 3 to be significantly higher than at lower temperatures. The IOM appears to be increasing even at $475^{\circ}C$ which indicates that coking is possibly occurring. In the temperature range examined the oils pass through a maximum at $475^{\circ}C$. In contrast, the asphaltenes exhibit a minimum at $475^{\circ}C$. The insoluble organic matter passes through a minimum at about $460^{\circ}C$. Likewise, the pre-asphaltenes reach a minimum at $475^{\circ}C$ and remain at that level. If gases produced during the reaction had been included in this product distribution, the apparent maxima and minima observed for each fraction would still be present but would probably be shifted slightly. The temperature $450^{\circ}C$ was chosen as

the reaction temperature for the study of various additives because it was noted at 450°C there was a large difference in oil production between a strongly catalyzed liquefaction reaction and a liquefaction reaction with no added catalyst. A similarly large difference was noted at 475°C, but there was no apparent advantage in using a reaction temperature of 475°C in order to compare the effects of the various mineral and by-product additives.

The effect of reaction parameters on the product distribution in the presence of a pyrite additive was examined. Pyrite, sized to +40, 40x80, 80x140, and 140x200 mesh, were used. The reaction conditions are given in the experimental section. The product distributions for the different sized pyrites along with that of -325 mesh Robena Mine pyrite are given in Table III. In the reaction system used, it is apparent from each fraction of the product distribution that each sized pyrite fraction has an equivalent effect on the reaction system.

An examination of reaction temperature on product distribution and conversion using 140x200 mesh pyrite was also undertaken. The temperatures studied ranged from 400°C to 500°C at 25°C intervals. The distribution of the products obtained at each reaction temperature is shown in Figure 4. A maximum in oil production is observed near 450°C. Both the asphaltenes and preasphaltenes decreased with increasing temperature. The IOM fraction passes through a minimum at about 440°C and appears to increase substantially at 500°C. The most dramatic change due to temperature in the product distribution is seen in the gas fraction produced from the coal which increases from 5% at the lower temperature range, 400 and 425°C, to 55% at 500°C. Concurrently, the oil fraction at 500°C declined to -11% from a high of 38% at 450°C. At 500°C, the liquefaction system does not make a sufficient quantity of oil

from the coal to maintain solvent balance; therefore, no net production of oil from coal is observed at 500°C. Coal conversion at 500°C is also lower than that at lower reaction temperatures. Since coal conversion is defined as 1-IOM, the decrease in conversion may be due to coke formation which is insoluble in methylene chloride and methyl alcohol.

To determine the effect of agitation rate on the product distribution using 140x200 mesh pyrite, reactions were performed at agitation rates ranging from 0 to 1000 RPM. The effect of agitation rate on product distribution is shown in Figure 5. When steel balls are used as agitators in the tubing bombs, the oil produced from coal increases from -39% at 0 and -26% at 200 RPM to ~39% at 400 RPM and above. Both the asphaltene and preasphaltene levels decrease slightly with increasing agitation rates when steel balls are used. Coal conversion increases radically from less than 35% at 200 RPM to greater than 85% at 300 RPM and above. One experiment was performed at 400 RPM without the steel ball agitators. Comparison of the product distribution at 400 RPM with and without steel balls shows a substantial decrease in oil production and coal conversion and an increase in IOM, preasphaltenes and asphaltenes without the steel balls. Considering the results of the above experiments, it is apparent that agitation rate has a strong influence on product distribution and that the agitation rate must be maintained at a sufficiently high level so that mass transfer is not limiting.

Minerals. The objective of this work is to determine the effect of coal minerals in a liquefaction reaction, how the minerals change during reaction, and if synergetic effects occur. The minerals examined in this study are those which commonly occur in United States coal.

The Elkhorn #3 coal used in the experiments has a high temperature ash content of 14.6 weight percent, and a mineral content of 17.8 weight percent as determined by low temperature ashing. Table IV gives the mineral composition of the Elkhorn #3 coal. The only minerals present in Elkhorn #3 coal which change during reaction as indicated by x-ray diffraction are pyrite (FeS_2) and gypsum ($CaSO_4 \cdot 2H_2O$) which become pyrrhotite ($Fe_{1-x}S$) and calcium sulfate ($CaSO_4$), respectively. Although it might be ideal to use a completely demineralized coal in a study of this type, by adding a relatively large quantity of a mineral to a reaction with a coal of as low an activity as Elkhorn #3, any significant effect of the mineral additive should be observable. Table V presents the product distribution and conversion obtained when the minerals used were added in a proportion of 33% of the coal. The original reaction mixture consisted of 60% solvent, 30% Elkhorn #3 coal, and 10% mineral additive by weight. The results are presented in order of increasing oils product. The commercial Co-Mo-Al catalyst is used for comparison. The Co-Mo-Al was presulfided before use.

Among the minerals tested, the most effective are molybdic oxide and compounds high in iron, such as ferric oxide and red mud. These compounds produce approximately 35% or more oils on a solvent free basis. Most of the other minerals added have minor but varying degrees of positive effects on oils production.

By-Product Metallic Wastes and Other Additives. Table VI shows the effect of various chemical additives and industrial waste materials on product distribution and conversion. The most noticeable effects were produced by Fe_2O_3 and red mud which consists of approximately 50% goethite, FeOOH, an iron oxide hydrate. Red mud is Bayer process waste from Kaiser Aluminum

Company. Using sulfur and red mud together produced the same effect as red mud alone. As with the minerals in Table VI, the chemicals or waste products high in iron gave the highest conversions and highest oil values.

Table VII shows the effects on product distribution and conversion of SRC residues ashed at three conditions: $800^{o}C$, $510^{o}C$, and low temperature ashing. The SRC residues used in this study were obtained by filtration or by Kerr McGee's Critical Solvent Deashing Process at the Wilsonville SRC Pilot Plant. In order to determine the effect of a diatomaceous earth filter aid normally present in SRC filtration residue, diatomaceous earth filter aid was also treated at the three ashing conditions and used as an additive. The diatomaceous earth filter aid produces identical product distributions at all three ashing conditions and essentially the same results as the SRC filtration residue ashed at $800^{o}C$ and $510^{o}C$. Filter aid does not appear to affect the oils production at the ashing temperatures used.

Table VIII presents the effects on product distribution and conversion when pyrite which has been reduced at several different conditions is used as an additive. X-ray analysis of the ground samples indicate that all the reduced pyrite used are essentially $Fe_{1-x}S$. The first column of Table VIII is the product distribution and conversion obtained with the untreated pyrite. As seen in Table VIII, all samples of reduced pyrite gave essentially identical results within experimental error. The reduced pyrite and the untreated pyrite distributions are also nearly identical within experimental error.

Table IX shows the effect of impregnating coal with compounds containing Co, Ni, and Mo. The weight of the impregnated species per gram of coal are: 0.01g Ni, 0.01g Co and 0.026g Mo. The liquefaction reaction, with an impregnated molybdenum compound, ammonium paramolybdate, showed one of the higher oil conversion, 58%, observed in the study. The coal impregnated with cobalt nitrate

hexahydrate and nickel nitrate hexahydrate and both show activity levels similar to that of coals reacted in the presence of pyrite.

Table X presents the product distribution results for several reactions using different fly ashes and bottom ashes as additives. A difference greater than experimental error is observed in the oil production using the various ashes. However, neither the composition nor whether the ash is a fly ash or a bottom ash appears to be a pertinent factor for the differences observed.

Table XI presents the effect of several coal preparation plant waste materials on product distribution and conversion of Elkhorn #3 coal. All of the materials show some enhancement of oils production.

Table XII shows the effect of varying proportions of Fe_2O_3 in the presence of either fly ash or silica on the product distribution and conversion of Elkhorn #3 coal. The product distributions and specifically the oils productions does not change within experimental error with the different proportions of the additives.

Table XIII shows that there were no substantial effects on product distribution or conversion produced when using four different mesh sizes of quartz. It is notable that these particular quartz samples seem ineffective compared with the quartz additive from a different source used in previous experiments shown in Table V. The quartz of Table V used in producing 30% oils was a naturally occurring crystalline SiO_2 ground to -325 mesh. In contrast to the crystalline quartz, the quartz used in producing the results in Table XIII, showing an average of 14% oils, was a precipitated silicon oxide which has a crystalline (quartz) core but an amorphous silicon oxide surface.

Table XIV presents the product distribution of experiments performed with Kentucky #9 coal. The coal without an additive converts more easily

to oil than does the Elkhorn #3 coal. The product distribution with Robena mine pyrite and Kentucky #9 coal is within experimental error of that of Elkhorn #3 coal and Robena mine pyrite.

Minerals Plus Pyrite. Since pyrite is present in most coals, and since pyrite generally has a positive effect on oils production in liquefaction processes, the enhancement or inhibition of oils production due to the presence of other minerals in addition to pyrite is of interest. Table XV presents the results of several liquefaction experiments with minerals plus pyrite. A modified solvent separation scheme using no sonication was used in obtaining the data of Table XV which resulted in slightly lower conversion data, lower oils fractions data, and higher asphaltenes fractions compared to data obtained using the sonifier in the separation scheme. Therefore, the data in Table XV are not directly comparable to data in other tables. In general, those minerals or additives which are beneficial in producing oils without pyrite are also beneficial in the presence of pyrite.

Mineral Alteration in Disposable Catalysts. Selected disposable catalysts were analyzed by x-ray powder diffraction methods to determine what if any changes occurred in the catalysts during a coal liquefaction reaction. The disposable catalysts used were:

(1) Robena pyrite (FeS_2)

(2) reduced Robena pyrite ($Fe_{1-x}S$)

(3) red mud from an alumina plant waste settling tank that is a mixture of goethite ($FeO(OH)$) and boehmite ($AlO(OH)$) plus amorphous iron and aluminum oxides

(4) hematite (Fe_2O_3)

(5) Elkhorn #3 coal LTA

(6) calcite ($CaCO_3$)

(7) quartz (SiO_2)

(8) bornite (Cu_5FeS_4)

(9) montmorillonite

The mineral alteration should be of three types: (1) recrystallization, (2) decrystallization, and (3) dehydration.

Recrystallization is a rearrangement of the internal structure of the mineral usually caused by either heat or pressure or both. Recrystallization may involve loss of an ion as in the case of pyrite going to pyrrhotite, or it may be only a rearrangement as in hematite to maghemite. Amorphous material may also crystallize to form a material that can be detected by XRD, but normally this requires conditions not found in the liquefaction reaction. Recrystallization is an easily detectable reaction and can be expected in many sulfide and easily reducible oxide minerals.

Decrystallization is the disruption of a structure to produce an x-ray amorphous state. An example of this is goethite which decomposes below 440°C into an amorphous iron oxide. Decrystallization is difficult to detect by XRD since the reaction product is amorphous and can be identified only as a reduced intensity of the diffraction peaks after the liquefaction reaction.

Dehydration is the loss of water without a disruption of the crystal structure. The effect is most often observed in clay minerals and zeolites. The amount of water contributed to the system may be negligible compared to that produced by the liquefaction reaction. Minerals that are easily re-hydrated, for example the iron sulfates, may be affected by this water, i.e. dissolved.

Within the limits of XRD, this investigation determined (1) the mineral composition of the original additive, (2) the type and amount of recrystallization, and (3) the amount of decrystallization of the disposable catalysts studied.

414

Alteration of Minerals During Coal Liquefaction. The Elkhorn #3 coal used in this study has an ash composition shown in Table IV and a total low temperature ash content of 17.8%. At a ratio of 3 grams coal to 1 gram catalyst this gives a dilution of 1 part catalyst residue to 0.534 parts coal ash residue. Because of this dilution, the calcite, gypsum, smectite, chlorite, and mica-smectite peaks were obscured and could not be detected after reaction; however, kaolinite, mica, and quartz had quite intense peaks and the reaction product of the pyrite, pyrrhotite, was also detectable. The reaction products of the disposable catalysts studied represent actual coal liquefaction runs in which the catalyst was added to the Elkhorn coal and then reacted. Before determining the amount and type of alteration the patterns were corrected for this ash dilution.

Major mineral alterations observed as being caused by the liquefaction process were:

(1) pyrite (FeS_2) recrystallized to pyrrhotite ($Fe_{1-x}S$) (the FeS_2 in the Elkhorn #3 coal is also recrystallized to $Fe_{1-x}S$).

(2) hematite (α Fe_2O_3) recrystallized in maghemite (γ Fe_2O_3).

(3) goethite (α $FeO(OH)$) and boehmite ($AlO(OH)$) decrystallized into an amorphous product.

(4) gypsum ($CaSO_4 \cdot 2H_2O$) dehydrated to anhydrite ($CaSO_4$) in Elkhorn #3 coal minerals.

In the reaction system used in these experiments, the amount of sulfur readily available for sulfiding the α Fe_2O_3 additive is less than 10% of the amount needed to form iron sulfide, FeS, from α Fe_2O_3. Consequently, after the reaction, the Fe_2O_3 present is a high temperature form of γ Fe_2O_3. The amount of iron sulfide stoichiometrically possible is below the limits of detection by x-ray diffraction analysis. The results are tabulated in Table XVI.

Minerals unaffected by the liquefaction reaction were: montmorillonite, calcite, quartz and reduced Robena pyrite. The montmorillonite was dehydrated slightly, but does not begin to loose structural water until above 400°C. Montmorillonite will absorb up to 5% water that is lost below 200°C on its cation exchange complex. The calcite and quartz used in this study were simply unreactive in the liquefaction reaction conditions. The reduced Robena pyrite was already converted to pyrrhotite so that it was not changed by the liquefaction reaction.

At this time, little is known of the synergistic or antagonistic effects coal ash may have on these types of catalysts nor is anything known about mixtures of catalysts and their interactions. A knowledge of the thermal stability of catalytic minerals would be an aid in predicting reaction products. While much is known about the endotherms and exotherms of minerals determined from DTA, DSC, and TGA little is known about what corresponding alterations have taken place in the minerals.

The information available from this study indicates that disposable catalysts show a wide response to liquefaction reactions ranging from no effect at all on the catalyst to complete conversion to another mineral. Easily reducible and thermally unstable minerals will recrystallize or de-crystallize depending on conditions. Hydrated minerals will dehydrate and add some water to the system.

ACKNOWLEDGEMENTS
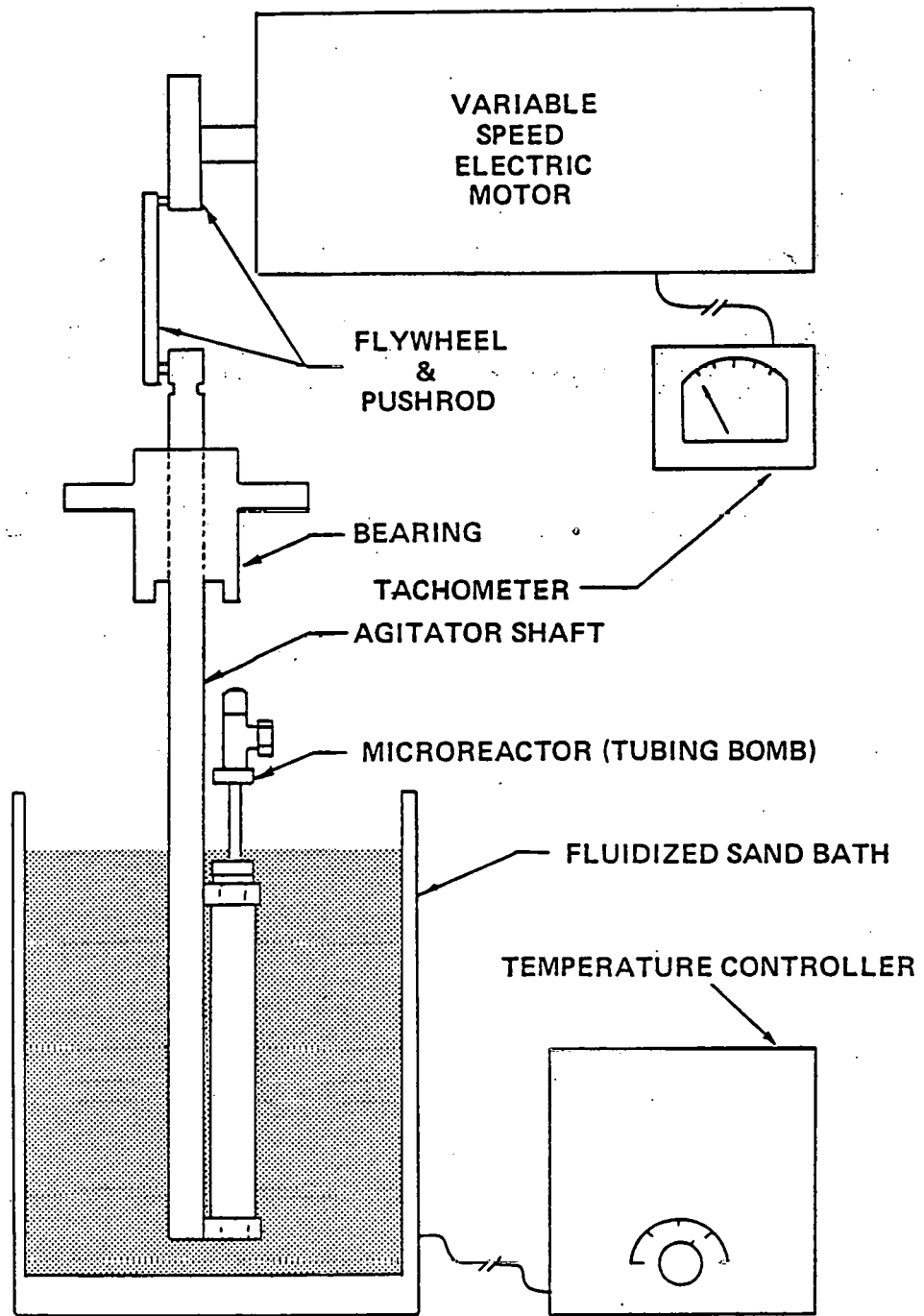
FIGURE 1: REACTOR SYSTEM USED IN LIQUEFACTION EXPERIMENTS

The labels in the figure are:

- VARIABLE SPEED ELECTRIC MOTOR
- FLYWHEEL & PUSHROD
- BEARING
- TACHOMETER
- AGITATOR SHAFT
- MICROREACTOR (TUBING BOMB)
- FLUIDIZED SAND BATH
- TEMPERATURE CONTROLLER
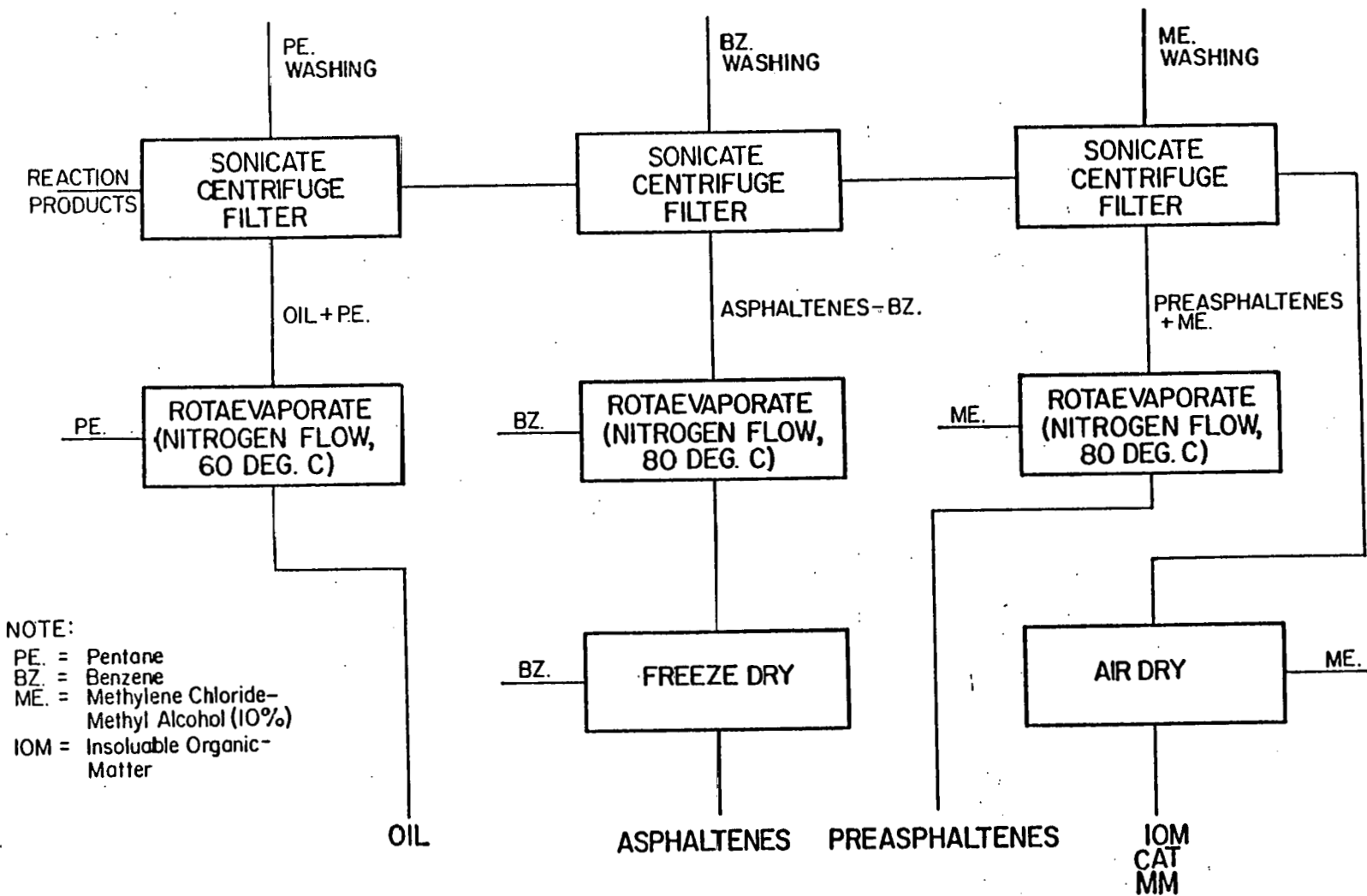
FIGURE 2. BLOCK DIAGRAM FOR PRODUCT SEPARATION
PROCEDURE

Reaction Conditions: 6g Solvent (Air Product, CPDU 121);
3g Elkhorn #3 coal; 1g presulfided Co-Mo-Al;
1250 psig initial H_2 pressure at ambient
temperature; 30 mins reaction time; 860 RPM;
46.3 cc reactor volume.
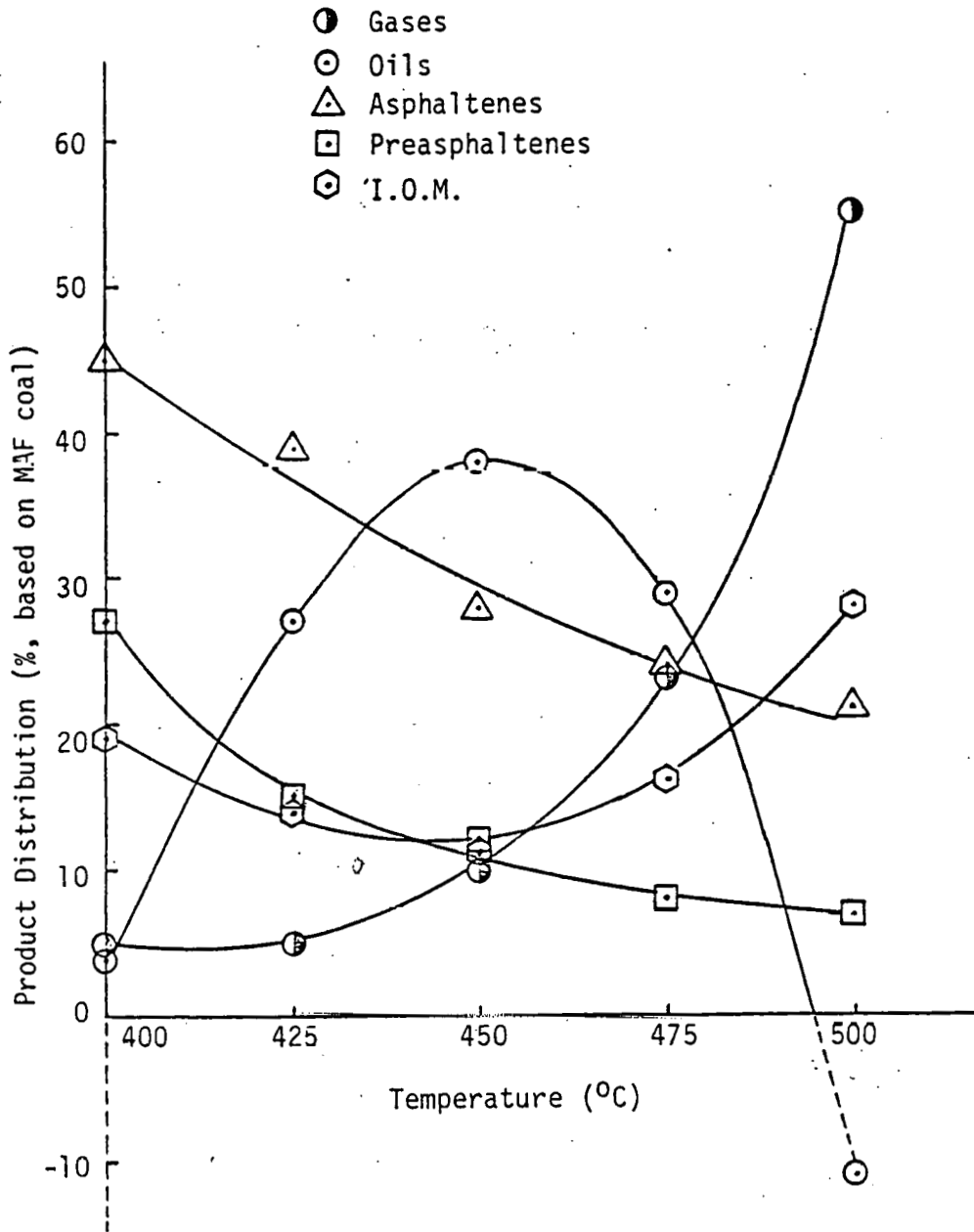
◐ Gas
⊙ Oils
△ Asphaltenes
⊡ Preasphaltenes
⬡ I.O.M.

Figure 3. Temperature Dependency of Oils, Asphaltenes,
Preasphaltenes, and Insoluble Organic Matter
(I.O.M.) in Coal Liquefaction Experiments
Catalyzed by Co-Mo-Al (Modified separation
technique used to determine fractions).

420

◐ Gases
⊙ Oils
△ Asphaltenes
⊡ Preasphaltenes
⊙ I.O.M.

Figure 4. Effect of Reaction Temperature
on Coal Liquefaction

421

Figure 5.

Effect of Agitation Rate on Coal Liquefaction

Reaction Conditions: 6g Solvent (Air Products, CPDU 121); 3g Elkhorn #3 coal; 1g (140 x 200 Mesh) pyrite; 1250 psig initial H_2 pressure at 25°C; 1 hour reaction time; 450°C; 46.3 cc reactor volume

* No Steel Balls

Gases
Oils
Asphaltenes
Preasphaltenes
I.O.M.

Product Distribution (%, based on MAF coal)

Agitation Rate (RPM)

Table I: Description and Source of Additives

1. All minerals are ground to -150 to -325 mesh as indicated below unless already in powder form. After grinding if necessary the minerals are dried at 100°C for 12 hours and allowed to cool in a desiccator before use unless otherwise indicated.

2. Albanian Chrome Ore Concentrates (Chromic oxide - 49%, Fe_2O_3-15%, Magnesia 19%) Interlake, Inc., Beverly, OH.

3. Apatite, $Ca_5(PO_4)_3(F,OH)_3$. Source: Stauffer Chemical Company; Westport, CT. (203) 222-3000. Received in powder form.

4. Bornite, Cu_5FeS_4 (copper ore); -115 mesh. Source: Mr. Rich Ramseier, Chief Geologist, The Anaconda Company, Geological Dept., 520 Hennessy Bldg., P.O. Box 621, Butte, MT 59701. (406) 723-4311.

5. Brown Fly and Bottom Ashes*, (SiO_2 - Fly 52%, Bottom 47%, Al_2O_3 - Fly 29%, Bottom 23%, Fe_2O_3 - Fly 12%, Bottom - 22%). Kentucky Utilities.

6. Calcite, $CaCO_3$, Gird Creek, Ravalli, MT, -115 mesh. Source: David New Minerals, Providence, UT.

7. Chabazite, $CaAl_2Si_4O_{12} \cdot 6H_2O$. W. R. Grace and Company, Upper Darby, Pennsylvania.

8. Co-Mo-Al, CoMox 451, presulfided at Auburn to 2.76% sulfur. Source: Laporte Industries, Inc.

9. Melanterite ($FeSO_4 \cdot 7H_2O$). Textile Chemical Company, Reading, PA.

10. Diatomaceous Earth Filter Aid, Filter Cel, 5/20/80, sample number 56678. Source: Catalytic, Inc., Wilsonville, AL.

11. Dolomite, $CaMg(CO_3)_2$. Source: David New Minerals, Providence, UT. Sample from Snarum, Norway. Ground to -115 mesh.

12. Feldspar, $KAl Si_3O_8$, Type NC-4, received in powder form. Source: Feldspar Corporation, Box 99, Spruce Pine, NC 28777. (704) 765-9051.

13. Fe_2O_3, Type I - 116, certified, received in powder form. Source: Fisher Scientific Co., Fairlawn, NJ 07410.

14. Green River Fly and Bottom Ashes*. Kentucky Utilities (SiO_2 - High Fly 41%, Blend Fly 48%, Bottom 50%, Al_2O_3 - High Fly 17%, Blend Fly 15%, Bottom 20%, Fe_2O_3 - High Fly 32%, Blend Fly 32%, Bottom 24%).

15. Gypsum, $CaSO_4 \cdot 2H_2O$ - #105 Terra Alba received in powder form. Source: C. A. Wagner, Philadelphia, PA. (215) 457-0600.

16. Illite, $KAl_2(Al,Si)_3O_{10}(OH)_2$. Source: Source Clay Minerals Repository (W.D. Johns), Dept. of Geology, University of Missouri, Columbia, MO 65211, (314) 822-3785. Screened to -115 mesh.

17. Kaolinite, $Al_2Si_2O_5(OH)_4$. Burgess #10, received in powder form. Source: Burgess Pigment Co. (Dan Adrian), P.O. Box 349, Sandersville, GA (912) 552-2544.

18. Kerr McGee Residue, KM-ME 103/V107 Ash Conc., Run 150-247, 10/19/78, S.N. 40478 #2. Source: Catalytic, Inc., Wilsonville, AL.

19. K_2CO_3. Source: Fisher Scientific Co., Number P-208 A.C.S. grade. In powder form.

20. Magnetite, $FeFe_2O_4$, Source: Received from Air Products and Chemicals, Inc., Box 538, Allentown, PA 18105. Sample Number CPDU-175 (originally from U.S. Steel).

21. Mica, $KAl_2(AlSi_3)O_{10}(OH)_2$. Source: Ontario Canada.

22. Molybdic Oxide, (MO-58.7%). Climax Molybdenum Company, Greenwich, CT.

23. Montmorillonite, $(Na,Ca)_{0.33}(Al,Mg)_2Si_4O_{10}(OH)\cdot nH_2O$, type -Hydrite PX, Source: Georgia Kaolin Co., 433 N. Broad St., Elizabeth, NJ (201) 352-9800.

24. Mordenite, $(Ca,Na_2K_2)Al_2Si_{10}O24\cdot7H_2O$. W. R. Grace and Company, Upper Darby, PA.

25. Sodium Carbonate Na_2CO_3. Source: Fisher Scientific Co., Number S-263.

26. Oil Shale, Source: John Ward Smith, Div. Manager, Div. of Resource Characterization, U.S. Department of Energy, Laramie Energy Technology Center, P.O. Box 3395, University Station, Laramie, Wyoming 82071. Preparation. The oil shale was received in a single piece. The oil shale was broken into 1/8 inch or smaller pieces, heated in air at 400°C for six hours to release the oil. The remaining solid residue was ground to -115 mesh.

27. Paradise Fly and Bottom Ashes*, (SiO_2 - 43%, Al_2O_3 - 18.5%, Fe_2O_3 - 30%), TVA.

28. Pyrite, FeS_2 from Robena Mine, -325 mesh. Prepared by Air Products and Chemicals, Co., Box 538, Allentown, PA 18105 (215) 398-4911. Original source, U.S. Steel Corporation, Robena Mine, Angelica, PA.

29. Quartz, SiO_2, U.S.A. type natural crystal, ground to -115 mesh. Source: Gary Johnson, Sawyer Research Products, 35400 Lakeland Blvd., East Lake OH (216) 951-8770. Typical analysis is 99.5% SiO_2. Impurities include Al 10 to 15 ppm, Fe<10 ppm, Mg<5ppm, Ti<5ppm, Ca<5ppm.

30. Quartz, 5μ, 10μ, 15μ, 30μ. Min-u-sil precipitated SiO_2. Received from Air Products and Chemicals, Inc., Allentown, PA 18105.

31. Red Mud, Bayer Process red mud waste from Kaiser Aluminum Co., -150 mesh. Source: Mr. I. L. Feld, Assistant to the Research Director, U.S. Dept. of Interior, Bureau of Mines, Tuscaloosa Research Center, P.O. Box L, University, AL 35486. (205) 758-0491.

32. Red Oxide, Ferro, Ottawa Chemical Division, Toledo, OH.

33. Reduced Robena Pyrite, Supplied by Dr. Diwakar Garg, Air Products and Chemicals, Inc., Box 538, Allentown, PA 18105. Sample No. 5429-76-7. Note: This sample was not dried at 100°C, but used as received.

34. Silica, -240 mesh, received from Air Products.

35. Speculite (Fe_2O_3 - 94%, SiO_2 - 5%). Chemalloy Company Inc., Bryn Mawr, PA.

36. SRC Residue, D102 Mineral Residue, 140-B-MB, 7/9/78, S.N. - 39198. Source: Catalytic, Inc., Wilsonville, AL.

37. X-Type Molecular Sieve, W. R. Grace and Company, Upper Darby, PA.

*Samples were supplied by Dr. Alan E. Bland of the Institute of Mining and Minerals, University of Kentucky, Lexington, KY

Table II

Analysis of Elkhorn #3 and Kentucky #9 Coal and 550°F+ Fraction of SRCII Fuel Oil Blend

	Coals		Solvent
	Elkhorn #3	Kentucky #9	SRCII Blend
Proximate Analysis (wt%)			
Moisture	1.81+0.03	1.6	
Volatile Matter	37.6+0.1	36.1	
Fixed Carbon	46.0	48.9	
Dry Ash	14.60+0.02	13.1	
Ultimate Analysis (wt%)			
Carbon	69.4	70.4	88.8
Hydrogen	4.88	4.76	7.40
Nitrogen	1.00	1.50	1.96
Sulfur	1.94	3.30	1.20
Oxygen (by difference)	8.18	6.07	0.48
Sulfur (wt%)			
Total Sulfur	1.94	3.30	
Sulfate Sulfur	0.04	0.10	
Pyrite Sulfur	1.19	1.60	
Organic Sulfur	0.75		
Product Distribution			
Oil			95.0
Asphaltenes			4.53
Preasphaltenes			0.42
I.O.M.			0.10

Table III

Effect of Pyrite Particle Size on Product Distribution and Conversion

Particle Size	+40 Mesh	40 x 80 Mesh	80 x 140 Mesh	140 x 200 Mesh	Robena pyrite -325 Mesh
Gases (g)	0.23	0.23	0.24	0.25	0.25
Oils (g)	5.87	5.97	5.94	5.90	5.74
Asphaltenes (g)	0.89	0.91	0.87	0.87	1.06
Preasphaltenes (g)	0.29	0.28	0.30	0.29	0.17
Residues (g)	1.36	1.37	1.34	1.33	1.16
Total (g)	8.64	8.76	8.69	8.64	8.38
Normalized	-	-	-	-	-
Gases (g)	0.23	0.23	0.24	0.25	0.25
Oils (g)	6.63	6.65	6.67	6.67	6.69
Asphaltenes (g)	1.00	1.01	0.98	0.98	1.24
Preasphaltenes (g)	0.33	0.31	0.34	0.33	0.20
Residues (g)	1.54	1.53	1.50	1.50	1.35
Total (g)	9.73	9.73	9.73	9.73	9.73
% Gases	9	9	9	10	10
% Oils	36	37	38	38	39
% Asphaltenes	29	30	28	28	38
% Preasphaltenes	12	11	13	12	7
% I.O.M.	14	13	12	12	6
% Conversion	86	87	88	88	94

427

Table III con't

Reaction Conditions: 6g Solvent (Air Products, CPDU 121); 3g Elkhorn #3 coal; 1g Additive; 1250 psig initial H_2 pressure at 25°C; 1 hour reaction time; 46.3 cc reactor volume; 860 RPM; 450°C.

1. For the purpose of calculations, all pyrites are assumed to form FeS during reaction.

2. Pyrite samples were obtained from Air Products and Chemicals, Inc. X-ray diffraction showed that the +40 mesh sample was 95% pure pyrite and 40x80 mesh, 80x140 mesh, and 140x200 mesh were 97% pure pyrite.

Table IV

Elkhorn Ky #3 Coal Minerals

Ash - 14.6%

Low Temperature Ash - 17.8% (Original Minerals)

Minerals: X-Ray Diffraction Results of Low Temperature Ash Material

Kaolinite	35%
Pyrite	12%
Quartz	15%
Mica	15%
Calcite	9%
Gypsum	9%
Smectite	1-5%
Chlorite	1-5%
Mica-Smectite	1-5%

Table V

Effect of Minerals on Product Distribution and Conversion

Additives[1]	% Gas	% Oils	% Asphal-tenes	% Preasphal-tenes	% I.O.M.	% Conversion
Dolomite	12	15	35	14	24	76
Bornite	11	15	40	10	24	76
Mordenite	13	19	29	12	27	73
None	11±1	21±5	36±5	12±1	20±2	80±2
Silica	14	22	32	11	21	79
Illite	11	22	37	13	16	84
Calcite	11	22	38	13	16	84
Apatite	12	23	34	11	20	80
Feldspar	10	24	34	12	20	80
Mica	10	25	28	14	23	77
Chabazite	11	25	31	12	21	79
Zircon	9	25	35	14	17	83
Montmorillonite	9	27	31	10	23	77
Kaolinite	13	27	29	12	19	81
Albanian Chrome Ore	11	29	30	12	18	82
Gypsum	14	29	31	12	14	86
Quartz	7	30	32	12	19	81
Magnetite	11	32	32	13	12	88
Red Oxide	11	35	32	10	12	88
Robena Mine Pyrite	9	35	40	7	9	91
Speculite	12	35	31	10	12	88
$FeSO_4 \cdot 7H_2O$	8	42	35	9	6	94
Molybdic Oxide	3	56	28	2	11	89
Co-Mo-Al	5	66	15	8	6	94

Reaction Conditions: 6g Solvent (Air Products CPDU 121); 3g Elkhorn #3 Coal; 1g additive; 1250 psig H_2 initial H_2 pressure; 450°C; 1 hour reaction time; 46.3 cc reactor volume; 860 RPM

1. For the purpose of calculations all additives are assumed to remain unchanged except $FeSO_4 \cdot 7H_2O$ which is assumed to lose the water of hydration, and pyrite (FeS_2) which is assumed to form FeS.

Table VI

Effects of Chemicals and Waste Materials
on Product Distribution and Conversion

	Lime	X-Type Molecular Sieve	Na_2CO_3	Oil Shale	Reduced Pyrite	K_2CO_3	Fe_2O_3	Red Mud
% Gas	6	15	13	13	10	11	8	7
% Oils	$(25)^a$	17	19	22	37	39	46	49
% Asphaltenes	22	28	37	34	36	19	38	31
% Preasphaltenes	11	16	7	14	8	5	7	6
% I.O.M.	86	24	24	17	9	26	1	7
% Conversion	14	76	76	83	91	74	99	93

[a] ( ) indicates a negative value

Table VII

Effect of Ashing Temperature of Residues and Filter Aid on Product Distribution and Conversion

Ashing Temperature (°C)	SRC-I Ash (Filter Separated)			SRC-I Ash (Kerr-McGee Critical Solvent Deashing Process			Diatomaceous Earth Filter Aid		
	800	510	LTA	800	510	LTA	800	510	LTA
% Gas	12	11	10	10	8	9	10	8	10
% Oils	31	34	42	37	39	45	32	33	34
% Asphaltenes	30	32	26	32	31	28	28	29	27
% Preasphaltenes	11	9	7	9	9	7	11	10	9
% I.O.M.	16	14	15	12	13	11	19	20	20
% Conversion	84	86	85	88	87	89	81	80	80

Table VIII

Effect of Pyrite Reduced at Different Conditions on Product Distribution and Conversion

Additive	1	2	3	4	5	6	7
% Gas	5	8	8	9	10	7	11
% Oils	44	38	38	37	38	37	37
% Asphaltenes	30	32	31	29	29	32	31
% Preasphaltenes	8	9	10	10	9	9	9
% I.O.M.	13	13	13	15	14	15	12
% Conversion	87	77	87	85	86	85	88

Reaction Conditions: 6g solvent (Air Products CPDU 121); 3g Elkhorn #3 Coal; 1g additive; 1250 psig H_2 initial H_2 pressure; 450°C; 1 hour reaction time; 46.3 cc reactor volume; 860 RPM

1.

Additive	Type	Reaction Conditions*
1	-200 Mesh Pyrite	
2	Reduced Pyrite	$T = 400°C$, $P = 1000$ psig H_2, $t = 10$ min.
3	Reduced Pyrite	$T = 450°C$, $P = 1000$ psig H_2, $t = 10$ min.
4	Reduced Pyrite	$T = 500°C$, $P = 1000$ psig H_2, $t = 10$ min.
5	Reduced Pyrite	$T = 600°C$, $P = 1000$ psig H_2, $t = 10$ min.
6	Reduced Pyrite	$T = 450°C$, $P = 1500$ psig H_2, $t = 10$ min.
7	Reduced Pyrite	$T = 450°C$, $P = 500$ psig H_2, $t = 10$ min.

2. For the purpose of calculation the pyrite (FeS_2) is assumed to form FeS during reaction. The Reduced Pyrite samples, 2 through 7 are assumed to remain unchanged.

Table IX

Effect of Impregnating Coal with Co, Ni, and
Mo Compounds on Product Distribution and Conversion

Coal Impregnated with Additive	$Co(NO_3)_2 \cdot 6H_2O$	$Ni(NO_3)_2 \cdot 6H_2O$	$(NH_4)_6Mo_7O_{24} \cdot 4H_2O$
% Gas	13	11	9
% Oils	35	37	58
% Asphaltene	32	32	21
% Preasphaltenes	8	12	5
% I.O.M.	12	8	7
% Conversion	88	92	93

Reaction Conditions: 6g solvent; 1250 psig H_2; 450°C, 1 hour reaction time, plus (1) 3.139g Elkhorn #3 coal impregnated with 4.57% $Co(NO_3)_2 \cdot 6H_2O$, (cobalt II nitrate), (2) 3.140g Elkhorn #3 Coal impregnated with 4.57% $Ni(NO_3)_2 \cdot 6H_2O$ (nickel nitrate, hexahydrate), (3) 3.149g Elkhorn #3 Coal impregnated with 4.98% $(NH_4)_6Mo_7O_{24} \cdot 4H_2O$, (ammonium paramolybdate).

1. For the purpose of calculations the following assumptions are made:

   (a) $Co(NO_3)_2 \cdot 6H_2O$ yields Co_9S_8 during reaction.

   (b) $Ni(NO_3)_2 \cdot 6H_2O$ yields Ni_2S_3 during reaction.

   (c) $(NH_4)_6Mo_7O_{24} \cdot 4H_2O$ yields MoS_2 during reaction.

Table X

Effect of Several Fly Ashes and Bottom Ashes
on Product Distribution and Conversion

Additive	Brown Fly Ash	Paradise Bottom Ash	Green River (Blend) Fly Ash	Green River (High) Fly Ash	Paradise Fly Ash	Brown Bottom Ash	Green River Bottom Ash
% Gas	13	14	12	15	14	15	13
% Oils	12	18	21	20	24	24	33
% Asphaltenes	27	27	31	27	31	29	29
% Preasphaltenes	20	13	12	12	12	11	12
% I.O.M.	28	28	24	26	19	21	13
% Conversion	72	72	76	74	81	79	87

Table XI

Effect of Coal Preparation Plant Waste Materials on Product Distribution and Conversion

Additives	1	4	6	8	2	5	7	3
% Gas	17	13	11	14	16	10	15	13
% Oils	18	23	28	30	30	31	32	33
% Asphaltenes	27	28	30	28	27	29	27	27
% Preasphaltenes	24	13	13	14	11	13	11	13
% I.O.M.	14	23	18	14	16	17	15	14
% Conversion	86	77	82	86	84	93	85	86

1. | Additive No. | Sample | Plant/Company |
|---|---|---|
| 1 | 100% Elkhorn #3 | Hendrix/Beth-Elkhorn |
| 2 | 100% Elkhorn #3 | Gund/Island Creek |
| 3 | 100% Elkhorn #3 | Gund/Island Creek |
| 4 | 55% Hazard #4 | Spurlock/Island Creek |
| | 33% Elkhorn #2 | |
| | 12% Elkhorn #1 | |
| 5 | 51% KY #11 | Gilbrator/Amax |
| | 28% KY #13 | |
| | 22% KY #12 | |
| 6 | 100% KY #11 | Fies/Island Creek |
| 7 | 100% KY #9 | Hamilton #1/Island Creek |
| 8 | 53% KY #14 | Colonial/P&M |
| | 47% KY #17 | |

2. Additives were heated at 500°C for 2 hours in air before use.

Table XII

Effect of Fe_2O_3 with Fly Ash or Silica
on Product Distribution and Conversion

Additive Identification	(1)	(2)	(2) Non Calcined	(1) Non Calcined	(3)	(3) Non Calcined	(5)	(4)	(6)
% Gas	13	15	9	12	9	10	13	12	13
% Oils	25	26	30	30	31	33	34	35	35
% Asphaltenes	29	27	30	26	29	27	27	26	27
% Preasphaltenes	17	12	11	15	12	12	14	12	10
% I.O.M.	16	20	20	17	19	18	12	15	15
% Conversion	84	80	80	83	81	82	88	85	85

1. Mineral Contents of Additives

(1)	75% Iron Oxide[a]	25% Fly Ash
(2)	25% Iron Oxide[b]	75% Fly Ash
Non Calcined(2)	25% Iron Oxide[b]	75% Fly Ash
(3)	25% Iron Oxide[b]	75% Silica
Non Calcined(1)	75% Iron Oxide[a]	25% Fly Ash
Non Calcined(3)	25% Iron Oxide[b]	75% Silica
(4)	25% Iron Oxide[a]	75% Fly Ash
(5)	50% Iron Oxide[b]	50% Fly Ash
(6)	50% Iron Oxide[b]	50% Silica

2. Additives were ground to -200 mesh before use.

[a]Reagent grade Fe_2O_3

[b]Fe_2O_3 from U.S. Steel

Table XIII

Effect of Quartz Size on Product
Distribution and Conversion

Quartz Size	5µ	10µ	15µ	30µ
% Gas	21	15	16	21
% Oils	14	16	13	13
% Asphaltenes	25	26	26	25
% Preasphaltenes	11	14	13	13
% I.O.M.	29	29	32	28
% Conversion	71	71	68	72

Table XIV

Liquefaction Experiments with Kentucky No. 9 Coal

Additive	None	Robena Mine Pyrite
% Gas	13	11
% Oils	27	39
% Asphaltenes	31	31
% Preasphaltenes	13	11
% I.O.M.	16	8
% Conversion	84	92

Reaction Conditions: 6g Solvent (Air Products, CPDU 121); 3g Ky #9 coal; 1g additive; 1250 psig initial H_2 pressure; 450°C; 860 RPM; 1 hour reaction time; 46.3 cc reactor volume

1. For the purpose of calculations FeS_2 is assumed to form FeS, and the KY #9 coal contains 13.1% ash.

Table XV

Effect of Minerals and FeS_2 on Product Distribution
and Conversion (Modified Separation Procedure)

Additive[1]	None	Lime & FeS_2	Bornite & FeS_2	Calcite & FeS_2	Reduced Robena Pyrite	Mort-moril-lonite & FeS_2	FeS_2 Base-line	Quartz & FeS_2	"Red Mud" & FeS_2	Fe_2O_3	Co-Mo-Al
% Gas	11	9	18	18	10	10	9	18	6	11	10
% Oils	7	12	19	21	25	25	28	35	36	36	71
% Asphaltenes	45	42	42	37	41	45	43	27	40	34	11
% Preasphaltenes	12	4	5	7	10	5	5	6	5	8	2
% I.O.M.	25	33	16	17	14	15	15	14	13	11	6
% Conversion	75	67	84	83	86	85	85	86	87	89	94

1. FeS_2 is assumed to form FeS.

Table XVI

Alteration of Minerals After Coal Liquefaction

Disposable Catalyst	Original Minerals Present	Reaction Products	% Change
Robena Pyrite	Pyrite FeS_2, 75% plus 5% quartz, 20% carbonates, sulfates, and clays	Pyrrhotite $Fe_{1-x}S$	100% of FeS_2
Reduced Robena Pyrite	Pyrrhotite $Fe_{1-x}S$	Unchanged	0
Fe_2O_3	Hematite αFe_2O_3	Maghemite γFe_2O_3	100%
Red Mud	Goethite $FeO(OH)$, Boehmite $AlO(OH)$	Amorphous	100%
Quartz	Quartz SiO_2	Unchanged	0
Calcite	Calcite $CaCO_3$	Unchanged	0
Bornite	Bornite (Ca_5FeS_4), Pyrite FeS_2), Chalcopyrite ($CuFeS_2$) and Quartz	Chalcopyrite, Quartz	
Montmorillonite	Montmorillonite	Unchanged	0
Elkhorn #3 Coal LTA	Kaolinite, Mica, Pyrite, Gypsum Quartz, Calcite, <10% others	Pyrite to Pyrrhotite, Gypsum to Anhydrite, others unchanged.	

REPRINTED

FROM

I&EC

PROCESS DESIGN
AND DEVELOPMENT

Pyrite Catalysis in Coal Liquefaction

Diwakar Garg and Edwin N. Givens

Pyrite Catalysis in Coal Liquefaction

Diwakar Garg* and Edwin N. Givens

Corporate Research and Development Department, Air Products and Chemicals, Inc., Allentown, Pennsylvania 18105

Significant liquefaction catalysis by pyrite was observed for both Elkhorn No. 3 and Kentucky No. 9 coals. For both coals conversion and oil yield increased on addition of 10% pyrite to the feed slurry. Oil yields increased from 27.3 to 41.0% for Elkhorn No. 3 and from 15.3 to 34.9% for Kentucky No. 9. Gas yields increased slightly for Elkhorn No. 3 and were essentially unchanged for Kentucky No. 9. Hydrogen consumption, after correction for the increased hydrogen sulfide make, was likewise favorable. Sulfur contents in the residual SRC material increased in both cases. Solvent hydrogen content remained constant in the presence of pyrite, whereas it decreased significantly in the absence of pyrite. Solvent in the presence of pyrite without any coal present showed little change at process conditions.

Introduction

Coal is a complex mixture of organic and inorganic constituents each of which has a unique response during liquefaction. Indigeneous coal minerals are not inert ingredients, but they undergo chemical and physical changes as well as catalyze the transformation of the organic phase.

The conversion of the coal to liquid products has been found to increase as the mineral matter content and the concentration of the iron and titanium in the coal increase (Mukhurjee and Choudhury, 1976).

The catalysis by iron compounds in the coal liquefaction reaction has been known for a long time. The Germans

found that adding iron to the feed slurry improved the liquefaction of coal (Wu and Storch, 1968). In certain cases the addition of sulfur to the system also improved the effect of the iron (Wu and Storch, 1968). Their stoichiometries suggested that they knew iron sulfide (FeS) was the ultimate form of the iron in the liquefaction residue. With the advent of X-ray diffraction technique this FeS was found to be in the form of pyrrhotite (Given et al., 1974).

Wright and Severson reported that the addition of iron as contained in the residues from coal liquefaction increased the hydrogen transfer capacity of anthracene oil (Wright and Severson, 1972). Seitzer (1978) magnetically separated the iron sulfur compounds in coal liquefaction residues and used them as catalysts in subsequent liquefaction reactions. He found that the magnetically separated material had, per weight of iron, about the same catalytic effect as ferrous sulfate. Furthermore, he found that the magnetically separated material catalyzed the addition of hydrogen to the dissolved coal.

Moroni and Fischer (1980), who reviewed many papers in the area of coal mineral catalysis, concluded that pyrite was by far the major if not the only mineral constituent in coal to effectively catalyze coal conversion. Neither the addition of the coal liquefaction residue nor the magnetically separated residue delineated whether pyrrhotite had better catalytic activity than pyrite. A significant amount of work has been done more recently to determine the true catalytic activity of pyrite and pyrrhotite. Although pyrite and pyrrhotite have been found at times not to have a significant effect on coal conversion (Given et al., 1979), substantial increases in coal conversion with the addition of pyrite and pyrrhotite have been reported (Given, 1979). Furthermore, Given and co-workers reported that pyrrhotite prepared from the pyrite in coal had even greater activity than the sample prepared from macrocrystalline mineral pyrite.

The addition of pyrite to the reaction mixture was found to affect the coal liquefaction product distribution. Small improvements in recycle solvent yield were observed with the addition of 3% hand-ground pyrite (Solvent Refined Coal, 1979). However, no further improvement was reported on addition of pyrite up to a 7.5% level. Granoff and Baca observed increased yield of pentane soluble oil and decreased yield of asphaltene and preasphaltene with the addition of pyrite (Granoff and Baca, 1979). They found that conversion to benzene solubles increased from 61% to 78% with the addition of either pyrite or pyrrhotite. Likewise, they found that pentane soluble oil increased from 14% to 31% on addition of pyrrhotite, and went to 36% when -325 mesh pyrite was used.

Apparently the particle size of the pyrite plays an important role in catalyzing the coal liquefaction reaction. The catalytic activity of pyrite was shown to improve with the reduction of particle size (Guin et al., 1979). Significantly more oil production was reported with the use of finely divided pyrite (Anderson, 1979) than with hand-ground pyrite (Solvent Refined Coal, 1979).

Hydrogen addition to both the recycle solvent and SRC increased on addition of a low level of pyrite (Solvent Refined Coal, 1979). Hydrogenation activity increased by increasing the concentration of pyrite in the reaction mixture. In this study no significant change occurred in the sulfur content of either the recycle solvent or SRC, which is consistent with another study in which mineral pyrite was shown to catalyze hydrogenation of creosote oil but not hydrodesulfurization (Tarrer et al., 1977; Guin et al., 1978). The desulfurization activity of reduced pyrite

Table I. Chemical Analysis of Coal Samples

	wt %	
	Elkhorn No. 3	Kentucky No. 9
Ultimate Analysis (as received)		
carbon	69.40	70.42
hydrogen	4.88	4.76
oxygen	8.18	6.07
sulfur	1.94	3.30
nitrogen	1.00	1.50
Proximate Analysis (as received)		
volatile matter	37.56	36.13
fixed carbon	46.03	48.90
ash	14.60	13.10
moisture	1.81	1.60

Table II. Analysis of 550-850 °F Fraction of SRC-II Fuel Oil Blend

element	wt %
carbon	88.79
hydrogen	7.40
oxygen	1.96
nitrogen	1.20
sulfur	0.48
molecular weight	210

was found to be insignificant whereas pyrite itself promoted the desulfurization of benzothiophene (Guin et al., 1979). The same authors reported insignificant hydrogenation of dibenzothiophene in the presence of pyrite as well as reduced pyrite. In another study, reduced pyrite was shown to give higher conversion of thiophene compared to pyrite (Hamrin, 1976).

The effect of pyrite and reduced pyrite on hydrogenation of model compounds has been investigated by several workers. Pyrite was shown to have no activity in dehydrogenation of tetralin, whereas reduced pyrite showed significant activity in the dehydrogenation of tetralin (Lee et al., 1978; Guin et al., 1979). Similarly, reduced pyrite was shown to have higher naphthalene hydrogenation activity than pyrite itself (Guin et al., 1978). In another study, pyrite was shown to have hydrogenation activity in the tetralin/naphthalene system (Gangwar and Prasad, 1979).

In the present paper data are presented which show the catalytic activity of pyrite for solvent hydrogenation as well as coal liquefaction. The catalytic activity of pyrite for hydrogenation of the solvent was measured for solvent alone as well as in the presence of coal. The catalytic activity for the coal conversion reactions is related to the product distribution including hydrocarbon gas make, oil yield, asphaltene and preasphaltene yields, and degree of coal conversion. All of the data reported in this paper refer to results in a continuous 100 pounds per day coal process unit.

Experimental Section

Materials. Elkhorn No. 3 was a run-of-mine sample taken from a mine in Floyd County. The Kentucky No. 9 coal was a sample taken from a preparation plant after washing. The coal samples were ground to 95% -200 mesh particles and dried in air. The coals were screened through a 150 mesh sieve prior to use. The detailed analysis of the screened coals is reported in Table I.

The 550-850 °F cut of SRC-II Fuel Oil Blend supplied by The Pittsburg and Midway Coal Mining Co. was used as a process solvent. The chemical analysis of the process solvent is shown in Table II. The solvent contained 90.8%

Table III. Analysis of Pyrite

	wt %
carbon	4.48
hydrogen	0.34
nitrogen	0.61
sulfur	41.34
oxygen	5.97
iron	42.30
other impurities (by difference)	4.96
total	100.0

surface area = 1.0 m²/g

pentane-soluble oils, 8.9% asphaltenes, and 0.3% preasphaltenes.

Pyrite sample was received from an operating mine in southwestern Pennsylvania. The sample was dried at 110 °C in nitrogen and then ground to 99.9% minus 325 U.S. mesh size in the presence of liquid nitrogen. The chemical analysis of the pyrite is given in Table III. The sample was comprised of 75% pyrite, 5% carbonaceous organic material, and 20% magnetite, quartz, and other inorganic materials. The BET surface area of the pyrite was 1.0 m²/g and it was relatively nonporous.

Equipment. Process studies were done in a continuous 100 pound/day coal liquefaction unit equipped with a continuous sitrred autoclave. The use of a stirred tank reactor ensured that solvent vaporization matched that of an actual SRC-I dissolver and that coal minerals did not accumulate. Since there was no slurry preheater, all of the sensible heat had to be provided by resistance heaters on the reactor. Because of this high heat flux, the reactor wall was about 27 °F hotter than the bulk slurry. Multiple thermocouples revealed that the slurry temperature inside the reactor varied by only 9 °F from top to bottom. A detailed description of the reactor is presented elsewhere (Skinner and Givens, 1980).

The products were quenched to 320 °F before flowing to a gas/liquid separator that was operated at system pressure. The slurry was throttled into the product receiver while the product gases were cooled to recover the product water and organic condensate. The product gases were then analyzed by an on-line gas chromatograph.

Procedure. Coal liquefaction runs were performed at 850 °F temperature, 2000 psig hydrogen pressure, 2000 rpm stirrer speed, hydrogen feed rate equivalent to 5.5 wt. % of the coal, and a superficial slurry space velocity of 1.5 inverse hours. The coal concentration in the feed was 30 wt %. The concentration of pyrite used was 10 wt % of feed slurry.

At least 10 reactor volumes of the product were discarded prior to collecting a product sample. A complete sample consisted of one 8-oz product slurry, one 1-L product slurry as back-up sample, a light condensate sample, and a product gas sample.

The product slurry from the continuous reactor was solvent separated into four fractions: (1) pentane-soluble material (oil), (2) pentane-insoluble and benzene-soluble material (asphaltene), (3) benzene-insoluble and pyridine-soluble material (preasphaltene), and (4) pyridine-insoluble material. The latter contains insoluble organic material (IOM) and mineral residue. A detailed procedure for performing this separation will be reported elsewhere. The overall coal conversion is calculated as the fraction of organic material (Moisture-ash-free coal) soluble in pyridine.

Results and Discussions

Solvent Hydrogenation. Process solvent was treated with hydrogen both in the presence and absence of pyrite.

Table IV. Solvent Hydrogenation in the Presence and Absence of Pyrite[a]

	feed compn		
	orig solv	100% solv	90% solv + 100% pyrite
temperature, °F	-	850	850
pressure, psig	-	2000	2000
hydrogen treat rate, wt % solvent	-	2.21	2.03
reaction time, min	-	61	60
product distribution, wt %			
HC	-	0.9	1.8
CO, CO$_2$	-	0.3	0.2
H$_2$S	-	0.2	0.2
NH$_3$	-	0.01	0.4
oil	90.8	87.3	92.9
asphaltene	8.9	7.6	3.2
preasphaltene	0.4	3.3	0.7
insoluble organic material	0.0	0.2	0.0
water	-	0.1	0.8
hydrogen consumption,[b] wt % solvent	-	-0.20	0.36

[a] Oil: pentane solubles; asphaltene: pentane insolubles, benzene solubles; preasphaltene: benzene insolubles, pyridine solubles; insoluble organic material: pyridine insolubles. [b] Hydrogen consumption does not include the hydrogen required for reducing pyrite (FeS$_2$) to reduced pyrite (FeS).

Table V. Elemental Analysis of Oil Fraction in Solvent Hydrogenation Reaction

	feed compn		
	orig solv	100% solv	90% solv + 10% pyrite
temperature, °F	-	850	850
oil fraction			
carbon	89.57	89.64	89.25
hydrogen	7.72	7.40	7.74
oxygen (direct)	1.32	1.30	1.39
nitrogen	0.88	1.17	1.19
sulfur	0.51	0.50	0.44

In the absence of pyrite lower molecular weight oils and asphaltenes shifted slightly to higher molecular weight preasphaltenes. The concentration of preasphaltenes increased from 0.4 to 3.3% (Table IV).

An elemental hydrogen balance showed that hydrogen in the solvent oil fraction decreased from 7.7 to 7.4% (Table V). The loss in hydrogen can be accounted for by the production of light hydrocarbon gases. Although no changes were noted in carbon, oxygen, and sulfur content of the oil, the nitrogen content increased from 0.9 to 1.2%.

In the presence of pyrite, process solvent underwent net solvent hydrogenation, the product distribution shifted to lower molecular weight material (Table IV), and the asphaltene fraction decreased from 8.9 to 3.2%. Also the hydrogen content of the oil fraction remained at its original 7.7%, which corresponds to a net consumption of hydrogen. Slight changes in carbon and oxygen content of the oil fraction were noted. The increase in nitrogen content of the oil from 0.9 to 1.2% was similar to that of the oil fraction obtained from reaction in the absence of pyrite. Surprisingly, the sulfur content of the oil fraction was found to decrease slightly. The yields of hydrocarbon gases, ammonia, water, and oil were higher in the presence of pyrite. The hydrogen content of the oil fraction remained constant in the presence of pyrite, whereas the oil fraction lost hydrogen in the absence of pyrite. This corresponds to a higher hydrogen consumption in the presence of pyrite. The hydrogen necessary to reduce the

Table VI.   Liquefaction of Elkhorn No. 3 Coal in the Presence and Absence of Pyrite

	feed compn	
	70% solv + 30% coal	60% solv + 30% coal + 10% pyrite
temperature, °F	850	850
pressure, psig	2000	2000
residence time, min	38	41
hydrogen treat rate, MSCF/T	19.9	21.9
product distribution, wt % MAF Coal		
HC	4.2	5.3
CO, CO$_2$	1.0	1.2
H$_2$S	1.3	2.8
NH$_3$	0.0	0.2
oil	27.3	41.0
asphaltene	14.8	11.3
preasphaltene	30.1	24.3
I.O.M.	18.1	10.4
water	3.2	3.5
conversion, % MAF	81.9	89.6
hydrogen consumption,[a] wt % MAF	1.4	2.0
oil hydrogen content, wt %		
start	7.7	7.7
finish	7.5	7.7
SRC sulfur, %	0.6	0.7

[a] Hydrogen consumption does not include the hydrogen required for reducing FeS$_2$ to FeS.

pyrite was 0.14% by weight of solvent. Even eliminating this added hydrogen consumption by pyrite, hydrogen was still consumed in the reaction. Again, hydrogen consumption was due to hydrocarbon gases, hydrogen sulfide, ammonia, solvent hydrogenation, and water production.

The solid residue from the solvent hydrogenation run was separated by filtration and analyzed by X-ray diffraction. No unreacted pyrite was detected. The sample pattern matched the pattern for pyrrhotite 11C which is FeS$_{1.099}$. Therefore, pyrite was completely reduced.

Coal Liquefaction

Liquefaction of Elkhorn No. 3 Coal. The conversion of Elkhorn No. 3 coal was reported earlier by Granoff and Thomas (1977) as having low conversion on liquefaction (62%), apparently due to the use of acetone as a wash solvent. In the studies reported here we also observed a low conversion (Table VI). In the presence of pyrite, coal conversion increased to 90%. The addition of pyrite increased not only coal conversion but also the yields of hydrocarbon gases, carbon monoxide, carbon dioxide, hydrogen sulfide, and ammonia. The oil yield increased from 27 to 41%, asphaltenes decreased from 15 to 11%, and preasphaltenes decreased from 30 to 24%. Pyrite also increased hydrogen consumption from 1.4 to 2.0% based on elemental hydrogen balance. An additional amount of 0.5 wt % hydrogen was consumed in reducing the added pyrite. The increased hydrogen consumption went to increasing the yields of gases and benzene solubles. In the absence of pyrite the hydrogen content of the oil fraction decreased while in the presence of pyrite the hydrogen content remained constant (Table VI).

The addition of pyrite resulted in an increase in sulfur contents of the oil and the SRC fractions. In the oil fractions the sulfur increased from 0.3 to 0.5% and in the SRC the sulfur increased from 0.6 to 0.7%. Also, pyrite caused a reduction in the nitrogen content of the oil fraction from 1.3 to 1.0% percent (Table VII). The in-

Table VII.   Distribution of Elements in Various Liquefaction Reaction Fractions (Elkhorn No. 3 Coal) in the Presence and Absence of Pyrite

Reaction without Pyrite

	wt %				
	C	H	O	N	S
oil	89.05	7.49	1.79	1.33	0.34
asphaltene	89.10	6.48	4.53	2.24	0.66
preasphaltene	84.06	5.50	5.44	3.30	0.58

Reaction with Pyrite

	wt %				
	C	H	O	N	S
oil	89.12	7.70	1.76	0.96	0.49
asphaltene	85.12	6.24	5.65	2.37	0.62
preasphaltene	83.17	5.65	-	3.28	0.71

Table VIII.   Liquefaction of Kentucky No. 9 Coal in the Presence and Absence of Pyrite

	feed compn	
	70% solv + 30% coal	60% solv + 30% coal + 10% pyrite
temperature, °F	850	850
pressure, psig	2000	2000
residence time, min	37	35
hydrogen treat rate, MSCF/T	20.6	21.8
product distribution, wt % MAF coal		
HC	5.1	4.9
CO, CO$_2$	0.6	0.8
H$_2$S	1.7	0.4
NH$_3$	0.0	0.3
oil	15.3	34.9
asphaltene	30.0	19.8
preasphaltene	28.2	25.6
I.O.M.	12.8	7.4
water	6.5	5.9
conversion, % MAF	87.2	92.6
H$_2$ consumption,[a] wt % MAF	1.5	2.4
oil H$_2$ content, wt %		
start	7.7	7.7
finish	7.3	7.7
SRC sulfur, %	1.0	1.2

[a] H$_2$ consumption does not include the hydrogen required for reducing FeS$_2$ to FeS.

creased nitrogen removal was reflected in an increased yield of ammonia in the off-gas stream. These results showed that for Elkhorn No. 3 coal pyrite catalyzed the oil and gas production, increased coal conversion, increased hydrogenation of process solvent, and catalyzed nitrogen removal from the oil fraction.

Liquefaction of Kentucky No. 9 Coal. Addition of pyrite increased the conversion of Kentucky No. 9 from 87 to 93%. Also, carbon monoxide, carbon dioxide, and ammonia production marginally increased. The oil yield increased from 15 to 35%, the asphaltene yield decreased from 30 to 20%, and the preasphaltene yield decreased from 28 to 26% (Table VIII). The additional converted coal ended up in the oil and gas product. The addition of pyrite increased hydrogen consumption from 1.5 to 2.4%. Also, an additional amount of 0.5% hydrogen was consumed in reducing the added pyrite. The oil hydrogen content decreased in the absence of pyrite but remained the same in its presence. The elemental compositions of the various fractions (Table IX) showed no significant

Table IX. Distribution of Elements in Various
Liquefaction Reaction Fractions (Kentucky No. 9 Coal)
in the Presence and Absence of Pyrite

Reaction without Pyrite

	wt %				
	C	H	O	N	S
oil	89.53	7.30	1.65	0.96	0.56
asphaltene	89.19	6.41	4.35	2.20	0.86
preasphaltene	83.94	5.39	6.03	2.42	1.17

Reaction with Pyrite

	wt %				
	C	H	O	N	S
oil	89.05	7.71	1.74	1.03	0.47
asphaltene	85.39	6.83	4.41	2.42	0.95
preasphaltene	83.52	5.69	5.76	2.53	1.68

differences except for an increase in asphaltene and preasphaltene sulfur content when pyrite was added. No reduction in nitrogen content of the various fractions was noted, but the total nitrogen content of the liquid product (oil + asphaltene + preasphaltene) decreased slightly from 2.0 to 1.9 wt % on addition of pyrite. This information showed that pyrite was active as a denitrogenation catalyst. Addition of pyrite to Kentucky No. 9 coal improved conversion and oil production and promoted rehydrogenation of the process solvent.

Conclusion

The addition of pyrite affects the process solvent hydrogenation reaction. Under the reaction conditions employed here, process solvent is found to dehydrogenate in the absence of pyrite. The product distribution also is shifted toward higher molecular weight product. The pyrite addition causes the hydrogenation of the process solvent as well as shifts the product distribution toward low molecular weight product. The pyrite addition also catalyzes the coal liquefaction reaction. It improves the coal conversion, increases the oil and gases production, increases hydrogen consumption, and rehydrogenates the process solvent. Pyrite addition also helps in denitrogenation of the total liquid product obtained with Elkhorn No. 3 and Kentucky No. 9 coals.

Literature Cited

Anderson, R. P. "Low Cost Additives in the SRC Processes"; paper presented in the Department of Energy Project Review Meeting on Disposable Catalysts in Coal Liquefaction held at Albuquerque, NM, June 1979.

Gangwar, T. E.; Prasad, H. Fuel 1979, 58, 577.

Given, P. H.; Spackman, W.; Davis, A.; Walker, D. L., Jr.; Lovell, H. L. "The Relation of Coal Characteristics to Coal Liquefaction Behavior"; Report No. 1 Submitted to NSF (RANN Division) by The Pennsylvania State University, Mar 15, 1974.

Given, P. H.; Spackman, W.; Davis, A.; Walker, P. L., Jr.; Lovell, H. L. "The Relation of Coal Characteristics to Coal Liquefaction Behavior"; Report No. 3 Submitted to National Science Foundation (RANN Division), Sept 1975.

Given, P. H. "Catalysis of Liquefaction by Iron Sulfide from Coals, With Some Thoughts on Coal Mineral Analysis"; paper presented at the Department of Energy Project Review Meeting on Disposable Catalysts in Coal Liquefaction held in Albuquerque, NM, June 1979.

Granoff, B.; Thomas, M. G. Am. Chem. Soc. Div. Fuel Chem. Prepr. 1977, 22, 183.

Granoff, B.; Baca, P. M. "Mineral Matter Effects and Catalyst Characterization in Coal Liquefaction"; Annual Report (Oct 1977–Sept 1978), Sandia Laboratories (SAND-79-0505), Albuquerque, NM, Apr 1979.

Guin, J. A.; Tarrer, A. R.; Prather, J. W.; Johnson, D. R.; Lee, J. M. Ind. Eng. Chem. Process Des. Dev. 1978, 17, 118.

Guin, J. A.; Tarrer, A. R.; Lee, J. M.; Lo, L.; Curtis, C. W. Ind. Eng. Chem. Process Des. Dev. 1979, 18, 371.

Hamrin, C. E., Jr. "Catalytic Activity of Coal Mineral Matter"; Interim Report for the Period April–September, 1976, prepared for ERDA by University of Kentucky (FE-2233-2).

Lee, J. M.; VanBrackle, H. F.; Lo, Y. L.; Tarrer, A. R.; Guin, J. A. "Catalytic Activity of Coal Minerals in Coal Liquefaction"; paper presented at the 84th National AIChE Meeting, Atlanta, Feb 26–Mar 1, 1978.

Moroni, E. D.; Fischer, R. H. "Disposable Catalysts for Coal Liquefaction"; paper presented at the 179th National Meeting of American Chemical Society, Houston, Mar 1980.

Mukherjee, D. K.; Chowdhury, P. B. Fuel 1976, 55, 4.

Seltzer, W. H. "Miscellaneous Autoclave Liquefaction Studies"; Final Report prepared for EPRI by Suntech, Inc., under the contract EPRI AF-612 (RP-799-7), Feb 1978.

Skinner, R. W.; Givens, E. N. "Effects of Solvent Hydrogen Content in the SRC Process"; paper presented at the 179th National Meeting of American Chemical Society, Houston, Mar 1980.

Solvent Refined Coal (SRC) Process, Quarterly Technical Progress Report FE/496-155 Prepared for U.S. Department of Energy by The Pittsburg and Midway Coal Mining Co., Shawnee Mission, KS, Mar 1979.

Tarrer, A. R.; Guin, J. A.; Pitts, W. S.; Hentey, J. P.; Prather, J. W.; Styles, G. A. "Effect of Coal Minerals on Reaction Rates During Coal Liquefaction"; American Chemical Society Preprints, "Liquid Fuel from Coal", Academic Press: New York, 1977.

Wright, C. H.; Severson, D. E. Am. Chem. Soc. Div. Fuel Chem. Prepr. 1972, 16 68.

Wu, W. R. K.; Storch, H. H. "Hydrogenation of Coal and Tar"; U.S. Department of the Interior, Bureau of Mines Bulletin 633, 1968; Chapter 4, p 74 ff.

EFFECT OF CATALYST DISTRIBUTION IN COAL LIQUEFACTION

Diwakar Garg and Edwin N. Givens
Corporate Research and Development Department

Air Products and Chemicals, Inc.
P.O. Box 538, Allentown, PA 18105

Effect of the mode of catalyst addition was studied for the liquefaction of Eastern Kentucky Elkhorn #2 coal in a continuously stirred tank reactor. Particulate addition of iron as pyrite significantly catalyzed the coal lique- faction reaction. Both coal conversion and oil yield increased on addition of pyrite to the feed slurry; oil production increased by more than a factor of two both at 825° and 850°F. Pyrite Concentration had negligible effect on product distribution, but the mode of catalyst addition had a big impact on coal liquefaction. Impregnation of coal with one weight percent iron gave a similar product distribution as obtained with addition of 3.5 weight percent iron in the form of particulate pyrite. Significantly lower hydrocarbon gas make and hydrogen consumption were noted with impregnation over particulate addition. SRC sulfur content was marginally higher with impregnation. Solvent hydrogen content increased with particulate addition whereas it decreased with impregnation.

Introduction

The basic non-catalytic process for liquefaction of coal was developed by Bergius[1] in Germany circa 1912. In 1925 Brown-coal tar was catalytically hydrogenated for the first time with molybdenum oxide. This advance led to the development of the catalytic hydrogenation of coal.

A number of catalysts were studied and reported to give improved yield and product quality[2]. Adding two percent molybdenum on coal as ammoniam molybdate substantially increased the liquefaction performance. Subsequent experiments showed that 0.05 percent molybdenum gave a yield equal to that obtained with two percent when the alkalinity of coal was reduced. Because molybdenum was expensive and in short supply in Germany, it was replaced by iron catalyst. The Germans found that adding iron as iron sulfate to the feed slurry improved the liquefaction of coal[2]. Bayermasse, an iron oxide-containing material obtained as by-product from aluminum manufacture was also shown to be active in coal liquefaction. In terms of iron content, twice as much Bayermasse as sulfate was needed to produce the same results in hydrogenation of coal. In certain cases the addition of sulfur to the system also improved the catalytic liquefaction effect of the iron[2]. The iron to sulfur ratio in the liquefaction residue suggested that iron sulfide (FeS) was the ultimate form of the iron. With the advent of x-ray diffraction technique the FeS was found to be in the form of pyrrhotite[3], $Fe_{1-x}S$.

Wright and Severson reported that the addition of iron as contained in the residues from coal liquefaction increased the hydrogen transfer capacity of anthracene oil.[4] Seitzer[5] magnetically separated the iron sulfur compound from coal liquefaction residues and used it as a catalyst in subsequent lique- faction reactions. He found that the magnetically separated material had, per

weight of iron, about the same catalytic effect as ferrous sulfate. Furthermore, he found that the magnetically separated material catalyzed the addition of hydrogen to the dissolved coal.

Moroni and Fischer[6], who reviewed many papers in the area of coal mineral catalysis, concluded that pyrite was active in coal conversion. Neither the addition of the coal liquefaction residue nor the magnetically separated residue delineated whether pyrrhotite had better catalytic activity than pyrite. A significant amount of work has been done more recently to determine the true catalytic activity of pyrite and pyrrhotite. A detailed summary of literature on pyrite and pyrrhotite catalysis has been made by Garg and Givens.[7]

The distribution of catalyst in the coal appears to be a critical factor in coal conversion. The method of applying the catalyst to the coal affects the catalyst distribution. For example, iron sulfate was shown to be much more effective when impregnated than when mixed mechanically.[2,8] Although prolonged mixing improved the effectiveness of the catalyst, the improvement was less than gained by impregnation. The method of impregnation is also quite important as was shown in one case in which an attempt to impregnate coal in-situ during hydrogenation gave poor results.[8]

A reduction in particle size of the pyrite, reported to play an important role in catalyzing the coal liquefaction reaction, improved the catalytic activity of the pyrite.[9] Significantly more oil production was reported with the use of finely divided pyrite[10] than with hand ground pyrite.[11]

The contact between catalyst and coal can be increased either by adding finely divided catalyst (two to three micron size) or impregnating it on coal using a water soluble compound like iron sulfate or dispersing it at the molecular level in the reaction mixture by using thermally unstable organic compounds like iron naphthenate. In the present paper data are presented which show the catalytic activity of pyrite and impregnated iron sulfate in coal liquefaction. The effect of simple particulate addition of pyrite is compared to catalyst impregnation. The catalytic activity for the coal conversion reactions are related to the product distribution including hydrocarbon gas make, oil, asphaltene and preasphaltene yields, and degree of coal conversion. All of the data reported in this paper refer to results in a continuous 100 pounds per day coal process unit.

Experimental

Materials: Elkhorn #2 was a washed sample taken from a preparation plant in Floyd County, Kentucky. The coal sample was ground to 95% minus 200 mesh particles and dried in air. The coal was screened through a 150 mesh sieve prior to use. The detailed analysis of the screened coal is reported in Table 1.

A 550-850°F cut of SRC-II heavy distillate supplied by The Pittsburg and Midway Coal Mining Company was used as a process solvent. The chemical analysis of the process solvent is shown in Table 2. The solvent contained 93.8% pentane-soluble oils, 5.0% asphaltenes and 0.4% preasphaltenes.

The pyrite sample was received from an operating mine in southwestern Pennsylvania. The sample was dried at 110°C in nitrogen and then ground to 99.9% minus 325 U.S. mesh size in the presence of liquid nitrogen. The chemical analysis of the pyrite is given in Table 3. The sample was comprised of 75%

pyrite, 5% carbonaceous organic material and 20% magnetite, quartz, and other inorganic materials. The BET surface area of the pyrite was 1.0 m^2/g and the material was relatively non-porous.

Iron sulfate (FeSO$_4$ · 7H$_2$O) was received from Textile Chemical Company, Reading, Pennsylvania. The chemical analysis of the iron sulfate is given in Table 4. The sample contained approximately 97% iron sulfate crystals.

Equipment: Process studies were done in a continuous 100 pound/day coal liquefaction unit equipped with a continuous stirred autoclave. The use of a stirred tank reactor insured that solvent vaporization matched that of an actual SRC-I dissolver and that coal minerals did not accumulate. Since there was no slurry preheater, all of the sensible heat had to be provided by resistance heaters on the reactor. Because of this high heat flux, the reactor wall was about 27°F hotter than the bulk slurry. Multiple thermocouples revealed that the slurry temperature inside the reactor varied by only 9°F from top to bottom. A detailed description of the reactor is presented elsewhere.[12]

The products were quenched to 320°F before flowing to a gas/liquid separator that was operated at system pressure. The slurry was throttled into the product receiver while the product gases were cooled to recover the product water and organic condensate. The product gases were then analyzed by an on-line gas chromatograph.

Procedure: Coal liquefaction runs were performed at 825 and 850°F, 2000 psig hydrogen pressure, 1000 rpm stirrer speed, hydrogen feed rate equivalent to 5.5 wt.% of the coal and a superficial slurry space velocity of 1.5 inverse hours. The coal concentration in the feed was 30 wt.%. Iron sulfate was impregnated on the coal by dissolving it in water and mixing it with coal. Impregnated coal sample was dried in nitrogen and ground to minus 200 mesh prior to use. The concentration of impregnated iron was 1.0 wt.% on the basis of coal. The concentration of pyrite was varied from 2.5 to 10 wt.% of feed slurry.

At least 10 reactor volumes of the product were discarded prior to collecting a product sample. A complete sample consisted of one 8-oz. sample of product slurry, one 1-liter sample of product slurry as back-up sample, a light condensate sample and a product gas sample.

The product slurry from the continuous reactor was solvent separated into four fractions: (1) pentane-soluble material (oil), (2) pentane-insoluble and benzene-soluble material (asphaltenes), (3) benzene-insoluble and pyridine-soluble material (preasphaltenes), and (4) pyridine-insoluble material. The latter contains insoluble organic material (IOM) and mineral residue. A detailed procedure for performing this separation will be reported elsewhere. The overall coal conversion is calculated as the fraction of organic material (moisture-ash-free coal) soluble in pyridine.

Results and Discussions

Effect of Pyrite on Coal Liquefaction - At 825 and 850°F, addition of pyrite increased the coal conversion from ~85 to ~92% (Table 5). The production of hydrocarbon gases, CO + CO$_2$ and water, marginally increased with pyrite. Oil production increased by more than a factor of two; 12 to 28% and from 8 to 27%

on addition of pyrite at 825 and 850°F, respectively. Production of preasphaltenes decreased and asphaltenes remained apparently unchanged. The additional converted coal and preasphaltenes with pyrite ended up in the oil fraction. Hydrogen consumption increased from 0.64 to 1.68% and from 0.53 to 2.41% on addition of pyrite at 825 and 850°F, respectively. Also, an additional amount of 0.5% hydrogen was consumed in reducing the added pyrite. X-ray diffraction analysis of coal liquefaction residue showed a complete conversion of pyrite to pyrrhotite. SRC sulfur content remained the same. Oil hydrogen content unchanged in the absence of pyrite but increased in its presence.

In summary, the addition of pyrite to coal during liquefaction improved conversion of coal and preasphaltenes, increased production of oil and hydrocarbon gases, promoted rehydrogenation of the process solvent and increased consumption of hydrogen. Increasing reaction temperature in the presence of pyrite increased conversion of preasphaltenes and increased production of hydrocarbon gases and hydrogen consumption. The conversion of coal and production of oil and asphaltenes marginally decreased with increasing temperature.

Effect of Pyrite Concentration on Coal Liquefaction - Conversion of coal and production of hydrocarbon gases remained the same upon increasing the pyrite concentration from 2.5 to 10 wt. percent. (Table 6, Figures 1 and 2). The production of $CO + CO_2$, water and oil shown in Table 6 and Figures 2 and 3 increased slightly as pyrite concentration increased. Asphaltenes remained the same and preasphaltenes decreased with increasing concentration of pyrite (Figure 4). Hydrogen consumption increased significantly as the pyrite concentration increased as shown in Table 6 and Figure 5. SRC sulfur content plotted in Figure 6 also marginally increased. Finally, increasing the concentration of pyrite from 2.5 to 10 wt.% of feed slurry had no significant effect on liquefaction of Elkhorn #2 coal.

Effect of Iron Impregnation on Coal Liquefaction - Conversion of coal was not significantly affected by impregnation at both 825 and 850°F. The production of hydrocarbon gases decreased considerably with iron impregnation while oil production increased by over a factor of two at both temperatures (Table 7). Asphaltene yield was unchanged but preasphaltene yield decreased considerably with iron impregnation. X-ray diffraction analysis of coal liquefaction residue showed a complete conversion of iron sulfate to pyrrhotite. Hydrogen consumption and SRC sulfur content were not significantly affected by iron impregnation. Oil hydrogen content was maintained without any additive but decreased with iron impregnation at both 825 and 850°F. Finally, iron impregnation significantly reduced the hydrocarbon gases and preasphaltenes production and increased the oil production.

Comparison of Iron Impregnated Versus Particulate Addition - The liquefaction of coal impregnated with one wt.% iron based on coal is compared with addition of 3.5 wt% particulate iron in the form of pyrite to coal-oil slurry. Conversion of coal was slightly lower with iron impregnation compared to pyrite addition. Iron impregnation gave signficantly lower hydrocarbon gases production and hydrogen consumption (Table 8, Figures 7 and 8). Oil, asphaltenes and preasphaltenes production with iron impregnation were comparable to that obtained by pyrite addition. SRC sulfur content was marginally higher with iron impregnation. Oil hydrogen content was improved with pyrite, whereas it decreased with iron impregnation.

The above data emphasize the importance of the method of catalyst distribution in coal liquefaction. The effectiveness of a metal catalyst can be enhanced significantly by increasing the intimate contact between catalyst and coal. The mode of catalyst distribution therefore determines the amount of catalyst required for the reaction.

Conclusion

Addition of pyrite significantly catalyzes the coal liquefaction reaction. It improves coal conversion, increases oil and gases production, increases hydrogen consumption and rehydrogenates the process solvent. Changing the concentration of pyrite does not significantly alter the coal liquefaction reaction. Mode of catalyst addition is very important in coal liquefaction. The activity of a catalyst depends on the level of intimate contact of catalyst with coal. Therefore, the concentration of the metal catalyst can be greatly reduced without affecting product distribution by insuring efficient contact between catalyst and coal. The reduction in catalyst loading will eventually increase the overall throughput of the plant, drastically reduce the load in the solid-liquid separation unit, and improve the overall process economics.

References

1. Bergius, F., and Billwiller, J., German Patent 301,231, August 1, 1913.
2. Wu, W. R. K., and Storch, H. H., "Hydrogenation of Coal and Tar", U.S. Department of the Interior, Bureau of Mines Bulletin 633, 1968.
3. Given, P. H., Spackman, W., Davis, A., Walker, P. L. Jr., and Lovell, H. L., "The Relation of Coal Characteristics to Coal Liquefaction Behavior", Report No. 1 Submitted to NSF (RANN Division) by the Pennsylvania State University, 15 March 1974.
4. Wright, C. H., and Severson, D. E., ACS Division of Fuel Chem., Preprints, 1972, 16, 68.
5. Seitzer, W. H., "Miscellaneous Autoclave Liquefaction Studies," Final Report Prepared for EPRI by Suntech, Inc., under the contract EPRI AF-612 (RP-779-7), February, 1978.
6. Moroni, E. C. and Fischer, R. H., "Disposable Catalysts for Coal Liquefaction," Paper Presented at the 179th National Meeting of American Chemical Society, Houston, March, 1980.
7. Garg, D. and Givens, E. N., "Pyrite Catalysis in Coal Liquefaction," Paper Accepted for Publication in I&EC Process Design and Development.
8. Weller, S. W. and Pelipetz, M. G., Ind. Eng. Chem., 1951, 43, 1243.
9. Guin, J. A., Tarrer, A. R., Lee, J. M., Lo, L. and Curits, C. W., Ind. Eng. Chem. Process Des. Dev., 1979, 18, 371.
10. Anderson, R. P., "Low Cost Additives in the SRC Processes," Paper Presented at the Dept. of Energy Project Review Meeting on Disposable Catalysts in Coal Liquefaction held in Albuquerque, New Mexico, June, 1979.
11. Solvent Refined Coal (SRC) Process, Quarterly Technical Progress Report FE/496-155 Prepared for U.S. Dept. of Energy by The Pittsburg and Midway Coal Mining Co., Shawnee Missio, Kansas, March, 1979.
12. Skinner, R. W., and Givens, E. N., "Effects of Solvent Hydrogen Content in the SRC Process," Paper Presented at the 179th National Meeting of American Chemical Society, Houston, March, 1980.

TABLE 5
LIQUEFACTION OF COAL IN THE PRESENCE AND ABSENCE OF PYRITE

FEED COMPOSITION	70% SOLVENT + 30% COAL		60% SOLVENT + 30% COAL + 10% PYRITE	
Fe CONCENTRATION, WT. % COAL	0.0	0.0	14.1	14.1
TEMP., °F	825	850	825	850
PRESSURE, PSIG	2000	2000	2000	2000
RESIDENCE TIME, MIN.	35	39	37	39
HYDROGEN TREAT RATE, MSCF/T	18.9	23.0	19.9	22.5
PRODUCT DISTRIBUTION, WT. % MAF COAL				
HC	5.2	7.0	5.7	10.6
CO, CO_2	0.7	0.6	0.9	1.2
H_2S	0.3	0.3	0.0	0.0
OIL	12.2	8.3	28.2	27.0
ASPHALTENES	21.2	21.6	24.3	22.3
PREASPHALTENES	44.2	43.4	29.6	25.6
I.O.M.	14.7	15.7	8.1	9.3
WATER	1.5	3.1	3.2	4.0
CONVERSION, % MAF	85.3	84.3	91.9	90.7
HYDROGEN CONSUMPTION,* WT. % MAF	0.64	0.53	1.68	2.41
OIL HYDROGEN CONTENT, WT. %				
START	7.2	7.2	7.2	7.2
FINISH	7.2	7.2	7.5	7.5
SRC SULFUR, %	0.61	0.55	0.60	0.57

*HYDROGEN CONSUMPTION DOES NOT INCLUDE THE HYDROGEN REQUIRED FOR REDUCING FeS_2 TO FeS

TABLE 6
EFFECT OF PYRITE CONCENTRATION ON COAL LIQUEFACTION

TEMP., °F	850	850	850
PYRITE CONCENTRATION, WT. % FEED SLURRY	2.5	5.0	10.0
IRON CONCENTRATION, WT. % COAL	3.5	7.1	14.1
PRESSURE, PSIG	2000	2000	2000
RESIDENCE TIME, MIN.	38	38	39
HYDROGEN TREAT RATE, MSCF/T	24.2	22.2	22.5
PRODUCT DISTRIBUTION, WT. % MAF COAL			
HC	10.2	9.9	10.6
CO, CO_2	0.9	1.0	1.2
OIL	25.6	24.3	27.0
ASPHALTENES	22.3	18.6	22.3
PREASPHALTENES	28.2	32.3	25.6
I.O.M.	9.3	10.4	9.3
WATER	3.2	3.5	4.0
CONVERSION, % MAF	90.7	89.6	90.7
HYDROGEN CONSUMPTION,* WT. % MAF	1.75	1.81	2.41
OIL HYDROGEN CONTENT, WT. %			
START	7.2	7.2	7.2
FINISH	7.3	7.5	7.5
SRC SULFUR, %	0.49	0.51	0.57

*HYDROGEN CONSUMPTION DOES NOT INCLUDE THE HYDROGEN REQUIRED FOR REDUCING FeS_2 TO FeS

TABLE 7
EFFECT OF IRON IMPREGNATION ON COAL LIQUEFACTION

IRON IMPREGNATION	NO	NO	YES	YES
Fe CONC., WT. % COAL	0.0	0.0	1.0	1.0
FEED COMPOSITION	70% SOLVENT + 30 COAL			
TEMPERATURE, °F	825	850	825	850
PRESSURE, PSIG	2000	2000	2000	2000
RESIDENCE TIME, MIN.	35	37	33	41
HYDROGEN TREAT RATE, MSCF/T	18.9	19.9	20.6	27.3
PRODUCT DISTRIBUTION, WT. % MAF COAL				
HC	5.2	7.0	3.5	4.4
CO, CO_2	0.7	0.6	0.6	0.5
H_2S	0.3	0.3	0.2	0.2
OIL	12.2	8.3	25.0	30.3
ASPHALTENES	21.2	21.6	19.1	20.8
PREASPHALTENES	44.2	43.4	35.8	27.5
I.O.M.	14.7	15.7	13.5	13.1
WATER	1.5	3.1	2.3	3.2
CONVERSION	85.3	84.3	86.5	86.9
HYDROGEN CONSUMPTION, WT. % MAF	0.64	0.53	0.40	0.60
OIL HYDROGEN CONTENT, WT. %				
START	7.2	7.2	7.2	7.2
FINISH	7.2	7.2	7.1	7.0
SRC SULFUR, %	0.61	0.55	0.61	0.57

TABLE 8
IRON IMPREGNATION VERSUS PARTICULAR ADDITION

IRON ADDITION	PYRITE	IMPREGNATION
Fe CONCENTRATION, WT. % COAL	3.5	1.0
TEMPERATURE, °F	850	850
PRESSURE, PSIG	2000	2000
RESIDENCE TIME, MIN.	38	41
HYDROGEN TREAT RATE, MSCF/T	24.2	27.3
PRODUCT DISTRIBUTION, WT. % MAF COAL		
HC	10.2	4.4
CO, CO_2	0.9	0.5
H_2S	0.3	0.2
OIL	25.6	30.3
ASPHALTENES	22.3	20.8
PREASPHALTENES	28.2	27.5
I.O.M.	9.3	13.1
WATER	3.2	3.2
CONVERSION, % MAF	90.7	86.9
HYDROGEN, CONSUMPTION,* WT. % MAF	1.75	0.60
OIL HYDROGEN CONTENT, WT. %		
START	7.2	7.2
FINISH	7.3	7.0
SRC SULFUR, %	0.49	0.57

*HYDROGEN CONSUMPTION DOES NOT INCLUDE THE HYDROGEN REQUIRED FOR REDUCING FeS_2 TO FeS

TABLE 1
CHEMICAL ANALYSIS OF COAL SAMPLE

	ELKHORN #2 WEIGHT %
ULTIMATE ANALYSIS (AS RECEIVED)	
CARBON	77.84
HYDROGEN	5.24
OXYGEN	7.20
SULFUR	1.08
NITROGEN	1.75
PROXIMATE ANALYSIS (AS RECEIVED)	
ASH	6.29
MOISTURE	1.55
DISTRIBUTION OF SULFUR	
TOTAL SULFUR	1.08
SULFATE SULFUR	0.04
PYRITE SULFUR	0.25
ORGANIC SULFUR	0.79

TABLE 2
ANALYSIS OF HEAVY DISTILLATE

ELEMENT	WEIGHT %
CARBON	89.44
HYDROGEN	7.21
OXYGEN	1.70
NITROGEN	1.10
SULFUR	0.55
NUMBER AVERAGE MOLECULAR WEIGHT	222

TABLE 3
ANALYSIS OF PYRITE

	WEIGHT %
CARBON	4.48
HYDROGEN	0.34
NITROGEN	0.61
SULFUR	41.34
OXYGEN	5.97
IRON	42.30
OTHER IMPURITIES (BY DIFFERENCE)	4.96
TOTAL	100.00

SURFACE AREA = $1.0 \ m^2/g$

TABLE 4
ANALYSIS OF IRON SULFATE

	WEIGHT %
FERROUS SULFATE, $FeSO_4$	53.78
IRON, Fe_2O_3	0.06
TITANIUM, TiO_2	0.33
MAGNESIUM SULFATE, $MgSO_4$	1.80
COPPER	0.0004
LEAD	0.0005
WATER OF CRYSTALLIZATION	42.28
TOTAL	99.25

Figure 1
Variation in the Conversion of Coal
With the Concentration of Pyrite

Figure 2
Variation in the Production of Gases and Water
With the Concentration of Pyrite

Figure 3
Variations in the Production of Oils
With the Concentration of Pyrite

Figure 4
Variation in the Production of Asphaltenes and Preasphaltenes
With the Concentration of Pyrite

Figure 5
Variation of Hydrogen Consumption With the
Concentration of Pyrite

Figure 6
Variation of SRC Sulfur Content With the Concentration
of Pyrite

Figure 7
Iron Impregnation Versus
Particulate Addition

Figure 8
Iron Impregnation Versus
Particulate Addition